Ellen J. Hagopian
Junji Machi *Editors*

Abdominal Ultrasound for Surgeons

VIDEOS
springerimages.com

Springer

Abdominal Ultrasound for Surgeons

Ellen J. Hagopian • Junji Machi
Editors

Abdominal Ultrasound for Surgeons

Springer

Editors
Ellen J. Hagopian, MD, FACS
Department of Surgery
Jersey Shore University Medical Center
Neptune, NJ
USA

Department of Surgery
Robert Wood Johnson Medical School
New Brunswick, NJ
USA

Department of Surgery
New York Medical College
Valhalla, NY
USA

Junji Machi, MD, PhD, FACS
Department of Surgery
John A. Burns School of Medicine
University of Hawaii and Kuakini Medical Center
Honolulu, HI
USA

Noguchi Medical Research Institute
JADECOM-NKP GME Center
Tokyo Bay Urayasu-Ichikawa Medical Center
(Noguchi Hideyo Memorial International
Hospital)
Urayasu, Chiba
Japan

Videos to this book can be accessed at http://www.springerimages.com/videos/978-1-4614-9598-7

ISBN 978-1-4614-9598-7 ISBN 978-1-4614-9599-4 (eBook)
DOI 10.1007/978-1-4614-9599-4
Springer New York Heidelberg Dordrecht London

Library of Congress Control Number: 2014938111

Printed on acid-free paper

Springer is part of Springer Science+Business Media (www.springer.com)

Preface

Surgical ultrasound has been a tool of the abdominal surgeon for a number of years. Ultrasound has been referred to as the stethoscope of the surgeon as it allows the unseen to be seen and is recognized as a vital component in many surgical procedures. Even with advances in preoperative imaging, such as computed tomography and magnetic resonance imaging, the evidence is clear that ultrasound is a practical and indispensable tool of the surgeon preoperatively, intraoperatively, and postoperatively. However, despite its well-recognized value, education and practice remain the major obstacles to the use of perioperative or intraoperative ultrasound. Furthermore, even for those using ultrasound in practice, advances not only in surgical procedure but also in ultrasound technology have emphasized the need to update the surgeon, fellow, and resident to the current status of surgical ultrasound. This book is intended to serve as the beginning or continuation of an education in ultrasound for the surgeon.

In the chapters that follow, experts in the field will detail the facts, lessons, and tricks to master this indispensable tool. The current and future applications of surgical ultrasound will be detailed to further underscore its need by the surgeon. Unlike other imaging methods, ultrasound is highly examiner dependent. Particularly in surgical ultrasound, surgeons must scan by themselves in order to maximize its benefits. We are certain that once learned, ultrasound can help improve surgeon-sonographers' practices, outcomes, and patient care. We hope this book provides the key to its use and execution to unlock the valuable insight that ultrasound can provide to the surgeon in practice or in training.

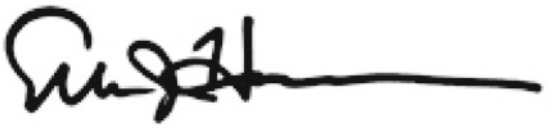

Ellen J. Hagopian, MD, FACS
Neptune, NJ, USA

Junji Machi, MD, PhD, FACS
Honolulu, HI, USA

Contents

Part I The Basics

1 Introduction: The Importance of Ultrasound in a Surgical Practice 3
Kevin Ryan Parks and Ellen J. Hagopian

2 Physical Principles of Ultrasound 7
Beth A. Schrope and Neha Goel

3 Instrumentation in Ultrasound 17
Halit Eren Taskin and Eren Berber

4 Scanning Techniques in Transabdominal and Intraoperative/ Laparoscopic Ultrasound 31
Reid B. Adams

5 Imaging Characteristics and Artifacts 61
Michael J. Giuffrida and Gary Gecelter

Part II Anatomy, Application, and Intervention: Transabdominal, Intraoperative, Laparoscopic

6 Abdominal Wall Anatomy, Pathology, and Intervention 71
Jose M. Velasco and Faaiza Vaince

7 Percutaneous Ultrasound Guidance Techniques and Procedures 89
Jose M. Velasco and Keith Hood

8 Trauma Ultrasound 109
Kazuhide Matsushima and Heidi L. Frankel

9 Abdominal/Retroperitoneal Vascular Ultrasound 121
Daniel R. Calderon and David C. Han

10 Laparoscopic Ultrasound in Staging of GI Malignancies 129
Ewen M. Harrison and O. James Garden

11 Endoscopic Ultrasound in the Upper Gastrointestinal Tract 151
Dominique Dempah, Moaz Abulfaraj, and Maurice E. Arregui

12 Intraoperative and Laparoscopic Ultrasound During Pancreatic Surgery 161
W. Scott Helton and J. Bart Rose

13 Intraoperative Ultrasound During Laparoscopic Cholecystectomy 177
Ezra N. Teitelbaum and Nathaniel J. Soper

14 Intraoperative Ultrasound During Biliary Tract Surgery 187
Ewen M. Harrison and O. James Garden

15 Intraoperative and Laparoscopic Ultrasound During Liver Surgery 201
Gabriella Pittau, Michele Tedeschi, and Denis Castaing

16 Techniques in Laparoscopic and Intraoperative Ultrasound Guidance 219
David J. Niemeyer, Kerri A. Simo, and David A. Iannitti

17 Ultrasound Techniques for Liver Tumor Ablation 229
Paul D. Hansen, W. Cory Johnston, and Chet Hammill

18 Computer-Assisted Navigation for Ultrasound "3-D Ultrasound" 243
John B. Martinie and Sharif Razzaque

19 Endoluminal Ultrasound: Anatomy, Technique, and Intervention of the Anorectum 255
Joseph L. Frenkel and John H. Marks

Part III Ultrasound in Surgical Practice

20 Getting Started 269
Christopher J. Kim and Junji Machi

21 Abdominal Ultrasound: Credentialing and Certification 279
R. Stephen Smith, William R. Fry, and Richard A. Hoppman

22 Coding and Billing for Ultrasound Examinations 283
Junji Machi

23 Future Perspective in Abdominal Ultrasound 287
Junji Machi, Fuminori Moriyasu, Shigeki Arii, Masahiko Yano, and Emi Saegusa-Beecroft

Index 305

Contributors

Moaz Abulfaraj, MD, FRCSC Department of General Surgery,
St. Vincent Hospital Indianapolis, Carmel, IN, USA

Reid B. Adams, MD, FACS Department of Surgery, The University of Virginia Cancer Center, University of Virginia Health System, Charlottesville, VA, USA

Shigeki Arii, MD, PhD Department of Hepato-Biliary-Pancreatic Surgery,
Tokyo Medical and Dental University, Bunkyo-ku, Tokyo, Japan

Maurice E. Arregui, MD, FACS Department of General Surgery, St. Vincent's Hospital, Indianapolis, IN, USA

Eren Berber, MD, FACS Department of General Surgery, Cleveland Clinic,
Cleveland, OH, USA

Daniel R. Calderon, MD Department of Surgery, Penn State Hershey Medical Center,
Penn State Heart and Vascular Institute, Hershey, PA, USA

Denis Castaing, MD HPB Surgery and Liver Transplantation,
AP-HP, Hopital Paul Brousse, Centre Hépato-biliaire, Villejuif, France

University Paris-Sud, UMR-S 785, Villejuif, France

Inserm, Unité 785, Villejuif, France

Dominique Dempah, MD Department of Surgery, St. Vincent's Hospital,
Indianapolis, IN, USA

Heidi L. Frankel, MD, FACS, FCCM Department of Surgery,
University of Southern California Keck School of Medicine, Los Angeles, CA, USA

Joseph L. Frenkel, MD Division of Colorectal Surgery, Lankenau Medical Center
and Lankenau Institute for Medical Research, Mainline Health Systems,
Wynnewood, PA, USA

William R. Fry, MD, FACS, RVT, RDMS Department of Surgery,
University of South Carolina School of Medicine, Columbia, SC, USA

O. James Garden, CBE, FRCSEd, FRSE Department of Clinical Surgery,
The University of Edinburgh, Royal Infirmary of Edinburgh, Edinburgh, UK

Gary Gecelter, MD, FACS, FACG Department of Surgery, St. Francis Hospital,
Roslyn, NY, USA

Michael J. Giuffrida, MD Department of Surgery, St. Francis Hospital, Roslyn, NY, USA

Neha Goel, MD Department of Surgery, Columbia University Medical Center,
New York, NY, USA

Ellen J. Hagopian, MD, FACS Department of Surgery, Jersey Shore University Medical Center, Neptune, NJ, USA

Department of Surgery, Robert Wood Johnson Medical School, New Brunswick, NJ, USA

Department of Surgery, New York Medical College, Valhalla, NY, USA

Chet Hammill, MD Department of Surgical Oncology, Gastrointestinal and Minimally Invasive Surgery, The Oregon Clinic, Portland, OR, USA

Providence Cancer Center, Portland, OR, USA

David C. Han, MD, MS, FACS, RPVI Department of Surgery, Penn State Hershey Medical Center, Penn State Heart and Vascular Institute, Penn State College of Medicine, Hershey, PA, USA

Paul D. Hansen, MD Department of Surgical Oncology, Gastrointestinal and Minimally Invasive Surgery, The Oregon Clinic, Portland, OR, USA

Providence Cancer Center, Portland, OR, USA

Ewen M. Harrison, MB, ChB, PhD, FRCS Department of Clinical Surgery, The University of Edinburgh, Royal Infirmary of Edinburgh, Edinburgh, UK

W. Scott Helton, MD, FACS Section of Hepatobiliary Surgery, Virginia Mason Medical Center, Seattle, WA, USA

Keith Hood, MD Department of General Surgery, Rush University Medical Center, Chicago, IL, USA

Richard A. Hoppmann, MD Department of Internal Medicine, University of South Carolina School of Medicine, Columbia, SC, USA

David A. Iannitti, MD Hepatobiliary and Pancreas Surgery, Department of General Surgery, Carolinas Medical Center, Charlotte, NC, USA

W. Cory Johnston, MD Department of Surgical Oncology, Providence Cancer Center, Portland, OR, USA

Christopher J. Kim, MD Department of Surgery, Regional Medical Center of San Jose, San Jose, CA, USA

Junji Machi, MD, PhD, FACS Department of Surgery, John A. Burns School of Medicine, University of Hawaii and Kuakini Medical Center, Honolulu, HI, USA

Noguchi Medical Research Institute, JADECOM-NKP GME Center, Tokyo Bay, Urayasu-Ichikawa Medical Center, (Noguchi Hideyo Memorial International Hospital), Urayasu, Chiba, Japan

John H. Marks, MD, FACS, FASCRS Division of Colorectal Surgery, Lankenau Medical Center and Lankenau Institute for Medical Research, Mainline Health Systems, Wynnewood, PA, USA

Department of General Surgery and Digestive Oncology, University Nice Sophia-Antipolis, Centre Hospitalier University, Nice, France

John B. Martinie, MD Department of Surgery, Carolinas Medical Center, Charlotte, NC, USA

Kazuhide Matsushima, MD Department of Surgery, University of Southern California, Los Angeles, CA, USA

Fuminori Moriyasu, MD, PhD Department of Gastroenterology and Hepatology, Tokyo Medical University, Shinjuku-ku, Tokyo, Japan

David J. Niemeyer, MD Hepatobiliary and Pancreas Surgery,
Department of General Surgery, Carolinas Medical Center, Charlotte, NC, USA

Kevin Ryan Parks, BA Department of Surgery, Jersey Shore University Medical Center, Neptune, NJ, USA

Department of Surgery, Robert Wood Johnson Medical School, New Brunswick, NJ, USA

Gabriella Pittau, MD HPB Surgery and Liver Transplantation,
AP-HP, Hopital Paul Brousse, Centre Hépato-biliaire, Villejuif, France

Sharif Razzaque, PhD InnerOptic Technology, Inc., Hillsborough, NC, USA

J. Bart Rose, MD, MAS Section of Hepatobiliary Surgery,
Virginia Mason Medical Center, Seattle, WA, USA

Emi Saegusa-Beecroft, MD, PhD Department of Surgery, JABSOM, University of Hawaii and Kuakini Medical Center, Honolulu, HI, USA

Beth A. Schrope, MD, PhD, FACS, RDMS Department of Surgery,
New York Presbyterian/Columbia University Medical Center, New York, NY, USA

Columbia University College of Physicians and Surgeons, New York, NY, USA

Kerri A. Simo, MD Hepatobiliary and Pancreas Surgery, Department of General Surgery, Carolinas Medical Center, Charlotte, NC, USA

R. Stephen Smith, MD, RDMS, FACS Department of Surgery,
University of South Carolina School of Medicine, Columbia, SC, USA

Nathaniel J. Soper, MD Department of Surgery, Northwestern University Feinberg School of Medicine, Chicago, IL, USA

Halit Eren Taskin, MD Division of Endocrinology and Metabolism Institute,
Cleveland Clinic, Cleveland, OH, USA

Department of General Surgery, Cleveland Clinic, Cleveland, OH, USA

Michele Tedeschi, MD HPB Surgery and Liver Transplantation,
AP-HP, Hopital Paul Brousse, Centre Hépato-biliaire, Villejuif, France

Ezra N. Teitelbaum, MD Department of Surgery, Northwestern University Feinberg School of Medicine, Chicago, IL, USA

Faaiza Vaince, MD Department of General Surgery, Rush University Medical Center, Chicago, IL, USA

Jose M. Velasco, MD Department of Surgery, NorthShore University HealthSystem, Skokie Hospital, Skokie, IL, USA

Department of General Surgery, Rush University Medical Center, Chicago, IL, USA

Masahiko Yano Ultrasound Systems Division, Ultrasound Systems Development Department, Toshiba Medical Systems Corporation,
Otawara-Shi, Tochigi, Japan

Part I

The Basics

Introduction: The Importance of Ultrasound in a Surgical Practice

1

Kevin Ryan Parks and Ellen J. Hagopian

Introduction

The surgeon relies heavily on diagnostics and imaging in addition to history and physical exam when evaluating a patient's clinical picture. Decisions based on this information are constantly under review and rereview. Information available is often the result of the surgeon's own practices and choices, such as where and how to palpate, and leads to information that can improve the outcome of the case, whether it means arriving at a diagnosis or an operative decision. Because of its diagnostic accuracy, intraoperative ultrasound has been a tool of the abdominal surgeon for a number of years. Intraoperative ultrasound (IOUS) allows the unseen to be seen and has been recognized as a vital component in many surgical procedures. This chapter will review the history and role of IOUS in abdominal surgery and will consider some of the challenges and eventual rewards when incorporating ultrasound into a surgical practice.

Brief History of Surgical Ultrasound

Although the use of intraoperative radiology, such as intraoperative cholangiography, began in the 1930s, the first use of intraoperative ultrasound was not until the early 1960s. Early use of ultrasound in the operating room utilized A-mode imaging (see Chap. 2), which consisted of one-dimensional amplitude spikes on a display screen. Schlegel and colleagues [1] introduced A-mode ultrasound to locate renal calculi during nephrolithotomy in 1961. Following this, other investigators used ultrasound in the operating room to locate biliary stones. The initial clinical report was by Hayashi and colleagues [2], followed by Knight and Newell [3]. Despite these reports, the use of ultrasound in the operating room did not gain widespread acceptance due to challenges in understanding and interpreting A-mode imaging.

By the 1970s, A-mode imaging had given way to the development of real-time brightness, or B-mode, imaging (see Chap. 2), which is the more familiar ultrasound used today. This refined imaging overcame the difficulties of previous technologies, given its real-time and two-dimensional image advantages. The initial reports of this ultrasound technology were in the mid- to late 1970s, when Cook and Lytton [4] reported the intraoperative detection of renal calculi and Makuuchi et al. [5] reported the intraoperative localization of liver tumors. The less-complicated image interpretation of this B-mode imaging led to A renewed interest in intraoperative ultrasound. Despite this, acceptance of intraoperative ultrasound was still slow in the 1980s.

In 1989, Machi and Sigel reported a 10-year experience in operative ultrasound during 2,299 abdominal (including liver, pancreas, biliary, gastrointestinal, kidney), thoracic, cardiovascular, neurologic, and endocrine operations [6]. Intraoperative ultrasound was deemed useful in 91.5 % of cases. In a subsequent report, Machi and colleagues wrote specifically on their experience in 357 hepatic, 735 biliary, and 242 pancreatic cases [7]. In this follow-up report, they found the sensitivity, specificity, and accuracy in diagnosing colorectal liver metastases to be 93, 95, and 94 %, respectively, and in diagnosing common bile duct stones to be 92, 99, and 99 %, respectively. Furthermore, intraoperative ultrasound of the pancreas was found to be beneficial in 73 %. With increasing numbers of reports focusing on the advantages and benefits of intraoperative ultrasound, such as those by Machi and Sigel [6, 7], the use

K.R. Parks, BA
Department of Surgery, Jersey Shore University Medical Center, Neptune, NJ, USA

Department of Surgery, Robert Wood Johnson Medical School, New Brunswick, NJ, USA
e-mail: parkskr@umdnj.edu

E.J. Hagopian, MD, FACS (✉)
Department of Surgery, Jersey Shore University Medical Center, Neptune, NJ, USA

Department of Surgery, Robert Wood Johnson Medical School, New Brunswick, NJ, USA

Department of Surgery, New York Medical College, Valhalla, NY, USA
e-mail: ellenhagopian@aol.com

E.J. Hagopian, J. Machi (eds.), *Abdominal Ultrasound for Surgeons*,
DOI 10.1007/978-1-4614-9599-4_1,

of ultrasound became more widespread and accepted. By the mid-1990s, surgeons had recognized the value of ultrasound during certain procedures and real-time B-mode imaging was applied routinely for various operations including liver, biliary, pancreatic, endocrine, and vascular surgeries. Even with the improvement of preoperative imaging in the new millennium, such as multidetector computed tomography and magnetic resonance imaging, intraoperative ultrasound remains a necessary and indispensable tool of the abdominal surgeon [8–15].

Training in Surgical Ultrasound

Realizing the value of surgical ultrasound is fundamental to motivating the surgeon to train for proficiency in performing, interpreting, and utilizing ultrasound in practice. While the challenge of training on a different imaging modality may seem formidable, it should be recognized that this situation is in no way unique. Surgeons routinely use techniques that require special training and time to master. Although the learning curve in ultrasound may appear steep, a surgeon's knowledge of three-dimensional anatomy enables his/her understanding of ultrasound images and thus the slope of the curve is lessened.

The main obstacle to overcome in incorporating ultrasound into a surgical practice is the difficulty in obtaining sufficient training in ultrasound. For those in training, ultrasound may be integrated within surgical residency and fellowship programs. However, for surgeons in practice, a formalized curriculum and consistent practice are paramount. Formalized training in surgical ultrasound can be obtained through the American College of Surgeons and, most recently, through the Americas Hepato-Pancreato-Biliary Association. Practical application following observational experience is extremely important to gaining skill in ultrasound. According to Machi and Sigel with their colleagues, the learning curve for intraoperative ultrasound depends on the purpose of intraoperative ultrasound, the target organ of interest, and the complexity of the imaging procedure [7]. They suggest that about 25 ultrasound examinations are required to overcome the learning curve for screening for colorectal liver metastases. Similarly, about 25 examinations are required for screening for bile duct stones. As ultrasound guidance procedures require two-handed skill, a greater number of examinations are needed. For ultrasound guidance operations, for example, about 25–40 pancreas and 50 liver examinations/procedures are needed. In Chap. 20, training issues are reviewed in detail.

Surgical Ultrasound in Practice

Incorporating ultrasound into a surgical practice has significant rewards, not only in terms of patient benefit and patient outcome but also in terms of surgical professional development.

Clinical Evaluation: Extension of the Physical Exam

Ultrasound can be used as an extension of the physical exam of the patient. In the same way that a stethoscope extends the auditory examination of the lungs and other organ systems, ultrasound extends the examination of the abdomen. Because of its dynamic and instantaneous nature, ultrasound has inherent advantages over other imaging modalities. One of the best examples of this use of ultrasound at the bedside is in trauma. In the trauma bay, ultrasound is routinely used as part of the physical exam to guide clinical decision-making.

Intraoperative Evaluation

Hepatic Resection

The use of ultrasound in the operating room can be viewed as an extension of the physical exam but is also essential to the localization of abnormalities and the planning, guiding, and ensuring of the completeness of surgery. Hepatic surgery is perhaps the clearest example of the surgical applications of intraoperative ultrasound. The dynamic nature of ultrasound imaging provides clear pictures of blood vessel variations, segmental anatomy, and the localization of not only known but also occult tumor(s) that might otherwise be unknown to the surgeon. Recognizing variations in portal venous and hepatic venous anatomy is critical in liver surgery. Intraoperative ultrasound can identify the presence of clinically significant abnormalities, which can help to guide the operation. For example, a significant percentage of patients have variations in both the number and organization of hepatic veins. An inferior right hepatic vein is found in 10–15 % of patients, which drains directly into the inferior vena cava caudal to the right hepatic vein. The presence of this accessory hepatic vein allows resection of segment 7 with the right hepatic vein, while allowing for preservation of segment 6. Less common are variations in the portal venous anatomy. One variation is the absence of the main right portal vein where the main portal vein divides into three veins: the right anterior, the right posterior, and the main left portal vein [16].

While identifying variations in vascular anatomy, the surgeon can also define the segmental anatomy and localize lesions. Furthermore, with its diagnostic accuracy, occult lesions not visualized on preoperative imaging can be defined. By clearly defining the extent of disease, resectability can be determined by the surgeon in the operating room. Following resection, IOUS can be utilized to ensure completeness of resection. Knowledge of anatomy is important to surgery, but knowledge of a particular patient's anatomy and extent of disease is paramount to planning liver resection and guiding surgery once it has begun.

Staging of Malignancy

The utility of ultrasound in abdominal surgery is also applied to staging of the extent of disease in many intra-abdominal malignancies. Preoperative staging of rectal cancer can be accomplished with transrectal endoluminal ultrasound and the extent of a pancreatic tumor can be evaluated using endoscopic ultrasound. Intraoperative ultrasound can also be integrated into the staging of pancreatic, gastric, and colorectal cancers while evaluating local disease and the presence of liver metastases [17]. Especially when combined with laparoscopy, intraoperative (laparoscopic) ultrasound can be instrumental in salvaging the patient from unnecessary laparotomy if occult metastatic disease is found.

Guidance of Procedures

Ultrasound can be used to guide operative procedures. Not only can ultrasound be used to target a liver lesion for biopsy or ablation, it can also be used to guide cannulation of the pancreatic duct. Minimally invasive approaches, such as percutaneous or laparoscopic techniques, utilize ultrasound in abdominal abscess drainage and have been recognized as a safe alternative therapy to open surgery [18]. Common bile duct stones can be identified during open or laparoscopic ultrasound to determine the need for common bile duct exploration or endoscopic retrieval. Furthermore, intraoperative ultrasound is essential for hepatectomy prior to resection by marking vasculature, during resection by guiding the line of parenchymal resection, and following resection by ensuring completion of resection.

Professional Development

It may be clear that utilization of ultrasound in a surgical practice is in the best interest of the patient, but it should be equally understood that using and understanding ultrasound are in the best interest of the surgical profession. Surgical ultrasound has had time to grow and refine as a technology and will continue to be introduced into procedures and practices not yet considered. Advances in technology will continuously influence surgical procedures. Less invasive surgery, such as laparoscopic liver resection and robotic-assisted pancreatoduodenectomy, displaces the surgeon's hand from the operation and thus increases the need for image guidance, such as what is provided for by ultrasound. As surgery evolves, new uses of ultrasound can be developed to continue to address the changing needs of the surgeon in the operating room. Newer technologies in ultrasound are reviewed in Chap. 23.

Our understanding and use of ultrasound in the daily practice of surgery are important when teaching the skill of surgery. For future surgeons, the understanding of how and when to utilize ultrasound in surgery becomes more imperative as new uses of this indispensible tool are developed.

Conclusion

Intraoperative ultrasound is an extremely useful tool for the surgeon, which demands presence at the forefront of patient care. In its beginnings, ultrasound was used primarily as a diagnostic tool but now has evolved to include multiple uses. Used not only in the mere diagnosis of conditions, but surgical ultrasound is also often used as an extension of the physical exam at the bedside and operating room in addition to use in surgical therapeutic procedures. Incorporating ultrasound into a surgical practice has significant rewards, not only in terms of patient benefit and outcome but also in terms of development of the surgical profession.

References

1. Schlegel JU, Diggdon P, Cuellar J. The use of ultrasound for localizing renal calculi. J Urol. 1961;86:367–9.
2. Hayashi S, Wagai T, Miyazawa R, Ito K, Ishikawa S, Uematsu K, Kikuchi Y, Uchida R. Ultrasonic diagnosis of breast tumor and cholelithiasis. West J Surg Obstet Gynecol. 1962;70:34–40.
3. Knight PR, Newell JA. Operative use of ultrasonics in cholelithiasis. Lancet. 1963;1(7289):1023–5.
4. Cook 3rd JH, Lytton B. Intraoperative localization of renal calculi during nephrolithotomy by ultrasound scanning. J Urol. 1977;117(5):543–6.
5. Makuuchi M, Torzilli G, Machi J. History of intraoperative ultrasound. Ultrasound Med Biol. 1998;24(9):1229–42.
6. Machi J, Sigel B. Overview of benefits of operative ultrasonography during a ten year period. J Ultrasound Med. 1989;8:647–52.
7. Machi J, Sigel B, Zaren HA, Kurohiji T, Yamashita Y. Operative ultrasonography during hepatobiliary and pancreatic surgery. World J Surg. 1993;17:640–6.
8. Lordan JT, Stenson KM, Karanjia ND. The value of intraoperative ultrasound and preoperative imaging, individually and in combination, in liver resection for metastatic colorectal cancer. Ann R Coll Surg Engl. 2011;93(3):246–9.
9. Sietses C, Meijerink MR, Meijer S, van den Tol MP. The impact of intraoperative ultrasonography on the surgical treatment of patients with colorectal liver metastases. Surg Endosc. 2010;24(8):1917–22.
10. Conlon R, Jacobs M, Dasgupta D, Lodge JP. The value of intraoperative ultrasound during hepatic resection compared with improved preoperative magnetic resonance imaging. Eur J Ultrasound. 2003;16(3):211–6.
11. D'Onofrio M, Gallotti A, Martone E, Nicoli L, Mautone S, Ruzzenente A, Mucelli RP. Is intraoperative ultrasound (IOUS) still useful for the detection of liver metastases? J Ultrasound. 2009;12(4):144–7.
12. Shukla PJ, Pandey D, Rao PP, Shrikhande SV, Thakur MH, Arya S, Ramani S, Mehta S, Mohandas KM. Impact of intra-operative ultrasonography in liver surgery. Indian J Gastroenterol. 2005;24(2):62–5.
13. Skrovina M, Bartos J, Cech B, Velkoborsky M, Czudek S, Kycina R, Bartos P, Adamcík L, Konvicna R, Soumarova R. Intra-operative liver ultrasound–a contribution to colorectal carcinoma staging. Acta Chir Belg. 2008;108(5):508–12.
14. Thaler K, Kanneganti S, Khajanchee Y, Wilson C, Swanstrom L, Hansen PD. The evolving role of staging laparoscopy in the treatment of colorectal hepatic metastasis. Arch Surg. 2005;140(8):727–34.
15. D'Hondt M, Vandenbroucke-Menu F, Préville-Ratelle S, Turcotte S, Chagnon M, Plasse M, Létourneau R, Dagenais M, Roy A, Lapointe R. Is intra-operative ultrasound still useful for the

detection of a hepatic tumour in the era of modern pre-operative imaging? HPB (Oxford). 2011;13(9):665–9.
16. Fang CH, You JH, Lau WY, Lai EC, Fan YF, Zhong SZ, Li KX, Chen ZX, Su ZH, Bao SS. Anatomical variations of hepatic veins: three-dimensional computed tomography scans of 200 subjects. World J Surg. 2012;36(1):120–4.
17. Machi J, Takeda J, Kakegawa T, Yamana H, Fujita H, Kurohiji T, Yamashita Y. The detection of gastric and esophageal tumor extension by high-resolution ultrasound during surgery. World J Surg. 1987;11(5):664–71.
18. Men S, Akhan O, Köroğlu M. Percutaneous drainage of abdominal abscess. Eur J Radiol. 2002;43(3):204–18.

Physical Principles of Ultrasound

2

Beth A. Schrope and Neha Goel

Acoustic Waves

Sound waves are defined as an oscillation of mechanical pressure waves through a medium. Unlike electromagnetic waves (where light is the most familiar example), which can travel through a vacuum, mechanical waves require a medium in order to transport their energy. Mechanical waves may have one of two forms: longitudinal (oscillation parallel to the propagation path) or transverse (oscillation perpendicular to the propagation path). Acoustic energy is a longitudinal wave, where particle displacement is parallel to the direction of wave propagation. The oscillation in this case can be described as a rarefaction and compression of the particles in the medium parallel to the path of propagation (Fig. 2.1).

Frequency is the number of times per second the wave is repeated, measured in cycles/second (Hz). The human ear can hear frequencies ranging from 20 to 20,000 Hz. Ultrasound, by definition, refers to frequencies greater than 20,000 Hz. The frequencies most often utilized in medical ultrasound imaging are between 2 and 20 million cycles/second (MHz).

Wavelength is defined as the distance covered by one complete cycle (measured from peak to peak or trough to trough) and is typically measured in millimeters (Fig. 2.2). Wavelength, λ, is inversely proportional to the frequency, f, and directly proportional to the propagation velocity, v, or speed at which a wave is traveling through a particular medium:

$$\lambda(\text{mm}) = v(\text{mm}/\mu\text{s})/f(\text{MHz})$$

The ability to distinguish objects along a sound beam depends on the wavelength of sound; one cannot differentiate objects whose dimensions are smaller than the wavelength of the incident wave. Thus, the higher the incident frequency, the greater the resolution of the image. As will be discussed shortly, better resolution attained with higher frequency comes at the cost of higher attenuation or loss of energy.

The *amplitude* of an acoustic wave represents the magnitude of the pressure in the medium as the wave travels (Fig. 2.2). The pressure is positive during the compression stage of the propagation and negative during the rarefaction stage. The logarithm of the square of the amplitude is measured in decibels (dB). *Power* is the amount of energy generated per unit time and is measured in joule/s or watts, where 0 dB (where decibel is a logarithmic unit expressing

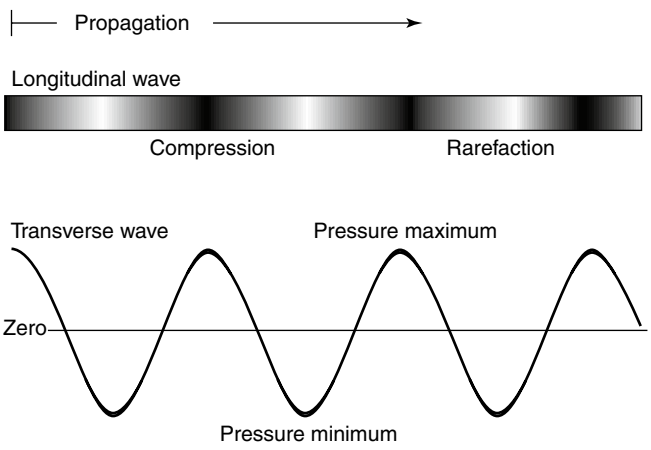

Fig. 2.1 Behavior of mechanical waves. Longitudinal waves oscillate parallel to the direction of propagation; transverse waves oscillate perpendicular to the direction of propagation

B.A. Schrope, MD, PhD, FACS, RDMS (✉)
Department of Surgery, New York Presbyterian/Columbia University Medical Center, 161 Fort Washington Avenue, Suite 810, New York, NY 10032, USA

Columbia University College of Physicians and Surgeons, 161 Fort Washington Avenue, Suite 810, New York, NY 10032, USA
e-mail: bs170@cumc.columbia.edu

N. Goel, MD
Department of Surgery, Columbia University Medical Center, 177 Fort Washington Avenue, MHB 7-313, New York, NY 10032, USA
e-mail: ng2362@columbia.edu

E.J. Hagopian, J. Machi (eds.), *Abdominal Ultrasound for Surgeons*,
DOI 10.1007/978-1-4614-9599-4_2, © Springer Science+Business Media New York 2014

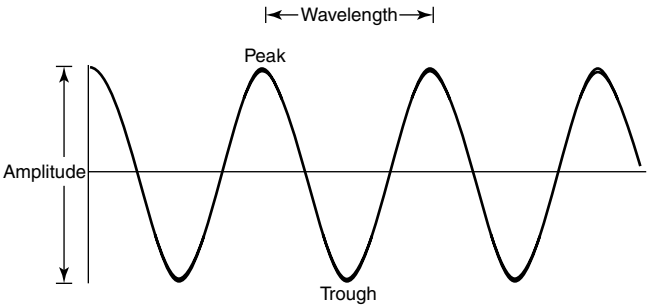

Fig. 2.2 Schematic representation of the properties of acoustic waves. See text for details

Table 2.1 Propagation velocity of sound through various biologic media

Medium	Speed of sound (m/s)
Air	330
Fat	1,460
Water	1,480
Brain	1,540
Kidney	1,560
Liver	1,580
Blood	1,580
Muscle	1,580
Eye lens	1,640
Bone	3,000–4,500

a quantity in relation to a reference level; in acoustics, it measures the intensity of sound pressure referred to a baseline pressure of 20 micropascals, commonly abbreviated as dB) refers to 1 milliwatt (mW). A 3 dB increase represents roughly doubling of power, which means that 3 dBm (where dBm is the power ratio in decibels (dB) of the measured power with a reference level of 1 mW) is equal to about 2 mW. For a 3 dB decrease, the power is reduced by half, making 3 dBm equal to about 0.5 mW. *Intensity* is the power density within an area and is expressed in W/m^2. Power and intensity describe the incident acoustic wave; *gain* refers to amplification of the returning echoes.

Tissue density and compressibility determine *propagation velocity*, which is a property of the medium through which sound travels. Higher density (mass/volume, measured in kg/m^3) and/or lower compressibility results in a faster speed of sound. More dense solids, therefore, have a faster propagation velocity than air. In soft tissue, propagation velocity is relatively constant at 1,540 m/s; this is the value assumed by ultrasound machines for all human tissue. Additional velocities through various media are listed in Table 2.1.

Attenuation

As a sound wave propagates through a medium, some of the acoustic energy is "lost" or transformed into other forms of energy. This phenomenon is known as

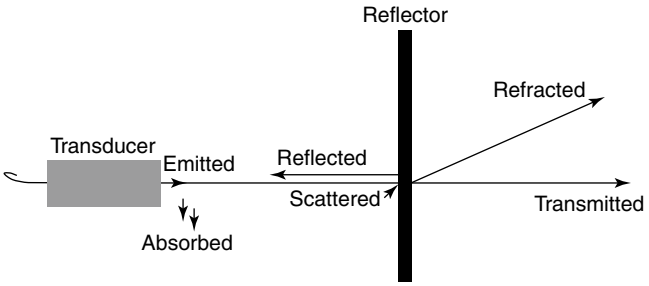

Fig. 2.3 Behavior of an acoustic wave as it travels through a medium

attenuation. Attenuation limits the depth of interrogation of a given frequency of the ultrasound beam, referred to as the penetration depth.

The attenuation of sound starts as soon as an electric pulse is converted to acoustic energy within the transducer and continues until the echo returns to the transducer to be processed into the image. Various factors contribute to attenuation including wavelength of the emitted sound, inherent properties of the medium, the number of interfaces encountered, and distance traveled. Attenuation is measured in decibels (dB), and the total attenuation in a specific medium is described by the "half-value thickness," which is the distance within the medium at which the intensity of the beam is reduced to half. In soft tissue, acoustic energy is lost at a rate of approximately 0.5 dB/cm/MHz. Homogeneous tissue, with similar density throughout, will have a decreased rate of attenuation versus tissue with varying densities (heterogeneous). Simple fluid, such as water and saline or serous fluid, will have nearly null attenuation.

To understand attenuation one must analyze the behavior of the wave as it travels through a medium with various interfaces (Fig. 2.3). *Reflection* is the redirection of part of the sound wave back to its source caused by the incident wave striking an interface; this serves as the basis for creation of the ultrasound image. Ideally, the ultrasound beam should evaluate the anatomy of interest at 90° incidence to maximize the reflection and visualization of anatomic structures. Absorption, refraction, scattering, and diffraction all lead to attenuation of ultrasound energy.

A wave hitting the interface at an angle less than 90° results in refraction of the wave away from the transducer at an angle equal to the angle of incidence but in the opposite direction (angle of reflection). When this happens, some of the returning echo is lost or attenuated. Diffuse reflection, or *scattering*, occurs where the dimensions of the interface are smaller than the acoustic wavelength, such as red blood cells or ultrasound contrast media. Depending on the size, shape, and orientation of the scatterers, scattering can redirect energy in all directions, or it can redirect energy primarily in the same direction as the incident energy, known as forward scattering, or in the reverse direction, known as backscattering. When received echoes are "translated" into

ultrasound images, these different types of reflection result in different types of images.

Absorption, generally accepted as thermal losses, depends on the viscosity of the medium as well as the incident energy. This is generally a minor effect at diagnostic ultrasound intensities but is central in many therapeutic ultrasound applications.

As stated above inherent properties of the medium influence attenuation. The degree to which a medium slows sound wave propagation is known as acoustic impedance and is defined as

$$z = \rho c$$

where z is acoustic impedance, ρ is the density of the material, and c is the sound velocity in that medium. The larger the difference in acoustic impedance between adjacent media (acoustic impedance mismatch), the more energy is lost as attenuation. Refraction is the redirection of part of the sound wave as it crosses a boundary of mediums with different acoustic impedances. Fortunately, the difference between the acoustic impedances of biologic tissues is very small, allowing for the creation of an ultrasound image without losing much to refraction.

Each of these attenuation phenomena is influenced by the frequency of the transmitted wave. The higher the frequency, the greater the energy loss or attenuation. In the application of medical ultrasound, this influences your choice of transducer; although a higher frequency of sound would result in higher resolution, this is limited by the attenuation of the sound wave. In other words, you would use a lower-frequency transducer to reach deeper structures (at the sacrifice of image clarity) and a higher-frequency transducer for more superficial structures (to optimize clarity).

Resolution

Resolution may be further categorized into spatial (lateral and axial), temporal, and contrast resolution. In order to gain a better understanding of resolution, it is important to understand the anatomy of an ultrasound beam (Fig. 2.4). An ultrasound beam consists of two regions: the near field or Fresnel zone and the far field or Fraunhofer zone. The near field is adjacent to the transducer face and has a converging beam profile; this results in complex interference patterns close to the face, which can distort the ultrasound image. The far field or Fraunhofer zone is characterized by beam divergence and loss of ultrasound intensity. The point of transition between these two zones is the location of the maximum signal intensity (also known as the spatial peak intensity), and the distance from the transducer face to this point is known as the focal distance. The focal zone is defined as the region over which the width of the beam is less than two times the width of the focal distance. The focal zone can be manipulated by focusing the beam with a lens or with electronic directional manipulation of the transducer.

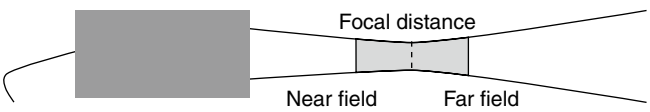

Fig. 2.4 Anatomy of an ultrasound beam

Lateral resolution is the ability to distinguish two closely spaced objects perpendicular to the direction of the beam. It depends on the diameter of the ultrasound beam and the depth of imaging. As the energy travels further away from the transducer face, the beam diverges, and lateral resolution suffers. Lateral resolution is best at the end of the near field.

Axial (also known as longitudinal) resolution refers to the ability to differentiate two objects that lie in a plane parallel to the direction of the sound wave. Axial resolution is determined by frequency and pulse duration; unlike lateral resolution, it is not affected by imaging depth. Axial resolution can be improved by decreasing the length of a pulse or increasing frequency.

Temporal resolution refers to the ability to detect moving objects over time and is determined by the frame (or refresh) rate. Temporal resolution can be improved by narrowing the image (thus decreasing the amount of time needed to refresh the image), decreasing the depth, or decreasing the line density of the image (at the sacrifice of spatial resolution).

Contrast resolution refers to the ability to distinguish differences in intensity in the image. It is generally accepted that the human eye can distinguish 256 shades of gray. Therefore, the range of detectable intensities of the received echoes is assigned across this spectrum.

The Doppler Effect

The Doppler effect refers to the shift in wavelength that occurs when a wave strikes a moving object. For example, as a moving object approaches a stationary observer, the frequency is increased; in contrast, a decrease in frequency is observed as the object moves away from the observer. The classic example is that of an ambulance siren appearing to have a higher pitch as the ambulance approaches and a lower pitch as it moves away. This change in audible frequencies can be described as Δf and is called the Doppler frequency shift, Doppler shift, or Doppler frequency.

The Doppler shift depends on the emitted frequency (f), the velocity of the object (v), the angle (α) between the observer and the direction of the movement of the sound emitter, and the velocity of the sound in the medium (c). Thus, the Doppler shift can be described as

$$\Delta f = 2f\left(v\cos\alpha\right)/c$$

Note that when the object and observer are perpendicular, there is no Doppler shift, as cosine 90 is zero. This is relevant in practical imaging of flow in blood vessels, for example, where one must be cognizant of the orientation of the transducer beam with respect to the direction of flow.

Imaging Modes

Commercial ultrasound devices offer several standard imaging modes. These are all created from the same basic information captured from the acoustic echoes at the transducer. The basic available modes are A mode, B mode, M mode, Doppler, and duplex imaging.

A mode, also known as amplitude modulation, depicts the amplitude of an acoustic waveform over time. This is the most basic, received echo from a single transmitted pulse. Increases in signal amplitude represent echoes from interfaces within the medium. Figure 2.5 depicts such a signal. A mode is generally not available for display on commercial ultrasound machines, but understanding this signal is key to understanding the more familiar two-dimensional grayscale image.

B mode, or brightness modulation, displays echoes as different shades of gray based on their intensity or amplitude. This is the most familiar image displayed on a commercial machine (Fig. 2.6). The B mode image is actually a two-dimensional reconstruction of the information obtained in the A mode over a given space at a given time point, where the amplitude of the spikes on the A mode image is now pixels whose brightness is dictated by the amplitude of the received signal.

M mode or TM mode (time-motion) depicts motion over time. Used often in echocardiography, this allows a real-time analysis of velocities, for example, to delineate abnormalities in valvular motion. M mode has also been applied to areas such as swallowing analysis, assessment of diaphragmatic movement, or deformation of vascular structures (Fig. 2.7).

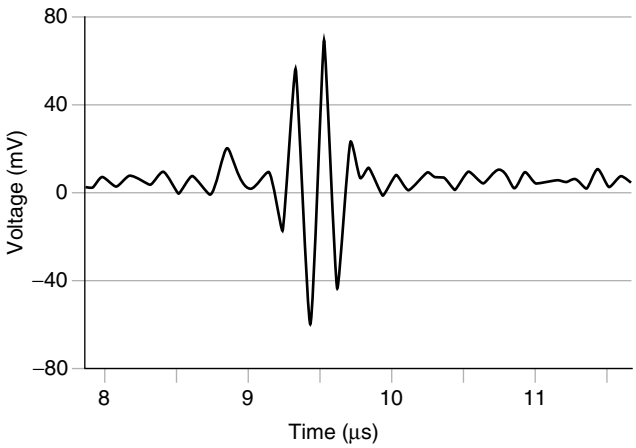

Fig. 2.5 A mode, or amplitude modulation

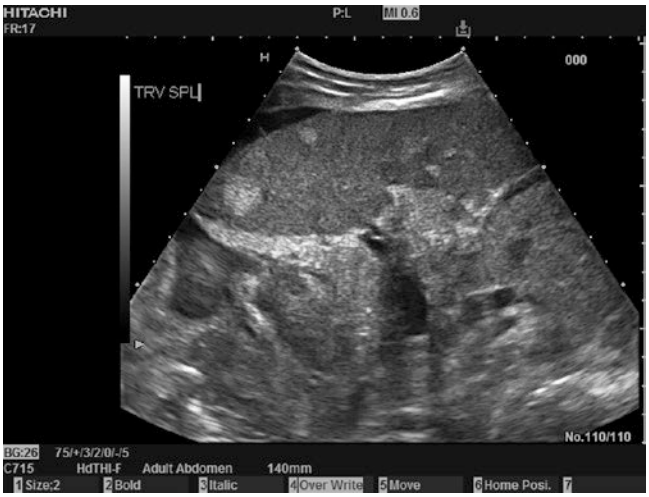

Fig. 2.6 A two-dimensional grayscale image, or B mode image

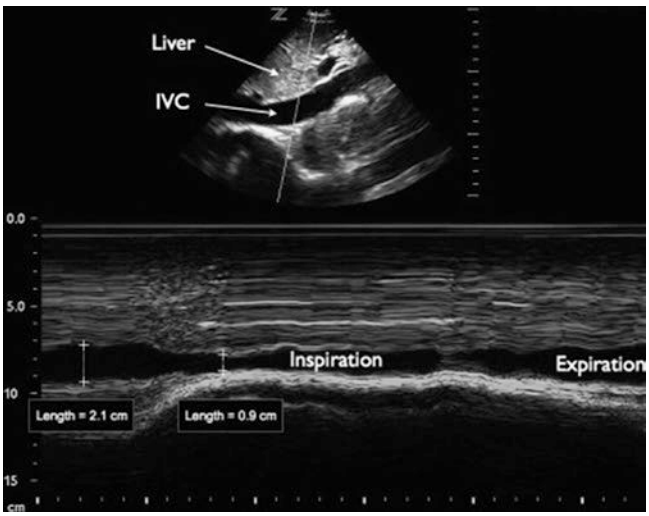

Fig. 2.7 IVC with M mode. Subcostal long axis view of the IVC imaged using M mode during inspiration (Used with permission: Byrne and Hwa [1])

Doppler ultrasound enables quantification of flow velocities. Both continuous and pulsed wave techniques are used in Doppler medical ultrasound. Continuous wave devices are used in the simplest audible probes used for velocity detection, such as fetal heart beat or arterial pulse. This form of imaging uses a transducer probe with two elements, an active one that continuously emits ultrasound and another passive element that receives the echoes. Because of the lack of distance information, continuous wave Doppler cannot be used to create two-dimensional images. A continuous wave system can be focused by altering the angle between the two elements of the transducer.

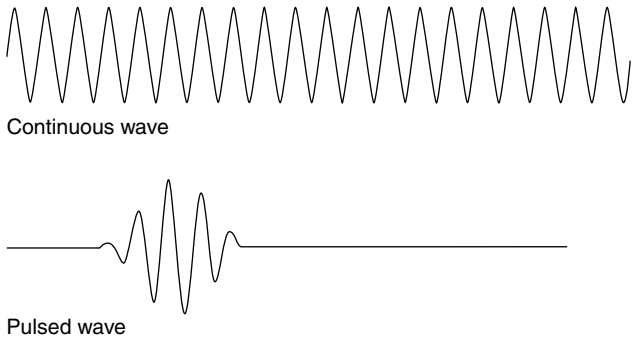

Fig. 2.8 Continuous wave and pulsed wave acoustic emissions

Pulsed wave ultrasound is most frequently used in ultrasound imaging. In this mode, a brief pulse of sound is applied to the medium, and the remaining time is spent "listening" for return echoes (as in the demonstration of A mode describe above). Figure 2.8 diagrams the difference between a continuous wave emission and a pulsed wave emission.

Blood flows through vessels as laminar flow, with the highest velocity in the center. Spectral Doppler is a form of ultrasound imaging where flow velocities are plotted on the y-axis with time on the x-axis. Flow that is moving toward the transducer is considered positive or above the x-axis, and flow moving away from the transducer is considered negative and plotted below the x-axis. Doppler ultrasound can be displayed simply as a color-flow map (blue and red mapped to flow toward and away from the transducer) or can be quantified. Color Doppler, another form of imaging that is integrated with B-scan, is used to color-code flow.

Quantitative Doppler utilizes the basic frequency shift information captured from various areas of the image. The volume of blood flow, Vol, is calculated by multiplying the cross-sectional area of a vessel, A, with the average flow velocity V_{mean}:

$$\text{Vol} = A \times V_{\text{mean}}$$

The resistance index (RI), which reflects how resistant a vessel is to flow, is calculated using the flow velocities as well. In particular, more resistant vessels have decreased flow and vice versa.

$$\text{RI} = \left(V_{\max} - V_{\min}\right) / \left(V_{\max}\right)$$

$V_{\max}$ is the peak systolic velocity, and $V_{\min}$ is the trough end-diastolic velocity. The pulsatility index, or PI, describes the variability in blood flow:

$$\text{PI} = \left(V_{\max} - V_{\min}\right) / V_{\text{mean}}$$

The grade of stenosis in a vessel ST is calculated using the following formula:

$$\text{ST} = 100\left(1 - V_1 / V_2\right)$$

where V_1 is flow prior to entering the stenotic region and V_2 is the flow within that region. Narrowing of a vessel due to atherosclerosis, or more acutely an embolus or thrombus, causes acceleration of flow within that stenotic region. Post-stenotic turbulence is seen as "spectral broadening" on a spectral Doppler display.

The echoes that arrive at the transducer between the pulses in a specific time interval, known as "the gate," are analyzed. The frequency of pulse emissions is called the pulse repetition frequency (PRF). If the flow velocity (Doppler frequency shift) is higher than one half the PRF, sampling error will occur and the velocity will be recorded erroneously low. When this happens, high velocities are displayed as low velocities in the opposite direction (spectral Doppler) or in the wrong color (color Doppler). This phenomenon is known as aliasing. A correct display is possible only for Doppler frequencies within the range of ± one-half the PRF; this is known as the Nyquist limit. Thus, in order to image high velocities, lower ultrasound frequencies with high PRF is necessary.

A B mode image combined with spectral Doppler is termed the duplex imaging, which localizes the vessel being examined and, importantly, the angle between the ultrasound wave and the vessel (the Doppler angle). Practically, the Doppler angle should be around 30° and certainly less than 60°. (Recall the Doppler equation, where cosine of the Doppler angle determines the frequency shift and where 90° results in nondetection of flow.) A B mode displayed with a color-flow map as well as quantified flow information is known as triplex ultrasound.

Newer Technologies

A newer technique called tissue harmonic imaging (THI) utilizes the second harmonic frequencies found in the received signal to produce higher-resolution images. This phenomenon occurs as the fundamental or first harmonic ultrasound signal encounters an interface it resonates at multiples of the transmitted frequency (twice the fundamental frequency is termed the second harmonic, third the fundamental frequency is termed the third harmonic, etc.). For the second harmonic imaging, as echoes return to the receiver, the receiver is tuned to twice the fundamental or transmitted frequency, removing the background "noise" generated from the fundamental frequency. Overall tissue harmonic imaging improves tissue visualization between interfaces and reduces scattering from tissues near the transducer. This method of imaging also improves lateral resolution since most of the echoes are produced along the center of the beam. An example of tissue harmonic imaging compared with conventional

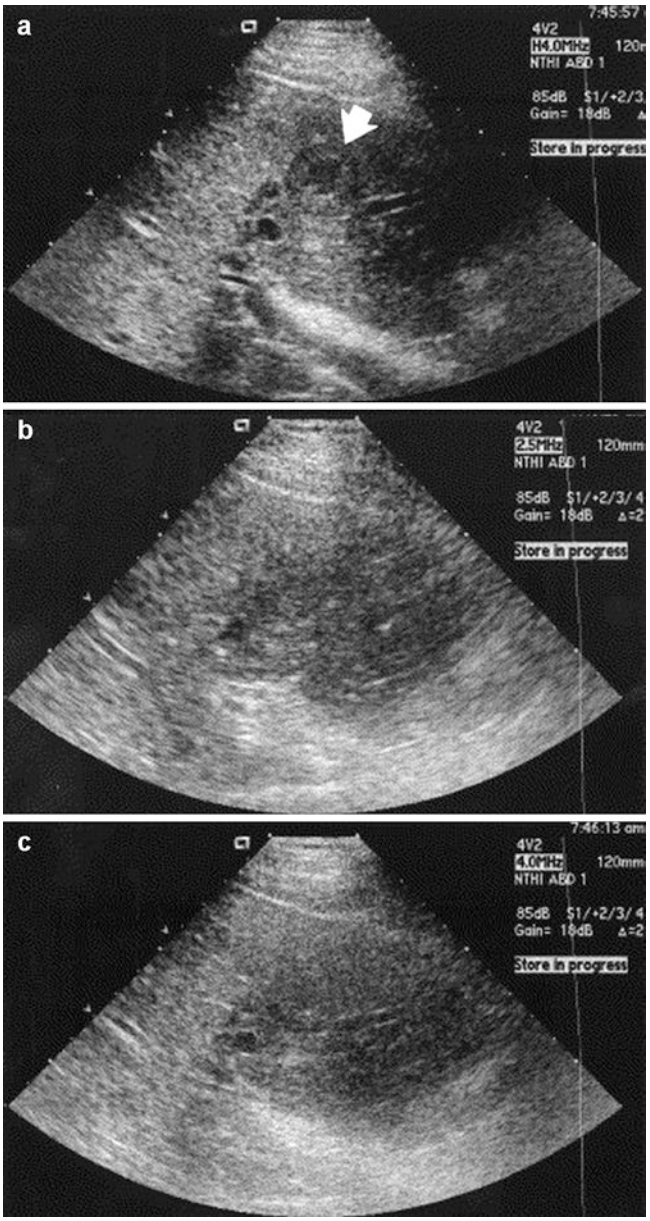

Fig. 2.9 Thirty nine-year-old man with liver mass. (**a**–**c**) Sonograms of the same anatomic area in the liver using tissue harmonic imaging (**a**), 2.5 MHz (**b**), and 4.0 MHz (**c**) show that the mass (*arrow*) is detectable in (**a**), but not in (**b**) or (**c**). Images (**b**) and (**c**) were graded as nondiagnostic (Used with permission: Shapiro et al. [4])

ultrasound imaging is seen in Fig. 2.9, where a liver mass is only detectable with the THI mode.

Contrast harmonic imaging uses the echoes from gas-filled microbubbles to delineate or enhance flow. These microbubble contrast agents are encapsulated gas bubbles, are smaller than red blood cells, and are injected intravenously into the systemic circulation. There are commercially available agents, composed of a capsule of albumin or lipid, with an air or perfluorocarbon gas core. This type of imaging can be used to detect flow in low-flow regions such as in very small vessels (in hypervascular tumors, e.g., as seen in Fig. 2.10) due to the contrast enhancement of these small microbubbles on the Doppler. In fact, bubbles have strong nonlinear characteristics, so that the regions occupied by the contrast agents appear brighter in the THI mode.

The nonlinear characteristics of bubbles can be understood as follows. When exposed to acoustic energy, gas bubbles pulsate or expand and contract. They contract at the peak of the ultrasound wave and expand at the trough. In bubbles this resonance generates nonlinear frequencies, or multiples of the fundamental frequency, to a greater extent than soft tissue. Thus, enhancement produced by contrast agents is greater in THI mode when compared to surrounding soft tissue.

With advances in data acquisition and processing speed, three- and four-dimensional ultrasound is now realized. Popularized by beautiful in utero baby pictures, 3D ultrasound is finding utility in volume rendering of solid organ tumors, for diagnosis and therapeutic applications. Figure 2.11 depicts a three-dimensional reconstruction of a breast tumor, with the addition of color enhancement for further visual delineation of the borders of the tumor. Three-dimensional imaging used in real time is termed four-dimensional imaging. Four-dimensional imaging has been used in vascular surgery to evaluate carotid disease (Fig. 2.12) and for such diverse applications as ophthalmology and the study of musculoskeletal disease.

Bioeffects

One of the attractions of ultrasound as a diagnostic imaging modality is its relative safety when compared to more conventional imaging such as CT or MRI. Yet, no action is without consequence, and ultrasound is no exception. As with all radiographic imaging, one must adhere to the concept of ALARA, or as low as reasonably achievable, where the lowest settings possible to obtain the appropriate diagnostic image are used.

The effects of ultrasound on biologic tissue are primarily due to two phenomena: thermal and mechanical. Thermal effects are related to the absorption of ultrasonic energy as it travels through tissue, as described earlier. The amount of absorption depends on several factors including power and frequency of the incident energy, ultrasound beam area, duration of exposure to ultrasound, and perfusion of the tissue medium. Higher frequency and insonation power lead to greater tissue heating, as does a wider beam area. Clearly a longer duration of exposure also leads to a greater thermal effect. Conversely, blood flow conveys the heat away, so a well-perfused tissue experiences relatively less heating. In addition, the presence of bone in the ultrasound field

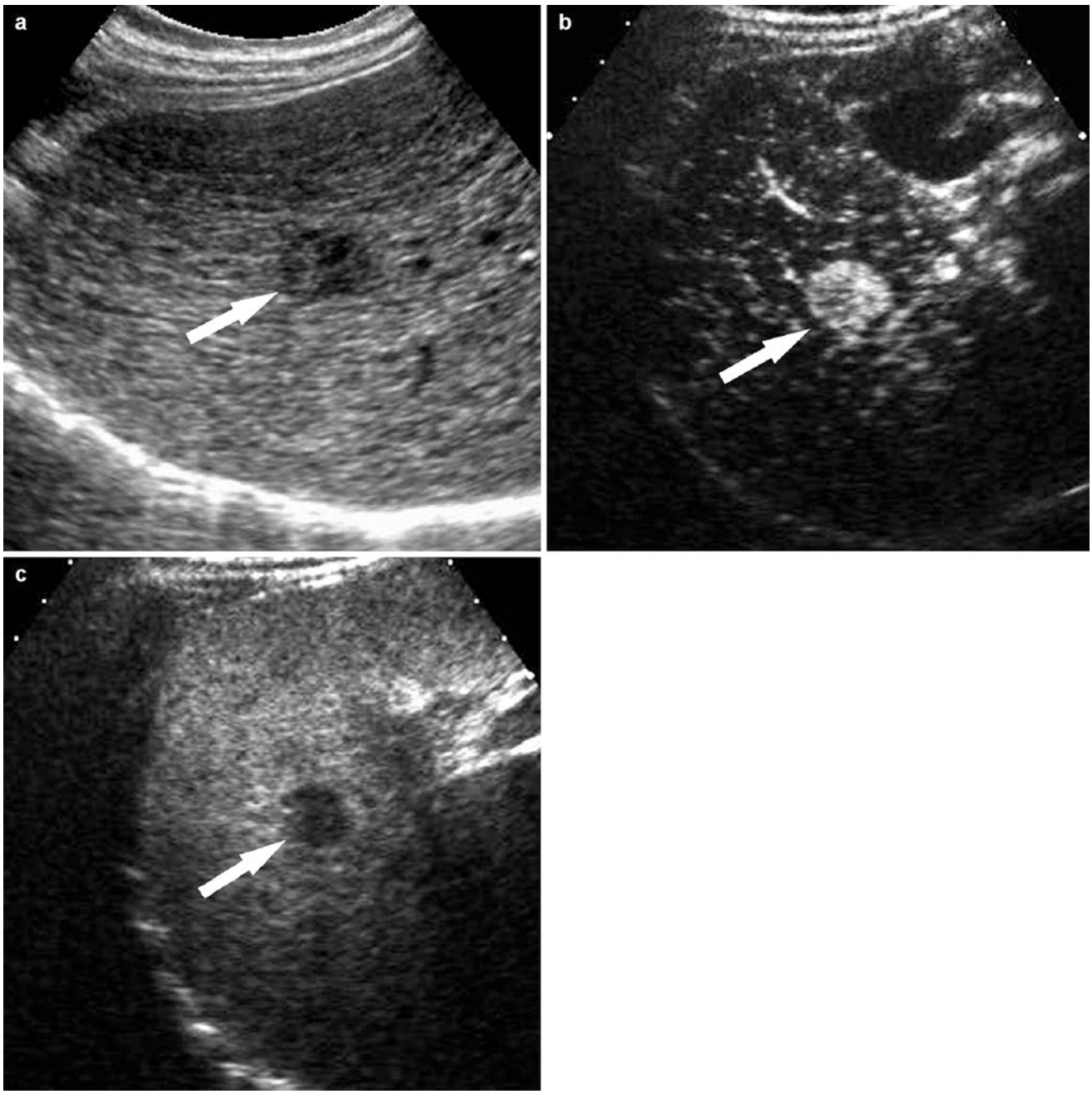

Fig. 2.10 HCC in a 77-year-old man with nonalcoholic steatohepatitis. (**a**) Grayscale ultrasound image shows a hypoechoic nodule (*arrow*) in the liver. (**b**) Contrast-enhanced ultrasound image obtained 18 s after injection of microbubbles shows diffuse hypervascularity within the nodule (*arrow*). The nodule continued to show hyperenhancement relative to the liver (not shown) until (**c**) 210 s after injection of microbubbles, when the nodule (*arrow*) shows negative enhancement (washout) relative to the normal liver (Used with permission: Jang et al. [2])

increases heating, as absorption is increased at the bone/soft tissue interface.

In 1992 the World Federation for Ultrasound in Medicine and Biology (WFUMB) released a position statement on the thermal consequences of ultrasound to the fetus. Based on evidence available at that time, a consensus panel concluded that "a diagnostic exposure that produces a maximum temperature rise of 1.5 °C above normal (37 °C) may be used without reservation in clinical examinations." Most commercially available equipment falls within these guidelines, with the possible exception of certain pulsed Doppler applications.

The mechanical effects of ultrasound relate to the influence of the vibrational aspect of ultrasound waves and include cavitation and acoustic streaming. Cavitation refers to the formation (from dissolved gas in the medium) and

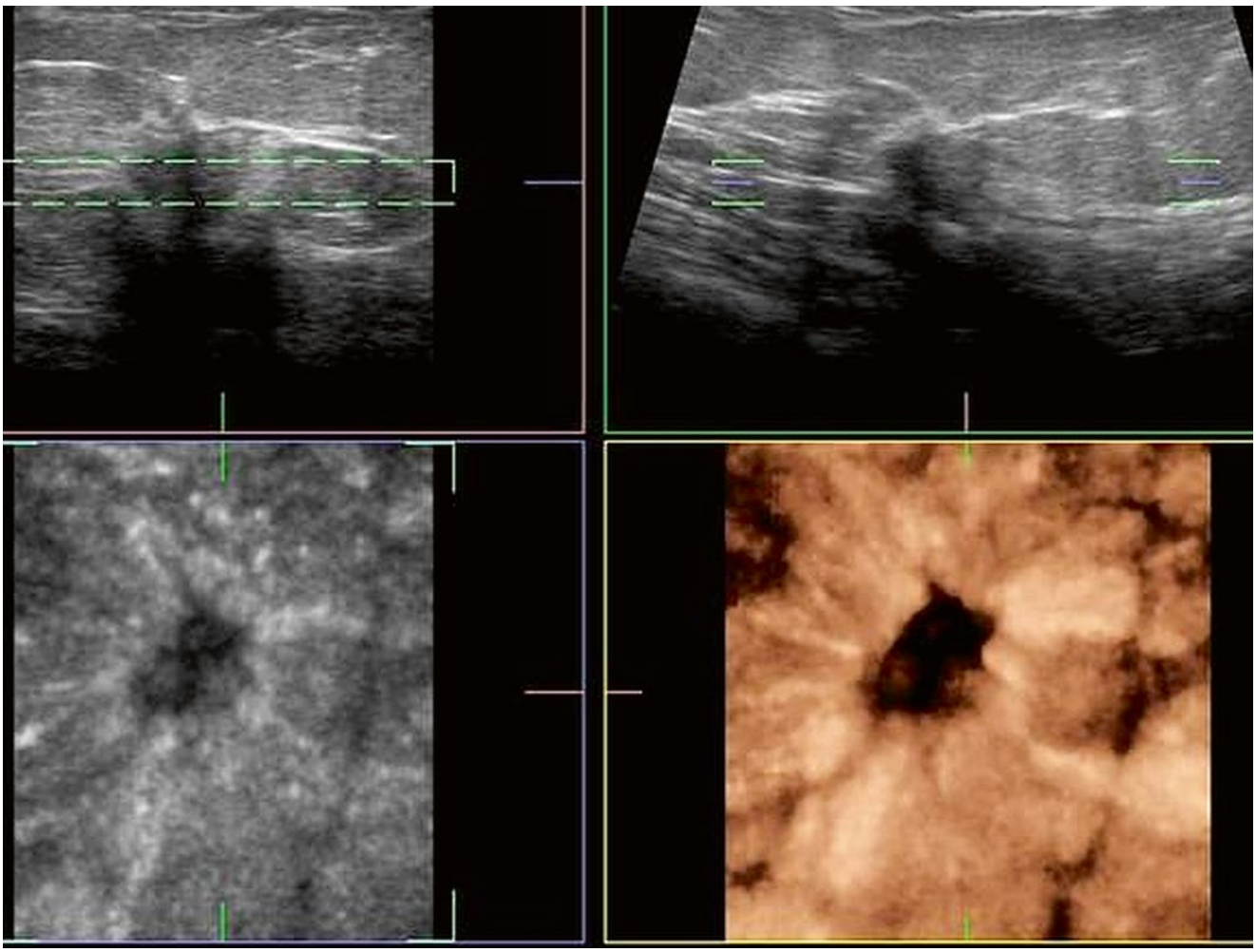

Fig. 2.11 Three-dimensional reconstruction of a breast tumor, with the addition of color enhancement for further visual delineation of the borders of the tumor (Courtesy of Hitachi-Aloka Medical, Ltd.)

oscillation of bubbles within the interrogated medium upon exposure to ultrasound waves. As the mechanical ultrasound wave rarefacts and compresses, it causes these bubbles to expand and contract. As introduced earlier, this effect can result in visible changes of the image which may be exploited for diagnostic purposes. The magnitude of the effect is influenced by frequency, power, pulse duration, and pulse repetition frequency. In typical diagnostic applications, cavitation is harmless to the patient.

Acoustic streaming refers to the behavior of the medium around the bubbles as they oscillate. Bubble vibration creates shear stresses in the surrounding tissues, which can displace ions or small molecules. This may affect membrane permeability, which has been exploited for therapeutic applications such as drug delivery and lithotripsy. As with cavitation, at typical diagnostic settings, acoustic streaming has negligible adverse effects.

With regard to the effects of ultrasound on biologic tissue, the Food and Drug Administration has endorsed an industry voluntary standard for reporting of bioeffects. The thermal index (TI) is the ratio of total acoustic power to the acoustic power required to raise the temperature of tissue by 1 °C. Thus, a TI of 1 means that the system has the potential of heating tissue by 1 °C. This is below the 1992 WFUMB standard of 1.5 °C, so equipment with a TI of 1 or less is not required to display the TI.

Mechanical effects are quantified by the mechanical index, MI. This is defined as the spatial peak of the peak rarefaction pressure, or

$$\mathrm{MI} = \mathrm{PNP} / \sqrt{F_c}$$

where PNP is the peak negative pressure of the ultrasound wave in MPa and F_c is the center frequency in MHz. The FDA endorses that diagnostic ultrasound equipment should not exceed an MI of 1.9, and those that cannot produce an MI of greater than 1 are not required to report the MI in real time on the user display.

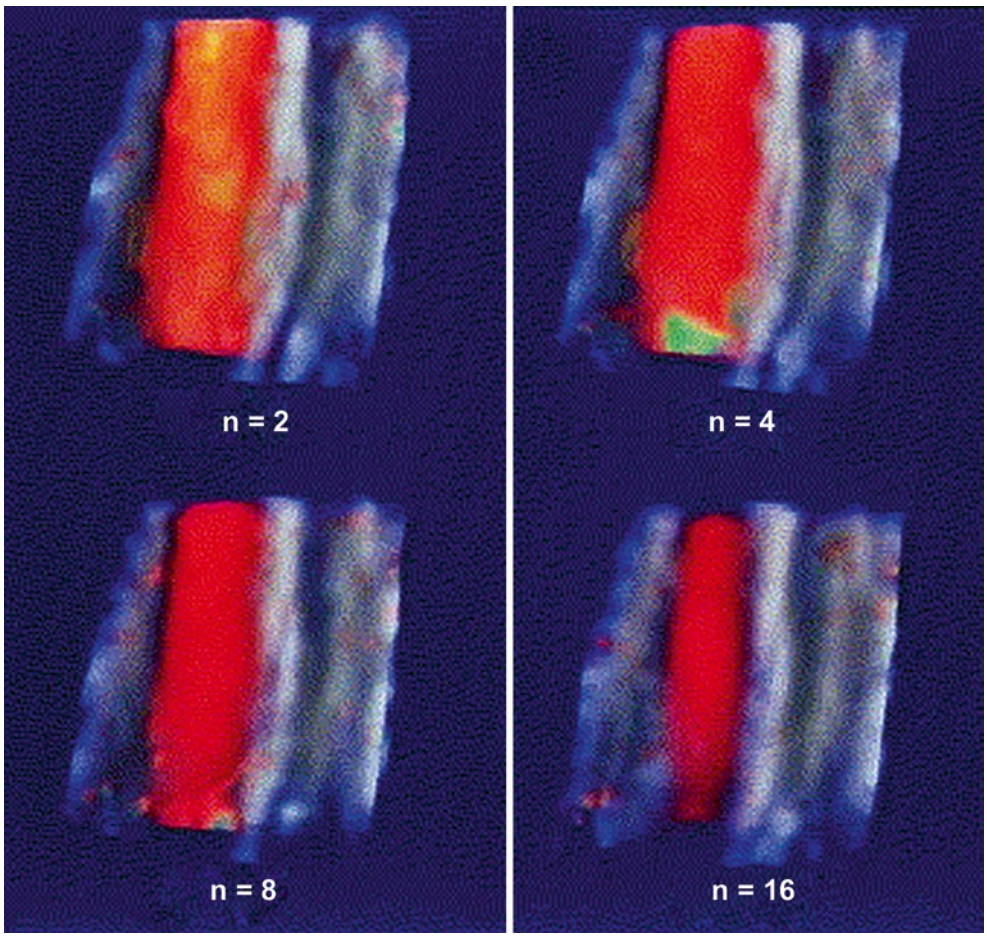

Fig. 2.12 4D color-flow imaging of the internal carotid artery with concurrent display of the B mode reconstruction of the arterial walls and surrounding tissue (Used with permission: Meairs et al. [3])

Summary

This chapter offers a basic knowledge of the physics of acoustics, with the intent to familiarize the surgeon sonographer so that he or she can utilize the technology to maximum diagnostic benefit. Admittedly to the surgeon, basic physics can seem tiresome, but hopefully, this discussion has highlighted the importance of its understanding and has clarified the salient points of wave characteristics and signal processing at least to the extent that turning the knobs and pressing the buttons are less intimidating.

References

1. Byrne MW, Hwang JQ. Ultrasound in the critically ill. Ultrasound Clin. 2011;6(2):235–59.
2. Jang H, Kim TK, Wilson SR. Small nodules (1–2 cm) in liver cirrhosis: characterization with contrast-enhanced ultrasound. Eur J Radiol. 2009;72(3):418–24.
3. Meairs S, Beyer J, Hennerici M. Reconstruction and visualization of irregularly sampled three- and four-dimensional ultrasound data for cerebrovascular applications. Ultrasound Med Biol. 2000;26(2):263–72.
4. Shapiro RS, Stancato-Pasik A, Sims SE. Diagnostic value of tissue harmonic imaging compared with conventional sonography. Comput Biol Med. 2005;35(8):725–33.

Instrumentation in Ultrasound

3

Halit Eren Taskin and Eren Berber

Abbreviations

LCD	Liquid crystal display
MHz	Megahertz
PACS	Picture archiving and communication system
PZT	Lead zirconate titanate
TGC	Time gain compensation

Overview

The ultrasound (US) probe has replaced the stethoscope for the surgeons in modern practice. Surgeon-performed ultrasound has become a part of the surgical examination being a cost-effective, repeatable, and mobile point-of-care procedure. Also, ultrasound can facilitate interventions. Surgeons should be aware of the basic principles and technical knowledge of the components of the ultrasound machine in order to obtain optimal results from an ultrasound examination. The surgeon, being a clinician, can perform ultrasound more effectively in real time with better knowledge of the anatomy and pathophysiology of the diseases than the sonographer, but a clear understanding of the technical jargon and effective and safe usage of the instruments are sine qua non principles of this diagnostic examination. Thus, herein, we will explain in detail the technical points about the instrumentation and knobology of the ultrasound machine in accordance with clinical practice. Although the instrumentation and machines might appear complicated for the surgeon, in fact, they are not if the basic principles and components are understood.

H.E. Taskin, MD • E. Berber, MD, FACS (✉)
Division of Endocrine Surgery,
Endocrinology and Metabolism Institute,
Cleveland Clinic, Cleveland, OH, USA

Department of General Surgery, Cleveland Clinic,
9500 Euclid Avenue F/20, Cleveland, OH 44196, USA
e-mail: taskinh@ccf.org; berbere@ccf.org

Components of the Ultrasound Machine

The modern ultrasound machine is composed of three main components: a transducer, a control panel, and a monitor.

Transducer (Probe)

An ultrasound transducer is a converter that converts electric energy into ultrasound energy and senses or listens to the reflected echoes by converting them into electric voltages.

An ultrasound probe is made of the following components (Fig. 3.1a, b):

- Piezoelectric materials
- Backing material
- Transducer housing
- Matching layer

Piezoelectric Materials

The term piezoelectric is derived from the Greek words *piezo*, which means "to press," and *electron*, which means "amber." When these elements are deformed by pressure, a voltage is produced. These elements also convert mechanical energy of the returning ultrasound echoes on the probe to produce electrical voltages. These electrical voltages are transmitted to the monitor where images are formed. This technique of image production is called the "pulse-echo technique." Echoes from anatomic structures correspond to the structures in a sonographic image.

Quartz, topaz, and amber are natural examples of piezoelectric materials, although various formulations of synthetic ceramics, such as lead zirconate titanate (PZT), are most commonly used in modern ultrasound probes as the transducer element. Some ceramics are made piezoelectric by placing the material in a strong electric field at high temperatures. Thus, these elements are heat sensitive, such that, if the critical temperature point (also called Curie point) is

E.J. Hagopian, J. Machi (eds.), *Abdominal Ultrasound for Surgeons*,
DOI 10.1007/978-1-4614-9599-4_3,

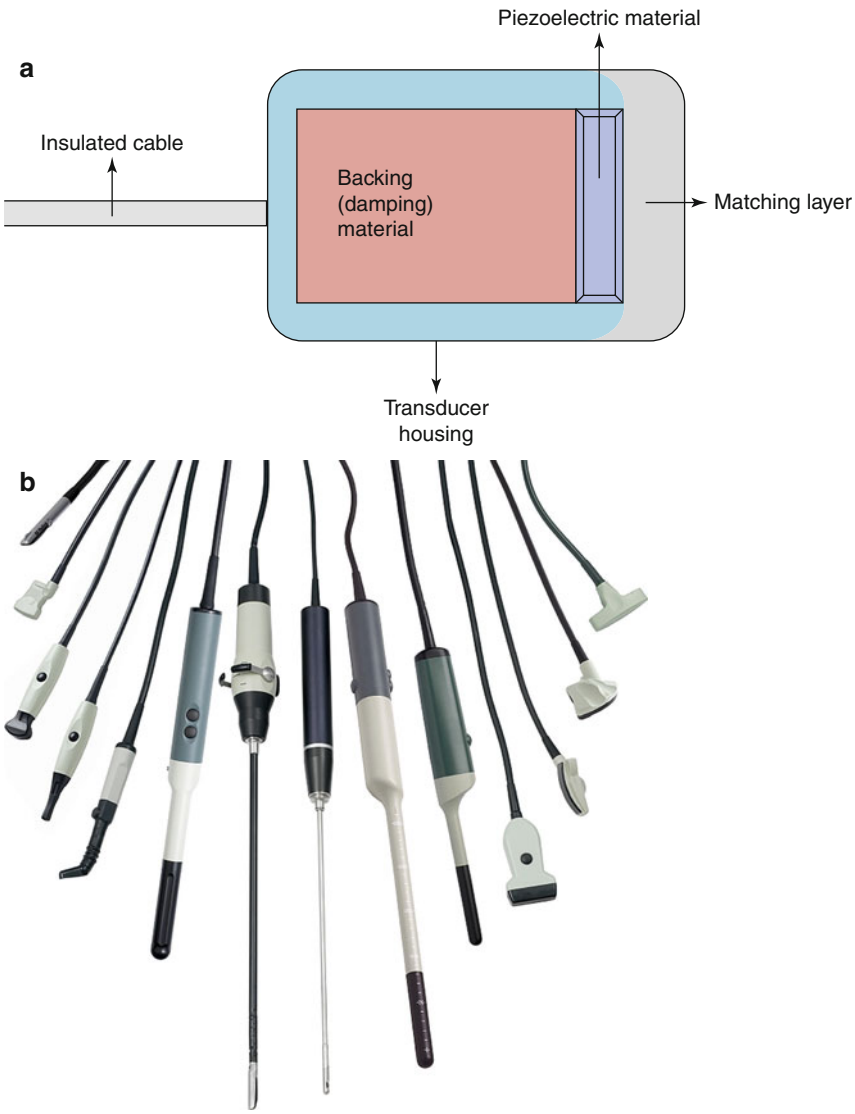

Fig. 3.1 (**a**) Diagram showing the structural parts of an ultrasound probe. (**b**) Figure showing various types of ultrasound probes

exceeded, then these elements would lose their piezoelectric properties. This is the reason why the ultrasound probes should never be autoclaved or exposed to extreme heat. These probes should be sterilized using either gas sterilization or high-level disinfection methods, making sure the electronic part is not soaked in the solution. The thickness of the crystal and the alternating voltage applied are factors that determine the frequency that the probe will create.

Backing (Damping) Material

Backing material is the material attached behind the piezoelectric material. This material is usually composed of metal powder and plastic epoxy resin. The function of this material is to reduce the vibrations of the piezoelectric material and, as a result, also reduce the pulse duration and spatial pulse length, thus improving resolution. In other words, ultrasound probe emits shorter pulses of ultrasound energy, so that more detailed high-quality images can be formed. However, the damping material causes a decrease in efficiency and sensitivity of the system by reducing the ultrasound amplitude. Some transducers intended for continuous wave Doppler do not have backing material, since pulses are not used. These transducers are more efficient because ultrasound energy is not lost during the damping process.

Transducer Housing

Transducer housing is usually composed of plastic and metal and encloses the piezoelectric material, damping material, and all the electrical connections. An intact transducer housing is important before attempting any sonographic examination, since broken transducer housings can cause serious injuries to the patient and the sonographer via electrical shock.

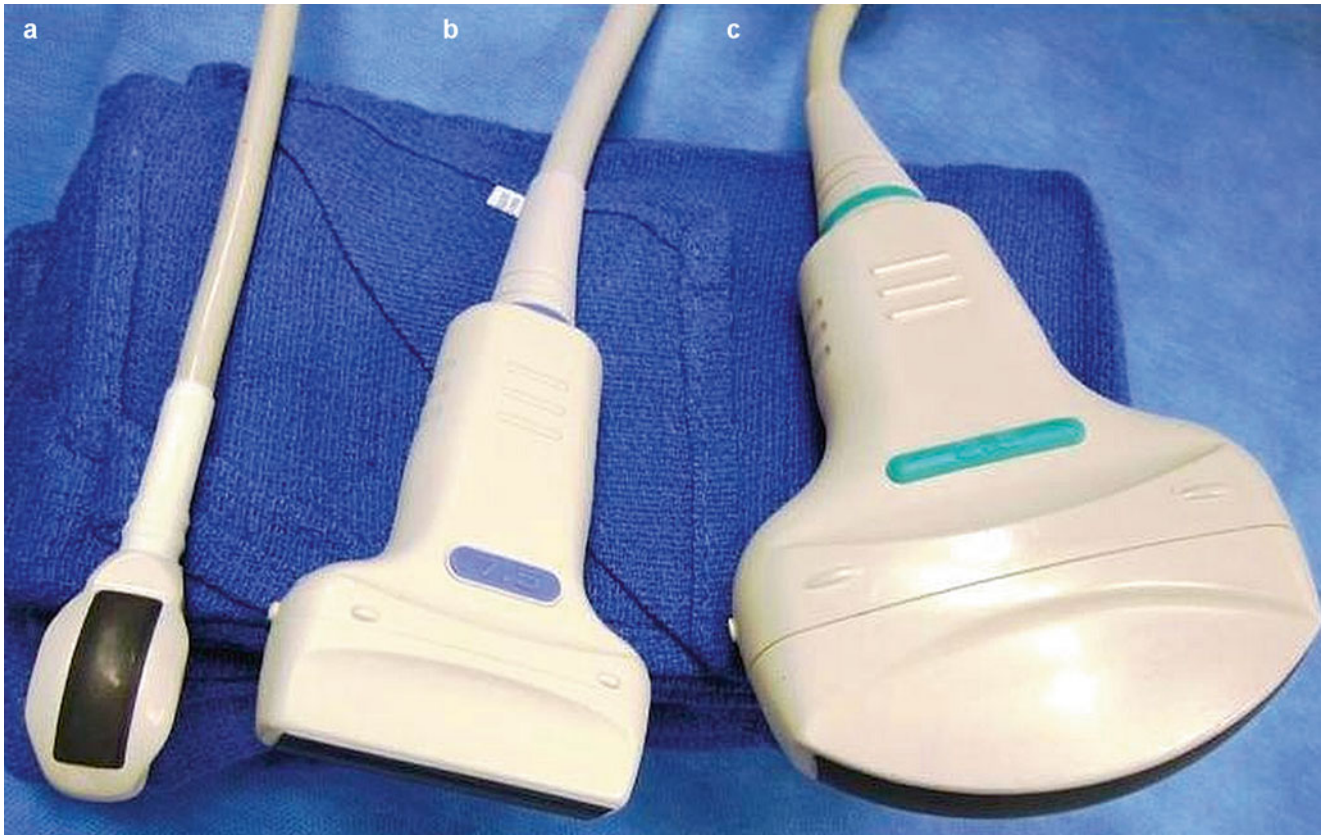

Fig. 3.2 Image depicting common probes which are used in different body regions with various frequency ranges. (**a**) Curvilinear array high-frequency small-parts probe. (**b**) Linear array high-frequency probe. (**c**) Curvilinear low-frequency probe

Matching Layer

Matching layer is the material that is on the face of the transducer located between the piezoelectric material and the patient. This layer matches the impedance difference between the solid probe and the body. This material has an intermediate impedance value and provides less reflection of the returning sound waves from the tissues to the transducer. Almost 80 % of the returning echoes would be reflected in the absence of this coating material since the transducer is solid and has an impedance value much higher than the tissues.

Since air has low impedance, a coupling medium, usually a gel, is required to avoid any contact of the ultrasound waves with air and to facilitate transmission of the sound waves to and from the tissues and the transducer. The gel also helps to diminish acoustic impedance mismatch between the skin and the transducer. Without the use of a coupling medium, most of the returning echoes would be reflected at the skin-transducer border and poor-quality images would be formed. Also, the inadequate use of coupling medium would result in artifacts that would cause an incorrect interpretation of the images.

Transducer (Probe) Types

Different types of transducers are needed for optimal imaging of the different structures in the body. Penetration of the ultrasound waves into tissues is inversely proportional to attenuation of the ultrasound signal. Attenuation is the weakening of the sound as it propagates. This concept is important as attenuation of the ultrasound energy limits the image depth and should be compensated by the ultrasound machine. This is why different transducers that generate ultrasound waves with different frequencies are needed for optimal imaging of the different parts of the body (Fig. 3.2).

Attenuation is directly proportional to the frequency of the ultrasound transducer (see section "Attenuation" in Chap. 2). The higher the frequency of the probe, the more quickly the sound energy is lost over distance. High-frequency transducers are therefore unable to penetrate into deeper tissues but provide better image resolution. Inversely, transducers with lower frequency can penetrate into deeper tissues, however, with decreased resolution. Nevertheless, low-frequency transducers (e.g., 3.5–5 MHz) are preferable to do transabdominal scanning of the solid abdominal organs where depth of penetration is important. On the other hand, high-frequency transducers

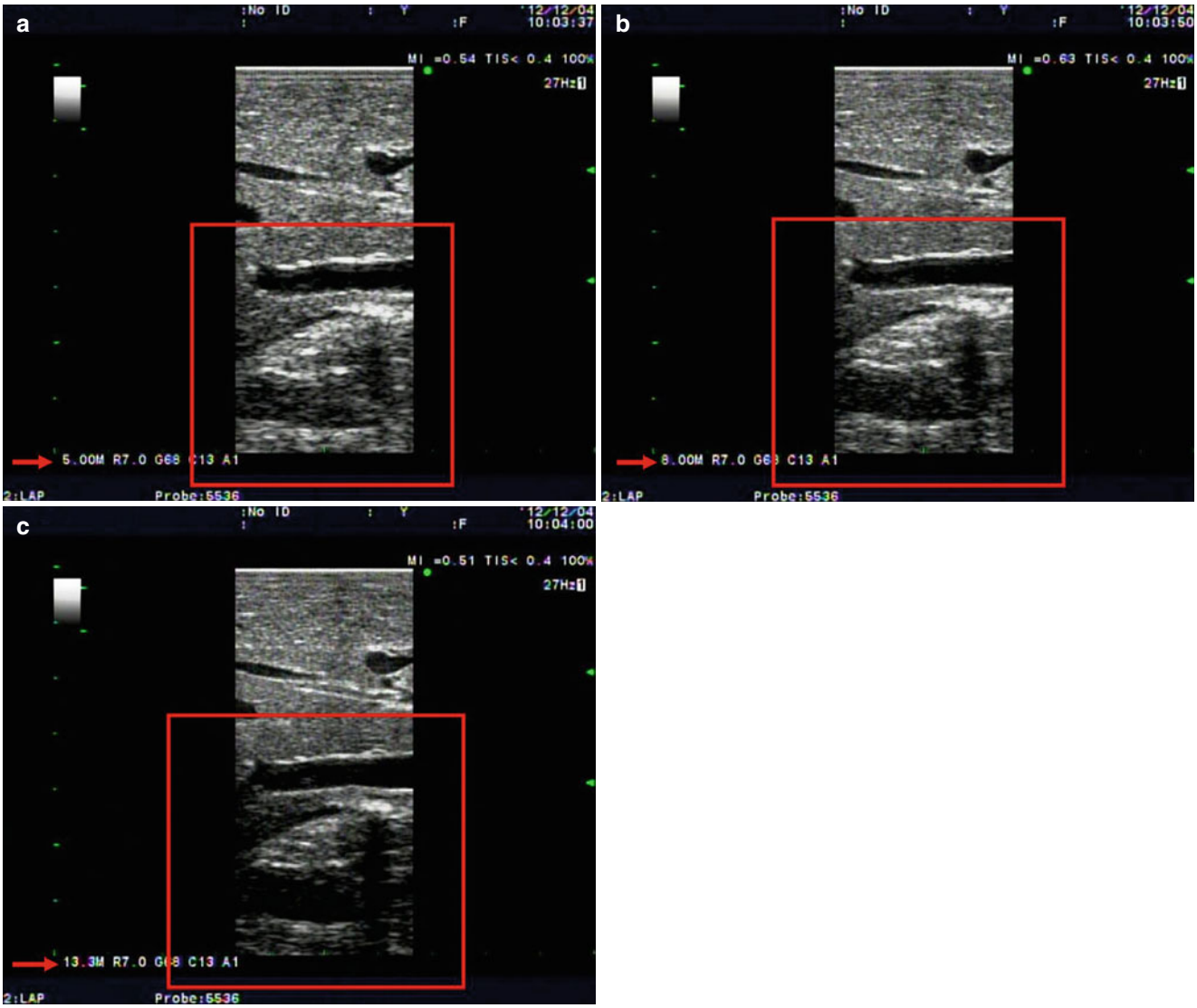

Fig. 3.3 (**a**–**c**) Figures showing ultrasound capture image of the liver parenchyma in (**a**) low, 5 MHz; (**b**) medium, 8 MHz; and (**c**) high, 13 MHz frequencies, respectively, adjusted by the surgeon intraoperatively. Note the changes in the image quality of the deep portion of liver scanned (*red box*) with different frequencies used

(e.g., 7.5–10 MHz) are ideal for thyroid and breast imaging, in addition to intraoperative ultrasound, where depth is less important and the image resolution is improved. The frequency of the probes can also be changed manually using the control panel of the ultrasound machine (Fig. 3.3a–c).

Mechanical Sector Probes

In mechanical sector-type transducers, a single crystal is attached to a rotating arm. Each time the probe sends a signal and receives the returning echo, a sector image is formed. This process is repeated so rapidly that formation of an image using one crystal is possible. These transducers are prone to breakage, since the motor of the arm rotates vigorously to obtain an image. Pie-shaped sector images are formed as a result of this type of scanning.

Endocavitary Probes

These probes also have a curved surface, and their unique extended design allows intracavitary evaluation of anatomic structures. Endocavitary probes provide wider views than curvilinear probes and also have higher frequency ranges (8–13 MHz). Thus, higher frequencies allow obtaining high-resolution images of close anatomic structures with a wider imaging area (see Chaps. 11 and 19 for more detail on endoluminal ultrasound).

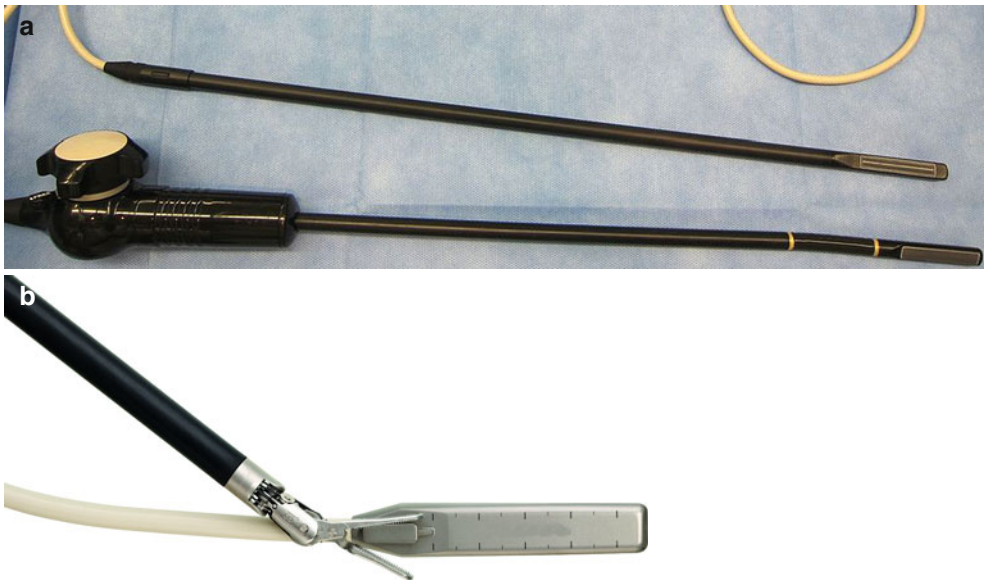

Fig. 3.4 (**a**, **b**) Photographs showing laparoscopic linear rigid and flexible (**a**) and drop-in robotic (**b**) probes

Intraoperative and Laparoscopic Probes

Although the idea of intraoperative ultrasound dates back to the 1960s, this concept has not been accepted and widely used until the introduction of real-time B-mode ultrasound scanners. Furthermore, the introduction of laparoscopy and minimal invasive techniques to the field of surgery led to a wider usage of intraoperative ultrasound for precise resection margins and detection and preservation of vital anatomic structures during surgical interventions. Today, both linear and convex probes are available for open or laparoscopic scanning. The technique for the laparoscopic examination is more demanding, since the ultrasound probe needs to be introduced to the target organ site from a trocar and manipulated in a limited space with limited range of motion. There are rigid, flexible, and robotic probes designed for easy manipulation (Fig. 3.4a, b). These probes have a frequency range between 5 and 12 MHz, and they provide high-resolution images of the scanned organs. They do not need any coupling media for imaging.

Array Types

Linear Array

Electronic scanning is achieved by arrays, which are transducer assemblies with multiple transducer elements. A linear array or linear-sequenced array consists of rectangular elements that are assembled in a straight line. A linear array forms rectangular images composed of many parallel vertical straight lines. This is achieved by pulses originating at different points across the surface of the array but traveling in the same vertical direction. This probe has higher frequencies ranging between 5 and 13 MHz, and as a result, it can be utilized for

- Imaging of superficial soft tissue
- Intraoperative imaging of solid organs
- Laparoscopic ultrasound
- Ultrasound-guided procedures (vascular access, biopsy, paracentesis, thoracentesis)

Curvilinear (Convex) Array

Curvilinear or convex probes are used for scanning deeper structures. The elements are assembled along a curved axis. The generated pulses travel out in different directions in contrast to linear arrays; so sector-type images are formed. The field of view is wider than the probe's face. The frequency range for these types of probes is between 1 and 8 MHz, which allows greater penetration with less resolution (Fig. 3.5a, b).

This probe is used in abdominal and pelvic imaging in the following scenarios:

- Evaluation of abdominal organs (liver, pancreas, gall bladder, spleen)
- Evaluation of the kidneys and bladder
- Abdominal FAST exam
- Abdominal aorta
- Musculoskeletal and soft tissue evaluation in obese patients
- Intraoperative ultrasound of the pancreas

Phased Array

Other than using a single crystal, many ultrasound crystals are cut from a single block of PZT, and each crystal is

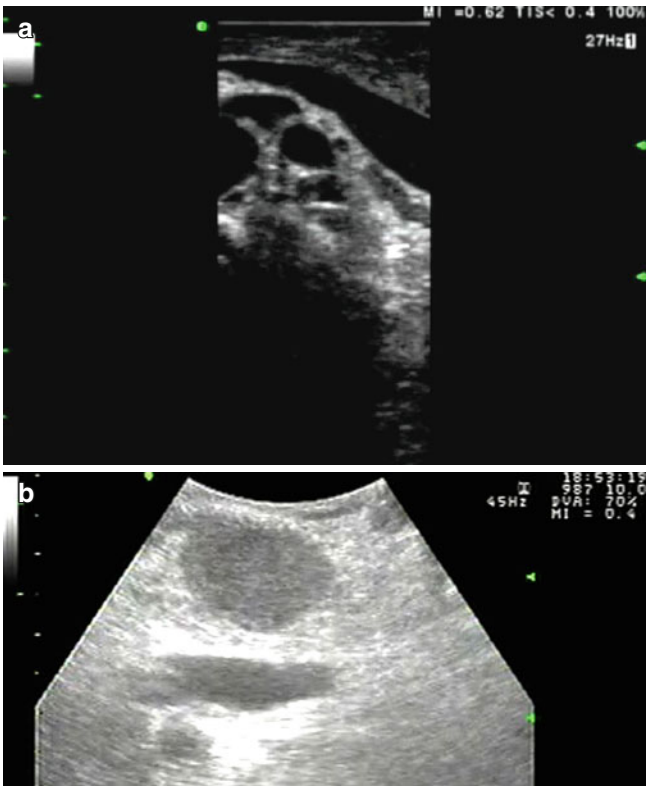

Fig. 3.5 (**a**) Intraoperative laparoscopic ultrasound image of pancreas using a linear array transducer. (**b**) Intraoperative ultrasound image of pancreas using a curvilinear small-parts transducer

assembled with electronic connections. This ensures each crystal to work independently but in a coordinated fashion. The sound waves originate from a single point; so sector-type images are created. This probe has a frequency range between 2 and 8 MHz. This probe is useful for

- Imaging of cardiac structures
- Imaging of the right upper quadrant via intercostal space
- Imaging of the abdomen in the absence of a curvilinear probe
- Ultrasound-guided procedures in small spaces and between the ribs

Control Panel

Modern ultrasound machines have many controls that allow adjustment of the ultrasound images and fine-tuning and amplification of the ultrasound energy sent to tissues. Basic controls are almost the same in every cart-based or portable ultrasound machine, though some machines have more sophisticated or slightly different control panels or touch pads (Fig. 3.6a, b). Surgeons should be familiar with the ultrasound machines in their institutions for optimal sonography. Surgeons performing ultrasound should practice with the ultrasound machines in their institutions in non-emergent situations to have a full understanding of the ultrasound system. In this section, we will review the components of the control panel essential for surgeons.

Presets

Many ultrasound machines have examination presets that allow the surgeon to easily perform basic examinations without the need for fine-tuning of parameters such as power, depth, focal zone, frequency, grayscale adjustments, and time gain compensations. Ultrasound machine presets are automatically changed when a different type of transducer is selected. Many ultrasound machines have categorized presets for each type of examination, such as cardiac, vascular, obstetrics/gynecology, small parts, and abdominal. When a surgeon chooses one of these categorized presets from the machine, the only control that can be modified would be the gain for appropriate brightness of the image displayed. However, these presets can be customized for more advanced imaging.

New Patient Control

This function will allow the surgeon to start a new ultrasound session and input patient information. Although most ultrasound machines allow scanning without entering patient information, this information is important to archive and retrieve images. In some institutions, the US images can also be sent to the hospital's picture archiving and communication system (PACS). This will allow the surgeon to store and recall previous examinations if needed for any reason.

Power Control

If returning echoes from the tissues are not strong enough to form an image, then the sonographer has two options to enhance the vision. Either increasing power or the gain will improve the image quality; however, increasing the gain is preferable. This control in some machines provides an increase or decrease of the ultrasound energy transmitted to tissues. Increasing power theoretically may cause thermal injuries to the patient since more ultrasound energy is transmitted to the tissues. Modern ultrasound machines have limits that do not allow power levels to be changed to degrees that might harm the patient. However,

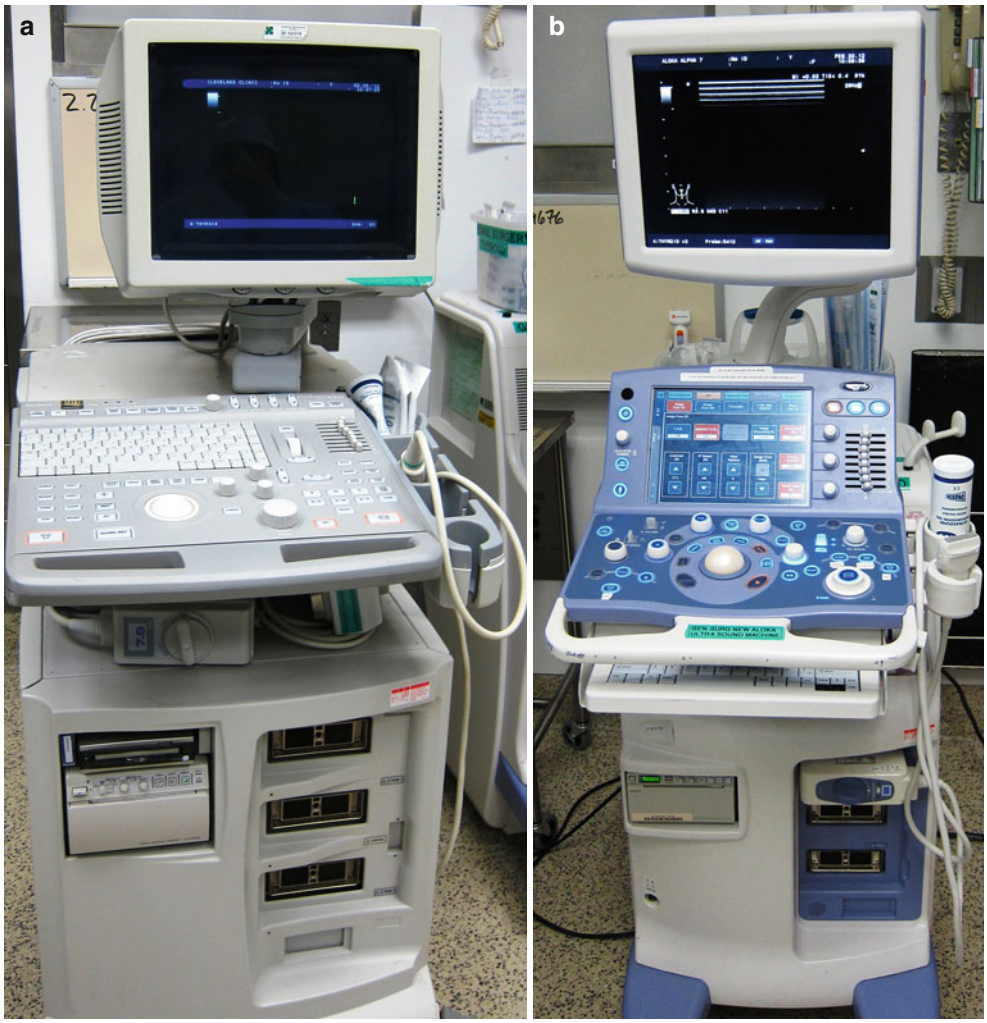

Fig. 3.6 (**a**, **b**) Two images showing different generations of machines

every sonographer should adapt the "ALARA" rule (as low as reasonably allowable) in their everyday practice (see Chap. 2).

Gain

Amplification is conversion of small voltages received from transducer elements to larger ones, which are suitable for evaluation and image formation. Gain control determines how much amplification is accomplished in the amplifier. Increasing the gain will amplify all the returning echoes from all depths and tissues. It is similar to increasing the volume in the radio. By decreasing or increasing the gain, the brightness of the image on the monitor changes. Because gain is set subjectively, there is a chance of missing vital structures or pathologies in the setting of inappropriate gain adjustment. With too little gain, weak echoes would not be able to be imaged, and conversely, with too much gain, saturation occurs and most echoes would appear bright and differences in echo strength would be lost (Fig. 3.7a–d).

Time Gain Compensation (TGC)

Time gain compensation (TGC) selectively allows modifying the amplification of returning echoes from structures in different depths for uniform image intensity. Thus, it is also called depth gain compensation. Because organs are located anatomically in different planes and depths in the human body and the ultrasound waves are attenuated as they traverse the tissues, there would be a mismatch of returning echoes even when imaging a single organ: less ultrasound energy would be reflected from deeper structures. The manipulation of TGC allows equivalent reflectors at different depths to have uniform brightness represented on the ultrasound monitor (Figs. 3.8a, b and 3.9a, b).

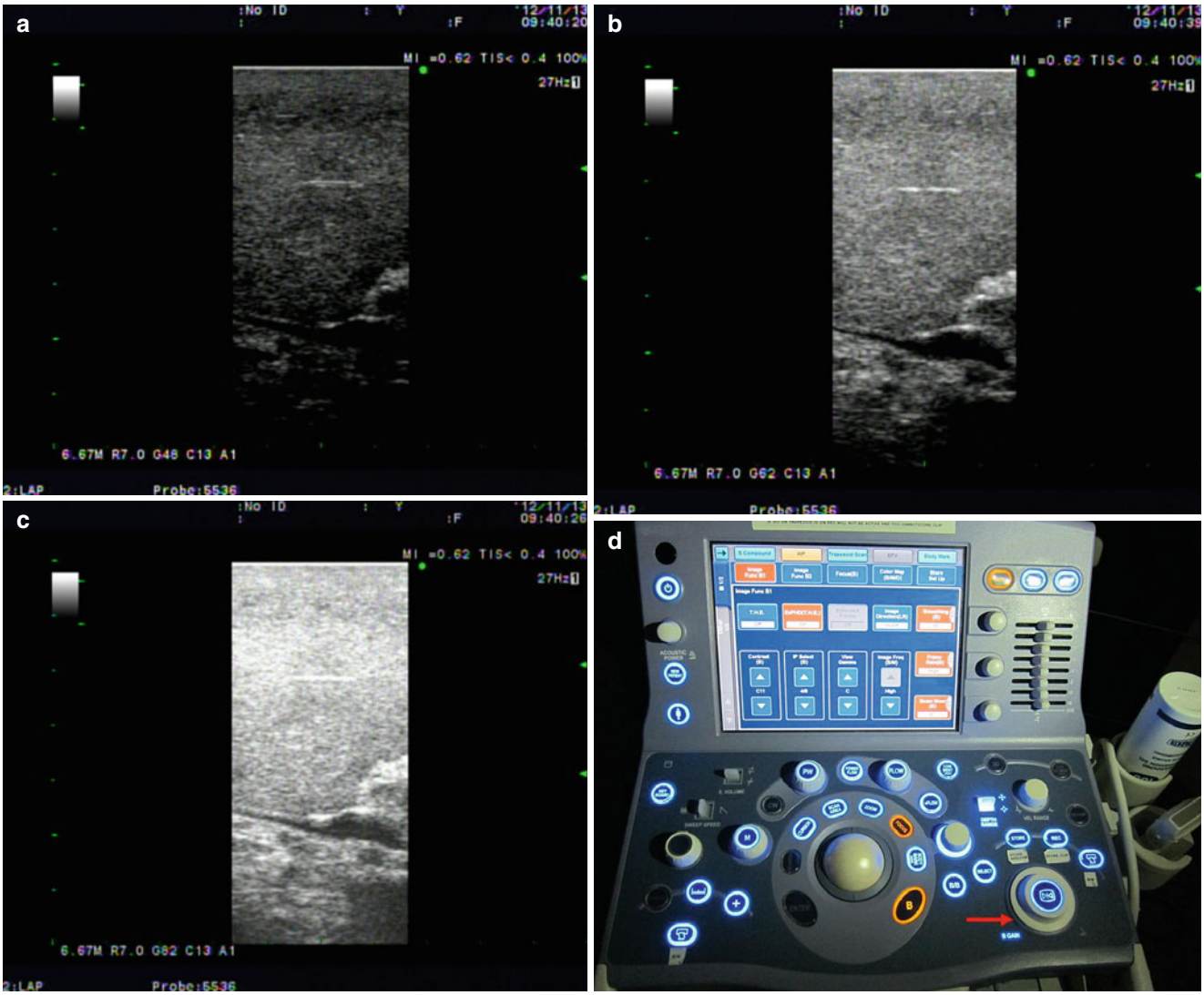

Fig. 3.7 (**a**) Ultrasound capture image showing liver parenchyma under inappropriate low-gain adjustment. (**b**) Ultrasound capture image showing liver parenchyma under appropriate gain adjustment. (**c**) Ultrasound capture image showing liver parenchyma under inappropriate high-gain adjustment. (**d**) Image showing gain control button on an ultrasound machine

Depth

Although the depth setting is usually pre-adjusted in a certain preset, depending on a patient's body habitus, obesity, or other anatomic factors, it can be further adjusted by the sonographer. For example, imaging of the liver in an obese patient would require a greater depth setting than imaging the liver in a pediatric slender patient. The depth is one of the factors affecting the frame rate and the image quality perceived by the sonographer. Since ultrasound waves would need to travel to tissues and reflected back in the setting of greater depth imaging, there would be a delayed perception of the returning echoes by the transducer. This would result in a slower frame rate. As a result, distorted poor-quality images would be formed (Fig. 3.10a–c).

Focus

The probe can be focused at any depth for enhancement of resolution. Focus control narrows the ultrasound beam to the point of interest. Focusing can be done either by an acoustic lens as in mechanical sector transducers or can be accomplished electronically as in the case of linear and curvilinear transducers. In more advanced ultrasound machines, multiple areas of focusing can be achieved by a component called "beam former." This component provides pulse delay sequences to the individual piezoelectric element of an ultrasound transducer to accomplish the focusing of the ultrasound beam. A single- or multiple-point focus could be used depending on the area imaged (Fig. 3.11a–d).

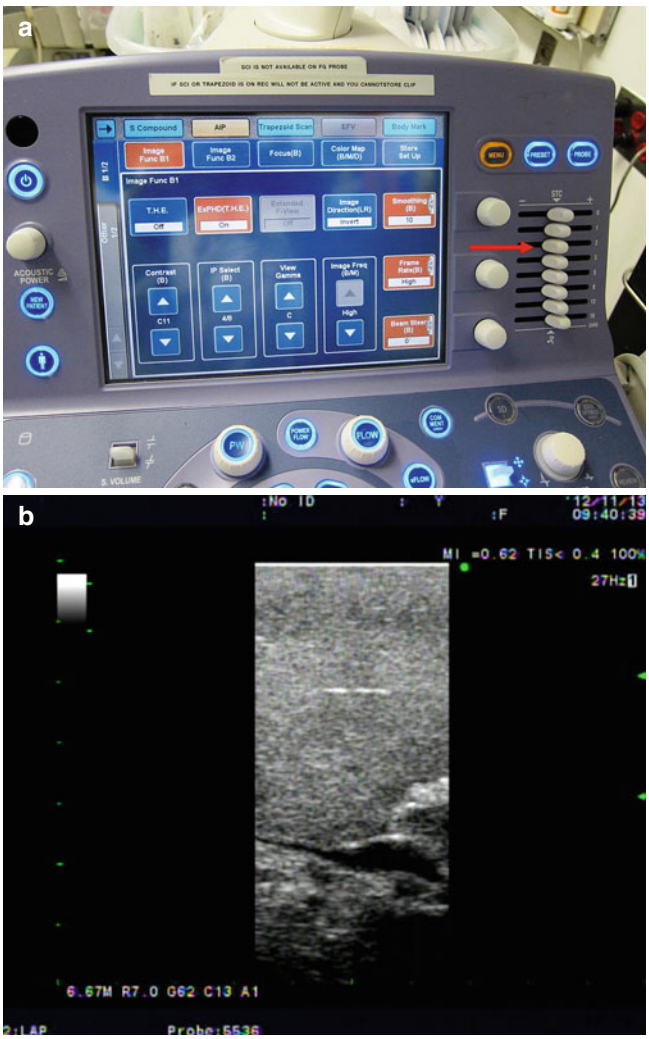

Fig. 3.8 (**a**, **b**) Image displaying time gain compensation (TGC) controls (**a**) and imaging with appropriately adjusted TGC (**b**) on an ultrasound machine

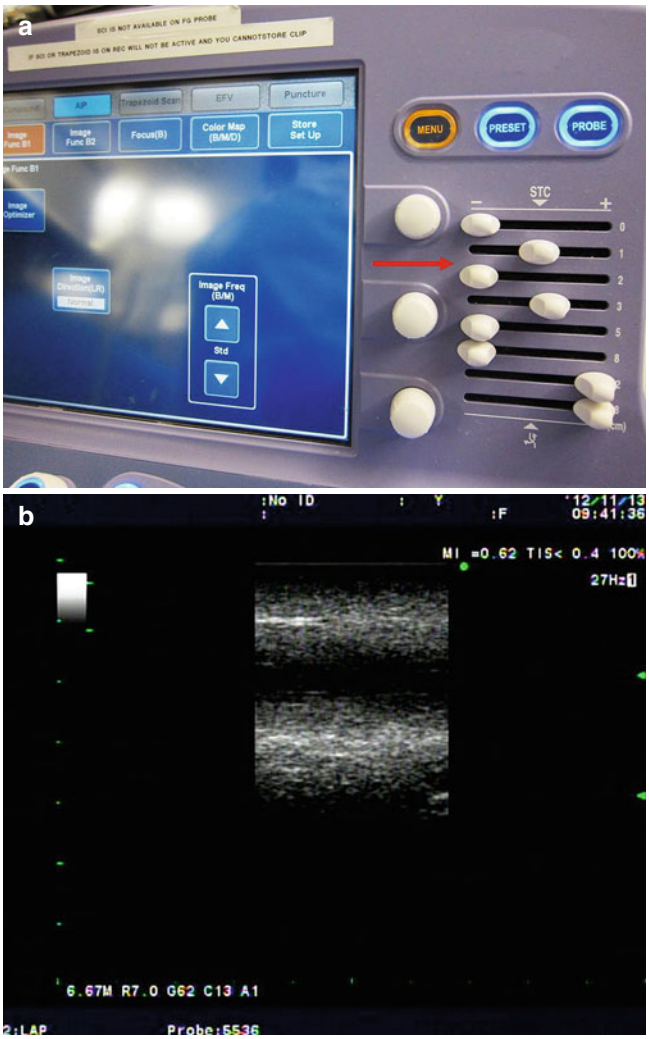

Fig. 3.9 (**a**, **b**) An intraoperative liver (*red arrow*) ultrasound image (**b**) with inappropriately adjusted time gain compensation controls (**a**)

Flow

The flow function is a useful feature that enables the surgeon to evaluate the vascularity of the organ imaged and also, in specific cases, to differentiate between vascular and other structures, such as the biliary duct. The addition of Doppler ultrasound on structural images provides physiologic information, which depends on the Doppler shift principle. While performing the ultrasound, pressing the flow button will activate this feature. The region of interest can be made smaller or larger, depending on the area of interest (Fig. 3.12a, b).

Image Display

Modern ultrasound machines use the pulse-echo principle with brightness mode (B-mode) display-quality, high-resolution images. In B-mode display, echoes are displayed in two dimensions as points of different grayscale brightness corresponding to the intensity (amplitude) of each signal. B-mode images may be displayed as still (static) or real-time images (see section "Imaging modes" in Chap. 2).

Formation of a Dynamic Ultrasound Image

The modern ultrasound system works according to the pulse-echo principle. This principle is based on creation of images from the voltages produced and received by the transducer. These images are processed and displayed by certain components of an ultrasound system such as a beam former, signal processor, image processor, and display unit to form real-time ultrasound images (Fig. 3.13).

Beam Former

A beam former is composed of a pulser, pulse delays, transmit/receive switch, amplifiers, analog-to-digital converters,

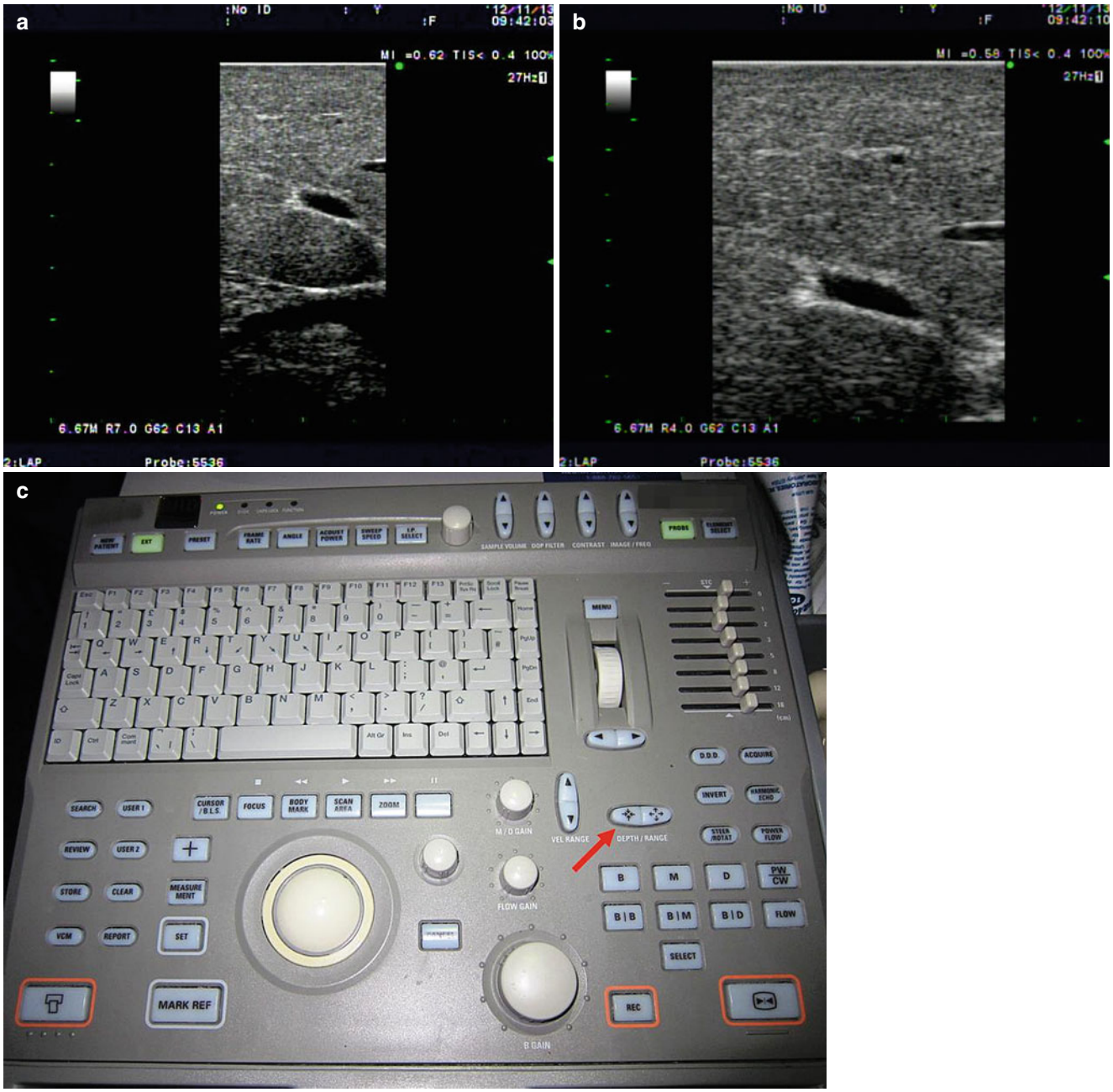

Fig. 3.10 (**a**–**c**) Ultrasound capture images of the liver in different depths: (**a**) decreased depth control, (**b**) increased depth setting, (**c**) depth control button (*red arrow*) on the unit

echo delays, and a summer. The beam former generates voltages for the transducer and amplifies the returning echoes from the transducer and directs and focuses the received beam. Also, amplification, adjustment, and filtering of the returning voltages are done by the transmit/receive switch. This switch prevents large transmitter signals from being transmitted to a sensitive signal processor. Failure of this action would result in damage to the signal processor and total loss of images or images with reduced brightness.

Signal Processor

Echoes initially processed by the beam former are transmitted to the signal processor where they are rendered into suitable inputs to the image processor. Signal processing embraces digital filtering, detection, and compression. Frequencies above or below the echo bandwidth are abolished so that the most suitable echoes are selected for optimal image processing. Another function of the signal processor is to compress or reduce the dynamic

range. Dynamic range is simply the ratio of the largest to smallest echoes that the ultrasound system can manage. This is done by two processes, TGC and rejection circuits, where TGC amplifies the echoes which are too weak and rejection circuits remove the low-amplitude noise.

Image Processor

The image processor converts the processed echoes through the beam former and the signal processor into images to be displayed on the display unit. This conversion of echo data to image format for image processing, storage, and display is called "scan conversion." Also, final signal processing to improve the image output in the display unit is done in the image processor and can be divided into two steps, preprocessing and postprocessing.

Preprocessing takes place as the data are being recorded to image memory. Edge enhancement, persistence, panoramic imaging, spatial compounding, and three-dimensional acquisition are various examples.

Postprocessing is done after the storage of the echo data into the image memory. A different level of numerical brightness is assigned to each pixel value displayed on the monitor as a result of this process. Each echo intensity is displayed in grayscale, varying from black to white with different brightness values. If there were less difference in echogenicity between the signals, then it would be difficult to differentiate between different types of tissues. This fact

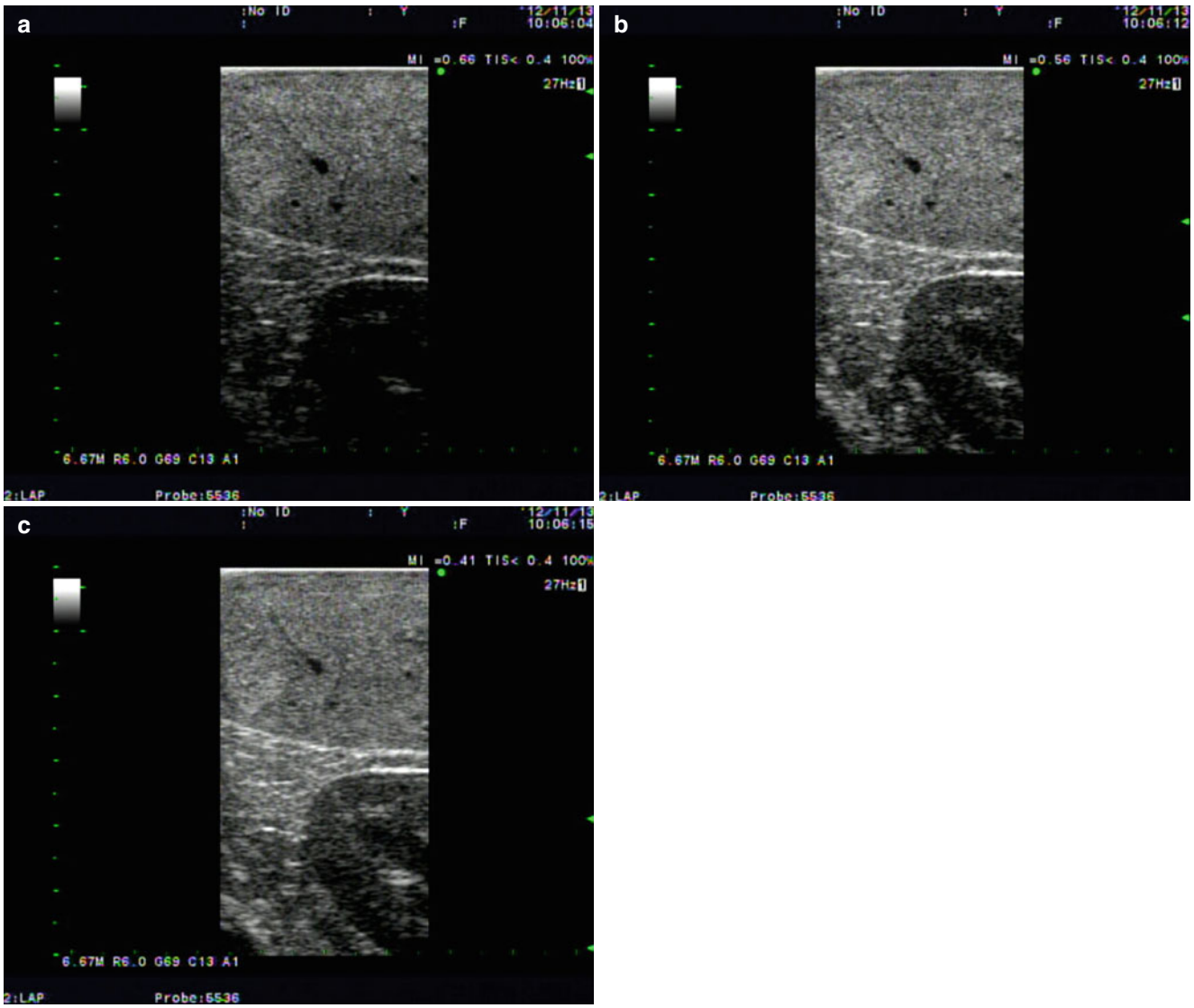

Fig. 3.11 (**a**–**d**) Ultrasound beam focused at different points during intraoperative sonography of the liver. More detail is seen as the beam is focused at three different points and is indicated between the *green arrowheads* on each ultrasound image (**a**–**c**). Focus control on an ultrasound touch pad shown by the *cpa* (**d**)

Fig. 3.11 (continued)

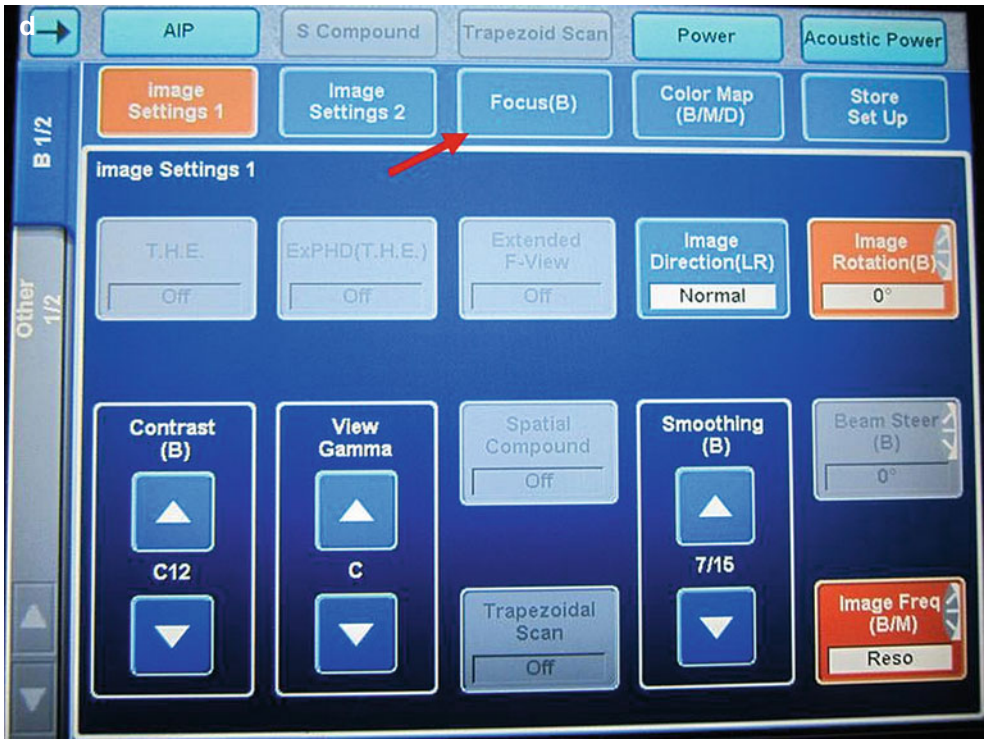

underscores the importance of contrast resolution, which is determined by this process.

Display Unit

Modern ultrasound machines usually have flat-panel liquid crystal display (LCD) units, whereas in the previous models, a monitor involving a cathode ray tube was used. The display unit is important since the real-time image quality is both related to frame rate and refresh rate. Frame rate is determined by images entered into image memory per second, and refresh rate is the number of times per second images are recalled from the image memory and displayed on the monitor. Modern LCD display monitors allow high-quality, high-frame-rate images and also four-dimensional reconstructed ultrasound images to be viewed in two dimensions.

Summary

Surgeon-performed ultrasound has become a part of routine surgical examination which also aids simple interventional procedures to complex operations. Although easy to practice and readily available, basic knowledge of the common terminology and basic technical knowledge should be a part of sonography training. Surgeons should be acquainted with the basic knowledge of the parts and operation of the ultrasound machine. If these principles are tailored, complex clinical sonographic applications can become readily available for every surgeon in practice.

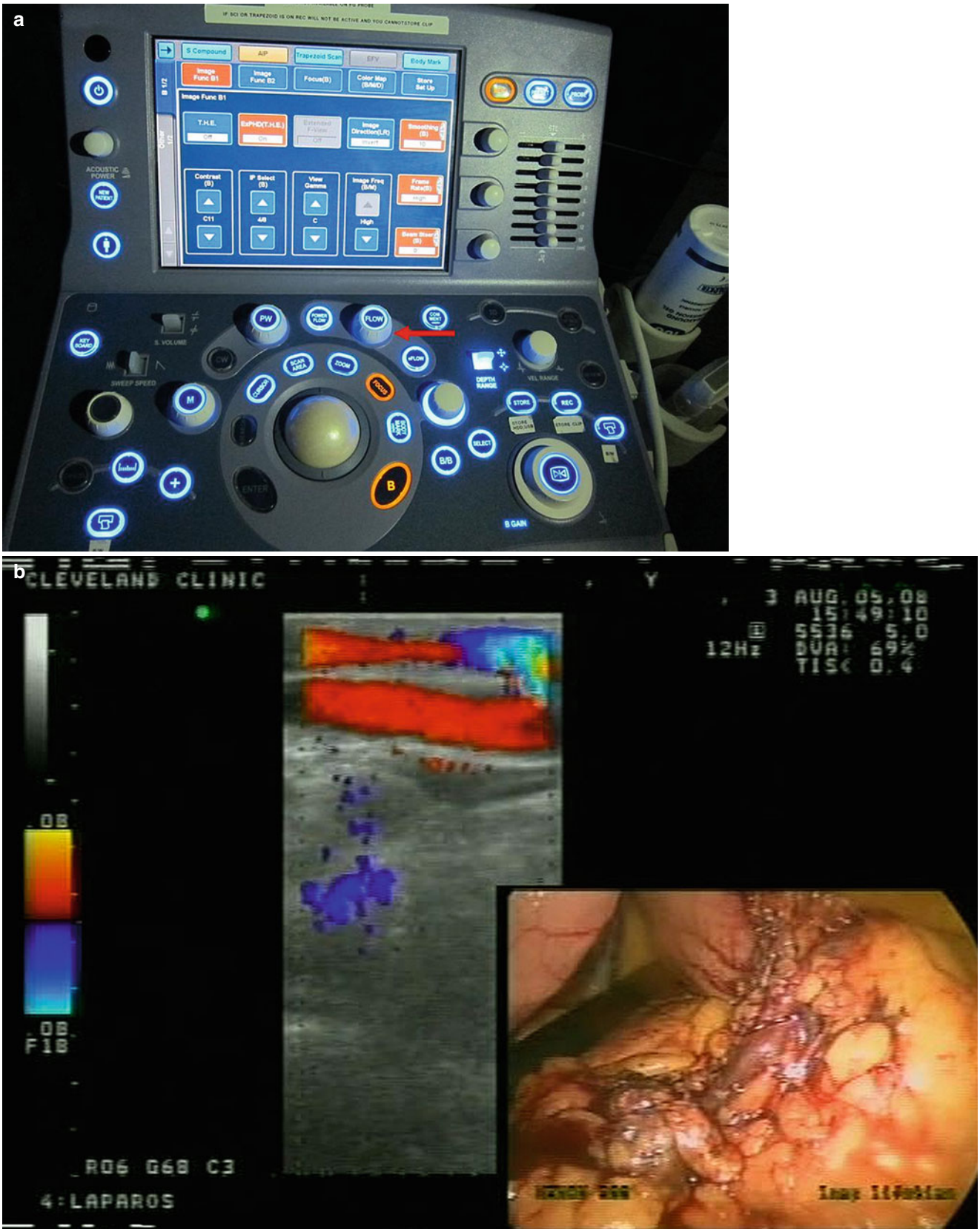

Fig. 3.12 (**a**) Image showing the flow control button (*red arrow*) on an ultrasound control panel. (**b**) The color Doppler image of splenic vein and artery

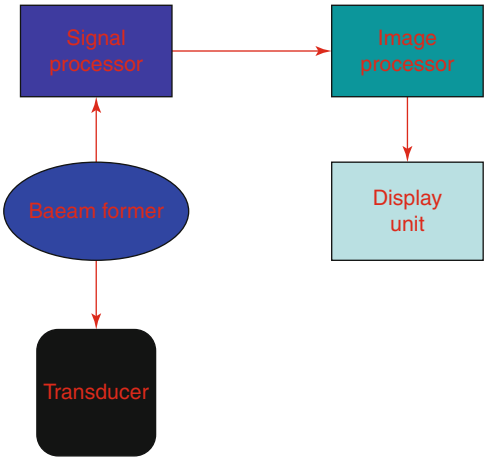

Fig. 3.13 Diagram showing the formation of a dynamic ultrasound image by the pulse-echo principle

Additional Reading

Abraham D, Silkowski C, Odwin C. Emergency medicine sonography: pocket guide to sonographic anatomy and pathology. Sudbury: Jones and Bartlett Publishers; 2010.

Carmody KA, Moore CL, Kopman DF. Handbook of critical care and emergency ultrasound. New York: McGraw-Hill Companies Inc.; 2011.

Dulchavsky SA, Fry WR, Gillman LM, Gittleman MA, Harness J, Kirkpatrick, AW et al. Ultrasound for surgeons: the basic course. 2nd ed [CDROM]. Chicago: American College of Surgeons; 2009.

Hendee WR, Ritenour ER. Medical imaging physics. 4th ed. New York: Wiley-Liss, Inc; 2002.

Jakimowicz JJ. Intraoperative ultrasonography in open and laparoscopic abdominal surgery: an overview. Surg Endosc. 2006;20 Suppl 2:S425–35.

Kremkau FW. Sonography principles and instruments. 8th ed. St. Louis: Elsevier/Saunders; 2011.

Lawrence JP. Physics and instrumentation of ultrasound. Crit Care Med. 2007;35(8 Suppl):S314–22.

Smith RS, Fry WR. Ultrasound instrumentation. Surg Clin North Am. 2004;84(4):953–71.

4 Scanning Techniques in Transabdominal and Intraoperative/Laparoscopic Ultrasound

Reid B. Adams

This chapter describes scanning techniques for transabdominal (TAUS), open intraoperative (IOUS), and laparoscopic (LUS) ultrasonography. The emphasis of the chapter is hepatic, biliary, and pancreatic scanning. Similarly, the discussion is based on performing a focused, not complete, diagnostic examination. The assumption is the surgeon will have a particular question in mind when performing the ultrasound examination, rather than performing a complete diagnostic examination.

The goal of this chapter is to describe techniques used to obtain optimal images of the liver, biliary tract, and pancreas. General principles, definitions, and standard imaging techniques, common to ultrasonography, are reviewed. Methods to avoid obstacles such as tissue-gas and tissue-bone interfaces and anatomic challenges are described. Techniques specific to each of the major target organs are detailed. Details not covered include ultrasound imaging physics and instrumentation, which are reviewed in Chaps. 2 and 3. Likewise, detailed specifics of liver, biliary, and pancreatic imaging are discussed in later chapters.

General Issues and Definitions

Equipment setup is determined by the type of scan, organ of interest, and the operator's position relative to the patient. Generally, TAUS scanning is done from the right side of a supine patient. The ultrasound machine and monitor are positioned on the patient's right and toward the head of the bed. This allows scanning while simultaneously changing machine settings as necessary. The bed height should be elevated to allow comfortable scanning for the ultrasonographer, either in a sitting or standing position (Fig. 4.1).

In the operating room, the machine and attached monitor are typically placed on the side of the bed opposite the surgeon (Fig. 4.2). In our case, this is most commonly on the patient's right. This has the disadvantage of requiring a third party to change machine settings when needed. If a remote monitor is available and displayed opposite the surgeon, the ultrasound machine can be placed next to the surgeon, covered with a sterile drape and settings changed by the ultrasonographer. During LUS, the use of the picture-in-picture feature is very helpful for matching external anatomic features with the corresponding ultrasound images.

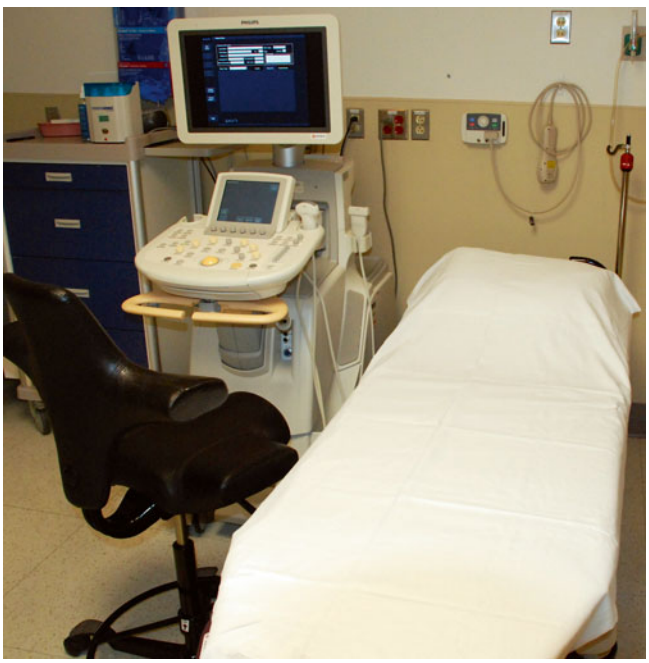

Fig. 4.1 Transabdominal ultrasound setup. The examiner sits or stands on the patient's right. The ultrasound controls and monitor sit to the right of the patient's head to allow easy use and viewing

R.B. Adams, MD, FACS
Department of Surgery, The University of Virginia Cancer Center, University of Virginia Health System, 800709, Charlottesville, 22908-0709, VA, USA
e-mail: rba3b@virginia.edu

E.J. Hagopian, J. Machi (eds.), *Abdominal Ultrasound for Surgeons*,
DOI 10.1007/978-1-4614-9599-4_4,

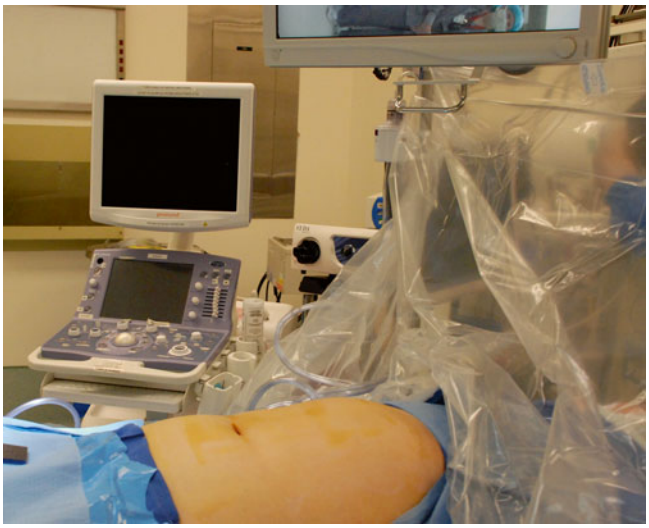

Fig. 4.2 Intraoperative ultrasound setup. The ultrasound machine and monitor are positioned to the patient's right. The operating surgeon stands on the patient's left. If the surgeon is positioned to the patient's right, the machine is on the opposite side of the table

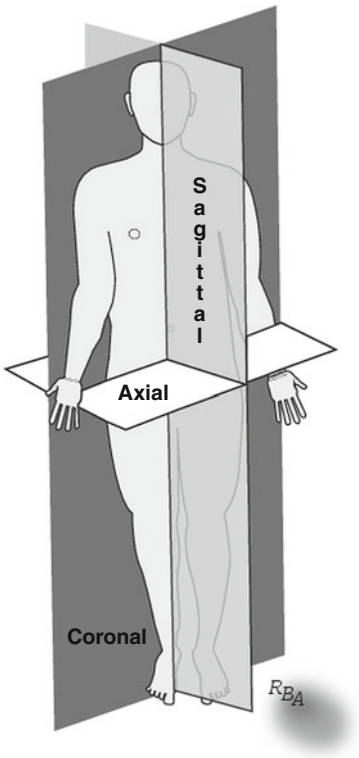

Fig. 4.3 Standard scanning planes for transabdominal ultrasound. Longitudinal planes include the sagittal and coronal planes. The single transverse plane is termed axial

Terminology and Image Display

A common terminology and display protocol are essential to allow clear interpretation of images and a reference standard for displaying static images. There are two primary imaging planes, longitudinal and transverse (Fig. 4.3). The longitudinal plane for TAUS is the long axis of the body; for IOUS or LUS, it is the long axis of the organ. Longitudinal planes include a sagittal view, when the transducer is oriented anterior to posterior, or coronal, when oriented side to side. The transverse plane gives a cross-sectional image similar to the familiar axial image seen on computed tomography (CT).

Image orientation and annotation are critical for clear communication of ultrasound images. Image orientation is standardized. When scanning in the longitudinal plane, the direction of the patient's head is oriented on the left side of the monitor screen (Fig. 4.4a). Scans done in the transverse plane are oriented such that the left side of the monitor image corresponds to the right side of the patient (Fig. 4.4b). Thus, when beginning a new scan, insure the transducer and monitor orientation are in alignment. Annotation should include the patient's name, medical record number, date of the examination, and the plane of the image.

Image acquisition consists of several important steps to obtain interpretable images: coupling, transducer placement, and transducer manipulation.

Coupling and the Acoustic Interface

To obtain adequate ultrasound images, a path for transmission of sound waves between the transducer and the object being imaged is necessary. This path is called an acoustic interface; it is achieved through coupling. Coupling is a process that displaces air (an inefficient sound transmitter) between the transducer and the object with a more efficient transmitter. In TAUS, a gel is the most common coupling agent (Fig. 4.5); for IOUS/LUS, a little saline placed on the surface of the organ works well.

Changing the thickness of the acoustic interface moves the transducer closer or farther from the object of interest, thereby altering the underlying image. This relationship allows several methods of scanning depending on the transducer's relationship to the structure of interest (Table 4.1). These different scanning techniques have specific uses as outlined in this and later chapters. This is particularly important for objects of interest in the near field (between the focal zone and the transducer); when they are too close to the transducer, they cannot be seen or the image suffers from low resolution.

Transducer Placement

The surgeons' intimate knowledge of three-dimensional anatomy facilitates recognition and interpretation of ultrasound images. This familiarity allows pattern recognition of organs and structures based on past experience. Transducer

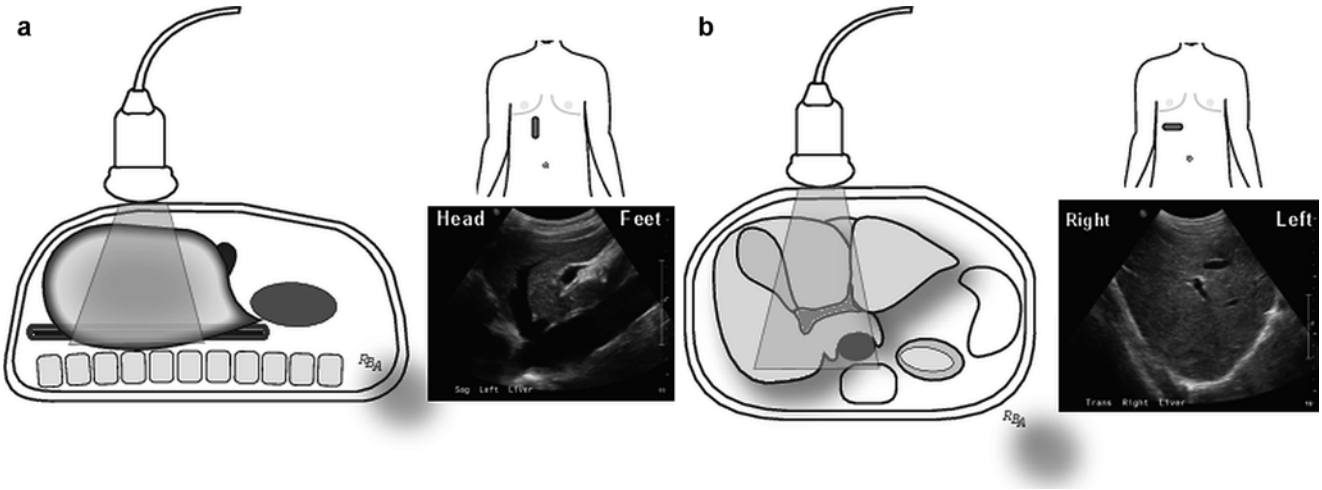

Fig. 4.4 Standard orientation and annotation of images is important for clearly communicating information represented by still images. (**a**) Transabdominal image with the transducer oriented in the longitudinal (sagittal) plane. By convention the image is oriented such that the patient's head is in the direction of the left side of the monitor. (**b**) Transabdominal image with the transducer oriented in the transverse (axial) plane. By convention the image is oriented such that the right side of the patients' body is oriented in the direction of the left side of the monitor

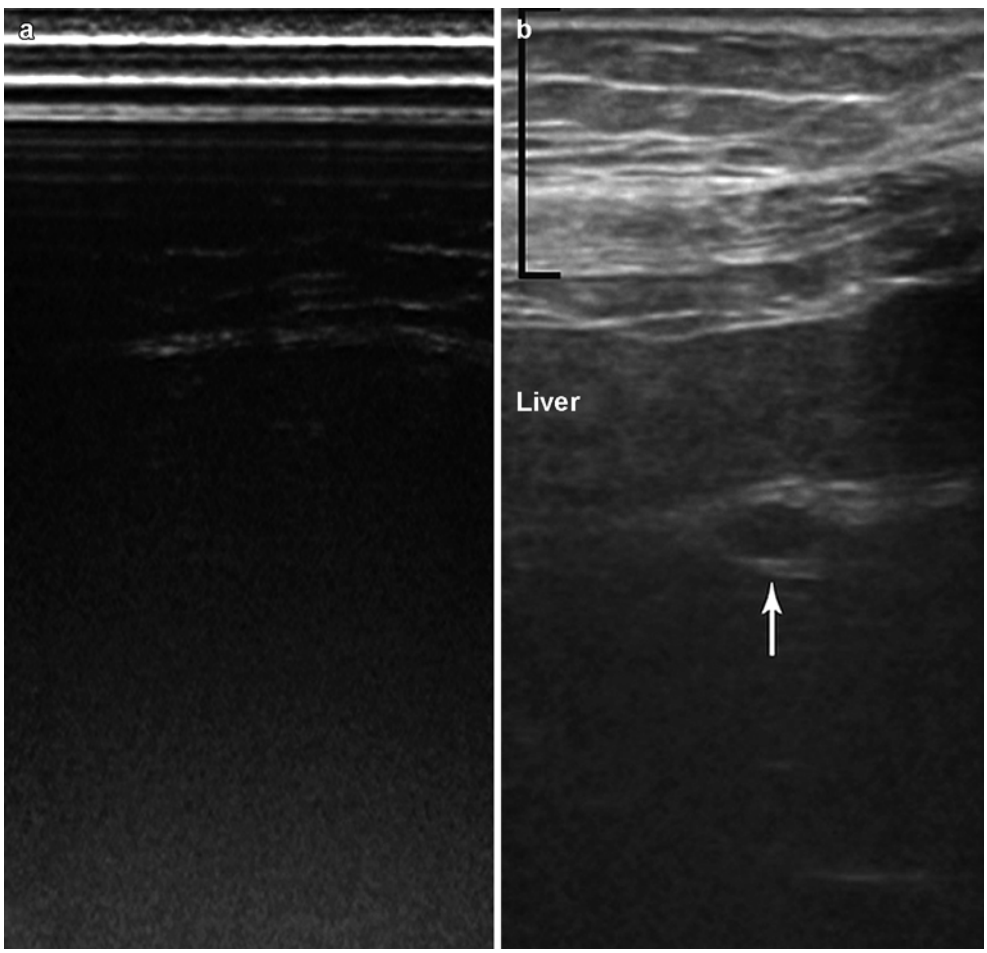

Fig. 4.5 Transabdominal ultrasound. (**a**) The transducer is placed on the skin without coupling gel. No discernible structures can be seen without an acoustic interface. (**b**) Gel is placed on the transducer and used to "couple" the transducer to the skin. This provides an acoustic interface that permits sound wave transmission and consequently an image. Seen in this image are the body wall (*black bracket*), the liver, and the left portal vein (*white arrow*)

Table 4.1 Types of scanning

Contact
Light contact
Graded compression
Deep compression
Probe standoff
Saline-filled bag/glove
Saline immersion of organs (intraoperative/laparoscopic ultrasonography)

Table 4.2 Probe standoff scanning advantages

Allows placement of the object of interest into the focal zone
Eliminates artifacts due to an irregular scanning surface
Objects within 1–1.5 cm of the scanning surface can be seen
Superficial objects are seen with high resolution
Lack of tissue compression eliminates distortion of underlying structures
Provides more angles of freedom for scanning maneuvers

Table 4.3 Transducer movements

Sliding – transducer remains in contact with scanning surface; it is slid in longitudinal or transverse plane
Rotating – transducer is spun clockwise or counterclockwise; central portion remains fixed to starting site
Rocking – transducer is moved (rocked) parallel to the scanning plane
Tilting – transducer is moved perpendicular to the scanning plane

placement is important to find "acoustic windows," which are transducer placement sites that allow examination and recognition of the organ of interest. This requires considerable practice, patience, and a few tricks. However, matching the acoustic window with the surgeon's deep understanding of the underlying anatomy makes learning this easier.

Transducer placement is determined by the type of scan being performed. These are reviewed in detail in the next sections. In addition, it is important to examine an organ or structure of interest in two planes to insure that the image is not due to an artifact. This includes both the longitudinal and transverse planes but also on occasion an oblique plane. Thus, transducer placement and movement is important to achieve this goal. Finally, the degree of transducer placement against the tissue alters the image and the scanning method may change based on the structure being imaged.

The next step for proper transducer placement is determining the type of contact between the transducer and the object for imaging (Table 4.1). *Contact scanning* occurs when the transducer is placed in direct contact with the tissue of interest. It can vary from light contact to deep compression, depending on the purpose of the scan. The majority of TAUS exams use light, direct contact scanning. If organ displacement is desirable during TAUS, for instance, to move a loop of bowel with gas lying over a structure of interest, then deep compression can be used to move it aside, exposing a better acoustic window. Similarly, light contact scanning is frequently used for liver scanning; occasionally deep compression is necessary to change the angle of viewing or to displace gas within an organ when viewing through the organ such as imaging the pancreas through the stomach or gastrocolic ligament. *Probe (transducer) standoff scanning* occurs when the probe is not in direct contact with the tissue of interest. Advantages of the probe standoff technique are outlined in Table 4.2. In probe standoff scanning, acoustic coupling is achieved by placing a fluid interface between the transducer and scanned structure. For instance, better images are obtained when scanning a superficial, subcutaneous object by placing a saline-filled glove on the skin and scanning through this to move the transducer 1–2 cm away from the surface of the skin. Probe standoff scanning is done frequently during IOUS/LUS, either by filling the abdominal cavity with saline or placing a saline-filled glove on the organ and scanning through the fluid-filled acoustic window.

Transducer Manipulation

After determining the type of probe contact, the next critical steps to master are the transducer movements (Table 4.3). Too much transducer movement is a common error early in the learning process. Most transducers have a wide viewing area, and movement of the transducer more than a few millimeters results in significant changes in the image. The novice becomes "lost" when the familiar patterns of a recognized image are no longer seen, requiring one to restart the process by identifying a recognizable structure or pattern. A second common error is lifting the transducer when moving it, which causes the image to disappear when the acoustic interface is interrupted, again causing the novice to lose a pattern they recognize. Lifting the transducer eliminates one of the unique and important features of ultrasound, that is, real-time image acquisition and viewing. To eliminate these errors, four basic types of transducer movement are outlined (Fig. 4.6).

Once the first acoustic window is identified and the transducer placed, the probe is moved by "sliding" it across the tissue surface (Fig. 4.6a), eliminating the need to lift from the scanning surface. Sliding can be done with the probe in a longitudinal or transverse orientation. Sliding gives a series of parallel images in relation to the original scan plane. Once the area of interest is identified, the probe can be rotated, rocked, or tilted to scan the object and its surrounding structures. Rotation involves spinning the probe as if the central part of the transducer was stuck to the tissue (Fig. 4.6b). This allows imaging of the structure of interest continually

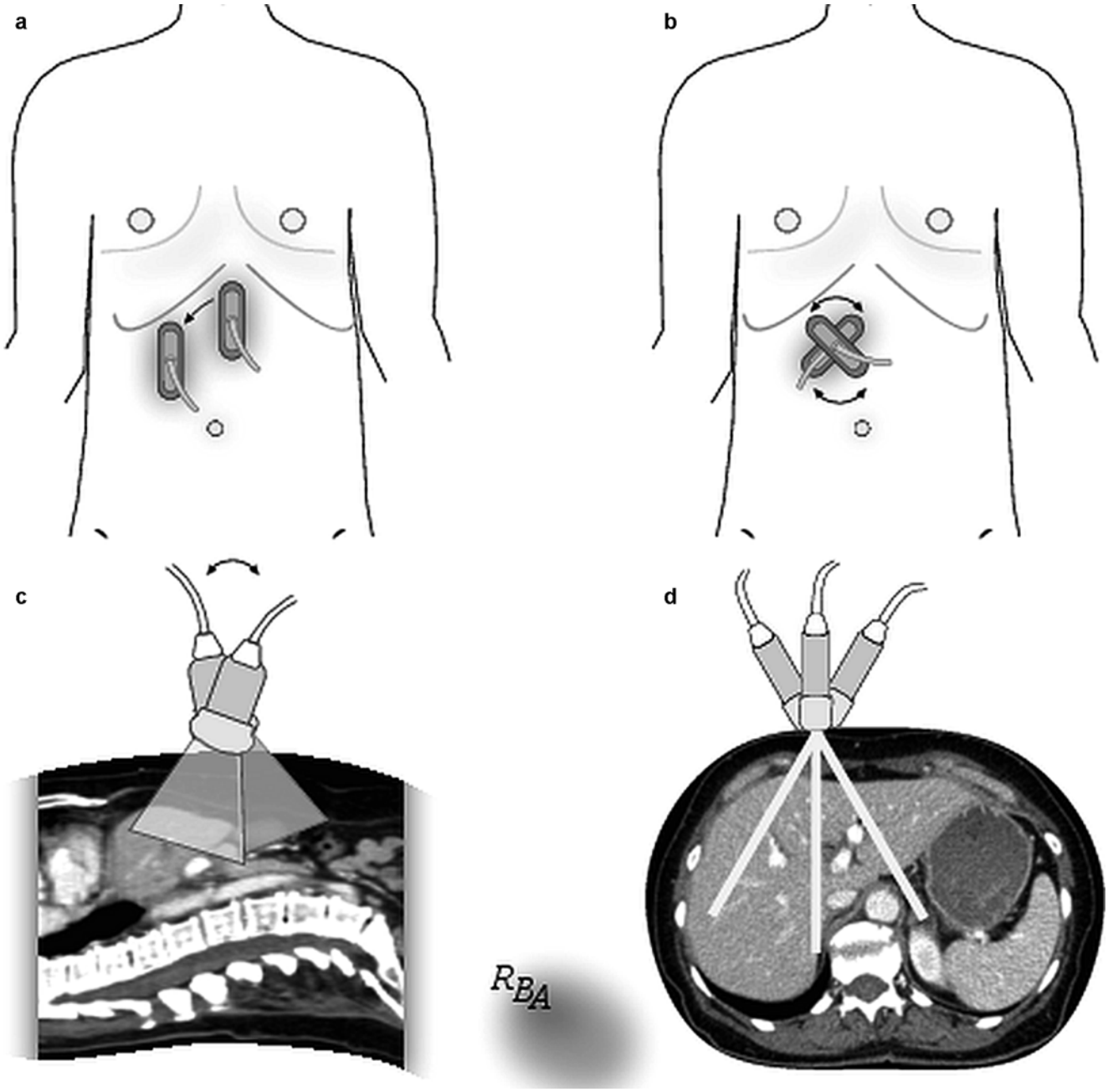

Fig. 4.6 Transducer movements. (**a**) Sliding. The transducer is moved without picking it up off the abdominal wall. (**b**) Rotating. The transducer is rotated clockwise or counterclockwise as if it were "pinned" to a central axis. (**c**) Rocking. The transducer remains in the same position relative to the skin while moving the back of the probe forward or backward in relationship to its long axis. This results in a series of images parallel to the scanning plane. (**d**) Tilting. The transducer remains in the same position relative to the skin while moving the back of the probe side to side relative to the long axis of the probe. This results in a series of images perpendicular to the scanning plane

through the longitudinal, oblique, and transverse planes, allowing one to develop a three-dimensional image. During rocking, the transducer moves parallel to the original plane of imaging (Fig. 4.6c). Tilting is the result of moving the probe perpendicular to the original scanning plane (Fig. 4.6d).

These small movements allow scanning of large areas with very little transducer movement in relationship to its site of contact with the tissue. Detailed images of the structures of interest can be achieved without getting lost during the scanning process. This allows scanning of the target in at least two dimensions to insure the object is not an artifact. In addition, scanning in multiple dimensions in real time allows one to develop a three-dimensional understanding of the structure or organ of interest.

Finally, it is critical to develop a systematic scanning approach for each type of scan you do and for each organ. To

insure a complete examination, this system should be followed fastidiously every time an ultrasound examination is performed.

Transabdominal Ultrasound

TAUS done by surgeons is typically a focused examination seeking specific information for diagnostic or therapeutic reasons. It does not substitute the need for radiological expertise or other imaging studies, but rather is complimentary to these.

TAUS usually begins with the patient in the supine position. The examiner is on the patient's right side and the ultrasound machine is on the same side toward the head of the bed. A 3.5 MHz curvilinear transducer is the most common one used in adults. The curvilinear transducer requires a larger, flatter surface for optimal contact. When a smaller "footprint" (size of the contact surface) is necessary, such as viewing through an intercostal space, a phased array transducer can be used. Ideally, prior to TAUS, the patient should fast for 6 h. This decreases bowel gas and allows gallbladder distension.

Standard scanning planes for TAUS are those previously described: longitudinal (sagittal, coronal) and transverse. Most TAUS scanning is done with light contact with coupling accomplished with gel. When holding the transducer, it is helpful to stabilize your hand by placing the base of the hypothenar eminence against the body (Fig. 4.7). This allows for fine probe movement during the examination. The initial transducer placement depends on the type of study or organ of interest. The same is true for the initial transducer orientation. Transducer movement during TAUS includes all the techniques previously described.

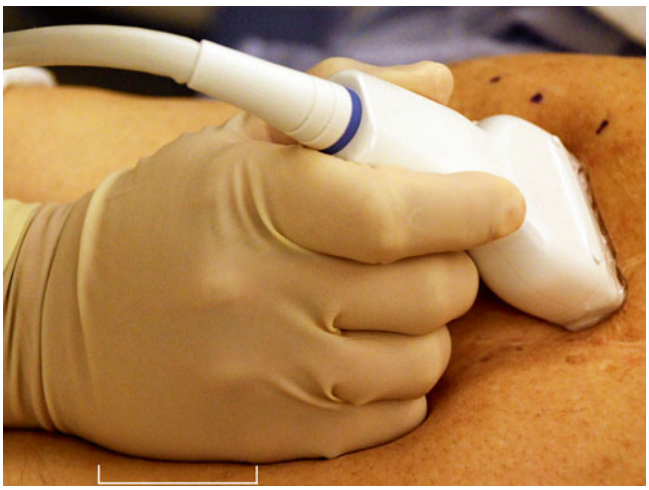

Fig. 4.7 During transabdominal ultrasound, it is helpful to hold the probe while lightly resting the hypothenar eminence (*white bracket*) against the body wall. This stabilizes the probe and allows for fine movements, steadies the image, and decreases fatigue

Liver Scanning Technique

Current transducers have a range of frequencies. A 3.0–3.5 MHz range is a good choice for most patients when evaluating the liver. A 5 MHz frequency may be better for very thin patients, while a 2.5 MHz frequency is helpful for obese patients or those with steatosis. Again, it is important to develop a systematic approach to scanning; it should be done every time. To begin liver imaging, place the probe transversely in the subxiphoid position and identify the hepatic veins as they join the vena cava. This is an easily recognized image that helps to orient the examiner (Fig. 4.8). If the patient has a steep, angulated costal margin, ask the patient to take a half to whole breath and hold it. This pushes the liver toward the costal margin, making the superior liver easier to see. Once this view is found, a systematic approach (Table 4.4) using a combination of transducer movements allows mapping of the segmental hepatic anatomy. For instance, a majority of the liver can be seen by rocking and tilting the probe while in the subxiphoid window (Fig. 4.9). Next, the probe is slid toward the left and then the right, allowing views of the remaining left and right livers, respectively. Upon completing the transverse views, the probe is reoriented in a sagittal plane and the process repeated. Sometimes the probe must be angulated sharply toward the head to scan beneath the costal margin. If this does not permit adequate viewing, an intercostal window allows access to structures hidden beneath the ribs. A smaller footprint probe is useful in this instance. Both an anterior and lateral approach through the costal margin may be necessary to image the structures of interest.

Biliary Scanning Technique

The transducer and techniques are similar to those described for the liver. Ideally, the patient should fast for 6 h prior to the study to allow maximal gallbladder distension. With the patient supine, position the probe subcostal in the midaxillary line while oriented in the sagittal plane. The initial step is to find the gallbladder. Slight sliding and tilting in this position allows a long axis view of the gallbladder (Fig. 4.10). Rotating the probe in the same position allows transverse and oblique views of the gallbladder. From here, several standard probe positions are helpful for complete biliary scanning (Fig. 4.11) [1]. Intercostal windows typically are necessary for complete biliary scanning. Rolling the patient into the left lateral decubitus position is important to distinguish

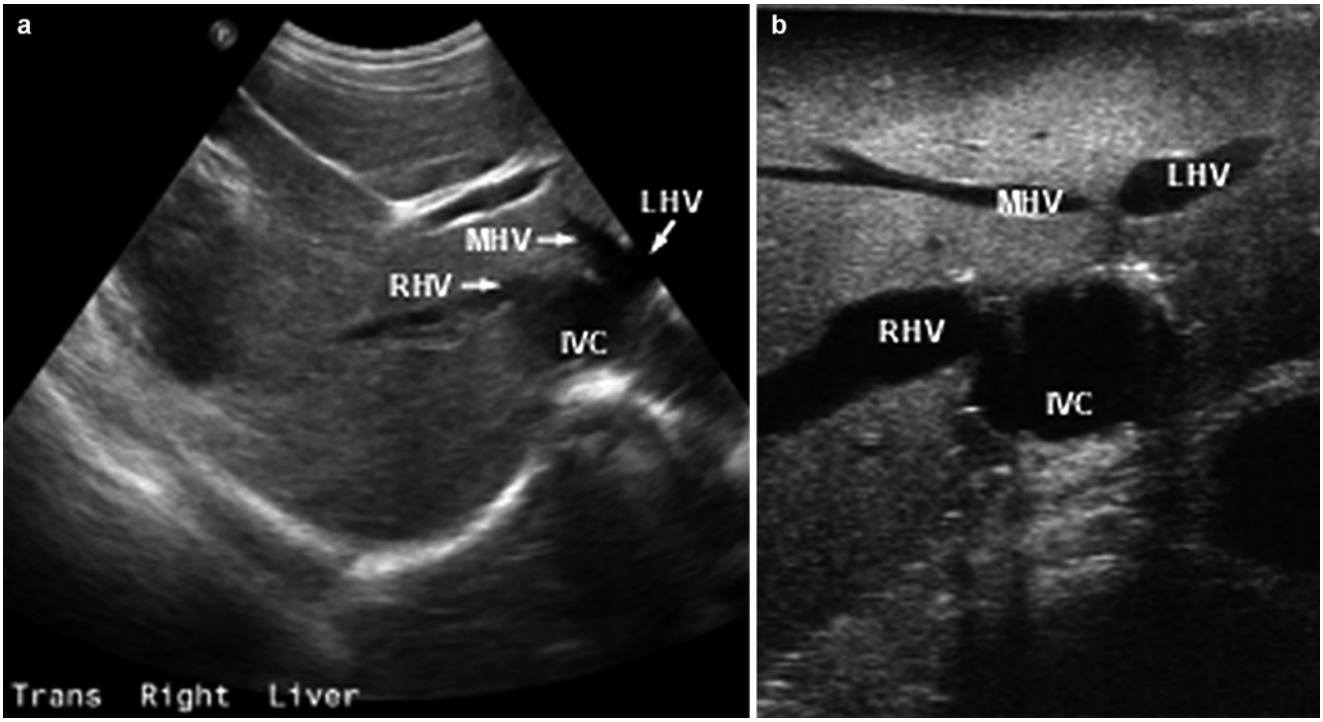

Fig. 4.8 Transabdominal ultrasound image with the transducer held transversely in the subxiphoid position. This allows a prototypical image of the hepatic veins as they join the vena cava (*IVC*). Right (*RHV*), middle (*MHV*), and left (*LHV*) veins are shown

Table 4.4 Stepwise approach to liver scanning: transabdominal

Identify hepatic veins
Find junction with vena cava
Follow to terminal branches
Identify any anomalous branches
Follow vena cava from hepatic vein branches to inferior liver
Identify portal branches
Find bifurcation, main, right, left portal veins
Follow right and left veins to their segmental branches
Systemic parenchymal scan
Develop a standard scanning approach
Examine all the parenchyma
Note lesion location, size, and features
Identify any vasculobiliary involvement or thrombosis

whether gallbladder masses are stones (move with repositioning) or polyps (stationary with repositioning) and sometimes to get an adequate view of the extrahepatic bile duct.

The extrahepatic bile duct is recognized by its position anterior to the portal vein. Place the probe in a longitudinal plane approximately perpendicular to the right costal margin between the midaxillary line and the epigastrium (Fig. 4.11, position b). Identify the portal vein at the hilar plate and follow it caudally to identify the bile duct in a longitudinal view anterior to the portal vein (Fig. 4.12). Sliding the probe toward the midline while in a longitudinal or oblique position allows viewing of the distal duct (Fig. 4.11, positions e and f). If the duct is not visible in this position, the best view may be obtained by placing the probe in a longitudinal, subcostal, and midaxillary position while the patient is in the left lateral decubitus position. Views of the retroduodenal duct are difficult to obtain as they often are obscured by duodenal or bowel gas. The intrapancreatic duct is best seen in transverse section through the head of the pancreas; however, this can be difficult to obtain due to bowel gas. Unless dilated, small intrahepatic ducts can be difficult to see. Intercostal windows facilitate imaging the right intrahepatic ducts, while the left ducts are viewed from a left subcostal window.

Pancreas Scanning Techniques

TAUS of the pancreas can be difficult due to bowel gas between the abdominal wall and the pancreas. The patient is examined in the supine position after fasting to minimize bowel gas. If the view still is impeded by gas, several other techniques can be used to improve the view. Deep inspiration and breath holding may push the liver below the costal margin where it can serve as an acoustic window to the pancreas. Compression scanning with deep pressure on the probe can push gas-filled structures aside. Placing the patient in a semi-upright position after drinking 500 ml of water may allow a viewing window through the fluid-filled stomach. A right

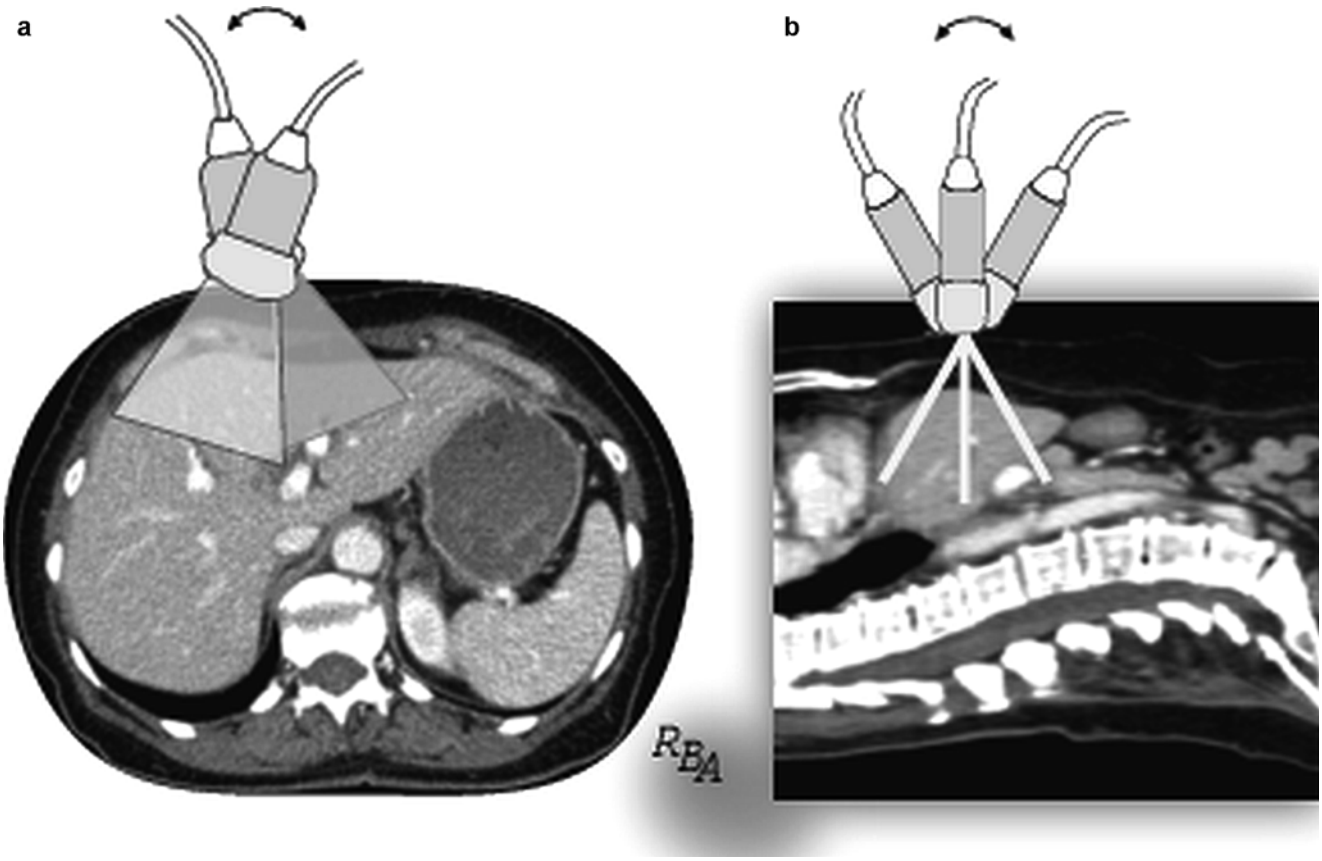

Fig. 4.9 Transabdominal ultrasound with the transducer placed transversely in the subxiphoid position. Rocking (**a**) and tilting (**b**) the probe in this single position allow one to image a large portion of the liver with relatively little probe movement relative to the body wall

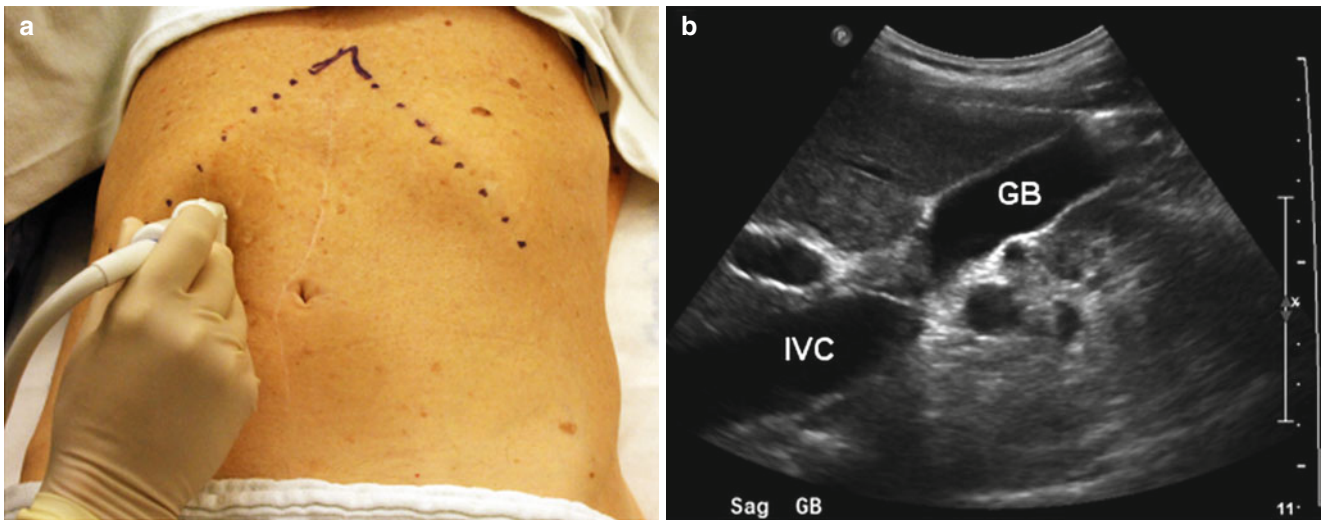

Fig. 4.10 Gallbladder imaging. (**a**) The transducer is oriented in the sagittal plane in the midaxillary line. (**b**) This allows a longitudinal view of the gallbladder (*GB*). Inferior vena cava (*IVC*)

lateral decubitus position may improve the image. Finally, the tail of the pancreas may be best seen from a left lateral flank view through the spleen.

The pancreas is difficult to find on TAUS. It is most easily identified by its relationship to surrounding landmarks. The transducer is positioned transversely in the subxiphoid,

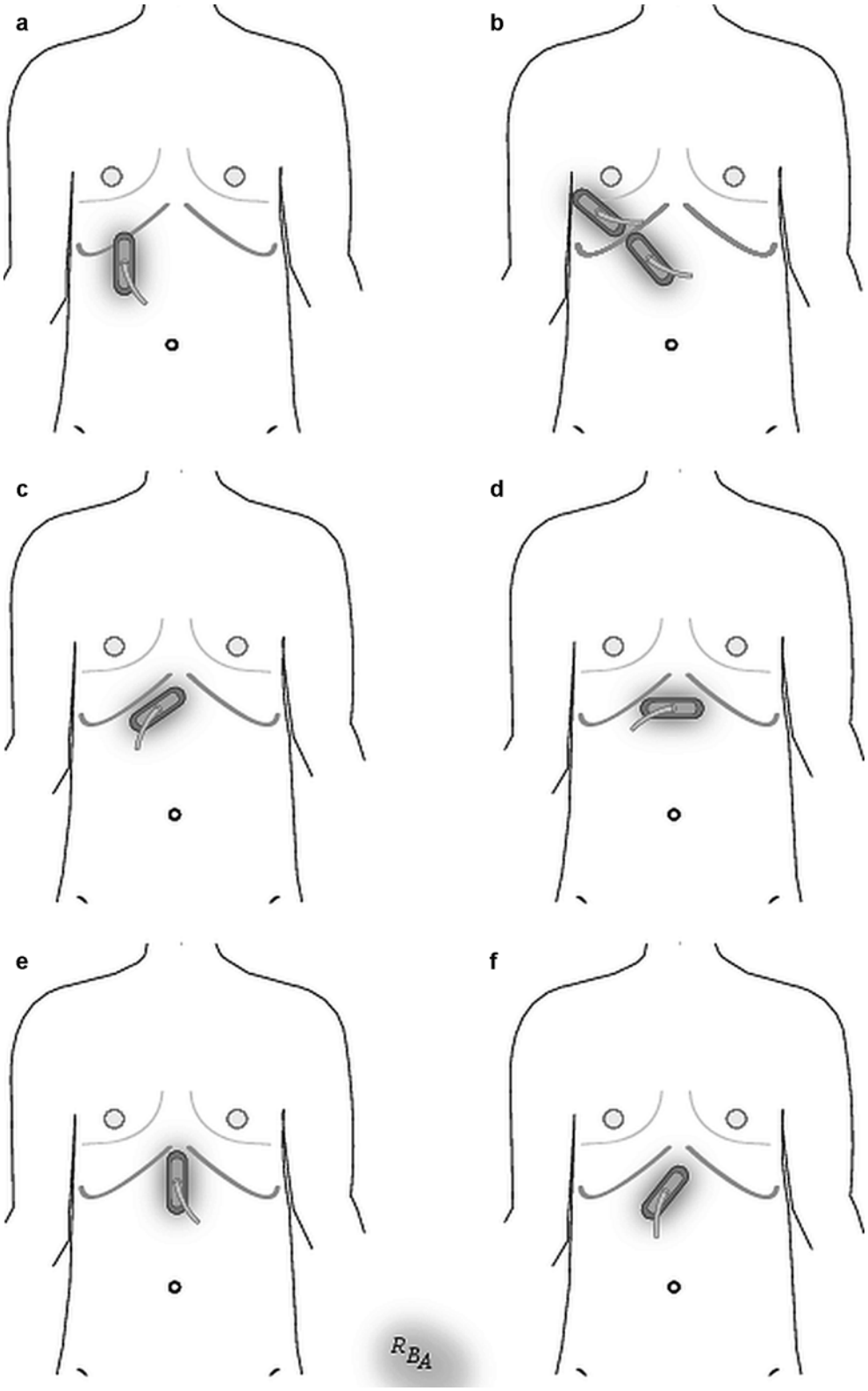

Fig. 4.11 Standard transducer positions for transabdominal biliary imaging. (**a**) The probe is positioned sagittally in the right subcostal, midaxillary position to view the gallbladder. (**b**) Right intercostal space, oblique position allows gallbladder, right intrahepatic duct, and right portal triad imaging. Right epigastric, oblique position allows viewing of the proximal extrahepatic porta hepatis. (**c**) Right subcostal, oblique position shows the right and left hepatic ducts. (**d**) Subxiphoid transverse position shows the left lateral section bile ducts. (**e**) Subxiphoid midline, or right paramedian, sagittal position allows imaging of the mid to distal extrahepatic bile ducts. (**f**) The distal-most portion of the common bile duct is seen from a left oblique upper abdominal position (Adapted from [1])

midline position. The pancreas is identified by first finding the vertebral body, aorta, vena cava, and the splenic vein junction with the superior mesenteric vein. The pancreas can be inferred by its relationship to these structures. Figure 4.13 shows the prototypical image used to identify the pancreas. Once the neck and body are seen, the remaining portions of the gland are examined in the transverse plane and then the longitudinal plane.

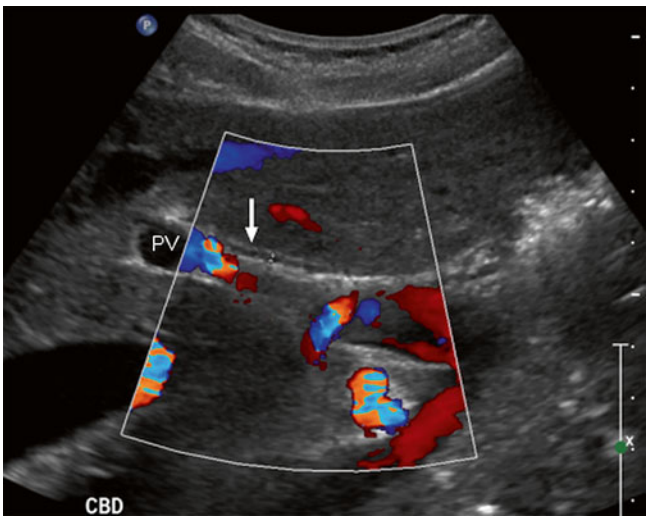

Fig. 4.12 Transabdominal ultrasound of the extrahepatic bile duct. The probe is positioned in the sagittal plane. The bile duct (*white arrow*) lies anterior to the portal vein (*PV*). Color Doppler is helpful to distinguish vascular structures from the bile duct

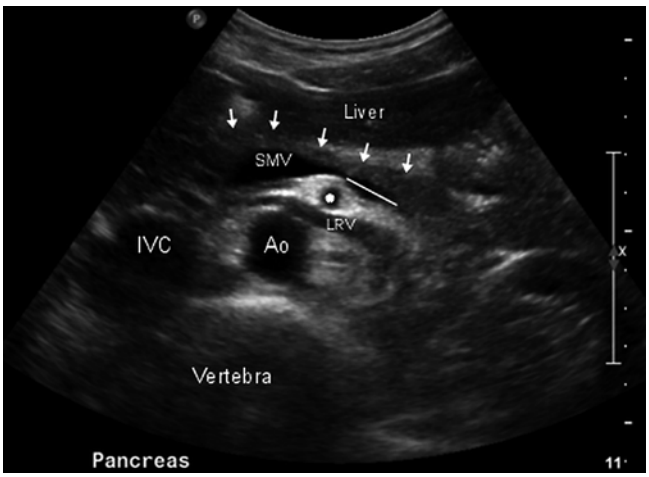

Fig. 4.13 Transabdominal ultrasound of the pancreas. The transducer is placed in the transverse plane in the midline just inferior to the xiphoid. This is the prototypical image of the vasculature surrounding the pancreas that facilitates its identification. The anterior border of the pancreas is denoted by the *white arrows*. The pancreas lies just anterior to the superior mesenteric vein (*SMV*) and the splenic vein (*white line*). Other vascular structures that comprise this prototypical image include the aorta (*Ao*), the inferior vena cava (*IVC*), and the superior mesenteric artery (*). The left renal vein (*LRV*) also can be seen

Open Intraoperative Ultrasound

Intraoperative ultrasound has become an indispensable part of abdominal surgery. It is a critical tool to evaluate and manage hepatic, biliary, and pancreatic diseases. IOUS has the advantage of being the only real-time, intraoperative imaging technique available in the operating room. Finally, it can be reused repeatedly throughout a procedure to reevaluate and guide the operation.

The ultrasound machine and monitor are placed on the side of the table opposite the ultrasonographer. Choosing the appropriate transducer type and frequency is determined by the nature of the examination and the target organ. If the transducer is sterilized, no cover is necessary and direct scanning without an acoustic interface is done. If a nonsterile transducer is covered by a sterile cover, gel must be placed into the cover around the probe to insure adequate coupling. IOUS, like TAUS, uses contact and standoff scanning techniques and similar probe movement and manipulation to obtain images. Unlike TAUS, IOUS scanning planes are in relationship to the organ being scanned, not the body, thus differing in some instances to conventional TAUS planes.

Liver Scanning Technique

A flat, side-viewing, linear array transducer is favored for liver scanning. The long footprint allows efficient imaging of the whole organ and gives a rectangular image of the underlying structures (Fig. 4.14). Images in this configuration make interventions, such as needle biopsy, relatively easier compared to a curvilinear array. The probe's low profile allows easy access in limited working spaces between the liver, abdominal wall, and diaphragm. While current probes are multifrequency, scanning in the 7.5 MHz range has the most utility for liver IOUS. This frequency allows adequate penetration to view the whole organ while showing the very fine detail of intrahepatic structures. A lower frequency, 5 MHz, may be necessary for a larger, steatotic, or cirrhotic liver since this frequency results in deeper sound penetration to examine the depths of the parenchyma in these organs.

Similar to TAUS, a critical component for successful IOUS is developing a systematic scanning approach for the liver. Fastidious adherence to this system insures an adequate and thorough evaluation every time an examination is performed. The first step of this approach is identifying the segmental anatomy. Once each segment is mapped, an evaluation for known and occult lesions is undertaken, noting their location and relationship to the segmental anatomy and intrahepatic structures.

Hepatic IOUS begins with contact scanning (Fig. 4.15, position A). Moistening the liver's surface with saline is sufficient to create coupling. The probe is placed in direct contact with the liver; knowing its exact position on the organ is an advantage of IOUS, making image interpretation easier. Contact scanning is useful for imaging most of the liver; however, it is of limited utility when a mass or structure is within 5–10 mm of the probe (Fig. 4.16). Thus, superficial areas directly beneath the probe represent a "blind spot" during

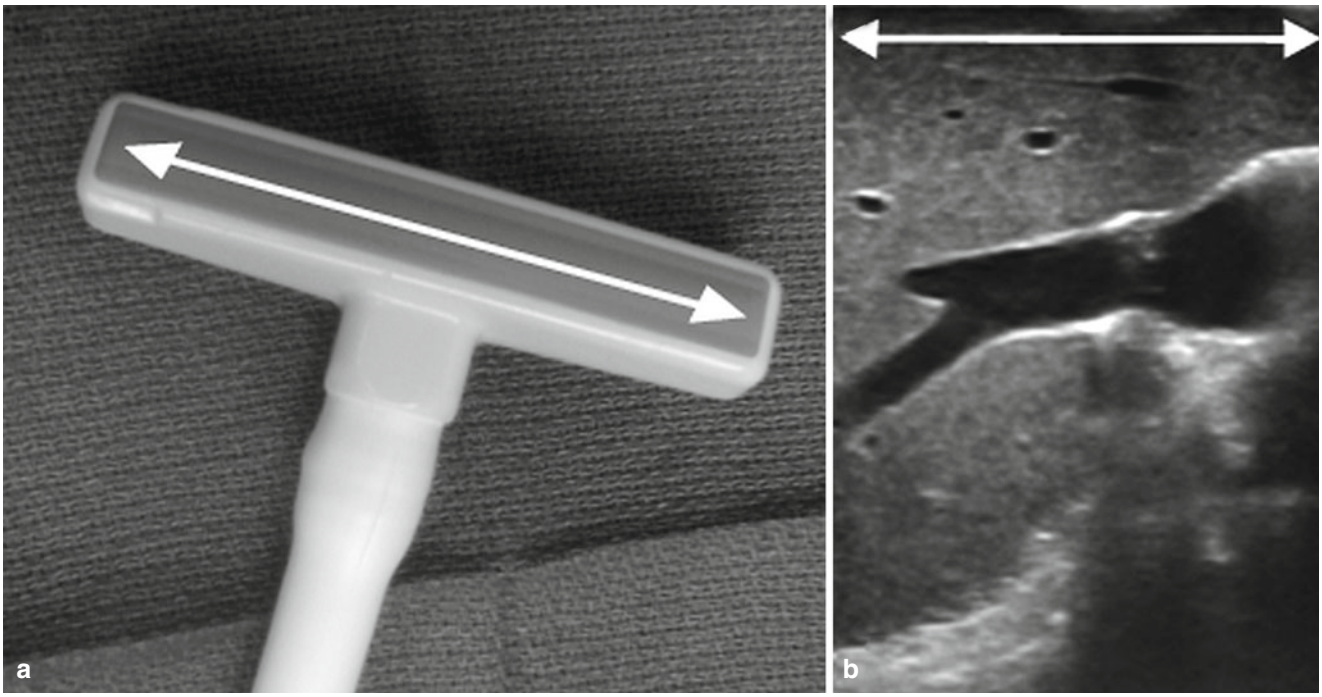

Fig. 4.14 (**a**) Intraoperative linear array transducer. This probe has a relatively large "footprint" due to its long crystal array (*white arrow*). (**b**) This results in a long, rectangular image

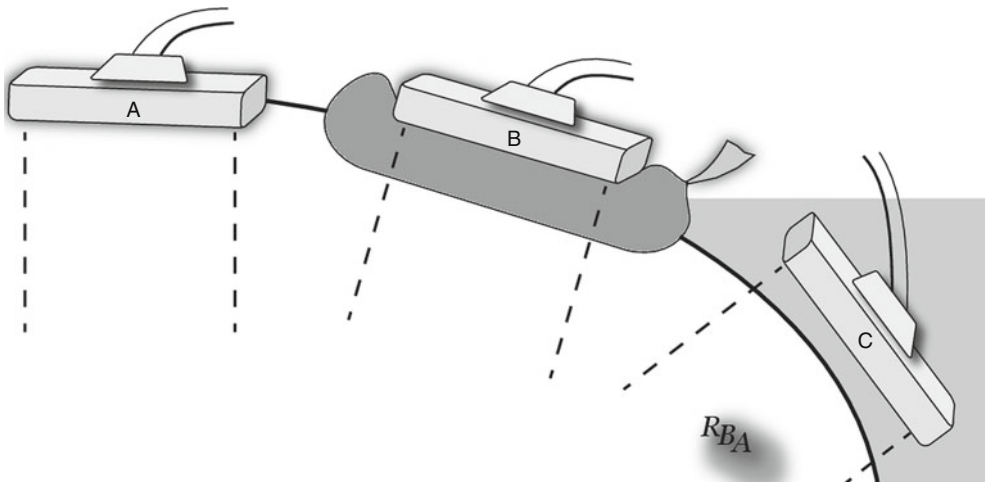

Fig. 4.15 Probe placement for intraoperative ultrasonography. (*A*) Contact scanning places the transducer directly in contact with the organ's surface. (*B*) Probe standoff scanning using a saline-filled glove. (*C*) Probe standoff scanning using saline (*gray area*) immersion. Probe standoff techniques hold the transducer away from the organ surface to allow imaging of superficial structures

contact scanning. Similarly, irregular surfaces (e.g., cirrhosis) make scanning difficult, leading to poor image quality. It is these circumstances when a probe standoff technique for scanning is of use (Fig. 4.15, positions B and C). Saline is an effective interface to establish an acoustic window between the probe and the surface of the liver for a probe standoff technique. With the transducer separated from the liver surface, superficial structures or the irregular surface are seen with better clarity and resolution than during contact scanning. Probe standoff scanning can be done in several ways as illustrated in Fig. 4.15. The difficulty with image resolution of superficial lesions by IOUS emphasizes the importance of combining inspection and palpation when examining abdominal organs, since these techniques are complementary to IOUS. Each of these examination methods should be used to insure complete evaluation of the liver.

The liver examination begins with transverse scanning followed by, longitudinal and oblique views (Fig. 4.17). Together, images in these planes define intrahepatic structures and verify lesions by demonstrating their presence in two or more dimensions. Rotating the probe over a fixed point allows examination of the underlying structure in several planes, a quick but important way to insure the object of interest is not an artifact (Fig. 4.18). A wider field of view is achieved by rocking or tilting the transducer without sliding it in relationship to the contact point. This allows delineation

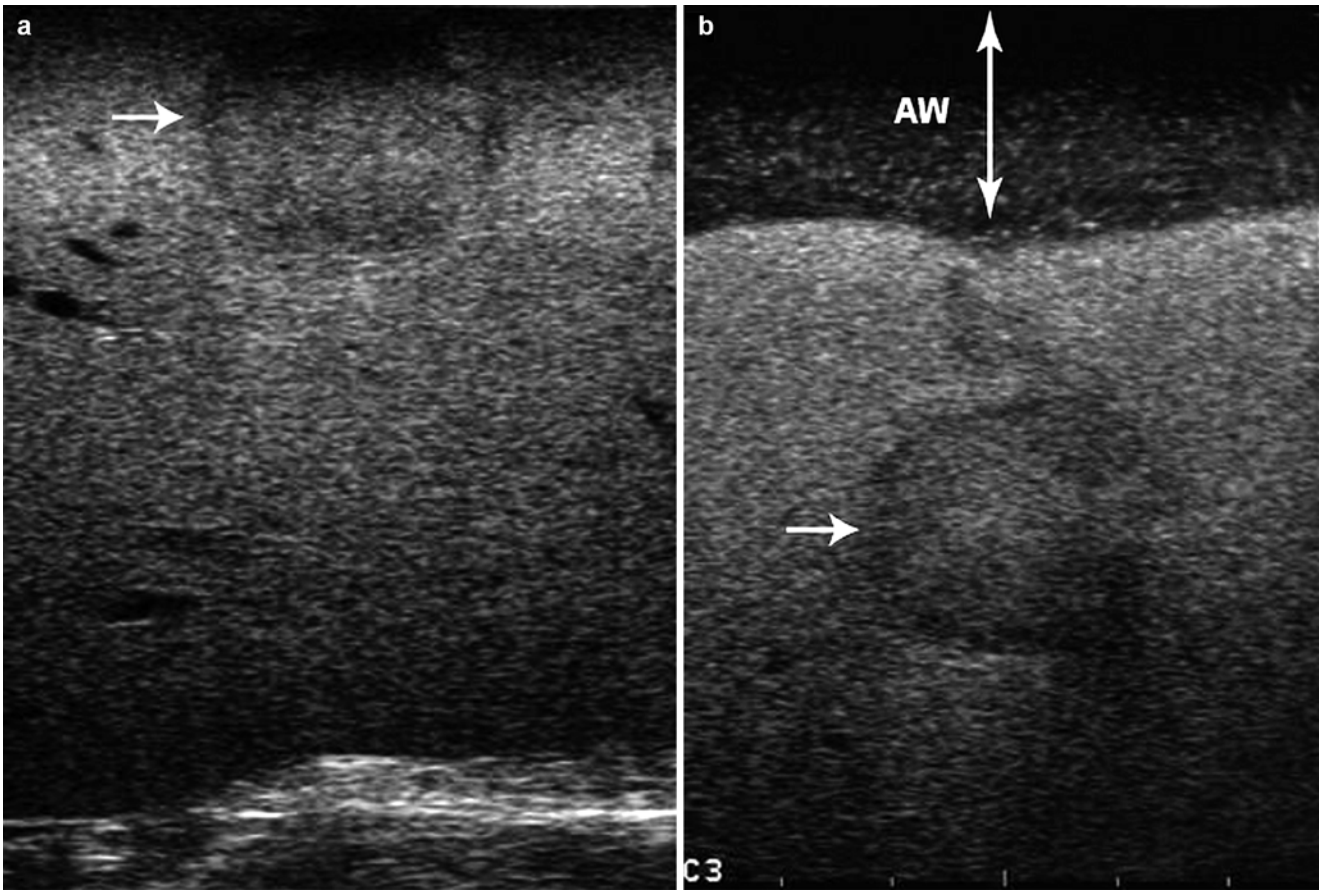

Fig. 4.16 Intraoperative imaging of a superficial liver mass (*white arrow*). (**a**) Contact scanning. (**b**) Probe standoff scanning using saline immersion allows a view of the entire mass, which cannot be seen in the contact scanning view. The saline provides the acoustic window (*AW*) for adequate viewing

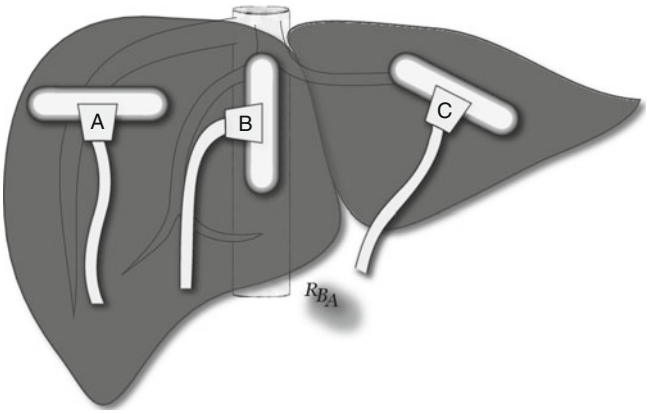

Fig. 4.17 Standard intraoperative transducer positions for liver scanning. (*A*) Transverse. (*B*) Longitudinal. (*C*) Oblique

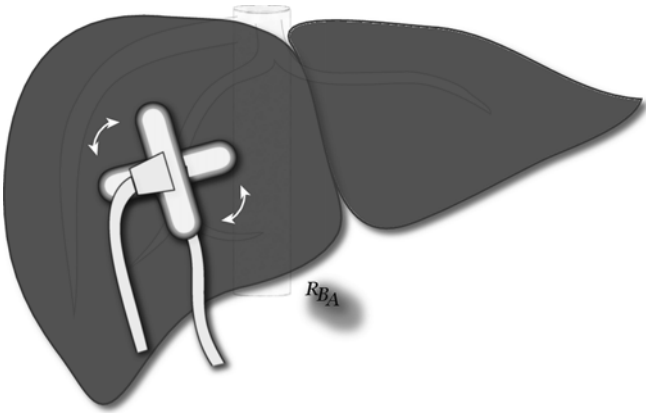

Fig. 4.18 Rotational transducer movement. The probe is rotated clockwise or counterclockwise on a fixed point. This allows examination of a structure or mass in two planes

of the relationship between structures in close proximity (Fig. 4.19). Rocking and tilting, when combined with saline immersion, allow superb views of the superior hepatic segments (Fig. 4.20).

Table 4.5 shows the steps for a systematic approach to liver scanning. The initial scanning is done without mobilizing the liver. This usually is sufficient for a screening examination. If resection or other intervention is planned, scanning before mobilization avoids artifacts, such as air, that may obscure the field of vision. A complete scan is repeated after mobilizing the liver. The primary goals of

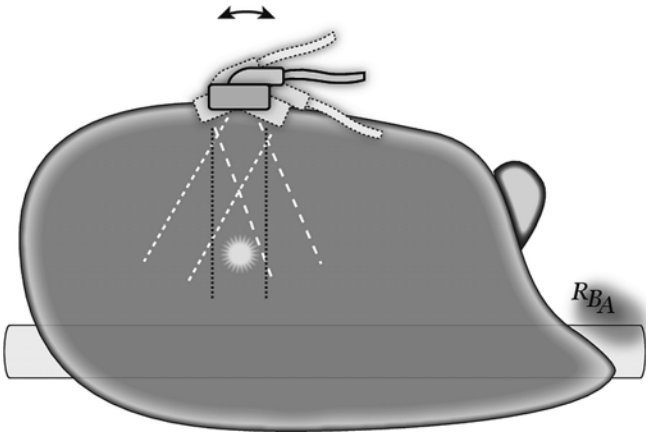

Fig. 4.19 Rocking/tilting transducer movement. The probe is "rocked" or "tilted" at a fixed point on the organ's surface. This allows examination of a wide area surrounding a structure of interest and prevents the examiner from "getting lost" by moving the probe too much

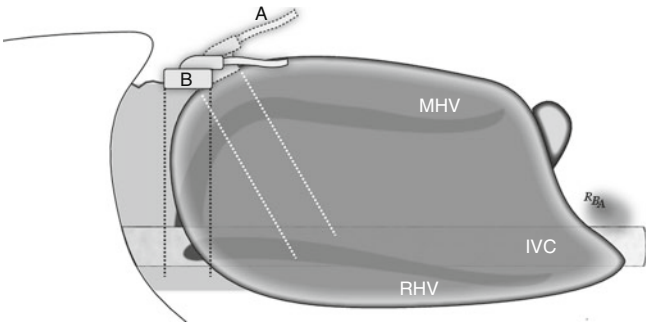

Fig. 4.20 Rocking/tilting combined with saline immersion. This technique allows an excellent view of the superior surface of the liver and its associated structures. (**a**) Contacting scanning along the superior liver gives a view of the central liver and portions of the hepatic veins (*MHV* middle hepatic vein, *RHV* right hepatic vein). However, imaging the junction of the hepatic veins with the inferior vena cava (*IVC*) can be difficult with contact scanning. (**b**) Probe standoff using saline immersion combined with rocking the transducer allows the crystal to be positioned in a way that allows imaging of the junction between the hepatic veins and the IVC

liver IOUS are evaluation of the segmental hepatic anatomy and vasculature and complete, systematic imaging of the parenchyma.

Prior to liver mobilization, initial attention is directed to:

1. Identify intrahepatic vascular anatomy. Segmental hepatic anatomy is defined by the hepatic veins and portal pedicles; these should be mapped first. They define the surgical anatomy of the liver.
   (a) Identify the junction of the major hepatic veins with the vena cava at the superior border of the liver. Follow each vein out to its terminal branches. The hepatic veins lie between sections of the liver [2]. Identify any anomalous hepatic veins, which are quite common. Identify any tumor involvement of the veins.
   (b) Identify the portal vein branches from the distal main portal vein to its bifurcation into the right and left branches and follow them out to their terminal branches. Again, vascular or biliary tract involvement by tumors should be identified.
2. Scan the entire liver parenchyma in a systematic fashion, identifying any known tumors and noting any occult lesions. Scan the liver in several planes and from various directions, including from the inferior and posterior surfaces, to fully evaluate any masses.
3. Establish the relationship between the portal and hepatic veins and any masses or anomalies. Multi-planar scanning allows construction of a three-dimensional mental model of the identified lesions and an understanding of their exact segmental locations and relationships to intrahepatic structures.

If the procedure requires liver mobilization, complete this and repeat the examination focusing on the following:

1. Repeat the systematic scan outlined above, but focus additional time on segment 7 (posterosuperior segment) and deeper portions of the liver that might not have been adequately seen on the initial survey prior to liver mobilization. Scan from the posterior and inferior surfaces of the liver if necessary.
2. Confirm the spatial relationship between identified lesions and the anatomic segments. Reassess the relationship or involvement of local vessels to any lesions. It is particularly important to develop a three-dimensional mental image of these relationships to understand how the anatomic relationships may appear different by IOUS when the liver's position is changed during resection or other interventions.

Table 4.5 Stepwise approach to liver scanning: intraoperative

Scan liver
Before mobilization
Repeat scan after liver mobilization
Contact scanning
Saline immersion probe standoff as necessary
Scan from inferior and posterior surfaces as necessary
Identify hepatic veins
Find junction with vena cava
Follow to terminal branches
Identify anomalous branches
Follow vena cava from hepatic vein branches to inferior liver
Identify portal branches
Find bifurcation, main, right, left portal veins
Follow right and left veins to their segmental branches
Systemic parenchymal scan
Develop a standard scanning approach
Examine all the parenchyma
Note lesion location, size, and features
Identify any vasculobiliary involvement or thrombosis

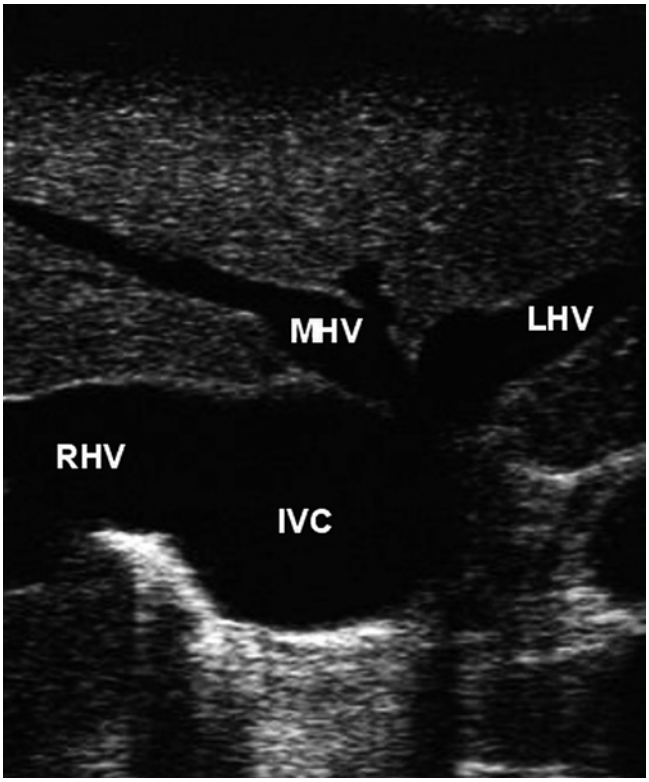

Fig. 4.21 Intraoperative ultrasound, transverse plane. This is the prototypical image seen at the superior border of the liver. The middle (*MHV*) and left (*LHV*) hepatic veins usually join to form a common trunk prior to joining the inferior vena cava (*IVC*). This has the appearance of "rabbit ears" and is a standard image that is helpful for orienting oneself during liver ultrasound. The right hepatic vein (*RHV*) is usually seen joining the vena cava in the same image

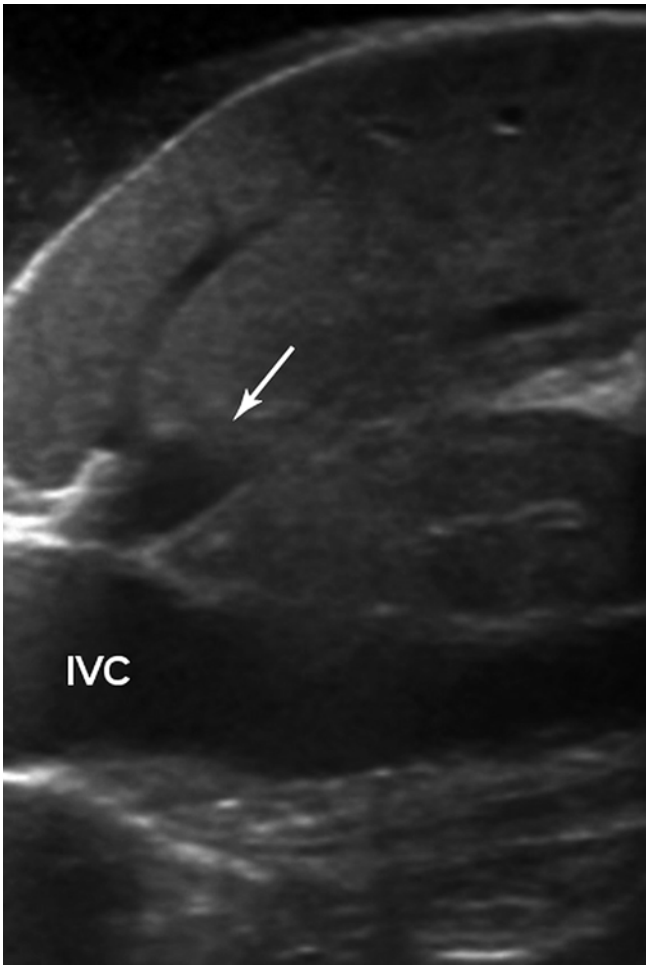

Fig. 4.22 Intraoperative ultrasound, longitudinal (sagittal) plane. The inferior vena cava (*IVC*) can be followed along its entire course in this plane. The middle hepatic vein (*white arrow*) is seen joining the vena cava

Begin contact scanning on the anterior liver surface and start the scan by identifying the intrahepatic vasculature. Find the junction of the three hepatic veins with the vena cava at the superior most portion of the liver by placing the probe over the upper portion of the falciform ligament. This gives a prototypical image of "rabbit ears" and is a fairly constant imaging feature that easily helps one get oriented at the beginning of the scan (Fig. 4.21). Once this image is obtained, each hepatic vein is followed peripherally to its terminal branches. Light contact scanning is necessary, as too much compression will cause the veins to collapse and they will not be visible. Next, reevaluate each vein in the longitudinal (sagittal) plane. In a similar way, the retrohepatic vena cava can be examined along its full length (Fig. 4.22).

A typical view of the hepatic hilum is acquired by contact scanning along the inferior aspect of the liver to the patient's right of the falciform ligament in the transverse plane (Fig. 4.23). The bifurcation of the portal vein is seen just distal to the termination of the main portal vein, allowing scanning of the right portal vein. It is followed peripherally to its division into the anterior (segments 5 and 8) and posterior (segments 6 and 7) sectorial branches (Fig. 4.24). Once the sectorial branches are seen, each can be followed to its superior and inferior segmental branches. In this fashion, the entire inflow to the right liver is mapped. Next, go back to the portal bifurcation view and follow the transverse portion of the left portal vein to the base of the umbilical fissure. At this point, the left portal vein travels anteriorly and inferiorly in the umbilical fissure. At this site, the left portal vein has the appearance of a tree trunk with branches coming off of the main trunk to its left and right (Fig. 4.25). Branches passing to the right of the umbilical fissure supply the medial section of the left liver (segment 4), while those traveling to the patient's left of the umbilical fissure supply the lateral section of the left liver (segments 2 and 3).

Completion of this portion of the study allows full delineation of the segmental anatomy of the liver and the intrahepatic vasculature. The systemic survey of the hepatic parenchyma follows next, seeking evaluation for diffuse and focal abnormalities, in particular mass lesions. Note the location of each previously known hepatic mass, as well as

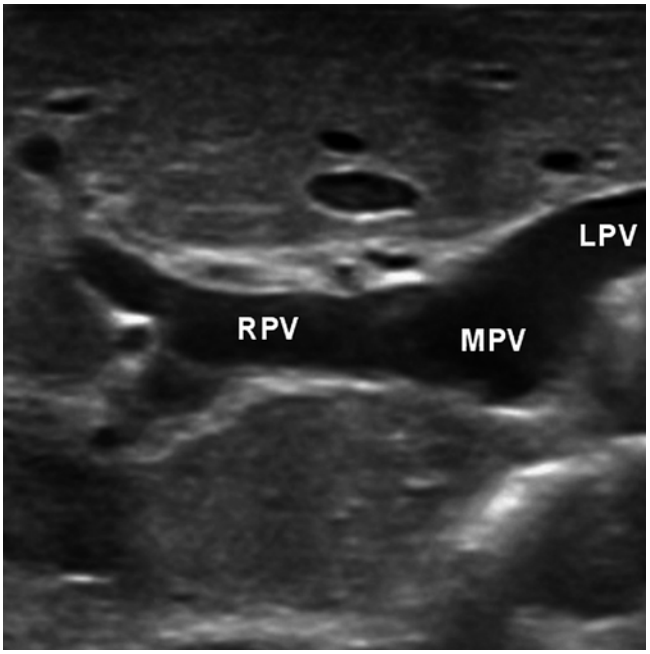

Fig. 4.23 Intraoperative ultrasound, transverse plane. View of the hepatic hilum through the anterior liver shows the main (*MPV*) portal vein as it branches into the right (*RPV*) and left (*LPV*) portal veins

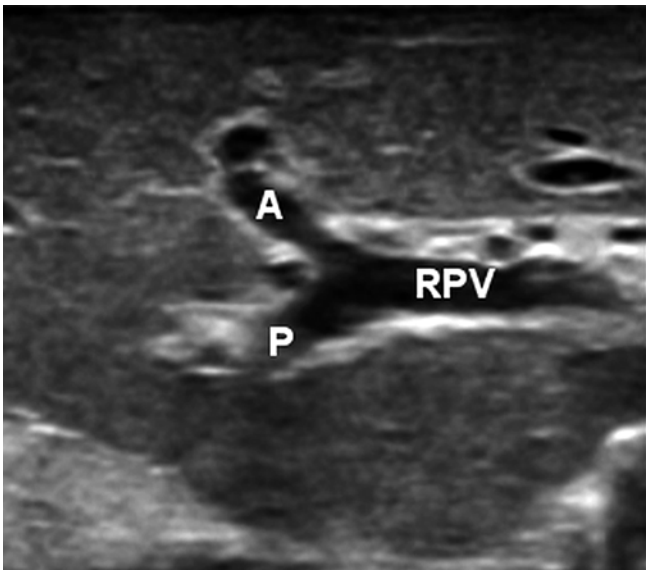

Fig. 4.24 Intraoperative ultrasound, transverse plane. View of the right portal vein (*RPV*) as it branches into its anterior (*A*) and posterior (*P*) sectorial branches

new, occult lesions found during the survey. Contact scanning should be done from the anterior and diaphragmatic surfaces of the liver. Again, develop a systematic approach that is used in every case to insure scanning of all segments of the liver. Finish the survey by scanning in the longitudinal plane. Alternative techniques may be necessary for complete scanning of segment 7 including a probe standoff technique or contact scanning from the posterior surface to see the entire segment. If the posterior sector is too deep to scan from the anterior surface, posterior contact scanning will allow adequate images. Finally, direct scanning of segment 1 may provide better images.

Strict adherence to this systematic approach for liver scanning will allow attainment of the goals outlined at the beginning of this section. A detailed knowledge of intrahepatic anatomy couple with these techniques will allow accurate localization of any structure or mass within the liver. This will facilitate intraoperative diagnosis of hepatic pathology and decision-making regarding the appropriate therapeutic approach.

Biliary Scanning Technique

Optimal biliary scanning often is best achieved using two different probes. Similar to hepatic scanning, a flat, side-viewing, linear array transducer is most useful for contact scanning of the gallbladder or extrahepatic bile ducts using the liver as the acoustic window or for imaging the intrahepatic bile ducts (Fig. 4.26). The gallbladder also can be scanned directly using a probe standoff technique, scanning the gallbladder from its inferior surface after filling the subhepatic fossa with saline. After scanning the gallbladder (Fig. 4.27a), the probe is slid toward the inferior edge of the liver, allowing a view of the hilar structures at the hepatic plate (Fig. 4.27b). Scanning further inferiorly gives transverse (cross-sectional) images of the hepatoduodenal ligament (Fig. 4.27c).

Scanning the extrahepatic bile ducts is best done with an end-viewing transducer at a frequency higher than 7.5 MHz. Table 4.6 shows a standardized technique for biliary scanning. Initial scanning should occur prior to any dissection of the gallbladder or hepatoduodenal ligament; this avoids introducing artifacts from the dissection. Likewise, if cholangiography is anticipated, ultrasonography is done prior to this. When learning biliary scanning, IOUS followed by cholangiography is an excellent way to compare the ultrasound findings to an accepted standard until you are comfortable performing and interpreting biliary IOUS images.

While contact scanning directly along the hepatoduodenal ligament may give adequate images if sufficient adipose surrounds the duct, the best views often are attained using a probe standoff technique following saline immersion of the ligament (Fig. 4.28). The longitudinal view (Figs. 4.29A and 4.30a) of the bile duct is the most useful, but transverse scanning (Fig. 4.29B, C) should be a part of the study. The supraduodenal bile duct can be examined from the hepatic plate to the superior edge of the duodenum or head of the pancreas using the standoff approach. Adequate images at the hilar plate may require probe angulation to fully examine the duct

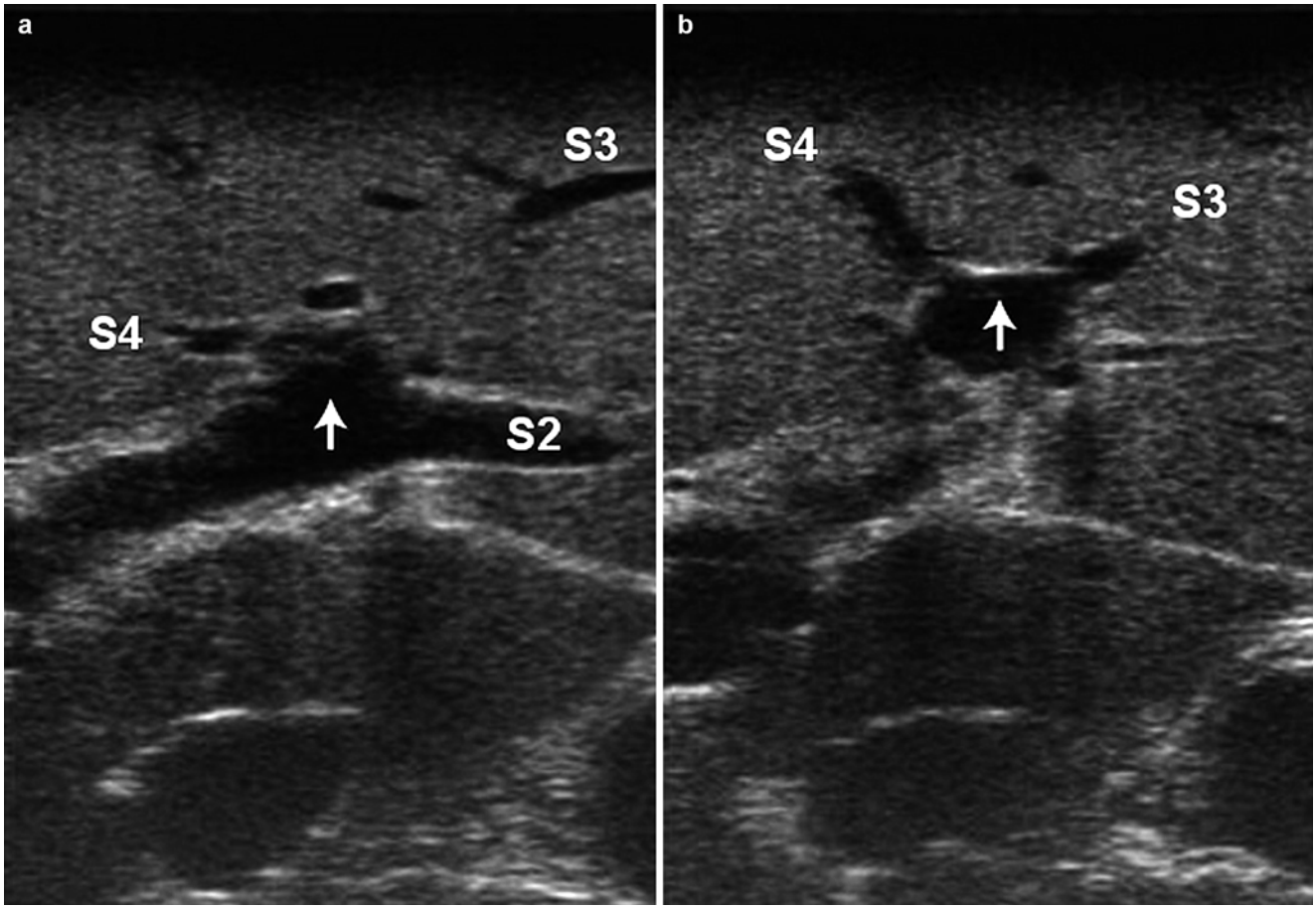

Fig. 4.25 Intraoperative ultrasound, transverse plane. View of the left portal vein (*white arrow*) and its segmental branches to segments 4 (*S4*), 3 (*S3*), and 2 (*S2*). The left portal vein and its branches often have a prototypical configuration, showing an image similar to a tree trunk with branches or a "dancing figure" with arms and legs. (**a**) View at the base of the umbilical fissure. (**b**) View further distal (more peripherally) from the umbilical fissure toward the ligamentum teres

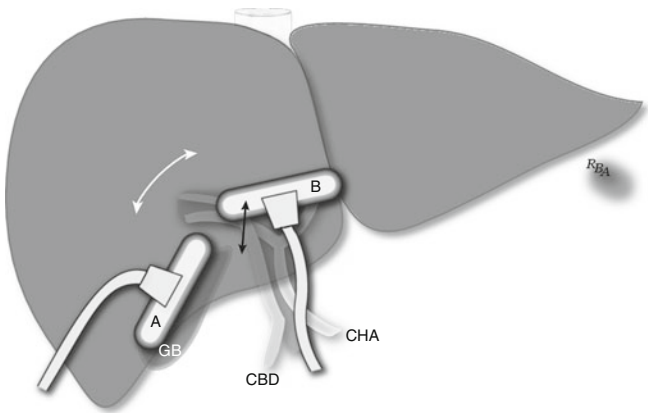

Fig. 4.26 Intraoperative biliary scanning. The gallbladder (*GB*) can be imaged using the liver as an acoustic window. The intrahepatic and proximal extrahepatic bile ducts (*CBD*) can be imaged similarly through the liver. The transducer can be oriented to show longitudinal (*A*) or transverse (*B*) images of these structures. Probe movement includes sliding (*black arrow*) or rotation (*white arrow*). Common hepatic artery (*CHA*)

at this site. The examination of the posterior duodenal and intrapancreatic bile duct requires use of compression scanning (Figs. 4.29C and 4.30b). Placement of the transducer on the anterior surface of the first portion of the duodenum followed by gentle compression will displace any duodenal air, giving a view of the bile duct. If the intrapancreatic portion is not visible from this position, move the probe over the pancreatic head, scanning through the pancreas itself. If the duct is not adequately seen with these techniques, standoff or compression scanning from a lateral (through the duodenum) or posterior approach after performing a Kocher maneuver to mobilize the duodenum and pancreatic head may provide better images. The junction of the bile duct with the duodenum is difficult to see unless the duct is dilated to the level of the ampulla or a stone is present in the very distal duct. Distinguishing between small bile ducts and vessels, particularly at the hepatic hilum can be difficult. Using color Doppler for this is very helpful in differentiating between these structures.

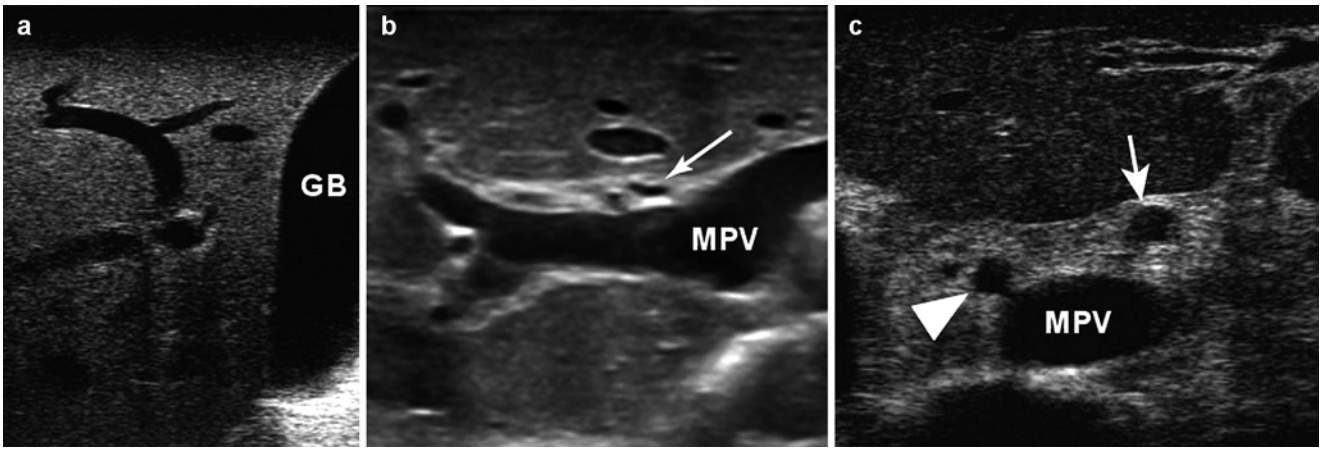

Fig. 4.27 (**a**) Longitudinal image of the gallbladder (*GB*) at the inferior edge of the liver. (**b**) Transverse view of the hepatic hilum. The *white arrow* points to the junction of the right and left hepatic ducts just proximal to the common hepatic duct. This lies anterior to the main portal vein (*MPV*). (**c**) Sliding the transducer further toward the inferior edge of the liver brings the hepatoduodenal ligament into view, showing the typical "Mickey Mouse" view of the common bile duct (*white arrowhead*), main portal vein (*MPV*), and common hepatic artery (*white arrow*)

Table 4.6 Stepwise approach to biliary scanning: intraoperative/laparoscopic

Scan gallbladder
Contact scanning, transhepatic
Saline immersion probe standoff from inferior surface
Scan extrahepatic bile duct
Contact scanning, transhepatic
Saline immersion probe standoff, transverse and longitudinal planes
Scan intrapancreatic bile duct
Transduodenal compression scanning
Transpancreatic contact/probe standoff scanning

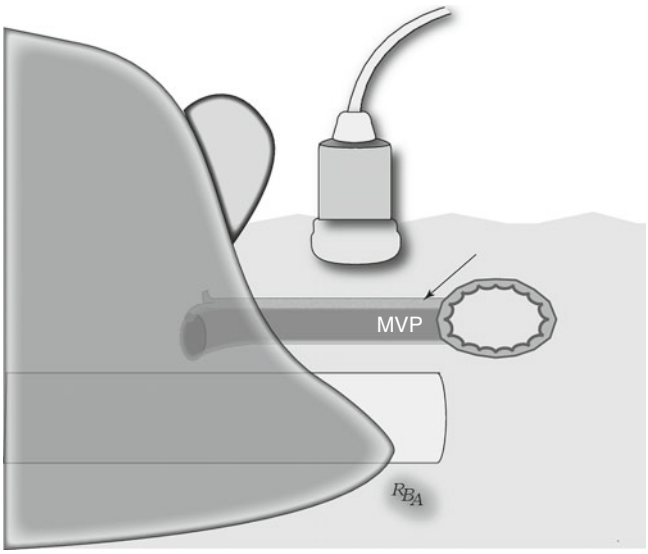

Fig. 4.28 Longitudinal (sagittal) scanning of the hepatoduodenal ligament a probe standoff, saline immersion technique. This allows very detailed images of the common bile duct (*black arrow*), which lies along the anterolateral surface of the main portal vein (*MPV*)

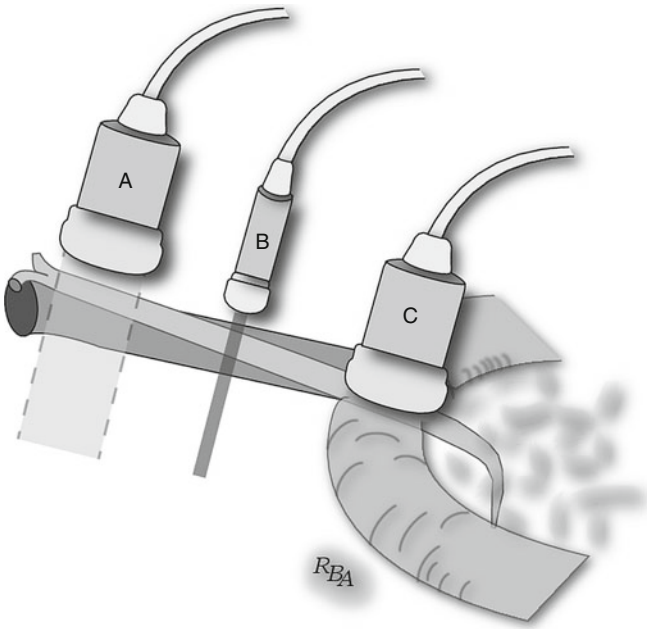

Fig. 4.29 (*A*) Longitudinal scanning of the bile duct during laparotomy. (*B*) Transverse scanning of the bile duct. (*C*) Compression of the duodenum displaces intraluminal air and allows imaging of the retroduodenal and intrapancreatic portions of the common bile duct

Pancreas Scanning Technique

IOUS of the pancreas can be done either with a side- or an end-viewing probe. Prior to any dissection, the gland can be seen by indirect scanning using the duodenum, stomach, gastrohepatic/gastrocolic ligaments, or the transverse mesocolon as an acoustic window (Fig. 4.31). Once the lesser sac is entered, direct contact scanning on the anterior surface of the gland is done. However, like the extrahepatic bile ducts, the

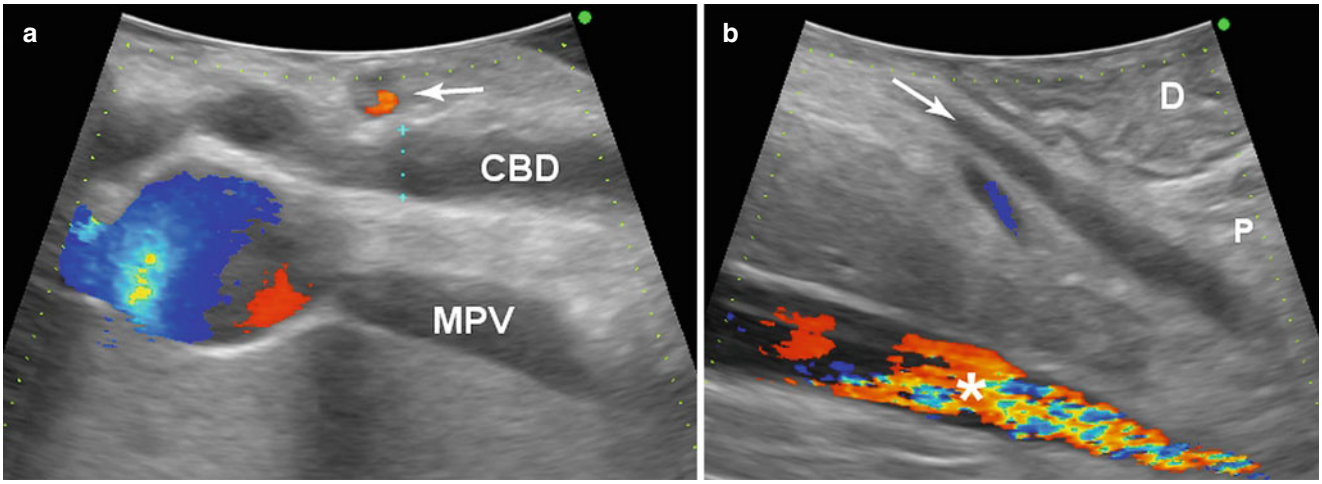

Fig. 4.30 (**a**) Contact scanning of the hepatoduodenal ligament in the longitudinal plane. This patient has aberrant anatomy. There is a right hepatic artery (*white arrow* and a signal on color Doppler) that courses anterior to the common bile duct (*CBD*, no flow signal). The main portal vein (*MPV* and a flow signal) is posterior to the bile duct. (**b**) Compression scanning through the duodenum (*D*) in the longitudinal plane shows the common bile duct (*white arrow*), the superior head of the pancreas (*P*), and the inferior vena cava (* and flow signal)

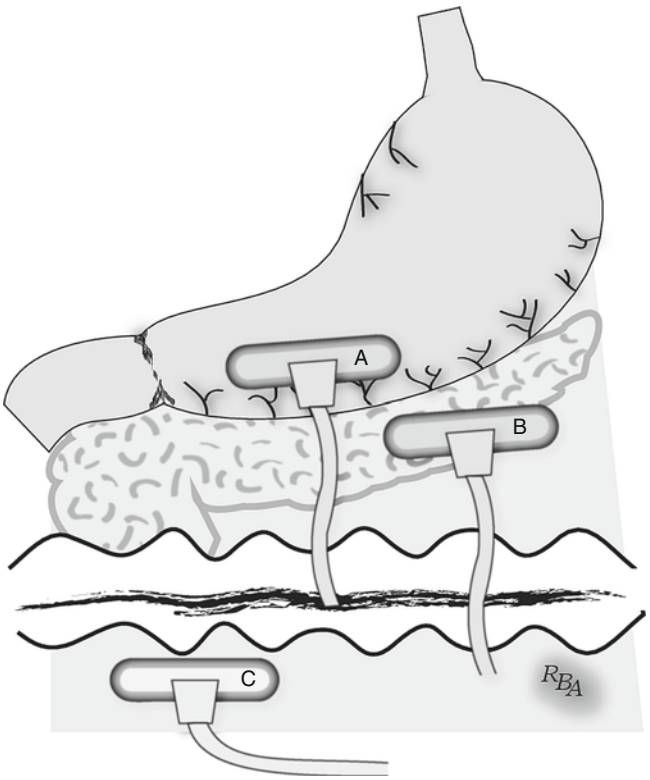

Fig. 4.31 Intraoperative pancreatic scanning. Several acoustic interfaces allow pancreatic imaging without dissection. (*A*) Transgastric. (*B*) Gastrocolic or gastrohepatic ligaments. (*C*) Transverse mesocolon

normal pancreas may be so thin from anterior to posterior that much of the gland immediately beneath the transducer is missed by being in the near field. Consequently, a probe standoff technique often is necessary to examine the entire gland (Fig. 4.32). A saline immersion technique works in most cases if the intent is diagnostic, but if an intervention is planned, a saline-filled glove may be useful to more easily guide a needle for biopsy or duct cannulation, rather than trying to do this while the gland is underwater.

As described for the liver and bile ducts, develop a standardized approach to pancreatic scanning to facilitate complete scanning and employ it every time (Table 4.7). Begin with indirect scanning, followed by direct scanning, if indicated. Longitudinal scanning is most common for the pancreas (Fig. 4.33). The principles are similar to TAUS, much of the pancreatic tissue can be inferred based on identification of surrounding vessels. Find the superior mesenteric or portal vein as it passes posterior to the pancreatic neck and scan the neck, body, and tail of the pancreas (Fig. 4.34). Change the probe to rescan these parts of the gland in the transverse dimension. Repeat these steps after immersing the pancreas in a saline bath. This allows a clear view of superficial structures or a very thin gland that may be lost in the near field during contact scanning. Pay careful attention to the pancreatic duct during the longitudinal portion of the study to identify its relationship to any adjacent lesions (Fig. 4.35). Examine the pancreatic head starting at the portal vein and working toward the patient's right. Much of the approach to scanning the head of the pancreas is similar to that described for examining the distal bile duct in the previous section. Adjacent vessels including the aorta, celiac axis, superior mesenteric artery, gastroduodenal artery, and the corresponding veins are clearly seen; mapping in relationship to masses is easily done with IOUS.

When a mass lesion is present in the pancreas, especially when dealing with neuroendocrine tumors, it is helpful after the initial scan to completely mobilize the gland. This includes Kocher's maneuver and elevating the body/tail out of the retroperitoneum. In this way a combination of

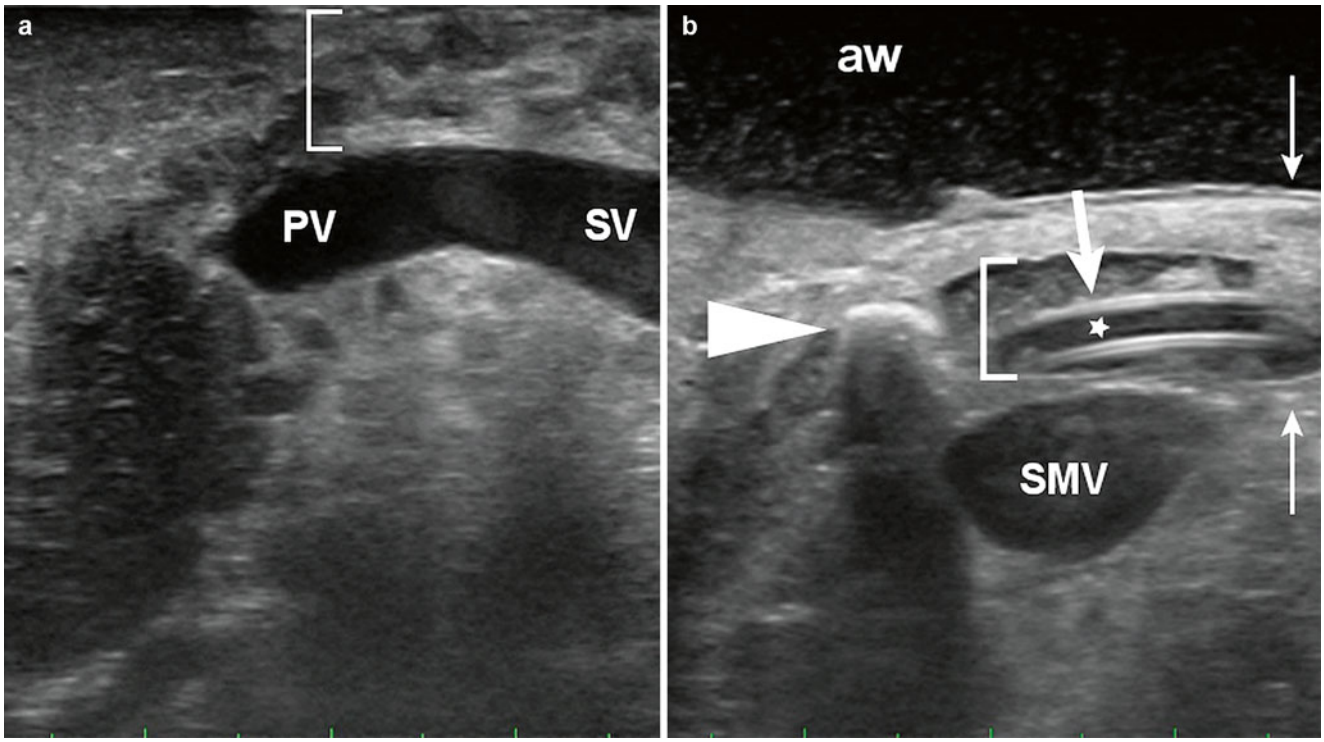

Fig. 4.32 (**a**) Contact scanning shows very little detail in the pancreas due to the thin gland (*white bracket*), which lies anterior to the portal (*PV*) and splenic (*SV*) veins. (**b**) Probe standoff scanning using a saline immersion technique to provide an acoustic window (*aw*) shows the detail missing with contact scanning. This patient has a very dilated pancreatic duct (*white bracket*) due to a pancreatic duct stone (*white arrowhead*) with posterior shadowing. A pancreatic duct stent (*white arrow*, * within the lumen of the stent) is present within the duct. The anterior and posterior surfaces of the gland are shown by the thin white opposing arrows. Superior mesenteric vein (*SMV*)

palpation and IOUS is used to find small tumors. Both contact and standoff scanning may be necessary to identify these small tumors in combination with palpation.

Laparoscopic Ultrasound

Laparoscopic ultrasonography has grown in importance as more procedures have transitioned to a minimally invasive approach. Its use is essential to overcome the lack of tactile feedback during laparoscopic procedures; it supplants the role of palpation that is so important during open surgery to identify specific anatomic structures or mass lesions. LUS can identify critical structures during dissection or screen organs for masses. It is indispensable in guiding resection or ablation procedures during minimally invasive operations since open IOUS or palpation are not feasible.

LUS probes have evolved considerably since their inception. Current probes typically are side-viewing, high-frequency transducers on flexible tip shafts. Most shafts are 10 mm in width allowing introduction through 12 mm trocars. The flexible tip allows much more freedom in scanning areas difficult to reach with the older rigid shaft probes. The relatively long footprint of the current transducers allows imaging of wide areas in an efficient manner. The positions for LUS trocar placement are determined by the type of examination being performed and the organ of interest, as illustrated in the following sections. The most common trocar positions used for LUS are shown in Fig. 4.36.

LUS has many similarities to IOUS in terms of probe placement and manipulation. However, there are some important differences. The first is image display. Placement of the ultrasound machine on one side of the patient or the other is less critical for LUS if a picture-in-picture setup is feasible. If this is not feasible, the ultrasound machine is positioned opposite the surgeon with placement of the ultrasound and laparoscopic monitors next to each other to allow easier coordination of the images. Displaying the ultrasound image on the laparoscopic monitor with both the ultrasound and laparoscopic images visible at the same time facilitates probe movement and LUS image interpretation. This is particularly helpful, allowing one to correlate the probe's position on an organ with the expected ultrasound image, an advantage described earlier that assists in image interpretation. The second difference is probe orientation. The configuration of the transducer on the shaft results in a longitudinal orientation of the probe, and this is often the easiest orientation to obtain images, particularly when a single port in the periumbilical position is used. However, to replicate a similar image to that

Table 4.7 Stepwise approach to pancreas scanning: intraoperative/laparoscopic

Techniques
Indirect scan
Direct scan
Contact
Saline immersion probe standoff
Probe standoff using saline-filled glove if intervention is necessary
Scan pancreatic neck, body, tail
Start in longitudinal plane, contact scanning
Identify portal vein/superior mesenteric vein
Move probe to the patient's left of the vein to scan neck, body, tail
Identify pancreatic duct
Note lesion location, size, and features
Identify any vascular/duct involvement or thrombosis
Repeat scan in the transverse plane
Scan pancreatic head
Start in longitudinal plane, contact scanning
Identify portal vein/superior mesenteric vein
Move probe to the patient's left of the vein to scan head, uncinate
Identify pancreatic duct
Note lesion location, size, and features
Identify any vascular/duct involvement or thrombosis
Repeat scan in the transverse plane
Identify retroduodenal bile duct using transduodenal compression scanning
Saline immersion probe standoff scanning
Repeat scan using probe standoff to view superficial portions of the gland
Mobilize pancreas
Repeat contact and probe standoff scanning after gland mobilization if necessary

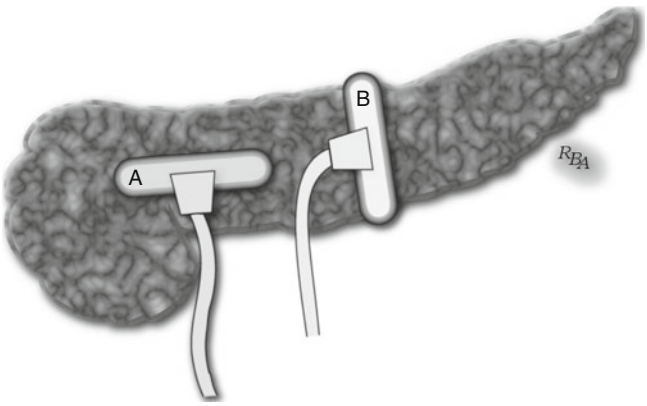

Fig. 4.33 Intraoperative pancreatic scanning. Longitudinal (*A*) and transverse (*B*) scanning of the pancreas

of a side-viewing IOUS probe, which typically is oriented in a transverse position relative to the probe cord, the LUS probe must be oriented likewise (Fig. 4.37a). In addition, because the probe may be changed from one trocar to another to allow complete organ examination, care should

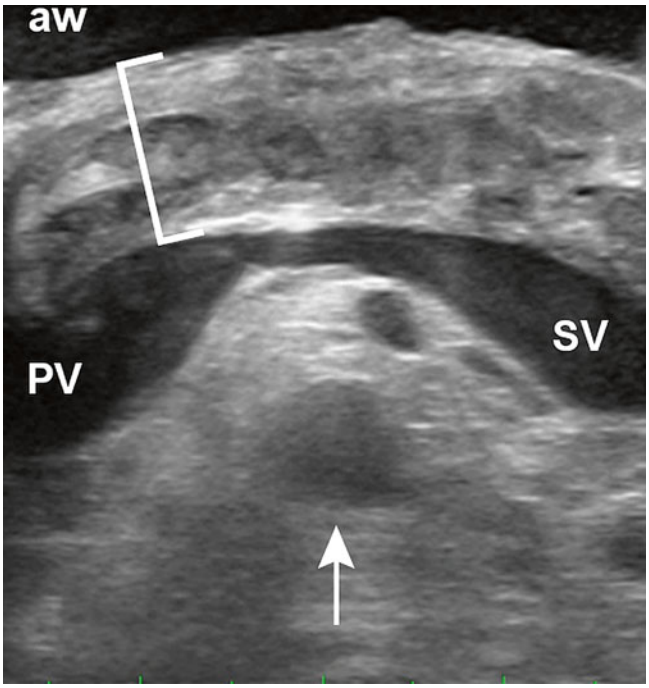

Fig. 4.34 Intraoperative ultrasound of the pancreas. The principles and images are very similar to those for transabdominal pancreatic scanning. The transducer is placed in the longitudinal plane with saline as an acoustic window (*aw*). This gives the prototypical image of the vasculature surrounding the pancreas that facilitates its identification. The pancreas is denoted by the *white bracket*. The pancreas lies just anterior to the portal vein (*PV*) and the splenic vein (*SV*). The superior mesenteric artery (*white arrow*) is seen posterior to the veins

be taken to reorient the image display to insure that the image is viewed in the conventional manner (Fig. 4.37b). This may require image inversion, usually an option button on the machine, which changes the orientation of the image display. Finally, because of the probe configuration (longitudinally on a long shaft), transverse image can be challenging when trying to replicate images traditionally seen by IOUS. Therefore, LUS can have a more difficult learning curve since one must often think in longitudinal images rather than transverse, particularly when imaging the liver. This can be disconcerting until sufficient experience and pattern recognition is gained.

LUS probe movements mimic those in open IOUS, but sliding (Fig. 4.38) and tilting (Fig. 4.39) are the most common. More difficult are rotational maneuvers, which make multi-planar scanning of an area of interest more tedious. Rocking the probe by flexing the tip up or down simulates the open technique (Fig. 4.40). Contact and probe standoff scanning techniques are used, but a probe standoff technique may be even more useful in LUS when imaging the superior aspects of the liver or the extrahepatic bile duct. A probe standoff technique may be particularly effective when combined with the rocking movement.

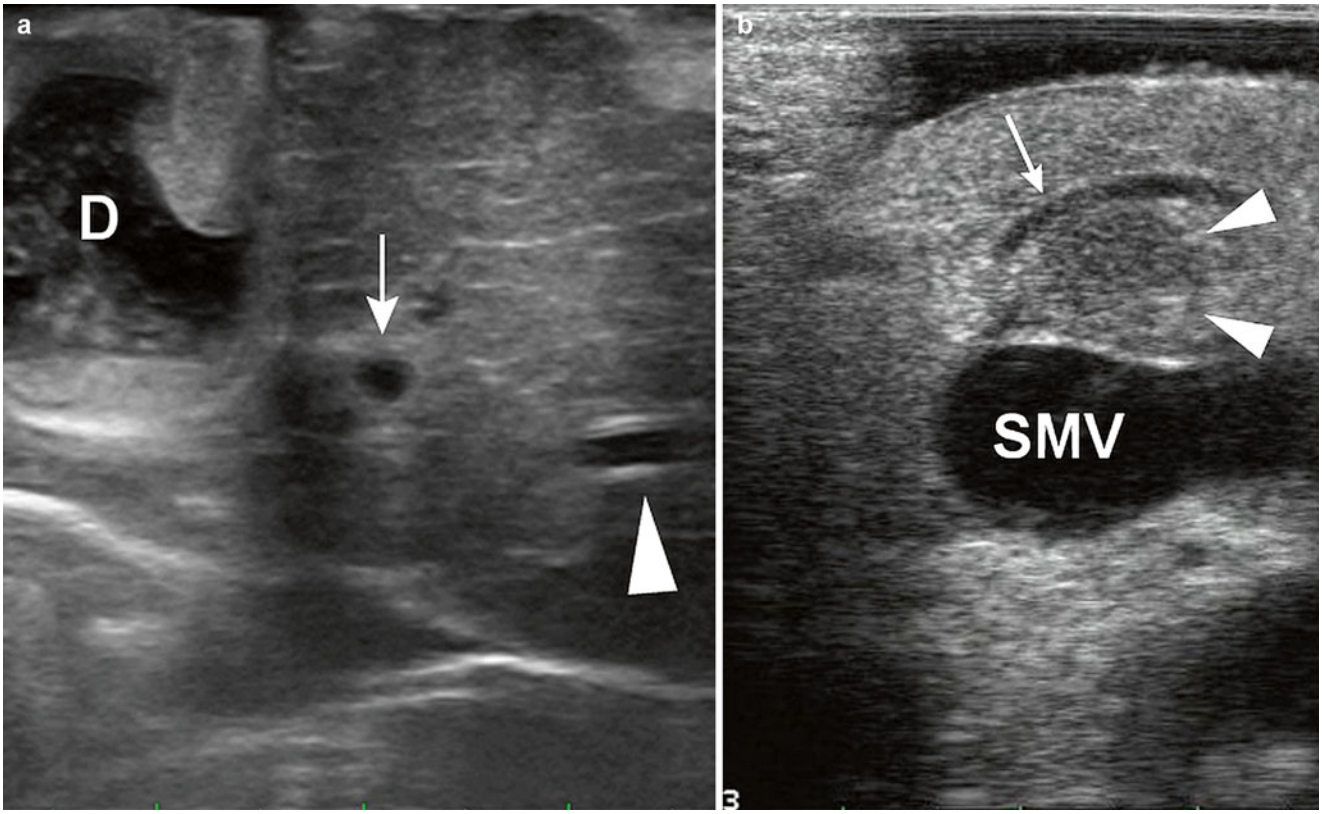

Fig. 4.35 Intraoperative ultrasound, pancreas, longitudinal plane. (**a**) An image through the head of the head of the pancreas shows the duodenum (*D*) just to the right of the pancreatic head. Within the head are a transverse view of the distal common bile duct (*white arrow*) and a longitudinal view of the distal pancreatic duct (*white arrowhead*). (**b**) Longitudinal view at the neck of the pancreas showing the pancreatic duct (*white arrow*) draped over a neuroendocrine tumor (*white arrowheads*). The tumor lies anterior to the superior mesenteric vein (*SMV*)

Liver Scanning Technique

The most useful initial trocar to begin hepatic scanning is one in the right subcostal position. We place a 5 mm trocar initially in the supra-umbilical midline to allow a visual examination of the peritoneal cavity and its contents. Choosing the appropriate distance superior to the umbilicus for trocar placement is based on the patient's body habitus. The simplest way to judge this is to place the tip of the LUS probe approximately at the level of the right nipple and measure the spot where the probe would exit in the midline if it was inserted to its full length. This should allow examination of the superior most portion of the liver when the probe is fully inserted through the trocar. Once the midline trocar is in position and no findings that would preclude the intended procedure are noted, place a right subcostal 12 mm trocar in the line of the intended subcostal incision. Scanning from the right subcostal position offers the closest approximation to a transverse view, although this is more likely to be somewhat oblique in orientation rather than truly transverse. If the liver is not completely visible from this trocar position, the midline trocar is exchanged for a 12 mm one and the LUS probe moved to this position. Remember to reorient the image on the monitor after changing positions. Occasionally, a left subcostal trocar is necessary to allow full examination of the liver. If the falciform ligament impedes probe placement to the other side of the liver, divide a portion of it and pass the probe through to the other side. The choice of which side to place the initial subcostal trocar is determined by the position of the liver as judged from the umbilical port site.

The steps for LUS scanning of the liver are similar to IOUS. A systematic approach is used each time and is the same as that described earlier for IOUS; define the vascular structures, followed by segmental parenchymal scanning. This can be difficult and unsettling, though, to the beginner because the familiar image orientation is more difficult to achieve through the relatively limited mobility allowed by moving a LUS probe through a fixed trocar(s). It is easiest to begin scanning from a trocar placed in the right subcostal position as it affords a view closest to the familiar transverse one (Fig. 4.41a). The transverse images are obtained mainly through sliding movements working from the superior portion of the liver to the inferior edge (Fig. 4.41c, e). The vessels are mapped out using a combination of transverse, oblique, and longitudinal views. Parenchymal scanning is more easily accomplished by scanning in the longitudinal plane

(Fig. 4.41b). With the probe longitudinal on the liver, the shaft is tilted side to side to cover a wide area of parenchyma without moving the probe in relationship to the surface of the liver. Begin parenchymal scanning at the superior border of the liver, tilt (roll) it side to side to view the segment, and then pull the probe toward the inferior edge of the liver and repeat the process (Fig. 4.41d and f). A series of overlapping movements done in this fashion allows complete scanning of the parenchyma. Several areas may pose imaging difficulties: the superior liver, segment 7, and the posterior liver when the liver is enlarged or steatotic. The superior liver is most easily scanned in the longitudinal plane using contact scanning. However, adequate images may require a probe standoff technique to fully view the superior liver and segment 7. When the posterior liver is difficult to see from an anterior position, moving the probe to the inferior liver may give a better view using either a contact or probe standoff technique. For a probe standoff technique, place the patient in the Trendelenburg position and fill the right upper quadrant with saline. As with IOUS, a probe standoff technique facilitates examination of a rough surface or lesions close to the surface of the liver.

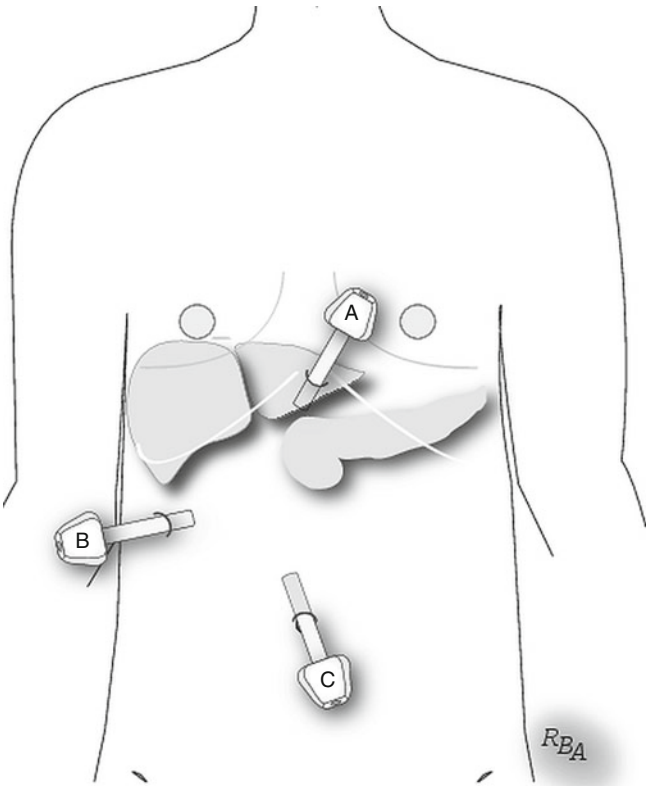

Fig. 4.36 Trocar placement for laparoscopic ultrasonography of upper abdominal organs. Common viewing sites include a subxiphoid port (*A*), a right subcostal port (*B*), and the periumbilical port (*C*)

Biliary Scanning Technique

Optimal biliary scanning is achieved through a two-trocar approach. Scanning is done through the umbilical port and an epigastric/subxiphoid port (Fig. 4.36). Similar to IOUS, LUS of the bile ducts should be done prior to dissection and cholangiography to avoid introducing artifacts. Contact scanning and saline immersion for a probe standoff technique may be necessary to obtain all the necessary images. Color Doppler can be particularly helpful to distinguish vessels from the bile ducts; it should be used liberally during biliary scanning.

Since the laparoscope usually is in the umbilical trocar, begin biliary scanning from the epigastric trocar. This allows transverse scanning of the hepatoduodenal ligament and its

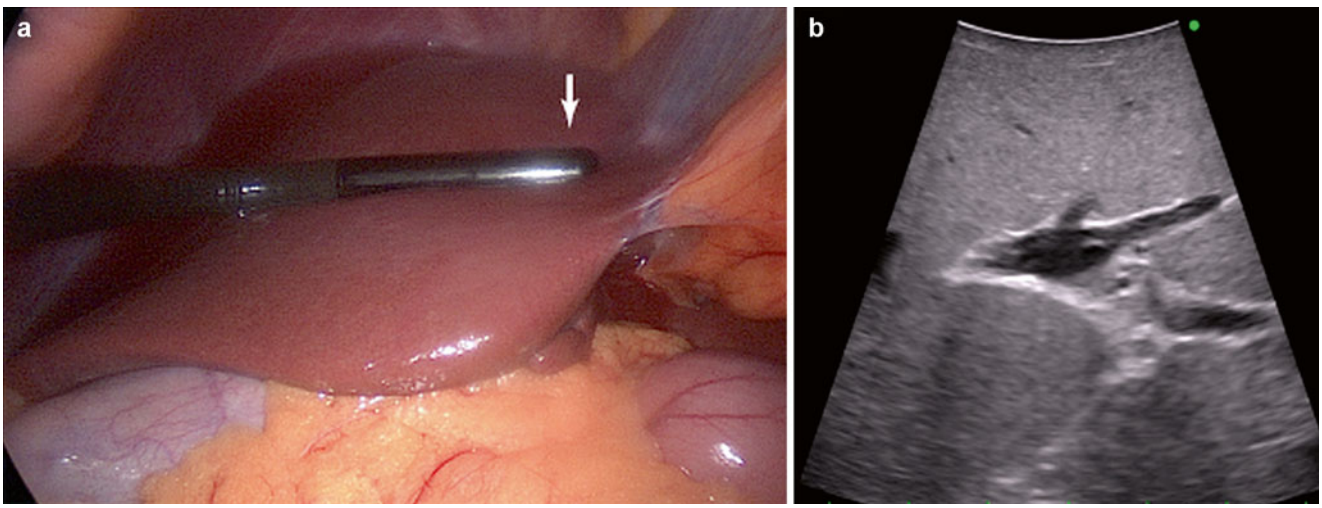

Fig. 4.37 Laparoscopic ultrasound examination of the liver in the transverse plane. (**a**) The probe is placed through the right subcostal port and the tip deflected to orient it transversely. Be sure the tip (*white arrow*) is oriented such that the image on the monitor (**b**) has it on the right side of the screen (*green dot* corresponds to *white arrow* in panel **a**)

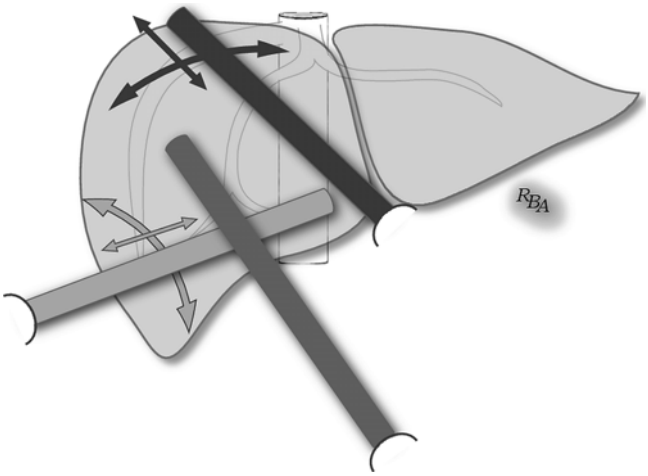

Fig. 4.38 Laparoscopic ultrasound, sliding probe movement for liver scanning. Nearly all the liver can be scanned in the transverse, longitudinal, and oblique planes using a sliding movement through the three standard port sites

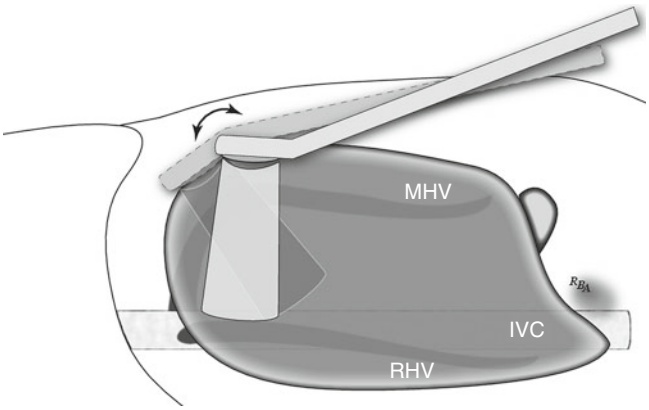

Fig. 4.40 Laparoscopic ultrasound, rocking probe movement for liver scanning. Flexing the tip of the probe up or down simulates the rocking motion of intraoperative ultrasonography. This allows examination of a wide area surrounding a structure of interest using multiple parallel images as the tip is flexed. Tip flexion also allows examination of the superior surface of the liver, something that is very difficult with a rigid probe. *MHV* middle hepatic vein, *RHV* right hepatic vein, *IVC* inferior vena cava

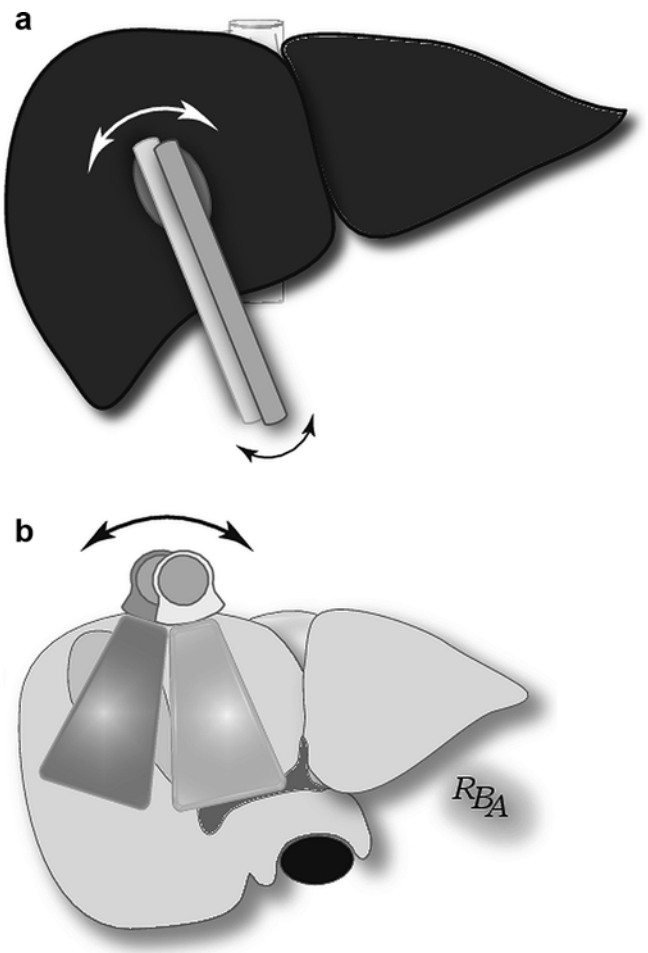

Fig. 4.39 Laparoscopic ultrasound, tilting probe movement for liver scanning. Rotating the ultrasound probe shaft clockwise and counterclockwise tilts the crystal array from side to side and is a very effective technique for scanning large areas of the liver with little movement in relationship to the liver surface. Anterior (**a**) and transverse (**b**) views of probe tilting movement

structures (Figs. 4.42 and 4.43). Grasp the gallbladder and push it cephalad to expose the hepatoduodenal ligament. Scan the gallbladder directly (Fig. 4.43a, b) and slide the probe along the inferior wall of the gallbladder to its junction with the hepatoduodenal ligament (Fig. 4.43c, d). To examine the duct proximal (toward the hilum) to this, rotate the shaft (counterclockwise) so the crystals move toward the hilum. Most, if not all, of the common hepatic duct should be visible with this maneuver. Once this is seen, rotate the shaft back to the neutral position and slide it inferiorly along the lateral side of the hepatoduodenal ligament. If adequate images cannot be obtained with contact scanning, instill saline to allow a probe standoff technique. When scanning directly along the biliary structures, it is important to apply the minimal pressure necessary to achieve coupling. Any pressure more than this will cause collapse of these very pliable structures and render them absent from the image.

As the probe slides from the proximal hepatoduodenal ligament to the inferior end, the structures visible will change. Along the superior portion of the ligament, the common hepatic duct between the right and left hepatic arteries can be seen anterior to the portal vein. As the probe moves inferiorly, the right hepatic artery will be seen passing beneath the common hepatic duct, followed by the characteristic "Mickey Mouse" view with the bile duct and hepatic artery anterior to the portal vein (Fig. 4.43 e, f). Depending on the location of its junction with the common hepatic duct, the cystic duct may be seen sweeping from near the transducer toward the common hepatic duct as the probe is moved inferiorly along the ligament (Fig. 4.43c, d).

After examination of the suprapancreatic portion of the bile duct, shift the focus to the intrapancreatic bile duct. Slide the probe over the duodenum to the anterior pancreatic head

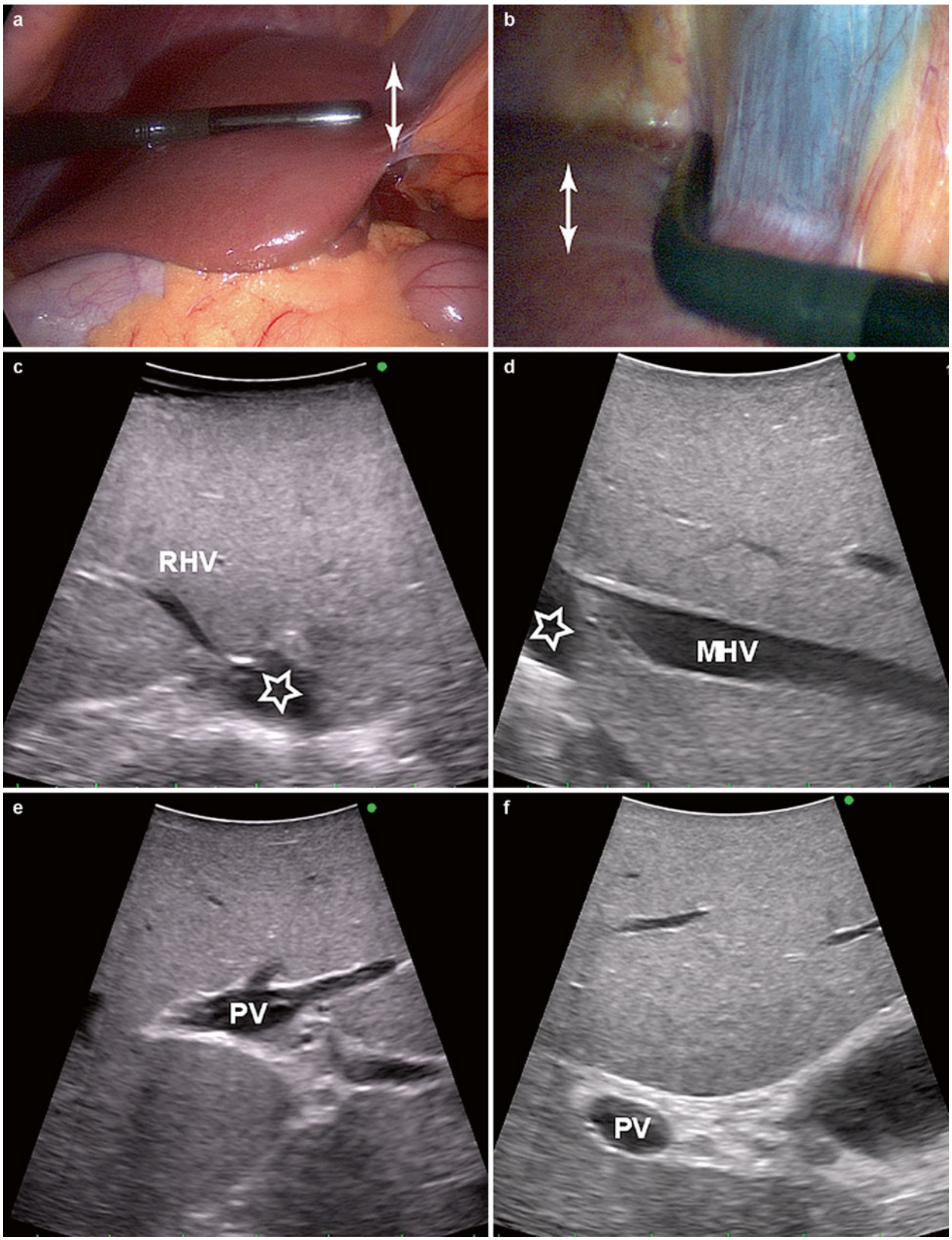

Fig. 4.41 Laparoscopic liver ultrasonography. (**a**) Transverse plane imaging. (**b**) Longitudinal plane imaging. (**c**) Transverse imaging at the superior edge of the liver shows the right hepatic vein (*RHV*) joining the inferior vena cava (*star*). (**d**) Longitudinal imaging at the superior border of the liver shows a longitudinal view of the middle hepatic vein (*MHV*) as it joins the inferior vena cava (*star*). (**e**) Sliding the probe toward the inferior edge of the liver (*white arrow*) while remaining in the transverse plane shows the left portal vein (*PV*) within the umbilical fissure. (**f**) Similarly, sliding the probe inferiorly while remaining in a longitudinal orientation shows the hepatic hilum with the portal vein (*PV*) in cross section

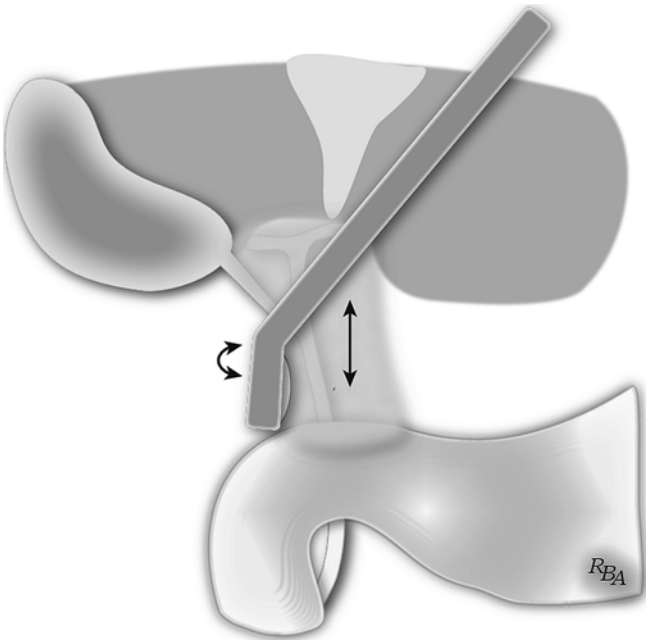

Fig. 4.42 Laparoscopic biliary ultrasonography. Biliary scanning is usually begun through the subxiphoid port. This results in transverse images of the ducts. The ducts are scanned using a combination of sliding (*straight arrow*) and tilting (*curved arrow*). Begin by contact scanning of the gallbladder; slide the probe along the cystic duct to its junction with the hepatoduodenal ligament. The shaft is rotated counterclockwise, tilting the crystal array toward the hilar plate. This images the proximal common hepatic duct. Through a combination of tilting back toward the common bile duct and sliding the probe inferiorly along the hepatoduodenal ligament, most, if not all, of the extrahepatic bile duct can be examined. The retroduodenal and intrapancreatic bile duct can be viewed using duodenal compression as done for the open technique

and scan directly through the head. The bile duct is seen in transverse section from this angle (Fig. 4.43 g, h). The pancreatic duct is seen in the longitudinal plane from this position; often the junction of the bile and pancreatic ducts is seen as the probe slides toward the duodenum (Fig. 4.44a). If the distal bile duct is not well seen, transduodenal compression scanning is the next step. Place the probe on the lateral duodenum and compress the air from the lumen until the pancreatic head and distal bile duct are seen (Fig. 4.44b).

If the common hepatic duct is not visible at the portal plate at the time of the initial examination, repeat the steps outlined above after the tissue in Calot's triangle is dissected free to obtain the critical view. Insert the probe into the triangle and rotate it counterclockwise toward the portal plate to view the proximal hepatic duct.

The second set of bile duct views are obtained through the umbilical port (Fig. 4.45). These show the long axis of the duct and vessels. First examine the gallbladder through the liver; release traction on the gallbladder and place the probe on the anterior hepatic surface over it (Fig. 4.45a, b). Likewise, better images of the proximal right, left, and common bile ducts often are obtained from this trocar using the liver as an acoustic window. After this view is seen, place the probe on the anterior hepatoduodenal ligament to perform direct contact scanning (Fig. 4.45c). Begin with the probe positioned as superiorly on the ligament as possible and then slowly slide it inferiorly to the edge of the duodenum. Prior to sliding the probe, rotate it slightly left and then right to view all the structures in the ligament with minimal probe manipulation. The extrahepatic bile duct, hepatic artery, and

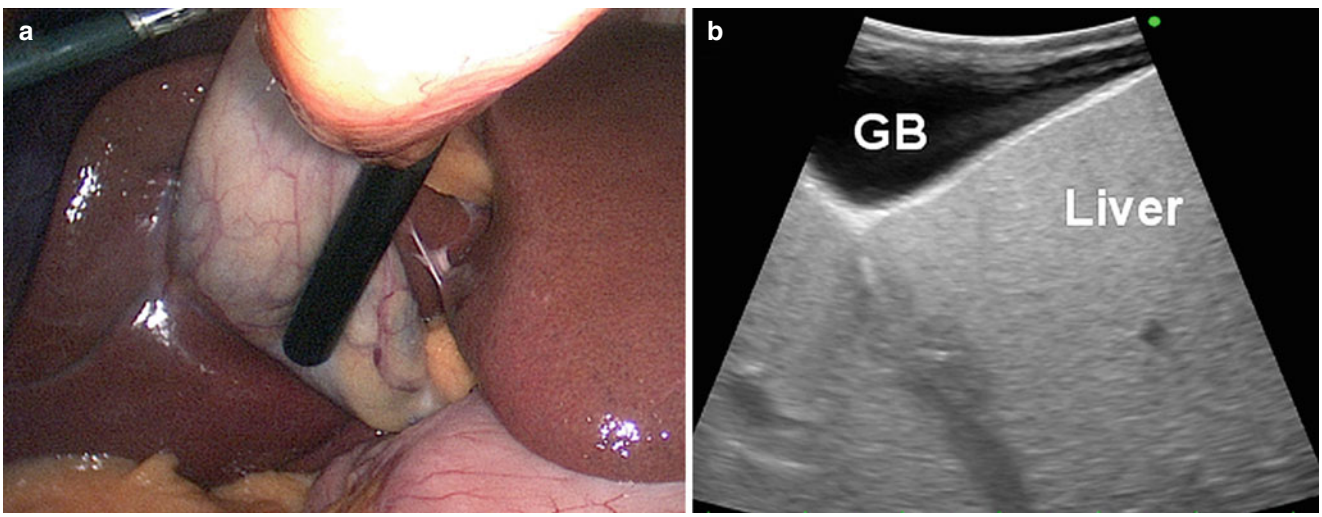

Fig. 4.43 Laparoscopic biliary ultrasonography. Initially, the gallbladder (*GB*) is scanned by direct contact (**a, b**). The probe is slid inferiorly to the cystic duct and its junction with the hepatoduodenal ligament (**c**). This allows viewing of the cystic duct (**d**, *white arrow*). Sliding the probe further inferiorly along the hepatoduodenal ligament (**e**) brings the portal triad into view (**f**) so that the common bile duct (*white arrow*), portal vein (*PV*), and common hepatic artery (*black arrowhead*) are seen ("Mickey Mouse" view). The inferior vena cava (*IVC*) is seen in this image. Finally, transduodenal compression views (**g**, **h**) allow imaging of the intrapancreatic bile duct (*black arrow*). Duodenum (*Du*)

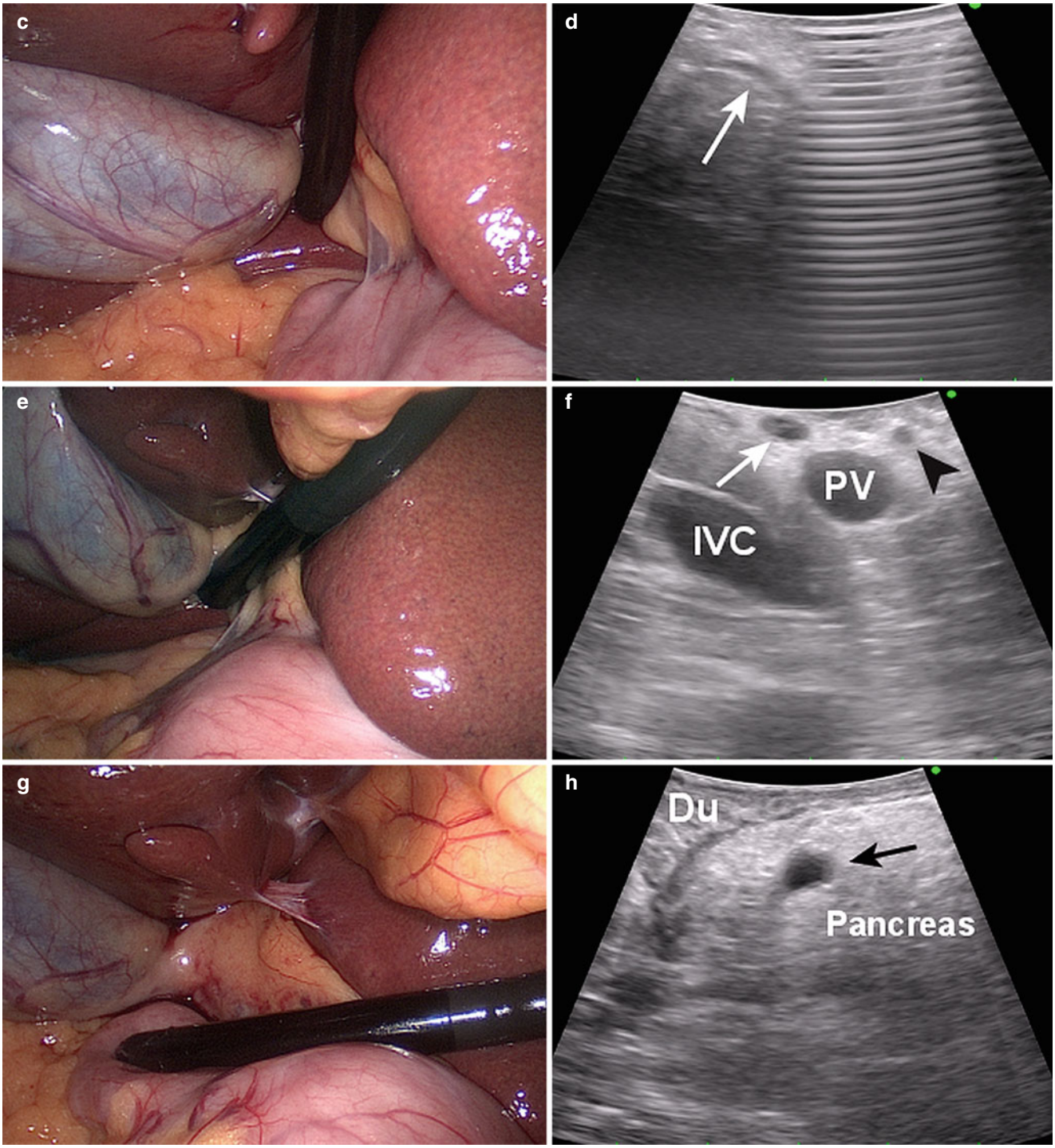

Fig. 4.43 (continued)

portal vein are viewed in their long axis using this approach (Fig. 4.45, image d). The retroduodenal bile duct is seen using a compression technique. Position the probe on the anterior duodenum and slowly compress the probe until the air is displaced from within the lumen (Fig. 4.45, image e and f). The intrapancreatic bile duct and pancreatic duct are seen in this fashion.

Pancreas Scanning Technique

LUS scanning of the pancreas is very similar to that outlined for IOUS. Longitudinal and transverse images are best acquired from right subcostal and periumbilical trocar sites (Fig. 4.46, images a and c). The simplest approach for scanning is a standoff technique using the stomach or

gastrohepatic/gastrocolic ligaments as an acoustic interface. For screening purposes, routinely entering the retrogastric space to allow direct contact scanning is unnecessary. Similar to TAUS and IOUS, identification of the surrounding vasculature facilitates recognition of the adjacent pancreas (Fig. 4.47).

Begin the scan through the right subcostal port. Remember to reorient the image on the monitor so that it is shown in the conventional fashion. Proceed in a systematic fashion as outlined for IOUS. Scanning from the right subcostal site allows longitudinal views of the neck, body, and tail (Fig. 4.46b). Scanning toward the patient's right beginning at the portal

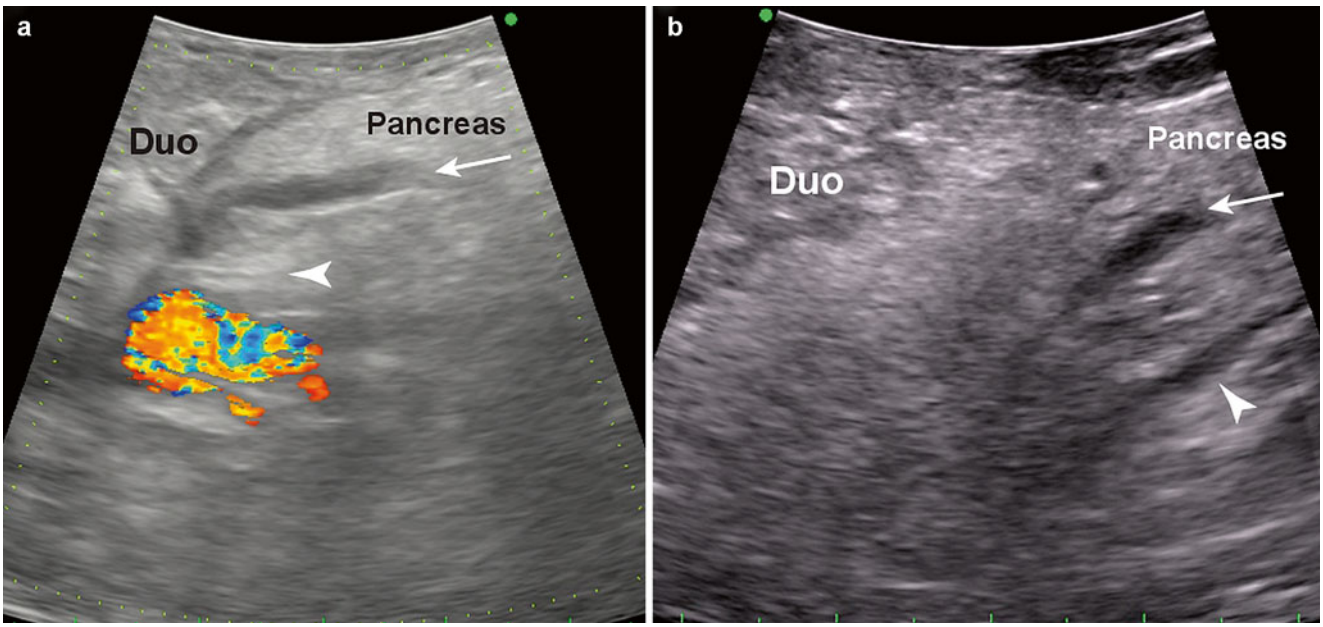

Fig. 4.44 Laparoscopic ultrasonography of the intrapancreatic bile duct and pancreatic duct. (**a**, **b**) Direct scanning through the pancreatic head or duodenal (*Duo*) compression scanning allow a detailed view of the common bile duct (*white arrow*) and the pancreatic duct (*white arrowhead*). Color Doppler shows no flow in the two ducts and a flow signal in the vena cava, directly posterior to the head of the pancreas (**a**)

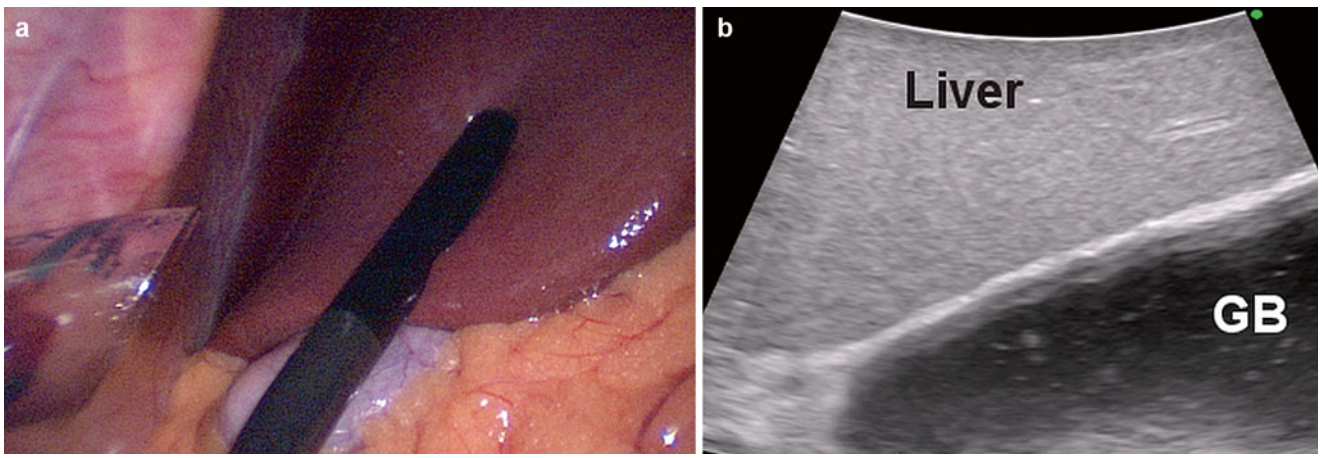

Fig. 4.45 Laparoscopic biliary ultrasonography. In this case, biliary scanning is done through the periumbilical port giving longitudinal views. (**a, b**) Gallbladder (*GB*). (**c**, **d**) Hepatoduodenal ligament with the common bile duct (*CBD*) and portal vein (*PV*). (**e**, **f**) Transduodenal (*Duo*) compression scanning showing the retroduodenal common bile duct (*black arrow*)

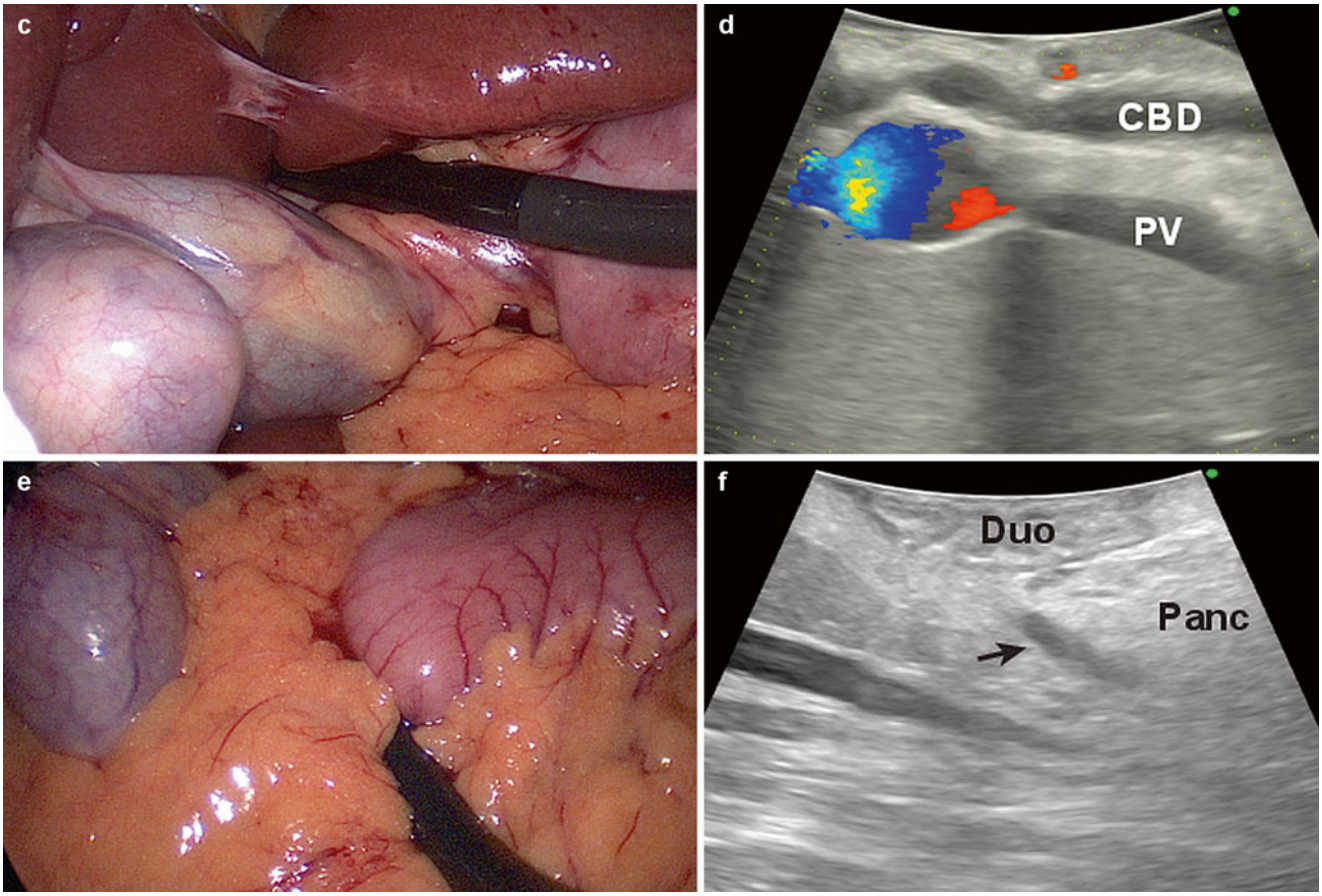

Fig. 4.45 (continued)

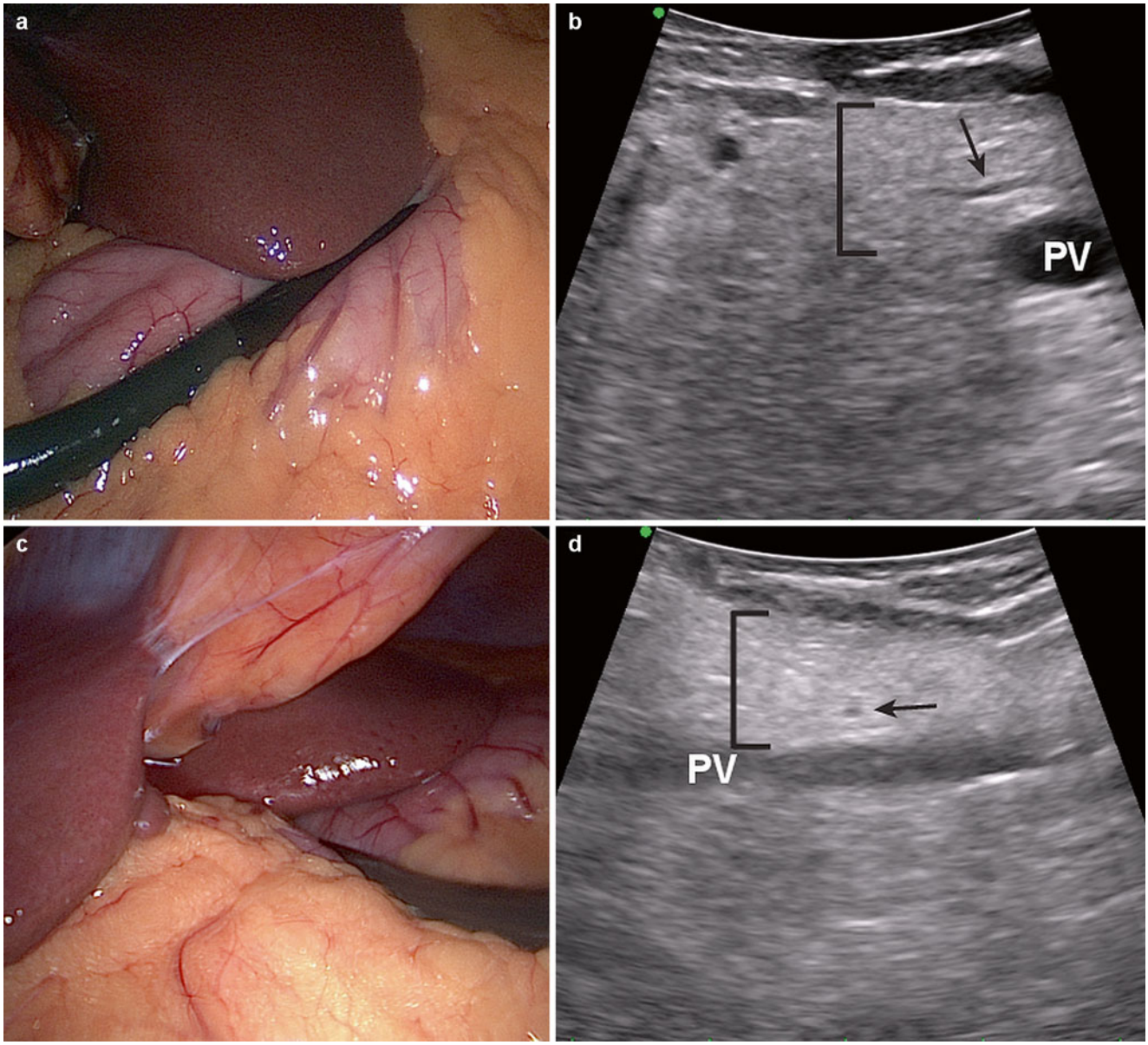

Fig. 4.46 Laparoscopic pancreatic ultrasonography. (**a**) Longitudinal scanning of the pancreas from the right subcostal trocar. A transgastric window is used to view the gland. (**b**) Longitudinal view of the head and neck of the pancreas (*black bracket*). The pancreatic duct is seen (*black arrow*), as well as the portal vein (*PV*). (**c**) Transverse scanning of the pancreas through the periumbilical trocar. Again, a transgastric window is used. (**d**) Transverse view of the neck of the pancreas (*black bracket*) with the pancreatic duct seen in transverse section (*black arrow*). The portal vein (*PV*) is seen in longitudinal section passing posterior to the neck of the pancreas

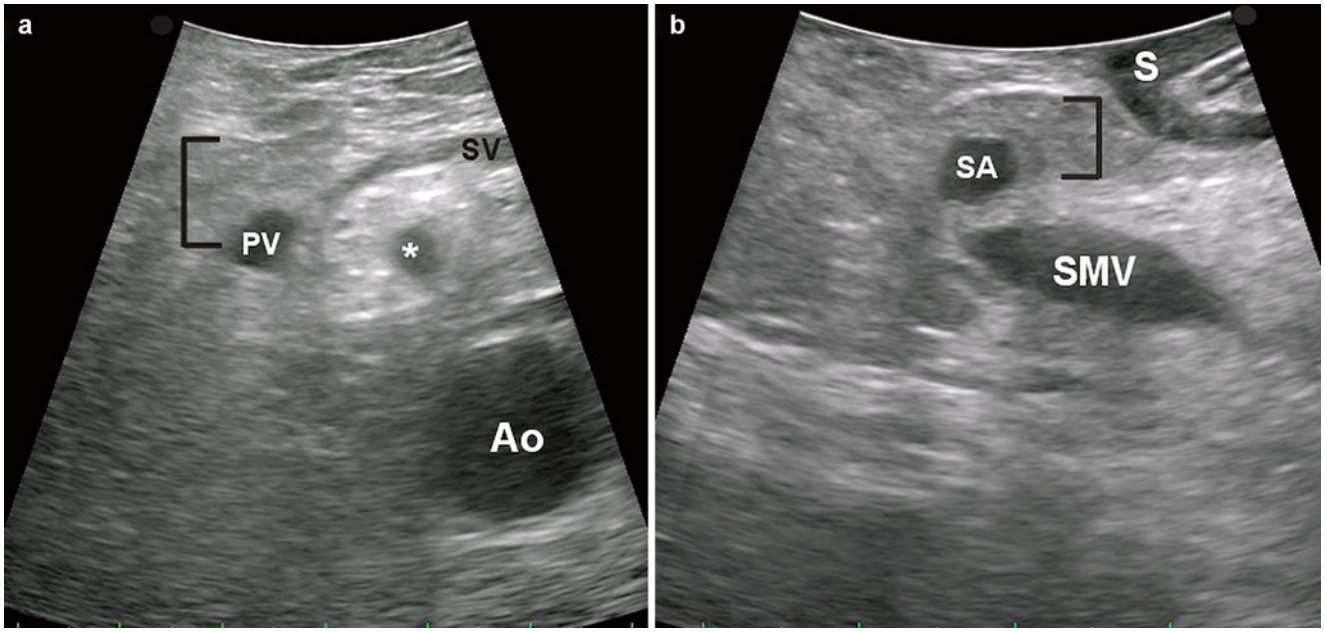

Fig. 4.47 Laparoscopic pancreatic ultrasound. The principles and images are very similar to those for transabdominal and intraoperative pancreatic scanning. (**a**) The transducer is placed in the longitudinal plane using a transgastric window. This gives the prototypical image of the vasculature surrounding the pancreas that facilitates its identification. The pancreas (*black bracket*) lies anterior to the portal vein (*PV*) and the splenic vein (*SV*). The superior mesenteric artery (*white* *) is seen posterior to the veins. The aorta (*Ao*) is posterior to the superior mesenteric artery. (**b**) Transverse position of the transducer using a transgastric (*S*) window. The pancreatic neck (*black bracket*) is seen with the splenic artery (*SA*) running along its anterior border, while the superior mesenteric vein (*SMV*) passes posterior to the neck of the pancreas

vein allows longitudinal examination of the pancreatic head. Moving the probe to the umbilical port permits examination of the gland in the transverse plane (Fig. 4.46d). If examination of the pancreatic head is inadequate, saline immersion and a probe standoff technique may provide better views of the head and uncinate of the pancreas. Again, subtle rotation of the probe clockwise and counterclockwise allows imaging of the entire gland with minimal probe manipulation.

Summary

TAUS, IOUS, and LUS all are effective for gathering additional information during a clinical examination, a procedure, or an operation. While there are differences in the probes and their placement between the approaches, the general principles are very similar. The most important aspect of hepatobiliary and pancreatic ultrasonography is developing a standardized approach and using it for every examination. This leads to readily recognizable images that help the novice gain experience and prevent the experienced sonographer from missing essential information.

References

1. Okuda K, Tsuchiya Y. Ultrasonic anatomy of the biliary system. Clin Gastroenterol. 1983;12:49–63.
2. Anonymous. The Brisbane 2000 terminology of hepatic anatomy and resections. HPB Surg. 2000;2:333–9.

Imaging Characteristics and Artifacts

5

Michael J. Giuffrida and Gary Gecelter

Ultrasound Characteristics of Abdominal Organs and Associated Lesions

The commonest terms in the ultrasound vernacular are those used to describe two distinct entities: the *relative "grayness"* of tissues and the *degree of uniformity*, or lack thereof, within each structure being described. They are as follows:

- Anechoic
- Isoechoic
- Hyperechoic
- Hypoechoic
- Homogenous
- Heterogeneous (mixed echogenicity)

Ultrasound signals travel as a beam through tissues and return to the transducer where the signals are interpreted as luminescence, or "brightness." This brightness mode is known at the B-mode display. After processing, the returning ultrasound signals are plotted on a pixel map and are displayed typically as a two-dimensional gray-scale image.

The strength of the reflected echo signals determines whether the pixel is black, gray, or white. In the case of an *anechoic* region, there is no relativity. Regarding the other degrees of gray scale, we select a reference "echogenicity" upon which we compare structures as being brighter, (*hyperechoic*), darker (*hypoechoic*), or similar (*isoechoic*) to the reference. It has been our routine to select the normal liver parenchyma as the reference standard against which we refer to surrounding organs as hyperechoic (pancreas, area on far side of cyst), hypoechoic (steatotic liver, necrotic pancreatic tumor center), or isoechoic (some liver tumors). Further, as the normal liver has a large volume of essentially homogeneous parenchyma, we set our transducer parameters ("knobology") so as to create an identical level of grayness throughout the visible depth of the transducer. This is done by placing the transducer over the liver so that the entire field is occupied by liver parenchyma and then set the slide rules in such a way as to see the liver appear uniform from near to far field (Fig. 5.1).

Anechoic regions of the image are areas that are not reflective and, therefore, do not produce a returning echo signal to the transducer; these objects have a black appearance.

One can think of an anechoic structure as being completely uniform with no tissue interfaces off which a signal can bounce. The classic example of a normal anechoic region is the lumen of the normal gallbladder, which is essentially a cyst cavity containing liquid bile (see discussion of "Clinical Classification" below). The classic abnormal anechoic image is that of a simple liver or kidney cyst (Fig. 5.1).

Hypoechoic tissues have less cellular interfaces per unit area and usually have a high fluid density making them less reflective than surrounding parenchyma. A good example of this is the hepatic carcinoid metastasis, which is homogeneously "darker" in gray scale than the surrounding liver parenchyma (Fig. 5.2).

The classic hyperechoic lesion is represented by the small hepatic hemangioma that is described as a sharp-edged, uniformly hyperechoic lesion that, when visualized, is said to illuminate like a light bulb (Fig. 5.3). A hyperechoic tissue is one that typically has denser cellular structure with more membrane interfaces than surrounding structures. For example, the pancreas is more echo-dense than the liver, and the renal collecting system, which is a dense connective tissue tubular structure, "whiter" than the surrounding renal cortex. Hyperechoic tissue can also be linear where there is a large difference in interface density between adjacent structures. The best example of this is the wall of the gallbladder and its juxtaposition with the lumen, which is anechoic (see discussion of "Artifacts of Modality Limitation" below).

An additional lesion is one of *mixed echogenicity* where, as the term implies, has components of its structure that vary from anechoic to hyperechoic. A typical example of this is

M.J. Giuffrida, MD • G. Gecelter, MD, FACS, FACG (✉)
Department of Surgery, St. Francis Hospital,
100 Port Washington Blvd, Roslyn, NY 11056, USA
e-mail: michael.giuffrida@chsli.org; gary.gecelter@chsli.org, ggecelter@gmail.com

E.J. Hagopian, J. Machi (eds.), *Abdominal Ultrasound for Surgeons*,
DOI 10.1007/978-1-4614-9599-4_5, © Springer Science+Business Media New York 2014

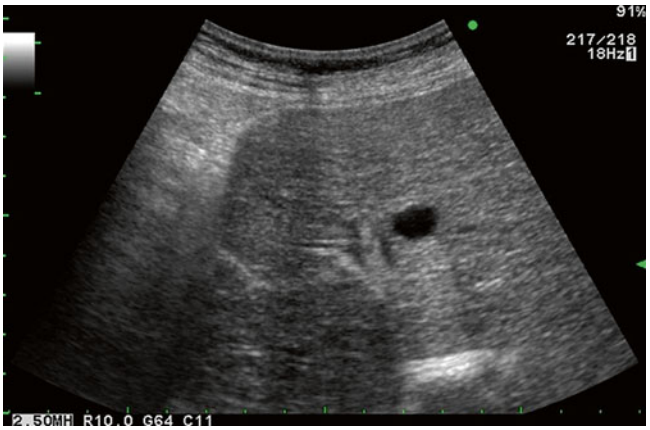

Fig. 5.1 Simple hepatic cyst seen on curvilinear 2.5 MHz transcutaneous transducer. There are 3 observations to be gleaned from this image. (i) Optimization of gray scale with liver parenchyma appearing the same throughout image depth of 10 cm as seen in the dotted scale on the left of the frame. (ii) *Anechoic* cyst with post-cyst enhancement. (iii) *Velocity displacement* with the far field liver capsule appearing as a hyperechoic linear structure in the path of the post-cyst enhancement (see Figs. 5.7 and 5.8)

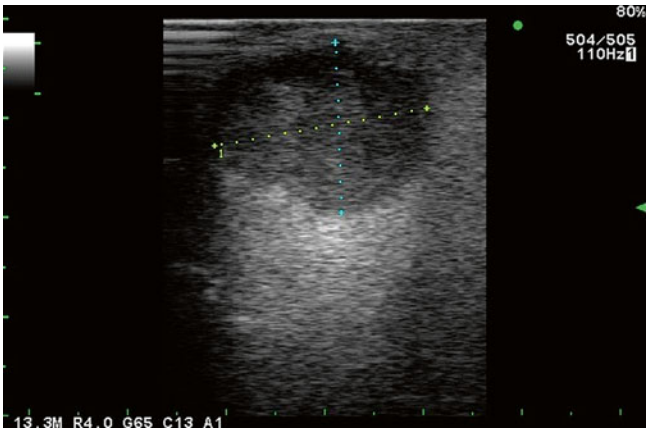

Fig. 5.2 Hypoechoic mass in liver seen on laparoscopic linear array imaging. This is typical of a metastatic carcinoid, exhibiting low to mixed echogenicity with significant post-lesion enhancement. Certain neuroendocrine lesions are so hypoechoic as to resemble cysts. Note the increased echogenicity (enhancement) beyond (or deep to) the lesion (1)

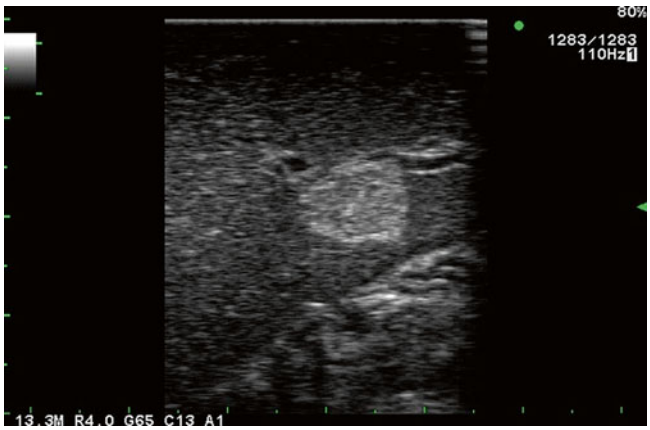

Fig. 5.3 Laparoscopic linear array 13.3 MHz transducer. Typical *hyperechoic*, well-circumscribed small hepatic hemangioma seen on laparoscopic ultrasound of segment III of the liver. In this image, there has been failure to create a uniform near-field gray scale of the liver when compared to Fig. 5.1

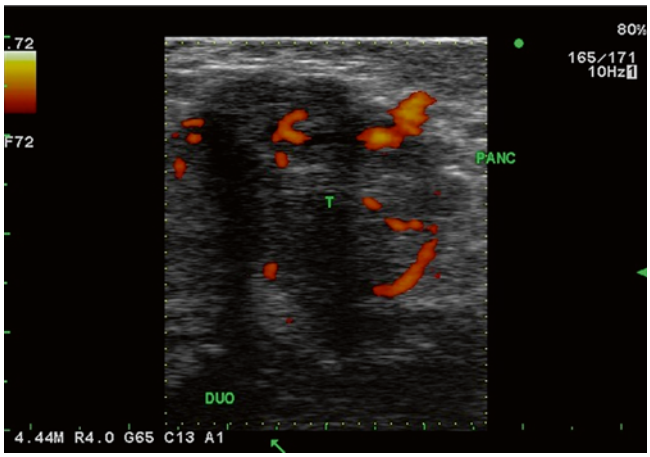

Fig. 5.4 *Mixed echogenicity*. Transverse image of head of pancreas (*PANC*) and duodenum (*DUO*) with pancreas tumor (*T*). Here demonstrated in this tumor is central hypoechoic necrosis with scalloped margins that are variably defined. The orange areas are blood vessels seen in color duplex mode

the necrotic pancreatic or hepatic tumor with an area of central anechoia surrounded by growing tumor and compressed parenchyma, giving it a spectrum of density as seen on ultrasound (Fig. 5.4).

Isoechoic regions of an image are those areas that have similar interface density to the surrounding structures but, by definition, have other characteristics that differentiate them from surrounding normal tissue. There is no reason to describe normal structures as isoechoic or "isodense" with surrounding tissue, but a pathologic entity can be described as isoechoic or isodense to its surrounding or host organ. An example of this is an isoechoic hepatic colorectal metastasis (Figs. 5.5 and 5.6), where there is a subtle visible margin that allows identification of the lesion within the adjacent liver tissue. This is usually possible because of the interruption of normal vascular arborization patterns within the liver that allow us to identify an isoechoic lesion. What makes this possible in ultrasound is the ability to see architecture in real time as the transducer moves over the organ and allows the examiner to identify a tissue interruption as evidenced by displacement or distortion of normal vascular architecture. In trying to save this as a static image, the isoechoic lesion is often indistinguishable from surrounding normal parenchyma, thereby reinforcing the value of surgeon-performed, real-time, image acquisition.

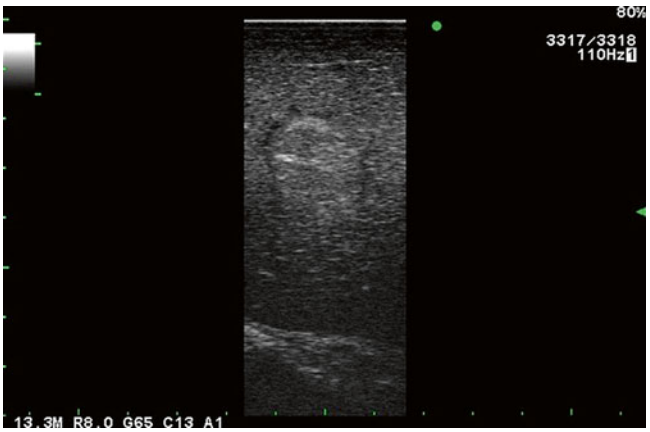

Fig. 5.5 Near isoechoic lesion in liver. This lesion is identified by the presence of a hypoechoic rim (margin) seen during laparoscopic side-fire, linear array imaging

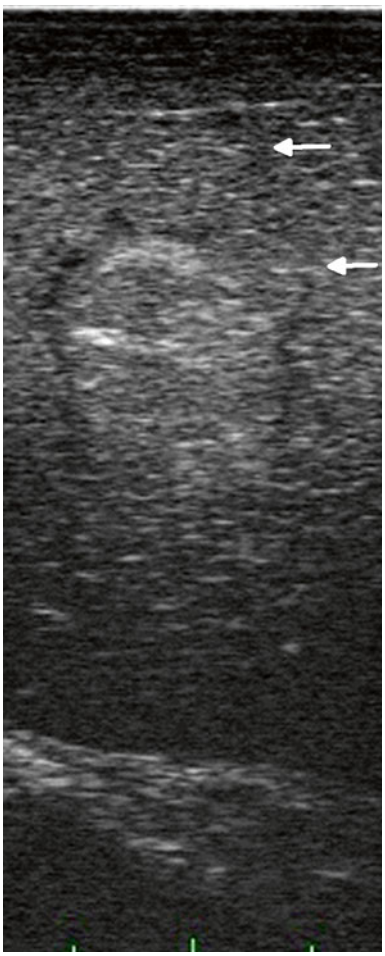

Fig. 5.6 On closer inspection, there are two truly isoechoic "daughter" lesions seen (*arrows*). These lesions are less subtle when real-time motion is used to scan the liver

Understanding Sonographic Artifacts

In the following discussion, we will describe ultrasound artifacts in two ways. First, we will address the *physics of ultrasound artifacts*. More relevant, however, we will attempt to provide a *clinical classification* of ultrasound artifacts that will help us use them as invaluable aids to better image the abdomen and arrive at more accurate sonographic diagnoses by their very existence.

The Physics of Ultrasound Artifacts

Ultrasound imaging is based upon using a transducer for converting electrical energy into pulsed mechanical sound energy via piezoelectric crystals into a scanned volume of tissue. The returning echoes are converted back into electrical energy that is then interpreted and converted into a two-dimensional gray-scale image. The device software is designed to receive signals from tissues that are predominantly water containing (the human body is comprised of approximately 53 % water), and the average transmission of sound waves in the human body is about 1,540 m/s. As a result, when an outgoing signal passes through a gas-containing structure (stomach or colon), the transmission of that signal slows down to approximately 330 m/s which upsets the ability of the "listening" cycle of the device to locate the echo.

Sonographic artifacts are images generated that do not have a true corresponding anatomic component. The ultrasound probe and processor rely on fixed assumptions of the pulsed echo they generate, including a constant speed of sound through human tissue (1,540 m/s), a uniform attenuation of signal as the beam travels further away from its origin, and the assumption that the beam travels straight and is reflected once. Often the beam is altered by its interaction with tissue, and the assumptions are no longer valid. Artifacts typically result from the following three common diversions from the above assumptions:

- Attenuation that is not uniform
- Wave propagation this is not straight and may have a variety of paths
- A change in the velocity of the signal

Understanding sonographic artifacts helps surgeons avoid pitfalls of misinterpretation of images, improve the quality of their scans, and use the peculiar characteristics of these artifacts to their advantage to clarify tissue morphology to improve their diagnostic capabilities.

In the following section, we will discuss the commonly encountered sonographic artifacts, the understanding of which will lead to a better ability to arrive at an accurate clinical diagnosis. This will give the *surgeon ultrasonologist* the ability to interpret findings as either representative of real

anatomy or pathology or arising from an artifact consequent to the nature of the physical principles governing ultrasonography.

Attenuation

The ultrasound is pulsed energy converted into mechanical waves. Piezoelectric crystals in the transducer are where packets of energy are converted into vibrations. These vibrations are then propagated as mechanical waves through tissues. As the pulses of the ultrasound beam travel through tissue, the signals can weaken and lose energy and intensity due to redirection (reflection, scatter) and absorption. The diversion of energy away from the detector results in decreased or weakened returned signals and, therefore, decreased signal intensity and is known as *attenuation*. Modern ultrasound devices have a combination of manual (slide rules) and automatic gain detection software that spontaneously compensates for signal attenuation. The automatic gain control (AGC) or time gain compensation (TGC) effectively acts to "increase the volume" of the listening device in order to augment the incoming echoes from structures further away from the transducer. Without this automatic device, an image seen, such as the homogeneous liver parenchyma in Fig. 5.1, would have to be manually adjusted using the slide rule devices on the ultrasound console.

If angle of incidence is perpendicular to a structure and the interface is "smooth," a portion of the pulse's energy is transmitted forward deeper through the tissue, while the remaining portion of the pulse's energy is reflected back to the detector. This partially reflected echo is weaker in intensity and is known as specular reflection, which is a specific cause of attenuation.

Reflection and Scatter

If the angle of specular reflection is not 90°, the echo will be reflected away from the transducer at an angle equivalent to the angle of incidence, similar to light *reflecting* off a mirror. If the angle of incidence is greater than 5°, the reflected waves do not return to the transducer and the object is not detected and is erroneously absent from the image.

"Rough" interfaces result in diffuse reflection of returning echoes in a wide variety of angles. When the object is smaller than the ultrasound wavelength, the echoes are also deflected in a wide range of angles and it is called *scatter*. Although this guarantees that some signal will return to the transducer regardless of the incident angle of the echo, the return signal is weaker and less intense.

Absorption

Absorption is another important source of signal attenuation. The wave's energy is not only decreased due to redirection (reflection/scatter), but can be lost to the surrounding tissue in the form of oscillating friction and localized heating, otherwise known as absorption. This is typically a function of the length of the pathway through tissue and the wavelength, with longer paths and higher frequencies resulting in greater attenuation.

Enhancement

This is essentially the opposite of attenuation. Enhancement is a bright band deep to a weakly attenuating structure. When the beam encounters a low or focal weakly attenuating object, less energy is dissipated and more energy returns to the transducer. More energy is preserved as the ultrasound beam energy passes through the low-attenuation tissue and returns to the detector. The tissue echoes beyond the object appear as a more intense, enhanced signal relative to the adjacent tissue signal at that same depth. This results a hyperechoic signal and is displayed as a brighter band extending beyond the object. Post-cyst enhancement refers to the bright echo pattern seen on the far side of a liver cyst (Fig. 5.1) and, occasionally, on the far side of a hypoechoic solid structure such as a pancreatic neuroendocrine tumor (PNET) (Fig. 5.2).

Additionally, structures beyond may appear more echogenic than normal; this is known as "increased through transmission." Through-transmission artifacts lead to incorrect conclusions about sonographic pathologic findings and can occur while scanning structures through fluid collections including soft tissue deep to cysts, liver or kidney through ascites, or testicles through hydroceles.

Velocity Displacement

Unlike the above artifacts which tend to diminish the visibility of structures in the transducer's path, velocity-related artifacts will malposition structures or lesions in such a way that their relevance will be most concerning in the role of ultrasound-directed localization for tissue acquisition and therapeutic interventions such as tissue ablation.

Velocity displacement is the false elongation or shortening of structures away or toward the transducer when the indecent angle is perpendicular. This form of range ambiguity is due to the transducer's assumption that the ultrasound beam is traveling a fixed, uniform rate of 1,540 m/s in human tissue. If the actual speed of the wave is faster or slower than the assumed speed, significant position changes can result in the display. A slower propagation will result in a longer return time which is interpreted as having traveled a longer, deeper distance, and the resulting image will be erroneously placed "deeper" than its true anatomic position. Conversely, faster propagation will result in a shorter return time which is interpreted as having traveled a shorter, shallower distance, and the resulting image will be erroneously placed more "superficial" than its true anatomic position (Figs. 5.7 and 5.8). A clinical example of velocity displacement artifact is seen in Fig. 5.1.

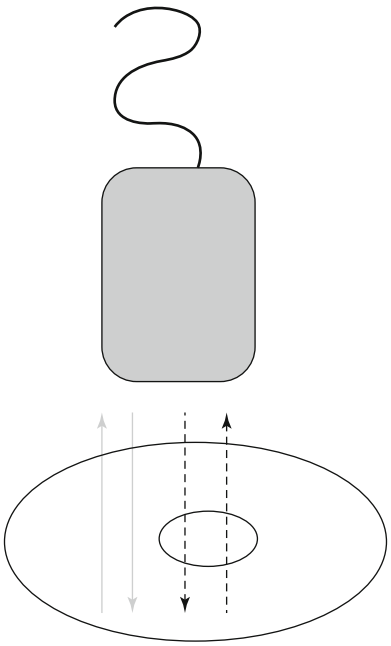

Fig. 5.7 *Velocity displacement artifact*. In this diagram, the gray arrows indicate the expected path of the ultrasound beam and the returning echoes are displayed properly. However, the black arrows represent the path of an ultrasound beam, which passes through an area of fatty infiltration (*gray ellipse*). This results in sound beams which travel slower and results in an image which appears to be deeper than in reality (From Feldman et al. [7])

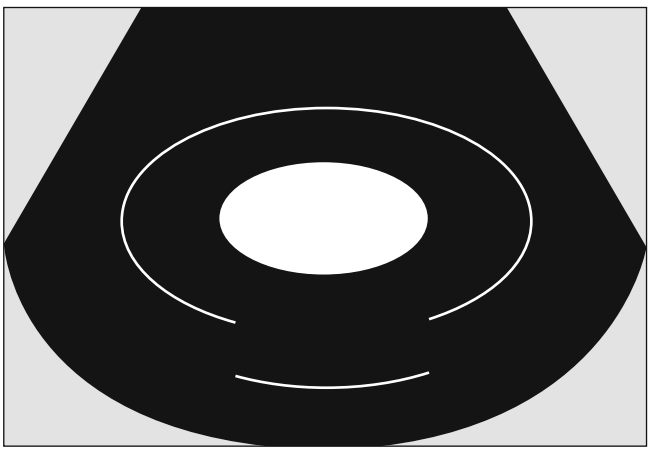

Fig. 5.8 *Velocity displacement artifact (2)*. The ultrasound beams pass through a focal area of steatosis (*central ellipse*) creating a velocity displacement artifact. The "broken" line is seen to be deeper as the steatotic area slows down the through transmission as the sound waves travel more slowly through fatty tissue than through tissues with more water content

Refraction

Refraction occurs when the ultrasound beam strikes the boundary of an object obliquely (particularly a convex, curved object) or it travels through two objects with different densities. The degree the beam will be redirected is based on both the incident angle and the difference in propagation speeds. The detector assumes the beams traveled in straight lines and will displace the objects to a side or magnify or reduce an object's size. The beams will magnify a structure's size as the beams diverge when transitioning between a lower velocity and a higher velocity medium and reduce a structure's size as they converge when transitioning between a higher velocity to lower velocity medium.

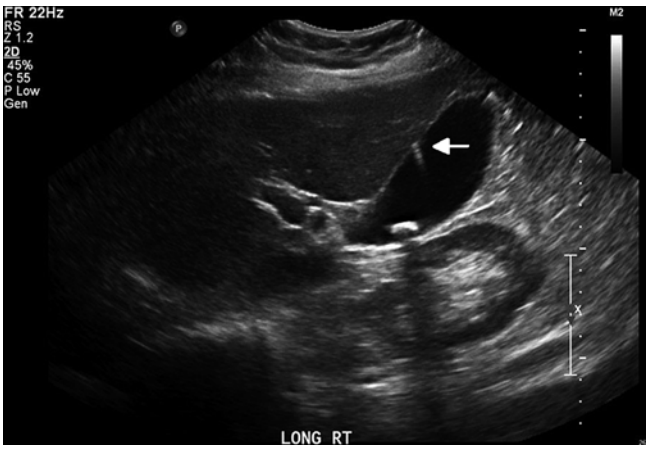

Fig. 5.9 Comet tail artifact (*arrow*). "Signature" artifact of gallbladder cholesterolosis seen in adenomyomatosis. Also seen is a gallstone (hyperechoic, space occupying structure in the dependent portion of the gallbladder lumen), which casts an acoustic shadow on the far side of the transducer (shadowing) and confirms the diagnosis of gallstone. Note the classic normal anechoic lumen of the normal gallbladder, which contains liquid bile

Clinical Classification of Ultrasound Artifacts

In thinking about a *clinical classification* of ultrasound artifacts, we have found that they all fall into one of three specific categories, unrelated to their physically derived properties. Some artifacts will result from *correctable technical errors*, such as poor transducer contact or excessive power, while others will occur as a result of *limitations of the modality* itself such as the presence of overlying bowel gas. Yet a third category is those artifacts that are created by the existence of a specific pathologic process that represent a "*signature artifact*," whereby that condition can be more readily recognized. A classic example of this last category is the comet tail artifact seen in gallbladder cholesterolosis (Fig. 5.9).

Occasionally, an expected artifact such as overlying gas in the left upper quadrant that ordinarily obscures the pancreatic tail is displaced by a large cyst or pseudocyst, making the pathology imminently visible. This consequently endorses the fact that one should always ultrasound the abdomen in a systematic, four-quadrant manner similar to that in which we perform a manual physical examination.

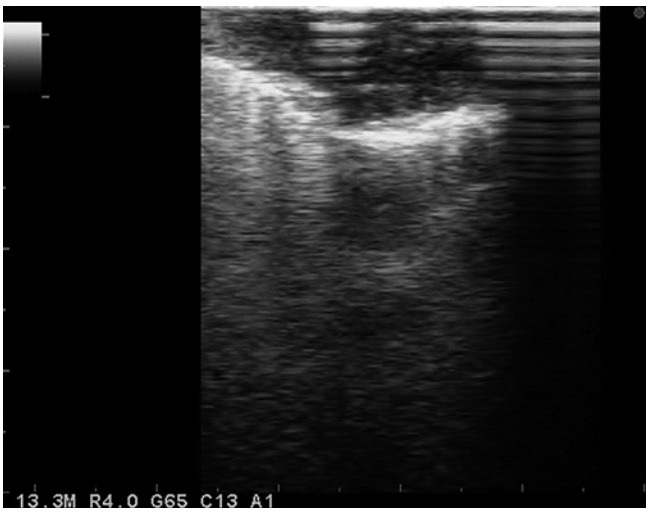

Fig. 5.10 Reverberation (contact) artifact. Typical technical, contact artifact seen as a reverberation artifact on the right side of this image. Note that this artifact appears as a continuous series of parallel bands radiating away from an object. This is a high-frequency laparoscopic side-fire linear array transducer attempting to make contact on the surface of the concave right hemidiaphragm in a patient with a metastatic ovarian carcinoma

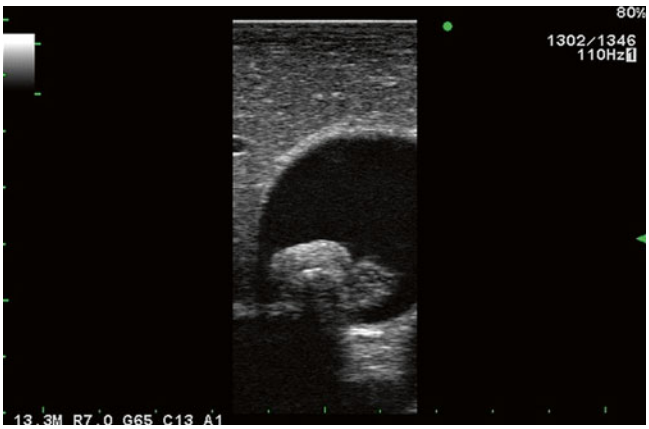

Fig. 5.11 The classic acoustic shadow. This is an image of two soft calculi, one of which contained internal calcifications seen on laparoscopic ultrasound. Note the shadowing, or darkened area, deep to the calculi

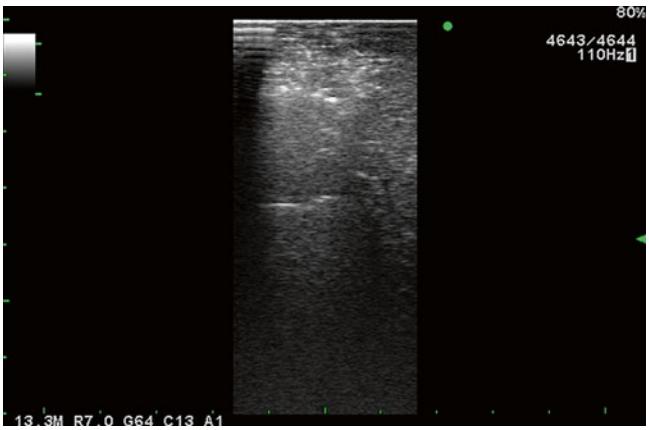

Fig. 5.12 Radiofrequency ablation of a liver lesion. Note the scattered hyperechocities within the lesion demonstrating microbubble formation. This leads to coalescing attenuating artifacts that result in smudging of margins resembling bowel gas

Correctable Technical Errors

Reverberation is a common phenomenon that refers to short-path "ricocheting" of ultrasound beams between highly reflective surfaces. The commonest reverberation artifact is that which results from poor *transducer contact* (Fig. 5.10).

Artifacts of Modality Limitation

Shadowing is a dark or hypoechoic band deep to a structure due to absorption and reflection due to highly attenuated or highly reflective structures. When a highly attenuated structure is encountered, the beam loses more energy in the form of scatter or absorption resulting in a low-intensity signal beyond the object. A highly reflective surface will also generate a shadow because most of the energy does not penetrate the object and is reflected back to the detector. The resultant hypoechoic signal is displayed as a dark band extending beyond the object. This shadowing can be seen beyond a gallbladder calculus (see Figs. 5.9 and 5.11) and beyond an air-filled structure, such as air within the bile duct (see discussion of "Signature Artifacts, Ring-down" below). Bone and bowel gas are the two commonest obstacles to transmission of ultrasound resulting in shadowing. Post-ablation tissue following radiofrequency ablation creates microbubbles that behave in a similar way, obscuring accurate delineation of the ablation zone (Fig. 5.12). Similarly, cryoablation will result in a temporary crescent-shaped shadow until the ablated tissue thaws.

Signature Artifacts

Edge shadowing is the result of beam interaction with a convex, curved interface of an object with significant acoustic impedance differences, such as a cyst in soft tissue (Fig. 5.13). There are two components: the transmitted component and the reflected component. The perpendicular beam will transmit a beam straight through as well as have a direct reflection to the transducer. When the beams start to strike the object off perpendicular, some of the beams pass through and are refracted while others are reflected. Not all of these beams will return to the transducer, especially as the angle becomes more oblique. Along the perimeter of the curved object, an edge shadow appears at a critical angle as a combination of refraction and reflection. These edges shadows are typically fuzzy because the objects are usually smaller than the beam's cross-section. Edge shadows are helpful in identifying the margins of structures that are otherwise difficult to identify.

Mirror images are the artificial creation of a duplicate pseudo-image. This artifact is based upon the assumption the beam returns after making one reflection. It usually occurs

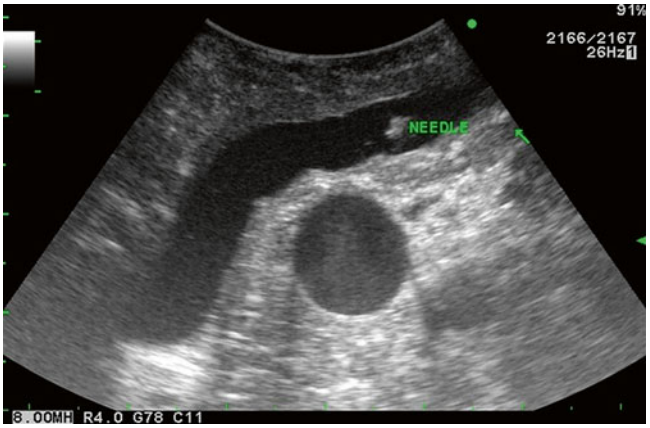

Fig. 5.13 *Edge shadowing*. Here depicted is a transverse image of the splenic artery (central circular hypoechoic structure). Note the hypoechoic lines deep to the edges of the splenic artery, indicating "edge" shadowing. The splenic artery is seen deep to a longitudinal image of a dilated pancreatic duct with a *NEEDLE* within

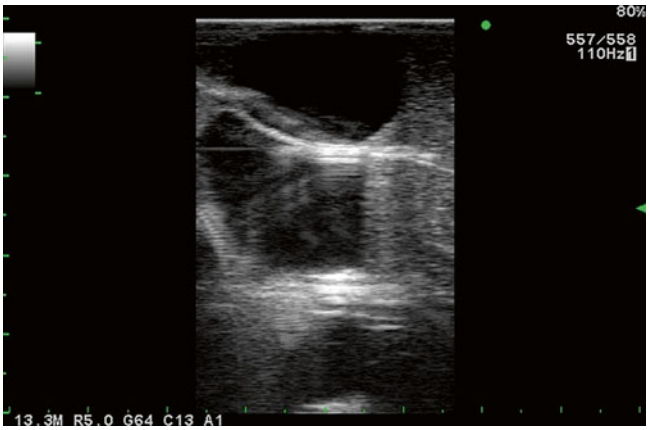

Fig. 5.14 Mirror imaging. A cystic lesion of the liver is seen adjacent to the diaphragm resulting in a mirror image as a result of the intensity of the interface between the anechoic cyst and the hyperechoic diaphragm

with a highly reflective interface. The beam will propagate through tissue and strike a highly reflective structure such as the diaphragm. The beam reflects off the structure heading back toward the transducer. Some of the beams will return to the transducer after one pass and the correct anatomy is displayed. However, some of the other beams strike tissue on the return trip and are then rebounded deeper, away from the transducer. The deflected beam then strikes the highly reflective structure a second time before it is returned to the transducer. The longer duration of the redirected signal places the duplicate image equidistant and deeper to the interface, creating a mirror image (Fig. 5.14).

A *comet tail* is a reverberation artifact that appears as a continuous series of parallel bands radiating away from an object (Fig. 5.9). The transducer assumes the beam reflects only once before returning to the detector. With reverberation,

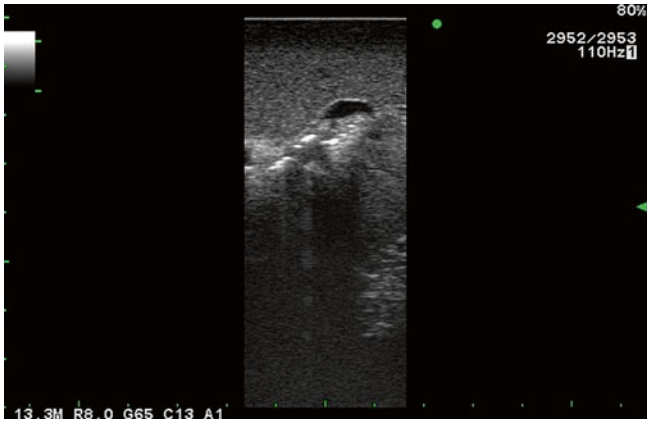

Fig. 5.15 Ring-down artifact. Intrabiliary air exhibits multiple artifacts within the center of the liver. In this image, the air exhibits an intensely hyperechoic "track" corresponding to the cavity of the intrahepatic bile ducts in the vicinity. Because of the echo disorganization at the level of the super slow velocity of sound conduction through the air, the far side of the air-filled duct is depicted as a shadow. In addition, a ring-down artifact is created by a presumed droplet of bile trapped between a cluster of bubbles in the duct

some the beams enter the object and reflect back to the transducer on the first reflection. However, additional beams continue to "ping-pong" between two highly reflective surfaces before returning to the detector. Longer time spent in rebounding within the object results in erroneously placing each successive signal "deeper." The automated ultrasound time compensation initially enhances the series of bands. As the echoes lose signal intensity due to attenuation, the characteristic tapered triangular shape of a comet tail results. Comet tails occur when a beam strikes a highly reflective object perpendicularly, such as stents, clips, needle tips, foreign objects, or cholesterol crystals (such as in the gallbladder).

Ring down is a variant of the comet tail. Ring down is a reverberation artifact created by an ultrasound beam rebounding within horn- or bugle-shaped fluid trapped within a tetrahedron of microbubbles of air. These ring-down artifacts are transient and are commonly encountered when the bowel is interrogated sonographically, but may also indicate the presence of air in the wall of viscera, such as an emphysematous gallbladder or air in the biliary tree after ERCP or stent placement (Fig. 5.15).

Conclusion

In this chapter we have discussed the essential descriptors used to recognize sonographic features of intra-abdominal pathology. We have outlined the common, clinically relevant artifacts that both identify the need to improve our image generation as well as those that, by their existence, aid us in making certain diagnoses. We have demonstrated that in virtually every sonographic image, there is at least one and sometimes multiple definable artifacts that

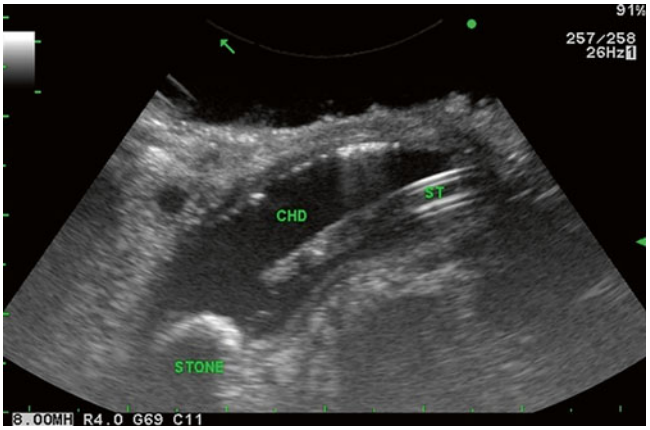

Fig. 5.16 Composite of multiple artifacts. This intraoperative sonogram obtained with an 8 MHz curvilinear array "finger probe" was achieved using an offset saline bath. The grossly dilated common hepatic duct (*CHD*) seen in longitudinal view contains a large solitary calculus (*STONE*) with a downstream stent (*ST*). The entire image appears brighter because of the water bath interface between the transducer and the anterior surface of the pancreas resulting in *enhancement* of subjacent structures. There is air in the lumen of the duct that has risen to the anti-dependent portion of the duct and casts a number of *ring-down artifacts* (note the hyperechocity in this area). The stent itself is seen as a double line (tram tracking) which is a *reverberation artifact* and is typical of plastic endobiliary stents. The stone (STONE) casts an *acoustic shadow* on the far side of the calcified structure, preventing any through transmission beyond the surface that is closest to the transducer. This creates a "crescent" appearance of the round stone

contribute to this modality's accuracy (Fig. 5.16). Ultrasound is an invaluable tool for the abdominal surgeon's diagnostic and therapeutic efficacy. A working, facile understanding of its strengths and limitations is essential for its safe and productive use by the abdominal surgeon.

Further Reading

Waldroup LD, Kremkau FW. Artifacts in ultrasound imaging. In: Goldberg BB, editor. Textbook of abdominal ultrasound. 1st ed. Baltimore: Williams & Wilkins; 1993.

Levitov A. Transducers, image formation, and artifacts. In: Levitov A, Mayo PH, Slonim AD, editors. Critical care ultrasonography. New York: McGraw-Hill Education; 2009.

Baker JA, Soo MS, Rosen EL. Pictoral essay: artifacts and pitfalls in sonographic imaging of the breast. AJR Am J Roengenol. 2001;176:1261–6.

Powers J, Kremkau F. Review: medical ultrasound systems. Interface Focus. 2011;1:477–89.

Wells PNT. Physics and instrumentation: non-Doppler. In: Goldberg BB, editor. Textbook of abdominal ultrasound. 1st ed. Baltimore: Williams & Wilkins; 1993.

Hangiandreou NJ. AAAPM/RSN physics tutorial for residents: topics in US: B-mode US: basic concepts and new technology. Radiographics. 2003;23:1019–33.

Feldman MK, Katyal S, Blackwood M. US artifacts. Radiographics. 2009;29:1179–89.

Ahrendt SA, Komorowski RA, Demeure MJ, Wilson SD, Pitt HA. Cystic pancreatic neuroendocrine tumors: is preoperative diagnosis possible? J Gastrointest Surg. 2002;6:66–74.

Part II

Anatomy, Application, and Intervention: Transabdominal, Intraoperative, Laparoscopic

Abdominal Wall Anatomy, Pathology, and Intervention

6

Jose M. Velasco and Faaiza Vaince

Abbreviations

CT	Computed tomography
MRI	Magnetic resonance imagining
TAP	Transversus abdominis plane
US	Ultrasound

Introduction

Ultrasonography is an extremely useful diagnostic tool with increasingly sophisticated equipment and imaging capabilities. Modern ultrasound machines have many advantages that enhance their usefulness, such as handheld ultrasound devices, multifrequency transducers, color Doppler, and reusable biopsy guide attachments. Furthermore, the use of ultrasound (US) is especially pertinent in the era of rising health-care costs for it is a relatively inexpensive and safe technology. Its portability and accessibility allow for its real-time use in the ambulatory or operative setting, particularly when other modalities, such as computed tomography (CT) or magnetic resonance imagining (MRI), are not available or are contraindicated. US can be used for diagnostic purposes to identify and localize pathology and is extremely effective in guiding therapeutic interventions (e.g., draining intra-abdominal fluid collections or guiding laparoscopic trocar insertion).

J.M. Velasco, MD (✉)
Department of Surgery, NorthShore University HealthSystem, Skokie Hospital, 9600 Gross Point Road, Skokie, IL 60076, USA

Department of General Surgery, Rush University Medical Center, 1653 W. Congress Parkway, Chicago, IL 60612, USA
e-mail: jvelasco@northshore.org, jose_velasco@rush.edu

F. Vaince, MD
Department of General Surgery, Rush University Medical Center, 1653 W. Congress Parkway, Chicago, IL 60612, USA
e-mail: faaiza_vaince@rush.edu

Ultrasound also plays a valuable role in the diagnosis and treatment of abdominal wall and groin pathology, especially as a first-line investigative modality. Surgeons quickly master and utilize ultrasonography for both diagnosis and intervention, given their technical background, their familiarity with the anatomy, and their ability to correlate the images to intraoperative findings. In this chapter, abdominal wall anatomy, pathology, and interventional ultrasound are reviewed.

Ultrasound Instrumentation and Technique

Examination of the abdominal wall with US should be done in a systematic fashion. The entire abdomen should be examined prior to focusing on a particular area of pathology. The examination should begin cephalad at the subxiphoid process moving laterally and caudally through each compartment. A multifrequency transducer (7.5–12 MHz), which allows for high resolution at the cost of lower penetration, can be utilized. Either a curvilinear array or linear array transducer probe with color Doppler can be used to examine the abdomen and to identify and differentiate vascular structures, particularly in the preperitoneal space. Most machines will also allow for the capture of video and picture so that images may be stored for clinical documentation and educational purposes.

Interventional Ultrasound Technique

Surgeons have utilized interventional ultrasound for decades as a diagnostic tool and to guide biopsies and drainage of fluid collections [1–3]. Since, it is an invasive procedure, it warrants a defined protocol; an informed consent from the patient must be obtained [4] and the patient should be advised on the low mortality and morbidity (less than 0.05 %) associated with interventional ultrasound [5]. A sterile environment should be maintained, including prepping and draping the patient's abdomen and ensuring that the ultrasound probe

E.J. Hagopian, J. Machi (eds.), *Abdominal Ultrasound for Surgeons*,
DOI 10.1007/978-1-4614-9599-4_6,

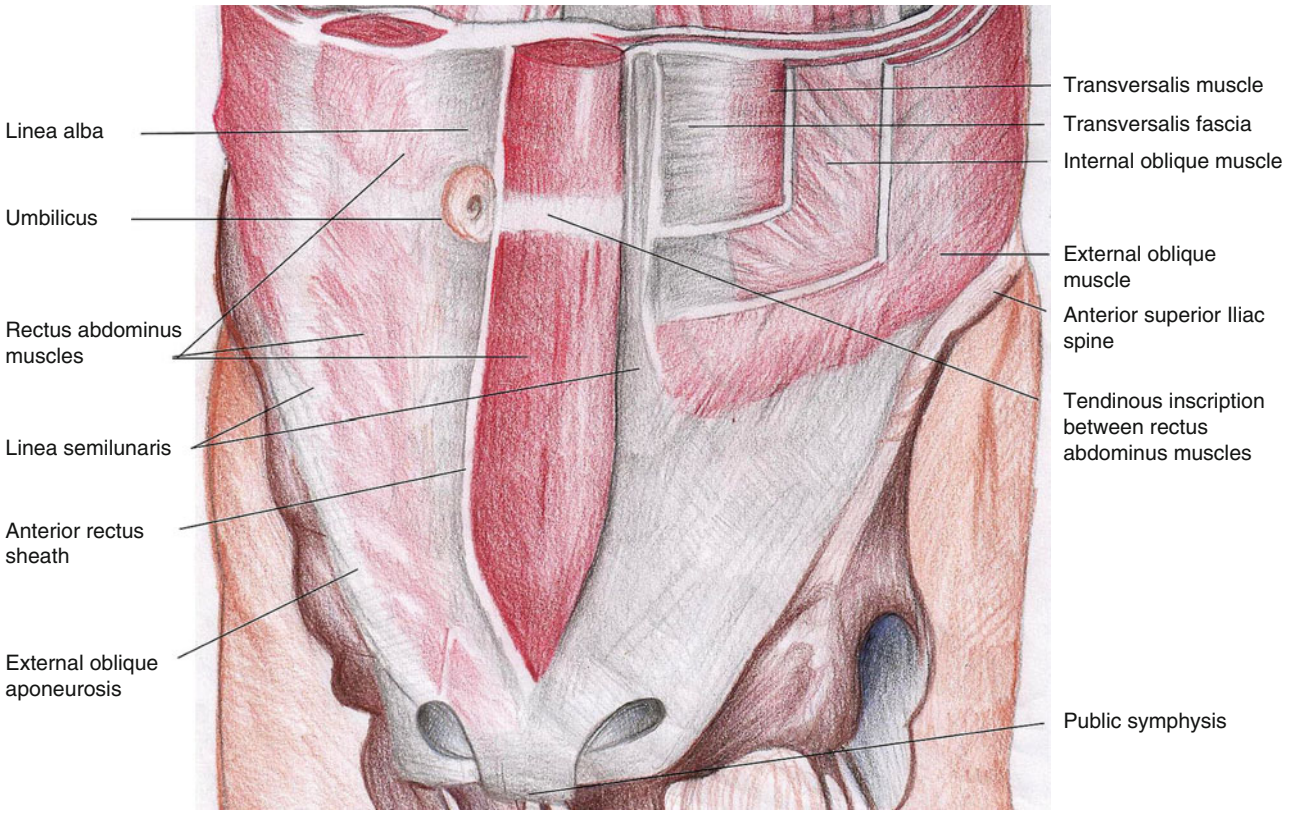

Fig. 6.1 Anterior abdominal wall musculature and fascia

is dressed with a sterile transparent drape. Administration of local anesthesia and sedation may also be warranted.

In interventional ultrasound, either a freehand technique or a biopsy guide device can be used. An echogenic needle facilitates precise placement and access to the area of pathology. These needles have different lengths and biopsy sampling sizes, which are used based on the patient's body habitus and the location of the pathology to be sampled. For abdominal wall pathology, a needle with a length of 3–4 cm and caliber ranging from 14 to 23 gauge is employed depending on the intended purpose of the intervention; it is generally advisable to use the thinnest needle allowable. An 18–20 gauge needle is advisable when aspirating fluid collections, cysts, and abscesses. A smaller 22–23 gauge needle is sufficient when obtaining a cytology sample. A Menghini or an automatic biopsy needle (14–21 gauge) can be used for obtaining a tissue sample. An adjustable needle-steering device (12–20 gauge) can be used alternatively [1].

Abdominal Wall Anatomy

Anterior Abdominal Wall Musculature and Fascia

Examination of the abdominal wall by ultrasound requires knowledge of the abdominal wall anatomy. The anterolateral abdominal wall is composed of nine layers: skin, subcutaneous tissue, superficial fascia, external oblique muscles, internal oblique muscle, transversus abdominis muscle, transversalis fascia, preperitoneal tissue, and peritoneum (Fig. 6.1). Anteromedially, the rectus abdominis muscles replace the oblique and transversus muscles and lie within the rectus sheath. The midline of the abdomen is marked by the linea alba, which is a band of crisscrossing fibers extending from the xiphoid process to the pubic symphysis (Fig. 6.2). Separating the rectus abdomini muscles from the oblique and transversalis muscles laterally on each side is the linea semilunaris (Fig. 6.3). The linea semicircularis, also known as the arcuate line of the rectus sheath, is an anatomical line (that is not always clearly defined) along the inferior posterior rectus sheath marking a change in its composition (Table 6.1).

On ultrasound, the skin is echogenic and measures a couple of millimeters in thickness. The subcutaneous tissue will appear as oval hypoechoic nodules demarcated by echogenic septae. Interspaced within the tissue are perforating vessels. Below the subcutaneous layer lie the muscles and their investing fascia (Fig. 6.4). Inferiorly the external oblique aponeurosis curves inward on themselves to form the inguinal ligament (Poupart's ligament), which is the shelf of the inguinal canal. The internal oblique muscles lie posterior to the external oblique muscles. Also, in males, inferiorly, the

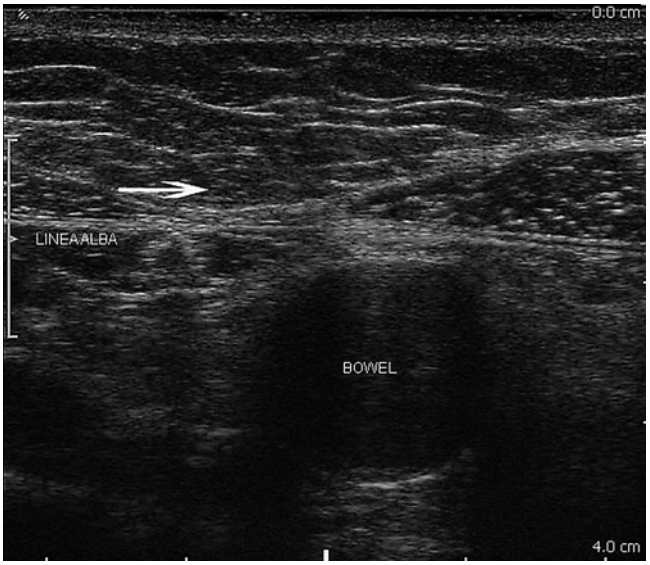

Fig. 6.2 Abdominal wall anatomy at the abdominal midline. The linea alba is noted by the *arrow*

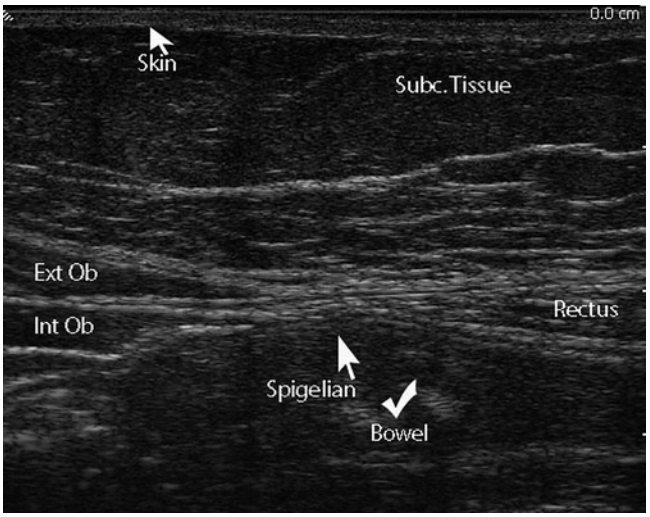

Fig. 6.3 Linea semilunaris. The linea semilunaris along the lateral margin of the inferior rectus muscle is where a Spigelian hernia is expected to occur

Table 6.1 Ultrasonographic appearance of abdominal wall anatomy

Abdominal wall component	Sonographic features
Skin	Hyperechogenic
Subcutaneous tissue	Oval hypoechoic nodules demarcated by echogenic septae
	Perforating vessels may be present
Fascia	Dense hyperechoic bands
Muscle	Intermediate echogenicity, echogenic dotting within each layer
Preperitoneal space	Hypoechoic adipose and areola tissue
	Inferior and superior epigastric vessels visible with Doppler

internal oblique aponeurosis fibers run alongside the spermatic cord to form the cremasteric muscles. The transversalis fascia lies posterior to the transversalis muscle and anteromedially forms the most posterior layer of the posterior rectus sheath prior to inserting at the linea alba. Medially, between the linea semilunaris and the linea alba lie the rectus abdominis muscles (Fig. 6.2). On ultrasound, the above muscle layers are of intermediate echogenicity and have echogenic dotting within each layer. The fascial layers separating the muscle layers appear as echogenic bands (Fig. 6.4).

Preperitoneal Space and Peritoneum

The preperitoneal space lies deep to the abdominal wall muscle layers and the transversalis fascia. This space contains adipose and areolar tissue and includes the inferior and superior epigastric artery and vein and the umbilical ligaments. The medial umbilical ligament is the obliterated remnant of the fetal umbilical artery, and the median umbilical ligament is the remnant of the urachus, which persists as fibrous cord along the midline extending from the bladder to the umbilicus. Superior to the umbilicus and extending towards the liver is the falciform ligament. The ligamentum teres, also known as the round ligament, is the free margin of this falciform ligament and is the obliterated remnant of the umbilical vein coursing from the left portal vein to the umbilicus. The preperitoneal fat layer is a relatively thin layer measuring less than a cm in thickness on ultrasound.

Vascular Supply of the Anterior Abdominal Wall

The inferior intercostal, lumbar, epigastric, and deep circumflex iliac arteries supply the arterial blood supply to the abdominal wall. The intercostal and lumbar arteries course alongside the nerves as bundles between the internal oblique and transversus abdominis muscles (Fig. 6.3). The superior epigastric artery is one of the terminal branches of the internal mammary artery and courses within the rectus sheath where it collateralizes with the inferior epigastric artery, which is a branch of the external iliac artery that courses superiorly in the preperitoneal space before piercing the rectus sheath. When imaging the abdominal wall with ultrasonography, it is important to identify the vessels in this preperitoneal layer prior to proceeding with any invasive intervention (Fig. 6.5a, b). The lymphatic drainage of abdominal wall is also similar to the venous outflow system whereby the supraumbilical lymph channels ultimately drain into the axillary basin while the infraumbilical channels drain into the superficial inguinal nodes. The lymphatic vessels from the liver also communicate with the periumbilical lymphatics via the ligamentum teres.

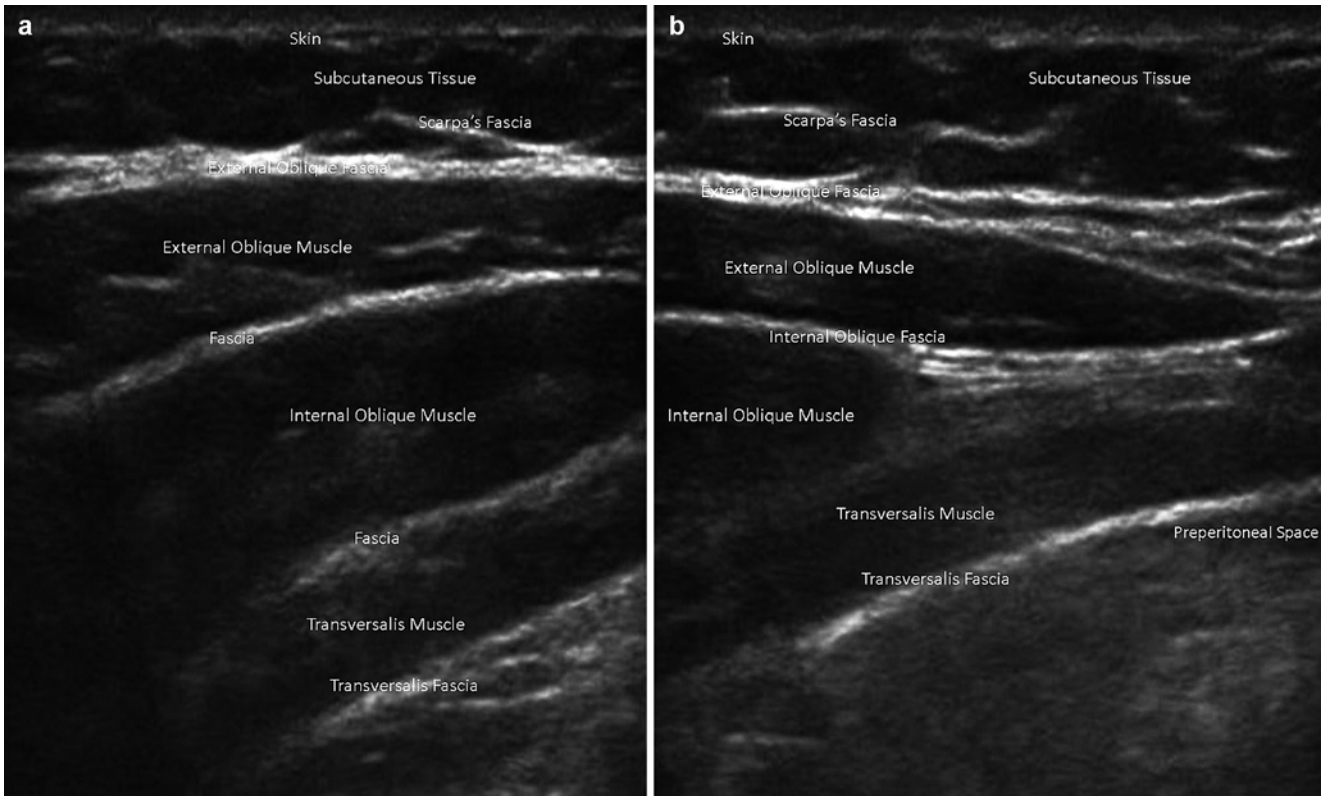

Fig. 6.4 Abdominal wall muscles and fascia on ultrasound. (**a**) Lateral abdominal wall. (**b**) Medial abdominal wall, lateral to linea semilunaris

Abdominal Wall Pathology and Intervention

A thorough physical examination will identify most pathological conditions within the abdominal wall. However, patient body habitus, edema, or complex masses can present a diagnostic dilemma for the clinician. US serves as a first-line tool in the identification, characterization, and management of abdominal wall pathology. Most pathology of the abdominal wall presents as a mass that may or may not be associated with skin changes. Ultrasound can further discern characteristics of the mass (solid versus cystic, complex versus simple, border regularity, etc.) as well as its location to the abdominal cavity and relationship to other abdominal wall structures. It is especially valuable in difficult-to-examine patients that are obese or comatose (Fig. 6.6). An image-guided biopsy using a #22 gauge needle or a #14 core biopsy can accurately and safely make a diagnosis after initial physical examination and ultrasound imaging [6, 7].

In this section, we review abdominal wall pathology and discuss US-guided interventions (Table 6.2).

Rectus Diastasis

Rectus diastasis is characterized by a thinning of the linea alba so that the distance between the rectus muscles is increased. There is no defect in the underlying aponeurosis and transversalis fascia; thus, there is no actual hernia. The patient may have a midline bulge as a result of this diastasis that is often mistaken as a hernia (Fig. 6.2). Management usually entails reassurance to the patient. If surgical correction is desired by the patient, abdominoplasty techniques are utilized. Ultrasound has been shown to be an accurate method of measuring the supraumbilical and periumbilical diastasis for the purposes of operative planning [8].

Rectus Sheath Hematomas

Hematomas within the rectus sheath are uncommon. They may develop spontaneously, yet, they often are associated with traumatic injury, pregnancy, coughing, or the use of anticoagulation therapy. They present with an acute onset of abdominal pain and tenderness that may be mistaken for peritonitis. In advanced cases, there may also be periumbilical or flank ecchymosis. Abdominal ultrasonography and CT scan aid in identifying the extent of a hematoma. The sonographic appearance of a rectus sheath hematoma varies with the age and location of the hematoma (Fig. 6.7). Above the arcuate line, the hematoma will have a lens-shaped appearance, whereas below the arcuate line, it may be more extensive, even crossing the midline or compressing the bladder [1].

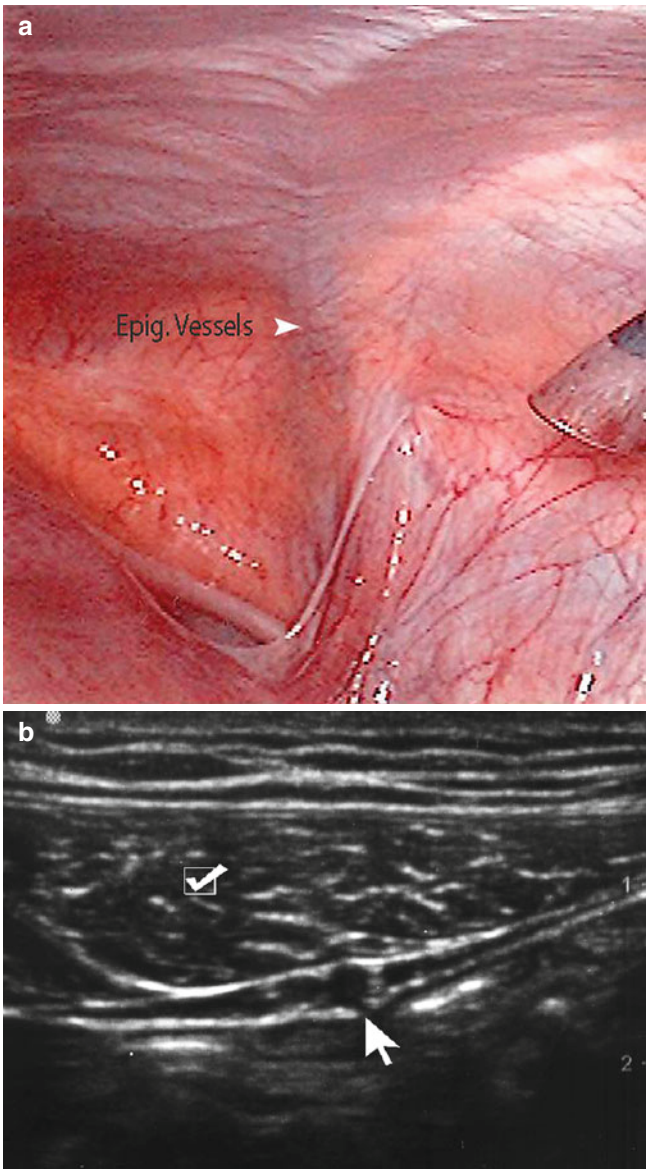

Fig. 6.5 (**a**) Note epigastric vessels through laparoscopic view. (**b**) Ultrasound imaging of epigastric vessels (*arrow*) and rectus abdominis muscle (*checkmark*)

Hematomas are primarily hypoechoic but can have septal or cystic components with echogenic borders [9]. Varying echogenicities within the hematoma represent different states of organized clot formation [10, 11]. Acute hematomas are homogenous and echogenic, while late-stage hematomas can be anechoic [10].

Management is usually conservative involving bed rest, analgesics, correction of coagulopathies, and blood transfusions as needed. If persistent bleeding is suspected, angiographic embolization of the bleeding of the vessel may be warranted, and if this is not available or successful, operative hemostasis and hematoma evacuation may be necessitated. Ultrasonography can be utilized to screen for hematomas

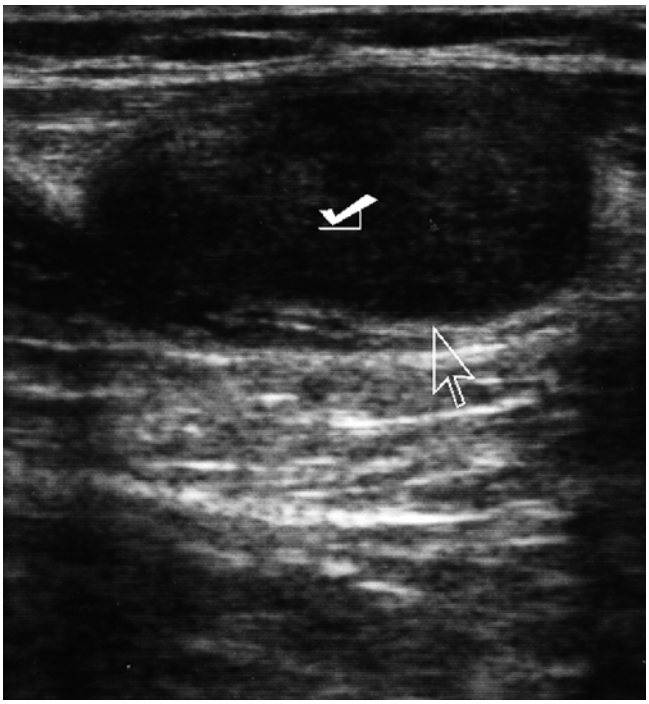

Fig. 6.6 Ultrasound of the abdominal wall depicting tumor implant (*check mark*). *Arrow* points to interface between tumor and wall

Table 6.2 Ultrasonographic appearance of abdominal wall masses

Abdominal wall pathology	Sonographic features
Rectus sheath hematoma	Primary hypoechoic but varies with age and location of the hematoma Acute hematomas are homogenous and echogenic while late-stage hematomas can be anechoic Above the arcuate line: lens-shaped appearance Below the arcuate line: more extensive and may cross midline
Hematoma	Variable echogenicity Acutely hyperechoic
Seroma/cyst	Simple fluid: anechoic, homogeneous appearance, posterior enhancement Complex: anechoic and hyper-/hypoechoic, heterogeneous
Abscess	Echogenic rim enhancement Variable echogenicity within cavity with presence of debris and septations
Urachal cyst	Well-circumscribed fluid collections Located along the lower midline Anechoic Varying internal echogenicity when infected with associated adjacent soft-tissue stranding
Abdominal wall varices	Dilated veins visible with Doppler Recanalized umbilical vein is anechoic in background of fatty falciform ligament
Endometriosis	Irregular hypoechoic mass Scattered internal echoes and internal vascularity

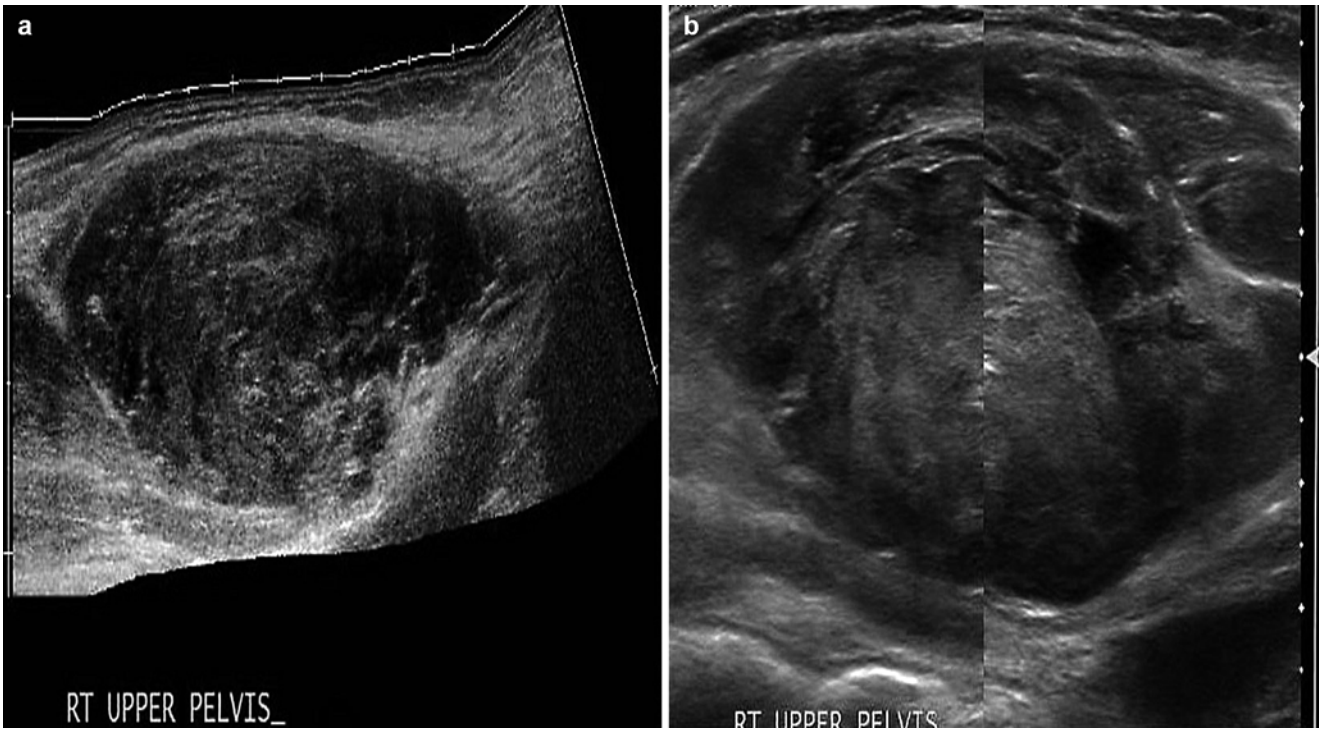

Fig. 6.7 Rectus sheath hematoma. (**a**) Rectus sheath hematoma below the arcuate line, with varying stages of echogenicity. (**b**) Acute-stage rectus sheath hematoma, with early organized clot formation (hyperechoic)

that may require surgical intervention. Hematomas that are larger in diameter and demonstrate the presence of intra-abdominal free fluid on ultrasound are more likely to benefit from surgical exploration [12]. Ultrasonographic treatment of rectus sheath hematomas, where repeated sessions of non-thermal pulsed sonography are employed, has also been reported in the physical therapy literature [13].

Abdominal Wall Fluid Collections

Abdominal wall fluid collections include cysts, hematomas, seromas, and abscesses. Ultrasonography is a useful modality in identifying a fluid collection and its characteristics. Hematomas may be spontaneous, postsurgical, or related to anticoagulation therapy or traumatic injury. If warranted, hematomas may be drained with image guidance. Abscesses have a variable appearance on ultrasound. They are typically irregular fluid collections containing septations and fluid debris and may have air-fluid levels (Fig. 6.8). They may also exhibit peripheral hyperemia with Doppler evaluation [10]. If gas bubbles are present with the abscess, they will be echogenic and demonstrate acoustic shadowing [14]. Seromas are usually more homogenous anechoic or hypoechoic fluid collections on ultrasound (Fig. 6.9). They are usually encountered following an abdominal operation, particularly following ventral hernia repairs. The development of postoperative seromas may be prevented with the use of pressure dressings and abdominal binders. If there is no evidence of superinfection, it is acceptable to observe a seroma without intervention, as there is a risk of introducing infection with needle aspiration. If a seroma or hematoma appears infected or an abdominal wall abscess is identified, operative drainage or needle drainage with image guidance is warranted in addition to antibiotic therapy. For larger fluid collections that are percutaneously drained, a drain may be left in place to facilitate additional drainage (Figs. 6.10 and 6.11).

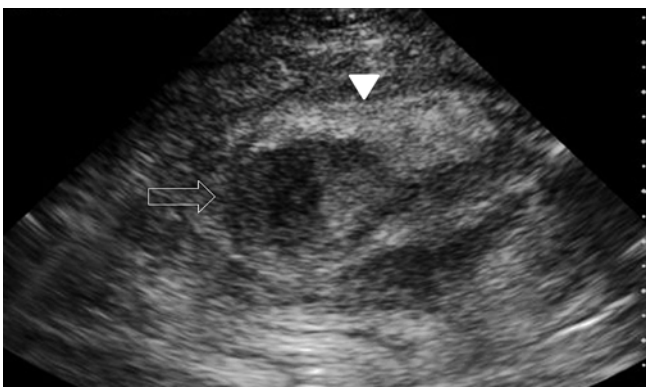

Fig. 6.8 Abdominal wall abscess (*solid arrow*). Abscess at umbilical incision site following laparoscopic appendectomy. Echogenic rim enhancement is seen. The abscess cavity demonstrates varying echogenicities with debris

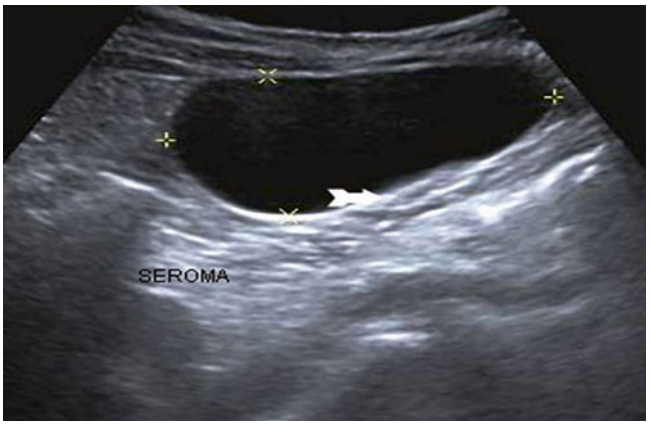

Fig. 6.9 Postoperative seroma. Anechoic fluid collection near umbilical incision consistent with postoperative seroma

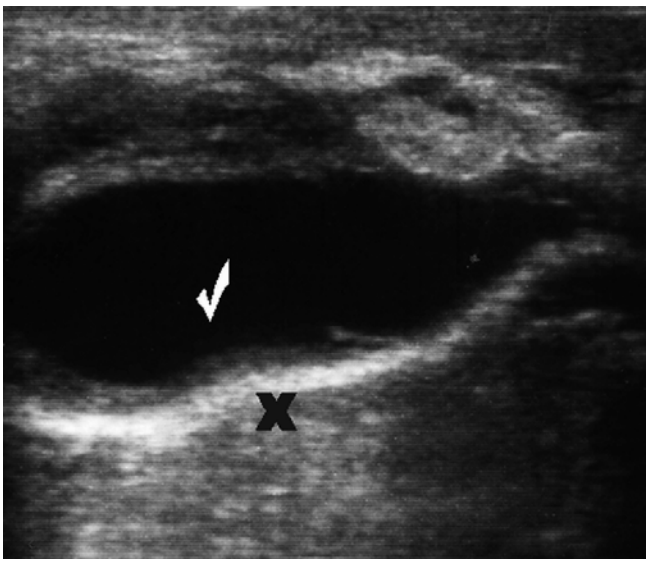

Fig. 6.11 Postoperative seroma (*checkmark*) following repair of ventral hernia. Note mesh (*X*)

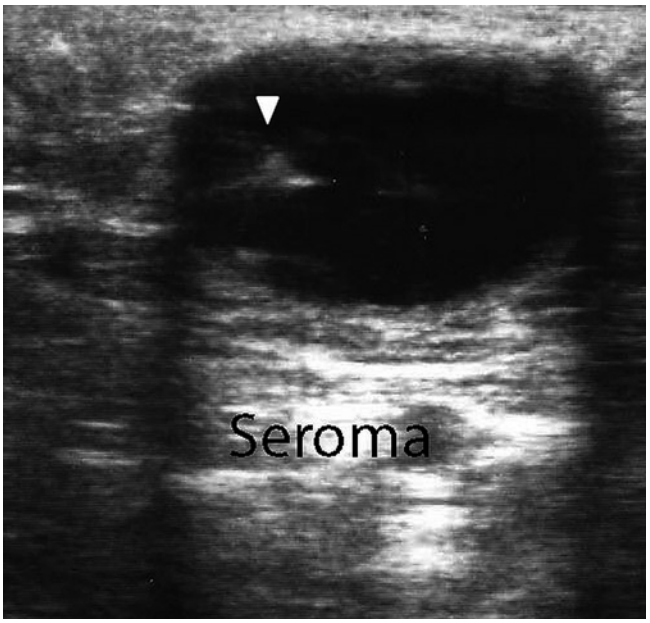

Fig. 6.10 Postoperative abdominal wall mass representing a seroma with enhancement. Note needle within the seroma (*arrowhead*)

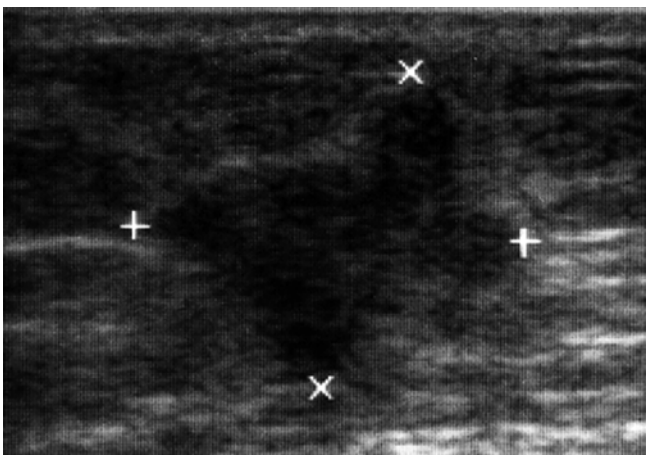

Fig. 6.12 Metastatic nodule in the abdominal wall following a resection for retroperitoneal sarcoma. The axis of the tumor (+, ×)

Abdominal Wall Neoplasms

Abdominal wall neoplasms present as painless palpable masses. Primary lesions may arise from any of the abdominal wall components: connective tissue, muscle, fat, blood vessels, or lymphoid tissue. These include benign soft-tissue neoplasms such as lipomas and desmoid tumors as well as malignant neoplasms such as sarcomas. Desmoid tumors and sarcomas are the most common primary malignancies of the abdominal wall. Metastatic neoplastic lesions may also be found in the abdominal wall, which often is associated with transperitoneal seeding of the abdominal wall by intra-abdominal malignancies (Fig. 6.12). Ultrasound examination permits precise definition of the mass as well as accurate biopsy. A diagnostic dilemma frequently occurs with these incisional wall masses where a recurrent tumor implant, a hernia, or a fluid collection could be found (Fig. 6.13). Ultrasound guidance is of value in obtaining a diagnostic biopsy of small nodules in the abdominal wall that are concerning for metastases (Table 6.3).

Benign Tumors

Lipomas, neurofibromas, and hemangiomas are the most common benign neoplasms of the abdominal wall. Lipomas are well-circumscribed mobile lesions. On ultrasound, they will have a variable echogenicity that is discrete from the

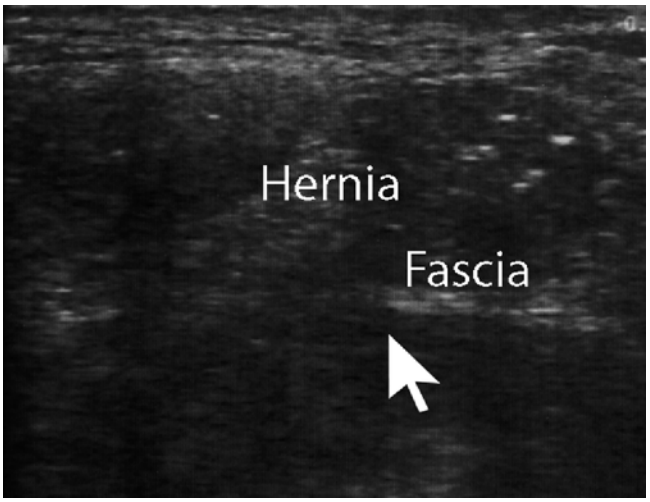

Fig. 6.13 Postoperative incisional hernia with incarcerated bowel

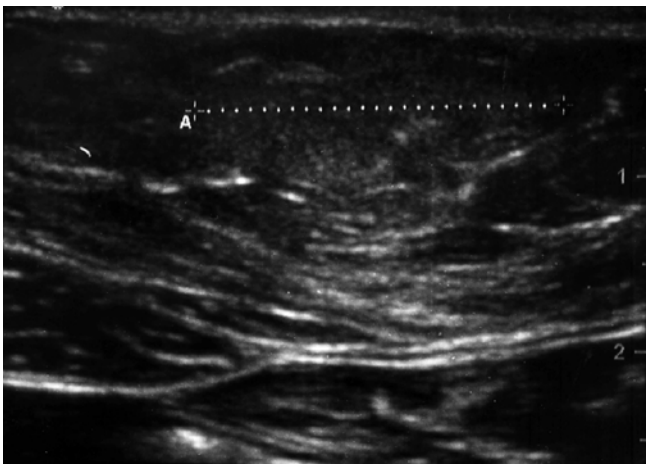

Fig. 6.14 Subcutaneous abdominal wall lipoma. Notice the smooth border and isoechoic content. Lipomas could present with bilateral or unilateral shadows

Table 6.3 Ultrasonographic appearance of abdominal wall tumors

Abdominal wall pathology	Sonographic features
Lipoma	Variable echogenicity that is discrete from the surrounding fat and muscle
	May have an echogenic capsule
Hemangioma	Multiple hypoechoic or anechoic cystic areas within an echogenic hypervascular background
Desmoid tumor	Solid
	Hypoechoic
	Abutting fascial planes or muscular tissue
Sarcomas	Irregular
	Solid
	Hypoechoic
	May have localized areas of necrosis or fluid
Metastatic lesions	Irregular
	Hyperechoic
	Irregular shadow

surrounding fat and muscle, and they may have an echogenic capsule [15] (Fig. 6.14). Hemangiomas are typically very small in diameter (millimeters) and on ultrasound will have multiple hypoechoic or anechoic cystic areas within an echogenic hypervascular background [10].

Desmoid Tumor

Desmoid tumors, or *aggressive fibromatosis*, are rare neoplasms that arise from fibroblast cells in either fascia or muscle. They may be intra-abdominal (pelvic and mesenteric), extra-abdominal (shoulder girdle or extremities), or abdominal wall tumors. When the tumor is superficial, it arises from the fascia and typically is slow growing in nature and of small size. These lesions are commonly referred to as *Dupuytren's fibromatosis*. Deeper lesions arise from the musculoaponeurotic tissues and are usually more aggressive in growth rate and size. Although these tumors do not metastasize and are thus considered benign lesions, they are locally aggressive and often recur following resection.

Additional characteristics of the mass and the extent of involvement may be delineated with the use of an ultrasound. If the lesion is solid, hypoechoic, and abutting fascial planes or muscular tissue, one should be suspicious for a desmoid lesion. If an ultrasound is inadequate, further extent of the lesion may be defined with the use of MRI. The lesion requires biopsy for diagnosis, which may be obtained with a core needle or as an incisional biopsy under ultrasound guidance.

The treatment of abdominal wall desmoids involves surgical resection with tumor-free margins. Local recurrence rate of these tumors can be as high as 40 % [16], and these recurrent tumors will also require resection. If a lesion is unresectable, primary radiation treatment may be considered as well as palliative chemotherapy with antiproliferative cytotoxic agents.

Sarcoma

The most common primary malignant neoplasm involving the abdominal wall is a sarcoma. These sarcomas, depending on what layers and cell types of the abdominal wall soft tissue are involved, can be of several subtypes: liposarcoma, fibrosarcoma, leiomyosarcoma, rhabdomyosarcoma, and malignant fibrous histiocytoma. The clinical progression of these tumors is reflective of their histology, size, and location.

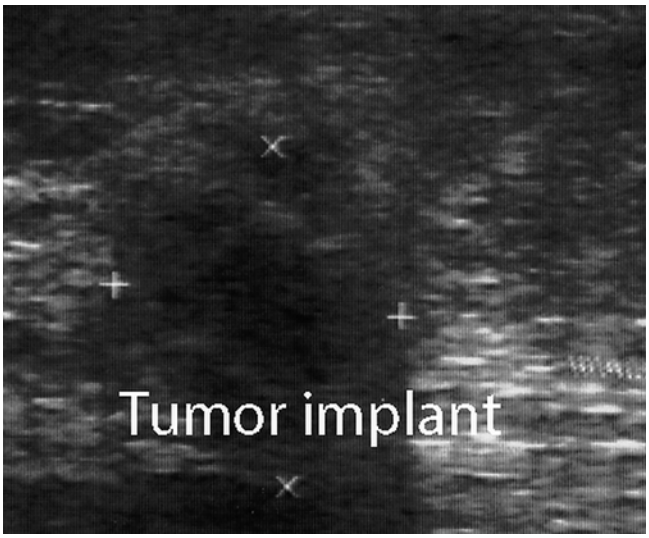

Fig. 6.15 Abdominal wall tumor implant in a patient with a history of colon cancer. The axis of the tumor (+, ×)

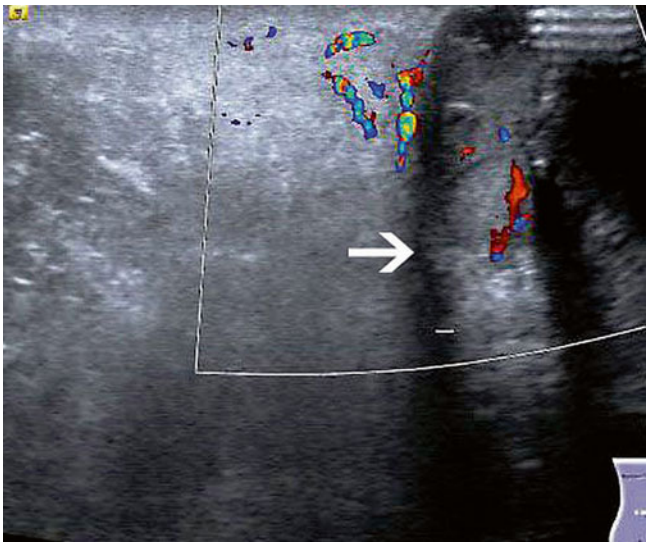

Fig. 6.16 Infected infraumbilical abdominal wall urachal cyst (*arrow* points at cyst wall)

These abdominal wall sarcomas can present as painless abdominal wall masses. Suspicion for malignancy arises with masses that are solid, large, fixated, and fast growing. On ultrasound, a sarcomatous lesion will be a hypoechoic solid lesion that may have localized areas of necrosis or fluid [10]. MRI can also be used to further delineate extent of disease. These lesions require guided biopsies, either incisional or percutaneous, to confirm their pathological diagnosis.

Metastatic Neoplasm

Transperitoneal, hematogenous, lymphatic seeding of intra-abdominal carcinomas or melanomas may result in metastatic lesions in the abdominal wall (Fig. 6.15). Cases of port-site seeding after laparoscopic surgery have also been reported in the literature, particularly following laparoscopic cholecystectomy where the cancer diagnosis was unknown at the time of operation. A metastatic deposit at the umbilicus is known as a Sister Mary Joseph's nodule. These lesions may be characterized and biopsied with sonographic guidance and are typically treated with surgical resection and radiation as needed. Ultrasound has also been reported to be of use in guiding insertion of applicator needles that can administer brachytherapy to abdominal wall metastases from colorectal cancer [17].

Other Abdominal Wall Masses

Urachal Cyst

An urachal cyst is a sinus remnant that persists between the umbilicus and bladder. It is usually present in the lower third of the urachus but may lie inferior to the umbilicus as well. These cysts can be depicted on ultrasound, where there will be well-circumscribed fluid collections that are anechoic, along the lower midline [15]. When infected, they have varying internal echoes and may be associated with adjacent soft-tissue inflammatory changes and urinary bladder wall thickening on ultrasound [18]. If symptomatic or associated with recurrent urinary tracts infections, these cysts should be surgically excised (Fig. 6.16).

Vascular Anomalies

Patients with portal hypertension often recannulate their umbilical vein as a means to shunt blood flow to the systemic veins (caput medusae). Ultrasound with color Doppler can be utilized as a means to avoid these varices when performing abdominal wall procedures such as a paracentesis or placement of a percutaneous endoscopic gastrotomy tube in patients with portal hypertension (e.g., cirrhotic patients) [19].

Scar-Related Masses

Common masses that present in relation to prior surgical scars include stitch granulomas, heterotropic calcifications, and endometrial implants. A stitch granuloma will occur near a retained nonabsorbable suture and will demonstrate irregular borders and heterogenicity on ultrasound. Heterotrophic calcifications are benign lesions, which on US examination have posterior acoustic shadowing [10]. Endometriosis of the abdominal wall may occur following a prior gynecologic operation. It is the most common site of extraovarian or extrauterine endometriosis following a cesarean section operation [20]. The lesion may present as a painful solid mass near a previous scar. On ultrasonography, it

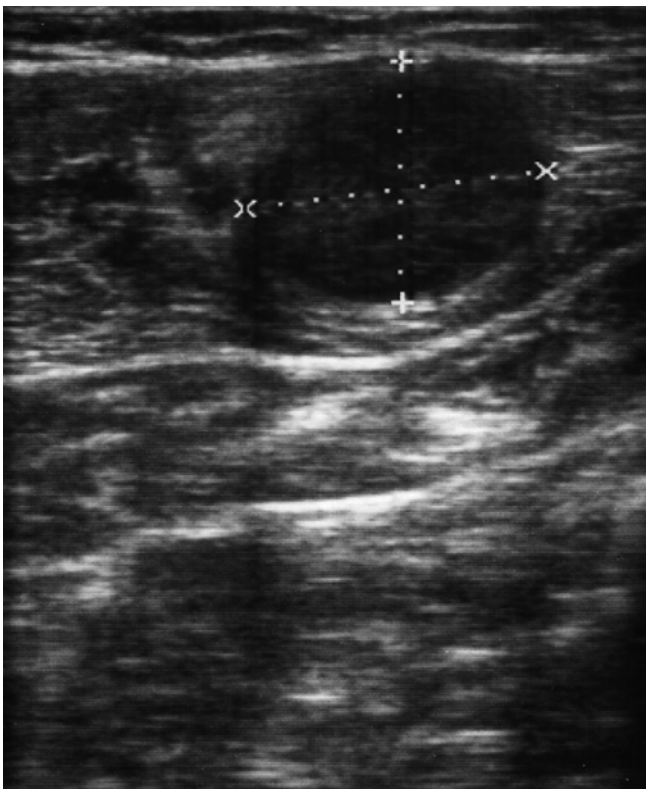

Fig. 6.17 Palpable mass in the abdominal wall following laparotomy for endometriosis. The axis of the tumor (+, ×)

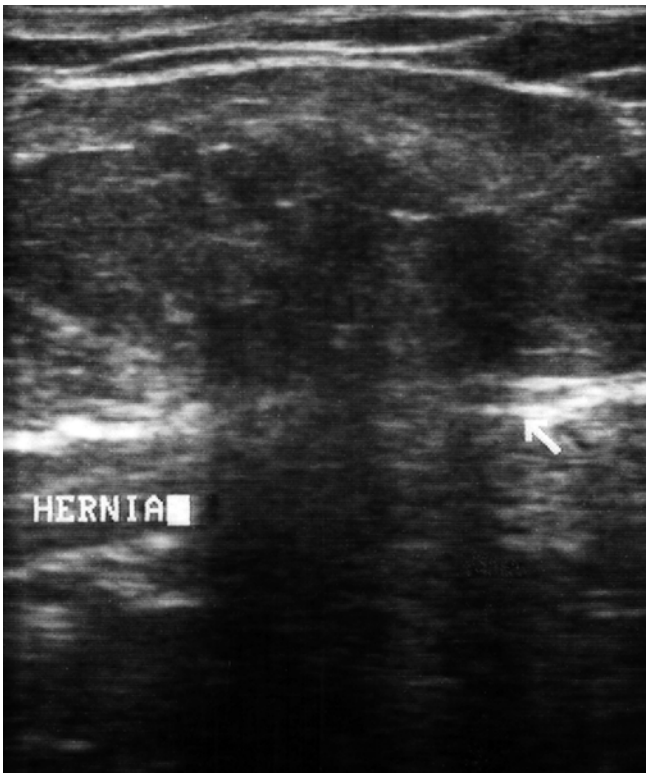

Fig. 6.18 Ventral hernia. Notice the hyperechoic fascia on both sides of the hernia sac. Points to fascia edge (*arrow*)

appears as a hypoechoic solid lesion, with scattered internal echoes and internal vascularity that can be demonstrated with color Doppler [21] (Fig. 6.17).

Abdominal Wall Hernias

In general, a hernia occurs when there is a protrusion of an organ or tissue through a defect in the surrounding fascia. Anterior abdominal wall hernias can be classified as either ventral hernias or groin hernias. Ultrasound can aid to diagnose a hernia, to define its contents, and to identify other possible defects. The hernia contents could be reducible, incarcerated, or strangulated. A strangulated hernia entails vascular compromise to the contents of the hernia sac that are irreducible through a small defect.

Ventral Hernias

Ventral hernias can be classified as umbilical, epigastric, or Spigelian hernias. In the event of acute incarceration, patients may present with strangulation or intestinal obstruction. Imaging, including ultrasonography and CT scan, may also play a role in diagnosis, particularly in evaluating the contents of the hernia sac and the size of the fascial defect. When bowel is contained with the hernia sac, US will demonstrate distinctive bright echoes from the intestinal gas [10]. Ultrasonography is also an especially useful and expedient way to screen for abdominal wall hernias, when there is no palpable mass or when there is a palpable mass of questionable etiology particularly in cases where there is pain and swelling in postoperative patients (Fig. 6.18).

Umbilical and epigastric hernias represent 10 % of all abdominal wall hernias [16]. Epigastric hernias can be found in 3–5 % of adults and are more common in men [16]. These hernias are located along the linea alba between the xiphoid process and the umbilicus, usually within 5–6 cm of the umbilicus. They are more common in patients with a single aponeurotic decussation at the linea alba as opposed to the usual decussation of fibers from all three muscle aponeuroses. There may be multiple defects, and most are off the midline. The fascial defect is usually small in size, and often pain is present due to incarceration of preperitoneal fat. Due to their association with pain and small size, operative repair is usually recommended. Ultrasound imaging of the abdominal wall can help to establish the diagnosis by identifying the mass, defining the fascial defect, and diagnosing possible multiplicity (Fig. 6.19).

Spigelian hernias are located along the Spigelian fascia, which is the aponeurotic layer between the rectus muscles medially and the semilunar line laterally (Figs. 6.3 and 6.20). They predominantly occur at the level of or below the arcuate line. Because the posterior rectus sheath comprises only

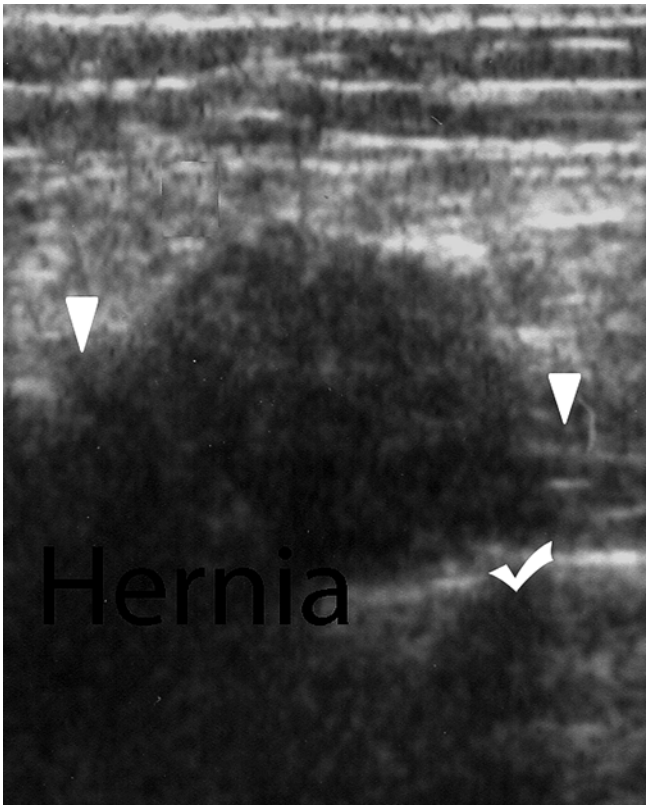

Fig. 6.19 Epigastric hernia. Notice the defect (→) in the aponeurosis (✓)

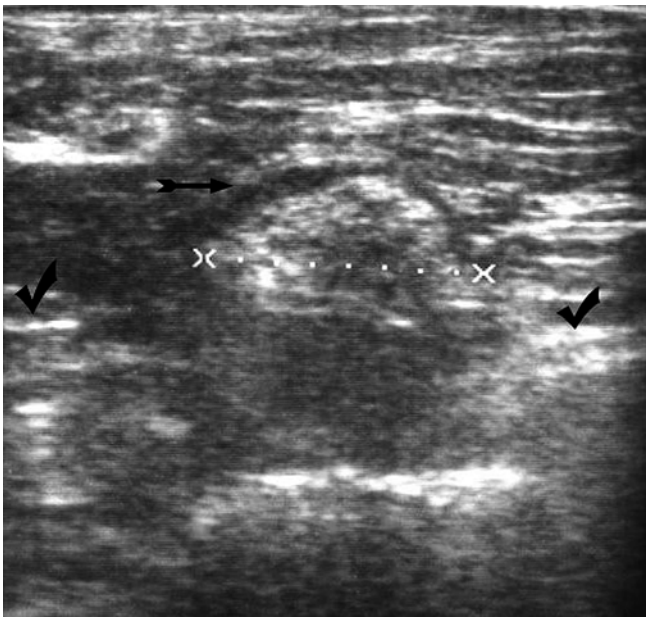

Fig. 6.20 Spigelian hernia. Note the defect in the aponeurosis (✓) and the hernia sac (→) containing small intestine (*dotted line*)

the transversalis fascia here, it is naturally weaker and more prone to herniation. The hernias are often intraparietal in that the hernia sac does not penetrate the external oblique

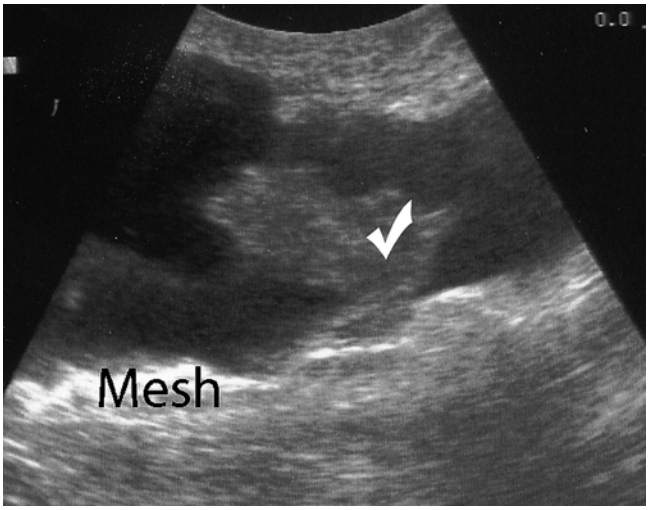

Fig. 6.21 Postoperative seroma following ventral hernia repair. Notice the mesh and the seroma with residual hematoma (✓)

aponeurosis. Because of their posterior location to the intact external oblique, a bulge is often not apparent on physical examination. An ultrasound of the abdominal wall often demonstrates a defect along the linea semilunaris, regardless of the presence of herniated bowel [22]. When evaluating with sonography, the transducer probe should be placed transversely at the lateral border of the rectus muscle (linea semilunaris) at the level of the umbilicus and should be shifted inferiorly in scanning for a Spigelian hernia [23].

Incisional hernias occur when intra-abdominal contents herniate through previous fascial incisions, the integrity of which may have been compromised by excessive tension, inadequate healing due to various conditions, conditions associated with increased intra-abdominal pressure, or surgical site infections. Following repair of large incisional hernias, usually with mesh, the incidence of seroma or hematoma within the cavity is rather high. In the postoperative period, questions concerning the nature of these masses frequently occur. US can define these collections, and if infection is present, drainage should be performed (Fig. 6.21). US-guided aspiration of these fluid collections is safer than blind aspiration. Presence of infected fluid permits immediate placement of drain.

Inguinal Region Anatomy

The inguinal region is a continuation of the abdominal wall muscles and fascia, yet it is an anatomically distinct region that warrants a separate discussion that is reviewed below.

At the inguinal region, the external oblique aponeurosis serves as the anterior, superficial border of the inguinal canal (Fig. 6.22). The inguinal ligament (Poupart's ligament) is actually the inferior edge of the external oblique aponeurosis

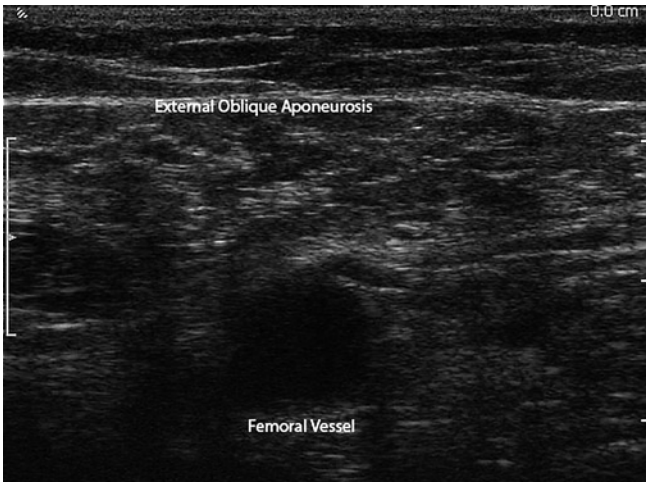

Fig. 6.22 Normal anatomy of the inguinal region (female)

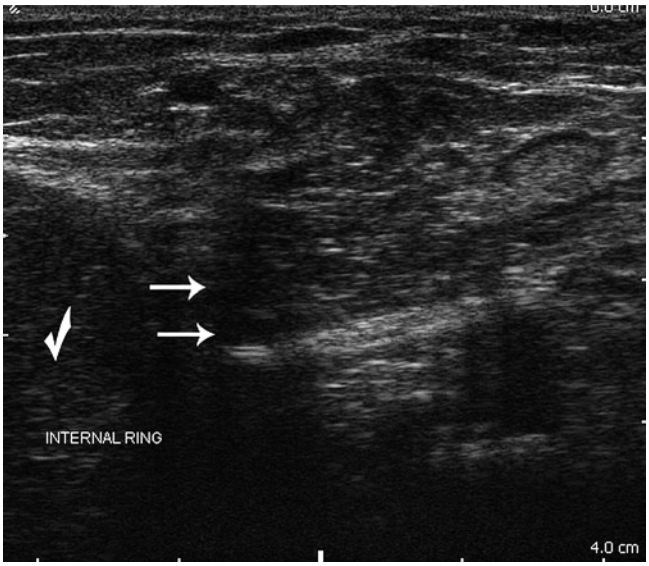

Fig. 6.24 Ultrasound of the inguinal region in a male without a demonstrable hernia. *Arrows* point to the epigastric vessels; *checkmark* indentifies internal ring

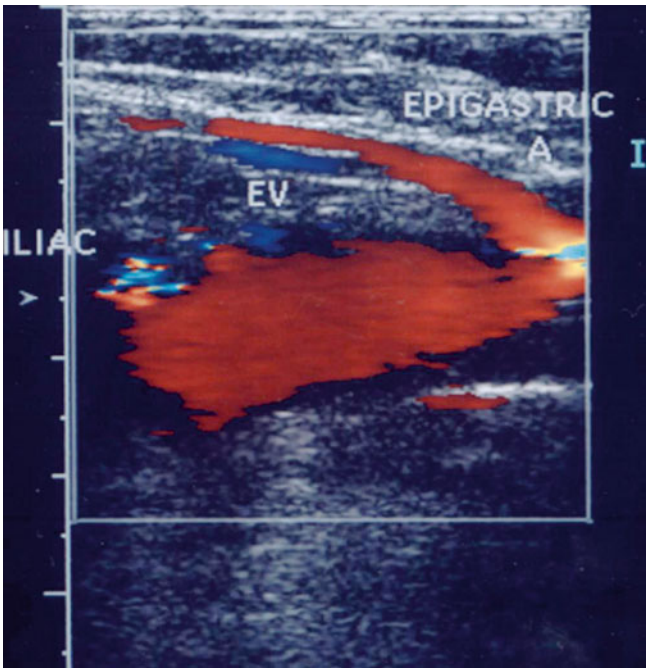

Fig. 6.23 Vasculature of groin with ultrasound using color Doppler

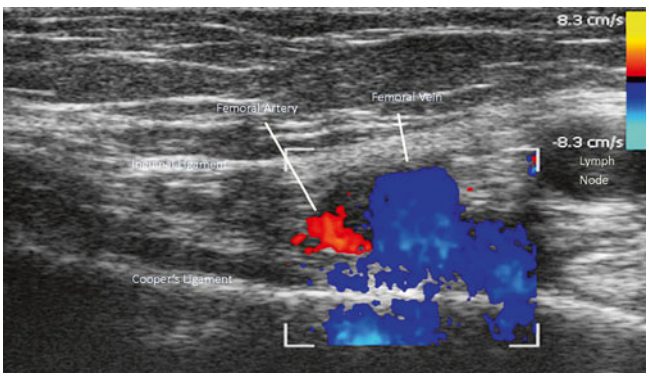

Fig. 6.25 Femoral canal anatomy on ultrasound with color Doppler. A femoral hernia occurs medial to the femoral vein

and runs from the anterior superior iliac spine to the pubic tubercle. The superior border of the canal is marked by the internal oblique muscle. As the internal oblique muscle and its aponeurosis courses medially towards the pubic tubercle, it joins the transversalis aponeurosis to form the conjoined tendon (which is actually present in only 5–10 % of patients) [16]. The floor of the inguinal canal is formed by the transversalis fascia and the margins of the inguinal floor are referred to as Hesselbach's triangle. The superolateral border of the triangle is marked by the inferior epigastric vessels (Fig. 6.23). The medial border is marked by the rectus sheath, and the inferior border is marked by the inguinal ligament.

The inguinal canal, which is about 4 cm in length, extends between the deep and superficial inguinal rings. The deep inguinal ring is an opening in the transversalis fascia through which the spermatic cord or round ligament pass prior to entering the inguinal canal. On ultrasonography, the cord can be seen in longitudinal and transverse planes as a heterogeneous echogenic structure with associated hypoechoic tubules and vessels, originating at the internal inguinal ring [23] (Fig. 6.24).

The femoral canal lies inferior to the inguinal ligament (Fig. 6.25). It is considered an anatomically distinct region from the inguinal canal. The iliopubic tract and Cooper's ligament constitute its anterior and posterior borders, respectively. The femoral vein lies laterally and medially; the pubic tubercle forms the apex of the femoral canal triangle [24].

Inguinal Region Pathology and Intervention

The etiology of groin masses may be difficult to diagnose based on clinical examination alone, especially in the obese and difficult-to-examine patients. Ultrasonography has proven to be a valuable tool in differentiating between the pathologies that may be encountered in the groin region. It is indicated in the preoperative setting as a tool to diagnose hernias as well as in the postoperative period when swelling of that region could be interpreted as a recurrent hernia, seroma, or hematoma. Seromas are frequently associated with laparoscopic repair of inguinal hernias.

Groin Masses

Superficial masses that appear as hypoechoic fluid collections in the groin region on sonography may be a cyst, hematoma, seroma, or abscess. In a patient who has had recent surgery in the groin region, a hematoma or seroma should be suspected (Fig. 6.26). An abscess may appear as a more complex fluid collection with septations and debris on sonography. Ultrasound-guided aspiration of the fluid collection can further aid in diagnosis if warranted.

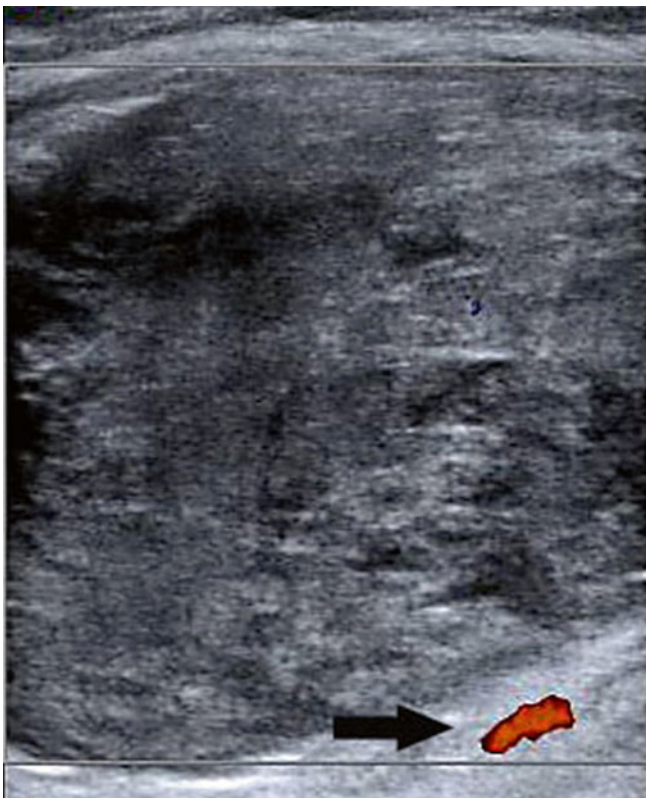

Fig. 6.26 Postoperative hematoma. Spermatic cord hematoma following inguinal hernia repair. *Arrow* points to epigastric vessel

A solid mass in the groin region may be a lymph node, an aneurysm, or a neoplasm (Fig. 6.27). On US, the pathologic lymph nodes may have varying echogenicities, can appear as multilobulated, and have varying amount of fat at the hilum [7]. Additionally, on ultrasound, nodes that are suspicious or metastatic may be spherical in shape (versus ellipsoid) and have a thickness-to-length ratio greater than 2:3 and a diameter greater than 5 mm [25]. The adenopathy may easily be confused with an abscess [7], and clinical correlation and ultrasound-guided aspiration or core biopsy may be warranted. Metastatic lymph nodes are most common from tumors arising from the genitourinary tract (vulva or vagina in females, penis or testes in males), the distal gastrointestinal tract (distal rectum and anus), or from the lower extremities. In general they are devoid of fat at the hilum. Ultrasonography is particularly useful in the surveillance of inguinal lymphatic and nodal basins in high-risk melanoma patients [26, 27] (Fig. 6.28).

Additional masses that can be encountered in the groin region are undescended and retractile testes (Fig. 6.29). The testes will appear as a homogeneous, predominantly hypoechoic mass with smooth borders and fine granularity on ultrasound [10]. Groin masses should be differentiated from scrotal masses for which there is an additional differential that includes hydroceles, varicocele, epididymitis or epididymal cyst, or testicular masses. Hydroceles are not continuous with the peritoneal cavity, and this can be confirmed with ultrasound. Varicoceles will demonstrate venous flow on Doppler ultrasound that is accentuated with the Valsalva maneuver [24]. There is a differentiation between the applicability of power Doppler and spectral (pulsed wave) color Doppler, which is especially important in the groin and scrotal region. Power Doppler allows for detection and direction of blood flow but is prone to motion artifact [28]. Spectral Doppler allows for the identification of artery versus venous flow and both must be identified in evaluating blood flow to the testes. Sonographic findings of

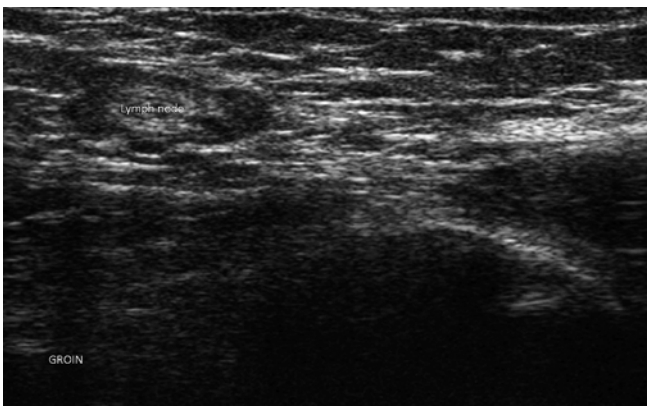

Fig. 6.27 Normal inguinal adenopathy. Notice the presence of increased echogenicity at the hilum indicating fat

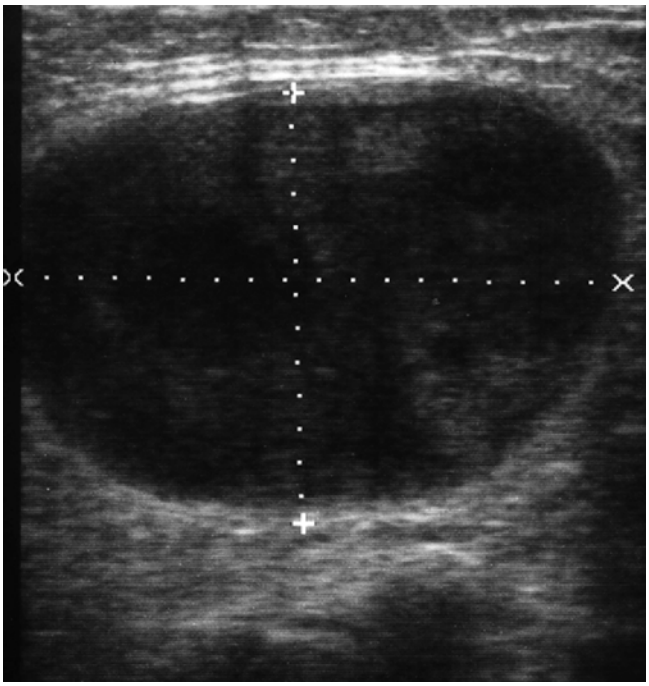

Fig. 6.28 A pathological lymph node may have irregular borders, is heterogeneous, and lacks hilar fat and thus appears hypoechoic. Fine-needle aspiration of the node showed melanoma

Table 6.4 Ultrasonographic appearance of groin masses

Inguinal region	Sonographic features
Undescended/retractile testes	Homogeneous Predominantly hypoechoic mass with smooth borders and fine granularity
Lymphadenopathy	Varying echogenicities May be multilobulated Metastatic nodes may be spherical in shape (versus ellipsoid), with diameter greater than 5 mm
Neoplasm	Solid Well defined, mobile, hypoechoic if benign Variable echogenicity, fixed, irregular if malignant
Scrotal masses	
Varicocele	Venous flow on Doppler ultrasound that is accentuated with the Valsalva maneuver
Epididymitis	Enlargement of the epididymis Decreased echogenicity due to edema Increased blood flow on Doppler ultrasound compared to the unaffected side
Hydrocele	Anechoic Does not communicate with peritoneal cavity
Testicular mass	Solid May be irregular

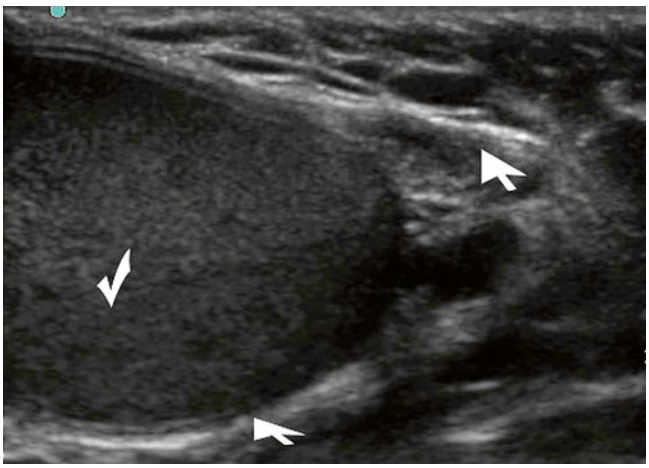

Fig. 6.29 Indirect inguinal hernia. Notice the location of the testicle (✓) within the inguinal canal. *Arrows* point to hernia sac

epididymitis include enlargement of the epididymis, decreased echogenicity due to edema, and increased blood blow on Doppler ultrasound compared to the unaffected side [28].

If the mass is in the femoral region, a femoral artery aneurysm or pseudoaneurysm should be suspected. Such a mass may be pulsatile and can easily be characterized as turbulent flow on sonography with color Doppler capabilities [24]. This flow of pseudoaneurysm is described as typical yin-yang flow on Doppler examination [29]. Ultrasound-guided injection of thrombin into pseudoaneurysm cavities has become more of common practice since its initial success was reported in 1997 [30] (Table 6.4).

Groin Hernias

The most common mass encountered in the groin region is a hernia. A groin hernia is either an inguinal hernia or a femoral hernia.

Inguinal Hernia

Inguinal hernias comprise up to 75 % of abdominal wall hernias [16]. Men are more likely, up to 25 times more, to have an inguinal hernia than woman. These hernias can be classified as either direct or indirect hernias. A direct inguinal hernia is marked by a defect in the floor of the inguinal canal, whereby the hernia sac protrudes medially to the deep inguinal ring inferior epigastric vessels. An indirect inguinal hernia is defined as a hernia sac and its contents passing though the deep inguinal ring, laterally to the inferior epigastric vessels, and alongside (usually medially) the spermatic cord or

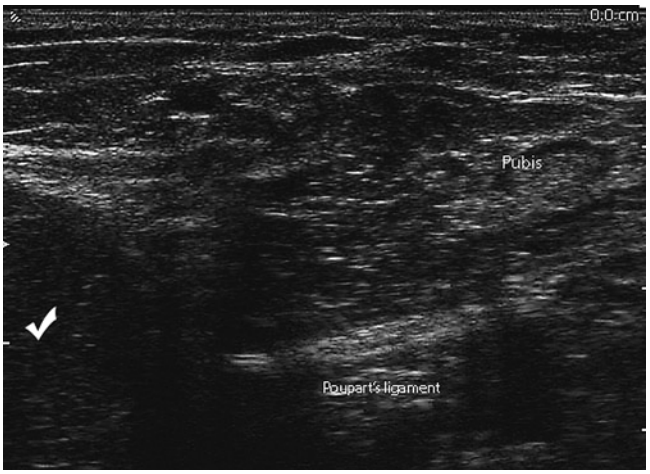

Fig. 6.30 Ultrasound of the inguinal region in a patient with a right indirect inguinal hernia (✓)

round ligament (Fig. 6.30). US is useful in diagnosing small indirect inguinal hernias in the patient presenting with acute onset of groin pain due to small incarcerated hernia containing preperitoneal fat.

An ultrasound, with its high degree of sensitivity and specificity in detection, can also aid in the diagnosis, particularly with occult hernias [31, 32]. Ultrasound has been shown to be quite accurate in identifying the presence of an inguinal hernia (>90 % accuracy) [32]. It can also be used to aid in identifying the type of hernia present (e.g., direct versus indirect) and in evaluating the viability of bowel that may be incarcerated [33, 34]. In identifying an indirect hernia on sonography, the transducer probe is positioned longitudinally (parallel to the inguinal canal), and the indirect hernia will be seen protruding anteriorly towards the transducer, lateral to the inferior epigastric vessel, at its origin, and then coursing medially along the canal towards the pubic tubercle and superficial ring [23]. In identifying a direct inguinal hernia, the transducer is again placed longitudinally along the inguinal canal and moved medially to identify a sac that protrudes anteriorly, originating medial to the inferior epigastric artery [23] (Figs. 6.30 and 6.31). The hernia sac's anterior protrusion can be accentuated with the Valsalva maneuver. The presence of peristalsis suggests the presence of viable bowel in the hernia sac [35]. Computed tomography (CT) of the abdomen/pelvis will also demonstrate an inguinal hernia.

Complications of an inguinal hernia repair include urinary retention, orchitis, groin pain from nerve injury, scrotal edema, seromas, hematomas, and abscesses. Postoperative fluid collections can be characterized with the use of ultrasonography. Seromas that are concerning for possible infection may be aspirated using ultrasound guidance. In cases of scrotal edema and hematomas following inguinal hernia repair, ultrasonography with Doppler can be utilized to ensure that vascular flow to the testes is not compromised (Fig. 6.26).

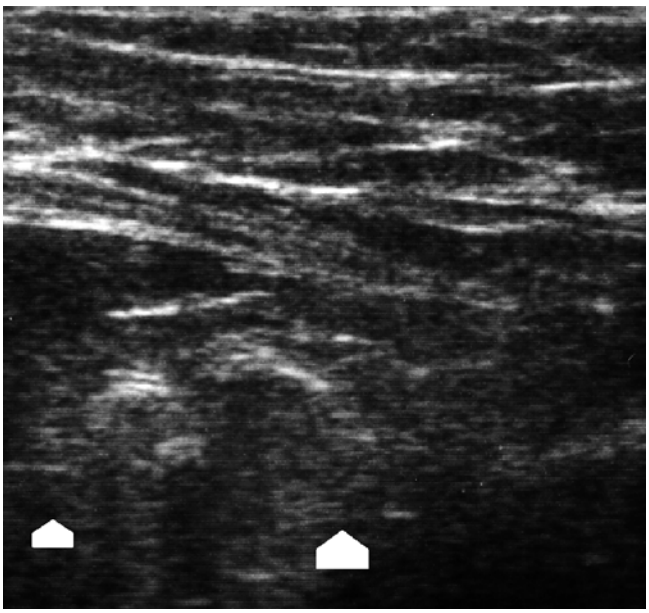

Fig. 6.31 Direct inguinal hernia. *Arrows* point to the defect in transversalis fascia

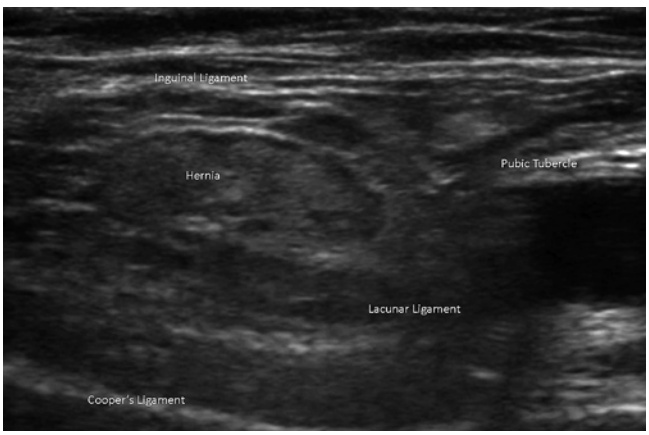

Fig. 6.32 Femoral hernia

Femoral Hernias

Femoral hernias are more likely to occur in women than men and are also associated with a higher risk of strangulation than inguinal hernias. In patients presenting with small bowel obstruction of uncertain origin, an ultrasound could be invaluable in the diagnosis of occult femoral hernias (Fig. 6.32). The transducer is placed inferior to the inguinal ligament and the femoral vein identified so that the area medial to it can be

Table 6.5 Ultrasound features of hernias

Abdominal wall hernias	May be reducible with transducer compression Distinctive bright echoes from the intestinal gas and presence of peristalsis if bowel presents with hernia sac
Groin hernia	May be reducible with transducer compression Distinctive bright echoes from the intestinal gas and presence of peristalsis if bowel present within hernia sac
Inguinal hernia	Indirect hernia: arises lateral to epigastric vessel (can be viewed with Doppler) Direct hernia: arises medial to epigastric vessel (can be viewed with Doppler)
Femoral hernia	Posterior to inguinal ligament and medial to femoral vessels
Femoral pseudoaneurysm	Turbulent flow, "yin-yang" flow on sonography with color Doppler

scanned for the presence of a hernia [23]. It is important to note that if the patient is asked to do the Valsalva maneuver during the exam, the femoral vein will dilate with the maneuver and could be mistaken for a hernia [23] (Table 6.5).

Interventional Ultrasound of the Abdominal Wall in the Perioperative Setting

Mapping of Abdominal Wall Adhesions

First described by Sigel et al., in 1991, the technique of graded compression, using ultrasound to detect and map abdominal wall adhesions prior to surgery has been utilized to identify safe access to the abdominal cavity [36, 37]. During real-time imaging, the abdominal viscera will demonstrate movement that varies with respiration. This movement, called visceral slide, can also be induced with manual graded compression with an ultrasound transducer. When this visceral slide appears restricted on manual compression, visceral adhesions to the abdominal wall are suspected in that particular region (Fig. 6.33). In this manner, one can map out the location of adhesions and thus avoid these areas when placing trocars during laparoscopic surgery. This technique has been shown to be reliable in preventing trocar-induced visceral injuries and its use is advocated in highly selective cases in planning abdominal wall cannulation for laparoscopy in patients with prior scars [38].

Perioperative Nerve Block

Abdominal wall nerve blocks have an established role in providing perioperative analgesia, and the majority of these blocks are now being performed with ultrasound guidance. Even though the majority of these nerve blocks are performed by anesthesiologists, the surgeon should be knowledgeable of the type of nerve blocks available in the perioperative setting to better select type of anesthesia given to the patient [39].

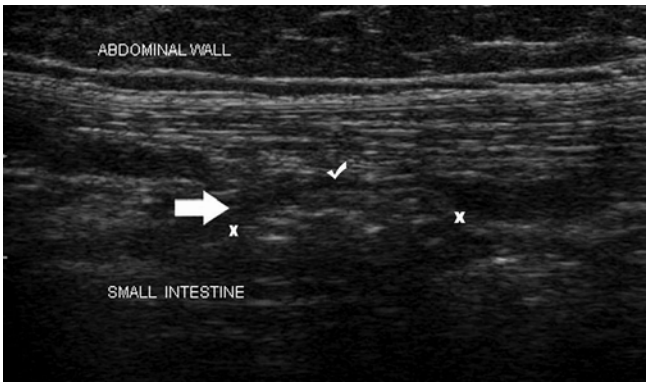

Fig. 6.33 Ultrasound-guided mapping of small bowel adhesions to abdominal wall. *Arrow* points to small intestine (*X*) adhesed to abdominal wall (✓)

The nerve supply to the abdominal wall arises from the anterior rami of the lower thoracic nerves and the first lumbar nerve. The seventh through twelfth thoracic nerves course anteromedially in the transversus abdominis plane anterior to the transversalis fascia and provide sensory and motor branches to the abdominal wall. The groin region includes several important nerves: iliohypogastric nerve, the ilioinguinal nerve, and the genital branch of the genitofemoral nerve. The iliohypogastric and ilioinguinal nerves are located medial and superior the anterior superior iliac spine beneath the external oblique aponeurosis, where they penetrate the internal oblique muscles and provide sensation to the skin, base of the penis, and upper medial thigh. The iliohypogastric nerve runs along the anterior surface of the internal oblique aponeurosis, medial and superior to the deep inguinal ring. The ilioinguinal nerve runs anterior to the spermatic cord in the inguinal canal. The genital branch of the genitofemoral nerve runs alongside the spermatic cord or round ligament in the inguinal canal and provides sensation to the cremasteric muscle and scrotal or labial skin.

The three most established ultrasound-guided nerve blocks of the abdominal wall are the ilioinguinal/hypogastric, transversus abdominis plane, and rectus sheath blocks (Table 6.6).

The ilioinguinal/hypogastric nerve block entails the infusion of local anesthetic typically 1–2 cm superior and medial to the anterior superior iliac spine. The use of ultrasound enhances the accuracy and efficacy of the block (Fig. 6.3). On ultrasound the nerve lies in the fascial layer between the internal oblique and the transversus abdominis muscles and appears as a hypoechoic structure surrounded by the more echogenic muscles and fat [40]. Since it is in close proximity to the deep circumflex artery, the use of color Doppler to

Table 6.6 Ultrasound-guided nerve blocks

Type of block	Location of anesthetic injection
Ilioinguinal/ iliohypogastric block	Within 2 cm to anterior superior iliac spine
	Inject below the external oblique muscle and internal oblique fascia
	Nerve appears as a hypoechoic structure surrounded by the more echogenic muscles and fat
	Ilioinguinal nerve lies in the same plane as the deep circumflex artery (can be seen with Doppler)
Transversus abdominis plane block	Inject below the internal oblique fascia within the transversus muscle, anterior to the transversalis fascia
	Location of administration most commonly within triangle of Petit or along midaxillary line
Rectus sheath block	Inject along the lateral margin of the plane between the rectus muscles and posterior sheath, where intercostal nerves enter the sheath

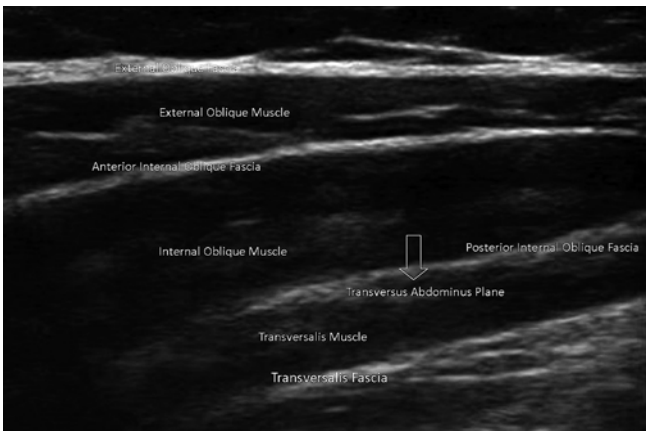

Fig. 6.34 Transversus abdominis plane block. Regional block for hernia repair is facilitated by infiltrating this space (*arrow*) with local anesthetic

identify this artery helps to identify the nerve [40]. The hypogastric nerve can be found medial to the ilioinguinal nerve. This ilioinguinal/hypogastric nerve block is routinely used for perioperative anesthesia during inguinal herniorrhaphies [41]. The nerve block can also be used in the postoperative setting to treat chronic pain following groin surgery [42], although its utility and long-term success have been questioned [43].

The transversus abdominis plane (TAP) block involves the ultrasound-guided infusion of the local anesthetic deep to the fascial layer (Fig. 6.34). They can be used for both laparoscopic and open procedures. There is no one method or protocol that has been demonstrated to be superior [44], but it is clear that the block in combination of local anesthesia offers better postoperative pain control than conventional local anesthesia alone [44, 45]. Long-term infusion of analgesics for chronic somatic pain via an indwelling catheter in the transversus abdominis plane has also been described [46].

Conclusion

Ultrasonography has a valuable role in the diagnosis and management of abdominal wall and groin pathology. The surgeon who is familiar with the anatomy and the wide differential of pathology that is reviewed in this chapter is especially equipped to utilize this modality for both diagnostic and therapeutic purposes in both the ambulatory and perioperative settings.

References

1. Velasco JM, Hieken TJ. Other transabdominal ultrasound. In: Machi J, Staren ED, editors. Ultrasound for surgeons. 2nd ed. Philadelphia: Lippincott Williams & Wilkins; 2005.
2. BERLYNE GM. Ultrasonics in renal biopsy: an aid to determination of kidney position. Lancet. 1961;2(7205):750–1. PubMed PMID: 13867961. eng.
3. Hancke S, Holm HH, Koch F. Ultrasonically guided percutaneous fine needle biopsy of the pancreas. Surg Gynecol Obstet. 1975;140(3):361–4. PubMed PMID: 1114427. eng.
4. Staren ED, Torp-Pedersen S. General interventional ultrasound. In: ED S, editor. Ultrasound for the surgeon. Philadelphia: Lippincott-Raven Publishers; 1997. p. 137–60.
5. Nolsoe C, Nielsen L, Torp-Pedersen S, Holm HH. Major complications and deaths due to interventional ultrasonography: a review of 8000 cases. J Clin Ultrasound. 1990;18(3):179–84. PubMed PMID: 2155937. eng.
6. Deitch EA, Engel JM. Ultrasonic diagnosis of surgical diseases of the anterior abdominal wall. Surg Gynecol Obstet. 1980;151(4): 484–6. PubMed PMID: 6447925. eng.
7. Lineaweaver W, Vlasak M, Muyshondt E. Ultrasonic examination of abdominal wall and groin masses. South Med J. 1983;76(5): 590–2. PubMed PMID: 6221409. eng.
8. Mendes DA, Nahas FX, Veiga DF, Mendes FV, Figueiras RG, Gomes HC, et al. Ultrasonography for measuring rectus abdominis muscles diastasis. Acta Cir Bras. 2007;22(3):182–6. PubMed PMID: 17546290. eng.
9. Fukuda T, Sakamoto I, Kohzaki S, Uetani M, Mori M, Fujimoto T, et al. Spontaneous rectus sheath hematomas: clinical and radiological features. Abdom Imaging. 1996;21(1):58–61. PubMed PMID: 8672974. eng.
10. Jain N, Goyal N, Mukherjee K, Kamath S. Ultrasound of the abdominal wall: what lies beneath? Clin Radiol. 2013;68:85–93. PubMed PMID: 22854266. ENG.
11. Lewiss RE, Wu S. Ultrasound diagnosis of rectus sheath hematoma. J Emerg Med. 2012;43(5):e337–8. PubMed PMID: 21820260. eng.
12. Klingler PJ, Wetscher G, Glaser K, Tschmelitsch J, Schmid T, Hinder RA. The use of ultrasound to differentiate rectus sheath hematoma from other acute abdominal disorders. Surg Endosc. 1999;13(11):1129–34. PubMed PMID: 10556453. eng.
13. Berná-Serna JD, Sánchez-Garre J, Madrigal M, Zuazu I, Berná-Mestre JD. Ultrasound therapy in rectus sheath hematoma. Phys Ther. 2005;85(4):352–7. PubMed PMID: 15794705. eng.

14. Yeh HC, Rabinowitz JG. Ultrasonography and computed tomography of inflammatory abdominal wall lesions. Radiology. 1982; 144(4):859–63. PubMed PMID: 6213981. eng.
15. Gokhale S. Sonography in identification of abdominal wall lesions presenting as palpable masses. J Ultrasound Med. 2006;25(9): 1199–209. PubMed PMID: 16929022. eng.
16. Turanage RH, Richardson KA, Benjamin DL, McDonald JC. Abdominal wall, umbilicus, peritoneum, mesenteries, omentum, and retroperitoneum. In: Townsend CM, Daniel Beauchamp R, Mark Evers B, Mattox KL, editors. Sabiston textbook of surgery. 18th ed. Philadelphia: Saunders/Elsevier; 2008.
17. Kishi K, Takifuji K, Shirai S, Sonomura T, Sato M, Yamaue H. Brachytherapy technique for abdominal wall metastases of colorectal cancer: ultrasound-guided insertion of applicator needle and a skin preservation method. Acta Radiol. 2006;47(2):157–61. PubMed PMID: 16604961. eng.
18. Lee RK, Cho CC, Tong CS, Ng AW, Liu EK, Griffith JF. Ultrasound of the abdominal wall and groin. Can Assoc Radiol J. 2013;64: 295–305. PubMed PMID: 23103240. ENG.
19. Höroldt BS, Lee FK, Gleeson D, McAlindon ME, Sanders DS. Ultrasound guidance in the placement of a percutaneous endoscopic gastrostomy (PEG): an adjuvant technique in patients with abdominal wall varices? Dig Liver Dis. 2005;37(9):709–12. PubMed PMID: 15925555. eng.
20. Gidwaney R, Badler RL, Yam BL, Hines JJ, Alexeeva V, Donovan V, et al. Endometriosis of abdominal and pelvic wall scars: multimodality imaging findings, pathologic correlation, and radiologic mimics. Radiographics. 2012;32(7):2031–43. PubMed PMID: 23150856. eng.
21. Hensen JH, Van Breda Vriesman AC, Puylaert JB. Abdominal wall endometriosis: clinical presentation and imaging features with emphasis on sonography. AJR Am J Roentgenol. 2006;186(3):616–20. PubMed PMID: 16498086. eng.
22. Deitch EA, Engel JM. Spigelian hernia: an ultrasonic diagnosis. Arch Surg. 1980;115(1):93. PubMed PMID: 7350893. eng.
23. Jamadar DA, Jacobson JA, Morag Y, Girish G, Ebrahim F, Gest T, et al. Sonography of inguinal region hernias. AJR Am J Roentgenol. 2006;187(1):185–90. PubMed PMID: 16794175. eng.
24. Shadbolt CL, Heinze SB, Dietrich RB. Imaging of groin masses: inguinal anatomy and pathologic conditions revisited. Radiographics. 2001;21 Spec No:S261–71. PubMed PMID: 11598262. eng.
25. Uren RF, Howman-Giles R, Thompson JF, Shaw HM, Roberts JM, Bernard E, et al. High-resolution ultrasound to diagnose melanoma metastases in patients with clinically palpable lymph nodes. Australas Radiol. 1999;43(2):148–52. PubMed PMID: 10901892. eng.
26. Voit C, Schoengen A, Schwürzer-Voit M, Weber L, Ulrich J, Sterry W, et al. The role of ultrasound in detection and management of regional disease in melanoma patients. Semin Oncol. 2002;29(4): 353–60. PubMed PMID: 12170438. eng.
27. Hofmann U, Szedlak M, Rittgen W, Jung EG, Schadendorf D. Primary staging and follow-up in melanoma patients–monocenter evaluation of methods, costs and patient survival. Br J Cancer. 2002;87(2):151–7. PubMed PMID: 12107834. Pubmed Central PMCID: PMC2376106. eng.
28. Blaivas M, Brannam L. Testicular ultrasound. Emerg Med Clin North Am. 2004;22(3):723–48, ix. PubMed PMID: 15301848. eng.
29. Mitchell DG, Needleman L, Bezzi M, Goldberg BB, Kurtz AB, Pennell RG, et al. Femoral artery pseudoaneurysm: diagnosis with conventional duplex and color Doppler US. Radiology. 1987; 165(3):687–90. PubMed PMID: 3317501. eng.
30. Liau CS, Ho FM, Chen MF, Lee YT. Treatment of iatrogenic femoral artery pseudoaneurysm with percutaneous thrombin injection. J Vasc Surg. 1997;26(1):18–23. PubMed PMID: 9240316. eng.
31. Robinson A, Light D, Kasim A, Nice C. A systematic review and meta-analysis of the role of radiology in the diagnosis of occult inguinal hernia. Surg Endosc. 2013;27:11–8. PubMed PMID: 22733195. ENG.
32. Light D, Ratnasingham K, Banerjee A, Cadwallader R, Uzzaman MM, Gopinath B. The role of ultrasound scan in the diagnosis of occult inguinal hernias. Int J Surg. 2011;9(2):169–72. PubMed PMID: 21059415. eng.
33. Zhang GQ, Sugiyama M, Hagi H, Urata T, Shimamori N, Atomi Y. Groin hernias in adults: value of color Doppler sonography in their classification. J Clin Ultrasound. 2001;29(8):429–34. PubMed PMID: 11745848. eng.
34. Babkova IV, Bozhko VV. Ultrasound assessment in diagnosis of uncomplicated inguinal hernia. Khirurgiia (Mosk). 1999;(2):46–50. PubMed PMID: 10081255. rus
35. Jamadar DA, Jacobson JA, Morag Y, Girish G, Dong Q, Al-Hawary M, et al. Characteristic locations of inguinal region and anterior abdominal wall hernias: sonographic appearances and identification of clinical pitfalls. AJR Am J Roentgenol. 2007;188(5):1356–64. PubMed PMID: 17449782. eng.
36. Sigel B, Golub RM, Loiacono LA, Parsons RE, Kodama I, Machi J, et al. Technique of ultrasonic detection and mapping of abdominal wall adhesions. Surg Endosc. 1991;5(4):161–5. PubMed PMID: 1839571. eng.
37. Kodama I, Loiacono LA, Sigel B, Machi J, Golub RM, Parsons RE, et al. Ultrasonic detection of viscera slide as an indicator of abdominal wall adhesions. J Clin Ultrasound. 1992;20(6):375–80. PubMed PMID: 1328308. eng.
38. Caprini JA, Arcelus JA, Swanson J, Coats R, Hoffman K, Brosnan JJ, et al. The ultrasonic localization of abdominal wall adhesions. Surg Endosc. 1995;9(3):283–5. PubMed PMID: 7597599. eng.
39. Herring AA, Stone MB, Nagdev AD. Ultrasound-guided abdominal wall nerve blocks in the ED. Am J Emerg Med. 2012;30(5):759–64. PubMed PMID: 21570238. eng.
40. Gofeld M, Christakis M. Sonographically guided ilioinguinal nerve block. J Ultrasound Med. 2006;25(12):1571–5. PubMed PMID: 17121952. eng.
41. Bærentzen F, Maschmann C, Jensen K, Belhage B, Hensler M, Børglum J. Ultrasound-guided nerve block for inguinal hernia repair: a randomized, controlled, double-blind study. Reg Anesth Pain Med. 2012;37(5):502–7. PubMed PMID: 22705951. eng.
42. Thomassen I, van Suijlekom JA, van de Gaag A, Ponten JE, Nienhuijs SW. Ultrasound-guided ilioinguinal/iliohypogastric nerve blocks for chronic pain after inguinal hernia repair. Hernia. 2013;17:329–32. PubMed PMID: 23015156. ENG.
43. Bischoff JM, Koscielniak-Nielsen ZJ, Kehlet H, Werner MU. Ultrasound-guided ilioinguinal/iliohypogastric nerve blocks for persistent inguinal postherniorrhaphy pain: a randomized, double-blind, placebo-controlled, crossover trial. Anesth Analg. 2012; 114(6):1323–9. PubMed PMID: 22467891. eng.
44. Abdallah FW, Chan VW, Brull R. Transversus abdominis plane block: a systematic review. Reg Anesth Pain Med. 2012;37(2):193–209. PubMed PMID: 22286518. eng.
45. Milone M, Di Minno MN, Musella M, Maietta P, Salvatore G, Iacovazzo C, et al. Outpatient inguinal hernia repair under local anaesthesia: feasibility and efficacy of ultrasound-guided transversus abdominis plane block. Hernia. 2013;17:749–55. PubMed PMID: 23160979. ENG.
46. Guirguis MN, Abd-Elsayed AA, Girgis G, Soliman LM. Ultrasound-guided transversus abdominis plane catheter for chronic abdominal pain. Pain Pract. 2013;13:235–8. PubMed PMID: 22734804. ENG.

Percutaneous Ultrasound Guidance Techniques and Procedures

7

Jose M. Velasco and Keith Hood

Abbreviations

CT	Computed tomography
FAST	Focused assessment with sonography for trauma
FNA	Fine-needle aspiration
ICU	Intensive care unit
MRI	Magnetic resonance imaging
MW	Microwave ablation
PT	Prothrombin time
PTC	Percutaneous transhepatic cholangiography
PTT	Partial thromboplastin time

Introduction

The field of interventional ultrasound has expanded dramatically since the 1980s when indications for interventional ultrasound included biopsy guidance and simple aspiration of fluid collections. Since then, interventional ultrasound has been increasingly utilized in clinical practice, in part due to improved sonographic imaging, newer multifrequency ultrasonic probes, as well as the development of less invasive therapies such as ablation techniques, ideally suited to work with ultrasonography. Because of the remarkable success of interventional ultrasound, combined with an outstanding safety record, the number and types of interventional procedures performed under sonographic guidance will continue to grow. Surgeons rapidly have embraced the use of ultrasound not only for diagnostic purposes but also for interventional procedures.

Both diagnostic and therapeutic interventional ultrasonography are now widely accepted techniques that can be used as adjuncts in nearly all areas of the body. Indications for interventional ultrasound are numerous and expanding: needle aspiration, biopsy, drainage, catheterization, tumor ablation, and tissue dissection. There are many advantages of using ultrasound as the imaging modality to guide interventional procedures. In particular, the ability to monitor the procedure in real time, its safety, relatively low cost, portability, and expediency make ultrasound an ideal modality to perform interventional procedures at various locations including the surgeon's office, critical care areas, as well as the operating room. Introduction and availability of newer ultrasound technology, such as ultrasound contrast enhancement, three-dimensional ultrasound, and high-intensity focused ultrasound, will be utilized more and should improve outcomes. Devices such as automated core biopsy needles have allowed for increased reliability in the performance of interventional ultrasound. It is expected that the recent changes in the healthcare environment with its emphasis on resource utilization and efficiency will further foster an expanded role for interventional ultrasound in clinical medicine. In such a clinical environment, surgeon-performed interventional ultrasound should be cost-effective and beneficial for surgical patients.

History

Needle guidance under sonographic direction was first developed in the early 1970s; however, the earliest work describing the use of ultrasound needle guidance can be traced a decade earlier. In 1961, Berlyne described the use of an A-mode apparatus to guide performance of renal biopsy in 20 patients with renal disease and advocated its use to check the needle tip for biopsy [1]. In 1967, Joyner and

J.M. Velasco, MD (✉)
Department of Surgery, NorthShore University HealthSystem, Skokie Hospital, 9600 Gross Point Road, Skokie, IL 60076, USA

Department of General Surgery, Rush University Medical Center, 1653 W. Congress Parkway, Chicago, IL 60612, USA
e-mail: jose_velasco@rush.edu; jvelasco@northshore.org

K. Hood, MD
Department of General Surgery, Rush University Medical Center, 1653 W. Congress Parkway, Chicago, IL 60612, USA
e-mail: keith_hood@rush.edu

E.J. Hagopian, J. Machi (eds.), *Abdominal Ultrasound for Surgeons*,
DOI 10.1007/978-1-4614-9599-4_7,

Table 7.1 Indications for interventional ultrasound

Technique	Methods
Aspiration	Contrast, alcohol
Biopsy	Cytology, core biopsies
Catheter guidance	Drainage: cholecystostomy, abscess, etc.
Definition of intra-abdominal anatomy	Fluid collections (e.g., blood, puss, cyst, etc.)
Injection	Operative approach
Probe guidance	Tumor ablation

associates used ultrasound to select a site for aspiration of pleural fluid [2]. At the First World Congress on Ultrasound in Vienna, Austria, in 1969, Kratochwil described an ultrasonic transducer with a central slot for needle insertion using the A-mode ultrasound [3]. This guide had a flexible cable attached to the transducer. This was easily maneuvered for biopsies. Gammelgaard et al. described the use of a static B-scanning transducer for guidance of needle puncture at the American Institute of Ultrasound in Medicine meeting in Cleveland, Ohio, in 1970 [4]. This transducer had a center slot in which the needle could be placed for aspiration techniques. In these initial phases of interventional ultrasound, the needle was not monitored by sonography; the target was only visualized and marked before insertion of the needle.

The first manuscripts documenting the use of ultrasound to guide invasive procedures appeared in 1972, and interventional ultrasound began to grow. Holm et al. described a special transducer with a central hole through which a needle could be placed [5]. Goldberg and Pollack American radiologists, independently developed an ultrasonic transducer with a central perforation for needle placement [6]. Holm and Goldberg described the use of a static bistable B-scanning technique in which the target was visualized by manual compound scanning. The transducer was angled until a marked line indicating the detection of the puncture needle intersected the target. The needle was inserted, and the needle tip echo, in many cases, could be visualized on the simultaneous A-presentation as a moving echo.

In 1972, Rasmussen et al., using Holm's transducer, compared two methods for liver biopsy of patients with suspected liver metastases. Blind liver biopsy was compared with a sonographically guided liver biopsy. The rate for successful targeting of liver metastases by the blinded technique was 23 % compared with 85 % by the sonographically guided technique [7]. In 1972, Bang and Northeved described the successful use of ultrasound to guide aspiration of amniotic fluid [8]. Bahlmann and Otto, Bartels and Jorgensen, and Kristensen et al. described ultrasound in guiding renal biopsy in the same year [9–11]. These initial studies more than 30 years ago laid the foundation for the field of interventional sonography and its broad application across numerous medical specialties.

Indications for Interventional Ultrasonography

Initially, the principal use of interventional ultrasound was as a diagnostic adjunct (i.e., indirect guidance of biopsies). Currently, interventional ultrasound is used to guide therapeutic interventions as well; examples include drainage, injection, ablation, or tissue dissection. The use of ultrasound in such settings directly affects the therapeutic outcome. In this chapter, general principles of interventional ultrasound, mainly for needle, catheter, and cannula placement, are discussed. Specific applications regarding surgeons are subsequently addressed. The specific applications of interventional ultrasound in different organs are described in relevant chapters, as well as the use of intraoperative and laparoscopic ultrasound (Table 7.1).

Interventional procedures guided by ultrasound for needle placement include biopsy, aspiration, and injection/ablation. Both fine-needle aspiration (FNA) cytology and core-needle biopsy can be guided by ultrasound. Ultrasound-guided FNA cytology is usually indicated for neck masses, including thyroid nodules, parathyroid nodules, cervical or other lymph nodes, and pancreatic lesions. On the other hand, ultrasound-guided core-needle biopsy is indicated more commonly for breast lesions, abdominal diseases such as liver tumors, retroperitoneal or pelvic masses, prostate lesions, and transplanted organs [12–14]. For both FNA and core-needle biopsy, ultrasound greatly facilitates the diagnosis and management of hepatic disorders, particularly neoplasms. Ultrasound-guided biopsy of the liver can be performed percutaneously in most circumstances and is frequently indicated for definitive diagnosis of liver tumors [15] (Fig. 7.1). Percutaneous biopsy of intra-abdominal, retroperitoneal, or pelvic masses can be guided by ultrasound as well as computed tomography (CT). Percutaneous ultrasound-guided biopsy of tumors of the liver or intra-abdominal masses may confirm metastatic or unresectable disease, thereby avoiding unnecessary laparotomy in a patient with incurable malignancy [15]. Ultrasound can be used to biopsy retroperitoneal masses including lymph nodes [16], even preventing unnecessary laparotomy in a patient with retroperitoneal lymphoma (Fig. 7.2). Ultrasound-guided core-needle biopsy of transplanted organs such as

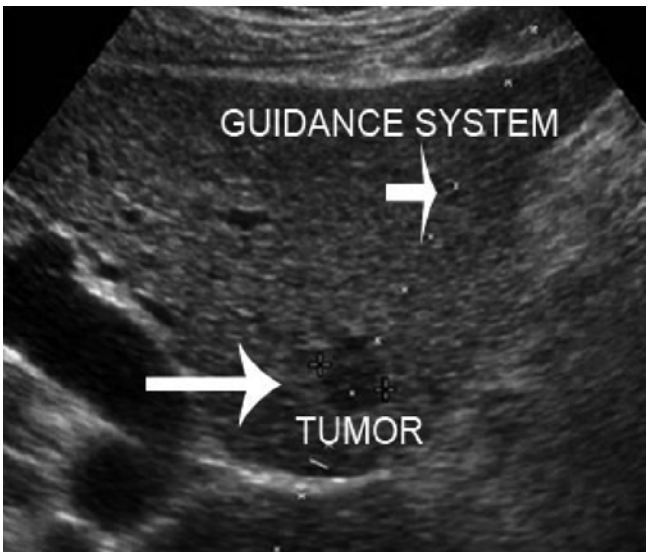

Fig. 7.1 Biopsy of liver tumor

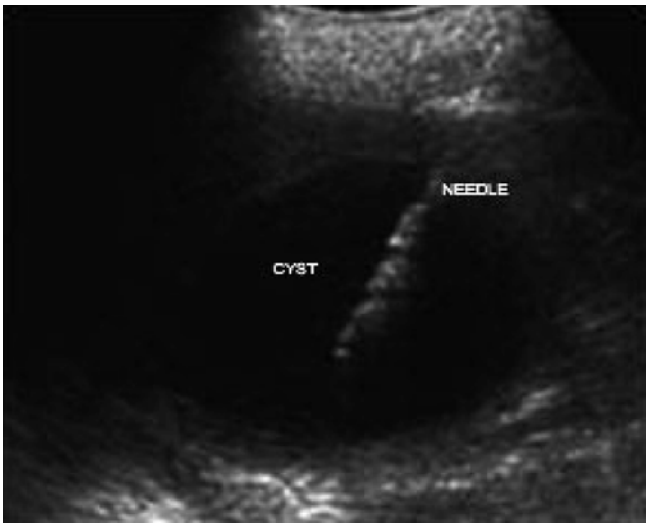

Fig. 7.3 Ultrasound-guided cyst aspiration

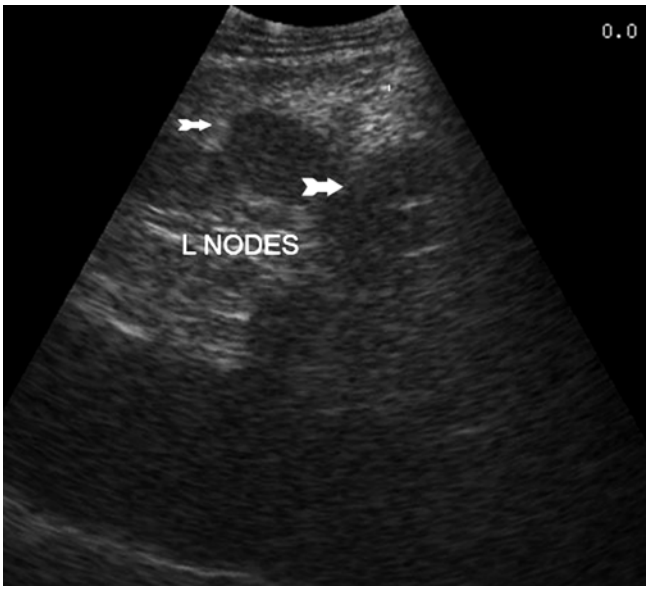

Fig. 7.2 Retroperitoneal lymph nodes (*arrows*)

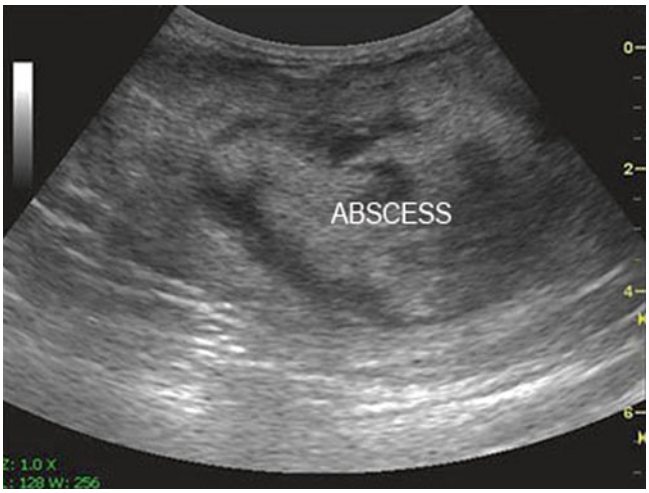

Fig. 7.4 Intra-abdominal abscess detected with ultrasound

the liver, kidney, and pancreas is indicated for histologic diagnosis of possible transplant rejection or other transplantation-related complications [17].

Ultrasound-guided needle placement is also indicated for aspiration of various fluids and cystic lesions involving the thoracic and abdominal cavities as well as other areas of the body. Ultrasound-guided aspiration is performed for both diagnostic and therapeutic purposes in the abdomen, for example, a paracentesis, and is much safer for the patient when done under ultrasound guidance. Abdominal cystic lesions that can be aspirated by ultrasound-guided needle placement are numerous and include, but are not limited to, liver cysts, renal cysts, and pancreatic cystic lesions [18] (Fig. 7.3).

Ultrasound-guided needle aspiration may be followed by ultrasound-guided catheter placement for drainage of various diseases. Intra-abdominal or pelvic abscesses and cysts can be aspirated and drained (Figs. 7.4 and 7.5). Some interventions require the placement of a catheter including percutaneous cholecystostomy, as well as percutaneous transhepatic cholangiography (PTC), nephrostomy, gastrostomy, and aspiration and drainage of abdominal wall and intra-abdominal fluid collections (Fig. 7.6).

Injection and/or tissue ablation of lesions is an important concept when discussing interventional sonography. Following needle placement, various agents can be injected under ultrasound guidance. Such agents include blue dye, radiographic contrast, or therapeutic agents such as alcohol. Blue dye injection may be used for marking the tissue or in the case of hepatic resections, injection into a branch of

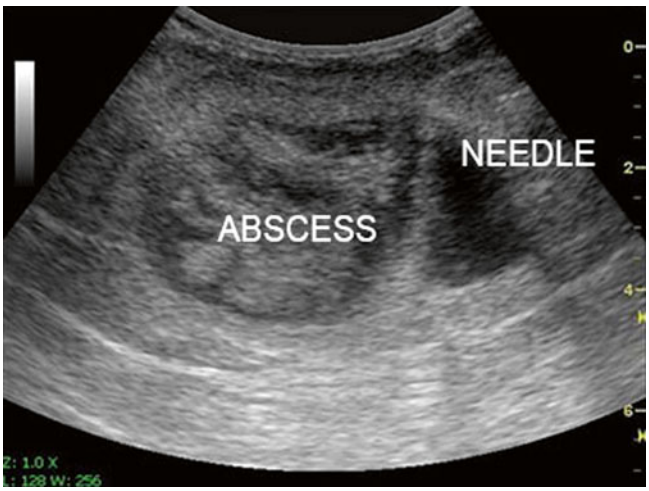

Fig. 7.5 Ultrasound-guided needle placement for abscess drainage

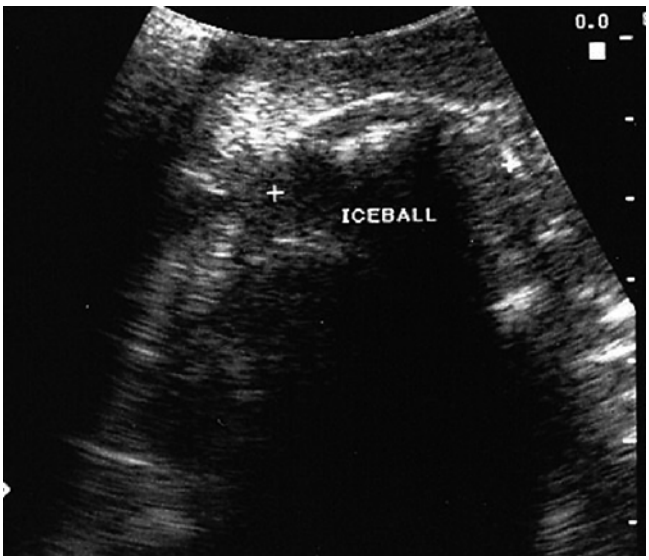

Fig. 7.7 Cryoablated liver lesion. Iceball between crossmarks

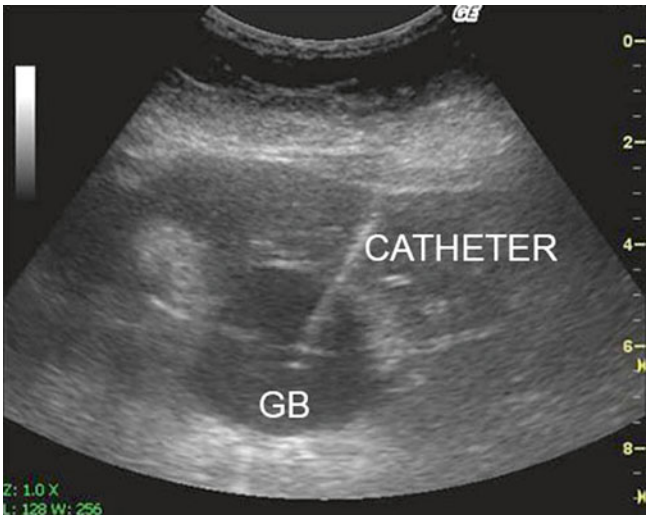

Fig. 7.6 Percutaneous cholecystostomy. *GB* Gallbladder

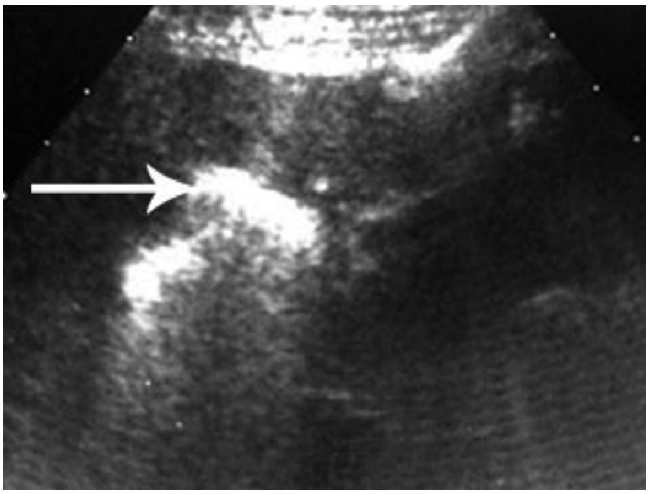

Fig. 7.8 Post-RFA of liver mass with hyperechoic residual effect

the portal vein to define the boundaries of a liver segment to facilitate subsegmental resection. Contrast can be injected into cystic lesions or biliary ducts for radiographic contrast studies (e.g., percutaneous transhepatic cholangiography). Ultrasound-guided ethanol injection has been used for management of hepatomas, parathyroid adenomas, thyroid nodules, and other diseases [19].

Tumor ablation is an effective therapeutic modality for the management of various types of cancers. Its success is dependent on accurate staging, precise targeting of the lesion, thorough ablation, and consecution of free margins. Cryoablation and thermal and microwave ablation have been extensively utilized in the treatment of liver tumors with good outcomes. Placement of the probes can be guided by ultrasound in an accurate, expeditious, and safe manner. Radiofrequency/microwave-ablated or cryoablated lesions become hyperechoic or hypoechoic, respectively, and associated with shadowing (Figs. 7.7 and 7.8) [20, 21].

Advantages and Disadvantages

With the wide variety of imaging modalities available to the surgeon presently, it is sometimes challenging to select the most effective method. What is best for the patient? Which modality will yield the greatest amount of information to guide clinical decision-making? Which one is the most cost-effective? (Table 7.2) The advantages of ultrasonography are numerous. The most significant is its visualization of an interventional procedure in real time, which allows for precise needle or cannula placement

Table 7.2 Advantages and disadvantages of interventional ultrasonography

Advantages	Disadvantages
Accurate	Difficult to image mid-abdomen and chest
Available	Interference from air and bone
Doppler capability	Learning curve
No ionizing radiation	Lower resolution
Portability	Sterilization of probes
Real-time visualization/dynamic study	
Repeatable: confirms procedure, complications	
Safe (no redirection)	
Versatile	

[22]. Ultrasound is a dynamic study with real-time imaging allowing for controlled intervention with a needle, catheter, etc. under visualization. With the exception of fluoroscopy, other image guidance modalities (e.g., CT and magnetic resonance imaging) require assessment of static images and, when necessary, subsequent adjustment of needle placement prior to rescanning. Precise placement of the needle and/or probe requires accurate definition of the target. If subsequent CT or magnetic resonance imaging (MRI) images are obtained without contrast, the risk for unsuccessful outcomes due to poor delineation of the lesion may be increased. Ultrasound also has the ability to be portable, which is extremely useful in the intensive care unit (ICU) setting or any setting in which a critically ill patient is involved. This minimizes any risk of transportation in a critically ill patient, and there is less of a burden on the collaborating departments (e.g., radiology) and the nursing staff. The portability of ultrasound also makes it ideal for the office or ambulatory setting. Focused assessment with sonography for trauma (FAST) in the emergency department to diagnose bleeding in the trauma patient has become extremely common and effective (Fig. 7.9). The uses of ultrasound to perform interventions due to its accessibility and portability will only continue to grow. Finally, ultrasound is considerably less expensive than CT, MRI, and other imaging modalities.

One of the main advantages to ultrasound is its lack of ionizing radiation. As a result, it can be used in circumstances in which image guidance would otherwise not be possible; examples include pregnant patients or radiation-sensitive areas (e.g., ultrasound-guided aspiration of amniotic fluid). Ultrasound also has the capability for immediate confirmatory imaging post-procedure. Successful aspiration of the fluid or drainage can be confirmed. Tumor-ablative procedures can be monitored by continuous ultrasound examination during the operation. During or at the end of the procedure, ultrasound may be used to detect early complications such as bleeding at the needle insertion site or hematoma formation [22].

Despite its myriad of uses and the abovementioned advantages, there are some disadvantages to ultrasonography [23]. Because ultrasound does not penetrate bone or air well, ribs or air within the lung, limits its use in evaluating the chest. Specifically in the abdomen, gas within the bowel lumen limits the value of ultrasound in evaluating the mid-abdominal region. Therefore, in most circumstances, CT guidance is required for intervention in those areas. The cumbersome mechanism for disinfection and sterilization of ultrasound transducers is a minor impediment to their use. Current transducers have limited tolerance to high temperature, preventing their sterilization by autoclaving. Alternative techniques necessitate time-consuming cold gas sterilization or soaking procedures with or without the use of sterile drape covers [20].

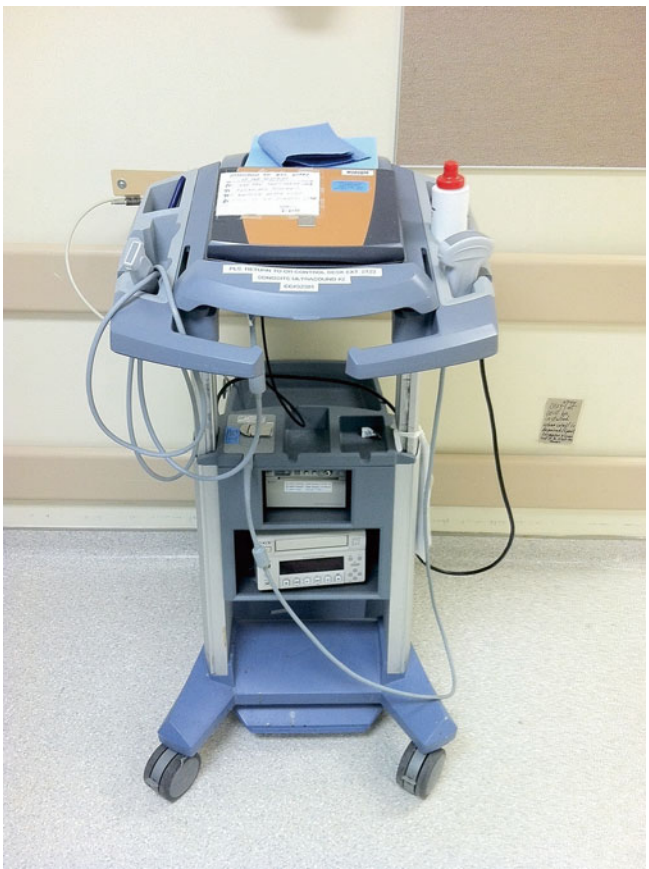

Fig. 7.9 Portable ultrasound used in the emergency department for FAST scan

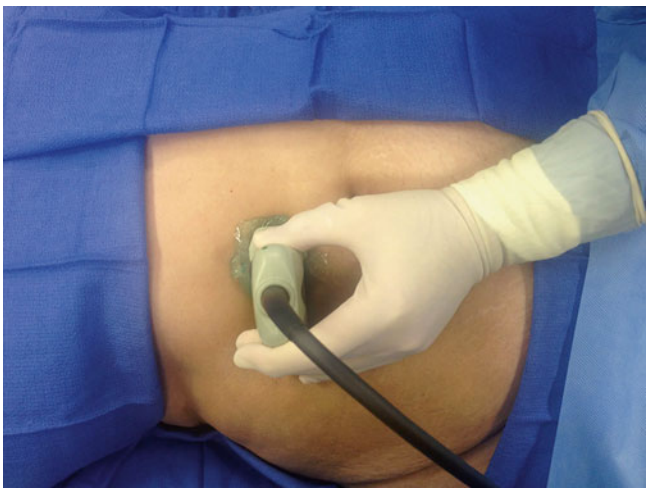

Fig. 7.10 Preliminary scan of abdomen prior to needle aspiration

Procedure Preparation

As with any interventional procedure, routine background information with attention to a history of bleeding disorders, liver disease, and medications is required. Specifically, the use of platelet-inhibiting drugs (e.g., aspirin, clopidogrel, etc.) and anticoagulants (e.g., warfarin, etc.) should be investigated. A review of the patient's coagulation profile including the prothrombin time (PT) and partial thromboplastin time (PTT) are always recommended before an interventional or invasive procedure. Informed consent must always be obtained before a procedure, outlining the procedure itself as well as the potential complications and morbidities associated with the specific procedure.

In most cases, optimal patient position for interventional ultrasound procedures is the same as that used for diagnostic ultrasonography of the area. In general, one should attempt to take the shortest possible path to a lesion. For example, to optimally visualize lesions in the abdomen (such as the liver), it may be necessary to move the patient from the supine to the left lateral decubitus position [22]. Raising the patient's right arm over the head, thereby moving the rib cage in a more cephalad direction, may further enhance exposure of the liver. Such maneuvers may be required to optimally visualize and access a liver mass. For most interventional ultrasound procedures, it is beneficial to perform a brief diagnostic scan of the patient prior to setting up for the planned intervention. This preliminary scan confirms the safest and most direct route to the area in question. When such a position is ascertained, the patient can be prepared in the usual manner (Fig. 7.10).

Skin preparation for ultrasound-guided procedures requires routine painting with antiseptic solutions and full operative drape of the patient and ultrasound equipment. The method will vary according to the nature and severity of the planned interventional ultrasound procedure. For acoustic coupling between the transducer and the skin, sterile ultrasound coupling gel can be used. During open surgical procedures, saline solution is used in the operative field for acoustic coupling.

The use and type of anesthesia varies depending on the nature and extent of the procedure and the anxiety and cooperation of the patient. Most percutaneous interventional ultrasound procedures are accomplished readily with a of local anesthetic. For more complex procedures, such as drainage of an intra-abdominal abscess or percutaneous biliary drainage, or for patients with anxiety, intravenous sedation is generally required (typically with a narcotic and benzodiazepine). When using sedation, the patient must be in a monitored setting, watching heart rate, blood pressure, respiratory rate, and oxygen saturation. Prolonged ultrasound-guided procedures, such as liver tumor ablation, are more frequently performed under general anesthesia.

Ultrasound Guidance and Visualization

Ultrasound guidance was a major advancement in the area of interventional sonography. Saitoh et al. first described the use of real-time guidance for sonographically guided puncture in 1979 [24]. Shortly thereafter, almost every manufacturer developed some type of transducer or needle guidance system for biopsy or aspiration techniques. There are advantages and disadvantages to each guidance system. Presently, the use of detachable guidance systems for sonographically guided needle puncture techniques is common, including the development of endoluminal transducers with biopsy guidance attachments to use with these transducers. These guidance techniques have become increasingly specialized and the equipment very specific for various ultrasound-guided procedures.

Various ultrasound guidance methods are utilized to optimally guide a needle, cannula, or probe. Indirect ultrasound guidance uses the ultrasound to select the site of intervention and aids in determining the angle of insertion for the needle. Despite this, it is essentially a blind technique. First, the size and the exact location of the lesion are evaluated by ultrasound. The needle puncture site is selected and marked with a marking pen or other convenient tool. The direction and depth of the needle insertion are determined by ultrasound. The needle is inserted from the predetermined site without concomitant use of ultrasound visualization. This method is less precise than direct ultrasound guidance, and thus inferior. However, skin and equipment preparation is easier because disinfection or sterilization of the ultrasound transducer is not needed. An indirect ultrasound guidance method is generally used when the target lesion is relatively large, e.g., aspiration or drainage of large fluid collections such as ascites, a large cystic lesion, or biopsy of a large tumor (Figs. 7.11 and 7.12).

Direct ultrasound guidance methods allow real-time needle visualization and therefore more precise needle placement. There are two techniques of needle insertion in

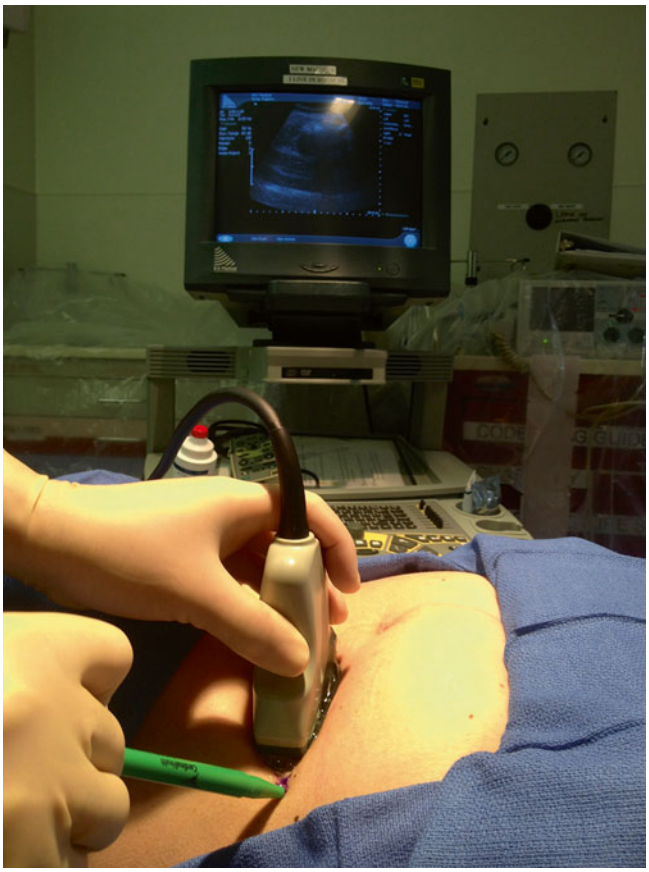

Fig. 7.11 Indirect ultrasound guidance method showing ascites

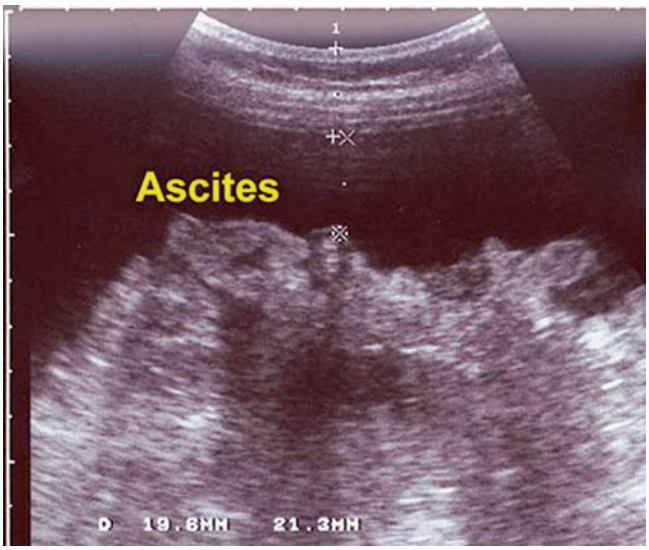

Fig. 7.12 Indirect ultrasound guidance method showing ascites

relation to the ultrasound scanning plane along the long axis of the transducer. The better and preferred technique is to insert and advance a needle in the plane parallel to the long axis of the transducer (i.e., ultrasound scanning plane). This allows for constant visualization of the shaft and tip of the needle throughout its entire path to the target. This is a safer and more accurate method because the needle tip is always demonstrated on the ultrasound monitor. The second and less preferable technique is to insert the needle perpendicular to the long axis of the transducer. This technique increases the difficulty of needle tip visualization because the tip is not seen until it enters the ultrasound scanning plane (Fig. 7.13a, b). This may increase the risk of significant past pointing of the needle tip, which may lead to complications such as pneumothorax and bleeding. For this reason, the use of this second technique should be limited to the situation in which the placement of transducer or access of the needle to the target cannot be achieved by the first technique [22].

Direct ultrasound guidance is the preferred method in interventional ultrasonography, and it can be accomplished typically in one of two ways: the "freehand" technique (Fig. 7.14) or by using the needle guidance system (so-called biopsy guide) (Fig. 7.15). In the freehand technique, the needle can be placed either adjacent to or remote from the transducer, and parallel or perpendicular to the ultrasound scanning. Another advantage of the freehand technique is that it allows independent movement of the transducer and the needle. The main disadvantage of the freehand technique is that it is sometimes difficult to keep or advance the needle within the ultrasound scanning plane for needle visualization. Various types of needle guidance systems are available. In this system, the needle is in a fixed location relative to the transducer. As a result, this guidance system allows for placement of the needle precisely along a predetermined course into the target site, which is often displayed as a needle guideline on the ultrasound monitor (Fig. 7.16). However, because of the fixation of the needle, it cannot be inserted from a remote site, which limits the usefulness of this system. Also, the transducer/needle devices can be somewhat cumbersome and more difficult to use.

Despite which technique the surgeon chooses to employ, it is the experience of the surgeon or the operator with that system that is paramount. The location and size of the target lesion will also aid one in determining which system to use. In general, more superficially located organs or lesions such as the thyroid or breast can be approached by the freehand technique. On the other hand, deeply situated lesions in locations such as the intra-abdominal organs often require a needle guidance system to access (Fig. 7.17).

Equipment

The transducers used for interventional ultrasound procedures have been either those that are biopsy dedicated or those that have the potential for needle guidance system (biopsy guide) attachment. Biopsy-dedicated transducers have fallen out of favor, primarily as a result of difficulty in needle visualization using such a transducer, but also because of the considerable difficulty in sterilizing the transducer's

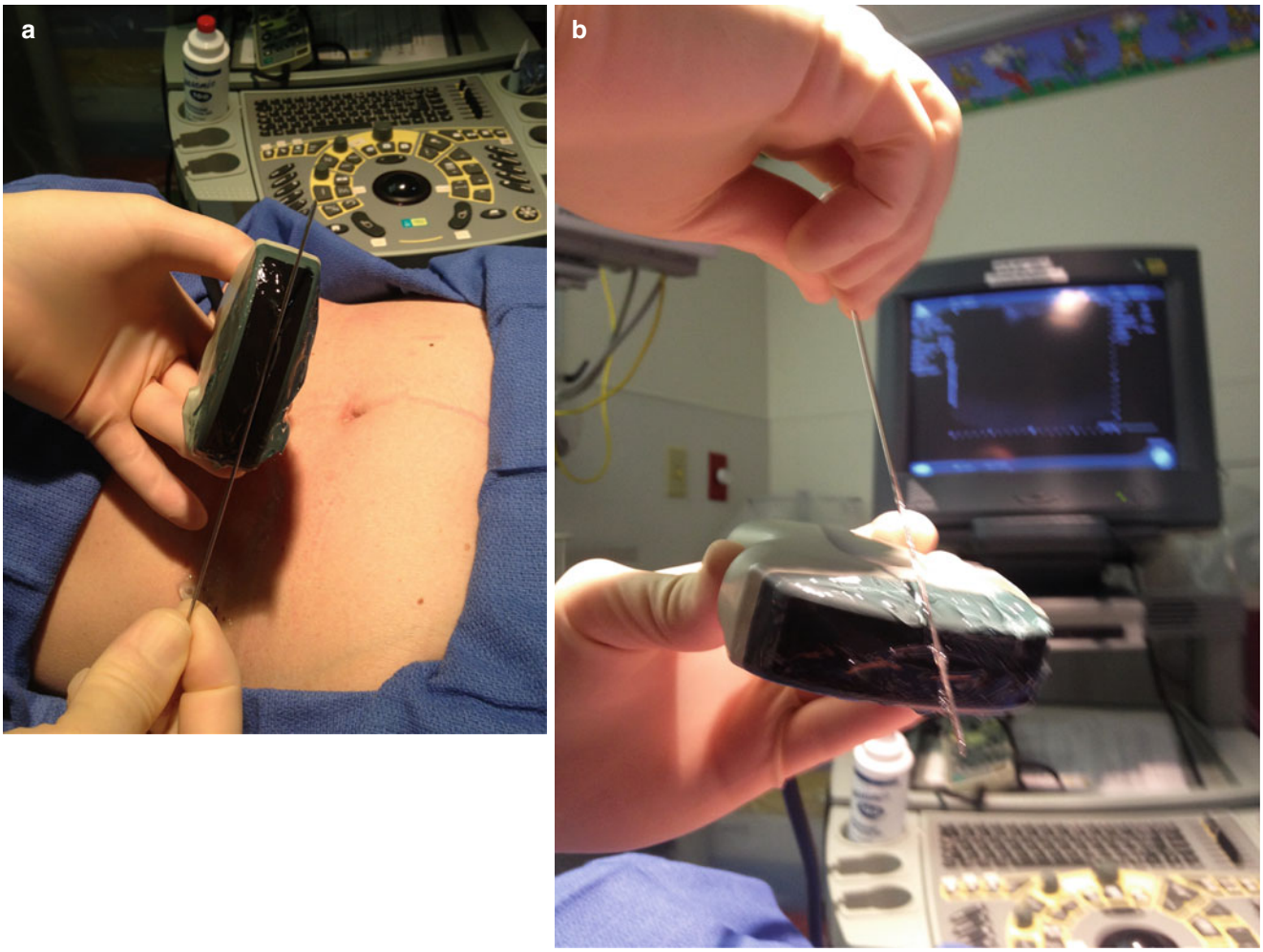

Fig. 7.13 (**a**, **b**) Two techniques of needle insertion: (**a**) demonstrates parallel insertion and (**b**) demonstrates perpendicular insertion to long axis of ultrasound scanning plane

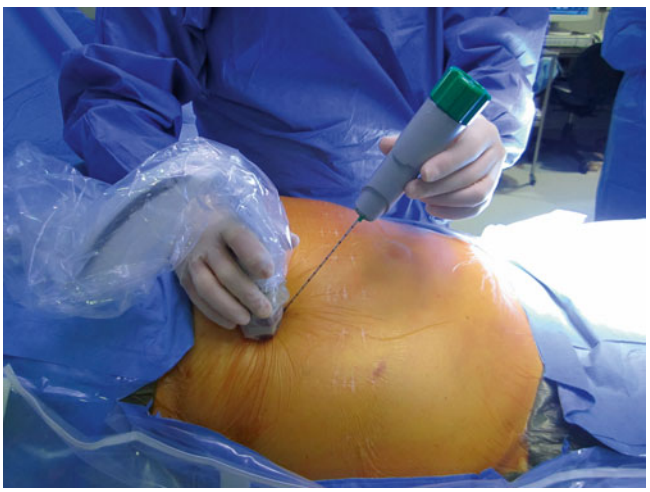

Fig. 7.14 Freehand technique

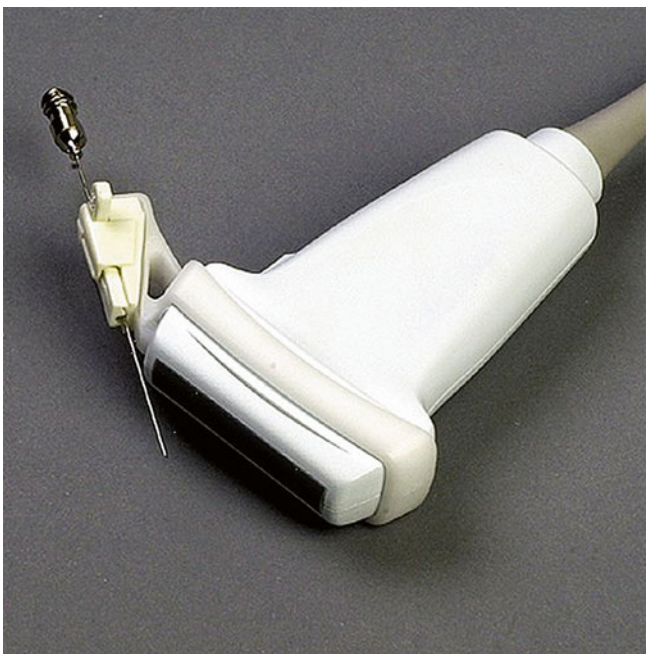

Fig. 7.15 Transducer equipped with needle guidance system

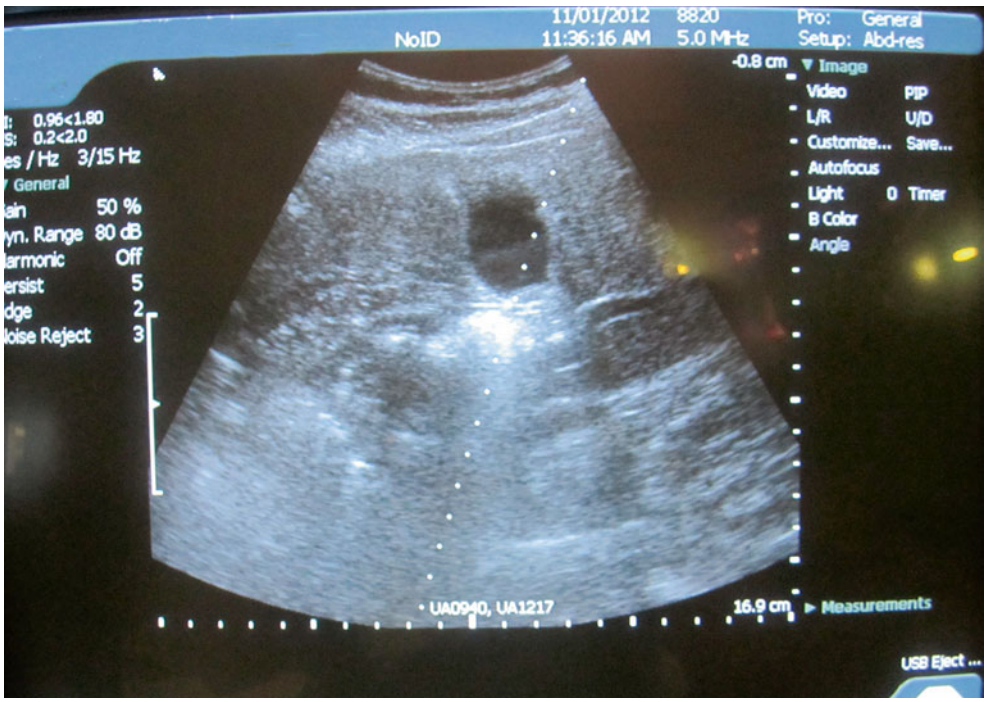

Fig. 7.16 Display of predetermined course into the target site on the monitor

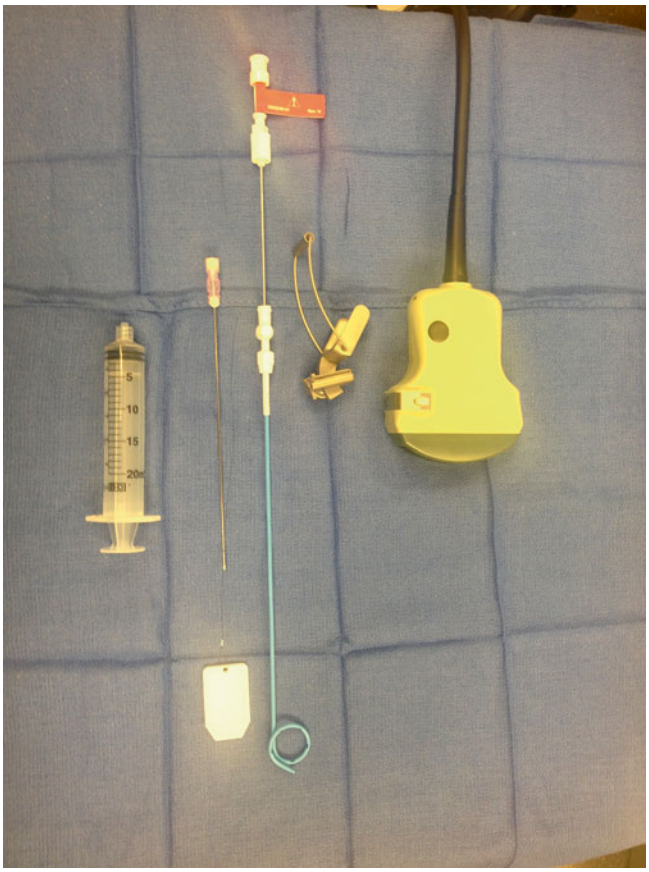

Fig. 7.17 Low-frequency transducer with needle-guided system used for percutaneous cholecystostomy

central canal. Needle guidance systems are available in multiple shapes and sizes to accommodate various types of transducers. Most systems hold the needle firmly in place along a predetermined angle. Some have variable angles of insertion, which greatly facilitates appropriate and safe approach of the needle into targets. Some systems keep the needle in the ultrasound scanning plane, but the insertion angle is not fixed. Needle guidance systems either can be reusable and require cleaning/sterilization or can be disposable.

Optimal visualization of the needle, cannula, or probe is the key for successful interventional ultrasound. Needle visualization is determined by many factors, one of which is the type of tissue or fluid. In general, needle visualization is much better in fluid than in soft tissues. Usually, the tip of needle is better visualized than the shaft. Ultrasound parameters such as transducer frequency and focal zone should be optimized to improve ultrasound image quality prior to intervention (Fig. 7.18).

Needles vary according to their echogenicity. The larger the needle diameter, the more easily it can be visualized by ultrasound. Needle echogenicity can be enhanced by maneuvers that roughen, scratch, or alter its outer surface or by coating with materials such as Teflon [25]. There are specific needles made for interventional sonography with these properties (Fig. 7.19).

Visualization of needles is dependent on the angle of needle insertion in reference to the ultrasound beam because it is determined by reflection of the sound. When the needle is placed perpendicular to the ultrasound beam (i.e., parallel to the transducer surface), much of the sound is reflected back to the transducer, thus providing better needle visualization.

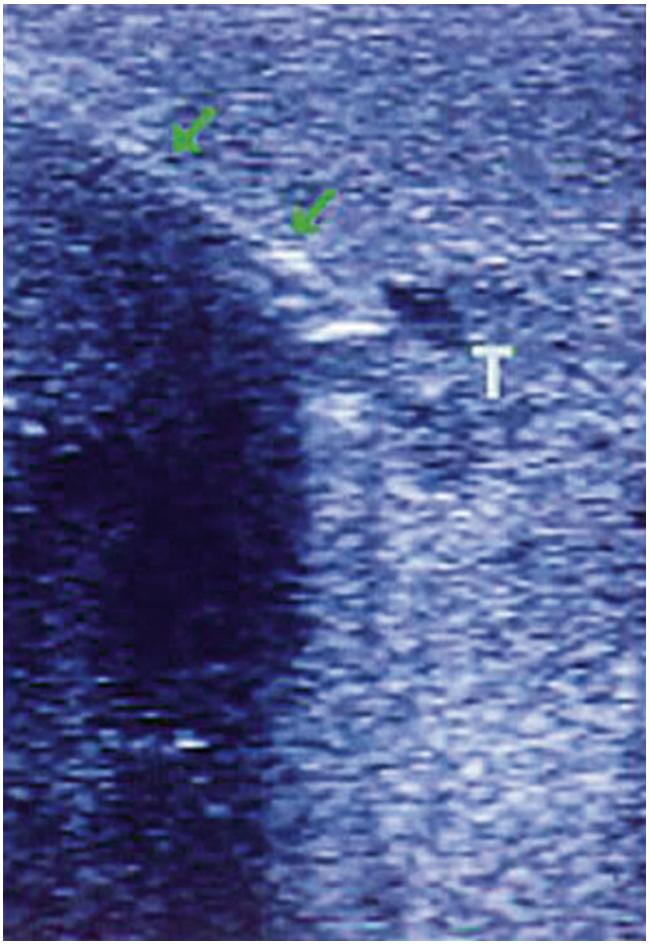

Fig. 7.18 Needle visualization during biopsy of a deep liver lesion. *Green arrow* depicts entire length of needle, note the acoustic shadowing inferior to the needle. "T" indicates lesion

Conversely, when the needle is parallel to the ultrasound beam, visualization is not as good. Another way in which the needle can be better visualized, specifically when using the freehand technique, is simply moving the needle. Also, the lumen of the needle may be made more anechoic relative to the needle wall by removal of the stylet and instillation of a fluid such as saline, thereby facilitating its visualization. Alternatively, introducing a guidewire or filling the needle lumen with air or air-gel mixture can make the lumen more echogenic. The use of color Doppler imaging when using the ultrasound can also aid in the identification and location of the needle.

There are a variety of types and gauges of needles used in interventional ultrasonography to perform the procedures described below. When a biopsy is to be obtained, determining whether or not the specimen needs to be evaluated cytologically or histologically is essential. This main division determines the type of procedure to be performed and the type/gauge of needle to be used. For core-needle biopsies for histologic examination, needles of 18 gauge or larger (up to 14 gauge) are usually required (Fig. 7.20).

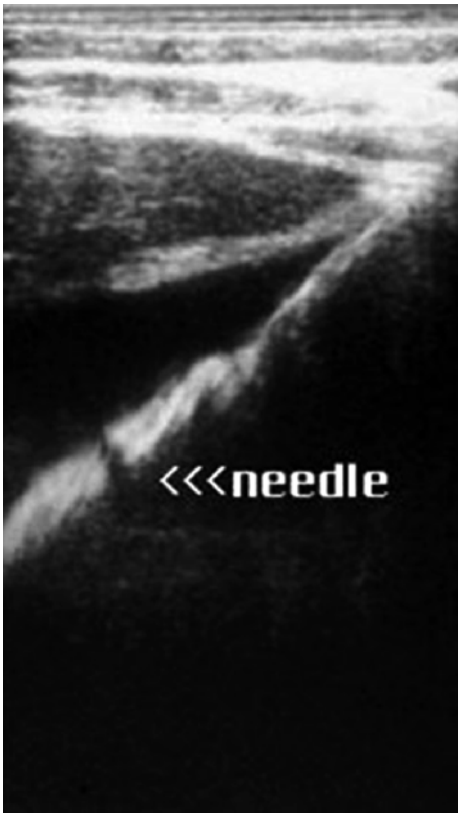

Fig. 7.19 Ultrasound image of a needle with an echogenic tip

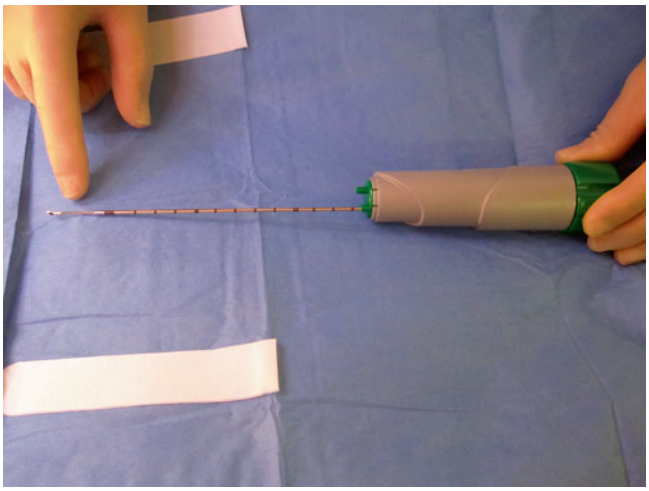

Fig. 7.20 Example of core-needle biopsy used for histologic biopsy specimens

Although there are a variety of means for distinguishing needle types, the primary discriminant involves gauge or diameter. The thin needles are those with a gauge less than or equal to 20–22, while the large-bore needles are those with a gauge greater than or equal to 18. Needles smaller than 18 gauge may safely transverse the bowel without consequent damage, whereas 18-gauge and larger needles have the potential

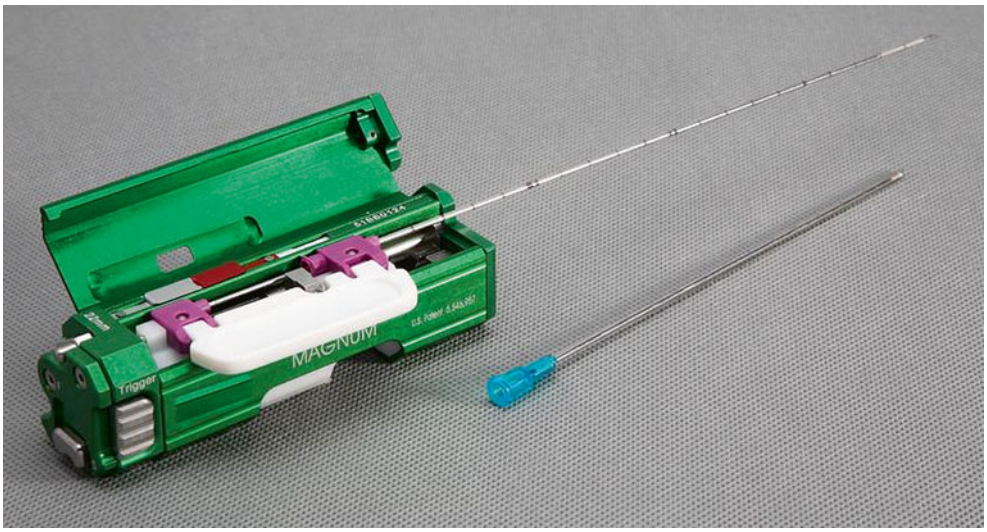

Fig. 7.21 Automatic core-needle biopsy system

to injure the bowel wall with resultant laceration and leak. Biopsy needles are available with several different tips. The needle tips fall somewhere within a spectrum that includes the spinal needle, which has an acutely angled, beveled tip, and the Greene needle, which has a non-angled, circumferentially sharpened tip. Most needle tips are somewhere between these two and have a less acutely angled end. Beveled-tip needles usually yield more suitable specimens than non-beveled ones. However, beveled-tip needles, particularly thin needles, tend to bend as they advance through tissues [22].

The use of spring-loaded automated biopsy needles is now readily available and effective (Fig. 7.21). As a result, it is now preferred over simple aspiration techniques alone. Such biopsy needles are available in a variety of gauges and specimen sizes and in both disposable and non-disposable forms; the latter may be used with single-use needles.

Procedures

Biopsy/Aspiration

Concomitant with the use of sonography as a method of guidance of needle puncture, a number of different pathologic techniques had been developed and refined. As a result, highly accurate pathologic specimen retrieval rates were seen, some with similar diagnostic accuracy rates to that of open surgical biopsies without the disadvantages and complications of surgery. Martin and Ellis and Stewart initiated the practice of aspiration cytologic examination [26, 27]. However, it was not until years later that this technique was widely applied, and it is now extensively used in almost all anatomic regions. Years later, another advancement in ultrasound-guided biopsy was the development of automated Tru-Cut-type needles. These automated Tru-Cut-type needles allowed for rapid performance of core biopsy for histologic diagnosis. These needles were described first in the prostate in 1987 and later described for use in other solid organs in 1989 [28, 29].

For aspiration or biopsy (particularly when using a needle of 20 gauge or larger), the use of a stylet within the needle is recommended to prevent contamination or obstruction of the lumen by tissue or blood clot before it reaches the target. When a relatively small amount of fluid is aspirated (e.g., aspiration of small cysts, diagnostic paracentesis), thin needles with or without stylets suffice using 5- to 20-mL syringes. Even with thin needles, when inserting through the skin is difficult, the skin may be punctured first using a no. 11 blade. When a large amount of fluid is aspirated (e.g., therapeutic paracentesis), the use of a flexible catheter (e.g., long angiocatheter) that is left in a fluid during aspiration is preferred because of a decreased risk of associated tissue injury. In addition, a three-way stopcock with tubing attached to a larger syringe (30–60 mL) is useful and convenient because the syringe need not be detached after each aspiration (Figs. 7.22 and 7.23).

FNA cytology is performed by either an aspiration or a non-aspiration method [25]. Under ultrasound guidance, a needle with a syringe attached is placed in appropriate position. Several millimeters to 1 cm of negative suction is applied to the syringe. At least three to four passes are made by withdrawing and advancing the needle back and forth 1–2 cm. The syringe is then detached and the needle withdrawn from the skin. The specimen is better if it is not aspirated into the syringe because this may cause fragmentation of cells. The specimen is then placed on a slide and smeared. A non-aspiration cytology method is performed in a similar technique. After removal of the stylet, a syringe is not attached. Several back-and-forth movements are performed. It is preferable for a cytopathologist to be available to examine the specimen immediately so that the adequacy of the specimen can be evaluated and determined (Fig. 7.24).

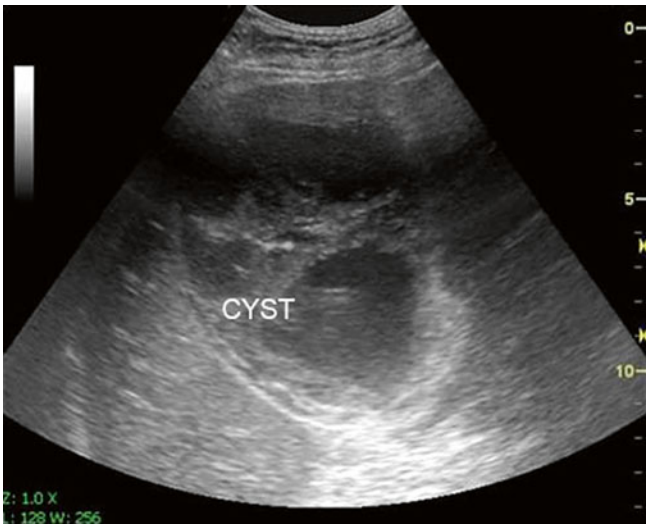

Fig. 7.22 Cyst identified by ultrasound

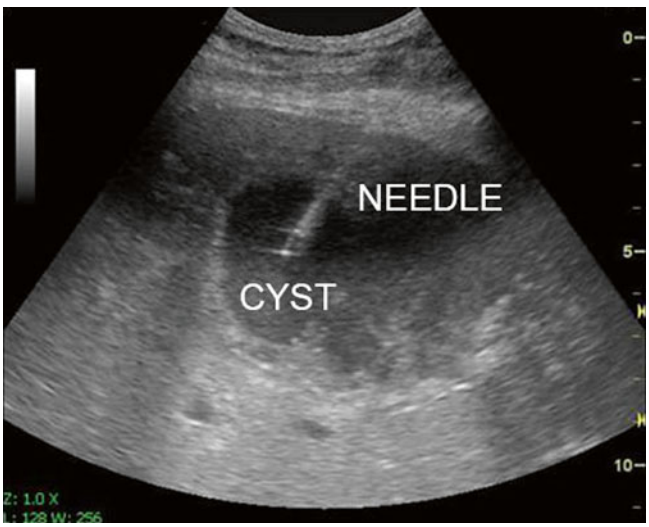

Fig. 7.23 Ultrasound-guided needle aspiration of cyst

As previously discussed, ultrasound guidance is ideal to procure core-needle biopsy specimens. For core-needle biopsy, availability of a pathologist for immediate frozen-section examination is also helpful. If such an examination is not possible, at least three or four core-needle specimens should be obtained from the lesion.

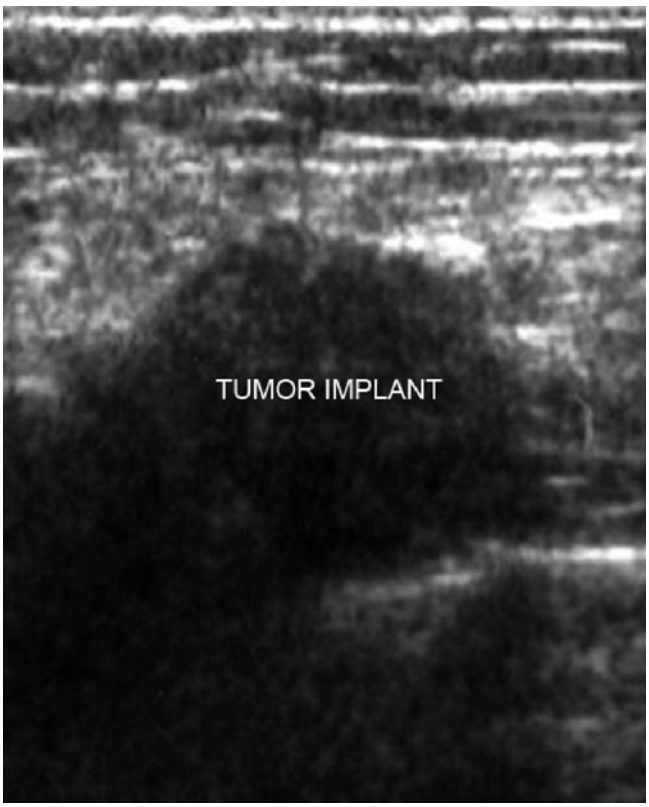

Fig. 7.24 Abdominal wall tumor implant following colectomy for carcinoma

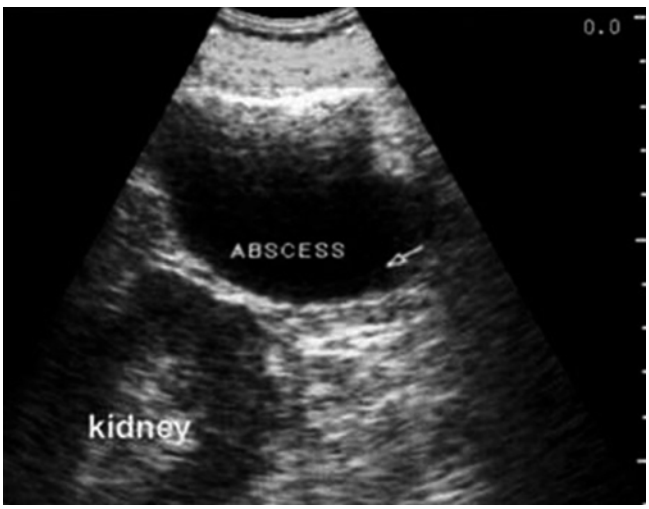

Fig. 7.25 Intra-abdominal abscess

Drainage

Percutaneous sonographically guided fluid aspiration/drainage techniques are applied to almost all areas of the body and allow the surgeon to treat a variety of pathology throughout the body. Again, Goldberg and Pollack first described sonographically guided thoracentesis and paracentesis as early as 1972. Holm et al. described the use of ultrasound to aspirate fluid collections throughout the chest and abdomen. These included aspiration of pericardial fluid, thoracentesis, paracentesis, and amniocentesis. Holm et al. also described abdominal abscess aspiration guided by sonography (Figs. 7.25 and 7.26). At the onset of interventional sonography, the majority of procedures being performed were obstetric and renal

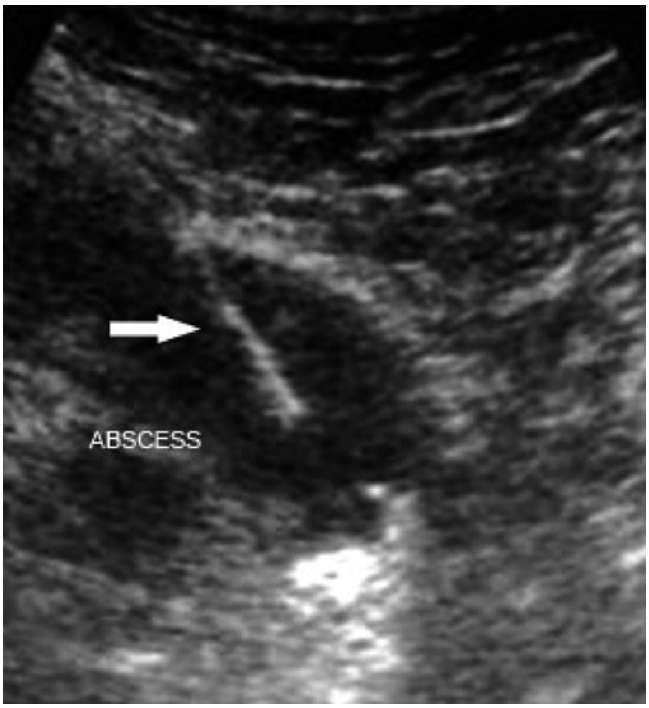

Fig. 7.26 Example of ultrasound-guided abscess drainage. *Arrow* indicates needle

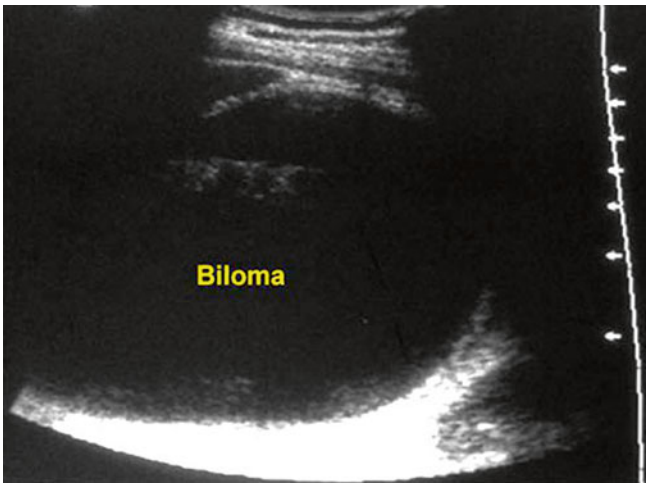

Fig. 7.27 Ultrasound-guided drainage of postoperative biloma

in origin. However, this soon evolved into use in the hepatobiliary tree, an area of particular interest to the surgeon. Cholangiographic techniques guided by sonography were described in 1978 by Makuuchi et al., including percutaneous transhepatic cholangiography [30]. After the initial applications of ultrasound-guided techniques proved to be extremely useful and successful, its uses grew exponentially. These included, among other procedures, pericardiocentesis, empyema drainage, pleural sclerotherapy, abdomen abscess drainage, transhepatic cholangiography, biliary drainage, cholecystostomy, cyst sclerosis, gastrostomy, nephrostomy, nephroureterolithotomy, and sonographically guided arterial and venous catheterization techniques (Fig. 7.27).

Various types of catheters and needle-catheter systems are commercially available for drainage. Two fundamental ultrasound-guided catheter placement methods are a guidewire exchange technique and a trocar technique [25]. A guidewire exchange technique (or Seldinger technique) is more commonly used. A large needle (usually 18 gauge) is introduced into the target lesion or organ under ultrasound guidance. A guidewire is introduced through the needle, and the needle is removed. The tract is then progressively dilated over the wire. Once the tract is appropriately dilated, a catheter is introduced and advanced into the lesion or organ. Ultrasound can be used to confirm the location of the catheter in the lesion (Fig. 7.28).

A trocar technique employs a special needle-catheter unit (e.g., McGahan drainage catheter), which includes a pigtail catheter, a cannula, an inner blunted obturator, and a sharp inner stylet [23]. Under ultrasound guidance, the unit is inserted through the skin and advanced. Once the tip of the cannula is confirmed to be in the lesion or organ, the catheter is pushed from the cannula. Reformation of a loop of the pigtail catheter can be visualized by ultrasound. In general, catheters are more difficult to visualize than needles [22] (Figs. 7.29 and 7.30).

One of the most common applications for ultrasound is the evaluation and treatment of acute cholecystitis. In some circumstances, patients may present with a diagnosis of acute cholecystitis and not being able to tolerate a cholecystectomy. The surgeon can use ultrasound to confirm the diagnosis and to perform a percutaneous cholecystostomy. Such would be the case in critically ill patients and patients following major cardiovascular procedures, etc. There are numerous indications for a percutaneous cholecystostomy besides those who cannot tolerate an operation in the setting of acute biliary sepsis. Because of this continued need, it is essential the surgeon is familiar with ultrasound of the hepatobiliary system and percutaneous interventions. Ultrasound is the least invasive radiologic modality for imaging the liver and biliary tract. Unlike CT scanning and MRI, the technique is portable and quick and can be used to guide interventional procedures. Ultrasound uses no ionizing radiation to create the image and is therefore the technique of choice in pregnant women, in patients with contrast.

When performing a percutaneous cholecystostomy, a catheter is inserted percutaneously under ultrasonographic guidance. First, the gallbladder is located ultrasonographically, and a transparietal puncture is performed by passing a Seldinger needle through the hepatic parenchyma and into the gallbladder. A sample of gallbladder fluid is collected for microbiology and culture. Typically, an 8.5-F pigtail catheter is then placed under US guidance via a two-step method

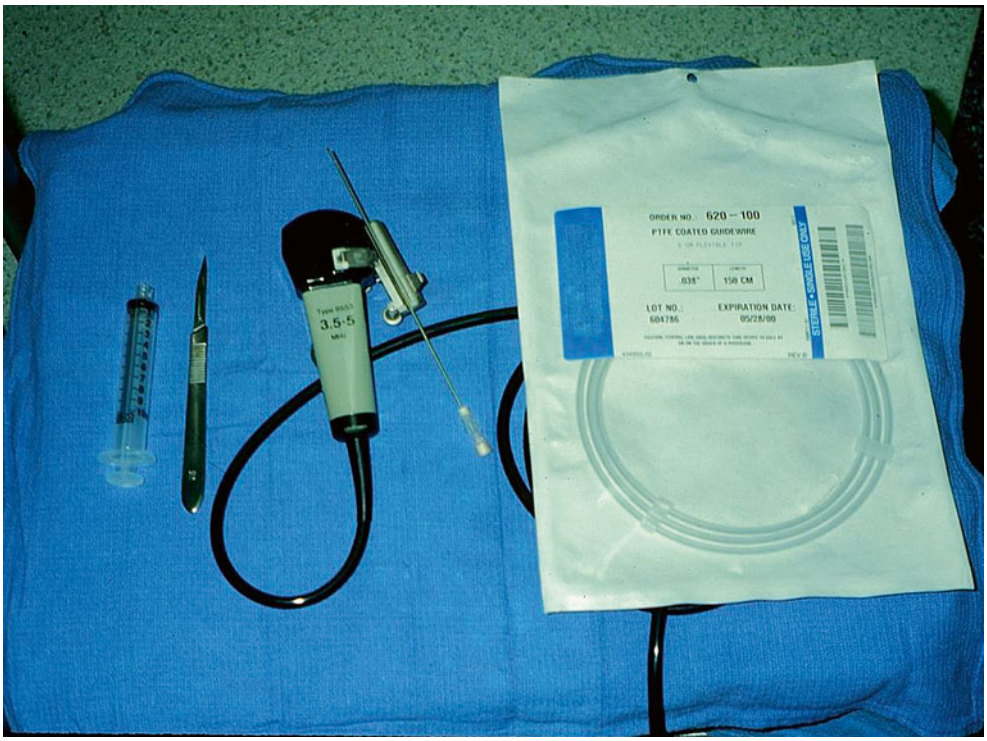

Fig. 7.28 Kit for ultrasound-guided drainage of intra-abdominal collections

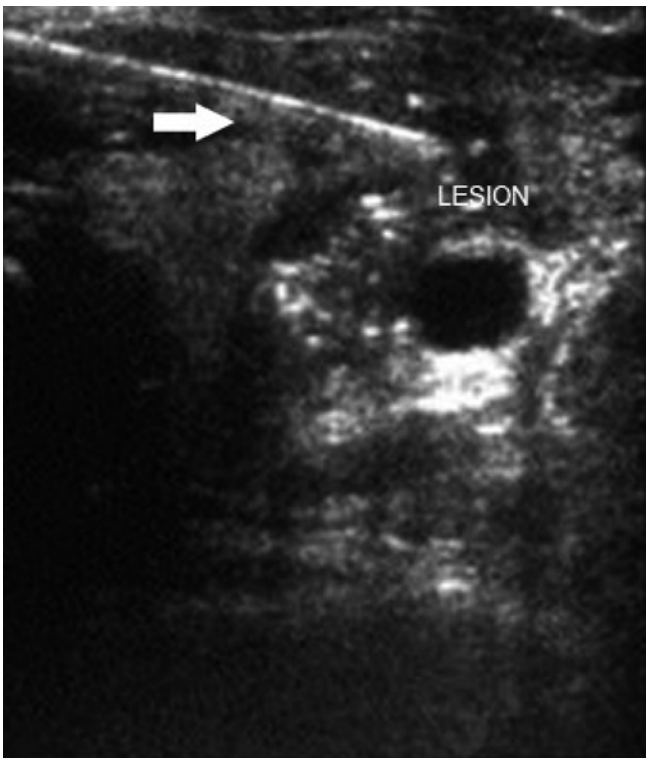

Fig. 7.29 *Arrow* points to needle used to drain cyst

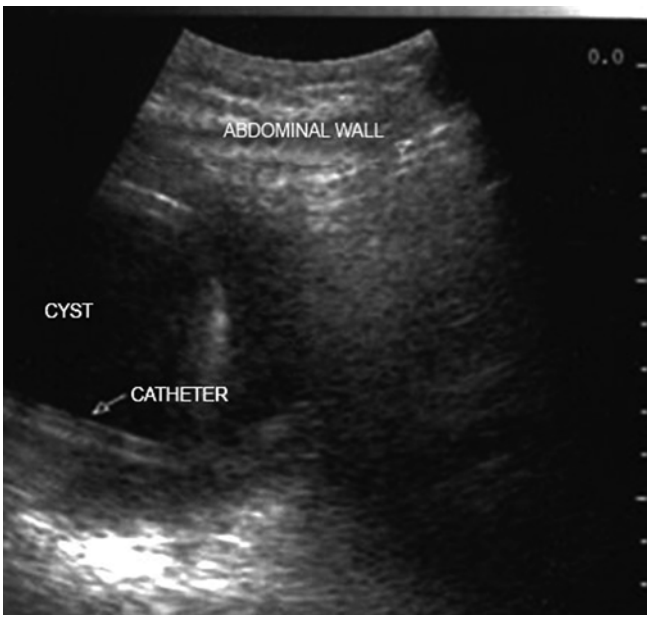

Fig. 7.30 Ultrasound confirming catheter placement

involving guidewire exchange. After all bile is aspirated from the gallbladder, cholecystography is usually performed via the catheter to confirm the type of pathology present (calculous or acalculous cholecystitis). The catheter is left in place for drainage and is flushed with saline solution. Repeat cholecystography can then be performed at the bedside is needed via the cholecystostomy tube to investigate cystic duct patency and assess the common bile duct (Figs. 7.31, 7.32, 7.33 and 7.34).

An additional indication for ultrasound-guided aspiration is in the setting of a symptomatic postoperative fluid collection after laparoscopic or open hernia repair. Abdominal wall

hernia repair is one of the most common surgical procedures worldwide. The use of mesh has been adopted as an important adjunct in the management of abdominal wall hernias. One of the most common complications following repair is an increased incidence of seroma formation with a reported incidence as high as 50 % following laparoscopic ventral herniorrhaphy. Wound complications after herniorrhaphy that result in the need for mesh excision have a high morbidity. In case of large fluid collections following hernia repair, ultrasound facilitates diagnosis and guides aspiration and even catheter drainage as needed. Furthermore, aspiration of fluid collection can facilitate diagnosis and management of suspected infected fluid collections (Fig. 7.35) [31, 32].

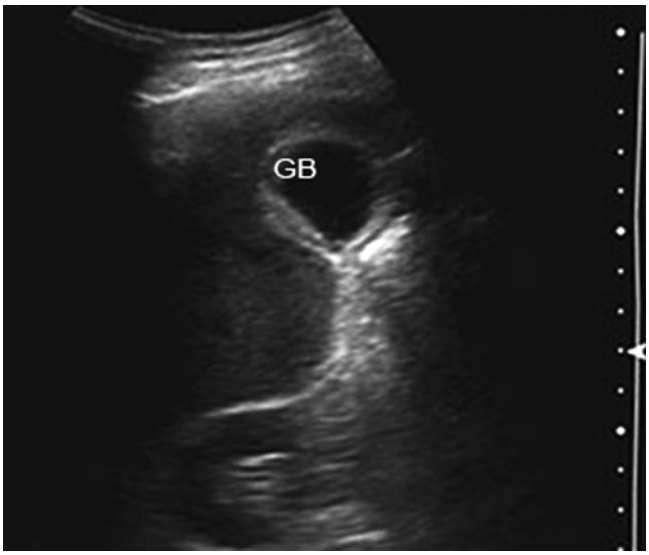

Fig. 7.31 Acute cholecystitis. *GB* Gallbladder

Ablation

Initially, ultrasound was used to guide puncture and instillation of sclerosing agents into renal cysts or recurrent lymphoceles; however, this technique can be applied to the sclerosis of cysts elsewhere in the body. Various agents have been used for sclerosis, including alcohol, povidone iodine, autologous clots, hot saline, and other agents. Ultrasound is used to guide puncture and aspiration of cyst content. To rule out the possibility of communication between the cyst and other structures, fluoroscopy can be used. Once ruled out, the cyst can be sclerosed under ultrasound, followed again by respiration. These techniques have proved more successful than simple cyst aspiration alone in permanent cyst or lymphocyst sclerosis [33].

In addition to cyst ablation, ultrasound has been used for ablation of soft tissue masses. Initially, this was done with alcohol alone. For the surgeon, this proved particularly useful in the thyroid, parathyroid, prostate, and liver. Sonographically guided ethanol injection has been used for ablation of hepatocellular carcinoma. In 1992, Livraghi et al. showed that patients with small hepatocellular carcinoma treated with absolute alcohol injections had better survival rates than those who underwent surgery [34]. Livraghi et al.

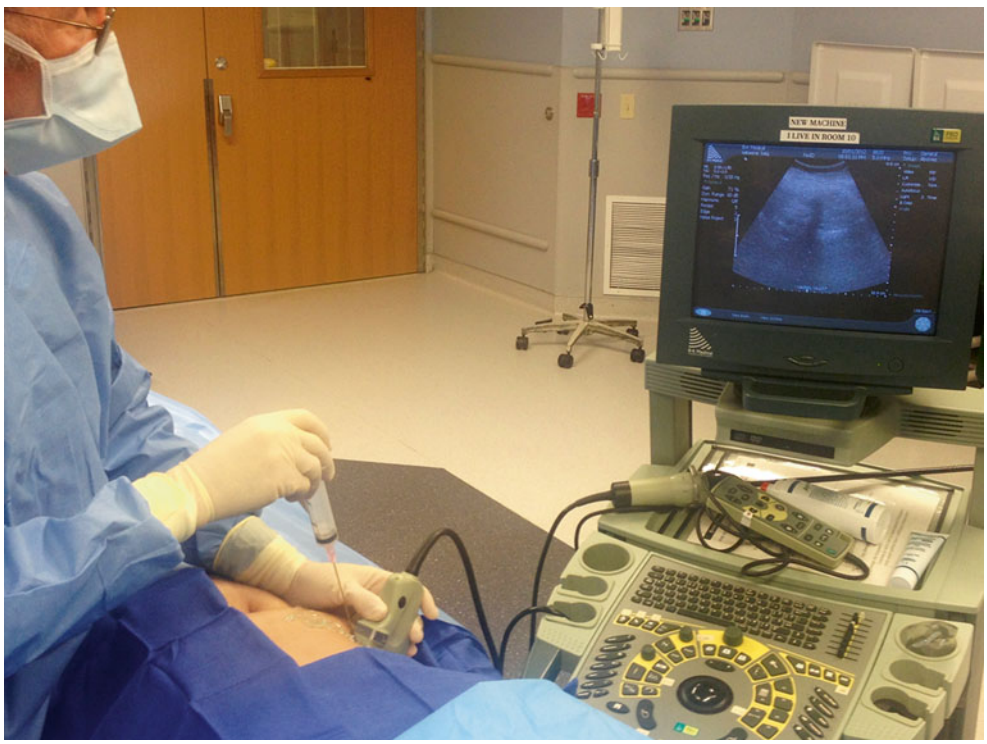

Fig. 7.32 Ultrasound-guided aspiration of gallbladder using a freehand technique

Fig. 7.33 Ultrasound-guided aspiration of gallbladder using a freehand technique

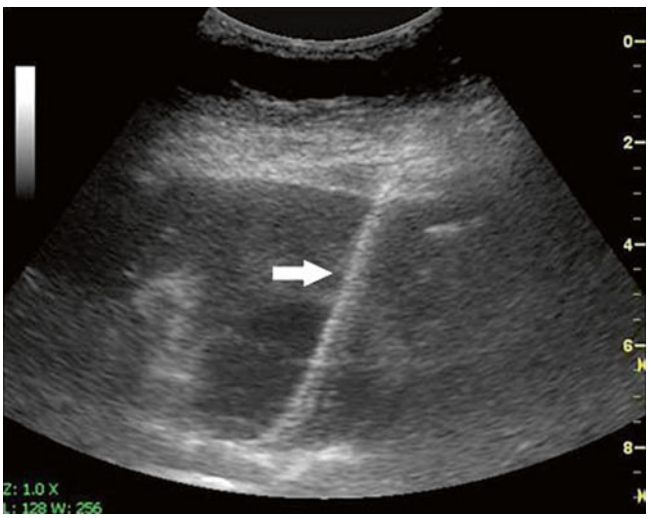

Fig. 7.34 Cholecystostomy catheter in place (*arrow*)

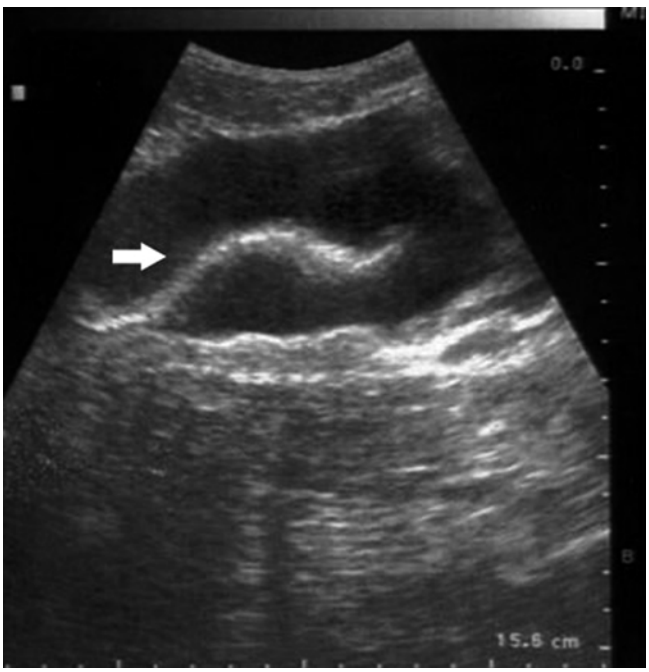

Fig. 7.35 Seroma following abdominal wall hernia. *Arrow* points to mesh

injected small amounts of absolute alcohol into hepatomas smaller than 3 cm in diameter. After injection, there is an increased echogenicity with dispersion of the alcohol in the tumor. This procedure, which is totally guided by sonography, is well tolerated by patients who have had low complication rates. It is still considered an effective alternative to surgery (Fig. 7.36).

Other types of tissue ablation that have been described under ultrasound guidance include microwave ablation, laser coagulation, and cryotherapy. Cryoablation of hepatic lesions was initially performed under sonographic guidance during laparotomy. More recently, with smaller probe designs, cryoablation can be performed percutaneously with sonographic guidance. When freezing a tissue, a very echogenic rim corresponding to the freeze zone is observed on sonography (Fig. 7.7). In 1990, two groups independently described the use of percutaneous ablation of liver tissue using radiofrequency waves: McGahan et al. and Rossi et al. described the use of a monopolar needle that was insulated

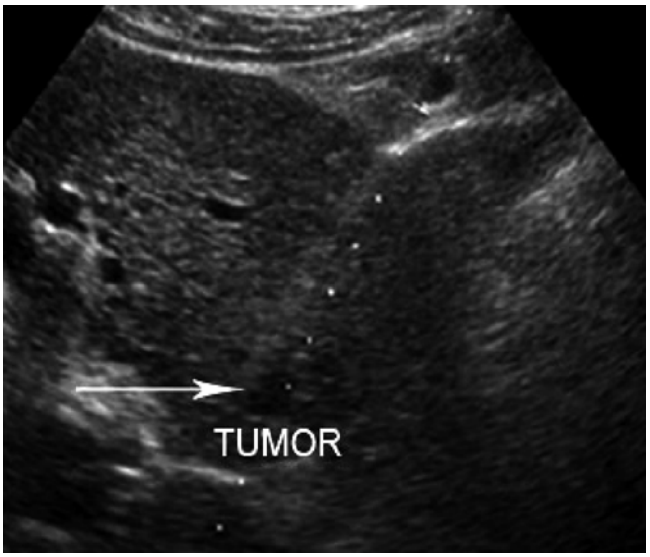

Fig. 7.36 Ultrasound showing needle used for ethanol tumor ablation of hepatocellular carcinoma

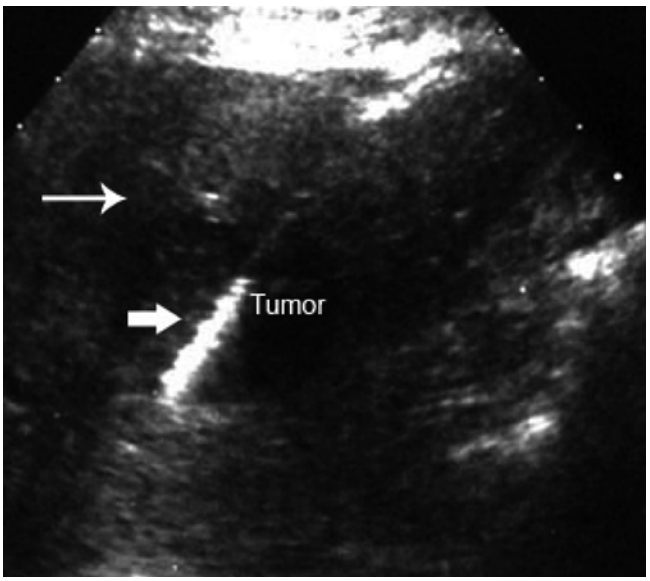

Fig. 7.37 Radiofrequency ablation of mass in the liver, tip of catheter seen in the mass with hyperechoic tip and "prongs" extended

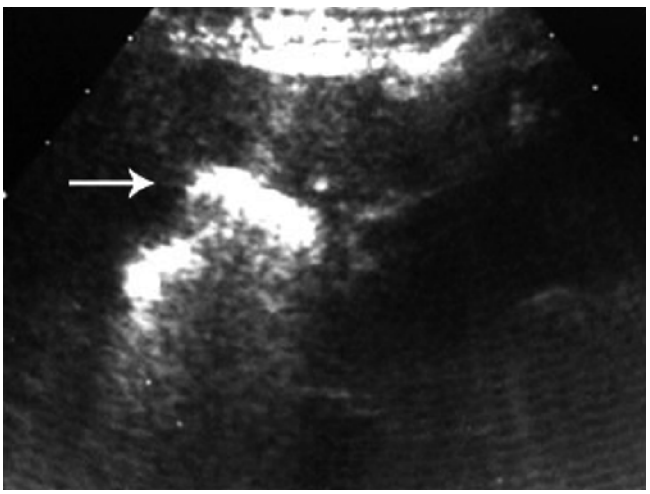

Fig. 7.38 Post-ablation of liver mass with hyperechoic residual effect (*arrow*)

at the distal tip to cause local tissue coagulation in the liver [35, 36]. This coagulation occurred at the needle tip, where radiofrequency energy was most concentrated. This technique was then later applied in ablating primary liver tumors in patients undergoing hepatic resections, as well as metastatic liver lesions. Radiofrequency electrocautery, guided by sonography, has been used to ablate tumors in the brain, thyroid, liver, kidney, and other sites. It has become a well-accepted, less invasive method of treatment of tumors throughout the body.

Radiofrequency thermal ablation management of abdominal pathology such as tumors of the liver can be performed percutaneously, laparoscopically, or via laparotomy [21]. Surgeons should use different approaches appropriately depending on the condition of patients and tumors to be ablated.

With ultrasound guidance, cannulas or needles (ranging from 14 to 18 gauge) are inserted into the tumor under needle guidance. The percutaneous approach has the advantage of being less invasive, possibly can be performed on an outpatient basis. However, it is less accurate in cancer staging, and some areas may not be easily accessible. In addition, it could result in possible adjacent thermal organ injury. Ultrasound allows for the advantage to monitor the region being ablated in real time, but in order to accurately do this, the tip of the needle must be confirmed at a specific location within the lesion prior to initiation. The ablated region becomes hyperechoic; however, this area does not always directly correspond to the true area of ablation. Depending on the size of the tumor and the achievable size of ablation, a single ablation or multiple overlapping ablation sessions are performed. A disadvantage of this technique is the hyperechoic area obscures the ultrasound images around the tumor, limiting surrounding visualization. Therefore, it is critical to make a good plan for multiple ablation sessions before the first ablation starts. When the cannula is withdrawn at the completion of ablation, the cannula track is also ablated under ultrasound visualization to prevent bleeding and possible tumor seeding. If color or power Doppler imaging demonstrates intra-tumoral blood flow prior to ablation, Doppler imaging can be repeated after ablation to confirm loss of blood flow within the tumor [37] (Figs. 7.37 and 7.38).

Microwave ablation (MW) is a treatment option for the management of many cancers. Frequencies of the electromagnetic spectrum between 915 MHz and 2.45 GHz have been most frequently used for ablation procedures. Recently, higher frequencies have been applied in an effort to achieve better outcomes. Preliminary reports indicate that this technology can be safely applied to the management of

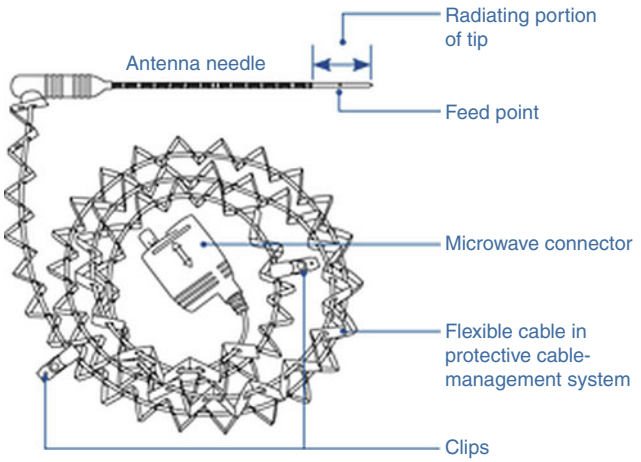

Fig. 7.39 Microwave ablation probe

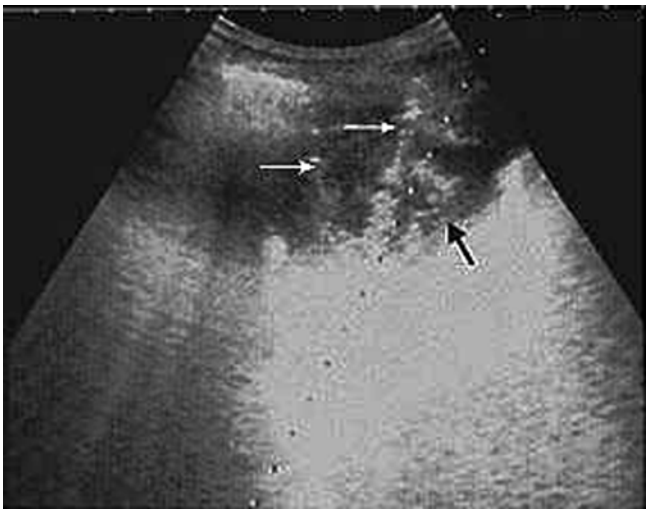

Fig. 7.40 Microwave ablation of liver tumor showing echoic effect. *Arrows* point to area of ablation

patients with bone, kidney, liver, and prostate tumors [38]. Microwave energy differs from other energies for thermal therapy in a number of ways. The most important is that microwaves propagate through all type of tissues, including water vapor, and dehydrated, charred, and dessicated tissues. During radiofrequency, laser, and ultrasound energies ablation, high-temperature heating of tissues can inhibit energy application unless the tissue is cooled and/or rehydrated. Furthermore, MW can ablate up to 3 mm in diameter vessels as opposed to radiofrequency ablation. A single application will ablate liver tumors between 3 and 4 cm in diameter. Liver tumors up to 7 cm can be successfully ablated provided multiple MW antennas are used. However, these properties require real-life monitoring of the ablative procedure to capture rapid heating and tissue changes since energy is rapidly absorbed. Thus, ultrasound guidance and monitoring of thermal ablation is paramount to the success of the procedure [39].

Microwave ablation requires an antenna usually composed of an applicator with a rigid shaft and distal radiating section (Fig. 7.39). Antenna properties include radiation pattern and reflection coefficient. Recently, antenna cooling has been utilized in an effort to eliminate excessive heat generation in the applicator, thus permitting the passage of higher power through the antenna and resulting in larger ablation zones. The primary benefit of using MW ablation in the liver appears to be the ability to overcome large heat sinks due to the vascularity of this organ. In a recently published series of 1,136 patients with 1,928 malignant liver tumors treated with percutaneous MW ablation, Liang et al. reported successful completion of the ablation with minimal mortality, 0.2 %, and major morbidity of 2.6 % of patients. Ultrasound guidance is used for guided biopsy, for introduction of the MW antenna (S), and for monitoring the ablation zone [40]. Ultrasound allows real-time monitoring of the ablation and facilitates identification of the treated zone by showing hyperechoic microbubbles enveloping the treated area (Fig. 7.40) (please refer to Chap. 17 for further information).

Conclusion

The use of ultrasound beyond diagnosis of abdominal conditions is now widely accepted. Surgeons can use interventional ultrasound for diagnostic and therapeutic purposes in most areas of the body. Indications for interventional ultrasound in the abdomen include but are not limited to aspiration, biopsy, drainage, placement of catheters, and tumor ablation. The portability, safety, low cost, and ability to observe a procedure on real time make ultrasound an ideal technology to embrace and master. Introduction of guiding systems, better automatic biopsy needles, and the increased utilization of ablation in the surgical field make learning these techniques an absolute necessity for the practicing surgeon. Furthermore, interventional ultrasound can be an effective and efficient adjunct to the surgeon in the operative approach to various intra-abdominal conditions. Both open and laparoscopic approaches to the management of hepatobiliary and pancreatic disease benefit from the use of ultrasound. The field of surgery is constantly evolving and interventional sonography continues to grow with it. As more applications for this field continue to be discovered, this will only further the practice of surgery.

References

1. Berlyne GM. Ultrasonics in renal biopsy. Lancet. 1961;1:750–1.
2. Joyner Jr CR, Herman RJ, Reid JM. Reflected ultrasound in the detection and localization of pleural effusion. JAMA. 1967;200:399–402.

3. Holm HH, Søren TP, Juul N, Larsen T. Instrumentation for sonographic interventional procedures. In: van Sonnenberg E, editor. Interventional ultrasound. New York: Churchill Livingstone; 1987. p. 9–40.
4. Gammelgaard PA, Holm HH, Kristensen JK, Rasmussen SN. Ultrasound in renal diagnosis. Film presented at American Institute of Ultrasound in Medicine annual meeting; Cleveland; 1970.
5. Holm HH, Kristensen JK, Rasmussen SN, Pedersen JF. Ultrasound as a guide in percutaneous puncture technique. Ultrasonics. 1972; 10:83–6.
6. Goldberg BB, Pollack HM. Ultrasonic aspiration transducer. Radiology. 1972;102:187–9.
7. Rasmussen SN, Holm HH, Kristensen JK, Barlebo H. Ultrasonically guided liver biopsy. Br Med J. 1972;2:500–2.
8. Bang J, Northeved A. A new ultrasonic method of transabdominal amniocentesis. Am J Obstet Gynecol. 1972;114:599–601.
9. Bahlmann J, Otto P. Perkutane Nierenbiopsie mit ultraschall-Lokalization. Dtsch Med Wochenschr. 1972;97:840–2. German.
10. Bartels ED, Jorgensen HE. Experiences with percutaneous renal biopsies. Scand J Urol Nephrol. 1972;6:57–63.
11. Kristensen JK, Holm HH, Rasmussen SN, Redersen JF, Gammelgaard PA. Ultrasonically guided percutaneous puncture of renal masses. Scand J Urol Nephrol. 1972;6:49–56.
12. Staren ED. Surgical office-based ultrasound of the breast. Am Surg. 1995;61:619–26.
13. Palombini L, Fulciniti F, Vetrani A, et al. Fine-needle aspiration biopsies of breast masses: a critical analysis of 1956 cases in 8 years (1976–1984). Cancer. 1988;61:2273–7.
14. Ballo MS, Sneiga N. Can core needle biopsy replace fine needle aspiration cytology in the diagnosis of palpable breast carcinoma: a comparative study of 124 women. Cancer. 1996;78:773–7.
15. Welch N, Reading CC. Imaging-guided biopsy. Mayo Clin Proc. 1989;64:1295–302.
16. Schwerk WE, Durr HK, Schmitz-Moormann P. Ultrasound guided fine-needle biopsies in pancreatic and hepatic neoplasms. Gastrointest Radiol. 1983;8:219–25.
17. Don S, Kopecky KK, Pescovitz MD, et al. Ultrasound guided pediatric liver transplant biopsy using a spring-propelled cutting needle (biopsy gun). Pediatr Radiol. 1994;24:21–4.
18. Gandini G, Grosso M, Bonardi L, et al. Results of percutaneous treatment of sixty-three pancreatic pseudocysts. Ann RadioI. 1988;31:117–22.
19. Verges BL, Cercuell JP, Jacob D, et al. Results of ultrasonically guided percutaneous ethanol injection into parathyroid adenomas in primary hyperparathyroidism. Acta EndocrinoI. 1993;129:381–7.
20. Gaitini D, Kopelman D, Soudak M, et al. Impact of intraoperative sonography on resection and cryoablation of liver tumors. J Clin Ultrasound. 2001;29:265–72.
21. Machi J, Uchida S, Sumida K, et al. Ultrasound-guided radiofrequency thermal ablation of liver tumors: percutaneous, laparoscopic and open surgical approaches. J Gastrointest Surg. 2001;5:477–89.
22. Machi J, Arregui M, Staren E. Interventional ultrasound. In: Machi J, Staren E, editors. Ultrasound for surgeons. Philadelphia: Lippincott Williams & Wilkins; 2004. p. 35–67.
23. McGahan JP, Brant WE. Principles, instrumentation, and guidance systems. In: McGahan JP, editor. Interventional ultrasound. Baltimore: Williams & Wilkins; 1990. p. 1–20.
24. Saitoh M, Watanabe H, Ohe H, Tanaka S, Itakura Y, Date S. Ultrasonic realtime guidance for percutaneous puncture. J Clin Ultrasound. 1979;7:269–72.
25. McGahan JP. Invasive ultrasound principles (biopsy, aspiration, and drainage). In: McGahan JP, Goldberg BB, editors. Diagnostic ultrasound: a logical approach. Philadelphia: Lippincott-Raven Publishers; 1998. p. 39–75.
26. Martin HE, Ellis EB. Biopsy of needle puncture and aspiration. Ann Surg. 1930;92:169–81.
27. Stewart FEW. The diagnosis of tumors by aspiration. Am J Pathol. 1933;9:801–12.
28. Ragde H, Aldape HC, Blasko JC. Biopty: an automatic needle biopsy device--its use with an 18 gauge Tru-cut needle (Biopty-cut) in 174 consecutive protate core biopsies. Endosonographique 1987; 3–5.
29. Parker SH, Hopper KD, Yakes WF, Gibson MD, Ownbey JL, Carter TE. Image-directed percutaneous biopsies with a biopsy gun. Radiology. 1989;171:663–9.
30. Makuuchi M, Beppu T, Kamiya K, et al. Echo-guided percutaneous transhepatic cholangiography with puncture transducer. Jpn J Surg. 1978;8:165–75.
31. Perrone JM, Soper NJ, Eagon JC, et al. Perioperative outcomes and complications of laparoscopic ventral hernia repair. Surgery. 2005;138:708–16.
32. Sains PS, Tilney HS, Purkayastha S, et al. Outcomes following laparoscopic versus open repair of incisional hernia. World J Surg. 2006;30:2056–64.
33. Bean WJ. Renal cysts: treatment with alcohol. Radiology. 1981;138:329–31.
34. Livraghi T, Bolondi L, Lazzaroni S, Marin G, Morabito A. Percutaneous ethanol injection in the treatment of hepatocellular carcinoma in cirrhosis. Cancer. 1992;69:925–9.
35. McGahan JP, Browing PD, Brock JM, Tesluk H. Hepatic ablation using radiofrequency electrocautery. Invest Radiol. 1990; 25:267–70.
36. Rossi S, Fornari F, Pathies C, Buscarini L. Thermal lesions induced by 480 KHz localized current field in guinea pig and pig liver. Tumori. 1990;76:54–7.
37. Kruskal JB, Newman PA, Sammons LG, Kane RA. Optimizing Doppler and color flow US: application to hepatic sonography. Radiographics. 2004;24:657–67.
38. Wright AS, Lee FT, Mahvi DM. Hepatic microwave ablation with multiple antennae results in synergistically larger zones of coagulation necrosis. Ann Surg Oncol. 2003;10:275–83.
39. Brace CL. Microwave tissue ablation: biophysics, technology and applications. Crit Rev Biomed Eng. 2010;38:65–78.
40. Liang P, Wang Y, Yu X, et al. Malignant liver tumors: treatment with percutaneous microwave ablation – complications among cohort of 1136 patients. Radiology. 2009;251: 933–40.

Trauma Ultrasound

8

Kazuhide Matsushima and Heidi L. Frankel

Introduction

Information obtained using ultrasound can often direct the management of injured patients. As an ultrasound study can be performed safely in the resuscitation room, ICU, or operating room, this technology is appropriate for use even in unstable patients. Over the past several decades, the indications for the use of ultrasound have expanded rapidly to a wide range of surgical diseases, with much enthusiasm by surgeons to perform studies independently [1–4]. It is important to note that other imaging modalities, particularly multidetector row computed tomography (MDCT), have also developed progressively over the same period [5]. The proper use of these advanced imaging modalities is key to improving the outcome of trauma patients. In this chapter, we will describe ultrasound techniques and their indications in the management of trauma patients.

History

At the beginning of the1970s, Goldberg and colleagues reported the successful visualization of as little as 100 mL of intra-abdominal free fluid using ultrasound [6]. The clinical significance of this ability was not recognized until the1980s, when care providers started using ultrasound to detect intra-abdominal free fluid (blood) in the injured patient [7, 8]. While small series on the use of ultrasound for diagnosis in trauma patients have been published in Europe and Asian countries since the1980s, it was not until the early 1990s when Tso and associates reported the first case series of trauma ultrasound in the United States [9]. Rozycki and colleagues conducted the first prospective study to investigate the sensitivity and specificity of ultrasound in injured patients [10]. They demonstrated that ultrasound studies performed by surgeons and their trainees were of high accuracy in the detection of free fluid. Their group initially named the ultrasound technique to detect pericardial effusion and intra-abdominal free fluid for the trauma patient, "FAST" (focused abdominal sonogram for trauma) [11, 12]. Subsequently, the acronym "focused assessment with sonography for trauma" has gained consensus [13].

FAST: Principle and Basic Technique

The main purpose of the FAST examination is to identify fluid in the pericardial and dependent spaces of the abdominal cavity of the patient in the supine position. The one pericardial and three intra-abdominal views are to be scanned within 5 min. FAST is currently incorporated in the ATLS (advanced trauma life support) algorithm, but the timing of performing the examination may be variable. It may be conducted during the primary survey as a part of "C: circulation" for hemodynamically unstable patients or as one of the adjunct imaging studies during the secondary survey for stable patients [14]. The ultrasound machine always needs to be powered on before a trauma patient presents to the resuscitation room. FAST can be performed by a trauma surgeon, surgical trainee, or emergency room physician. The technique for FAST examination is summarized in Table 8.1.

K. Matsushima, MD
Department of Surgery,
University of Southern California,
Los Angeles, CA USA
e-mail: mkazu45@gmail.com

H.L. Frankel, MD, FACS, FCCM (✉)
Department of Surgery,
University of Southern California Keck School of Medicine,
Los Angeles, CA, USA
e-mail: heidileefrankel@gmail.com

E.J. Hagopian, J. Machi (eds.), *Abdominal Ultrasound for Surgeons*,
DOI 10.1007/978-1-4614-9599-4_8,

Table 8.1 Summary of FAST techniques

Goal: to detect and rule out fluid collection in pericardial space and intra-abdominal cavity
Transducer: 2.5–5.0 MHz sector- or convex-type transducer
Image mode: regular abdomen image mode
Timing of study: during the primary survey for unstable patient or during the secondary survey for stable patient
Pericardial examination: longitudinal or transverse view in the subxiphoid area
Abdominal examination: longitudinal views in right and left upper quadrants, and longitudinal or transverse view of the pelvis

Pericardial Examination

The examination is typically conducted with the ultrasound machine positioned on the patient's right side, although some perform a FAST from the patient's left (personal experience, authors). A low-frequency transducer (2.5–5.0 MHz), sector or convex type, is used to maximize penetration. The pericardial examination should be performed prior to the abdominal examination to optimize the ultrasound settings (e.g., gain, depth). The transducer is first oriented in the sagittal plane in the subxiphoid area. The transducer may then be rotated 90° counterclockwise to provide a transverse view of the heart. As the primary goal of FAST is to identify free fluid which appears as an anechoic (dark) space, fluid (blood) inside the atria and ventricles can be used to adjust the settings, particularly the gain to improve image quality (Figs. 8.1 and 8.2). The examination focuses on the identification of free fluid in the pericardial space. Spending extra time to survey for a structural abnormality of the heart during the initial assessment is not necessary and may be harmful if it delays resuscitation or further diagnostic testing. For the patient who is morbidly obese, who has a narrow costal angle, or who has subcutaneous emphysema, the subxiphoid window may be difficult to visualize, and alternate views may need to be acquired.

Abdominal Examination

Next, an examination is performed to survey for free fluid in the abdominal cavity. Three dependent areas are visualized: the hepatorenal recess (Morison's pouch) in the right upper quadrant, the splenorenal recess in the left upper quadrant, and the pelvic region around the bladder. First, a long-axis view is obtained at the level of 10th to 11th intercostal space in the right mid- to posterior axillary line for surveillance of the hepatorenal recess (Figs. 8.3 and 8.4). Appropriate transducer placement varies based on the patient's body habitus or history of pulmonary disease. To minimize the false-negative rate, the area of interest should be surveyed entirely by changing the angle of the transducer (fanning). Next, a longitudinal view of the splenorenal recess is obtained in the left upper quadrant (Figs. 8.5 and 8.6). Trauma patients often present with a full stomach that can obscure the penetration of ultrasound. Therefore, transducer placement should be

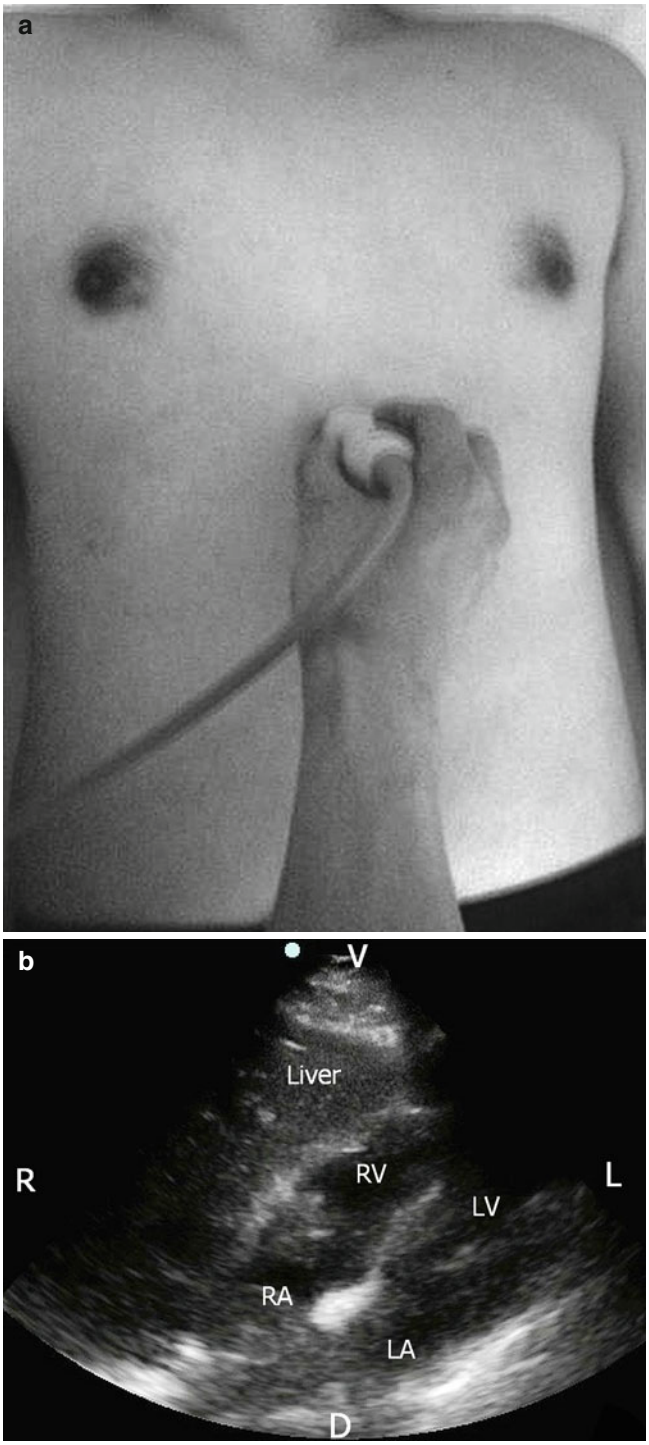

Fig. 8.1 (**a**, **b**) Transducer placement for pericardial examination and transverse view of normal pericardial examination with transducer in abdominal preset. *RA* right atrium, *LA* left atrium, *RV* right ventricle, *LV* left ventricle, *R* right, *L* left, *V* ventral, *D* dorsal

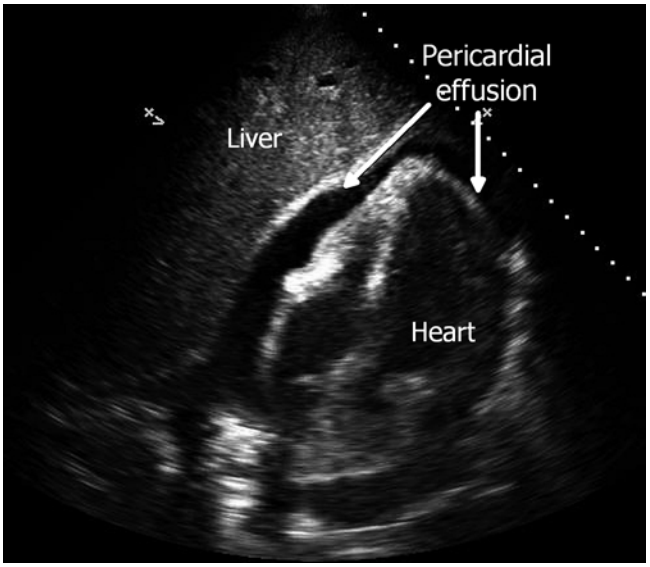

Fig. 8.2 Transverse view of the pericardial examination in an abdominal preset demonstrating a pericardial effusion. Note the small cavity size of the RV. Diastolic collapse of the RV would demonstrate tamponade physiology. *RV* right ventricle

more cephalad and posterior than the analogous view on the right side for better visualization. Finally, the transducer is moved to the pelvis just above the pubic symphysis (Figs. 8.7 and 8.8). The transducer is oriented in either the sagittal or transverse plane.

FAST: Clinical Data

Blunt Torso Injury

In the United States, the first prospective study of surgeon-performed FAST was conducted by Rozycki and colleagues in 1995 [11]. They showed 78.6 % sensitivity and 100 % specificity for the detection of free fluid among 295 blunt injury patients. Their group reported on a larger number of patients in 1998 [15]. Among 1,227 patients, the sensitivity and specificity was 78.3 and 97.4 %, respectively. While FAST could accomplish a very low false-positive rate, more than 20 % of free fluid was missed according to these data. Friese and associates reported that the sensitivity of FAST was as low as 26 % among the patients with pelvic fractures [16]. Hypotensive patients with positive FAST in the abdomen should be taken to the operating room immediately for exploratory laparotomy. In contrast, intra-abdominal bleeding should not be ruled out just based on a negative or indeterminate FAST in hypotensive patients. These patients need to undergo repeat FAST or an alternate test such as diagnostic peritoneal aspiration (DPA) to confirm the result [17]. However, repeat FAST might not be ideal in the face of

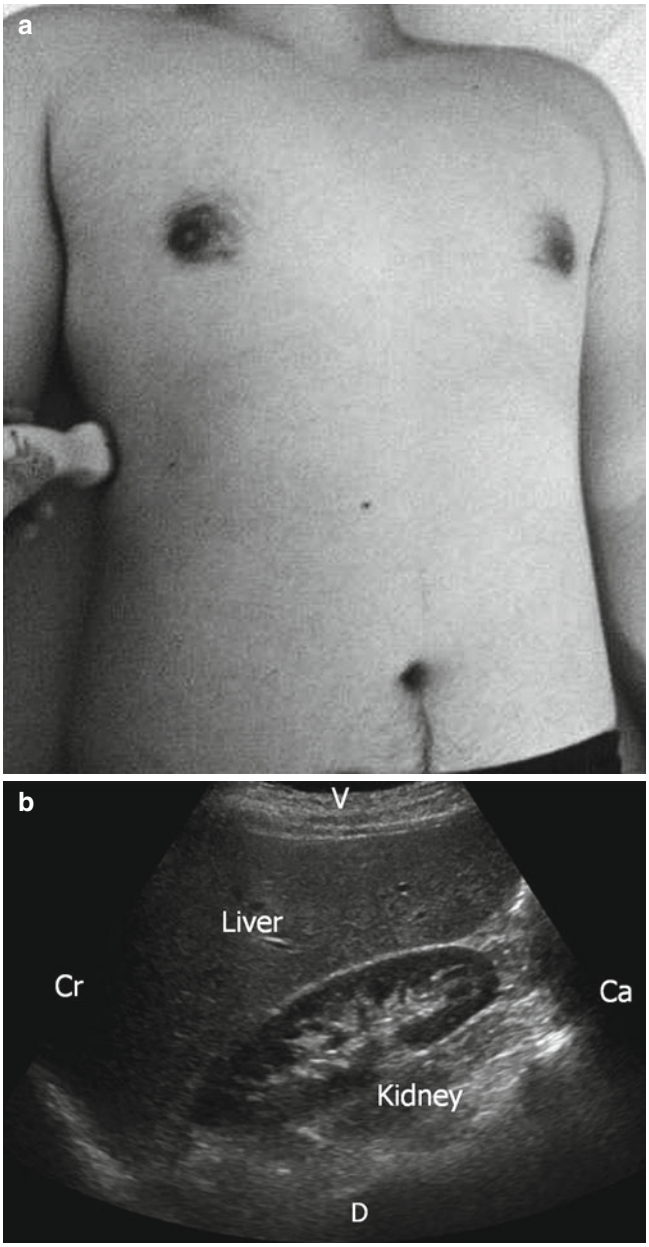

Fig. 8.3 (**a**, **b**) Transducer placement for the right upper examination and normal longitudinal view. *Cr* cranial, *Ca* caudal, *V* ventral, *D* dorsal

continued hemodynamic instability. We also prefer DPA over lavage (DPL) because fluid instilled during the procedure can be confusing on CT images once the patient is stabilized and sent for scanning.

With the development of MDCT, the role of FAST in hemodynamically stable trauma patients is currently of little value (except for triage and education), particularly among the adult population. In addition to a higher sensitivity for intra-abdominal bleeding, the information regarding organ-specific injury can be obtained more accurately by MDCT. In a single-center retrospective study, Natarajan showed that the sensitivity

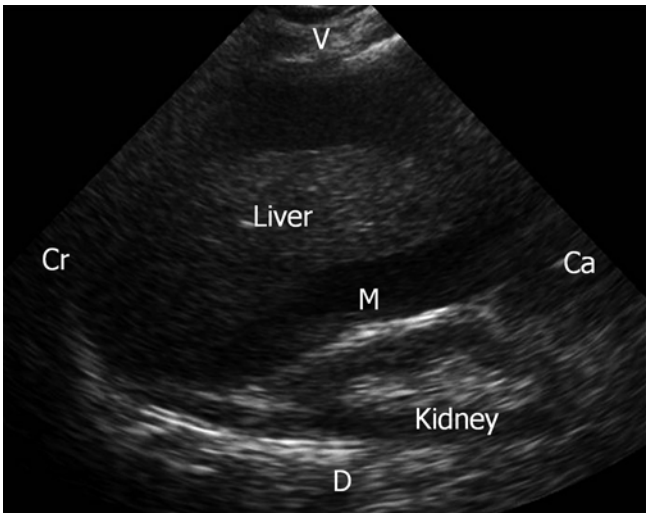

Fig. 8.4 Longitudinal view of the right upper quadrant demonstrating free fluid in Morrison's pouch and above the liver. *Cr* cranial, *Ca* caudal, *V* ventral, *D* dorsal, *M* Morrison's ouch

of FAST performed by residents under attending trauma surgeons' supervision was impressively low (40.8 %). Further, 22 % of false-negative cases required exploratory laparotomy [18]. Additional study will be needed to explore the utility of FAST for stable patients as the risk of radiation exposure by CT to trauma patients is now well recognized [19].

Penetrating Torso Injury

For the patient with penetrating injury to the area known as the "box" or "kill zone" defined as an area bounded by the nipple line bilaterally, sternal notch superiorly, and xiphoid process inferiorly (Fig. 8.9), FAST is a rapid and effective tool for the diagnosis of cardiac injury by detecting pericardial free fluid. From early experience in the 1990s, Rozycki demonstrated that the sensitivity and specificity of FAST approached100 % for the detection of pericardial fluid in the patient with cardiac injury [20]. Of note, in their multicenter study, they showed that FAST could expedite the treatment of cardiac injury (the mean time from a positive pericardial fluid FAST to operation was 12±5 min) [21]. A false-negative FAST is possible in the patient whose pericardial blood decompresses into the chest cavity. The patient usually presents with a large hemothorax with unstable vital signs. Thus, an unstable patient with a "box" injury may need a surgical pericardial window despite a negative FAST. In contrast, epicardial fat pads may be mistaken for pericardial fluid because fat tissue appears as hypoechoic in ultrasound. For the patient in whom visualization of the heart is difficult due to body habitus or injury pattern (wound to the subxiphoid area), an alternate view can be obtained in the second intercostal space (parasternal view) or left nipple area (apical view). Pericardial FAST may also be beneficial to assist in

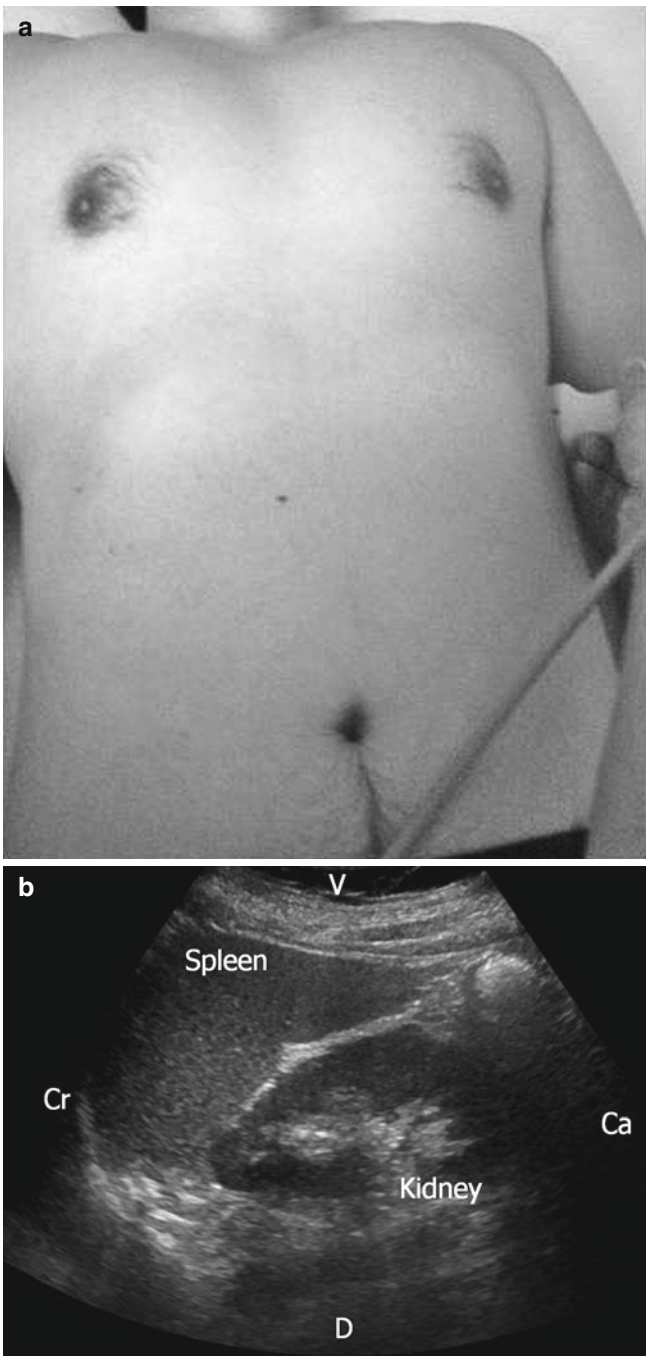

Fig. 8.5 (**a**, **b**) Transducer placement for the left upper quadrant and normal longitudinal view. *Cr* cranial, *Ca* caudal, *V* ventral, *D* dorsal

the decision to terminate resuscitative efforts in penetrating (or even blunt) torso trauma, particularly if no injury is visualized in the chest [22, 23].

In contrast to its use in blunt abdominal injury, FAST is not currently considered the standard imaging modality of choice for penetrating abdominal injury [24]. The accuracy of FAST for penetrating torso injury has been studied since the 1990s [11, 25, 26]. An early study by Rozycki showed that the sensitivity and specificity of FAST for penetrating

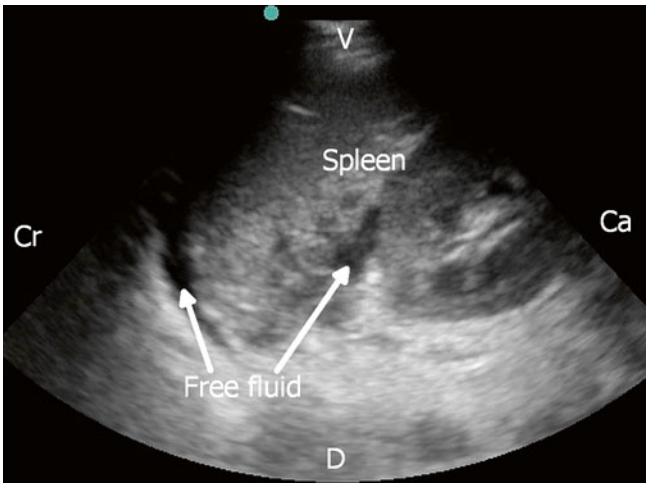

Fig. 8.6 Longitudinal view of the left upper quadrant demonstrating free fluid in the splenorenal recess and above the spleen. *Cr* cranial, *Ca* caudal, *V* ventral, *D* dorsal

injury were 83.8 and 97.4 %, respectively [11]. This result is comparable to that for blunt injury. However, a subsequently performed study showed much lower sensitivity, ranging from 46 to 67 % [27]. The biggest reason why FAST is not used for penetrating abdominal injury as often as blunt injury is its low sensitivity for detecting hollow viscus and diaphragm injury that are far more common in penetrating than blunt injury. In other words, a negative FAST cannot safely exclude these injuries. Thus, hemodynamically stable patients with abdominal gunshot or stab wounds with fascial violation may still require exploratory laparotomy to exclude visceral injury that may not be associated with an appreciable amount of free fluid [28]. Soffer demonstrated this low sensitivity of FAST (48 %) in their patients with penetrating injury performed by trauma surgeons and surgical trainees [29]. Not surprisingly, they found a significant number of missed hollow viscus and diaphragm injuries. Likewise, they showed that a positive FAST rarely added any information to change the management of the patient with penetrating torso injury. There were only three patients whose initial management was altered by a positive FAST. All these patients had unclear bullet trajectory with no signs or symptoms for immediate exploration. FAST may be helpful in the situation of the hemodynamically unstable patient with multicavitary penetrating injury to assist in deciding which body cavity to enter first or in the instance of multiple simultaneously penetrating injured patients for triage purposes.

E-FAST: Extended FAST

Principles and Technique

The incidence of pneumothorax or hemothorax is astoundingly common in injured patients [30]. In addition to physical examination during the initial ATLS protocol, chest radiography (CXR) has historically been the diagnostic study of choice to identify these potentially life-threatening injuries. However, the utility of CXR for identifying both pneumothorax and hemothorax is somewhat suspect, with surprisingly low sensitivity, as will be discussed in detail below [31]. For trauma patients, CXR is usually performed with the patient in the supine position to maintain spinal immobilization. As air tends to be loculated anteriorly and fluid (blood) posteriorly, an anterior-posterior view of CXR may not visualize air or blood. For hemodynamically unstable patients with suspected thoracic injury, a so-called normal CXR cannot safely (or often rapidly) exclude the potential for pneumothorax or hemothorax. For example, CXR diagnosis of hemothorax requires the presence of at least 175 mL of fluid in the chest cavity [32]. A recent multicenter study demonstrated that 6 % of patients with occult pneumothoraces (defined as those visualized on CT (or ultrasonography), but not on CXR) eventually required tube thoracostomy due to the progression [33].

E-FAST is performed with the patient in the supine position with the same machine position as with a conventional FAST and starts using a low-frequency transducer (Fig. 8.10). The examination typically adds no more than 2 min to a conventional FAST examination [34]. The initial portion of the E-FAST involves retracing the abdominal right and left upper quadrant views with the transducer oriented in a more cephalad fashion to search for free fluid above the diaphragm. Hemothorax (fluid) is detected as an anechoic (black) area above the diaphragm (Fig. 8.11). Ultrasound can detect as little as 20 mL of fluid in the chest cavity. Clot-bearing hemothoraces might be seen as more hypoechoic (gray). Finally, in patients with moderate to large hemothoraces, the atelectatic (collapsed) lung parenchyma will be a hyperechoic (white) structure floating in the fluid. Also, the thoracic spine can be visualized above the level of diaphragm when the transducer is aimed toward the midline ("spine sign") as ultrasound penetrates through fluid in the chest cavity. In normal individuals, air in the lung parenchyma obscures the spine in these levels.

The remainder of the E-FAST examination is typically performed with a high-frequency (7.5–10 MHz) transducer; however, it can be accomplished with a low-frequency transducer as well. As air is usually located in the anterior chest of a patient in the supine position, the ultrasound images are obtained through the anterior intercostal spaces (high, mid, and low levels) in the midclavicular line bilaterally. The transducer is oriented in the sagittal or long-axis plane. The sonographic finding of a normal lung includes lung sliding and the comet-tail sign (Fig. 8.12). Real-time observation of the parietal and visceral pleura moving in apposition to each other is called "lung sliding" [35]. Comet tails or lung rockets, characterized as vertical, narrow-based, and hyperechoic lines arising from pleural line, represent artifacts resulting

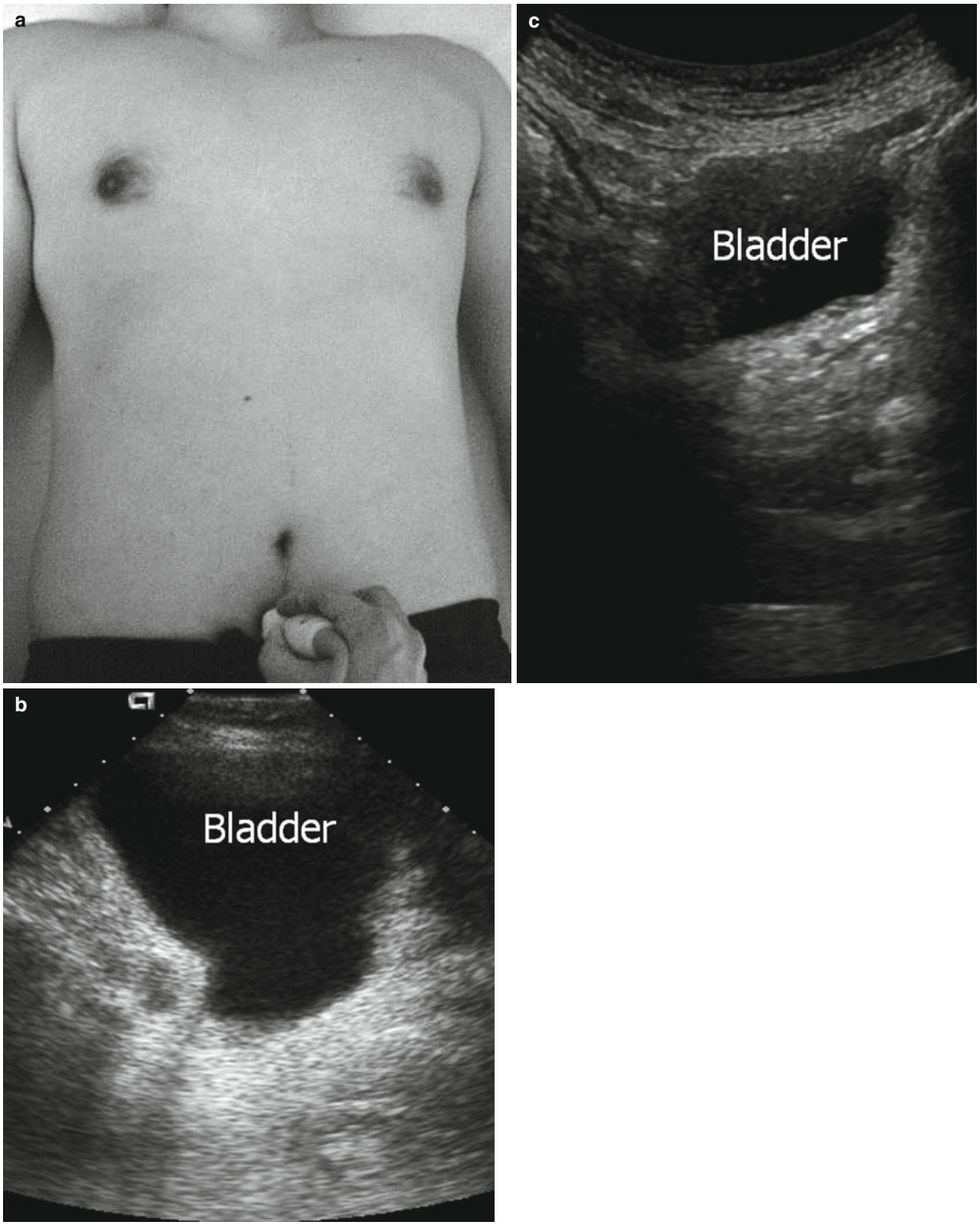

Fig. 8.7 (**a–c**) Transducer placement for the pelvic view and normal transverse and longitudinal views. (**b**) Transverse view. (**c**) Longitudinal view

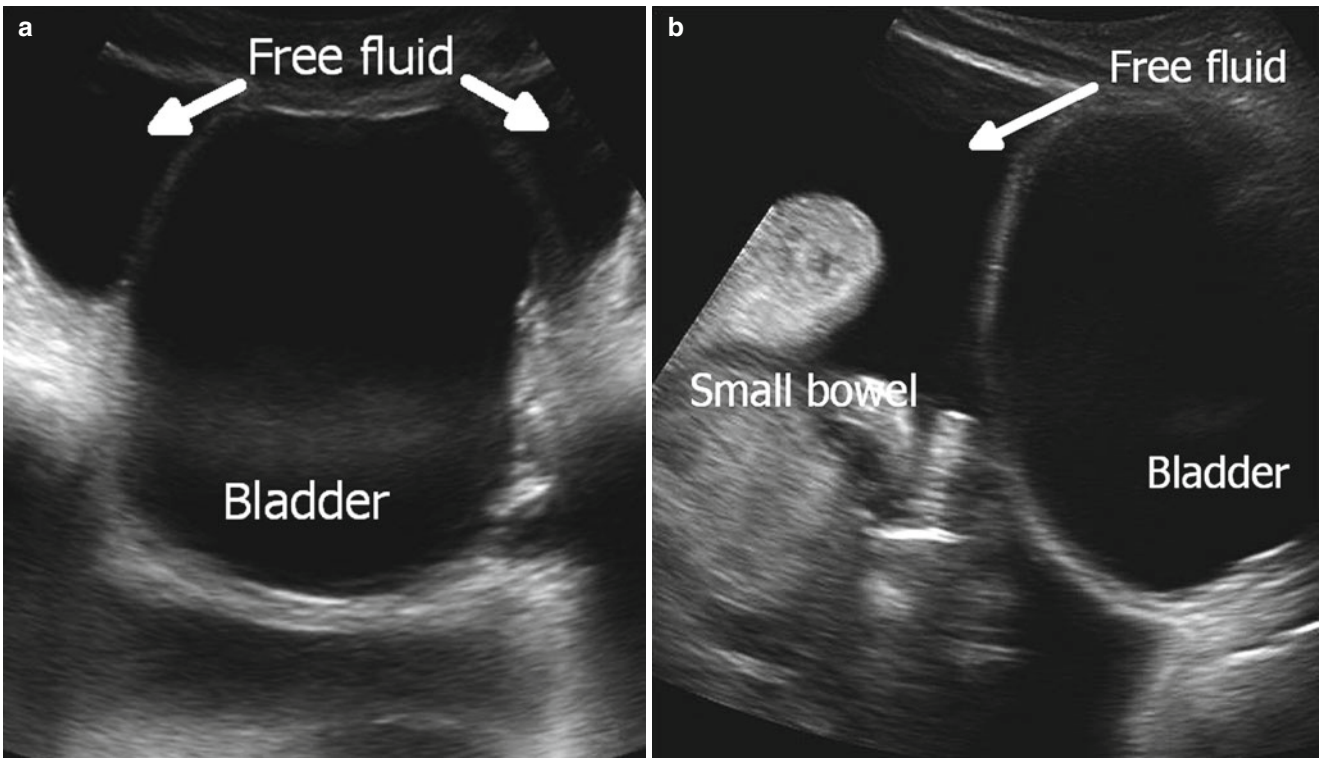

Fig. 8.8 (**a**, **b**) Pelvic view demonstrating free fluid. (**a**) Transverse view. (**b**) Longitudinal view

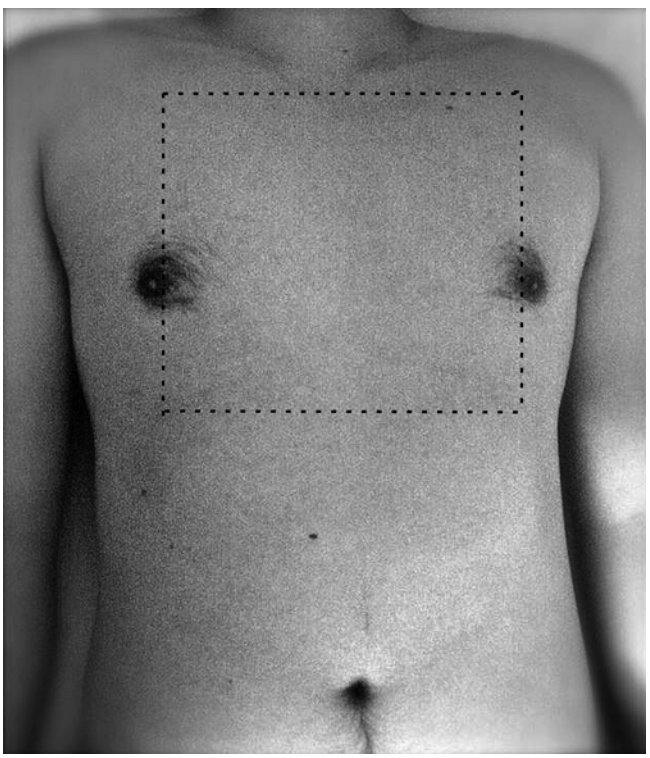

Fig. 8.9 "Box" or "kill zone" demonstrating topographic region where the heart and the great vessels are at risk of injury

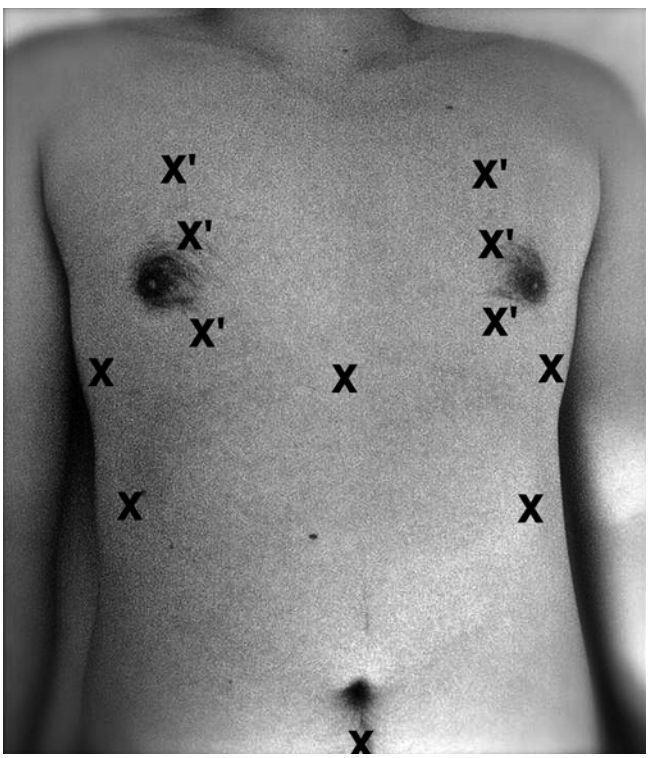

Fig. 8.10 Transducer placement for extended focused assessment with sonography for trauma. *X* low-frequency transducer, *X′* high-frequency transducer

from reverberation of ultrasound. Another technique to detect pneumothorax is performed using the M-mode (motion-mode) view as opposed to the B-mode (brightness mode) used in other portions of the E-FAST (see section "Imaging modes"). In the normal lung, a linear pattern of ultrasound image above the pleural line and a granular pattern below the pleural plane are seen, the so-called seashore sign (Fig. 8.12). Pneumothorax can be diagnosed by both the absence of comet tails and of lung sliding. The M-mode view shows loss of the seashore sign, with a similar linear pattern above and below the pleural line, the so-called barcode sign (Fig. 8.13).

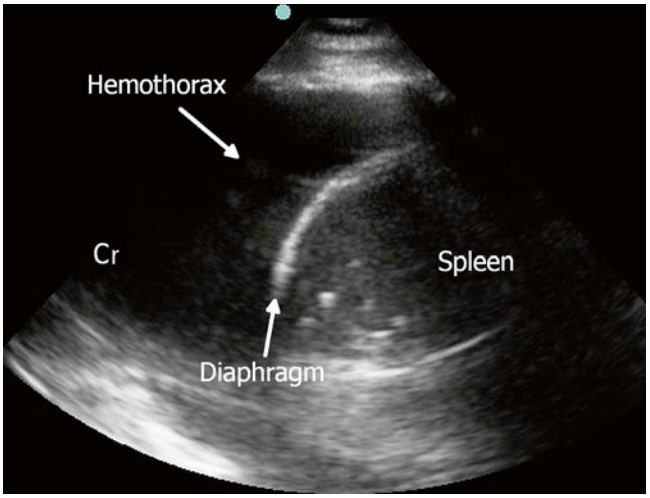

Fig. 8.11 Extended focused assessment with sonography for trauma: free fluid in the thorax (hemothorax) in a longitudinal view of the left upper quadrant with low-frequency transducer directed cranially. *Cr* Cranial

Clinical Data

In 1993, Röthlin and colleagues first described, in the English literature, using ultrasound to detect hemothoraces in injured patients [36]. In 1996, Ma and associates conducted a retrospective analysis comparing the sensitivity of ultrasound performed by emergency physicians to CXR for the detection of hemothorax [32]. For 26 patients with hemothoraces, they found a comparable sensitivity and specificity of these imaging modalities (96.2 and 100 %, respectively in both CXR and ultrasound). Sisley and colleagues conducted a prospective study to evaluate the accuracy of surgeon-performed

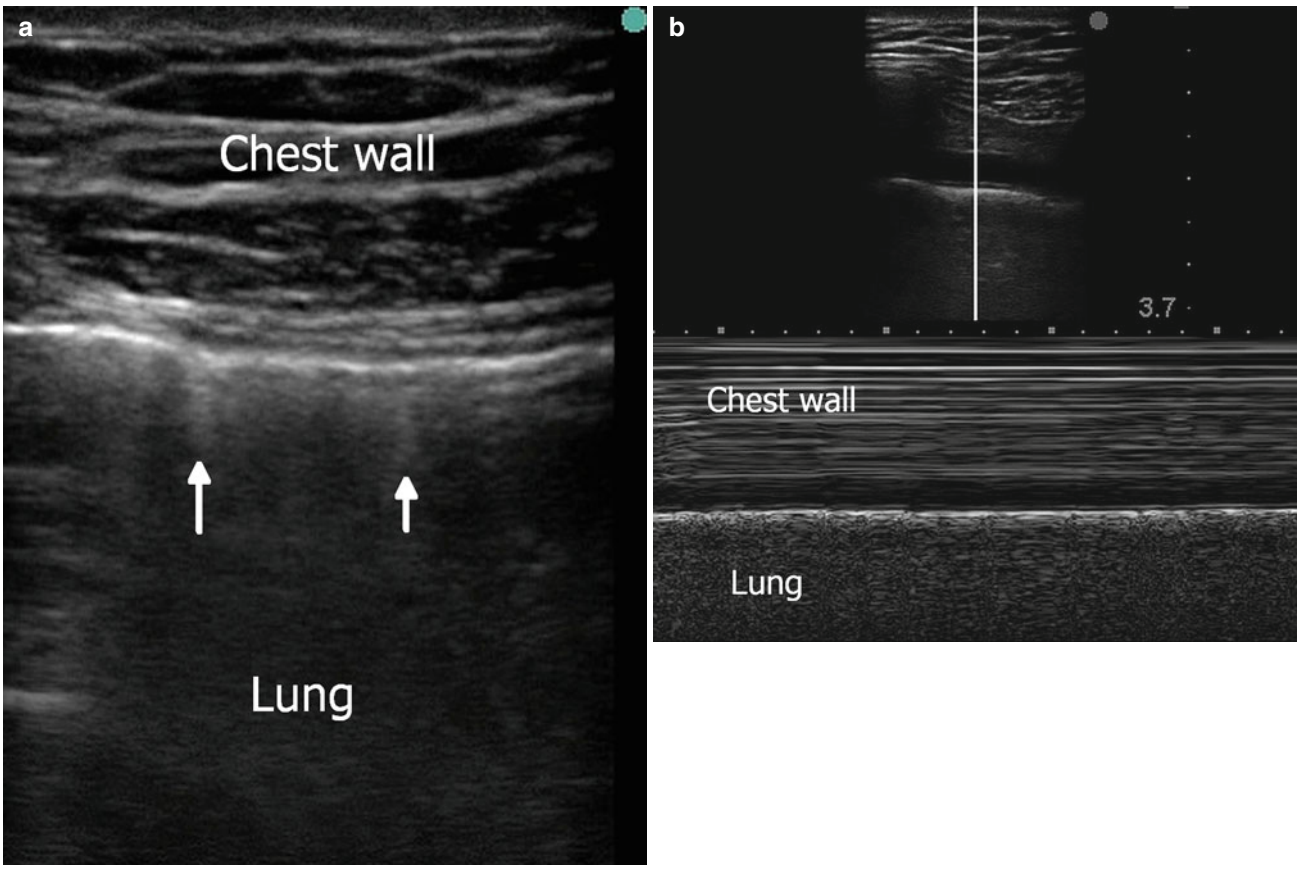

Fig. 8.12 Normal view in thoracic view of extended focused assessment with sonography for trauma using a high-frequency transducer. (**a**): In B (brightness)-mode view, pleural sliding (see text) and comet-tail sign (*arrows*) are identified. (**b**): In M (motion)-mode view, seashore sign (see text) is observed

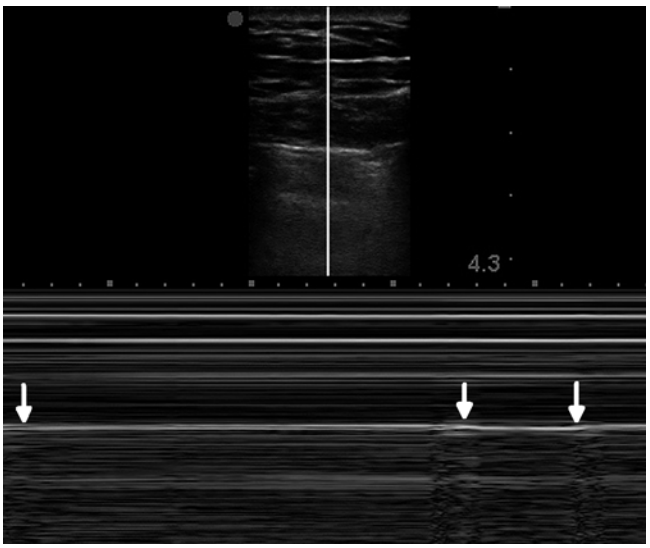

Fig. 8.13 Positive finding (pneumothorax) in thoracic view of extended focused assessment with sonography for trauma using a high-frequency transducer. Loss of seashore sign (*barcode sign*) is observed. With respiration, normal lung sliding is identified as known as "lung point" (*arrows*)

ultrasound for the detection of hemothorax [37]. Again, thoracic ultrasound and CXR had similar sensitivity and specificity (97.5 % sensitivity and 99.7 % specificity for ultrasound and 92.5 % sensitivity and 99.7 % specificity for CXR). Notably, study time for ultrasound was significantly shorter than CXR (1.30 vs. 14.18 min, $p<0.0001$). Another prospective study by Brooks documented a high sensitivity of ultrasound for hemothorax [38]. Hyacinthe and colleagues recently reported the diagnostic accuracy of ultrasound compared to clinical examination plus CXR for the detection of thoracic trauma including pneumothorax, hemothorax, and lung contusion [39]. Using CT as a comparison, thoracic ultrasound was superior to clinical examination plus CXR for pneumothorax and lung contusion while similar results were found for hemothorax.

Rantanen and associates described the utility of ultrasound for the diagnosis of pneumothorax in horses in 1986 [40]. Lichtenstein subsequently applied this thoracic ultrasound technique to critically ill patients (using a low-frequency transducer) [35]. The sensitivity and specificity of ultrasound for the detection of pneumothorax were 95.3 and 91.1 %, respectively. Dulchavsky first reported on the accuracy of ultrasound in detecting pneumothorax in injured patients [41]. Compared to CXR, the sensitivity of ultrasound was 95 %. Of note, two pneumothoraces were missed because of concomitant subcutaneous air. Similarly, Knudtson reported 100 % sensitivity and specificity in penetrating trauma and 88.9 % sensitivity and 99.7 % specificity in blunt trauma for ultrasound for the diagnosis of pneumothorax [42]. Subsequently, comparison of the sensitivity between CXR and thoracic ultrasound was performed using

Table 8.2 Summary of the bedside echocardiographic assessment in trauma/critical care (BEAT) examination

	View	Task	Goal
*B*eat	Parasternal long	Stroke volume	Cardiac function
*E*ffusion	Parasternal long	Subjective assessment	Pericardial effusion
*A*rea	Parasternal short, apical four chamber	Subjective assessment	Right and left ventricular size, movement
*T*ank	Subcostal	IVC measurement	Volume status

IVC inferior vena cava

CT as a gold standard. Kirkpatrick reported on E-FAST performed by trauma surgeons with a handheld portable ultrasound [34]. The sensitivity of E-FAST for pneumothorax detection was 48.8 %, while the sensitivity of CXR was 20.9 % in 266 patients with CT as a gold standard. A higher sensitivity (>90 %) for thoracic ultrasound in diagnosing pneumothoraces has been observed in more recent studies [43]. A meta-analysis by Alrajhi included eight studies with 1,048 patients [44]. Ultrasound was 90.9 % sensitive and 98.2 % specific for the detection of traumatic or iatrogenic pneumothorax, which was superior to that of CXR (50.2 % sensitivity and 99.4 % specific). In a subgroup analysis of trauma patients, similar results were shown.

Trauma Ultrasound in the ICU Setting

An accurate and real-time assessment of hemodynamic status is crucial to improve the outcome of critically ill patients. Historically of value, pulmonary artery catheters (PAC) have largely been abandoned based on multiple randomized studies failing to demonstrate an outcome benefit [45–47]. Currently, a myriad of options are available for hemodynamic monitoring in the ICU setting [48, 49]. Of these, noninvasive monitoring of preload status and cardiac function using ultrasound has obtained popularity in the last decade [50, 51]. Moreover, it has been demonstrated that bedside echocardiography performed by intensivists can provide accurate information on the patient in a timely fashion [52, 53]. Favorable data have been also reported among critically ill trauma patients [54–57].

Gunst and colleagues reported an ultrasound technique for hemodynamic monitoring, entitled "the BEAT exam (bedside echocardiographic assessment for trauma/critical care)" [58]. The BEAT exam consists of the assessment of (1) (B)eat, cardiac function; (2) (E)ffusion, pericardial effusion; (3) (A)rea, right and left ventricle function; and (4) (T)ank, volume status (Table 8.2). Unlike FAST, all images for BEAT are acquired using a cardiac software package. A 3.5–5.0 MHz sector-type transducer is used. Patients can be positioned in the lateral decubitus position when supine

position views are not optimal. Cardiac function is evaluated both by a subjective assessment of cardiac morphology and by calculated objective values (e.g., stroke volume, cardiac output, ejection fraction) (Figs. 8.14 and 8.15). Intravascular volume status (preload) is assessed by measuring the diameter of the inferior vena cava (IVC) within 2 cm of its entrance to the right atrium (Fig. 8.16). This view is normally obtained using a longitudinal view through subxiphoid region. An IVC of smaller diameter (<20 mm) with >50 % collapsibility with patient respiration suggests intravascular volume depletion. The accuracy of the BEAT exam for the assessment of cardiac function and volume status was evaluated by comparing it to PAC for surgical ICU patients (57 % trauma) [54]. Good quality images were obtained in 59 % of cardiac index examinations and 97 % of IVC measurements performed by six trauma surgeons or trainees. For both cardiac index and IVC measurements, there were significant correlations between BEAT exam and PAC values. Similarly, Murthi and associates compared the bedside ultrasound technique, "FREE (focused rapid echocardiographic evaluation)," with PAC or pulse contour analysis via arterial line for the measurement of cardiac index [55]. They showed FREE and PAC agreement in 87 % of patients and FREE and pulse contour analysis in 76 % of patients. This technique might be too complicated for a trauma or general surgeon to perform. However, Ferrada and colleagues showed that a limited transthoracic echocardiogram for the evaluation of cardiac contractility, fluid status, and pleural effusion was successfully implemented after 1-day course including a didactic and hands-on session [59].

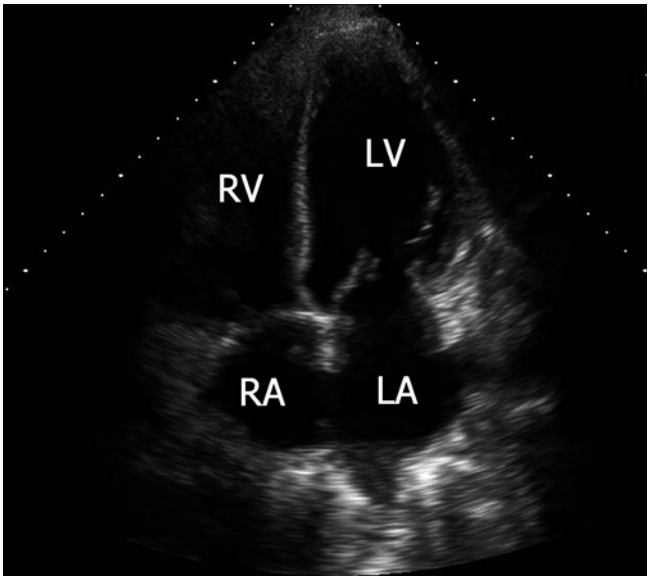

Fig. 8.14 The evaluation of heart contractility is performed with an apical four chamber view. *LA* left atrium, *LV* left ventricle, *RA* right atrium, *RV* right ventricle

Other Indications of Trauma Ultrasound

The indications of ultrasound continue to expand rapidly in trauma setting. Most of the techniques can be performed by a surgeon, intensivist, or emergency physician at bedside. Several types of fracture can be detected using portable

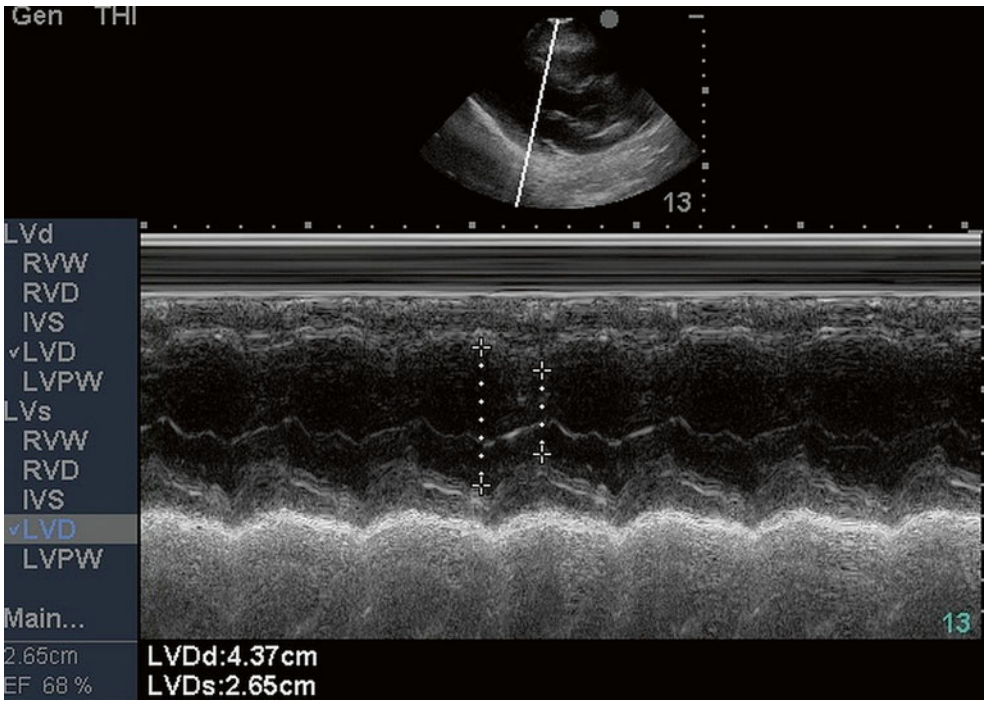

Fig. 8.15 In parasternal long-axis view, the ejection fraction of heart is calculated using the fractional shortening method

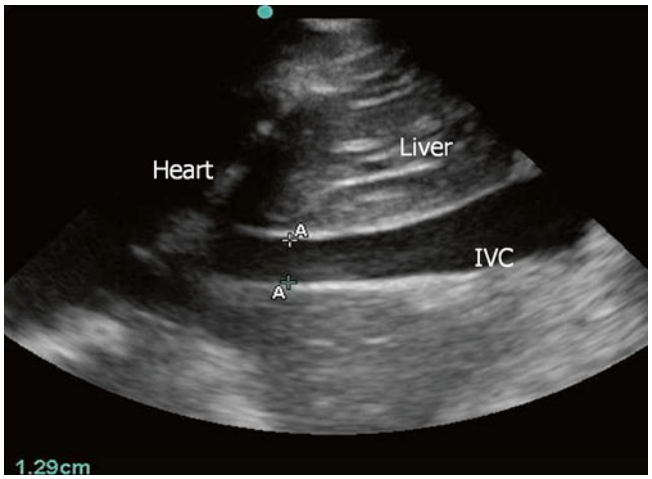

Fig. 8.16 Measurement of the inferior vena cava diameter for the assessment of volume status in a longitudinal view of the right upper quadrant in an abdominal preset

ultrasound [60, 61]. You and colleagues reported 100 % of sensitivity and specificity by ultrasound in the emergency department for the detection of sterna fracture [62]. Similarly, an ocular ultrasound has been increasingly used in the emergency department [63]. A bedside ultrasound technique to measure the diameter of optic nerve sheath is reported to be effective in identifying the patient with elevated intracranial pressure secondary to brain injury [64, 65].

Conclusion

In the last 20 years since FAST was introduced, its accuracy in diagnosing different types of injury has been studied extensively. While FAST has proven to be accurate in detecting free fluid in hemodynamically unstable blunt trauma patients and patients with penetrating injury to the "box" area, its accuracy in diagnosing stable blunt injured patients or those with abdominal penetrating injury appears to be limited. E-FAST is a useful technique to detect pneumothorax and hemothorax more quickly and accurately than CXR. Further prospective studies are needed to clarify how to choose the imaging modality between ultrasound and CT, particularly for the stable patients with suspected blunt torso injury. Surgical intensivist-performed ultrasound has been shown to be an effective tool to perform hemodynamic monitoring in the severely injured ICU patient. The use of ultrasound is expected to expand further for the management of trauma patients.

References

1. Ballard RB, Rozycki GS, Knudson MM, et al. The surgeon's use of ultrasound in the acute setting. Surg Clin North Am. 1998;78:337–64.
2. Goldfarb M, Gondek S, Solorzano C, et al. Surgeon-performed ultrasound can predict benignity in thyroid nodules. Surgery. 2011;150:436–41.
3. Kell MR, Aherne NJ, Coffey C, et al. Emergency surgeon-performed hepatobiliary ultrasonography. Br J Surg. 2002;89:1402–4.
4. Burford JM, Dassinger MS, Smith SD. Surgeon-performed ultrasound as a diagnostic tool in appendicitis. J Pediatr Surg. 2011;46:1115–20.
5. Huber-Wagner S, Lefering R, Qvick LM, et al. Effect of whole-body CT during trauma resuscitation on survival: a retrospective, multicentre study. Lancet. 2009;373:1455–61.
6. Goldberg BB, Goodman GA, Clearfield HR. Evaluation of ascites by ultrasound. Radiology. 1970;96:15–22.
7. Grüessner R, Mentges B, Düber C, et al. Sonography versus peritoneal lavage in blunt abdominal trauma. J Trauma. 1989;29:242–4.
8. Kimura A, Otsuka T. Emergency center ultrasonography in the evaluation of hemoperitoneum: a prospective study. J Trauma. 1991;31:20–3.
9. Tso P, Rodriguez A, Cooper C, et al. Sonography in blunt abdominal trauma: a preliminary progress report. J Trauma. 1992;33:39–44.
10. Rozycki GS, Ochsner MG, Jaffin JH, Champion HR. Prospective evaluation of surgeons' use of ultrasound in the evaluation of trauma patients. J Trauma. 1993;34:516–26; discussion 526–7.
11. Rozycki GS, Ochsner MG, Schmidt JA, et al. A prospective study of surgeon-performed ultrasound as the primary adjuvant modality for injured patient assessment. J Trauma. 1995;39:492–8; discussion 498–500.
12. Han DC, Rozycki GS, Schmidt JA, Feliciano DV. Ultrasound training during ATLS: an early start for surgical interns. J Trauma. 1996;41:208–13.
13. Scalea TM, Rodriguez A, Chiu WC, et al. Focused Assessment with Sonography for Trauma (FAST): results from an international consensus conference. J Trauma. 1999;46:466–72.
14. American College of Surgeons. Advanced trauma life support for doctors. Student course manual. 8th ed. Chicago: American College of Surgeons; 2008.
15. Rozycki GS, Ballard RB, Feliciano DV, et al. Surgeon-performed ultrasound for the assessment of truncal injuries: lessons learned from 1540 patients. Ann Surg. 1998;228:557–67.
16. Friese RS, Malekzadeh S, Shafi S, et al. Abdominal ultrasound is an unreliable modality for the detection of hemoperitoneum in patients with pelvic fracture. J Trauma. 2007;63:97–102.
17. Blackbourne LH, Soffer D, McKenney M, et al. Secondary ultrasound examination increases the sensitivity of the FAST exam in blunt trauma. J Trauma. 2004;57:934–8.
18. Natarajan B, Gupta PK, Cemaj S, et al. FAST scan: is it worth doing in hemodynamically stable blunt trauma patients? Surgery. 2010;148:695–700; discussion 700–1.
19. Brenner DJ, Hall EJ. Computed tomography – an increasing source of radiation exposure. N Engl J Med. 2007;357:2277–84.
20. Rozycki GS, Feliciano DV, Schmidt JA, et al. The role of surgeon-performed ultrasound in patients with possible cardiac wounds. Ann Surg. 1996;223:737–44; discussion 744–6.
21. Rozycki GS, Feliciano DV, Ochsner MG, et al. The role of ultrasound in patients with possible penetrating cardiac wounds: a prospective multicenter study. J Trauma. 1999;46:543–51; discussion 551–2.
22. Schuster KM, Lofthouse R, Moore C, et al. Pulseless electrical activity, focused abdominal sonography for trauma, and cardiac contractile activity as predictors of survival after trauma. J Trauma. 2009;67:1154–7.
23. Cureton EL, Yeung LY, Kwan RO, et al. The heart of the matter: utility of ultrasound of cardiac activity during traumatic arrest. J Trauma Acute Care Surg. 2012;73:102–10.

24. Biffl WL, Kaups KL, Cothren CC, et al. Management of patients with anterior abdominal stab wounds: a Western Trauma Association multicenter trial. J Trauma. 2009;66:1294–301.
25. Boulanger BR, Kearney PA, Tsuei B, Ochoa JB. The routine use of sonography in penetrating torso injury is beneficial. J Trauma. 2001;51:320–5.
26. Udobi KF, Rodriguez A, Chiu WC, Scalea TM. Role of ultrasonography in penetrating abdominal trauma: a prospective clinical study. J Trauma. 2001;50:475–9.
27. Quinn AC, Sinert R. What is the utility of the Focused Assessment with Sonography in Trauma (FAST) exam in penetrating torso trauma? Injury. 2011;42:482–7.
28. Como JJ, Bokhari F, Chiu WC, et al. Practice management guidelines for selective nonoperative management of penetrating abdominal trauma. J Trauma. 2010;68:721–33.
29. Soffer D, Cohn SM. Futility of abdominal ultrasound in penetrating abdominal injuries. J Trauma. 2009;67:1130.
30. Shorr RM, Crittenden M, Indeck M, et al. Blunt thoracic trauma. Analysis of 515 patients. Ann Surg. 1987;206:200–5.
31. Ball CG, Kirkpatrick AW, Feliciano DV. The occult pneumothorax: what have we learned? Can J Surg. 2009;52:E173–9.
32. Ma OJ, Mateer JR. Trauma ultrasound examination versus chest radiography in the detection of hemothorax. Ann Emerg Med. 1997;29:312–15; discussion 315–6.
33. Moore FO, Goslar PW, Coimbra R, et al. Blunt traumatic occult pneumothorax: is observation safe? Results of a prospective, AAST multicenter study. J Trauma. 2011;70:1019–23; discussion 1023–5.
34. Kirkpatrick AW, Sirois M, Laupland KB, et al. Hand-held thoracic sonography for detecting post-traumatic pneumothoraces: the Extended Focused Assessment with Sonography for Trauma (EFAST). J Trauma. 2004;57:288–95.
35. Lichtenstein DA, Menu Y. A bedside ultrasound sign ruling out pneumothorax in the critically ill. Lung sliding. Chest. 1995;108:1345–8.
36. Röthlin MA, Näf R, Amgwerd M, et al. Ultrasound in blunt abdominal and thoracic trauma. J Trauma. 1993;34:488–95.
37. Sisley AC, Rozycki GS, Ballard RB, et al. Rapid detection of traumatic effusion using surgeon-performed ultrasonography. J Trauma. 1998;44:291–6; discussion 296–7.
38. Brooks A, Davies B, Smethhurst M, et al. Emergency ultrasound in the acute assessment of haemothorax. Emerg Med J. 2004;21:44–6.
39. Hyacinthe AC, Broux C, Francony G, et al. Diagnostic accuracy of ultrasonography in the acute assessment of common thoracic lesions after trauma. Chest. 2012;141:1177–83.
40. Rantanen NW. Diseases of the thorax. Vet Clin North Am Equine Pract. 1986;2:49–66.
41. Dulchavsky SA, Schwarz KL, Kirkpatrick AW, et al. Prospective evaluation of thoracic ultrasound in the detection of pneumothorax. J Trauma. 2001;50:201–5.
42. Knudtson JL, Dort JM, Helmer SD, Smith RS. Surgeon-performed ultrasound for pneumothorax in the trauma suite. J Trauma. 2004;56:527–30.
43. Wilkerson RG, Stone MB. Sensitivity of bedside ultrasound and supine anteroposterior chest radiographs for the identification of pneumothorax after blunt trauma. Acad Emerg Med. 2010;17:11–7.
44. Alrajhi K, Woo MY, Vaillancourt C. Test characteristics of ultrasonography for the detection of pneumothorax: a systematic review and meta-analysis. Chest. 2012;141:703–8.
45. Sandham JD, Hull RD, Brant RF, et al. A randomized, controlled trial of the use of pulmonary-artery catheters in high-risk surgical patients. N Engl J Med. 2003;348:5–14.
46. Binanay C, Califf RM, Hasselblad V, et al. Evaluation study of congestive heart failure and pulmonary artery catheterization effectiveness: the ESCAPE trial. JAMA. 2005;294:1625–33.
47. Richard C, Warszawski J, Anguel N, et al. Early use of the pulmonary artery catheter and outcomes in patients with shock and acute respiratory distress syndrome: a randomized controlled trial. JAMA. 2003;290:2713–20.
48. Slagt C, Breukers RM, Groeneveld AB. Choosing patient-tailored hemodynamic monitoring. Crit Care. 2010;14:208.
49. Hadian M, Kim HK, Severyn DA, et al. Cross-comparison of cardiac output trending accuracy of LiDCO, PiCCO, FloTrac and pulmonary artery catheters. Crit Care. 2010;14:R212.
50. Beaulieu Y, Marik PE. Bedside ultrasonography in the ICU: part 1. Chest. 2005;128:881–95.
51. Beaulieu Y, Marik PE. Bedside ultrasonography in the ICU: part 2. Chest. 2005;128:1766–81.
52. Melamed R, Sprenkle MD, Ulstad VK, et al. Assessment of left ventricular function by intensivists using hand-held echocardiography. Chest. 2009;135:1416–20.
53. Vignon P, Dugard A, Abraham J, et al. Focused training for goal-oriented hand-held echocardiography performed by noncardiologist residents in the intensive care unit. Intensive Care Med. 2007;33:1795–9.
54. Gunst M, Ghaemmaghami V, Sperry J, et al. Accuracy of cardiac function and volume status estimates using the bedside echocardiographic assessment in trauma/critical care. J Trauma. 2008;65:509–16.
55. Murthi SB, Hess JR, Hess A, et al. Focused rapid echocardiographic evaluation versus vascular catheter-based assessment of cardiac output and function in critically ill trauma patients. J Trauma Acute Care Surg. 2012;72:1158–64.
56. Ferrada P, Murthi S, Anand RJ, et al. Transthoracic focused rapid echocardiographic examination: real-time evaluation of fluid status in critically ill trauma patients. J Trauma. 2011;70:56–62; discussion 62–4.
57. Stawicki SP, Braslow BM, Panebianco NL, et al. Intensivist use of hand-carried ultrasonography to measure IVC collapsibility in estimating intravascular volume status: correlations with CVP. J Am Coll Surg. 2009;209:55–61.
58. Gunst M, Sperry J, Ghaemmaghami V, et al. Bedside echocardiographic assessment for trauma/critical care: the BEAT exam. J Am Coll Surg. 2008;207:e1–3.
59. Ferrada P, Anand RJ, Whelan J, et al. Limited transthoracic echocardiogram: so easy any trauma attending can do it. J Trauma. 2011;71:1327–31; discussion 1331–2.
60. Jin W, Yang DM, Kim HC, et al. Diagnostic values of sonography for assessment of sternal fractures compared with conventional radiography and bone scans. J Ultrasound Med. 2006;25:1263–8.
61. Chien M, Bulloch B, Garcia-Filion P, et al. Bedside ultrasound in the diagnosis of pediatric clavicle fractures. Pediatr Emerg Care. 2011;27:1038–41.
62. You JS, Chung YE, Kim D, et al. Role of sonography in the emergency room to diagnose sternal fractures. J Clin Ultrasound. 2010;38:135–7.
63. Blaivas M. Bedside emergency department ultrasonography in the evaluation of ocular pathology. Acad Emerg Med. 2000;7:947–50.
64. Tayal VS, Neulander M, Norton HJ, et al. Emergency department sonographic measurement of optic nerve sheath diameter to detect findings of increased intracranial pressure in adult head injury patients. Ann Emerg Med. 2007;49:508–14.
65. Cammarata G, Ristagno G, Cammarata A, et al. Ocular ultrasound to detect intracranial hypertension in trauma patients. J Trauma. 2011;71:779–81.

Abdominal/Retroperitoneal Vascular Ultrasound

9

Daniel R. Calderon and David C. Han

Introduction

Significant advances in technology have resulted in both better visualization and the development of smaller and more portable ultrasound units. The combination of brightness mode (B-mode) imaging with Doppler analysis, or so-called duplex ultrasound (DUS), has been a long-standing tool of the vascular surgeon. An understanding of the capabilities of the vascular laboratory is a central piece of the educational curriculum of vascular trainees; no other imaging modality plays as central a role in the overall care of the vascular patient. While the physical principles of ultrasound are discussed elsewhere, an understanding of ultrasound physics, in particular, the Doppler equation, is a key concept in the use of DUS.

Ultrasound Physics

Sound is the propagation of an energy wave through vibration of particles that make up the medium through which the sound travels. The wave proceeds as a succession of an area of high pressure, known as compression, followed by an area of low pressure, known as rarefaction. Every sound wave has a wavelength that is determined by the distance between the peaks (or troughs) of the energy wave. The number of these pulses that pass in a given period of time refers to the wave frequency (cycles per second, or Hertz). The human ear can detect a frequency between approximately 20 and 20,000 Hertz (Hz). Ultrasound represents higher-frequency sound and those frequencies used in medical applications typically fall between 2 and 20,000 megahertz (MHz).

The Doppler effect refers to the predictable change in frequency of a sound wave that is produced by the relative motion between a sound source and a listener. In the case of DUS, Doppler shifts occur between the frequency of the transmitted and reflected sound wave when it encounters a moving object. In the bloodstream, the red blood cells act as the spectral reflectors. This frequency shift is directly proportional to the velocity of the moving reflector. The angle between the incident ultrasound beam and the direction of blood flow also affects the frequency shift. In clinical practice, this angle is defined as the angle between the axis of the ultrasound beam and the adjacent vessel wall. This is based on the assumption that blood cell motion is parallel to the vessel wall. By convention, an angle of 60° is used to obtain Doppler velocity measurements.

The simplest clinical use of Doppler does not require either simultaneous B-mode ultrasound or determination of the Doppler angle. Pocket-sized Doppler machines, known as continuous-wave or CW Doppler, are often used to determine the presence of arterial flow such as when measuring ankle-brachial indices. These instruments house both a transmitting and receiving element into a single transducer, sometimes shaped like a pencil (so-called pencil Doppler). Because they are unable to identify flow at a specific depth or site within the body, multiple vessels in the path of the sound beam result in a combination of superimposed signals.

The use of pulsed Doppler, along with B-mode imaging, overcomes this limitation, by allowing measurement of the velocity of blood in a specific location or sample volume. In this case, a single ultrasound transducer alternates between sending a short burst or pulse of ultrasound and then receiving the returning signal. The B-mode image provides the distance from the probe to the sample volume, which allows the machine to calculate the time required for the pulse to be sent and then subsequently received (see Fig. 9.1).

Spectral Broadening: Normal arterial flow is laminar, and spectral waveforms taken in a discrete sample volume will display a relatively narrow band of frequencies. In areas of

D.R. Calderon, MD
Department of Surgery, Penn State Hershey Medical Center, Penn State Heart and Vascular Institute, Hershey, PA, USA
e-mail: dcalderon@hmc.psu.edu

D.C. Han, MD, MS, FACS, RPVI (✉)
Department of Surgery, Penn State Hershey Medical Center, Penn State Heart and Vascular Institute, Penn State College of Medicine, 500 University Drive, MC H053, Hershey, PA 17033, USA
e-mail: dhan@psu.edu

E.J. Hagopian, J. Machi (eds.), *Abdominal Ultrasound for Surgeons*,
DOI 10.1007/978-1-4614-9599-4_9,

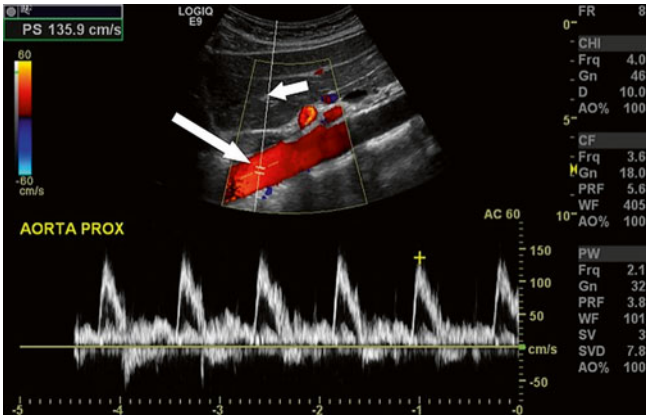

Fig. 9.1 Sagittal view of the abdominal aorta. Note the sample volume (*large arrow*) within the lumen of the aorta. The Doppler beam (*small arrow*) is adjusted to an angle of 60° relative to the direction of flow

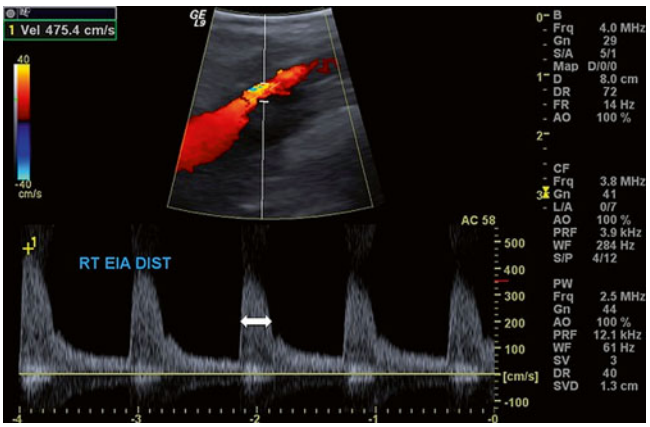

Fig. 9.2 Sagittal view of the right external iliac artery with elevated velocity (475 cm/s) and spectral broadening (*arrow*) consistent with turbulence and flow limiting stenosis

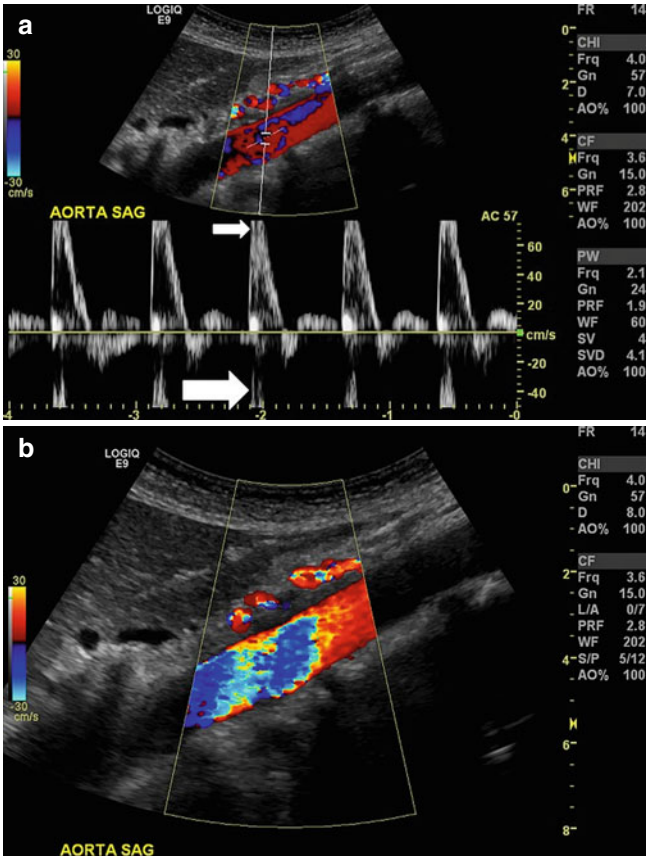

Fig. 9.3 Aliasing. (**a**) Sagittal view of the aorta where the relationship between the pulse repetition frequency and velocity causes the spectral waveform to be cut off (*small arrow*) and wrap around below the baseline (*large arrow*). (**b**) Color flow used in sagittal view of the same aorta as in (a). While multiple colors (color bruit) suggest turbulence, this is in fact an artifact of aliasing

stenosis or other abnormalities that disrupt laminar flow, these disturbances will display a broader range of frequencies at any given point in time. This increase in width of the displayed frequency shifts is referred to as *spectral broadening* and along with increases in the peak-systolic and end-diastolic velocities is used as a criterion to define stenosis within arterial beds (see Fig. 9.2).

Aliasing: One of the physical limitations of ultrasound is the frequency at which ultrasound pulses can be sent in order to ensure that the reflected signal from each pulse is received before the transmission of the next pulse. The limitation of this pulse repetition frequency (PRF) is defined as

$$\mathrm{PRF}(\max) = \frac{C}{2d}$$

where C is the speed of sound in tissue and d is the distance from the transducer to the sample volume. Higher PRF values result in more ultrasound pulses to provide a better representation of the Doppler signal. When the pulsed Doppler provides less than two samples for each cycle of the Doppler signal, a phenomenon called *aliasing* occurs where the spectral waveform appears to be "cut off" and then "wraps around" and appears as flow below the baseline. This is an artifact of the sampling process and can occur in an area with high flow velocity, such as a jet of blood associated with a severe stenosis, or in deep structures where low PRF values are needed to detect flow due to the attenuation of the additional tissue. The same effect can be seen in color flow imaging, where aliasing results in flow appearing to be present in opposite directions (colors) at a single sample volume. This is often referred to as a "color bruit" (see Fig. 9.3a, b).

Anatomy

Vascular structures in the abdomen and retroperitoneum that are typically imaged with ultrasound include the aorta and its branches, as well as the vena cava and associated branches,

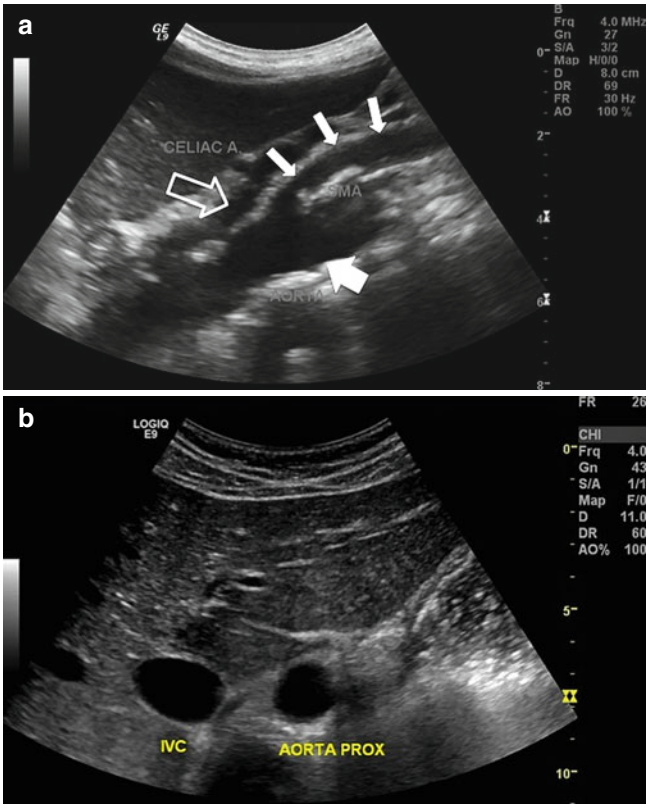

Fig. 9.4 (**a**) Gray-scale sagittal image of the aorta visualizing the proximal aorta (*large arrow*), celiac trunk (*hollow arrow*), and superior mesenteric artery (*small arrows*). Note the use of the liver as an acoustic window to visualize the proximal aorta. (**b**) Gray-scale transverse view of the aorta and adjacent inferior vena cava (IVC). The liver is used as an acoustic window

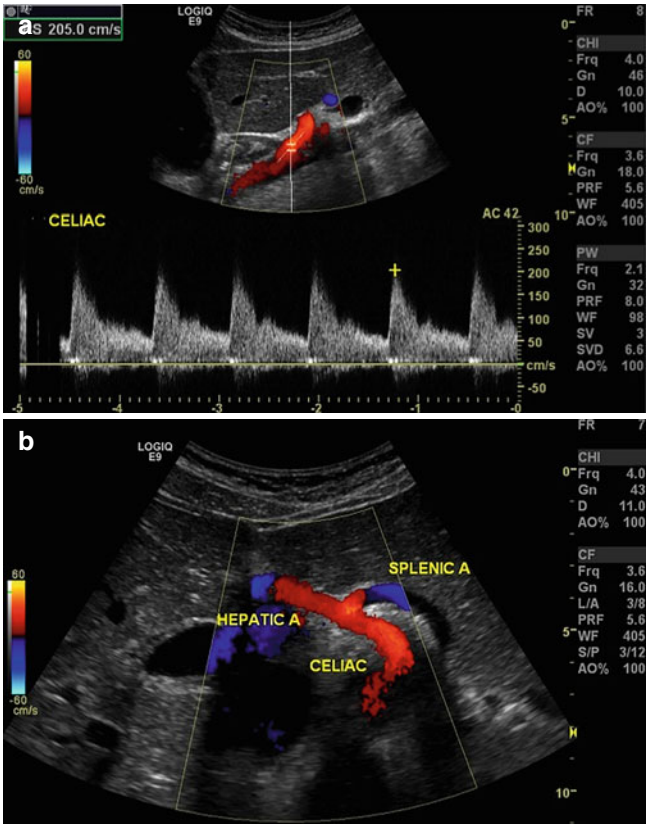

Fig. 9.5 (**a**) Longitudinal view of the aorta with Doppler interrogation of origin of the celiac trunk. Peak systolic velocity is 205 cm/s suggesting no evidence of significant stenosis. (**b**) Transverse view of the celiac trunk and hepatic and splenic arteries. Color flow is useful to identify vascular structures

and the portal circulation. Variations in anatomy can provide challenges, but many of these variations are well described, and an experienced technician can typically identify them. Obesity provides perhaps the greatest challenge to accurate identification of disease within the abdominal vascular structures. Bowel gas also limits visualization and these tests are best performed in the morning or at a time when the patient has had limited oral intake to limit associated bowel gas.

Aorta: The abdominal aorta lies in the retroperitoneum and is typically imaged from the midline. Lower-frequency transducers will sacrifice resolution but are required to adequately image structures at this depth. An ultrasound unit with color flow Doppler capabilities is necessary, and proper imaging requires range-gated spectral Doppler that has the ability to adjust the depth and position of the range gate within the area of interest. Both longitudinal and transverse views are required to assess the aorta for flow and size. The aorta should be visualized in its proximal, mid-, and distal portions, and aneurysm size should be determined at its widest diameter measured outer wall to outer wall (see Fig. 9.4a, b).

Visceral/Renal Arteries: Imaging of these vessels in any significant detail is best performed in a qualified and accredited facility by experienced operators. These challenging studies require a thorough understanding of both typical and variant anatomy among these adjacent structures. The celiac trunk and the superior mesenteric artery, the two most cephalad aortic branches, can be imaged in both a transverse and longitudinal axis. From a transverse image, the celiac trunk can be followed to its bifurcation into the splenic and hepatic arteries. The superior mesenteric artery can be visualized at its origin from the aorta in a longitudinal plane, with the left renal vein seen between it and the aorta. The renal arteries can also be imaged from an anterior position; however, in order to accurately identify and quantify flow in the distal arteries, a flank approach may be necessary with the kidney serving as an acoustic window (see Figs. 9.5a, b, 9.6a, b and 9.7a, b).

Vena Cava: The vena cava is imaged in a similar fashion to the abdominal aorta. Transverse and longitudinal views can be used, and color flow is often helpful to identify these large vascular structures that lie in the retroperitoneum. The vena cava can be imaged both centrally (at the hepatic vein confluence) and more distally (between the renal veins and the caval bifurcation). Overlying bowel gas is the most

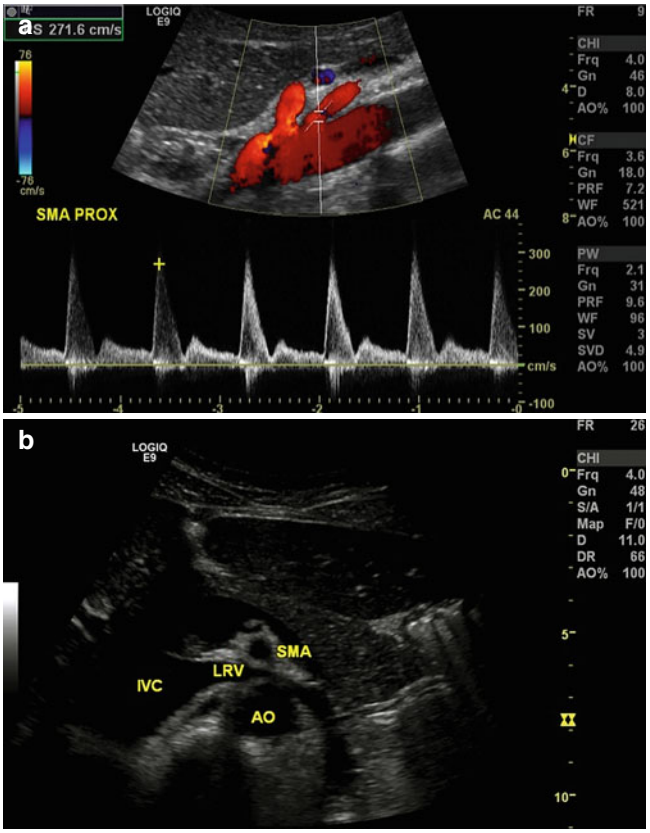

Fig. 9.6 (**a**) Longitudinal view of the aorta with Doppler interrogation of origin of the superior mesenteric artery. Peak systolic velocity is 271.6 cm/s suggesting no evidence of significant stenosis. (**b**) Transverse view of the aorta (*AO*) and superior mesenteric artery (*SMA*), with the left renal vein (*LRV*) interposed between as it empties into the inferior vena cava (*IVC*). Note the similarity between this and a familiar view from cross-sectional imaging such as CT or MRI

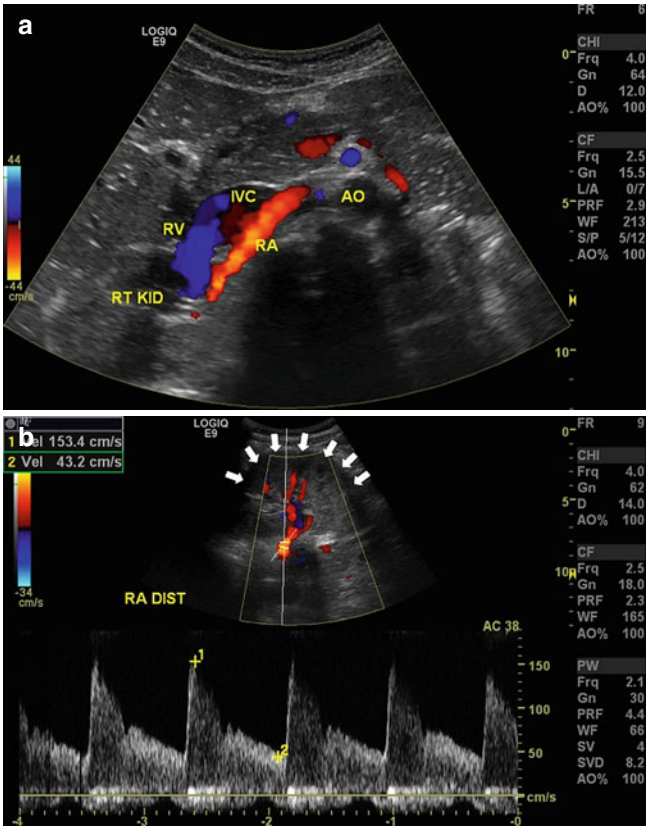

Fig. 9.7 (**a**) Transverse view of the right renal artery (*RA*) as it exits the aorta (*AO*) and lies posterior to the inferior vena cava (*IVC*). *RV* renal vein, *RT KID* right kidney. (**b**) The distal renal artery (*RA DIST*) may sometimes need to be imaged by placing the transducer on the flank and using the kidney (*arrows*) as an acoustic window

consistent challenge to overcome adequate imaging of these structures (see Fig. 9.8a, b).

Portal Venous Structures: Diagnostic imaging of the hepatoportal system is best left to the highly trained technicians in the vascular laboratory and radiology suite and to those who perform routine intraoperative assessment (see Chap. 15). An understanding of these structures can be helpful for diagnostic and therapeutic interventions on the liver, which is discussed elsewhere (see Chap. 16) (see Fig. 9.9).

Application

Aneurysmal Disease: Perhaps the most common application of abdominal vascular ultrasound is to identify and determine the size of abdominal aortic aneurysms (AAA). Because it is noninvasive and portable, ultrasound is the study of choice when assessing AAA. B-mode ultrasound can identify the maximum diameter of the AAA, as well as extension of aneurysmal disease into the paravisceral aorta and the iliac arteries. For the general surgeon, the use of ultrasound for the diagnosis of AAA falls into two basic categories: acute and chronic.

Acute Diagnosis: In the acute setting, the old axiom "gray hair + back pain = ruptured aortic aneurysm until proven otherwise" still holds true. While rapid diagnosis and treatment are important to obtain good outcomes, it is just as important to be able to exclude the presence of AAA to allow other diagnoses to be considered. The performance of surgeon-performed ultrasound by appropriately trained providers clearly has a role in this abbreviated and directed study [1–3]. Perhaps the greatest impediment is the presence of overlying bowel gas that can make imaging more challenging. While rapid diagnosis can allow patients to be taken straight to surgery, adequate preoperative planning with the use of cross-sectional imaging (CT scanning) is becoming more common, particularly in the endovascular era (see Fig. 9.10a–c).

Chronic Diagnosis and Follow-up: The majority of AAA are not detectable on physical examination [4]. Imaging is most commonly performed in a dedicated radiology or vascular laboratory and typically includes assessment for

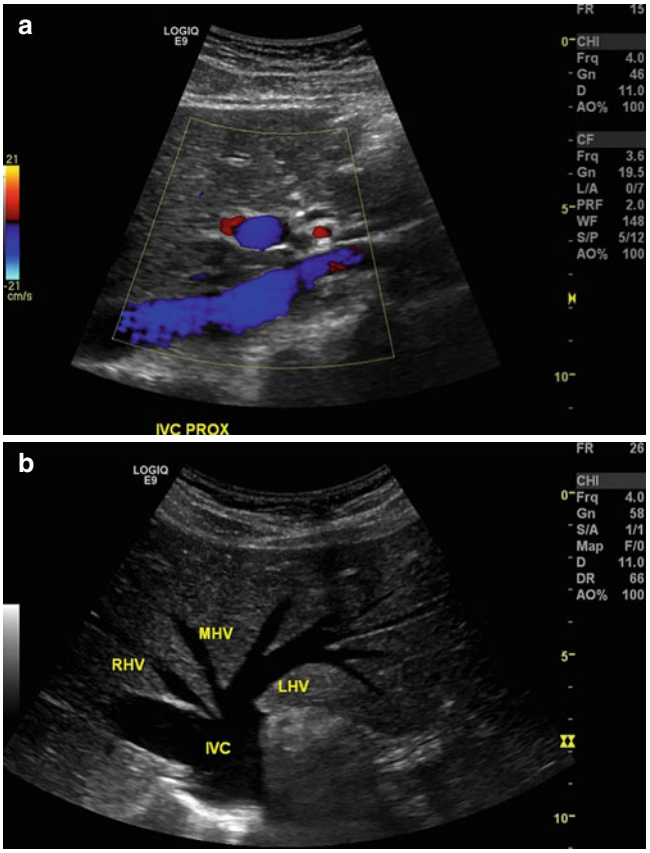

Fig. 9.8 (**a**) Longitudinal view of the proximal inferior vena cava at the level of hepatic veins. Note the use of the liver (*arrows*) as an acoustic window. (**b**) Transverse view of the inferior vena cava (*IVC*) at the level of hepatic veins. *RHV* right hepatic vein, *MHV* middle hepatic vein, *LHV* left hepatic vein

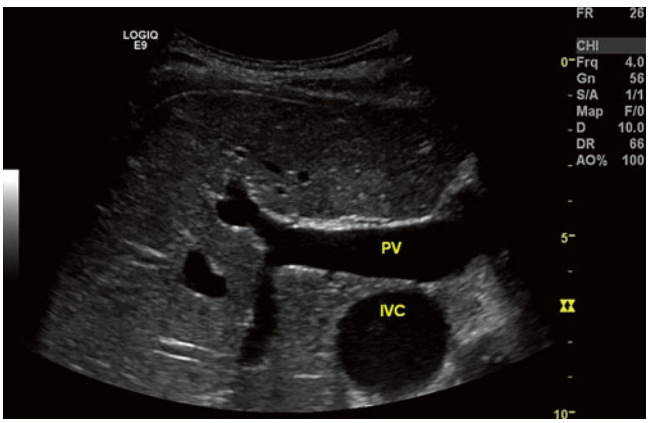

Fig. 9.9 Transverse view of the extrahepatic portal vein (*PV*). The portal vein can be distinguished from the hepatic vein by both its anatomy and its characteristic bright echogenic wall. *IVC* inferior vena cava

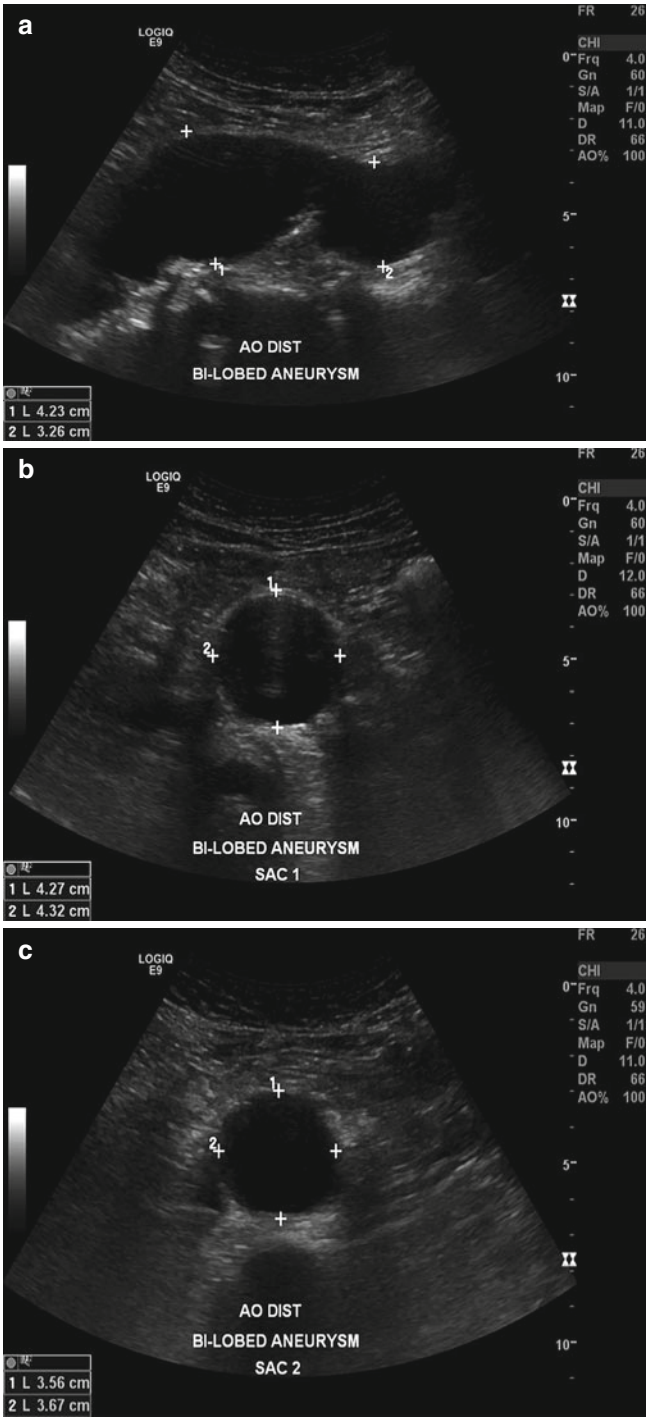

Fig. 9.10 Abdominal aortic aneurysm. (**a**) Sagittal view of a bilobed abdominal aortic aneurysm. (**b**) Transverse view of the more proximal larger lobe of the aneurysm. (**c**) Transverse view of the more distal smaller lobe of the aneurysm

screening purposes, suspected physical findings, or follow-up [5]. Screening is currently recommended in certain populations by the U.S. Preventive Services Task Force with follow-up studies performed at routine intervals depending on aneurysm size [6]. DUS evaluation of endovascular repair of abdominal aortic aneurysms continues to be studied and compared to CT scan for the detection of endoleaks [7]. Because of the hazards of ionizing radiation and contrast

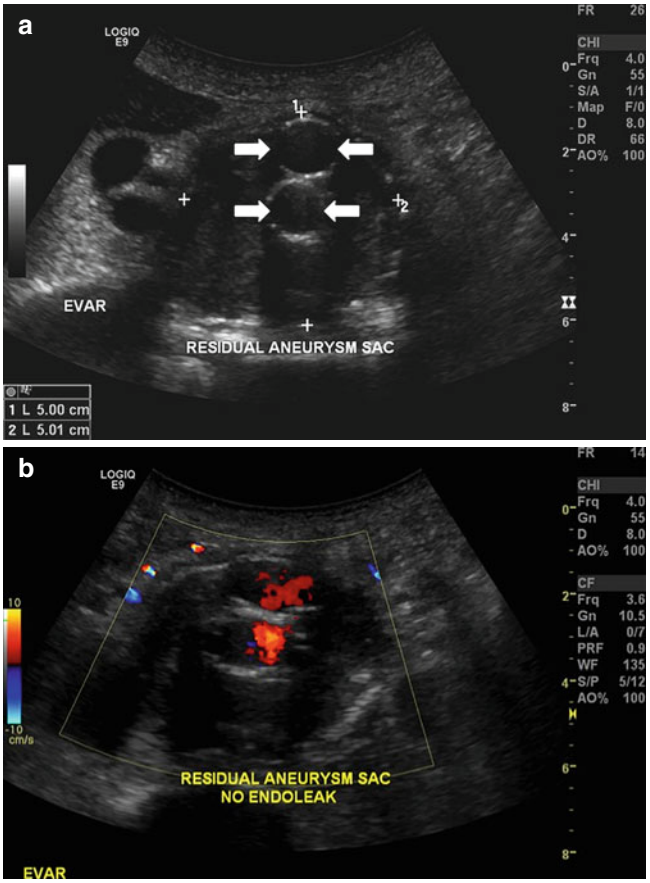

Fig. 9.11 (**a**) Gray-scale transverse image of residual abdominal aortic aneurysm sac after endovascular repair of aortic aneurysm (*EVAR*). Note the presence of the graft limbs within the aneurysm sac (*arrows*). The residual sac measures 5 cm. (**b**) Color flow image showing no evidence of endoleak, i.e., no flow outside of the graft limbs that is within the aneurysm sac

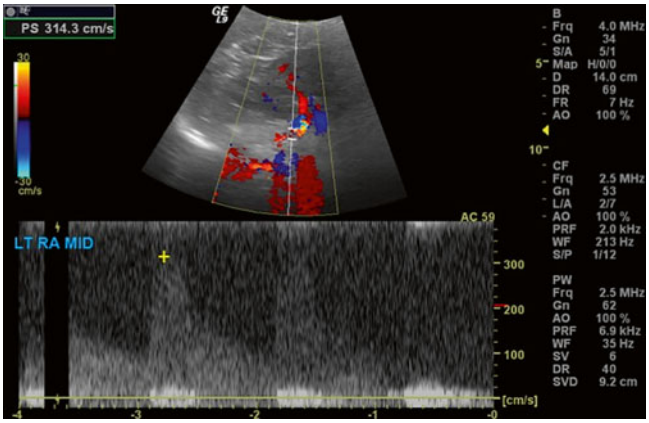

Fig. 9.12 Elevated velocity (314.3 cm/s) within the midportion of the left renal artery (*LT RA MID*) consistent with a hemodynamically significant stenosis. This view has been obtained through the flank using the kidney as an acoustic window

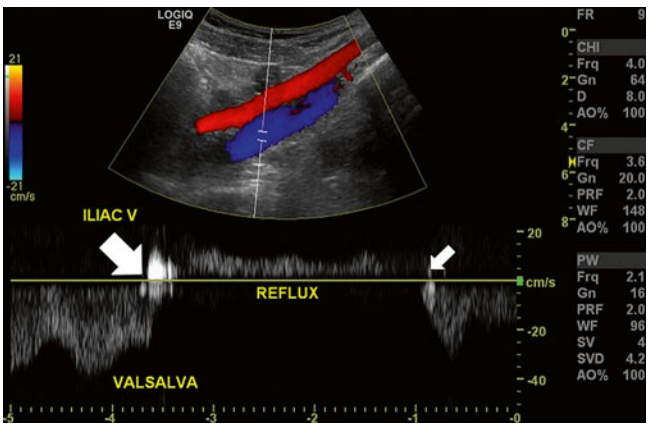

Fig. 9.13 Longitudinal view of the iliac vein demonstrating reflux. At time 0 (−5 on the horizontal scale), venous flow is toward the heart. Valsalva maneuver (*large arrow*) produces sustained reversal of flow in the iliac vein which persists approximately 2.5 s (*small arrow*). A total of 5 s of data is collected in this spectral analysis

nephropathy, ultrasound clearly has a role in the postoperative surveillance of these patients [4] (see Fig. 9.11a, b).

Vascular Stenoses and Occlusions: DUS can provide a significant amount of information in real-time regarding blood flow. Using the Doppler equation, velocity measurements within a particular vessel can be made which can then provide reproducible estimates of degrees of stenosis based on these velocities or on the ratio of the velocity relative to the velocity in an adjacent vessel. Well-established criteria exist for determining degrees of stenosis within the iliac, mesenteric, and renal vessels (see Fig. 9.12).

Venous: Ultrasound evaluation of the vena cava and iliac veins is helpful to determine the extent of deep venous thrombosis that originates in the lower extremities. As in the lower extremities, DUS can not only diagnose thrombotic occlusions but can also identify reflux, such as postthrombotic reflux from dysfunctional valves that have been recanalized after previous deep venous thrombosis. Valve closure times greater than 0.5 sec are generally defined as significant reflux [8]. In those patients undergoing intervention such as endoluminal angioplasty and/or stenting, intravascular ultrasound plays a significant adjunctive role to contrast venography to determine the size and length of the devices to be used (see Fig. 9.13).

Portal: Assessment of portal venous blood flow is an excellent application of DUS. While operator dependent, it is a noninvasive and repeatable method to assess the portal circulation. Thrombosis of the splenoportal circulation is readily identified with ultrasound and can be used as a surveillance imaging modality for splenoportal thrombosis after surgical intervention such as splenectomy [9]. With the use of color flow and spectral analysis, hepatopetal (toward the liver) and hepatofugal (from the liver) flow directions can be determined. Using flow characteristics as well as B-mode diameter measurements, estimates of portal venous flow and pressures can then be made [10, 11] (see Fig. 9.14a, b).

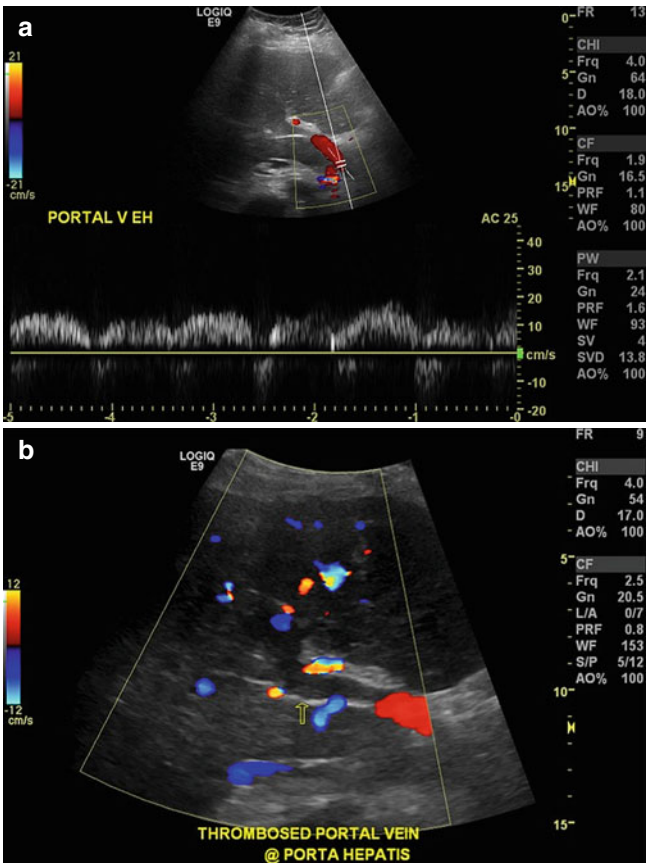

Fig. 9.14 (**a**) The extrahepatic portal vein is identified and has flow within it. (**b**) The intrahepatic portal vein is thrombosed

Intervention

Unlike the peripheral vessels, direct percutaneous access to the visceral vessels is uncommon, and thus ultrasound-guided percutaneous abdominal vascular interventions are relatively rare. The use of intraoperative ultrasound, however, is quite helpful to assess the adequacy of mesenteric vascular reconstructions such as bypass or endarterectomy. In these circumstances, velocity elevations relative to the adjacent vessel can identify areas that may require technical correction, such as retained vein valves in a bypass conduit, anastomotic stenoses, or residual plaque at an endarterectomy site.

While the use of intravascular ultrasound (IVUS) is beyond the scope of this text, its use has become significant in abdominal vascular interventions, including endoluminal interventions such as balloon angioplasty or stenting, as well as during placement of abdominal aortic endografts. Catheters with lower frequencies (relative to those used in coronary applications) allow identification of visceral branches within the aorta and can lessen the amount of intravenous contrast required during complex endovascular reconstructions. In the treatment of arterial occlusive disease, IVUS interrogation after stent placement can be used to determine the adequacy of stent apposition against the arterial wall. Finally, IVUS can more accurately determine intraluminal diameters, optimizing size selection of devices, particularly when dealing with central venous reconstructions.

The use of ultrasound to direct placement of vena cava filters has been well described with both transabdominal and intravascular ultrasound [12–14]. The limitations of poor visualization using transabdominal ultrasound, particularly in the obese patient, have been overcome by the use of intravascular ultrasound. As smaller-diameter probes have become available, this can be performed through acceptably small-diameter sheaths. Both double-puncture and single-puncture techniques are well described, with excellent results [14].

Conclusion

Because of its noninvasiveness, repeatability, and portability, ultrasound plays a key role in the imaging of the vascular structures of the abdomen and retroperitoneum. Experience, an awareness of anatomic variations, and a healthy amount of patience will lead to the best results. In any given individual, optimal DUS imaging of the vascular structures may be accomplished through various angles, planes, and acoustic windows. The number of nondiagnostic or incomplete studies can be limited by performing these studies as early in the day as possible to minimize the effects of overlying bowel gas. Additionally, at times success will be achieved when the study is performed at another time or by another sonographer. Because the quality of the study is highly operator dependent, familiarity with the physical principles of ultrasound and the Doppler equation allows an understanding of the strengths and limitations of the use of ultrasound in this setting.

References

1. Hendrickson RG, Dean AJ, Costantino TG. A novel use of ultrasound in pulseless electrical activity: the diagnosis of an acute abdominal aortic aneurysm rupture. J Emerg Med. 2001;21:141–4.
2. Kuhn M, Bonnin RL, Davey MJ, Rowland JL, Langlois SL. Emergency department ultrasound scanning for abdominal aortic aneurysm: accessible, accurate, and advantageous. Ann Emerg Med. 2000;36:219–23.
3. Shuman WP, Hastrup Jr W, Kohler TR, Nyberg DA, Wang KY, Vincent LM, Mack LA. Suspected leaking abdominal aortic aneurysm: use of sonography in the emergency room. Radiology. 1988;168:117–9.
4. Chaikof EL, Brewster DC, Dalman RL, Makaroun MS, Illig KA, Sicard GA, Timaran CH, Upchurch GR, Veith FJ. The care of patients with an abdominal aortic aneurysm: the Society for Vascular Surgery practice guidelines. J Vasc Surg. 2009;50:2–49S.
5. Thompson SG, Ashton HA, Gao L, Buxton MJ, Scott RA. Final follow-up of the Multicentre Aneurysm Screening Study (MASS)

randomized trial of abdominal aortic aneurysm screening. Br J Surg. 2012;99:1649–56.
6. Screening for abdominal aortic aneurysm. Clinician Fact Sheet. June 2009. Rockville: Agency for Healthcare Research and Quality; 2009. http://www.ahrq.gov/clinic/cvd/aaaprovider.htm
7. Manning BJ, O'Neill SM, Haider SN, Colgan MP, Madhavan P, Moore DJ. Duplex ultrasound in aneurysm surveillance following endovascular aneurysm repair: a comparison with computed tomography aortography. J Vasc Surg. 2009;49: 60–5.
8. Raju S, Hollis K, Neglen P. Obstructive lesions of the inferior vena cava: clinical features and endovenous treatment. J Vasc Surg. 2006;44:820–7.
9. Tran T, Demyttenaere SV, Polyhronopoulos G, Séguin C, Artho GP, Kaneva P, Fried GM, Feldman LS. Recommended timing for surveillance ultrasonography to diagnose portal splenic vein thrombosis after laparoscopic splenectomy. Surg Endosc. 2010; 24:1670–8.
10. Chow PK, Yu WK, Ng TH, Ong HS, Ooi PJ, Chan ST, Aw SE, Soo KC. Influence of respiration and portal pressure on transabdominal duplex Doppler ultrasound measurement of portal blood flow: a porcine model for experimental studies. J Surg Res. 2000;89: 66–73.
11. Singal AK, Ahmad M, Soloway RD. Duplex Doppler examination of the portal venous system: an emerging novel technique for the estimation of portal vein pressure. Dig Dis Sci. 2010;55:1230–40.
12. Corriere MA, Passman MA, Guzman RJ, Dattilo JB, Naslund TC. Comparison of bedside transabdominal duplex ultrasound versus contrast venography for inferior vena cava filter placement: what is the best imaging modality? Ann Vasc Surg. 2005;19:229–34.
13. Kassavin DS, Constantinopoulos G. The transition to IVUS-guided IVC filter deployment in the nontrauma patient. Vasc Endovascular Surg. 2011;45:142–5.
14. Jacobs DL, Motaganahalli RL, Peterson BG. Bedside vena cava filter placement with intravascular ultrasound: a simple, accurate, single venous access method. J Vasc Surg. 2007;46:1284–6.

Laparoscopic Ultrasound in Staging of GI Malignancies

10

Ewen M. Harrison and O. James Garden

Introduction

Surgical resection is the treatment of choice for most GI malignancies. Whether resection with curative intent is possible will be determined by the stage of the malignancy. Staging is the process by which the primary malignancy is assessed and its degree of progression beyond the site of origin determined. Of particular importance is the presence of local invasion, lymph node metastases and metastases to distant organs.

The accuracy by which the stage of a GI malignancy can be determined prior to resection has greatly improved in recent years, directly as a result of advances in diagnostic imaging. Computed tomography (CT), magnetic resonance imaging (MRI), positron emission tomography (PET-CT) and endoscopic ultrasound (EUS) are now widely employed in the assessment of malignancy and planning of treatment. Despite improvements in the spatial resolution of cross-sectional imaging modalities, these remain relatively poor in determining the presence of peritoneal disease, and all have limitations in the assessment of local progression.

Staging laparoscopy is a quick, safe, but invasive investigation with which the presence of peritoneal disease can be determined. It has few disadvantages and can avoid an unnecessary nontherapeutic laparotomy. Critics of the technique complain that its accuracy is low, that it is an additional procedure and that it ignores the possibility of palliative surgery. The addition of direct contact laparoscopic ultrasonography (LUS) provides the ability to further assess the local stage of disease and to evaluate the liver for metastases. Although laparoscopy is widely used in the assessment of many gastrointestinal malignancies, the indications and sensitivity/specificity of LUS in contemporary practice remain poorly defined. There are no randomised controlled trials of laparoscopy or LUS, and in many areas, the case series are small in size.

Principles of Laparoscopy for Staging

The clear benefit of laparoscopy over cross-sectional imaging is its ability to diagnose peritoneal disease that may not be apparent even on high-quality CT imaging.

There are three potential advantages of laparoscopy over cross-sectional imaging in the staging of GI malignancy:

1. The diagnosis of peritoneal disease
2. The determination of local resectability and formulation of an operative plan
3. The ability to obtain tissue for diagnosis

Technique

Laparoscopy

As with all laparoscopy, some thought should go into the operating room set-up to allow the surgical team to work comfortably (Fig. 10.1). High-definition (HD) camera systems are now common and provide excellent visualisation of the peritoneal cavity (Fig. 10.1a). The laparoscopic monitor and stack should be positioned beyond the patient in the direction the surgeon is working. The laparoscopic ultrasound monitor can be placed beside this. Although, in our practice, facilities are available for 'picture-in-picture' – the ultrasound monitor view being placed on the same screen as the laparoscopic image – this may obstruct the laparoscopic view. HD recordings of the laparoscopic camera feed can be undertaken, and facilities for recording video images of the ultrasonography are useful.

E.M. Harrison, MB, ChB, PhD, FRCS
O.J. Garden, CBE, FRCSEd, FRSE (✉)
Department of Clinical Surgery,
The University of Edinburgh, Royal Infirmary of Edinburgh,
51 Little France Crescent, Edinburgh EH16 4SA, UK
e-mail: ewen.harrison@ed.ac.uk; o.j.garden@ed.ac.uk

Electronic supplementary material The online version of this chapter (doi:10.1007/978-1-4614-9599-4_10) contains supplementary material, which is available to authorized users. Videos can also be accessed at http://www.springerimages.com/videos/978-1-4614-9598-7

E.J. Hagopian, J. Machi (eds.), *Abdominal Ultrasound for Surgeons*,
DOI 10.1007/978-1-4614-9599-4_10, © Springer Science+Business Media New York 2014

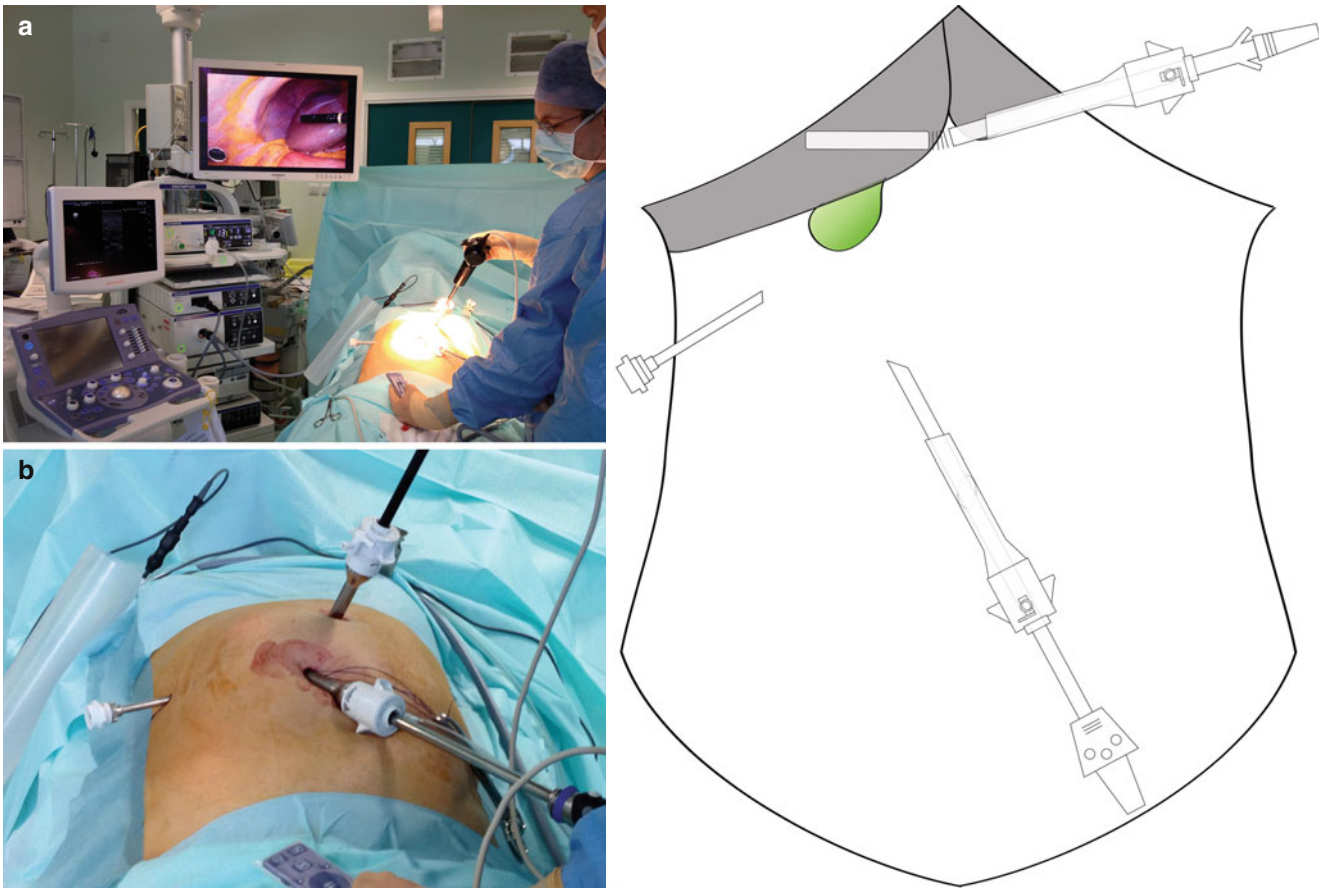

Fig. 10.1 Setting-up staging laparoscopy. The laparoscopic monitor is placed beyond the patient in the direction the surgeon is working (**a**). The laparoscopic ultrasound machine is placed to the left of this. An assistant is controlling the laparoscopic camera while the primary surgeon manipulates the ultrasound probe. Note the remote control unit for the ultrasound machine in the surgeon's left hand with which he is recording images and turning the Doppler flow on and off. There are many options for port placement and this is our preferred (**b**). A pneumoperitoneum is established through an infraumblical port inserted with an open technique. A further 10–12 mm port is placed in the epigastrium to the left of the midline and well below the costal margin. A 5 mm port for a grasper is placed in the right upper quadrant

There are a number of options for laparoscopic port placement, and this depends on the primary organ for investigation. Our standard approach (Fig. 10.1b, c) involves establishing a pneumoperitoneum (12 mmHg) via a 10 mm infraumbilical port placed under direct vision. A further 10 mm port is placed in the epigastrium to the left of the midline well below the costal margin. A 5 mm port is usually placed on the right side for use of a grasper. These positions allow easy access to the liver, gallbladder and portal pedicle. In the staging of oesophagogastric cancer, it can be preferable to place the 10–12 mm port on the right side of the abdomen and the 5 mm port on the left. The right-sided and umbilical ports can then be used to gain easy access to the stomach and oesophageal hiatus.

A 30° laparoscope is inserted through the umbilical port and a careful inspection of the intra-abdominal organs and peritoneum performed (Fig. 10.2a, b). Particular attention is paid to the falciform ligament, liver (including the under surface, Fig. 10.2a), diaphragm, hepatoduodenal ligament and lesser omentum. The greater omentum is retracted superiorly to allow the small bowel mesentery and ligament of Treitz to be directly visualised.

Laparoscopic Ultrasonography

A high-resolution flexible tip linear array transducer is inserted through the epigastric port (Fig. 10.2c). Systematic scanning of the liver should start with identification of standard landmarks and of the liver parenchyma. A window may be made in the falciform ligament to aid visualisation of the hepatic outflow. Intrahepatic liver metastasis can appear as hyper-, iso- or hypoechoic lesions on imaging. It can also be useful to position the probe on the underside of the liver, particularly on the right lobe (Fig. 10.2f). This manoeuvre can be used to better visualise lesions in the posterior section (segments VI/VII) of the liver.

Depending on the location of the primary tumour, identification of structures in the portal triad is now performed

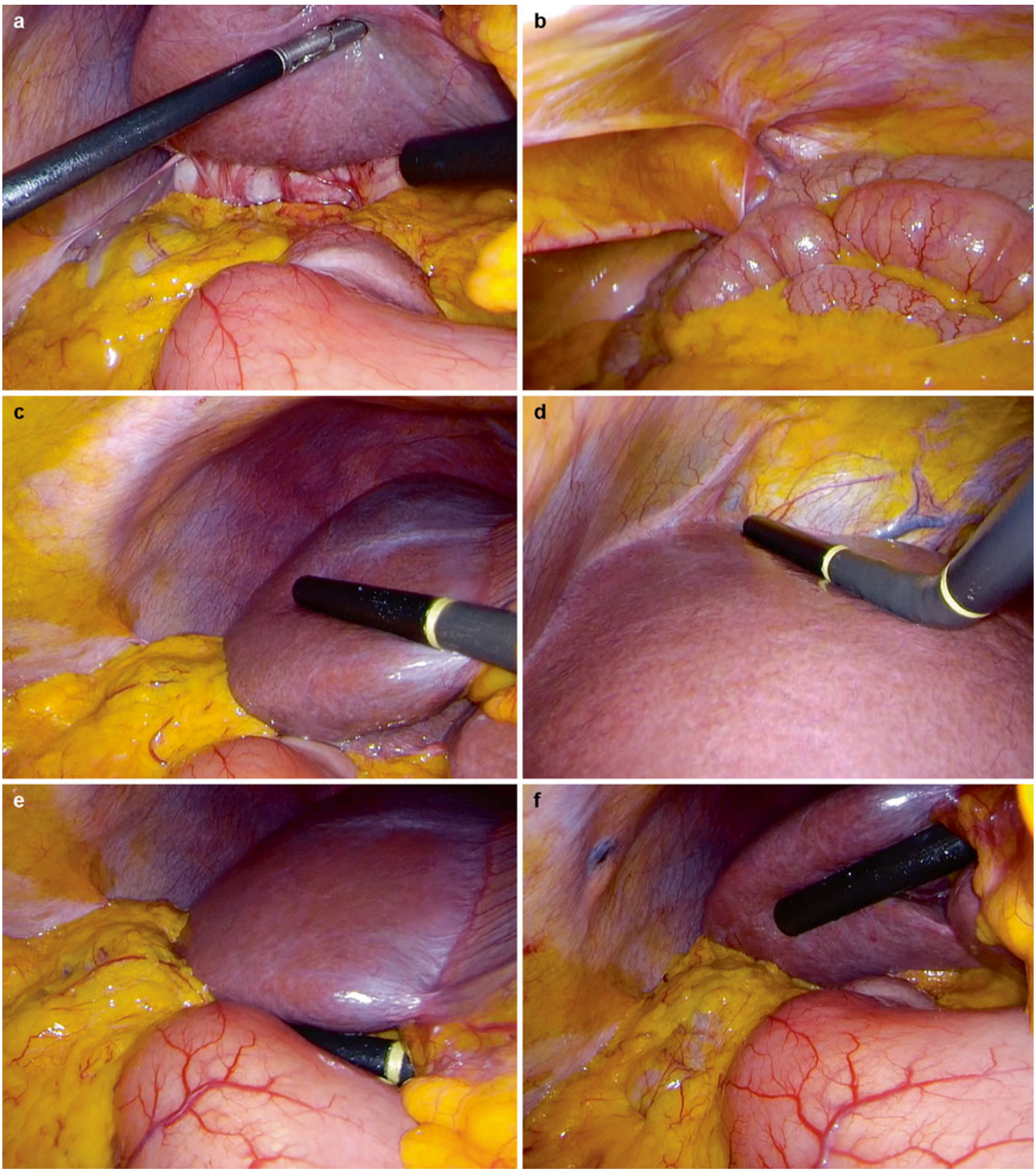

Fig. 10.2 Staging laparoscopy. Begin with a full inspection of the peritoneal cavity lifting the left and right liver to view the underside (**a**) and paying particular attention to the peritoneum (**b**). Use laparoscopic ultrasound to orientate on the origin of the left and right portal vein branches and carefully visualise the parenchyma of the right lobe (**c**). Look on the left side of the falciform ligament and scan segments II and III (**d**). Place the probe on the hepatoduodenal ligament in the transverse plane to examine the portal pedicle (**e**). The probe can also be placed on the underside of any part of the liver and orientated anteriorly (**f**). Adhesions around the gallbladder can be seen as a result of recent acute cholecystitis (**a**)

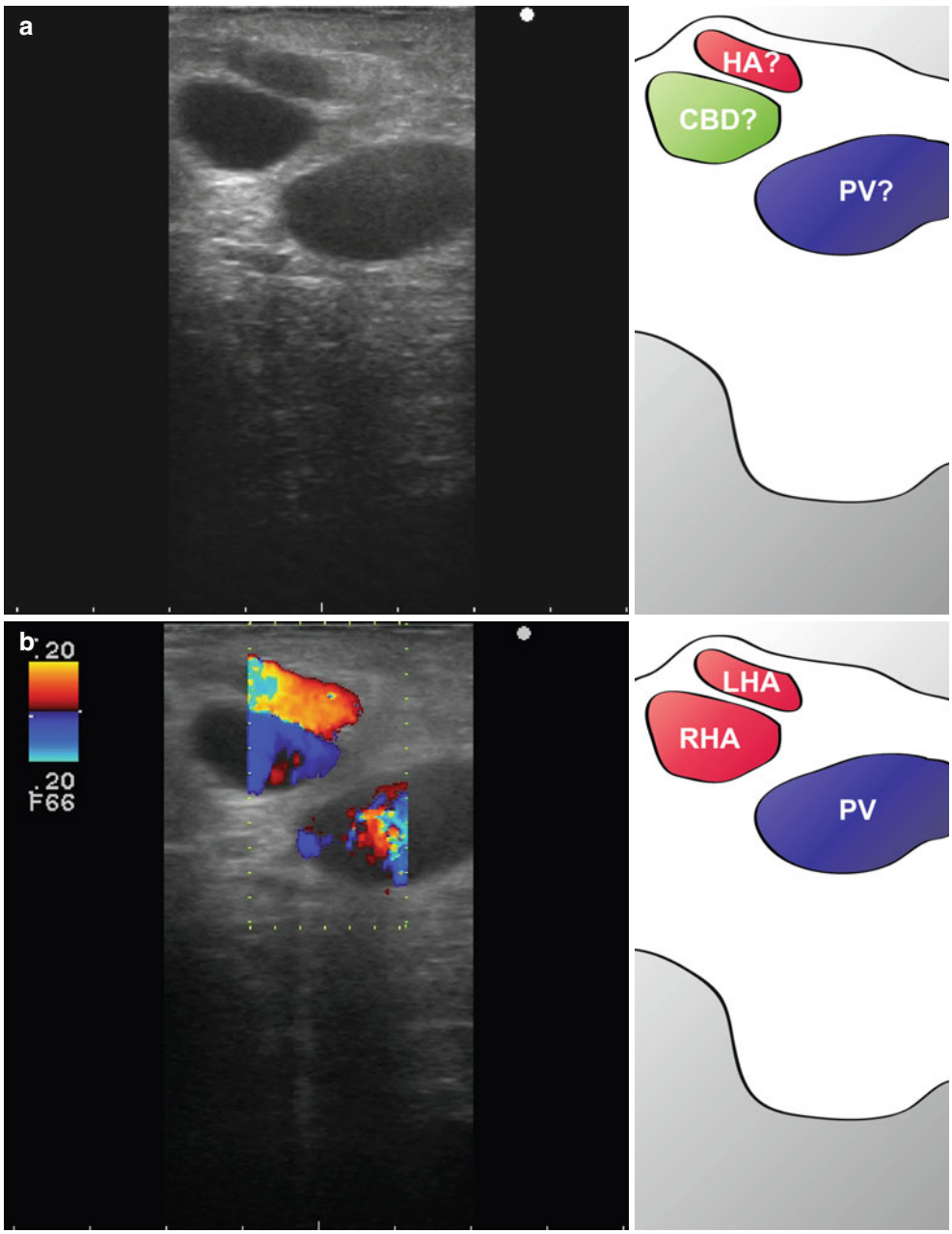

Fig. 10.3 Colour flow Doppler in the identification of structures. Three structures are apparent in the hepatoduodenal ligament (**a**). These appear to have the configuration of the portal vein (*?PV*), hepatic artery (*?HA*) and bile duct (*?CBD*) (see Chap. 14). However, when colour flow Doppler is used, it is apparent that all three structures (*LHA* left hepatic artery, *RHA* right hepatic artery, *PV* portal vein) are blood vessels (**b**). In this patient, the hepatic artery bifurcates early, and the bile duct was small and lateral. Colour flow was useful in differentiating the bile duct from the artery

(Fig. 10.2e). Visualisation of the portal structures can be aided by inserting the probe through the infraumbilical port and placing it on the hepatoduodenal ligament (see Chap. 14 for further information). By identifying the inferior vena cava posteriorly and rotating the probe counterclockwise, the portal vein, bile duct and hepatic artery are visualised. The portal vein can be followed to the splenoportal confluence and continued down the superior mesenteric vein. This manoeuvre is clearly important in tumours of the head of pancreas and distal common bile duct.

Vascular invasion is suggested by the absence of the tissue plane between the tumour and blood vessel. Avoid excessive pressure with the probe as this can emulate the appearance of tumour involvement into vessels when this has not occurred. The presence of a fixed stenosis in a vessel in more than one plane suggests tumour involvement. If views are not adequate due to poor probe contact or as a result of the pneumoperitoneum, CO_2 can be released and saline injected into the peritoneum to improve probe contact, though is rarely required.

In pancreas and biliary tumours, the primary lesion should be assessed to determine the proximal and distal extent, radial extension (particularly arterial and venous invasion) and the presence of lymph node metastases. Lymph nodes invaded by tumour are hypoechoic with a loss of definition. While enlarged lymph nodes may represent the presence of

metastatic disease, this finding is non-specific and should be confirmed pathologically (Fig. 14.4b, c).

Careful examination should be made of the coeliac trunk and aortocaval window for suspicious nodes. Large coeliac trunk nodes can sometimes be accessed through the less omentum and biopsy made. Care needs to be taken to avoid bleeding in this area. Colour Doppler can be helpful in differentiating vessels from nodes during these manoeuvres (Fig. 10.3).

Laparoscopic Biopsy

A patient presenting with painless obstructive jaundice and a mass in the head of pancreas on CT underwent staging laparoscopy (Fig. 10.4). A full staging laparoscopy was performed followed by laparoscopic ultrasound through an epigastric port (Fig. 10.4a, b). Suspicious lesions were seen in segment II/III (Fig. 10.4a, c) and segment V (Fig. 10.4b, d) of the liver. These were firm on direct pressure with a grasper and had a 'target' appearance on ultrasonography suggesting metastatic disease.

Any suspicious lesions identified can then be biopsied directly or using ultrasound guidance. The lesion in segment II/III was accessible and biopsied directly using scissors (Fig. 10.5). It is best not to use diathermy when taking the biopsy to avoid thermal artefact, particularly when the specimen is small. Bleeding can be controlled with diathermy after the specimen is removed (Fig. 10.5f). In this case, the biopsy was sent for direct frozen-section analysis and adenocarcinoma was confirmed.

Oesophagogastric Junctional Cancer and Gastric Cancer

The epidemiology of gastric cancer has altered over the last 40 years. The site of origin within the stomach has changed in frequency in the USA and Europe, with a reduction in the incidence of cancer arising in the distal half of the stomach and a rapid increase in the number of cases of the cardia and gastro-oesophageal junction [1]. The overall incidence of cancer at these sites has also risen rapidly, especially in patients younger than 40 years.

The prognosis of patients with these cancers is related to local tumour extent, including both nodal involvement and direct tumour extension beyond the gastric wall [2]. Importantly, the presence of metastases in the peritoneal cavity or distant organs renders the disease incurable and the prognosis is usually very poor. Following resection, the peritoneum is the most common site of recurrence as a result of malignant cells shed from the primary tumour [3].

Radical surgical resection is the only curative treatment for patients with oesophagogastric cancers and is the first-choice treatment in patients with early-stage disease [4]. However, the majority of patients have advanced disease at the time of diagnosis, and accurate preoperative staging is essential to guide management. The objectives of cancer staging are to confirm the diagnosis of malignancy and to determine the extent of the disease, enabling the most appropriate treatment modality to be selected [5]. Given that radical surgery provides the only curative treatment of oesophagogastric cancer, the number of falsely over-staged patients must be minimised to ensure that the possibility for cure is not missed. Yet the sensitivity of any test measuring dissemination of oesophagogastric cancer must be high to avoid unnecessary explorative laparotomies. It has been widely shown that despite improvements in quality, CT still has a low sensitivity for detecting peritoneal disease, hence the proposed need for laparoscopic staging [6].

High-quality contrast-enhanced computerised tomography is the most accurate, widely used, non-invasive modality for detecting distant metastases in oesophagogastric cancer [7]. The introduction of endoscopic ultrasound (EUS) has also been successful in improving the accuracy of preoperative staging in oesophagogastric cancers and is more accurate than CT in determining T and N stages [8] (see Chap. 11 for further information). An added benefit of EUS is the ability to sample suspicious lymph nodes using needle aspiration/mini-core biopsy. As in other diseases described here, CT is inaccurate in the evaluation of peritoneal disease, with sensitivity ranging from 30 to 73 % and specificity from 83 to 100 % [9].

A number of small observational studies have been published comparing imaging modalities in the staging of oesophagogastric cancer. In a study from the authors' own centre, LUS was compared with CT and EUS. Thirty-six patients with histologically proven carcinoma of the oesophagus or stomach who were considered fit for surgery underwent CT, EUS and LUS. The findings of these investigations were compared with final histopathology or intraoperative findings where the tumour was irresectable. Locally advanced tumours were accurately identified by CT in 15/16 (94 %), EUS in 14/16 (88 %) and LUS in 10/12 (83 %). In the assessment of locoregional lymph node involvement, EUS was superior to both CT and LUS: accuracy 21/29 (72 %) versus 17/29 (59 %) and 17/29 (59 %). Although the specificity of LUS in assessment of lymph node involvement was good compared to CT and EUS, the sensitivity was poor: sensitivity/specificity, EUS 79 %/60 %, CT 68 %/40 % and LUS 42 %/90 %. LUS was clearly superior in the identification of metastatic disease, with an accuracy of 21/32 (81 %) versus 23/32 (72 %) for CT. The authors concluded that although the numbers were small, CT, EUS and LUS act in a complimentary manner to provide the most complete preoperative staging for patients with oesophagogastric cancer [10].

In an earlier study aiming to determine the added benefit of LUS over laparoscopy, of 93 patients who underwent

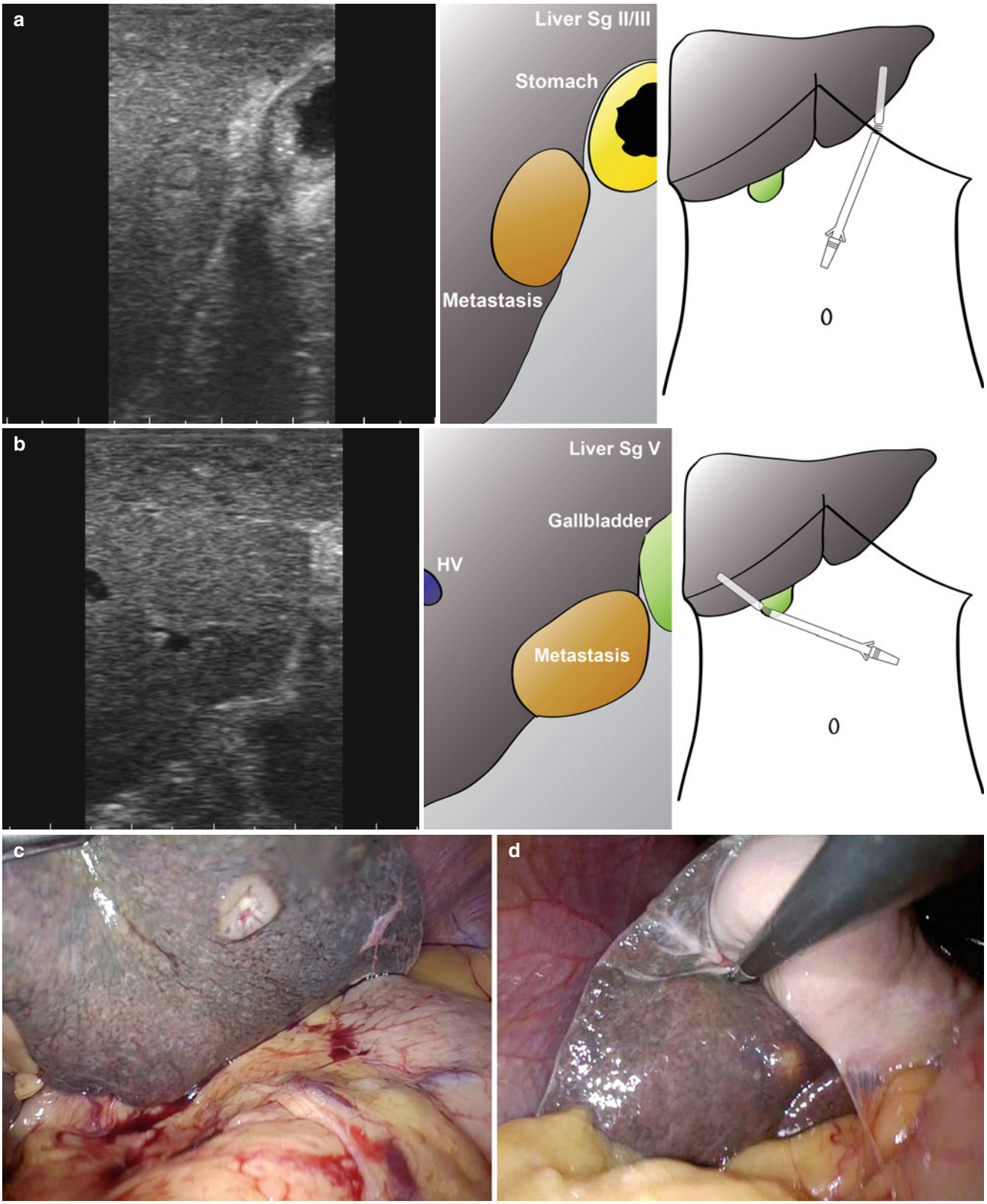

Fig. 10.4 Staging laparoscopy in a patient with a head of pancreas mass. A small lesion had been seen in the right liver on CT and MRI but was too small to characterise. At laparoscopy a lesion was seen in segment II/III of the liver (**a**, **c**) and segment V (**b**, **d**). These looked suspicious and on biopsy with frozen-section analysis, the left-sided lesion was confirmed to be adenocarcinoma (**c**)

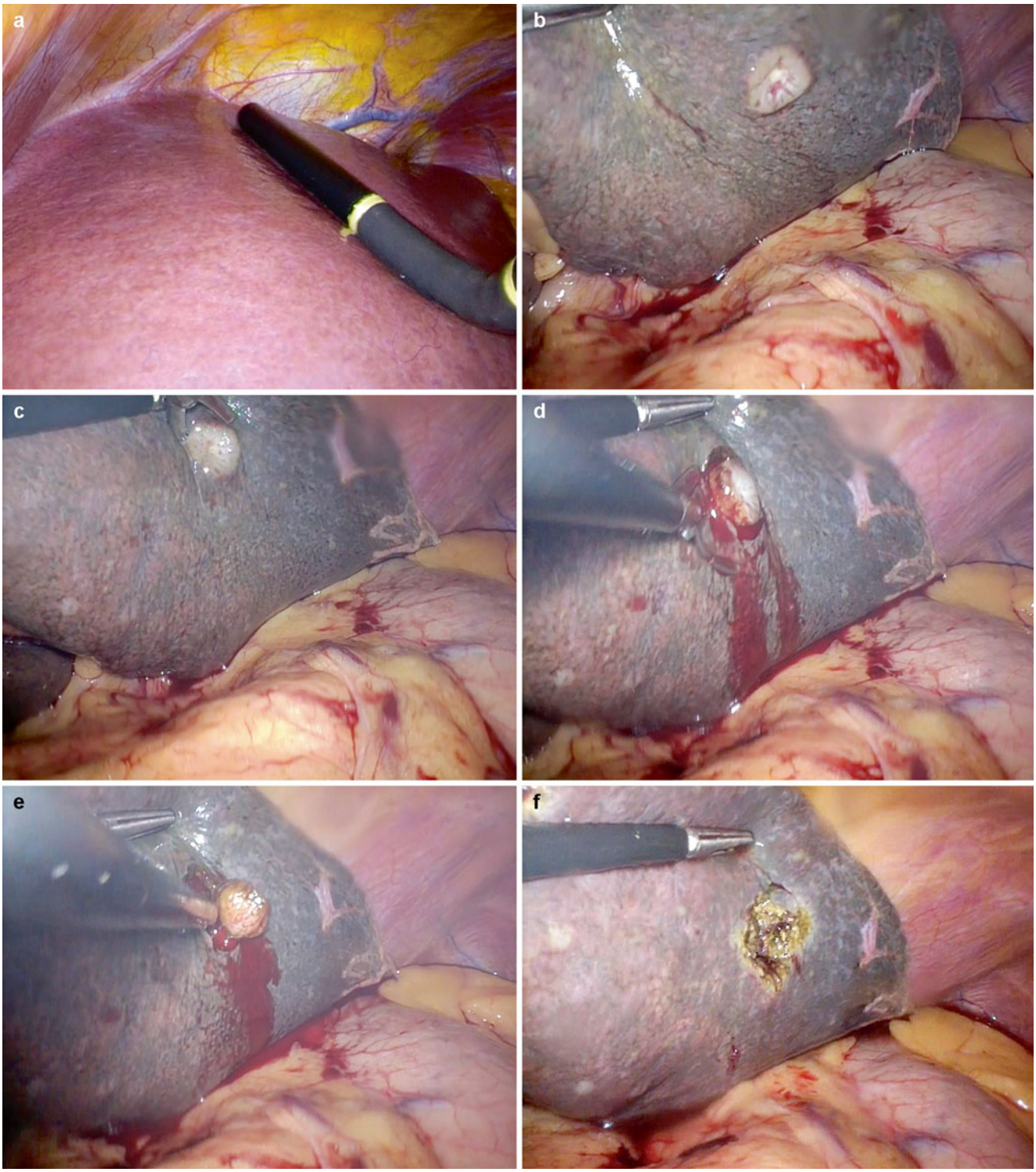

Fig. 10.5 Laparoscopic ultrasound and biopsy of suspicious liver lesion in a patient with head of pancreas mass. The lesion is identified with the ultrasound (**a**) and visualised (**b**). Using scissors without diathermy (**c**), the lesion is excised and subjected to frozen-section analysis (**d**, **e**). Diathermy is used to achieve haemostasis (**f**)

laparoscopy, 18/93 (19.4 %) were shown to have irresectable disease and avoided an inappropriate laparotomy. With the addition of LUS, a further 7/93 (7.5 %) were found to have advanced disease [11]. The unnecessary laparotomy rate reduced from 5/25 (20 %) in those without laparoscopy to 9/75 (12 %) with laparoscopy and 2/68 (3 %) in those who

had LUS. These findings suggesting a positive role for LUS in the staging of OG malignancy were mirrored in other studies [12–15]. However, more recent studies have shown less benefit with the addition of LUS to laparoscopy, possibly as a result of the improved quality of CT and EUS.

In one such study comparing CT, transabdominal ultrasound, laparoscopy and LUS in the assessment of 47 patients with gastric cancer, laparoscopy was accurate in determining overall clinical stage (31/37, 84 %) compared with transabdominal ultrasound (20/37, 54 %) and CT (23/37, 62 %) [6]. However, the addition of laparoscopic ultrasonography did not change the stage of the disease or the decision of whether to proceed with laparotomy for any of the patients, which was correctly predicted in 95 % of the cases. Laparoscopy was superior for detecting peritoneal seeding and ascites, characteristic features of advanced gastric carcinoma. Laparoscopy was also superior in identifying local extension of gastric carcinoma, but the additional information from LUS was minor. The lack of benefit with LUS was also seen in another smaller study, which looked at 18 patients [16].

One of the advantages of staging laparoscopy is the ability to sample tissues. Specifically in gastric cancer, the use of peritoneal lavage cytology can be used to determine operability. In this procedure, fluid is instilled in the upper abdominal cavity at laparoscopy, aspirated and spun-down for cytological examination. In a study examining the value of this procedure in oesophagogastric adenocarcinoma, 255 patients had peritoneal washings at laparoscopy of which 48/255 (18.8 %) had overt peritoneal metastases at staging laparoscopy. Of the remaining patients, 15/207 (7.2 %) had positive cytology. These patients had a median (95 % confidence interval) survival of 13 (3.1–22.9) months versus 9 (7.4–10.6) months for those with overt peritoneal metastases ($p=0.517$). The authors conclude that positive peritoneal cytology in the absence of overt peritoneal metastases was a marker of poor prognosis and should be considered to signify incurable disease [17].

Overall, laparoscopy increases the demonstrated disease stage in 40 % of gastric cancer patients and avoids unnecessary laparotomy in around 25 % (Level II evidence) [18]. It has also been suggested that laparoscopy may downstage tumours thought to be T4 on EUS to T3 by demonstrating the absence of direct invasion into surrounding structures [18]. Early series showed the addition of LUS to be an advantage, but this has been questioned in more recent studies. While the requirement for staging laparoscopy with peritoneal washings is supported by the NCCN Clinical Practice Guidelines in the USA [19] and the SIGN guidelines in the UK [7], neither specifically recommend the use of LUS. The Society of American Gastrointestinal and Endoscopic Surgeons (SAGES) guidelines conclude that LUS for gastric cancer staging can be performed safely and adds little time to the duration the procedure (Grade A). The routine use of staging laparoscopy and LUS after a negative preoperative workup is recommended (Grade B) [18].

Colorectal Liver Metastases

Colorectal cancer (CRC) is the third most common cancer worldwide and the second most frequent cause of cancer death in the USA [20]. The liver is the most frequent site of metastases, and liver resection and ablation are accepted as standard treatment strategies [21]. Outcomes after surgical management of colorectal liver metastases (CRLM) are improving, with 5-year survival now approaching 50 % [22]. Accurate preoperative staging is essential if treatments are to be targeted to those who will benefit most.

Factors associated with poor long-term outcome after liver resection for CRLM include positive margin (hazard ratio (HR) = 1.7, $p=0.004$), extrahepatic disease (HR = 1.7, $p=0.003$), node-positive primary (HR = 1.3, $p=0.02$), disease-free interval from primary to metastases < 12 months (HR = 1.3, $p=0.03$), number of hepatic tumours > 1 (HR = 1.5, $p=0.0004$), largest hepatic tumour > 5 cm (HR = 1.4, $p=0.01$) and carcinoembryonic antigen level > 200 ng/ml (HR = 1.5, $p=0.01$) [23].

Laparoscopy or LUS is not generally recommended for the staging of patients with CRC without evidence of CRLM. In patients with CRC and suspected or proven CRLM, US and European guidelines recommend staging with CT with intravenous contrast, positron emission tomography (PET) CT and/or MRI imaging [21, 24]. As the quality and resolution of these modalities improve, the role of laparoscopy and laparoscopic ultrasound in the staging of colorectal cancer becomes less clear.

The UK guidelines suggest that patients with 'high-risk' primary disease (T4 (perforated), C2 (apical node)) should have careful preoperative investigations that might include laparoscopy. Laparoscopy may identify occult metastatic disease and prevent unnecessary laparotomy in some patients with potentially resectable colorectal liver metastases, and LUS may provide additional information in selected patients [21]. Laparoscopy/LUS may also be useful in the presence of multiple bilobar disease when there are concerns regarding the feasibility of liver resection or imaging is indeterminate.

Conversely, Dutch guidelines for the management of CRLM state that there is no role for diagnostic laparoscopy in routine daily practice due to its invasiveness and the low prevalence of small subcapsular liver lesions and extrahepatic disease. Small liver metastases 'missed' on preoperative imaging also have less clinical consequence as these can generally be resected [25].

A recent meta-analysis examined the role of laparoscopy and laparoscopic ultrasound in the preoperative staging of patients with resectable colorectal liver metastases (Tables 10.1 and 10.2) [38]. The authors identified 12 studies that described a total of 1,047 patients who underwent staging laparoscopy and/or LUS. The difficulty in comparing studies of this type is the assessment of inclusion criteria for the diagnostic test. Significant heterogeneity exists between studies making data synthesis difficult. Clearly, older studies using low-resolution CT imaging are likely to have less

Table 10.1 Meta-analysis of studies examining the role of laparoscopy and laparoscopic ultrasound in the preoperative assessment of patients with resectable colorectal liver metastases: study characteristics

Study	Year	Country	Study type	Preoperative investigation	Patients, *n*	Median age, years	STARD score[a]
Biondi [26]	2010	Italy	Not defined	CT/MRI/PET	65	63	10
Muntean [27]	2009	Romania	Prospective	CT/MRI/PET	18	NA	13
Pilkington [28]	2007	England	Retrospective	CT/MRI	73	NA	12
Khan [29]	2007	England	Retrospective	CT/MRI	210	NA	8
Mann [30]	2007	England	Retrospective	CT/CEA/PET/MR	200	60	13
Mortensen [31]	2006	Denmark	Retrospective	CT	45	62	13
de Castro [32]	2004	The Netherlands	Prospective	US/CT/MR	43	NA	15
Koea [33]	2004	New Zealand	Prospective	CT/CEA	59	65	14
Metcalfe [34]	2003	Australia	Retrospective	CT/CEA	24	NA	12
Grobmyer [35]	2004	United States	Retrospective	CT/CEA/PET/MR	264	62	16
Gholghesaei [36]	2003	The Netherlands	Retrospective	CT/CEA/PET/MR	56	NA	16
Rahusen [37]	1999	The Netherlands	Not defined	CT/CEA/US/MR	50	61	14
Overall	–	–	–	–	1,107		–

Adapted from Hariharan et al. [38]

[a]The STARD statement is a 25-item checklist and recommends the use of a flow diagram, which describes the design of the study and flow of the patients

Table 10.2 Meta-analysis of studies examining the role of laparoscopy and laparoscopic ultrasound in the preoperative assessment of patients with resectable colorectal liver metastases: study results

Study	Lap	Lap/LUS	Sensitivity, %	Specificity, %	PPV, %	NPV, %	True yield, %
Biondi [26]	62	62	72.7 (54.50–86.70)	100	100	76.3	38.7
Muntean [27]	18	18	75.0 (19.4–99.40)	92.9 (66.10–99.80)	75	92.8	16.6
Pilkington [28]	73	73	69.6 (47.10–86.80)	100	100	87.7	21.9
Khan [29]	202	202	39.3 (21.50–59.40)	100	100	91.1	5.45
Mann [30]	178	178	61.9 (48.80–73.90)	100	100	82.7	21.9
Mortensen [31]	38	38	57.1 (18.40–90.10)	100	100	91.1	10.5
de Castro [32]	32	32	71.4 (29.00–96.30)	100	100	92.5	15.6
Koea [33]	54	41	37.5 (8.50–75.00)	100	100	90.2	7.3
Metcalfe [34]	24	24	66.7 (34.90–90.01)	100	100	75	33.3
Grobmyer [35]	264	168	41.3 (29.0–54.0)	100	100	84.4	15.4
Gholghesaei [36]	55	48	73.1 (52.50–88.40)	100	100	80.5	39.5
Rahusen [37]	47	47	75.0 (53.30–90.20)	100	100	79.3	38.3
Overall	1,047	931	59.1 (53.20–64.70)	99.9 (99.30–100)	99.4	86	18.90 (16.44–21.57)

Adapted from Hariharan et al. [38]

contemporary relevance, while trials using the best available cross-sectional imaging with tighter inclusion definitions are likely to demonstrate the greatest utility in laparoscopy, at the expense of the total proportions of their practice numbers included. None of the considered trials were randomised or blinded. The true yield of laparoscopy/LUS for CRLM was 19 % (95 % CI, 16–22 %) with an overall sensitivity of 59 % (95 % CI, 53–65 %). Subgroup analysis for detection of other liver and peritoneal lesions showed a sensitivity of 59 % (95 % CI, 49–67 %) and 75 % (95 % CI, 63–85 %), respectively.

The use of a clinical risk score (CRS) may be a valid method of identifying patients most likely to benefit from LUS. In a study of 79 patients, LUS prevented unnecessary laparotomy in 15/74 patients by predicting the benign nature of lesions or demonstrating unresectability [39]. A CRS was determined based on lymph node-status of primary tumour, disease-free interval, number of metastases, largest metastasis and CEA. In those with a CRS < 2, LUS prevented a laparotomy in only 7 % of patients. However, in those with a CRS > 2, LUS prevented an operation in 24 % of patients. The authors concluded that selecting those likely to benefit from LUS will increase the utility of the investigation.

The best indication for laparoscopy and laparoscopic ultrasound in CRLM is in patients with resectable disease, but a suspicion of peritoneal disease that is not well defined on cross-sectional imaging or PET-CT. This is with the intention of avoiding an unnecessary laparotomy in patients with extrahepatic disease. As laparoscopic liver resection becomes more common, this step will be part of the resection procedure anyway.

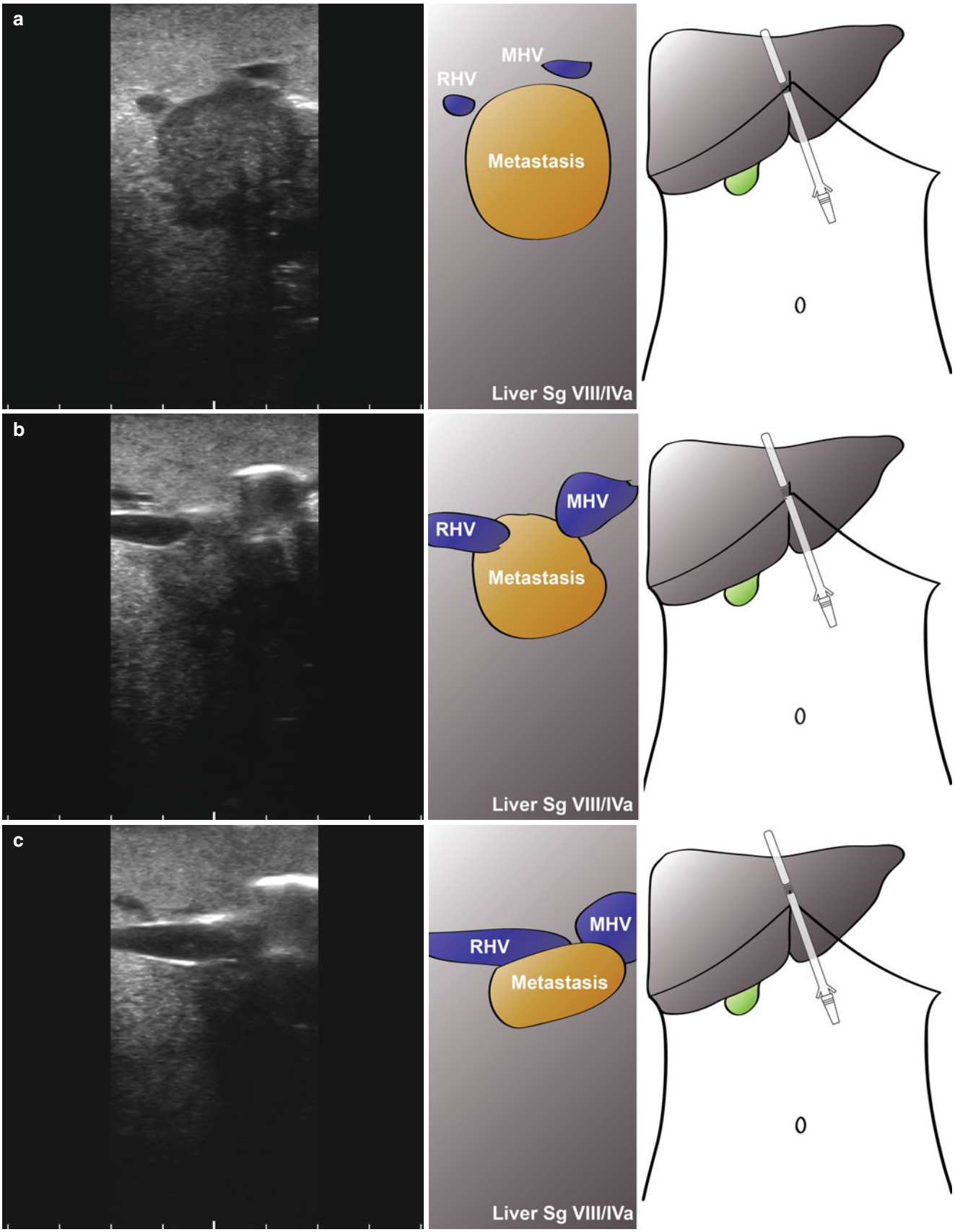

Fig. 10.6 Laparoscopic ultrasonography in a patient with large colorectal liver metastasis at the hepatic outflow (**a**; RHV, right hepatic vein; MHV, middle hepatic vein). As the probe is moved up towards the suprahepatic vena cava (**b**), a large metastasis can be seen sitting between the right and middle hepatic veins (**c**)

The final area in which LUS may be of use is in patients with borderline resectable disease. Figure 10.6 shows images from a patient with a colorectal liver metastasis high in segment VIII. A right hepatectomy was being considered, but significant progression of disease had occurred since the last cross-sectional imaging. LUS shows clear impingement of the metastasis upon the middle hepatic vein. The procedure was abandoned, and the patient had radiological embolisation to the right lobe and segment IV. A successful extended right hepatectomy was performed 6 weeks later. In a different case, local resection was being considered for a right-sided CRLM (Fig. 10.7). Again, there has been significant progression of disease and with ultrasonography clearly showing tumour abutting the segment VIII pedicle (Fig. 10.7a, b, Video 10.1) and indenting the right hepatic vein with possible invasion (Fig. 10.7c, d, Video 10.2). This patient went on to have a successful open right hepatectomy.

In summary, the ratio of patients benefiting from laparoscopy/LUS (i.e. those avoiding an unnecessary laparotomy) to those submitted to the procedure (the true yield) is around 20 %. It is likely that this could be increased by selecting the patients most likely to benefit. Ultrasound has a place in the assessment of borderline resectable disease, and the rise in the number of laparoscopic liver resections will naturally encourage an increased use in LUS assessment.

Hepatocellular Carcinoma

Hepatocellular carcinoma (HCC) is a leading cause of cancer-related death worldwide [40]. The incidence is particularly high in East Asia and sub-Saharan Africa and is rising in North America and Europe. Around 80 % of cases develop on a background of chronic liver disease with aetiology varying by geography and the primary factor being infection with hepatitis B or hepatitis C virus [41]. Liver resection and liver transplantation provide an opportunity for cure. Ablation of lesions and transarterial chemoembolisation can be used to control disease while awaiting transplantation or as palliative measures in advanced disease. The role of chemotherapy has expanded in recent years and will likely become more prominent in the future.

Staging of HCC is important in determining suitability for transplantation. The original 'Milan criteria' of one lesion smaller than 5 cm or 3 lesions smaller than 3 cm, together with no extrahepatic disease or vascular invasion, have been broadened [42]. Patients with no cirrhosis or good preservation of liver function are considered for resection. The use of magnetic resonance imaging (MRI) with liver-specific contrast agents has become the primary mode of investigation of suspected HCC [43]. The requirement, therefore, of laparoscopic staging of HCC is now limited. In centres without access to MRI, LUS can still be useful in guiding treatment decisions [41]. Figure 14.8 and accompanying video demonstrates the typical ultrasound features of HCC. Lesions can be hypo- or hyperechoic with reference to the background liver and often demonstrate a peripheral hypoechoic ring.

Laparoscopic radiofrequency or microwave ablation is becoming an important technique in the management of HCC [44]. LUS is an absolute requirement during laparoscopic ablation. This is discussed in further detail in Chap. 17.

Cholangiocarcinoma

Cholangiocarcinoma is an uncommon malignancy with a poor prognosis: the majority of patients will only be suitable for palliative measures [45]. Tumours may be intrahepatic (IHC), proximal extrahepatic (hilar, HC) or distal (DC) and may be multifocal. Surgery offers the only potential cure in patients with localised disease but is associated with significant morbidity and mortality. Accurate preoperative staging is essential to avoid unnecessary morbidity and to plan the surgical approach to treatment. While improvements in cross-sectional imaging have made a great impact in the staging of other GI malignancies, the evaluation of cholangiocarcinoma remains a challenge even to the most experienced clinician.

Staging laparoscopy and laparoscopic ultrasound (LUS) are commonly used in the evaluation of all types of cholangiocarcinoma, but no randomised controlled trials have been published examining their use. As in other diseases, the great benefit in of laparoscopy is the ability to detect previously undiagnosed peritoneal disease. Laparoscopic ultrasound can detect intrahepatic metastases and provide further information regarding local involvement. In cholangiocarcinoma, the use of staging laparotomy avoids unnecessary laparotomy in a significant proportion of patients with overall yields ranging between studies from 35 to 96 % [2].

Hilar Cholangiocarcinoma

In hilar cholangiocarcinoma, patient- and local tumour-related factors, as well as the presence of metastatic disease, determine resectability (Table 10.3). A study from the authors' own centre showed a yield from laparoscopy alone of 20/82 (24.3 %), where yield is defined as the number of irresectable patients detected at laparoscopy divided by the total number of patients undergoing laparoscopic assessment. This number increased to 35/82 (41.5 %) with the addition of LUS.

An earlier observational study from the Memorial Sloan-Kettering Cancer Center failed to show any benefit with the addition of LUS [46]. In this study, however, LUS was only used in a subset of patients (23/100, 23 %), and a significant proportion went straight to laparotomy with no laparoscopy (76/176, 43 %). In this latter group, 39/76 (51 %) were

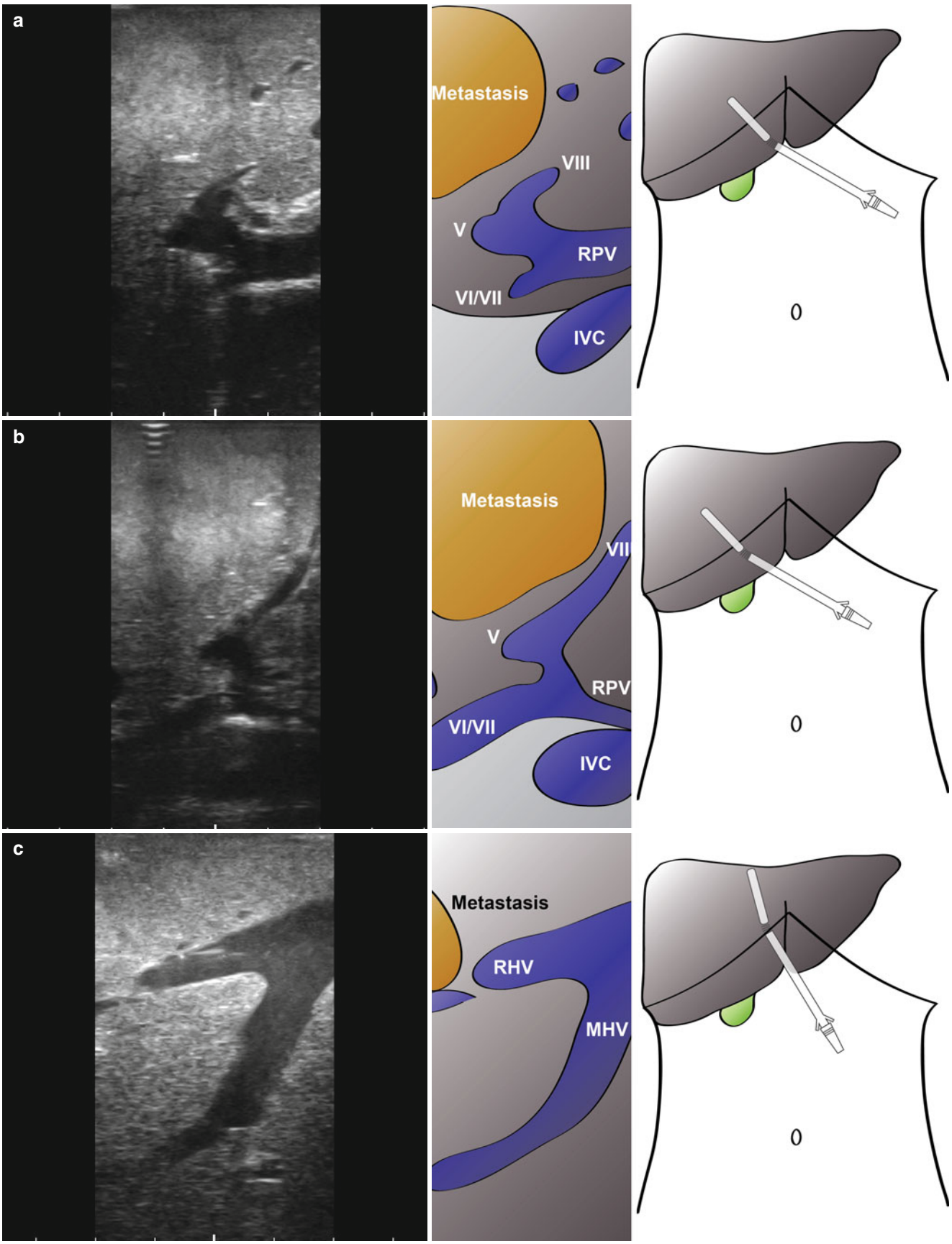

Fig. 10.7 Intraoperative ultrasonography to determine relationship of large colorectal liver metastasis to vascular structures. A local resection was being considered, but ultrasonography clearly shows the tumour abutting the segment VIII pedicle (**a**, **b**, Video 10.1) with no resection margin possible at this structure. In addition, there is indenting and possible invasion of the right hepatic vein (**c**, **d**, Video 10.2; RHV). The patient has a successful open right hepatectomy. MHV, middle hepatic vein; IVC, inferior vena cava; V, segment V pedicle; VI/VII, segement VI/VII pedicle

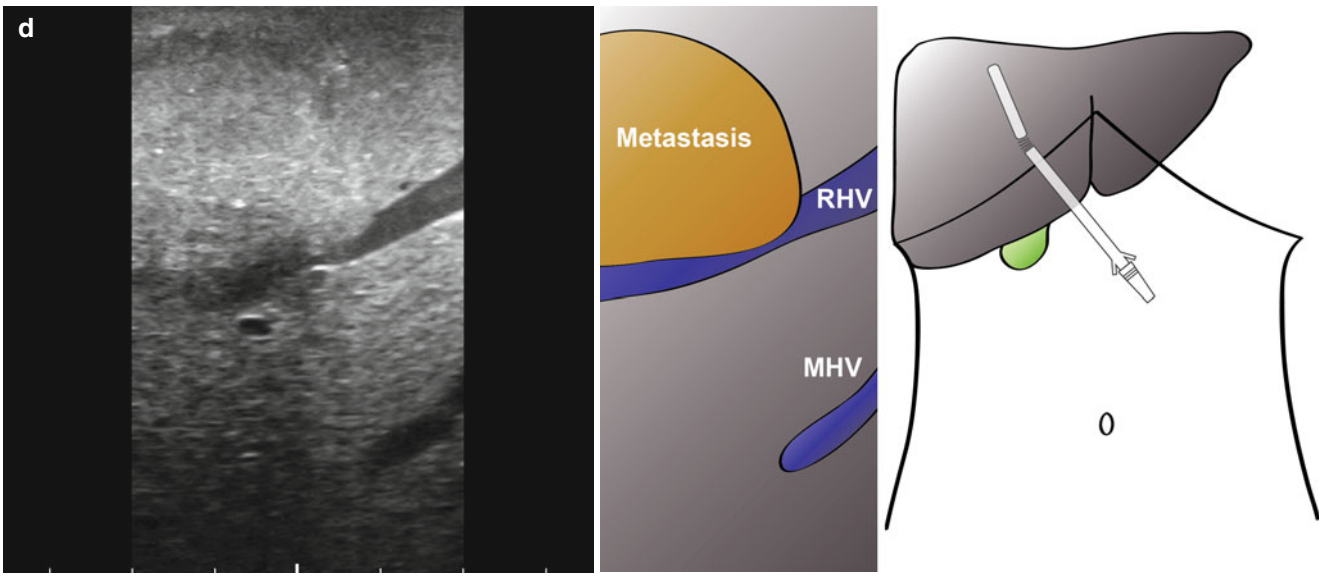

Fig. 10.7 (continued)

Table 10.3 Factors associated with inoperable disease in hilar cholangiocarcinoma

Factors associated with inoperable disease	Evaluable by laparoscopy alone	Evaluable by LUS
Patient factors		
Medically unfit or otherwise unable to tolerate a major operation	–	
Liver cirrhosis	+	++
Local tumour-related factors		
Tumour extension to secondary biliary radicles bilaterally	–	+
Encasement or occlusion of the main portal vein proximal to its bifurcation	–	+
Atrophy of one hepatic lobe with contralateral portal vein branch encasement or occlusion	–	+
Atrophy of one hepatic lobe with contralateral tumour extension to secondary biliary radicles	–	+
Unilateral tumour extension to secondary biliary radicles with contralateral portal vein branch encasement or occlusion	–	+
Metastatic disease		
Histologically proven metastases to N2 lymph nodes	–	+/–
Liver or peritoneal metastases	+	+++

Adapted from Blot et al. [1]

irresectable with 73/176 (41 %) overall having inoperable disease. The authors comment correctly that although LUS might appear useful in the assessment of locally advanced disease, particularly in assessing vascular involvement, its accuracy can be limited by inflammation secondary to biliary stents. Moreover, patients with extensive vascular involvement, which would be readily detected on LUS, are usually identified with cross-sectional imaging prior to surgery.

In our own study, patients judged to be irresectable upon the addition of LUS were, on the whole, found to have locally advanced disease (13/14). Making a decision on resectability on the basis of LUS can be difficult, and surgeons may be uncomfortable doing this. Some may prefer to 'give the patient the benefit of doubt' and perform an exploratory laparotomy to provide further information. Certainly, in most studies, a significant proportion of patients are found to be irresectable at laparotomy despite being deemed resectable on laparoscopy/LUS. In our series, of those that underwent trial dissection, 19/44 (43.2 %) were irresectable: 4 for with peritoneal disease, 10 with locally advanced disease, 3 with metastatic disease and 2 unknown [47].

In a meta-analysis of the role of laparoscopy and LUS in the preoperative staging of pancreaticobiliary cancers [48], 7 studies with 478 patients were examined which focussed on

Table 10.4 Meta-analysis of data from studies analysing staging laparoscopy/LUS in proximal biliary cancers

First author	Year	Laparoscopic examinations	Diagnostic odds ratio[a]	Overall yield (%)
Goere [49]	2006	39	42.8	35.8
Agarwal[b]	–	91	135	43.9
Weber [46]	2002	100	64.8	35
Vollmer [50]	2002	11	35	63.6
Connor [47]	2005	80 (4 failed)	22.2	45
Tilleman [51]	2002	110	105.9	40.9
Kriplani [52]	1992	47	91	95.7
Total (95 % CI)		478	61 (19–189)	47 (42–51)
Heterogeneity, I^2		–	0 %	–

Adapted from Hariharan et al. [48]

[a]Diagnostic odds ratio: the odds of irresectable disease given a positive laparoscopy divided by the odds of irresectable disease given a negative laparoscopy

[b]Error in citation in study, correct citation could not be identified

hilar cholangiocarcinoma. The overall sensitivity and specificity of laparoscopy/LUS in detecting irresectable disease were 63 % (95 % CI 58–68) and 100 % (95 % CI 97–100). Significant variation in sensitivity was seen between studies but could not be explained by further regression analyses. In sensitivity analyses, studies making specific inclusion of LUS were not shown to result in any improvement of diagnostic parameters. A subgroup analysis revealed a high sensitivity for liver and peritoneal lesions but low sensitivity for local/vascular tumour invasion, despite the results of our own study. Again, the overall yield for the use of laparoscopy was 46 % (95 % CI 42–51) (Table 10.4).

Is there a role for targeted laparoscopy/LUS on the basis of the suspected stage of disease? Jarnagin and colleagues have proposed T-stage criteria for hilar cholangiocarcinoma which correlates well with survival [45] and resectability [47]. Palliation in the past has included bypass of the obstructed common bile duct by means of a segment III hepaticojejunostomy. In recent years, this procedure has been superseded by endoscopic metal stent placement, which is superior both in patient tolerability and efficacy. In the past, it may have made sense to have a low threshold for proceeding directly to laparotomy in patients without distant metastases, given that a surgical bypass procedure would be required if the disease was irresectable. However, this is no longer the case, and given the benefits of palliative endoscopic treatment and the necessity to avoid unnecessary laparotomy, all patients with potentially resectable hilar cholangiocarcinoma should undergo staging laparoscopy/LUS prior to open surgical exploration.

Intrahepatic Cholangiocarcinoma

Little has been written about LUS in intrahepatic cholangiocarcinoma. In a small series by Goere, previously undiagnosed peritoneal disease was demonstrated in 4/11 (36 %) [49]. Importantly, of those who went on to attempted resection, 3/7 (42.9 %) were irresectable due to peritoneal disease missed at laparoscopy, vascular involvement or lymph node spread.

In an earlier series from Japan between 1984 and 2001, 62 patients with intrahepatic cholangiocarcinoma underwent laparotomy without a prior staging laparoscopy. Fourteen (23 %) were shown to have peritoneal, liver and lymph node metastases at laparotomy. It has been suggested that an equivalent number of unnecessary laparotomies could have been avoided if staging laparoscopy had been used [53].

On occasion it can be difficult to differentiate malignant and benign lesions of the intrahepatic biliary tree. Figure 10.8 demonstrates a so-called pseudo-tumour, where a suspicious lesion seen on CT is shown on LUS to have a clear acoustic shadow and to be an intrahepatic gallstone (Fig. 10.8, Video 10.3).

Pancreatic and Peri-pancreatic Carcinoma

In this section, pancreatic, ampullary and duodenal cancer, as well as distal cholangiocarcinoma, are considered. Pancreatic cancer is an important cause of cancer-related deaths yet the majority of patients are irresectable at presentation due to liver metastases, peritoneal metastases or locally advanced disease. In the experience of the authors, the median survival of patients who do not undergo a surgical resection is 6 months [55] and is only extended to 24 months in those resected. Given that the outcome for the majority of patients is poor, accurate staging is essential to guide appropriate treatment selection, which unfortunately is most commonly palliation.

The question of whether to perform staging laparoscopy/LUS partly depends on the consequence of identifying irresectable disease. In the recent past, the only effective palliation for the often present biliary obstruction and occasional gastric outlet obstruction has been open surgical bypass. Our

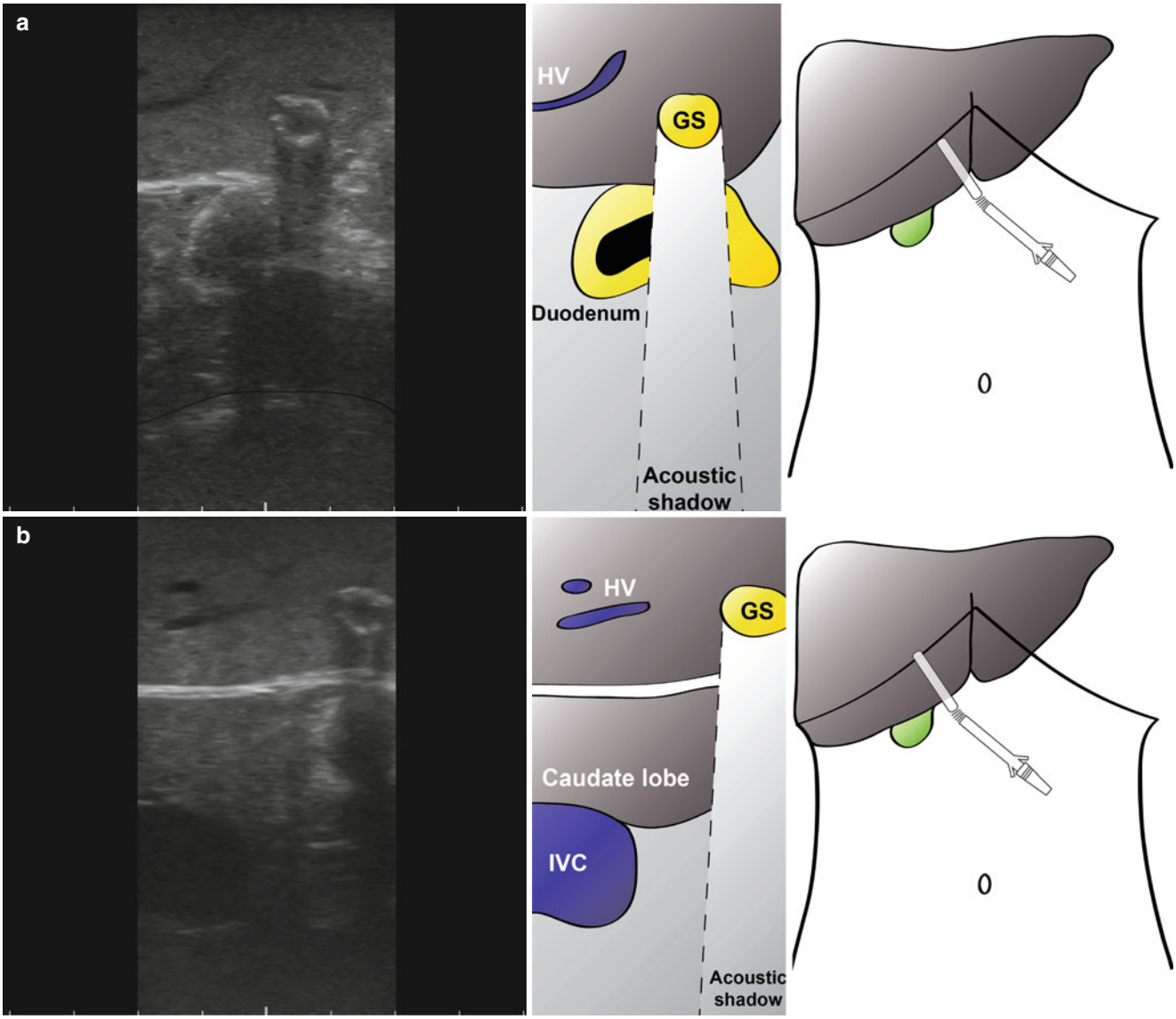

Fig. 10.8 A patient with a suspicious liver lesion which on LUS is demonstrated to be an intrahepatic gallstone (**a**, **b**; see Video 10.3). Benign and malignant lesions can be difficult to differentiate in the biliary tree, as a number of case reports of similar instances describe [54]

own experience reflects a broader appreciation of the benefits of nonoperative palliation: although surgical bypass may be more effective (at the cost of a significant operative procedure), survival is similar following surgical bypass or biliary stenting for jaundice [55]. While the threshold for open exploration used to be low, if preoperative imaging now demonstrates inoperable disease, then endoscopic placement of a self-expanding metal biliary stent and laparoscopic gastrojejunostomy may be considered. The question, therefore, is which group of patients may laparoscopy/LUS benefit?

In an early study from the authors' centre, laparoscopic ultrasonography was used to evaluate 12 patients with suspected adenocarcinoma of the head of the pancreas [56]. Preoperative transabdominal ultrasonography and CT had suggested these patients were all resectable. LUS demonstrated hepatic metastases in four patients, peritoneal disease in two and malignant ascites in one. Overall, LUS demonstrated a contraindication to resection in six patients (50 %). In the six patients subjected to laparotomy, one was found to be resectable due to lymph node metastases.

These observations were followed with a prospective study comparing LUS with USS, CT and selective visceral angiography in determining the TNM stage in 50 patient with pancreatic or peri-ampullary cancers [57]. The gold standard defining resectability in these patients was either biopsy at the time of laparoscopy or subsequent open surgical exploration. The ability to demonstrate irresectability based on T-stage was similar for the four techniques (sensitivity 60–71 %); however, laparoscopic ultrasound was significantly more specific (100 %), i.e. all patients ultimately

resected were thought to be resectable by T-stage on LUS. No modality was accurate in determining N-stage, but laparoscopy was required to identify metastases (sensitivity, USS (29 %), CT (33 %), laparoscopy/LUS (94 %)). LUS though did not significantly improve on laparoscopy alone in this study, as all metastases were superficial and easily visualised. Overall diagnostic accuracy was better with LUS than the other modalities (PPV LUS (97 %) versus CT (79 %)). This study was performed 20 years ago, and since then, the quality of CT imaging has improved dramatically. Does LUS still have a place given this greatly improved non-invasive staging?

Our group revisited the question with a study published in 2006 which aimed to identify a subgroup of patients who may benefit from LUS based on CT assessment of vascular involvement [58]. A CT grade was assigned based on the degree of vascular involvement observed, following which LUS was performed. Of 152 patients who underwent LUS, 56 (37 %) had irresectable disease. In patients with pancreatic and biliary duct dilatation but no mass, three of 26 (12 %) were irresectable, compared with 27 of 88 (31 %) in those with a mass seen not to encircle vessels. However, as expected, the number of irresectable patients was much higher in those with tumour encircling vessels (17 of 29 (59 %)) and all nine patients with tumour occluding vessels. The accompanying Venn diagram (Fig. 10.9) summarises the reasons patients were found to be irresectable at LUS. It was concluded that selective use of LUS in patients with a mass adjacent to but not encircling or obstructing vessels could further differentiate those who are actually resectable. LUS was not deemed useful in those with biliary/pancreatic duct obstruction but no mass or those with clear vessel involvement.

A meta-analysis published in 2010 on the use of staging laparoscopy and LUS in pancreatic-biliary cancers identified

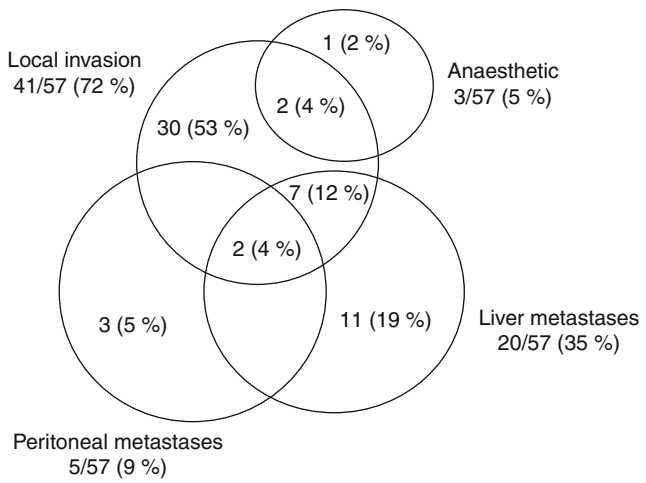

Fig. 10.9 Reason pancreas/ampullary cancer irresectable at laparoscopic ultrasound (From Thomson et al. [58])

22 studies examining pancreatic/peri-pancreatic cancer that satisfied inclusion criteria [48]. The study examined 2,827 patients in studies published over a 13-year period (Table 10.5). The overall sensitivity and specificity of laparoscopy/LUS in this group was 64 % (95 % CI 61–66) and 99 % (95 % CI 99–100) with a true yield of 25 % (95 % CI 24–27) and a diagnostic odds ratio of 104 (48–227). Importantly, the use of laparoscopy/LUS improved the resection rate from 61 to 80 %. In sensitivity analyses, no improvement in diagnostic accuracy was seen in larger studies or studies that fulfilled reporting guidelines. However, studies employing LUS over those using only staging laparoscopy show improved sensitivity and diagnostic odds ratio: 137 (50–376) from 104 (48–227). Similarly, subgroup analysis revealed a high sensitivity for liver and peritoneal lesions but a low sensitivity for local/vascular tumour invasion. The analysis concluded that staging laparoscopy appeared beneficial for the detection of peritoneal disease and surface liver metastases and that laparoscopy should be routine in clinical practice. It made no recommendation on the place of LUS in addition to laparoscopy.

The potential benefits in avoiding an unnecessary laparotomy are reflected in an economic analysis [79]. Using decision modelling, costs and benefits in hypothetical patients with suspected pancreatic cancer were calculated under various scenarios. With best estimates, CT followed by laparoscopy/LUS had an incremental cost-effectiveness ratio of $87,502 per life-year gained, compared with best supportive care, which was significantly more cost-effective than CT/MRI and was less expensive than other imaging strategies. Immediate surgery with no additional imaging for staging was more expensive and less effective than all imaging strategies. The study concluded that a strategy involving CT/laparoscopy/LUS would consistently result in lower costs compared with any other combination of imaging tests under a wide range of scenarios.

Endoscopic ultrasound has become an essential investigation in the assessment of patients with pancreatic cysts or suspected intraductal pancreatic mucinous neoplasm (IPMN), where the underlying diagnosis is in question [80]. Although it is invasive, it does not usually require a general anaesthetic and has the advantage of being to sample tissue from suspicious pancreatic lesions or lymph nodes. Its place in the routine staging of patients with typical features of pancreatic ductal adenocarcinoma on cross-sectional imaging is less clear, although early studies reported EUS to be more sensitive than CT [81] or angiography [82] in the detection of vascular involvement. A recent review concluded that EUS is useful in assessing suspicious lesions that are not well defined on cross-sectional imaging and potentially in the assessment of cases deemed ‘borderline resectable’ due to vascular involvement [83]. This is supported by a recent prospective observational study comparing EUS with CT in

Table 10.5 Individual and overall results following homogenisation of data from studies analysing staging laparoscopy/laparoscopic ultrasound in pancreatic/peri-pancreatic cancers

First author	Year	Laparoscopic examinations	Diagnostic odds ratio[a]	Overall yield (%)
White [59]	2008	1,045	27,308.1	13.8
Enestvedt [60]	2008	86	138.1	27.9
Thompson [58]	2006	152	204.7	36.8
Doucas [61]	2007	98	80.5	56.1
Ahmed [62]	2006	37	103.4	24.3
Karachristos [63]	2005	63	58.9	19
Nieveen Van Dijkum [64]	2003	286	13.6	24.1
Doran [65]	2004	216	40.9	15.2
Zhao [66]	2003	22	153	59
Vollmer [50]	2002	84	46	28.5
Kwon [67]	2002	52	826.3	34.6
Taylor [68]	2001	51	250.6	52.9
Menack [69]	2001	27	111	25.9
Schachter [70]	2000	67	454.1	44.7
Jimenez [71]	2000	125	29.2	31.2
Pietrabissa [72]	1999	42	177	23.8
Durup Scheel-Hincke [73]	1999	34	139.3	55.8
Reddy [74]	1999	98	60.7	29.5
Andrén-Sandberg [75]	1998	24	21.5	37.5
Conlon [76]	1996	108	785.3	37.9
Bemelman [77]	1995	70	22.9	22.8
John [78]	1995	40	50.6	57.5
Total (95 % CI)		2,827	104 (48–227)	25 (24–27)
Heterogeneity χ^2 (p-value), I^2		–	47 ($p=0.001$), 56 %	–

From Hariharan et al. [48]

[a]Diagnostic odds ratio: the odds of irresectable disease given a positive laparoscopy divided by the odds of irresectable disease given a negative laparoscopy

the detection, staging and resectability of pancreatic cancer [84]. In 120 patients enrolled, 104 (87 %) underwent EUS and CT. Of 80 patients with pancreatic cancer, 27 (34 %) were managed nonoperatively, and of the 53 (66 %) who underwent laparotomy, 25 (31 %) had a resection. For these 53 surgical patients, EUS was superior to CT for tumour staging accuracy (67 % vs. 41 %; $P<0.001$) but equivalent for nodal staging accuracy (44 % vs. 47 %; $P>0.2$). In the 25 patients resected, operability was correctly identified by EUS in 88 % and CT in 92 %. Of the 28 patients with irresectable tumours, inoperability was correctly identified by EUS in 68 % and by CT in 64 %. The authors concluded that EUS is superior to CT for T-staging but similar for nodal staging and resectability. It is our own practice to use EUS when there is doubt about the diagnosis or when a patient is clearly irresectable and a tissue diagnosis is required prior to palliative chemotherapy. EUS is not part of our standard preoperative assessment in suspected pancreatic cancer. Please refer to Chap. 11 for more information on EUS.

Distal cholangiocarcinoma and ampullary carcinomas are disease entities in their own right but are usually investigated and staged in the same manner as pancreatic cancer. In an interesting study from 2002, Vollmer examines these different diagnostic categories with the aim of determining the utility of preoperative staging for each [50]. Is laparoscopy +/– LUS equally useful in staging biliary malignancies arising from different sites? Staging laparoscopy was performed in 157 patients. Patients were identified to be irresectable by the following categories: head of pancreas (24/72, 33 %), distal pancreas (2/12, 17 %), gallbladder (7/11, 64 %), distal cholangiocarcinoma (4/23, 18 %) and ampullary/duodenal (0/22, 0 %). LUS was most useful in head of pancreas cancer, where eight patients were demonstrated to be irresectable with the addition of LUS. If the proportions in this study are representative, laparoscopy/LUS seems very useful in head of pancreas and gallbladder cancer, of limited use in distal cholangiocarcinoma and distal pancreas cancer and of no use in ampullary/duodenal cancer.

LUS has also been reported in the investigation of other pancreatic neoplasms and in particular neuroendocrine tumours [18]. A number of studies exist demonstrating the ability of intraoperative in the detection of insulinomas with an accuracy of 83–100 % [85–88].

In conclusion, the benefit of LUS in addition to standard laparoscopy is sensitive to many factors. In studies specifically reporting the added benefit of LUS, irresectable disease is

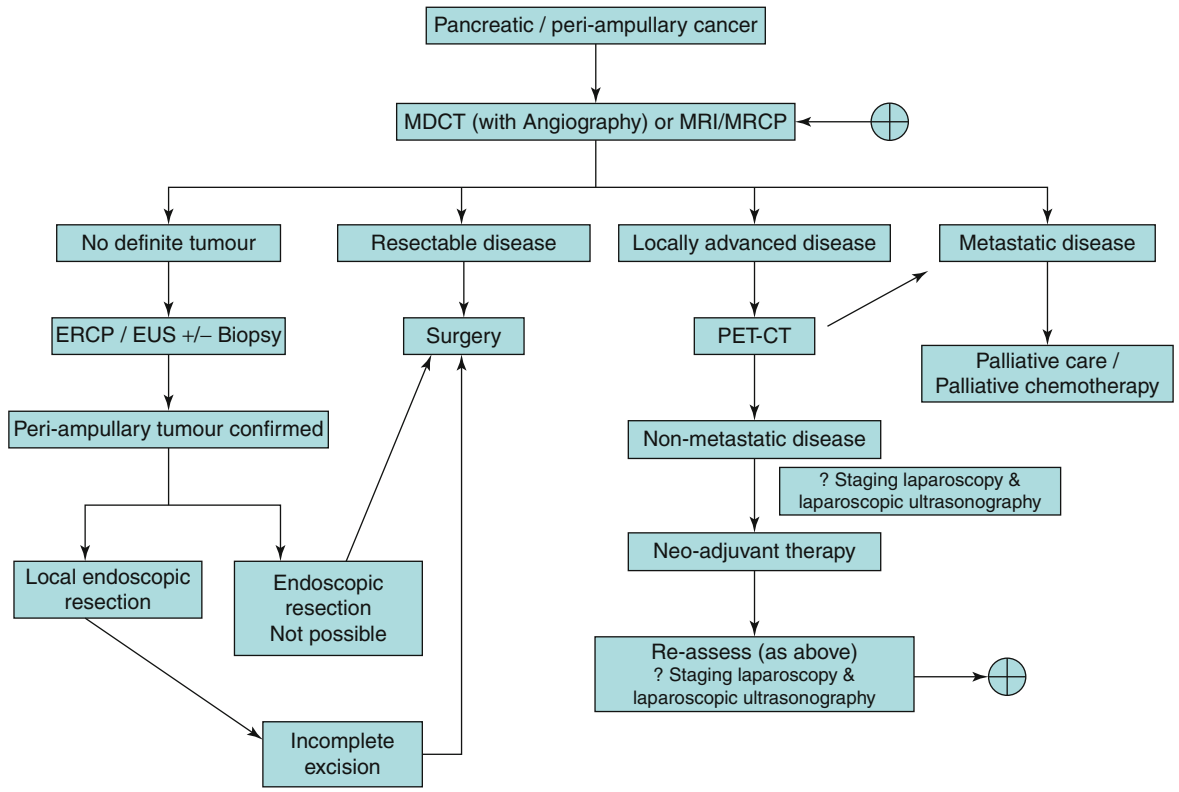

Fig. 10.10 A proposed algorithm outlining the role of the individual imaging modalities in the management of pancreatic and peri-ampullary cancers. *MDCT* multi-detector computed tomography, *MRI* magnetic resonance imaging, *MRCP* magnetic resonance cholangiopancreatography, *PET-CT* positron emission tomography-computed tomography, *EUS* endoscopic ultrasonography, *ERCP* endoscopic retrograde cholangiopancreatography (From Shrikhande et al. [83])

detected in 11–28 % of patients who would have been deemed resectable on laparoscopy alone, with a false-negative rate of 1–8 % [18]. Overall, unnecessary laparotomy can be avoided in 34 % of patients. Patients presenting with gastric outlet obstruction and a CT/MRI demonstrating a potentially resectable tumour should proceed directly to laparotomy, as a hepaticojejunostomy and gastroenterostomy can be performed readily if the tumour is irresectable. In the situation where CT/MRI shows irresectable disease, endoscopic biliary metal stenting should be performed and consideration given to laparoscopic gastroenterostomy in the presence of gastric outflow symptoms. In patients with a CT/MRI that suggests malignancy, but the diagnosis is uncertain, EUS should be considered (Fig. 10.10).

Gallbladder Carcinoma

As suggested in the previous section, laparoscopy/LUS may be useful in the staging of gallbladder carcinoma. A number of older studies have suggested laparoscopy is associated with a yield of 38–62 % [46, 49, 89–92]. There have been few studies that have looked specifically at the added benefit of LUS. The study by Vollmer mentioned above examined 11 patients gallbladder carcinoma [50]. Of those, laparoscopy alone identified 6 (55 %) of patients with metastatic disease. The other six patients all underwent LUS, and a further one of those patients was found to be irresectable.

In a study by Weber and colleagues, 44 patients with potentially resectable gallbladder carcinoma underwent staging laparoscopy +/– LUS. The overall yield was 21/44 (48 %), but a further 15/23 patients were found to be irresectable at laparotomy, giving an accuracy for laparoscopy/LUS of 21/36 (58 %). In this study, LUS did not identify any patients deemed irresectable based strictly on LUS findings alone. Despite the operating surgeons being very experienced, nine patients found to be irresectable at laparotomy had locally advanced disease and a further two had liver metastases.

The largest series of staging laparoscopy in gallbladder cancer was published recently by Agarwal and colleagues, although LUS was not used at all [93]. Of 409 patients with gallbladder cancer who underwent laparoscopy, 95/409 (23 %) had disseminated disease: surface liver metastasis ($n=29$) and peritoneal deposits ($n=66$). The overall yield laparoscopy was 23 % (95/409). Of the 314 patients who underwent laparotomy, an additional 75 had unresectable disease due to missed surface liver metastasis ($n=5$), deep

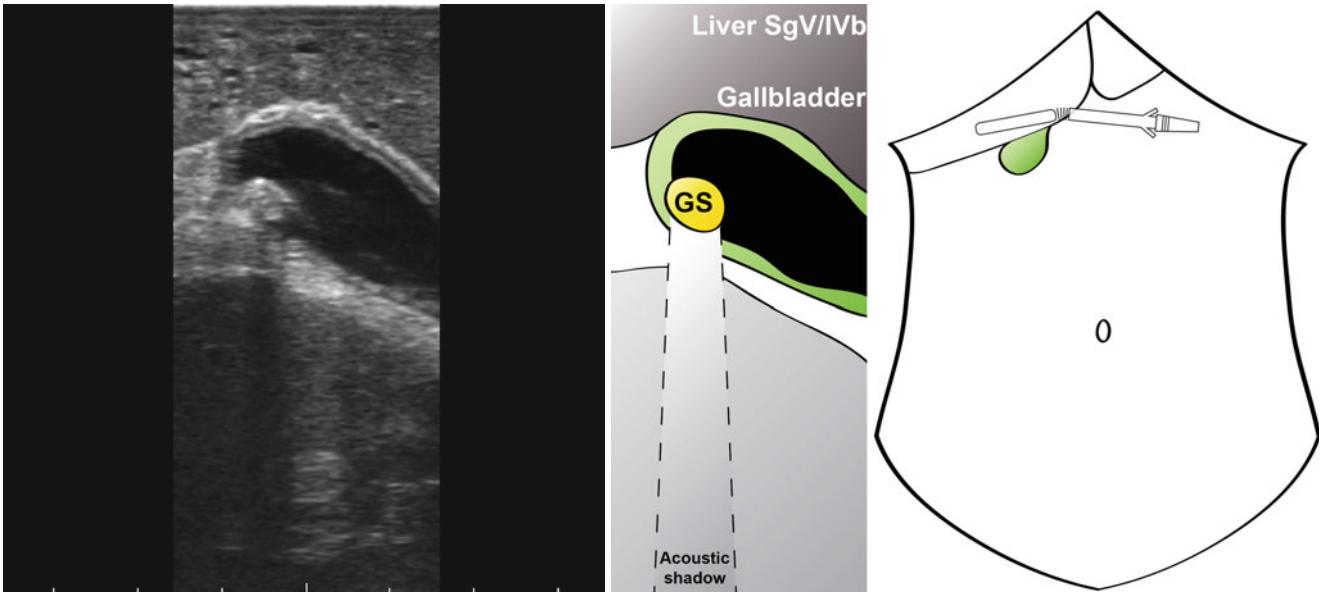

Fig. 10.11 Laparoscopic ultrasound the in the assessment of the gallbladder. In this patient, a suspicious polyp was reported on preoperative imaging. On LUS, only a simple gallstone (*GS*) is seen in the gallbladder, with no wall thickening or infiltrating lesion

parenchymal liver metastasis ($n=4$), peritoneal deposits ($n=1$), non-locoregional lymph nodes ($n=47$) and locally advanced disease ($n=18$). Therefore, the accuracy of laparoscopy for detecting unresectable disease was 55.9 % (95/170). A subgroup analysis of early ($n=56$) versus locally advanced ($n=353$) gallbladder cancer showed an expected greater yield in the latter with accuracy being similar between groups. In this series, would the inclusion of LUS have increased the yield? Four patients had deep parenchymal liver metastases, which would likely have been detected with LUS. A further five patients with surface liver metastases were missed in the early part of the series. If the addition of LUS would have identified these lesions, then the yield would increase from 23.2 to 24.7 % and the accuracy for irresectable disease from 55.9 to 59.4 %.

LUS can be used in patients with indeterminate preoperative imaging. A relatively common situation is the finding of a gallbladder polyp with or without wall thickening in the presence of gallstones. CT can demonstrate the presence of liver infiltration; however, characterisation of the lesion itself can often be difficult. In Fig. 10.11, LUS is used to assess the gallbladder prior to a decision about the appropriateness of a laparoscopic cholecystectomy. In this case, the suspicious lesion had typical appearances of a gallstone on LUS, and a standard laparoscopic cholecystectomy was performed without incident.

A final situation to consider which is unique to the gallbladder is the identification of early-stage carcinoma found incidentally following cholecystectomy for gallstones [94]. Factors determining the outcome of this group include the histological grade of the tumour, involvement of the cystic lymph node if included in the specimen, and whether there was spillage of gallbladder contents during primary cholecystectomy. Curative resection even in patients with advanced disease is possible, although results for patients with T4 disease are poor. Patients should be formally staged with cross-sectional imaging after the histological diagnosis has been made. Little evidence exists, but it is the authors' experience that laparoscopy in this situation is also useful, particularly if there has been bile spillage, given the propensity for peritoneal metastases.

In conclusion, evidence exists of a benefit associated with the use of laparoscopy in the staging of gallbladder cancer. Little has been written specifically about the added benefit of LUS. However, it seems reasonable to suppose that surgeons with experience of LUS are likely to increase the yield and accuracy of in diagnosing irresectable disease given the rate of missed liver metastases on laparoscopy alone.

Complications Associated with Laparoscopy/ LUS

Laparoscopy is a relatively safe procedure, but of course, risks exist related to the anaesthetic, bleeding, damage to structures (including trocar injuries), infection and port-site herniae. In a meta-analysis on the use of laparoscopy in pancreaticobiliary cancers, 9 of 29 studies included information on complications [48]. These included haemorrhage requiring laparotomy ($n=3$), port-site abscess/infection ($n=3$), postoperative pneumonia ($n=2$), post-procedure pancreatitis ($n=2$), bile leak ($n=2$), port-site haematoma ($n=2$) and port-site recurrence ($n=1$). In addition, there was one reported death following laparoscopy due to myocardial infarction.

Conclusion

Laparoscopy with LUS still has a clear benefit over cross-sectional imaging in its ability to diagnose peritoneal disease and to directly biopsy abnormalities. The great improvement of equipment in recent years has delivered to the surgeon a high-resolution flexible tool which can be used to guide treatment decisions. There is a learning curve associated with the technique, but developing LUS skills is essential for those performing many advanced laparoscopic procedures such as liver ablation or resection.

The utility of LUS for staging differs by diagnosis. Laparoscopy is still common in oesophagogastric surgery, and although LUS may downstage gastric cancer, its use is not recommended in guidelines. In colorectal liver metastases and hepatocellular carcinoma studies quote useful LUS yields, but its use in staging alone is now less common given the improved sensitivity of cross-sectional imaging for these conditions. It is a particularly useful though in aiding laparoscopic interventions such as ablation. In pancreaticobiliary cancers including pancreas carcinoma and cholangiocarcinoma, LUS has a useful place in identifying irresectable patients who can be palliated by endoscopic or percutaneous means, thus avoiding a laparotomy. It is in these conditions that LUS still plays a significant role in staging in many centres worldwide.

References

1. Blot WJ, Devesa SS, Kneller RW, Fraumeni Jr JF. Rising incidence of adenocarcinoma of the esophagus and gastric cardia. JAMA. 1991;265(10):1287–9.
2. Siewert JR, Böttcher K, Stein HJ, Roder JD. Relevant prognostic factors in gastric cancer: ten-year results of the German Gastric Cancer Study. Ann Surg. 1998;228(4):449–61.
3. Bryan RT, Cruickshank NR, Needham SJ, Moffitt DD, Young JA, Hallissey MT, et al. Laparoscopic peritoneal lavage in staging gastric and oesophageal cancer. Eur J Surg Oncol (EJSO). 2001;27(3):291–7.
4. NCCN Clinical Practice Guidelines in Oncology: gastric cancer [Internet] [cited 2013 Jan 13]. Available from: http://www.nccn.org/professionals/physician_gls/f_guidelines.asp.
5. De Graaf GW, Ayantunde AA, Parsons SL, Duffy JP, Welch NT. The role of staging laparoscopy in oesophagogastric cancers. Eur J Surg Oncol (EJSO). 2007;33(8):988–92.
6. Lavonius M, Gullichsen R, Salo S, Sonninen P, Ovaska J. Staging of gastric cancer: a study with spiral computed tomography, ultrasonography, laparoscopy, and laparoscopic ultrasonography. Surg Laparosc Endosc Percutan Tech. 2002;12(2):77–81.
7. Scottish Intercollegiate Guidelines Network. Management of oesophageal and gastric cancer: a national clinical guideline. Edinburgh: Scottish Intercollegiate Guidelines Network; 2006.
8. Kelly S, Harris KM, Berry E, Hutton J, Roderick P, Cullingworth J, et al. A systematic review of the staging performance of endoscopic ultrasound in gastro-oesophageal carcinoma. Gut. 2001;49(4):534–9.
9. Burbidge S, Mahady K, Naik K. The role of CT and staging laparoscopy in the staging of gastric cancer. Clin Radiol [Internet] [cited 2013 Jan 15]. Available from: http://www.sciencedirect.com/science/article/pii/S0009926012004205.
10. Wakelin SJ, Deans C, Crofts TJ, Allan PL, Plevris JN, Paterson-Brown S. A comparison of computerised tomography, laparoscopic ultrasound and endoscopic ultrasound in the preoperative staging of oesophago-gastric carcinoma. Eur J Radiol. 2002;41(2):161–7.
11. Smith A, Finch MD, John TG, Garden OJ, Brown SP. Role of laparoscopic ultrasonography in the management of patients with oesophagogastric cancer. Br J Surg. 1999;86(8):1083–7.
12. Romijn MG, van Overhagen H, Spillenaar Bilgen EJ, Ijzermans JNM, Tilanus HW, Laméris JS. Laparoscopy and laparoscopic ultrasonography in staging of oesophageal and cardiac carcinoma. Br J Surg. 1998;85(7):1010–2.
13. Hünerbein M, Rau B, Schlag PM. Laparoscopy and laparoscopic ultrasound for staging of upper gastrointestinal tumours. Eur J Surg Oncol. 1995;21(1):50–5.
14. Gouma DJ, de Wit LT, Nieveen van Dijkum E, Van Delden O, Bemelman WA, Rauws EA, et al. Laparoscopic ultrasonography for staging of gastrointestinal malignancy. Scand J Gastroenterol Suppl. 1996;218:43–9.
15. Goletti O, Buccianti P, Chiarugi M, Pieri L, Sbragia P, Cavina E. Laparoscopic sonography in screening metastases from gastrointestinal cancer: comparative accuracy with traditional procedures. Surg Laparosc Endosc. 1995;5(3):176–82.
16. Velasco JM, Rossi H, Hieken TJ, Fernandez M. Laparoscopic ultrasound enhances diagnostic laparoscopy in the staging of intra-abdominal neoplasms. Am Surg. 2000;66(4):407–11.
17. Nath J, Moorthy K, Taniere P, Hallissey M, Alderson D. Peritoneal lavage cytology in patients with oesophagogastric adenocarcinoma. Br J Surg. 2008;95(6):721–6.
18. Richardson W, Stefanidis D, Mittal S, Fanelli RD. SAGES guidelines for the use of laparoscopic ultrasound. Surg Endosc. 2010;24(4):745–56.
19. NCCN Clinical Practice Guidelines in Oncology: esophageal and esophagogastric junctional cancer [Internet] [cited 2013 Jan 13]. Available from: http://www.nccn.org/professionals/physician_gls/f_guidelines.asp.
20. Akin O, Brennan SB, Dershaw DD, Ginsberg MS, Gollub MJ, Schöder H, et al. Advances in oncologic imaging. CA Cancer J Clin. 2012;62(6):364–93.
21. Garden OJ. Guidelines for resection of colorectal cancer liver metastases. Gut. 2006;55(suppl_3):iii1–8.
22. De Jong MC, Pulitano C, Ribero D, Strub J, Mentha G, Schulick RD, et al. Rates and patterns of recurrence following curative intent surgery for colorectal liver metastasis. Trans Meet Am Surg Assoc. 2009;127:84–92.
23. Fong Y, Fortner J, Sun RL, Brennan MF, Blumgart LH. Clinical score for predicting recurrence after hepatic resection for metastatic colorectal cancer: analysis of 1001 consecutive cases. Ann Surg. 1999;230(3):309.
24. NCCN Clinical Practice Guidelines in Oncology: colorectal [Internet] [cited 2012 Dec 28]. Available from: http://www.nccn.org/professionals/physician_gls/f_guidelines.asp#site.
25. Bipat S, van Leeuwen MS, Ijzermans JN, Comans EF, Planting AS, Bossuyt PM, et al. Evidence-base guideline on management of colorectal liver metastases in the Netherlands. Neth J Med. 2007;65(1):5–14.
26. Biondi A, Tropea A, Tropea DA, Basile F. Clinical rescue evaluation in laparoscopic surgery for hepatic metastases by colorectal cancer. Surg Laparosc Endosc Percutan Tech. 2010;20(2):69–72.
27. Muntean V, Oniu T, Lungoci C, Fabian O, Munteanu D, Molnar G, et al. Staging laparoscopy in digestive cancers. J Gastrointestin Liver Dis. 2009;18(4):461–7.
28. Pilkington SA, Rees M, Peppercorn D, John TG. Laparoscopic staging in selected patients with colorectal liver metastases as a prelude to liver resection. HPB. 2009;9(1):58–63.

29. Khan AZ, Karanjia ND. The impact of staging laparoscopy prior to hepatic resection for colorectal metastases. Eur J Surg Oncol. 2007;33(8):1010–3.
30. Mann CD, Neal CP, Metcalfe MS, Pattenden CJ, Dennison AR, Berry DP. Clinical Risk Score predicts yield of staging laparoscopy in patients with colorectal liver metastases. Br J Surg. 2007;94(7):855–9.
31. Mortensen FV, Zogovic S, Nabipour M, Tønner Nielsen D, Pahle E, Rokkjaer M, et al. Diagnostic laparoscopy and ultrasonography for colorectal liver metastases. Scand J Surg. 2006;95(3):172–5.
32. De Castro SM, Tilleman EH, Busch OR, van Delden OM, Laméris JS, van Gulik TM, et al. Diagnostic laparoscopy for primary and secondary liver malignancies: impact of improved imaging and changed criteria for resection. Ann Surg Oncol. 2004;11(5):522–9.
33. Koea J, Rodgers M, Thompson P, Woodfield J, Holden A, McCall J. Laparoscopy in the management of colorectal cancer metastatic to the liver. ANZ J Surg. 2004;74(12):1056–9.
34. Metcalfe MS, Close JS. The value of laparoscopic staging for patients with colorectal metastases. Arch Surg. 2003;138(7):770–2.
35. Grobmyer SR, Fong Y, D'Angelica M, Dematteo RP, Blumgart LH, Jarnagin WR. Diagnostic laparoscopy prior to planned hepatic resection for colorectal metastases. Arch Surg. 2004;139(12):1326–30.
36. Gholghesaei M, van Muiswinkel JM, Kuiper JW, Kazemier G, Tilanus HW, Ijzermans JNM. Value of laparoscopy and laparoscopic ultrasonography in determining resectability of colorectal hepatic metastases. HPB. 2003;5(2):100–4.
37. Rahusen FD, Cuesta MA, Borgstein PJ, Bleichrodt RP, Barkhof F, Doesburg T, et al. Selection of patients for resection of colorectal metastases to the liver using diagnostic laparoscopy and laparoscopic ultrasonography. Ann Surg. 1999;230(1):31–7.
38. Hariharan D, Constantinides V, Kocher HM, Tekkis PP. The role of laparoscopy and laparoscopic ultrasound in the preoperative staging of patients with resectable colorectal liver metastases: a meta-analysis. Am J Surg. 2012;204(1):84–92.
39. Shah AJ, Phull J, Finch-Jones MD. Clinical risk score can be used to select patients for staging laparoscopy and laparoscopic ultrasound for colorectal liver metastases. World J Surg. 2010;34(9):2141–5.
40. Venook AP, Papandreou C, Furuse J, de Guevara LL. The incidence and epidemiology of hepatocellular carcinoma: a global and regional perspective. Oncologist. 2010;15(Supplement 4):5–13.
41. Lai ECH, Tang CN, Ha JPY, Tsui DKK, Li MKW. The evolving influence of laparoscopy and laparoscopic ultrasonography on patients with hepatocellular carcinoma. Am J Surg. 2008;196(5):736–40.
42. Mazzaferro V, Regalia E, Doci R, Andreola S, Pulvirenti A, Bozzetti F, et al. Liver transplantation for the treatment of small hepatocellular carcinomas in patients with cirrhosis. N Engl J Med. 1996;334(11):693–9.
43. Bartolozzi C, Battaglia V, Bozzi E. HCC diagnosis with liver-specific MRI–close to histopathology. Dig Dis. 2009;27(2):125–30.
44. Herbold T, Wahba R, Bangard C, Demir M, Drebber U, Stippel DL. The laparoscopic approach for radiofrequency ablation of hepatocellular carcinoma–indication, technique and results. Langenbecks Arch Surg. 2013;398(1):47–53.
45. Jarnagin WR, Fong Y, DeMatteo RP, Gonen M, Burke EC, Bodniewicz J, et al. Staging, resectability, and outcome in 225 patients with hilar cholangiocarcinoma. Ann Surg. 2001;234(4):507–19.
46. Weber SM, DeMatteo RP, Fong Y, Blumgart LH, Jarnagin WR. Staging laparoscopy in patients with extrahepatic biliary carcinoma: analysis of 100 patients. Ann Surg. 2002;235(3):392.
47. Connor S, Barron E, Wigmore SJ, Madhavan KK, Parks RW, Garden OJ. The utility of laparoscopic assessment in the preoperative staging of suspected hilar cholangiocarcinoma. J Gastrointest Surg. 2005;9(4):476–80.
48. Hariharan D, Constantinides VA, Froeling FEM, Tekkis PP, Kocher HM. The role of laparoscopy and laparoscopic ultrasound in the preoperative staging of pancreatico-biliary cancers – a meta-analysis. Eur J Surg Oncol (EJSO). 2010;36(10):941–8.
49. Goere D, Wagholikar GD, Pessaux P, Carrère N, Sibert A, Vilgrain V, et al. Utility of staging laparoscopy in subsets of biliary cancers. Surg Endosc. 2006;20(5):721–5.
50. Vollmer CM, Drebin JA, Middleton WD, Teefey SA, Linehan DC, Soper NJ, et al. Utility of staging laparoscopy in subsets of peripancreatic and biliary malignancies. Ann Surg. 2002;235(1):1–7.
51. Tilleman EHBM, de Castro SMM, Busch ORC, Bemelman WA, van Gulik TM, Obertop H, et al. Diagnostic laparoscopy and laparoscopic ultrasound for staging of patients with malignant proximal bile duct obstruction. J Gastrointest Surg. 2002;6(3):426–30; discussion 430–1.
52. Kriplani AK, Jayant S, Kapur BM. Laparoscopy in primary carcinoma of the gallbladder. Gastrointest Endosc. 1992;38(3):326–9.
53. Joseph S, Connor S, Garden OJ. Staging laparoscopy for cholangiocarcinoma. HPB. 2008;10(2):116–9.
54. Worley PJ, Roberts-Thomson IC, Dymock RB, Maddern GJ. Benign inflammatory pseudotumour of the biliary tract masquerading as a Klatskin tumour. HPB (Oxford). 2001;3(2):179–81.
55. Engelken FJF, Bettschart V, Rahman MQ, Parks RW, Garden OJ. Prognostic factors in the palliation of pancreatic cancer. Eur J Surg Oncol. 2003;29(4):368–73.
56. Murugiah M, Paterson-Brown S, Windsor JA, Miles WF, Garden OJ. Early experience of laparoscopic ultrasonography in the management of pancreatic carcinoma. Surg Endosc. 1993;7(3):177–81.
57. John TG, Wright A, Allan PL, Redhead DN, Paterson-Brown S, Carter DC, et al. Laparoscopy with laparoscopic ultrasonography in the TNM staging of pancreatic carcinoma. World J Surg. 1999;23(9):870–81.
58. Thomson BNJ, Parks RW, Redhead DN, Welsh FKS, Madhavan KK, Wigmore SJ, et al. Refining the role of laparoscopy and laparoscopic ultrasound in the staging of presumed pancreatic head and ampullary tumours. Br J Cancer. 2006;94(2):213–7.
59. White R, Winston C, Gonen M, D'Angelica M, Jarnagin W, Fong Y, et al. Current utility of staging laparoscopy for pancreatic and peripancreatic neoplasms. J Am Coll Surg. 2008;206(3):445–50.
60. Enestvedt CK, Mayo SC, Diggs BS, Mori M, Austin DA, Shipley DK, et al. Diagnostic laparoscopy for patients with potentially resectable pancreatic adenocarcinoma: is it cost-effective in the current era? J Gastrointest Surg. 2008;12(7):1177–84.
61. Doucas H, Sutton CD, Zimmerman A, Dennison AR, Berry DP. Assessment of pancreatic malignancy with laparoscopy and intraoperative ultrasound. Surg Endosc. 2007;21(7):1147–52.
62. Ahmed SI, Bochkarev V, Oleynikov D, Sasson AR. Patients with pancreatic adenocarcinoma benefit from staging laparoscopy. J Laparoendosc Adv Surg Tech A. 2006;16(5):458–63.
63. Karachristos A, Scarmeas N, Hoffman JP. CA 19–9 levels predict results of staging laparoscopy in pancreatic cancer. J Gastrointest Surg. 2005;9(9):1286–92.
64. Nieveen van Dijkum EJM, Romijn MG, Terwee CB, de Wit LT, van der Meulen JHP, Lameris HS, et al. Laparoscopic staging and subsequent palliation in patients with peripancreatic carcinoma. Ann Surg. 2003;237(1):66–73.
65. Doran HE, Bosonnet L, Connor S, Jones L, Garvey C, Hughes M, et al. Laparoscopy and laparoscopic ultrasound in the evaluation of pancreatic and periampullary tumours. Dig Surg. 2004;21(4):305–13.
66. Zhao Z-W, He J-Y, Tan G, Wang H-J, Li K-J. Laparoscopy and laparoscopic ultrasonography in judging the resectability of pancreatic head cancer. Hepatobiliary Pancreat Dis Int. 2003;2(4):609–11.
67. Kwon AH, Inui H, Kamiyama Y. Preoperative laparoscopic examination using surgical manipulation and ultrasonography for pancreatic lesions. Endoscopy. 2002;34(6):464–8.
68. Taylor AM, Roberts SA, Manson JM. Experience with laparoscopic ultrasonography for defining tumour resectability in carcinoma of the pancreatic head and periampullary region. Br J Surg. 2001;88(8):1077–83.
69. Menack M, Spitz J, Arregui M. Staging of pancreatic and ampullary cancers for resectability using laparoscopy with laparoscopic ultrasound. Surg Endosc. 2001;15(10):1129–34.

70. Schachter PP, Avni Y. The impact of laparoscopy and laparoscopic ultrasonography on the management of pancreatic cancer. Arch Surg. 2000;135(11):1303–7.
71. Jimenez RE, Warshaw AL. Impact of laparoscopic staging in the treatment of pancreatic cancer. Arch Surg. 2000;135(4):409–15.
72. Pietrabissa A, Caramella D, Candio GD, Carobbi A, Boggi U, Rossi G, et al. Laparoscopy and laparoscopic ultrasonography for staging pancreatic cancer: critical appraisal. World J Surg. 1999;23(10):998–1003.
73. Durup Scheel-Hincke J, Mortensen MB, Qvist N, Hovendal CP. TNM staging and assessment of resectability of pancreatic cancer by laparoscopic ultrasonography. Surg Endosc. 1999;13(10):967–71.
74. Reddy KR, Levi J, Livingstone A, Jeffers L, Molina E, Kligerman S, et al. Experience with staging laparoscopy in pancreatic malignancy. Gastrointest Endosc. 1999;49(4 Pt 1):498–503.
75. Andrén-Sandberg A, Lindberg CG, Lundstedt C, Ihse I. Computed tomography and laparoscopy in the assessment of the patient with pancreatic cancer. J Am Coll Surg. 1998;186(1):35–40.
76. Conlon KC, Dougherty E, Klimstra DS, Coit DG, Turnbull AD, Brennan MF. The value of minimal access surgery in the staging of patients with potentially resectable peripancreatic malignancy. Ann Surg. 1996;223(2):134–40.
77. Bemelman WA, de Wit LT, van Delden OM, Smits NJ, Obertop H, Rauws EJ, et al. Diagnostic laparoscopy combined with laparoscopic ultrasonography in staging of cancer of the pancreatic head region. Br J Surg. 1995;82(6):820–4.
78. John TG, Greig JD, Carter DC, Garden OJ. Carcinoma of the pancreatic head and periampullary region. Tumor staging with laparoscopy and laparoscopic ultrasonography. Ann Surg. 1995;221(2):156.
79. McMahon PM, Halpern EF, Fernandez-del Castillo C, Clark JW, Gazelle GS. Pancreatic cancer: cost-effectiveness of imaging technologies for assessing resectability. Radiology. 2001;221(1):93–106.
80. Khashab MA, Kim K, Lennon AM, Shin EJ, Tignor AS, Amateau SK, et al. Should we do EUS/FNA on patients with pancreatic cysts? The incremental diagnostic yield of EUS over CT/MRI for prediction of cystic neoplasms. Pancreas. 2013;42(4):717–21.
81. Tierney WM, Francis IR, Eckhauser F, Elta G, Nostrant TT, Scheiman JM. The accuracy of EUS and helical CT in the assessment of vascular invasion by peripapillary malignancy. Gastrointest Endosc. 2001;53(2):182–8.
82. Ahmad NA, Kochman ML, Lewis JD, Kadish S, Morris JB, Rosato EF, et al. Endosonography is superior to angiography in the preoperative assessment of vascular involvement among patients with pancreatic carcinoma. J Clin Gastroenterol. 2001;32(1):54–8.
83. Shrikhande SV, Barreto SG, Goel M, Arya S. Multimodality imaging of pancreatic ductal adenocarcinoma: a review of the literature. HPB. 2012;14(10):658–68.
84. DeWitt J, Devereaux B, Chriswell M, McGreevy K, Howard T, Imperiale TF, et al. Comparison of endoscopic ultrasonography and multidetector computed tomography for detecting and staging pancreatic cancer. Ann Intern Med. 2004;141(10):753–63.
85. Lo CY, Lo CM, Fan ST. Role of laparoscopic ultrasonography in intraoperative localization of pancreatic insulinoma. Surg Endosc. 2000;14(12):1131–5.
86. Huai JC, Zhang W, Niu HO, Su ZX, McNamara JJ, Machi J. Localization and surgical treatment of pancreatic insulinomas guided by intraoperative ultrasound. Am J Surg. 1998;175(1):18–21.
87. Hiramoto JS, Feldstein VA, LaBerge JM, Norton JA. Intraoperative ultrasound and preoperative localization detects all occult insulinomas. Arch Surg. 2001;136(9):1020–5; discussion 1025–6.
88. Brown CK, Bartlett DL, Doppman JL, Gorden P, Libutti SK, Fraker DL, et al. Intraarterial calcium stimulation and intraoperative ultrasonography in the localization and resection of insulinomas. Surgery. 1997;122(6):1189–93; discussion 1193–4.
89. Jarnagin WR, Bodniewicz J, Dougherty E, Conlon K, Blumgart LH, Fong Y. A prospective analysis of staging laparoscopy in patients with primary and secondary hepatobiliary malignancies. J Gastrointest Surg. 2000;4(1):34–43.
90. Corvera CU, Weber SM, Jarnagin WR. Role of laparoscopy in the evaluation of biliary tract cancer. Surg Oncol Clin N Am. 2002;11(4):877–91.
91. Agrawal S, Sonawane RN, Behari A, Kumar A, Sikora SS, Saxena R, et al. Laparoscopic staging in gallbladder cancer. Dig Surg. 2005;22(6):440–5.
92. D'Angelica M, Fong Y, Weber S, Gonen M, DeMatteo RP, Conlon K, et al. The role of staging laparoscopy in hepatobiliary malignancy: prospective analysis of 401 cases. Ann Surg Oncol. 2003;10(2):183–9.
93. Agarwal AK, Kalayarasan R, Javed A, Gupta N, Nag HH. Role of staging laparoscopy in primary gall bladder cancer-an analysis of 409 patients: a prospective study to evaluate the role of staging laparoscopy in the management of gallbladder cancer. Ann Surg. 2013;258:318–23.
94. Fong Y, Jarnagin W, Blumgart LH. Gallbladder cancer: comparison of patients presenting initially for definitive operation with those presenting after prior noncurative intervention. Ann Surg. 2000;232(4):557.

Endoscopic Ultrasound in the Upper Gastrointestinal Tract

11

Dominique Dempah, Moaz Abulfaraj,
and Maurice E. Arregui

Outline

Introduction to EUS
Development of EUS
EUS equipment
  Scopes
    Linear
    Radial
    Forward viewing minicatheter
    Intraductal ultrasound
  Ultrasound console
General technique of use
Clinical uses of EUS in the foregut
    EUS in esophageal diseases
    EUS in gastric diseases
    EUS in biliary diseases
    EUS in pancreatic diseases
    EUS in diagnosis of upper abdominal masses
The future of EUS in the upper abdomen

Development of EUS

Endoscopic ultrasound was developed in the early 1980s and introduced into practice in the late 1980s. It was used to remedy the radiologic shortcomings in visualizing the pancreas, which is located deep in the abdomen and obscured by air in the bowel lumen. It shortly became apparent that EUS would also provide outstanding imaging of the different layers of the esophageal, gastric, and intestinal wall as well as visualization of the lymph nodes close to the digestive tract. These findings led to the prominent role of EUS on the preoperative staging of gastrointestinal tumors. The development of linear probes in the early 1990s ushered the era of interventional EUS while greater miniaturization led to the development of intraductal ultrasound for direct access into the bile ducts and the pancreatic duct [1, 2].

D. Dempah, MD
Department of Surgery, St. Vincent's Hospital,
8235 Spyglass Dr. Apt 2A, Indianapolis, IN 46260, USA
e-mail: ddempah@gmail.com

M. Abulfaraj, MD, FRCSC
Department of General Surgery, St. Vincent Hospital Indianapolis,
635 Danforth St., Carmel, IN 46032, USA
e-mail: dr_moaz82@yahoo.com

M.E. Arregui, MD, FACS (✉)
Department of General Surgery, St. Vincent's Hospital,
8402 Harcourt Rd. Suite 815, Indianapolis, IN 46260, USA
e-mail: arregui@ameritech.net

Equipment

Echoendoscopes

The technique of EUS combines endoscopy which enables direct visualization of the mucosal surface of any enteric surface that can be reached by an endoscopic instrument and echography through a small ultrasound transducer fitted on the tip of an endoscope (echoendoscope) and thus brought into the close vicinity of the area or the organ to be studied. The close proximity of the ultrasound probe allows use of high ultrasonic frequencies (generally 5–20 MHz but can be as high as 30 MHz). As a result, excellent definition in the order 1/10 of 1 mm can be achieved, and lesions as small as 1–2 mm can be visualized in the GI wall, pancreas, bile ducts, etc. [1].

Currently, there are two distinct types of echoendoscopes used for clinical practice: radial and linear (Figs. 11.1 and 11.2). Both of these have a 4-cm distal rigid tip that houses the optics, ultrasound transducer, and electronic components. This is an important feature to note as it can make intubation of the esophagus and duodenum technically challenging. Care must be taken to avoid bowel perforation when negotiating these scopes into the duodenum as the distal segment of the echoendoscope is inflexible [2]. The radial and linear echoendoscopes provide both video endoscopy and sonographic imaging. The radial echoendoscope creates a sonographic image that is 360° and is perpendicular to the shaft

E.J. Hagopian, J. Machi (eds.), *Abdominal Ultrasound for Surgeons*,
DOI 10.1007/978-1-4614-9599-4_11, © Springer Science+Business Media New York 2014

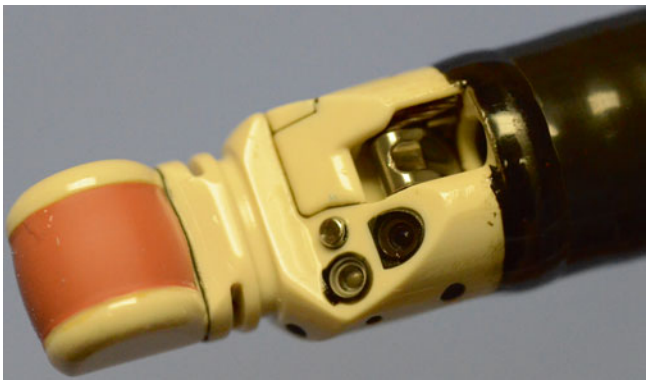

Fig. 11.1 Shown here is a linear tip echoendoscope. This type of tip creates a sagittal view

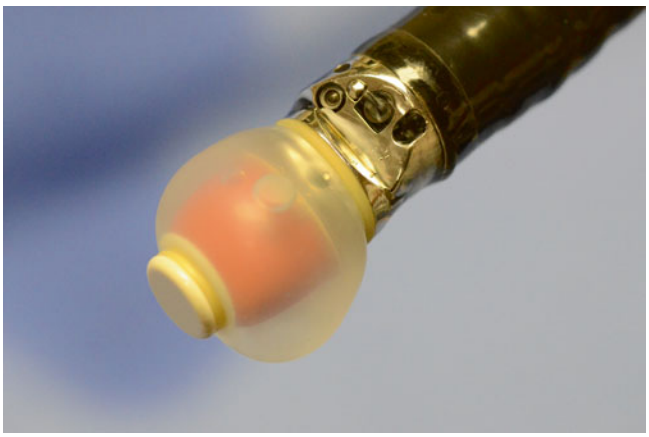

Fig. 11.2 Shown here is a radial tip echoendoscope with the balloon inflated. This type of tip creates axial views

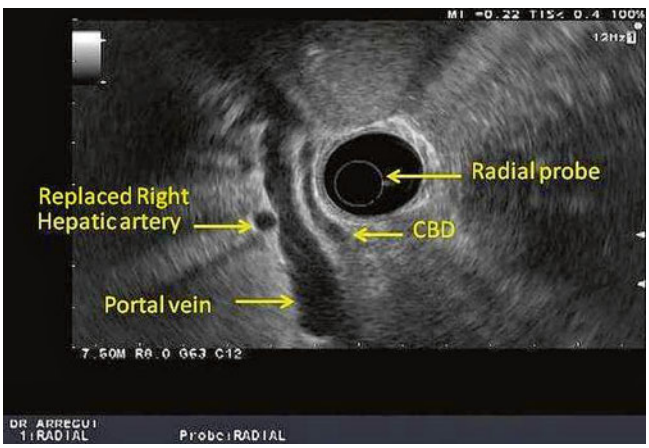

Fig. 11.3 This is a radial view of the porta hepatis obtained with a radial echoendoscope. *CBD* common bile duct

of the scope resulting in a cross-sectional image (Fig. 11.3). There are two types of radial echoendoscopes that are commercially available, mechanical and electronic. They differ in the way the sonographic image is produced. The mechanical radial scope creates an ultrasound image with rotating piezoelectric crystals in the transducer that detect a sound wave and convert it to an electronic signal. The electronic radial scope has improved spatial and contrast resolution as its transducer consists of multiple fixed nonrotating elements, where each transmits and receives ultrasound waves that are converted to an image by an electrical signal. Furthermore, the electronic radial array echoendoscope has the added features of pulse wave and color Doppler to identify vascular and ductal structures [2]. Overall, the image quality is better with the electronic echoendoscope, but the mechanical echoendoscope is cheaper and can image with higher frequencies. The radial echoendoscopes are only used for diagnostic purposes as the images are more easily interpreted due to the 360° feature.

The linear echoendoscope creates a sonographic image that is parallel to the shaft of the scope resulting in a sagittal sector image as opposed to the circumferential cross-sectional image of the radial echoendoscope [3]. This allows the operator to trace the path of a needle as it is inserted out of the operating channel in real time and thus enables therapeutic capabilities and interventions such as EUS-guided FNA (fine needle aspiration biopsy), EUS-guided injection therapies, and EUS-guided drainage procedures [2]. The standard linear echoendoscope is actually curvilinear and oblique viewing, similar to the side-viewing duodenoscope used for ERCP. It also has a lever on the handle called the elevator that raises the instruments passed through the accessory channel and thus allows fine movements. This configuration carries some inherent drawbacks. First, linear and radial echoendoscopes only allow side-viewing endoscopy as opposed to the more intuitive forward viewing of a gastroscope, for example. There is also a "push back phenomenon," where the force of the needle advancement might cause the scope to push back. Finally, the size of the accessory device is limited by the angulation of the accessory channel at the endoscope tip and the elevator [4]. Forward-viewing curvilinear echoendoscopes have been recently developed to overcome these challenges with the theoretical advantages of superior endoscopic visualization, easier deployment and manipulation of devices and needles, as well as better transmission of force to the needle. These forward-viewing scopes also have an increased tip deflection, but they also have a narrower ultrasound scanning range and lack an elevator. Early data on forward-viewing echoendoscopes suggest EUS visualization is comparable to the oblique-viewing linear echoendoscope in the upper gastrointestinal tract. Furthermore, endoscopists have reported increased ease of device deployment and better force transmission [4]. Currently, these forward-viewing echoendoscopes are mainly used for research purposes.

In addition to the conventional linear and radial echoendoscopes, catheter mini-ultrasound probes and intraductal

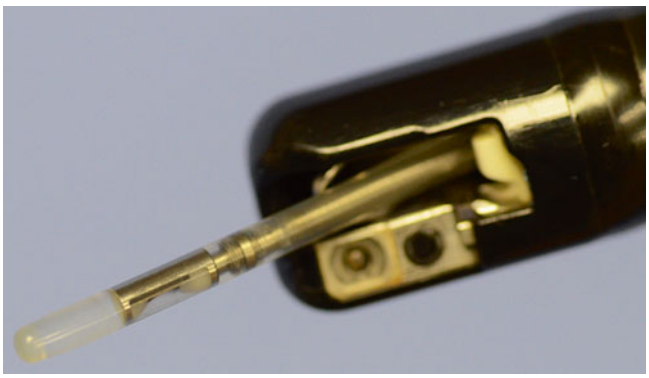

Fig. 11.4 A minicatheter can be seen through the working port of a duodenoscope

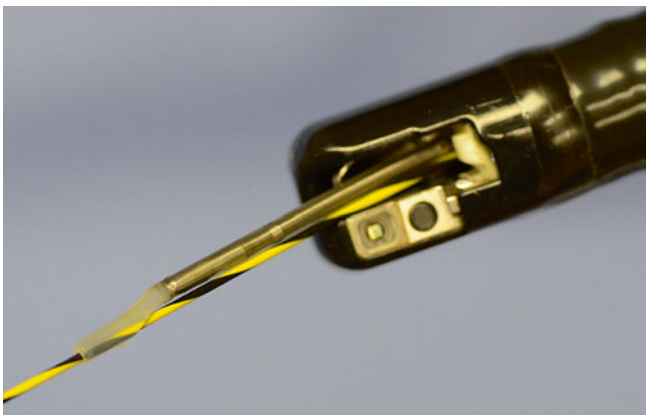

Fig. 11.5 An intraductal ultrasound is passed on a guidewire catheter through the working port of a duodenoscope

ultrasound (IDUS) probes have been developed. The catheter miniprobes can be used for lesions in or near the gastrointestinal mucosa or when an obstruction precludes the safe use of an echoendoscope. Their outer diameter ranges from 1.7 to 3.1 mm, which allows their passage through the working channel of an upper endoscope or duodenoscope (Fig. 11.4). These probes have a limited life span due to breakdown of the driveshaft that spins the ultrasound transducer tip, especially when used through a duodenoscope because the elevator causes repeated trauma to the probe.

Transpapillary IDUS catheters (Fig. 11.5) are high-frequency wire-guided catheters that are typically used during endoscopic retrograde cholangiopancreatography (ERCP). These probes produce high-quality cross-sectional images of the pancreatic and biliary ducts with resolution ranging from 0.07 to 0.18 mm. Not only are these probes high frequency, but the fluid in the ducts where they are inserted serves as an excellent acoustic window which improves resolution [2]. The use of IDUS to evaluate the biliary tree was first published in 1992, but despite reports indicating its value in decreasing the rate of recurrent biliary stones after endoscopic sphincterotomy, its utilization in clinical practice remains low [5]. Other indications include cholangiocarcinoma, evaluation of pancreatic cystic tumors, pancreatic islet cell tumors, and biliary and pancreatic duct strictures.

Console Function

It is essential to be familiar with the various functions of the EUS console as well as to understand when to apply the different US functions when acquiring images in order to make more accurate clinical diagnosis. We will discuss some of the important functions. The depth/range function changes the display depth of the image. It is helpful to start with the greater depth range for initial scanning and identify any gross abnormality and magnify the near-field view for more detailed study. Similarly, using the frequency function, one should start with a lower frequency to scan through a wide range of structures. Indeed lower frequency allows greater penetration but lower resolution. Once a lesion is identified, frequency can be increased to obtain a better resolution, which refers to the ability to discriminate between two points along the beam path. The focus function allows convergence of the US beam to a particular depth to achieve an image with a higher lateral resolution. The gain function adjusts the overall sensitivity of the gray-scale image. If it is turned too high, the image will be too white, and if it is turned too low, the image will be too dark. The Doppler function not only allows identification of blood flow in vessels but also provides information regarding the direction of the flow and its velocity. The power Doppler function has a higher sensitivity in detecting blood flow because background noise is reduced. However, it does not give any information on flow direction and velocity. Annotations features are also available to measure and mark any structures or lesions [6]. (Refer to section "Control panel" in Chap. 3 for more information.)

General Technique of Use

Most echoendoscopes are oblique viewing and the process of pharyngeal intubation is nearly blind similar to a duodenoscopy. The echoendoscope is inserted into the pharynx with the tip deflected downward. Once in the pharynx, the tip is gently advanced in the esophagus. Forceful intubation must be avoided to prevent perforation. In difficult cases, excluding a Zenker's diverticulum or other unusual anatomic abnormalities, a diagnostic gastroscopy may be advisable. For both radial and linear EUS, recognition of key landmarks is vital for proper orientation. Filling the GI lumen with water is helpful when the GI wall is being examined. Radial images are axial circumferential images that are more easily interpreted partly because axial imaging is more familiar to most. Linear images are sagittal sector images that are more

limited and more difficult to interpret. To facilitate performance of the exam and interpretation of the image, linear EUS requires the use of key movements, which include advancement and withdrawal, clockwise and counterclockwise torquing, and angulation. Torquing is achieved either by using the right hand to torque the shaft of the echoendoscope or by changing the direction of the handle by turning the left wrist or body. Angulation of the tip is mainly performed by using the up-down control. It is also important to ensure proper coupling by continuous suction and by keeping the tip of the echoendoscope pressed against the mucosa. For example, with a linear scope in the mediastinum, the abdominal aorta should be identified first as a large hypoechoic tubular structure with the echoendoscope shaft held at neutral position. Doppler can confirm vascularity. As the scope is advanced distally in the esophagus into the proximal stomach, the celiac artery (Fig. 11.6) and superior mesenteric artery should be seen next arising from the aorta. At the level of the celiac artery, clockwise rotation allows examination of the left adrenal gland (Fig. 11.7) superior to the kidney, while counterclockwise rotation will allow visualization of the left lobe of the liver [3].

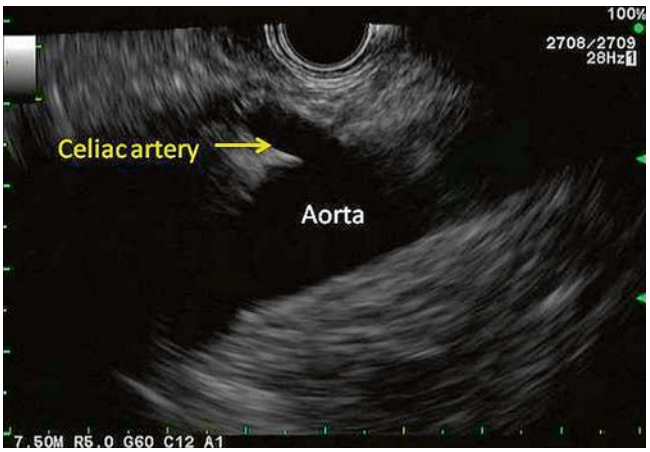

Fig. 11.6 The celiac artery can be seen coming off the aorta. This view is obtained through a linear echoendoscope

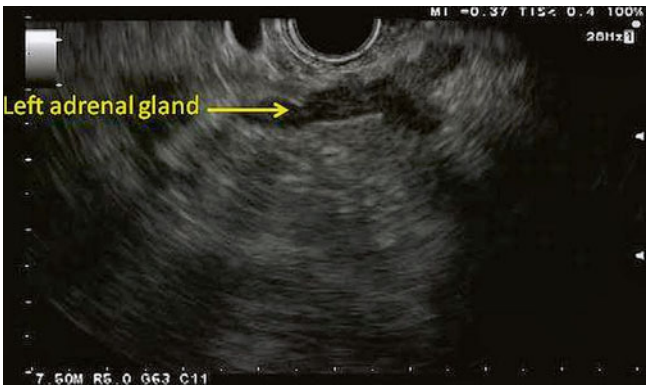

Fig. 11.7 Depicted here is the typical sonographic appearance of a left adrenal gland. It is a V- or Y-shaped organ with a hypoechoic cortex and a hyperechoic inner medulla

Clinical Uses of Endoscopic Ultrasound in the Foregut

Esophageal Disease

The esophagus is the easiest part of the gastrointestinal tract to evaluate with EUS and thus plays an important role in the staging of esophageal cancer particularly with the increasing use of neoadjuvant therapy. EUS allows accurate assessment of depth of invasion and the nodal status. However, its role in identifying metastatic disease is limited. The esophagus has five ultrasonographic layers, namely, mucosa, muscularis mucosa, submucosa, muscularis propria, and adventitia (Fig. 11.8). Puli et al. conducted a meta-analysis and reported a sensitivity of 81–90 % and specificity of 99 % for T staging. The accuracy of T staging with T4 tends to be higher in comparison to T1 [7]. In advanced tumors where the lumen is too narrow to allow examination with the echoendoscope, a mini-ultrasound probe can be used through the endoscope to assess the depth of the invasion. EUS can identify local lymph nodes including paraesophageal, paratracheal, subcarinal, and aortopulmonary groups. In addition, it allows biopsy of any suspicious nodes. EUS has a sensitivity and specificity of 84.7 and 84.6 %, respectively, which improves to 96.7 and 95.5 % with the use of FNA [7]. EUS allows visualization and biopsy of metastatic lymph node, particularly celiac adenopathy with sensitivity of 67 % and

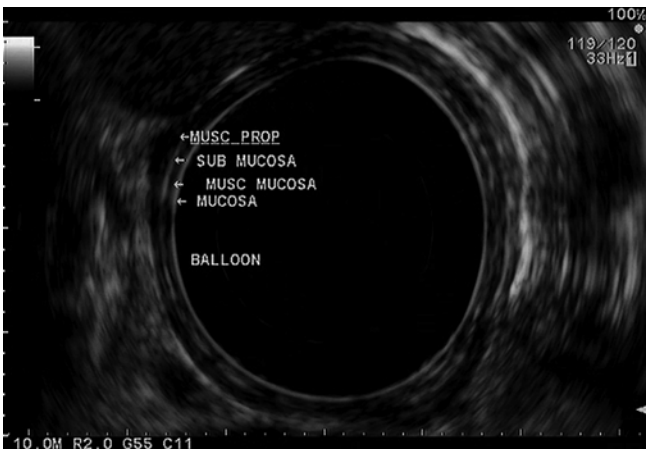

Fig. 11.8 A radial view of the esophageal layers is obtained with a radial echoendoscope. Beginning from the lumen (balloon) and extending outward, the mucosa, muscularis mucosa (musc mucosa), submucosa, and muscularis propria (musc prop) layers can be seen. The mucosal layers (mucosa and submucosa) are hyperechoic, while the muscular layers (muscularis mucosa and muscularis propria) are hypoechoic

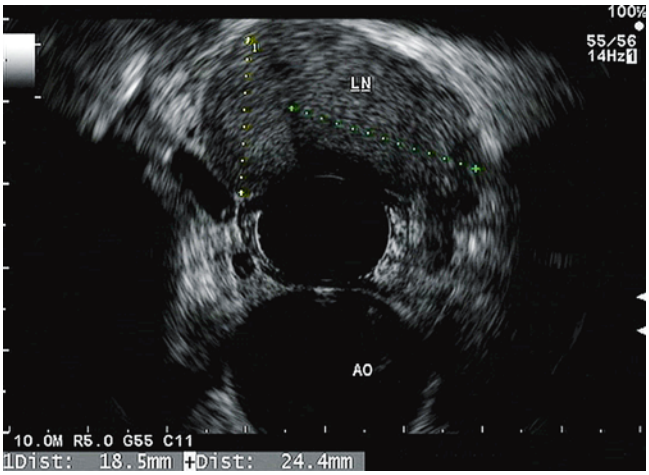

Fig. 11.9 An enlarged lymph node (*LN*) is seen in the mediastinum. The aorta (*AO*) can also be seen at 6 o'clock

specificity of 98 %. EUS can also be helpful to visualize much of the liver, with exception to the subdiaphragmatic part of the right lobe.

Gastric Disease

Similar to the esophagus, EUS plays an important role in the management of gastric cancer. It can help in determining if the patient requires neoadjuvant treatment and also if the patient is a candidate for endoscopic resection. The overall accuracy of EUS for T staging is 75 %, and the accuracy tends to be higher for more advanced disease. It has an accuracy of 77 % for T1, 65 % for T2, 85 % for T3, and 79 % for T4 [8]. However, EUS is 86 % sensitive and 91 % specific in differentiating early "T1/T2" from advanced "T3 and T4" lesions [9]. Higher-frequency (12–20 MHz) ultrasound probes have lower depth of penetration and lower accuracy to stage advanced lesions. Nevertheless, higher frequencies have a higher accuracy for differentiating smaller lesions, which can be particularly helpful for tumors that appear to be amenable for endoscopic resection. Endoscopic ultrasound has a sensitivity of 74 % and specificity of 80 % in lymph node staging and allows biopsy of any clinically suspicious lymph nodes. Suspicious lymph nodes are usually hypoechoic, round, and larger than 10 mm in size (Fig. 11.9). EUS can also identify ascites and can evaluate many parts of the liver.

Biliary Disease

Transabdominal US is the gold standard for evaluation of gallbladder stones. However, it can miss small stones. In patients with suspected gallbladder stones and a nondiagnostic transabdominal US, EUS can be used to evaluate for occult cholelithiasis given its higher-frequency resolution and its closer proximity to the biliary system as compared with transabdominal US. Similarly in patients with acute idiopathic pancreatitis, EUS can be used to rule out occult cholelithiasis or microlithiasis. EUS has also emerged as a minimally invasive procedure for the evaluation of choledocholithiasis, especially among patients with intermediate probability of common duct stones. In this setting, transabdominal US is not very sensitive, and ERCP is associated with a small but not insignificant risk of serious complications. Because of these potential complications such as pancreatitis, cholangitis, perforation, and hemorrhage, ERCP should ideally be reserved for patients with proven common bile duct stones. EUS allows detection of common bile duct stones with sensitivities similar to MRCP and even ERCP in some studies. The exam is usually started with the echoendoscope in the long position in the duodenal bulb. The scope is advanced to the superior angle of the duodenal bulb and the tip is deflected downward. The transducer is then moved slowly along the course of the gallbladder using torque and tip deflection as needed to image the body, fundus, and neck of the gallbladder. The normal gallbladder appears as a large fluid-filled (anechoic) structure with a thin-layered wall. The common bile duct, common hepatic duct, and portal vein are also seen in their long axis with the scope in this position. Doppler can be used to distinguish blood vessels such as the portal vein and gastroduodenal artery from the bile ducts. The scope can then be placed in the short position at the level of the papilla similar to the endoscope position when performing ERCP. This allows identification of the bile duct in the periampullary area. The bile duct can also be followed proximally to the gallbladder and also the level of the bifurcation [10].

EUS can also be used in the management of biliary obstruction. ERCP remains the gold standard for drainage of biliary obstruction caused by benign or malignant diseases. However, conventional ERCP may be difficult in cases of impacted stone at the ampulla, ampullary stenosis, or ampullary carcinoma. In such cases, other options, which are considered to be more invasive and morbid, would include PTC or CBDE. In addition, ERCP may be impossible in patients who have altered anatomy due to previous gastric surgery or duodenal bulb obstruction. More recently, EUS has been used to drain the biliary tree as a safe valid alternative to other options with adequate clinical and technical success. EUS-guided cholangiogram was first reported by Wiersema in 1996 [11] and EUS-guided drainage was first reported by Giovannini in 2001 [12]. A therapeutic linear echoendoscope with a large working channel is used to access and stent the biliary tree using a technique similar to EUS-guided cystgastrostomy. The CBD is visualized through the duodenal bulb or the left hepatic duct is visualized through the stomach by

ultrasound. Doppler is used to avoid puncturing a vessel. A 19-gauge needle then is used to puncture the duct and bile aspirated. Afterward, contrast is injected under fluoroscopy and a cholangiogram is performed to delineate the biliary tree and area of obstruction. This is followed by advancing a guidewire into the hepatic duct. The needle then is removed, and dilator is inserted to dilate the tract. A double-pigtail or metallic stent is inserted across the area of obstruction [13]. Early complications include bleeding, right hepatic duct obstruction, cholangitis, and pneumoperitoneum. Late complications include stent migration and cholangitis.

Pancreatic Disease

EUS plays a tremendous diagnostic and therapeutic role in the management of benign and malignant pancreatic disease. For pancreatic cancer, EUS has a high sensitivity, comparable to dual-phase CT for tumors greater than 15 mm, but it is more sensitive than CT for tumors less than 15 mm. Therefore, although a pancreas protocol CT with intravenous contrast should be the initial imaging technique for diagnosis and staging of pancreatic cancer, EUS is a valuable complementary study especially when the CT findings are equivocal. EUS-guided FNA also allows tissue diagnosis, which is sine qua non for neoadjuvant therapies. In regard to pancreatitis, multiple EUS criteria have also been established for the diagnosis of chronic pancreatitis.

Evaluation of the pancreas includes a transduodenal view and transgastric view. The transduodenal view allows visualization of the head of the pancreas. The echoendoscope is inserted in the second portion of the duodenum, which contacts the duodenal mucosa and is slowly withdrawn into the duodenal bulb with counterclockwise torque. The pancreatic head and pancreatic duct can be traced, and at the apex of the duodenal bulb, the portal vein and the common bile duct can be seen parallel to each other. The scope is then withdrawn in the stomach until the pancreas can be visualized again. At this point, counterclockwise torque and advancement of the scope allow visualization of the body and neck of the pancreas, while clockwise torque and withdrawal allow visualization of the tail of the pancreas [3]. EUS offers various therapeutic options in pancreatic disease.

A pancreatic pseudocyst is a collection of fluid around the pancreas with a wall that lacks epithelium and develops secondary to pancreatitis and pancreatic ductal disruption (Fig. 11.10). Most pseudocysts are asymptomatic and usually resolve spontaneously. Indications for intervention include biliary obstruction, gastric outlet obstruction, bleeding, infection, and increasing in size. Surgical drainage was the treatment of choice for symptomatic pancreatic pseudocyst. However, in recent years endoscopic drainage has emerged as a less invasive alternative to surgery and is gaining more acceptance as an effective approach in the therapy

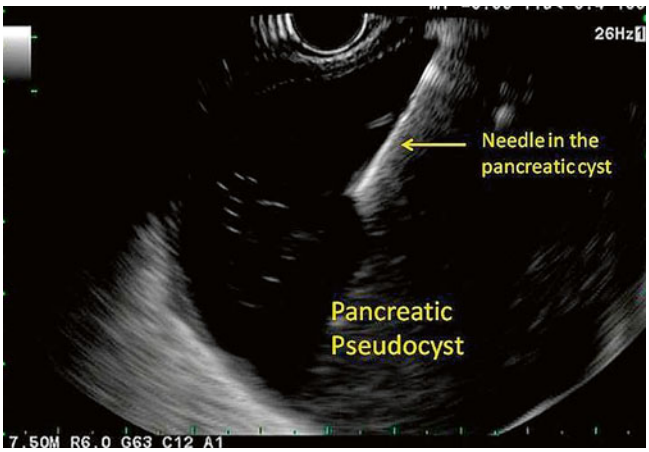

Fig. 11.10 A needle is inserted in a pancreatic pseudocyst during an endoscopic cystgastrostomy. One can clearly see the hyperechoic needle

of symptomatic pancreatic pseudocysts. More recently, EUS guidance has been advocated to increase technical success rate and to decrease the risk of bleeding and perforation, particularly in patients who fail to demonstrate bulging on endoscopy and in those with portal hypertension [14]. EUS-guided drainage might not be feasible in cases where there is an interposing vessel between the cyst and stomach or duodenal wall. Absence of direct contact between the cyst and the stomach, which usually occurs in small cysts (<6 cm), is a contraindication. Coagulopathy is a relative contraindication due to the risk of bleeding that might be difficult to control with endoscopic measures. Several studies confirm advantages of endoscopic ultrasound including a shorter hospital stay, lower total costs, and its less invasive approach. It is also a more appropriate approach for high-risk patients and in those who cannot tolerate a general anesthetic. Varadarajulu et al. compared surgical to EUS-guided cystgastrostomy and reported similar treatment success rate in both groups with a shorter hospital stay using the mean hospital stay (2.65 vs. 6.5 days, $P<0.05$) as well as a lower cost in the EUS group [15]. Several complications have been reported including bleeding, perforation, stent migration, aspiration, and infection. Infection occurs as a result of premature occlusion of the stent and contamination of the cyst. To perform an endoscopic cystgastrostomy, a therapeutic linear echoendoscope with a large working "3.8-mm" channel is used to access and stent the pseudocyst in one step. The pseudocyst is visualized through the stomach or duodenal bulb to confirm that there is no fatty tissue in between, and color Doppler is applied to avoid puncturing a vessel or pseudoaneurysm. The cystotome (a needle knife and an outer catheter with diathermic ring) is used to puncture the pseudocyst (Figs. 11.10 and 11.11a, b). Fluid can be withdrawn and sent for analysis, cytology, lipase, CEA, gram stain, and culture, when infection is suspected. Afterward, contrast is injected under fluoroscopy to delineate the boundaries of the

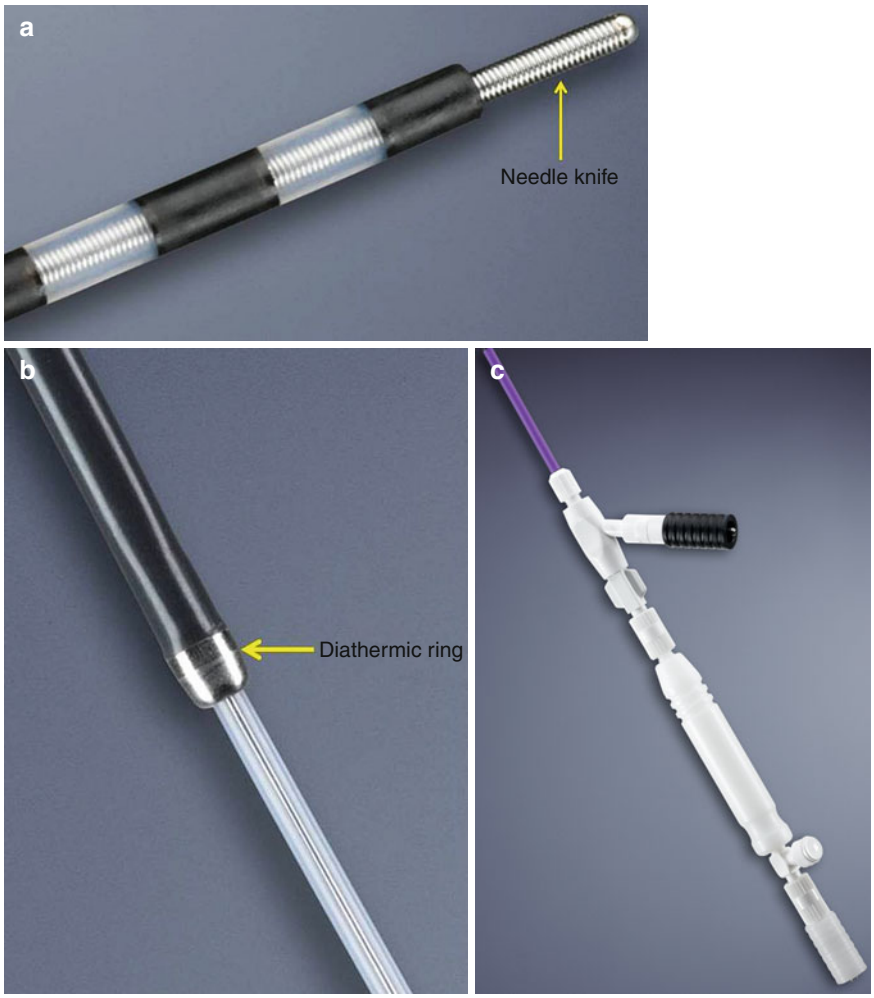

Fig. 11.11 (**a**) The cystotome: the needle knife at the tip uses electrocautery energy to puncture the wall of a pseudocyst during an endoscopic cystgastrostomy. (**b**) The cystotome: the diathermic ring allows dilation of the tract created by the needle knife by cauterizating through the pseudocyst wall during an endoscopic cystgastrostomy. (**c**) The cystotome: the handle has a black connector for energy and a distal port for contrast injection

cyst (Fig. 11.11c). The outer catheter is introduced and the diathermic ring is used to dilate the tract by applying electrocautery. A guidewire is advanced and coiled inside the pseudocyst and a double-pigtail stent is inserted unless pancreatic necrosis or if a thick fluid containing significant amount of debris is encountered. In this case, multiple larger-caliber stents are placed followed by a nasocystic catheter for continuous irrigation and lavage of the cyst. If necrosis is persistent despite irrigation, the tract can be dilated with balloon dilator to over 12 mm at a later date and a direct endoscopic necrosectomy can be performed using forceps and snare to debride the cyst cavity [16]. Some studies advocate routine nasocystic catheter for irrigation in all patients with pseudocysts regardless presence or absence of abscess or necrotic debris to increase the clinical success rate and decrease the rate of recurrence [17]. Perforation and bleeding are the two most feared complications of the EUS-guided cystgastrostomy. Perforations tend to occur more commonly with pseudocysts, which arise from the uncinate process and are drained transgastrically [18]. This usually happens after the pseudocyst is decompressed and the distance between the stomach and the pseudocyst increases which might cause dislodgment of the stent and leakage of gastric contents. Patients with such complications can be treated conservatively with gastric decompression, intravenous antibiotics, and close observation in the absence of sepsis and peritonitis. Bleeding can originate from the gastric or duodenal wall, which is usually controlled with endoscopic measures, or it can originate from a branch of the splenic artery, which requires angioembolization. Aspiration is a major complication in patients with giant pseudocyst. These patients should have the procedure done under general anesthetic with endotracheal intubation to protect the airway. Other complications include stent migration and infection.

Pain of pancreatic origin is a significant problem in patients with chronic pancreatitis and inoperable pancreatic cancer. This pain is usually difficult to control and has a major significant negative impact on patients' quality of life. These patients usually require a significant amount of analgesia including opioids, which are associated with significant side effects such as addiction, tolerance, and constipation. Non-pharmacological options include ERCP and stenting of the pancreatic duct, celiac nerve block, or neurolysis. Celiac nerve block can be done percutaneously, surgically, or more recently EUS guided. EUS celiac nerve block has been found to be more effective than a percutaneous approach [19].

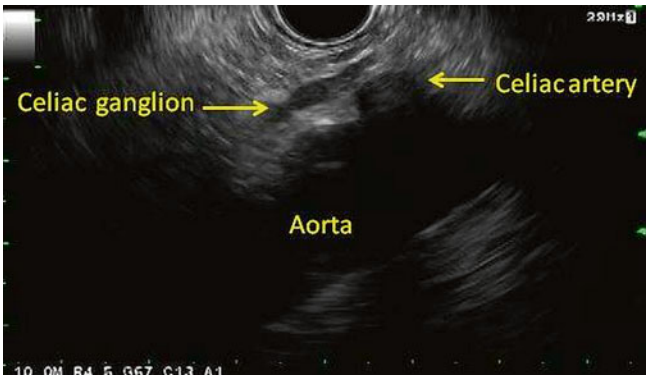

Fig. 11.12 The celiac ganglion can be seen as hypoechoic almond- or oval-shaped structure usually to the left of the celiac artery takeoff and proximal to the superior mesenteric artery

Multiple studies reported the effectiveness of EUS celiac block with a success rate up to 94 % [20]. The effectiveness increases when the ganglion is visualized and with the use of alcohol rather than steroids [20]. However, the ganglia are not visible up to 19 % of the time. In such cases, injection on both sides of the celiac trunk was found to be more effective than injecting just one side in one prospective trial [21]. Complications from the procedure are diarrhea and transient hypotension. Some patients have exacerbation of pain after the procedure, which starts in the recovery room and can last up to 2 days. Interestingly, these patients tend to have better long-term response to the treatment once the pain subsides. To perform a celiac ganglion block, a linear echoendoscope is advanced to about 40 cm, and the aorta is visualized and traced to the celiac trunk. The celiac ganglia are usually located along the celiac artery or between the celiac artery and the origin of the superior mesenteric artery. The average number of ganglia is 3 with size ranging from few millimeters to few centimeters (Fig. 11.12). A 22–25-gauge needle is inserted through the working channel and color Doppler is applied. Color Doppler is helpful to avoid puncturing a vessel and to prevent injecting bupivacaine intravascularly, which can cause a potentially lethal cardiac arrest. The toxic effects of an intravascular injection of bupivacaine can be treated by infusion of lipid emulsion [22]. The needle is applied to the center of each ganglion and injected with 10–30 ml of 50 % bupivacaine. Twenty ml of absolute alcohol in cases of pancreatic cancer or 40 mg of triamcinolone in cases of chronic pancreatitis is injected in addition to the bupivacaine. Most endoscopists avoid using alcohol in chronic pancreatitis [23] despite a higher efficacy in controlling pain because of alcohol's permanent effect, which can lead to chronic diarrhea that can be difficult to control by antidiarrheal medications. Some patients develop agitation during direct ganglia injection, which usually lasts for a few seconds. If there is no visible ganglion, then injection to the right, left, and base of the celiac trunk can be performed.

EUS in Diagnosis of Upper Abdominal Masses

Aside from FNA biopsy of pancreatic, biliary, and hepatic masses as described earlier, EUS can be used in the diagnosis of retroperitoneal masses, especially left adrenal masses that are accessible through EUS. Many studies have demonstrated the safety and utility of EUS-guided biopsy of left adrenal masses. Dewitt et al. from the Indiana University School of Medicine described their experience with EUS-guided biopsy of the left adrenal gland. They found that EUS-guided FNA of the left adrenal gland had a high sensitivity for cancer and that nondiagnostic biopsies were more common with diffusely enlarged glands compared with glands with a focal mass [24]. Bodtger et al. from the Copenhagen University Hospital showed that EUS-FNA of an enlarged left adrenal gland altered the TNM staging in 70 % and treatment in 48 % in patients with established or suspected lung cancer with adrenal metastasis [25].

The Future of EUS in the Upper Abdomen

EUS has already established itself as a powerful diagnostic and therapeutic tool in the management of diseases in the upper abdomen. Further advances in imaging such as sono-elastography, contrast enhancement, tridimensional EUS, and real-time optical diagnosis can potentially increase the diagnostic accuracy of EUS. Sono-elastography allows real-time visualization of tissue strain and hardness displayed in a transparent layout over the gray-scale images in a similar fashion to color Doppler. It can potentially help to select which lymph node to biopsy and help to differentiate between masses from chronic pancreatitis and pancreatic cancer in the setting of a nondiagnostic FNA. Microbubble contrast agents can be used as vascular signal enhancers to detect low-velocity and low-volume flow. This can also help to differentiate between focal pancreatitis and pancreatic cancer. Contrast harmonic imaging with microbubble-specific software allows visualization of vascular and parenchymal phases similar to computer tomography but with the advantage of being real time. Microbubble contrast agents can also be used to target specific endothelial cell surface receptors in vivo when coupled to monoclonal antibodies. This could lead to in vivo quantification of the targeted receptors and monitoring of treatment response. Furthermore, there is some evidence that enhanced cellular uptake of drugs and gene occurs in the presence of ultrasound, a process called sonoporation. Therefore, the combination of sonoporation and targeted contrast agents when coupled with chemotherapeutic agents could lead to targeted treatment. Tridimensional EUS can improve depiction of the spatial relationship between tumors and major surrounding vessels and thus improve staging especially in the case of pancreatic cancer where the assessment of mesenteric vessels involvement is

critical. Confocal laser endomicroscopy probes have been miniaturized to allow EUS-guided placement near the lesion of interest. Images obtained through these probes are high quality and essentially yield real-time histopathology [26].

EUS holds an important therapeutic role in the management of benign pancreaticobiliary disorders. Its role as a therapeutic vector in malignant disorders appears to be expanding and is the subject of much research. EUS-guided injection of antitumor agents in pancreatic cancer, EUS-guided brachytherapy, and EUS-guided alcohol ablation of left adrenal metastasis from small cell lung carcinoma [27] are being reported. Furthermore, the transfer of ablative technologies to the EUS field could make EUS-guided radiofrequency or microwave ablation along with EUS-guided electroporation new therapeutic options.

Conclusion

The applications of EUS have been expanding since its introduction. Standard equipment and technique have made EUS reproducible, reliable, and amenable to teaching. It is now an essential diagnostic and therapeutic tool in the management of benign and malignant upper gastrointestinal diseases. A thorough understanding of the current and future uses of EUS will enhance one's ability to properly manage diseases of the foregut.

References

1. De Angelis C, Martini M, Recipi A, et al. Instruments and accessories for diagnostic endoscopic ultrasound (radial scanning and miniprobes). Minerva Med. 2007;98:253–60.
2. Leblanc JK. An overview of endoscopic ultrasound equipment. Minerva Gastroenterol Dietol. 2008;54:177–87.
3. Seewald S, Ang TL, Soehendra N. Basic technique of handling the linear echoendoscope and how it differs from the radial echoendoscope. Gastrointest Endosc. 2009;69:S78–80.
4. Iwashita T, Nakai Y, Lee JG, et al. Newly-developed, forward-viewing echoendoscope: a comparative pilot study to the standard echoendoscope in the imaging of abdominal organs and feasibility of endoscopic ultrasound-guided interventions. J Gastroenterol Hepatol. 2012;27:362–7.
5. Ang TL, Fock KM. Intraductal ultrasound in biliary disorders. J Gastroenterol Hepatol. 2008;23:1520–7.
6. Lee YT. Basic functions of linear EUS processor and when to use them. Gastrointest Endosc. 2009;69:S64–7.
7. Puli SR, Reddy JB, Bechtold ML, Antillon D, Ibdah JA, Antillon MR. Staging accuracy of esophageal cancer by endoscopic ultrasound: a meta-analysis and systematic review. World J Gastroenterol. 2008;14:1479–90.
8. Cardoso R, Coburn N, Seevaratnam R, Sutradhar R, Lourenco LG, Mahar A, Law C, Yong E, Tinmouth J. A systematic review and meta-analysis of the utility of EUS for preoperative staging for gastric cancer. Gastric Cancer. 2012;15 Suppl 1:S19–26. Epub 2012 Jan 12.
9. Mocellin S, Marchet A, Nitti D. EUS for the staging of gastric cancer: a meta-analysis. Gastrointest Endosc. 2011;73:1122–34.
10. O'Neill DER, Saunders MD. Endoscopic ultrasonography in diseases of the gallbladder. Gastroenterol Clin North Am. 2010;39:289–305.
11. Wiersema MJ, Sandusky D, Carr R, et al. Endosonography-guided cholangiopancreatography. Gastrointest Endosc. 1996;43:102–6.
12. Giovannini M, Moutardier V, Pesenti C, Bories E, Lelong B, Delpero JR. Endoscopic ultrasound-guided bilioduodenal anastomosis: a new technique for biliary drainage. Endoscopy. 2001;33(10):898–900.
13. Siddiqui AA, Sreenarasimhaih J, Lara LF, et al. Endoscopic ultrasound-guided transduodenal placement of a fully covered metal stent for palliative biliary drainage in patients with malignant biliary obstruction. Surg Endosc. 2011;25:549–55.
14. Park DH, Lee SS, Moon SH, Choi SY. Prospective randomized trial. Endoscopic ultrasound-guided versus conventional transmural drainage for pancreatic pseudocysts. Endoscopy. 2009;41(10):842–8. Epub 2009 Oct 1.
15. Varadarajulu S, Lopes TL, Wilcox CM, et al. EUS versus surgical cyst-gastrostomy for management of pancreatic pseudocysts. Gastrointest Endosc. 2008;68:649–55.
16. Gardner TB, Coelho-Prabhun N, Gordon SR, et al. Direct endoscopic necrosectomy for the treatment of walled-off pancreatic necrosis: results from a multicenter U.S. series. Gastrointest Endosc. 2011;73:718–26.
17. Puri R, Mishra SR, Thandassery RB, Sud R, Eloubeidi MA. Outcome and complications of endoscopic ultrasound guided pancreatic pseudocyst drainage using combined endoprosthesis and naso-cystic drain. J Gastroenterol Hepatol. 2012;27(4):722–7. doi:10.1111/j.1440-1746.2012.07089.x.
18. Varadarajulu S, Christein JD, Wilcox CM. Frequency of complications during EUS-guided drainage of pancreatic fluid collections in 148 consecutive patients. J Gastroenterol Hepatol. 2011;26(10):1504–8. doi:10.1111/j.1440-1746.2011.06771.x.
19. Santosh D, Lakhtakia S, Gupta R, et al. Clinical trial: a randomized trial comparing fluoroscopy guided percutaneous technique vs endoscopic ultrasound guided technique of coeliac plexus block for treatment of pain in chronic pancreatitis. Aliment Pharmacol Ther. 2009;29:979–84. This is a well-designed randomized trial evaluating the efficacy of EUS-directed versus percutaneous celiac plexus block. This paper is a good example of the type of prospective research that is needed to evaluate EUS-directed therapies.
20. Levy MJ, Topazian MD, Wiersema MJ, et al. Initial evaluation of the efficacy and safety of endoscopic ultrasound-guided direct ganglia neurolysis and block. Am J Gastroenterol. 2008;103:98–103.
21. Lemelin V, Lam E, Sahai A. A prospective trial of central versus bilateral celiac plexus bloc/neurolysis in 160 patients: bilateral injection is safe and is more effective. Gastrointest Endosc. 2005;61(5):AB77.
22. Foxall G, McCahon R, Lamb J, et al. Levobupivacaine-induced seizures and cardiovascular collapse treated with intralipid. Anaesthesia. 2007;62(5):516–8.
23. Puli SR, Reddy JB, Bechtold ML, Antillon MR, Brugge WR. EUS-guided celiac plexus neurolysis for pain due to chronic pancreatitis or pancreatic cancer pain: a meta-analysis and systematic review. Dig Dis Sci. 2009;54(11):2330–7. Epub 2009 Jan 10.
24. Dewitt J, Alsatie M, Leblanc J, et al. Endoscopic ultrasound-guided fine needle aspiration of left adrenal gland masses. Endoscopy. 2007;39:65–71.
25. Bodtger U, Vilman P, Clementsen P, et al. Clinical impact of endoscopic ultrasound-fine needle aspiration of left adrenal masses in established or suspected lung cancer. J Thorac Oncol. 2009;4(12):1485–9.
26. Saftoiu A. State-of-the-art imaging techniques in endoscopic ultrasound. World J Gastroenterol. 2011;17(6):691–6.
27. Artifon ELA, Lucon A, Sakai P, et al. EUS-guided alcohol ablation of left adrenal metastasis from non-small-cell lung carcinoma. Gastrointest Endosc. 2007;66(6):1201–5.

Intraoperative and Laparoscopic Ultrasound During Pancreatic Surgery

12

W. Scott Helton and J. Bart Rose

Abbreviations

Ao	Aorta
CBD	Common bile duct
Co	Colon
Du	Duodenum
GDA	Gastroduodenal artery
HIFU	High-intensity focused ultrasound
IOUS	Intraoperative ultrasound
IVC	Inferior vena cava
L	Liver
L/RA	L/R renal artery
LUS	Laparoscopic ultrasound
M	Mass
MEN1	Multiple endocrine neoplasia type 1
NET	Neuroendocrine tumor
P	Pancreas
PD	Pancreatic duct
PV	Portal vein
S	Stomach
SA	Splenic artery
SMA	Superior mesenteric artery
SMV	Superior mesenteric vein
SV	Splenic vein

The utility of laparoscopic or handheld intraoperative ultrasound in pancreatic surgery is well established, having been in use for over three decades [1–4]. Glazer and Lane first utilized real-time B-mode ultrasound in 1980 to help identify biliary calculi [5]. This work was quickly expanded upon by Sigel et al. to the investigation of pancreatic adenocarcinomas. should be plural [6]. Advances in technology over the last 30 years have seen the application of intraoperative ultrasound expand beyond its initial limited diagnostic role to assisting in: tumor staging, guiding intervention, assessing anatomic relationships, and directed therapy [7]. Laparoscopic ultrasound (LUS) has developed as a subset of intraoperative ultrasound (IOUS) and allows surgeons to obtain comparable imaging without the need for laparotomy.

Within this chapter we will explore the current use of ultrasound in pancreatic surgery. The first section is dedicated to the discussion of proper preoperative patient setup, IOUS technology, normal anatomic findings, and general indications for use. The second portion of the chapter will focus on disease-specific indications and the ultrasonographic findings associated with these conditions. We will conclude by briefly touching on emerging uses of IOUS in pancreatic surgery.

Instrumentation and Technique

Instrumentation

Ultrasonographic imaging of the pancreas is obtained with both laparoscopic and handheld transducers utilizing real-time B-mode transduction, often complimented by color Doppler imaging systems. An in-depth review of this equipment can be found in Chaps. 2 and 3.

The two most common handheld transducers utilized in pancreatic ultrasound assessment are end-fire linear-array or side-fire curvilinear-array models operating at a frequency range of 7.5–15 MHz. The pencil-like end-fire transducer often provides the best imaging but is limited by the need for direct exposure. The side-fire transducer was originally

W.S. Helton, MD, FACS (✉) • J.B. Rose, MD, MAS
Section of Hepatobiliary Surgery, Virginia Mason Medical Center, 1100 9th Ave C6-GTS, Seattle, WA 98101, USA
e-mail: scott.helton@vmmc.org; bart.rose@vmmc.org

Electronic supplementary material The online version of this chapter (doi:10.1007/978-1-4614-9599-4_12) contains supplementary material, which is available to authorized users. Videos can also be accessed at http://www.springerimages.com/videos/978-1-4614-9598-7

E.J. Hagopian, J. Machi (eds.), *Abdominal Ultrasound for Surgeons*,
DOI 10.1007/978-1-4614-9599-4_12, © Springer Science+Business Media New York 2014

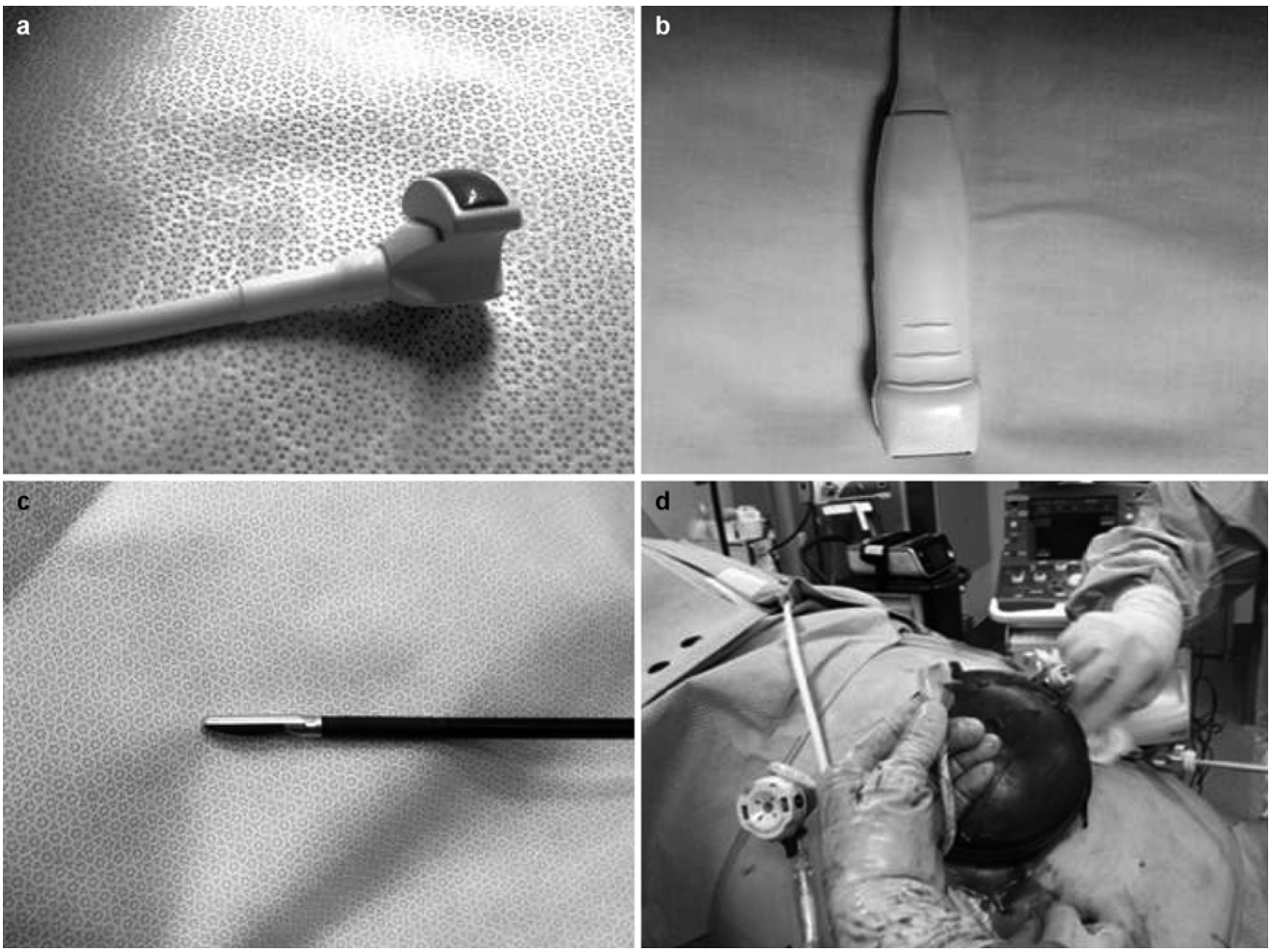

Fig. 12.1 *Transducer probes* – (**a**) Handheld side-fire curvilinear-array transducer. (**b**) Handheld end-fire linear-array transducer. (**c**) Laparoscopic side-fire linear-array transducer. (**d**) Hand-assisted laparoscopic approach

developed for imaging the liver within tight anatomic confines and provides an alternative when direct exposure is not possible (Fig. 12.1a, b).

Laparoscopic transducers are either fixed or articulating (generally with 6° of freedom) side-fire linear or curvilinear arrays operating at a slightly lower frequency range of 5–10 MHz. The use of a laparoscopic transducer with an articulating head increases the ability of the operator to view different anatomic regions of the pancreas through the same port (Fig. 12.1c).

A hand-assisted laparoscopic approach should be considered if accurate laparoscopic imaging is difficult to obtain. This hybrid technique allows the use of handheld side-fire transducers to view anatomy often impossible to view with traditional laparoscopic access while still maintaining many of the benefits of laparoscopic resection. However, this added variability should not preclude well-thought-out preoperative patient, equipment, and port placement (Fig. 12.1d).

Preoperative Setup

Proper setup can significantly reduce case length and operator stress and improve patient outcomes. The patient should be supine on an operating table in a neutral position. The ultrasound monitor should be placed in a direct line-of-sight across from the operator (Fig. 12.2). If laparoscopic instruments are to be utilized, their monitors should be placed directly next to or above the ultrasound monitor. Modern laparoscopic and ultrasound equipment provide a "picture-in-picture" feature that allows viewing of ultrasonic images within a dedicated space on the laparoscopic monitor (see Fig. 12.3). The monitor should be at eye level and in the line-of-sight to reduce operator neck and/or eyestrain. When using a fixed laparoscopic probe, port placement should be well planned before the patient is prepped. Table 12.1 lists the common port placement locations and the associated anatomic region best visualized in this location when a fixed probe is utilized. The use of a laparoscopic probe with an

Fig. 12.2 *Line-of-sight viewing* – Aligning laparoscopic and ultrasound monitors in an ergonomically advantageous position will reduce operator stress

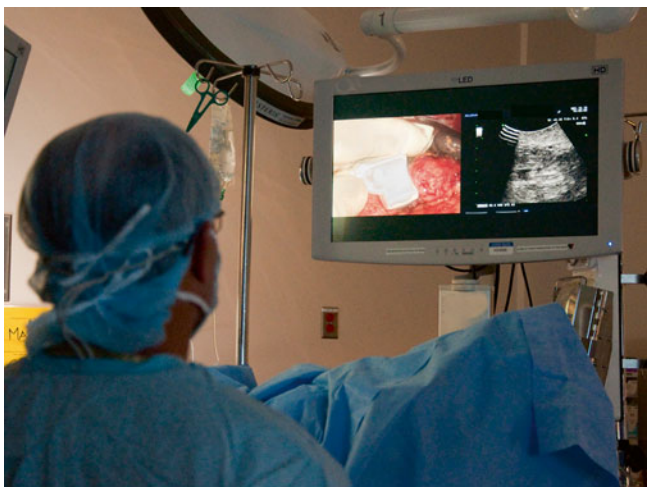

Fig. 12.3 *Picture-in-picture* – Modern laparoscopic equipment may have picture-in-picture capabilities, allowing for line-of-sight viewing without an additional monitor

articulating head can usually scan the pancreas in two planes when placed anywhere in the abdomen.

Scanning Techniques

The timing and method of pancreatic intraoperative ultrasonographic evaluation should be carefully planned. If the operative goal is disease staging, then IOUS should be performed immediately after entering the abdomen to assess for metastasis and local invasion that would prohibit resection. In patients with limited intra-abdominal fat, ultrasonographic views of the pancreas may be obtained via indirect acoustic coupling through the stomach, duodenum, mesocolon, or liver by utilizing low frequency and steady compression of overlying structures (Fig. 12.4). The use of acoustic coupling allows imaging of pertinent structures without disrupting anatomic planes. For cases in which patient anatomy precludes indirect viewing or violation of anatomic spaces is not a concern, direct imaging of the exposed pancreas is preferred for superior resolution (Fig. 12.5). Since a direct scan does not need to penetrate through overlying structures, a higher frequency may be utilized. It is important that minimal compression of the pancreas be performed with all scanning techniques, as even light compression can limit the ability to accurately view surface lesions and pancreatic

Table 12.1 Ports placed in the locations listed below provide optimal viewing of the corresponding anatomic regions of the pancreas when using a fixed laparoscopic transducer

Port location	View of the pancreas best provided
Umbilicus	Longitudinal images of the portal vein and common bile duct
	Transverse images of the pancreas neck, body
Right upper quadrant	Transverse images of the pancreatic tail
	Longitudinal, axial images of the pancreatic head, neck, tail
Left upper quadrant	Oblique images of the pancreatic head

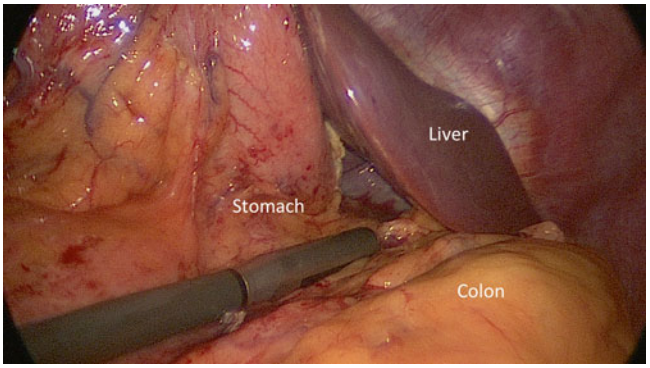

Fig. 12.4 *Indirect scanning* – The pancreas may be viewed through surrounding structures via acoustic coupling. This allows for initial evaluation of pathology with minimal disruption of anatomic planes

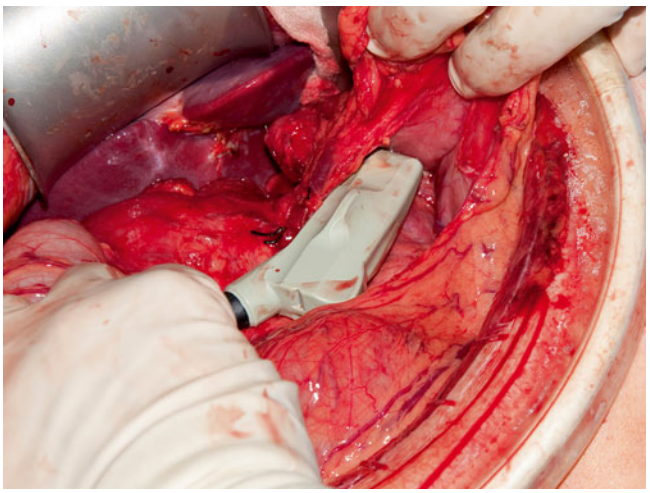

Fig. 12.5 *Direct scanning* – Superior imaging of the pancreas and surrounding structures is obtained via placement of the probe directly on the organ's surface

ductal anatomy in a soft gland. Imaging of surface lesions may be improved by utilizing a "probe-standoff" technique, in which the field to be viewed is flooded with sterile saline and the transducer is immersed within this conductive medium and held just off the area of interest. Alternatively, a fluid-filled glove can be placed between the transducer and the gland to provide the conduction medium. Both techniques facilitate excellent acoustic coupling without the need to compress the gland (Fig. 12.6).

Once the choice between indirect and direct visualization has been made, the next focus of examination should be complete assessment of anatomic structures. This is best achieved via systematic scanning of the organ in both and transverse planes. The longitudinal plane is also referred to as "sagittal" and is obtained with the probe oriented along the long axis of the pancreas. Similarly, the transverse plane is also known as "axial" and is obtained with the probe oriented along the short axis (Fig. 12.7). Overlapping sweeps of the gland in both planes should begin at the head and work toward the tail on the ventral surface, providing longitudinal and cross-sectional views of the main pancreatic duct and parenchyma. Examination of the head and/or uncinate process may benefit from additional scanning from the right lateral or anterolateral aspect. Visualization of the intrapancreatic and/or periampullary bile duct is best achieved via acoustic coupling transduodenally (Fig. 12.8). The duodenal luminal gas is usually easily compressed with the probe to provide adequate imaging. Rarely, a nasogastric tube may be required to introduce saline into the duodenum to displace the luminal gas or a Kocher maneuver employed to provide a more lateral approach to the periampullary region. Lateral movement, rotation, angulation, and swing maneuvers (see Table 12.2 for definitions) may be employed to visualize key structures listed in the normal anatomy section below. Color Doppler may be employed if evaluation of vessel patency is of clinical importance. (Video 12.1 depicts laparoscopic pancreas scanning technique.)

Normal Pancreatic Anatomy

Normal pancreatic parenchyma should have a homogeneous echogenicity similar to the liver, and the pancreatic duct should appear hypoechoic with well-defined borders (Fig. 12.9). The confluence of the splenic vein and superior mesenteric vein should be well visualized as it transitions to the portal vein beneath the neck. The relationship between the pancreatic duct, common bile duct, and gastroduodenal artery should be delineated. The aorta, inferior vena cava, celiac plexus, and superior mesenteric artery should all be visible as the surface of the pancreas is scanned. Doppler imaging may be useful in confirming structures (Fig. 12.10).

Benign fatty infiltration of the pancreas is becoming more common with increasing Body Mass Indexes and appears as diffuse hyperechoic appearance of the gland often with head or uncinate sparing (Fig. 12.11). This sparing anomaly is thought to be due to the different embryologic origins of the dorsal and ventral pancreatic buds. It is important to understand this differentiation as this contrast in relative echogenicities can be misinterpreted as a mass [8].

Guidance Techniques

One of the key benefits of IOUS over other imaging modalities is its ability to provide real-time imaging guidance for needle localization or tissue dissection. Needle localization is often employed to locate the pancreatic duct prior to exposure or to aspirate cystic structures for analysis. Specialty devices are available commercially to aid in

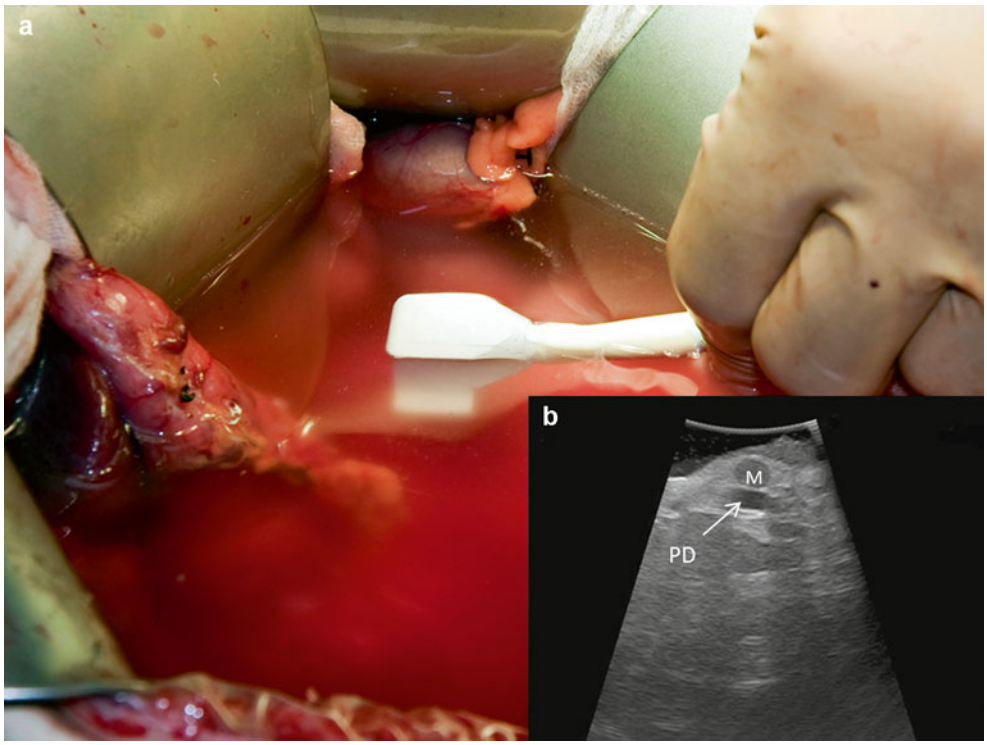

Fig. 12.6 *Standoff technique* – By immersing the probe in saline (**a**), a view of the surface of the gland is obtained without compression. This method (**b**) offers superior imaging of a surface lesion (*M*) and small pancreatic duct (*PD*)

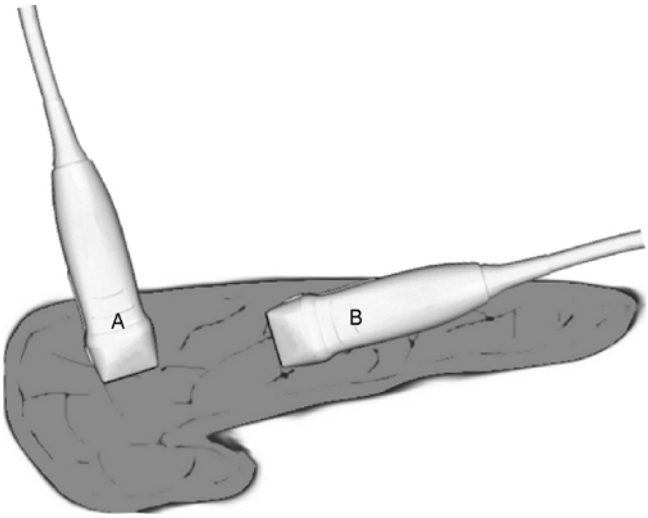

Fig. 12.7 *Probe orientation* – The transducer may be used to provide images in either a longitudinal (sagittal) plane (*A*) or in a transverse (axial) plane (*B*)

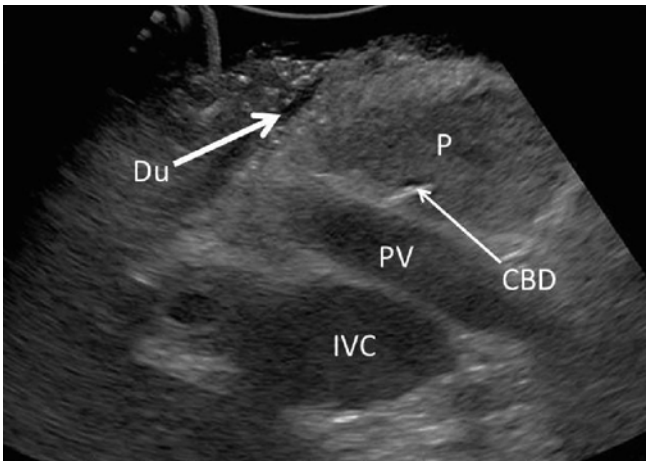

Fig. 12.8 *Transduodenal view* – By placing the probe anterolaterally on the duodenum (*Du*), an excellent view of the pancreatic head (*P*) at the level of the portal vein (*PV*) may be obtained with compression. Common bile duct (*CBD*), inferior vena cava (*IVC*), and portal vein (*PV*)

needle placement; however, a significantly cheaper freehand approach is similarly effective. With the freehand method the structure of interest is first identified with the ultrasound transducer, its center aligned with center of the probe, and the approximate anatomic depth noted. This can be done in either longitudinal or transverse planes, but the former will allow visualization of needle advancement through the entire gland. A long 21- to 27-gauge needle is then placed at an equidistance from the structure of interest related to the depth, in the plane between the operator and the probe, and aligned with the center of the probe (Fig. 12.12). The needle is then advanced under ultrasound guidance at an approximate 45° angle into the structure of interest. A syringe may be attached to the finder needle at this point and gently aspirated to confirm placement into a duct or cyst if relevant. If the intent is to expose the pancreatic duct, the needle may then be utilized as a guide for cut-down with electrocautery if the course of the duct is

Table 12.2 The various movements utilized in the systematic scanning of pancreatic structures

Maneuver	Description of technique
Lateral movement	Lateral movement of the probe along either the transverse or longitudinal path of the structure, with the probe in constant contact with the structure's surface. The most common technique during scanning
Rotation	Rotation of the probe along the direction of the ultrasonic beam. May be utilized to change between transverse and longitudinal views without having to pick up the probe
Angulation	The transducer surface is kept fixed on the organ, while the angle of the ultrasound beam is changed by pivoting the probe along its long axis. Utilized to obtain three-dimensional information or within confined spaces
Swing	Using the probe cable as a fulcrum, the probe head is swung in a pendulous motion while in contact with the structure surface. May be utilized in either transverse or longitudinal pathways

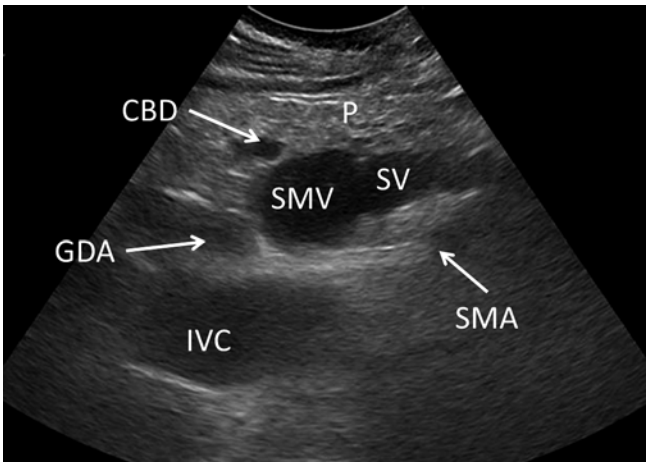

Fig. 12.10 *Normal vessel anatomy* – Vasculature visible through the head and neck of the pancreas (*P*) should include: the superior mesenteric artery (*SMA*) and vein (*SMV*), inferior vena cava (*IVC*), splenic vein (*SV*), and gastroduodenal artery (*GDA*). The aorta, portal vein, and splenic artery may also be visible in alternate planes. The common bile duct (*CBD*) is seen in this image

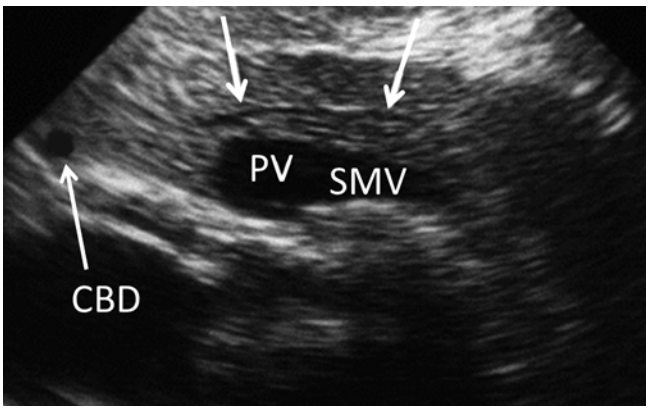

Fig. 12.9 *Normal ductal anatomy* – A normal main pancreatic duct (*white arrows*) is visualized in a longitudinal view. Also seen are the common bile duct (*CBD*) and the confluence of the portal (*PV*) and superior mesenteric veins (*SMV*) (With kind permission from Lichtenstein [76])

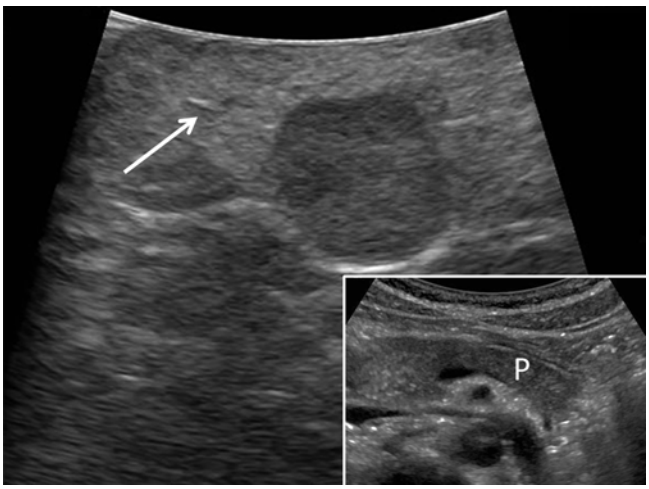

Fig. 12.11 *Fatty infiltrate* – Fatty infiltration of the pancreas showing diffuse hyperechogenicity of pancreatic parenchyma (*white arrow*) compared to normal parenchyma (*P*) shown within inset

evident. If the duct is narrow and difficult to visualize, an appropriately sized wire may be advanced through the needle in order to cannulate the entire length of the duct and subsequently utilized for exposure.

Contrast Enhancement

The use of contrast-enhanced ultrasound (CEUS) is relatively new to the surgeon's armamentarium, with the first reports of its clinical use published in 2000 [9]. The initial application of this technology was limited to the evaluation of the right heart due to the first generation of contrast agents being destroyed after passing through the pulmonary circulation. Second-generation contrast agents are more stable, can be administered peripherally, and have indications in evaluating a variety of organ systems [10]. While the main utility of this technique has been in the investigation of liver lesions, it has found some use in differentiating pancreatic lesions. The European Federation of Societies for Ultrasound in Medicine and Biology (EFSUMB) periodically releases guidelines for CEUS, with its last revision in 2011 [11]. Based on the recommendations of the EFSUMB, CEUS has a sufficient level of evidence for use in the following pancreatic conditions:

1. Characterizing ductal adenocarcinomas (evidence level: A;1b)
2. Differentiating pseudocysts from cystic tumors (evidence level: A;1b)

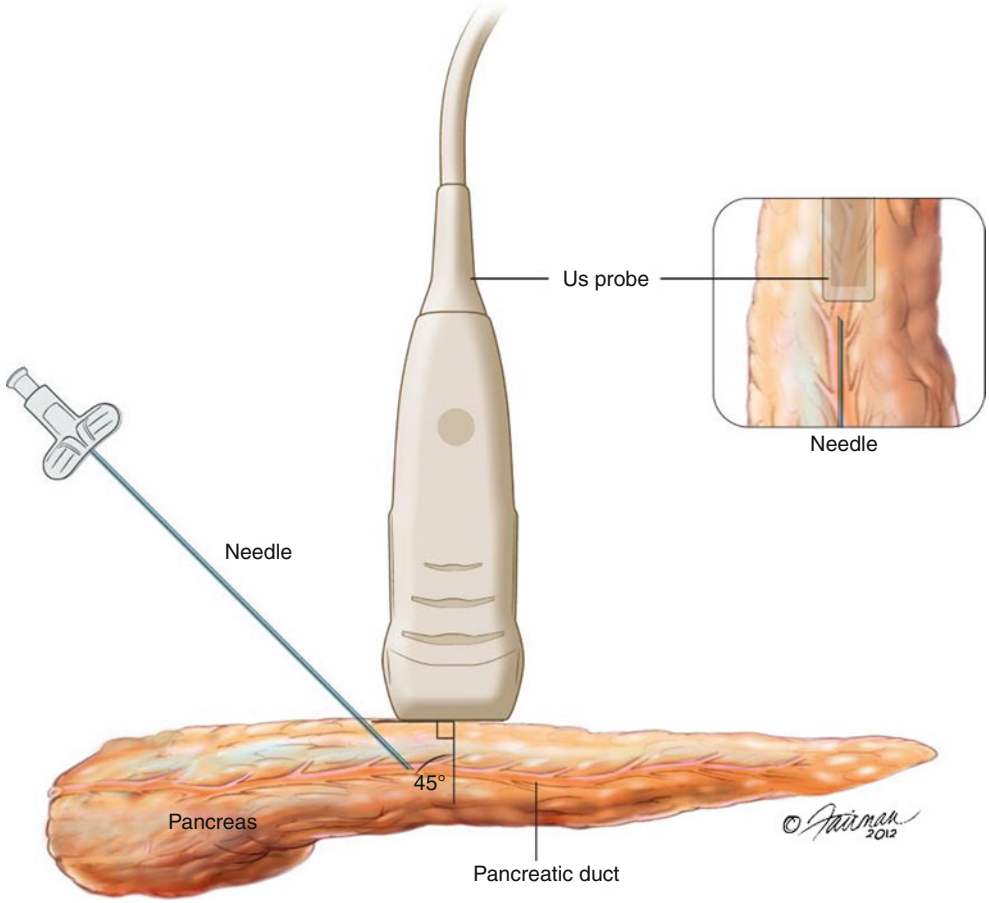

Fig. 12.12 *Needle guidance* – The needle should be placed in-line with the probe, enter the gland at a distance equal to the depth of the lesion, and follow a 45° angle. The needle tip should be visible throughout the advancement

3. Differentiating solid from liquid/necrotic components of a lesion (evidence level: A;1b)
4. Defining lesion dimensions and anatomic relationships with surrounding structures (evidence level: B;2b)

Contrast enhancement of the pancreatic arteries begins immediately after aortic enhancement, lasts 10–30 s, and is immediately followed by a 90-s venous phase [12]. The liver should then be assessed for metastasis after the pancreatic venous phase, using the same contrast injection [13]. The specific ultrasonic findings for each indication will be discussed below in the corresponding pathologic section. Although there is no significant evidence to recommend the routine use of CEUS to evaluate pancreatic lesions, the technique should be considered if previous diagnostic work-up is equivocal. (See Chap. 23, section "Contrast-enhanced ultrasound," for more information.)

Condition-Specific Indications

The following sections will discuss indications of IOUS for various pancreatic pathologies and focus on their typical ultrasonographic features. Images were obtained via handheld and/or LUS.

Pancreatitis

Indications: Operative treatment of acute and/or chronic pancreatitis and its major sequelae have been on the decline with the advancement of various percutaneous and endoscopic treatments such as dual drainage and rendezvous techniques [14, 15]. However, for lesions not amenable to these techniques or for institutions without access to advanced subspecialist, operative drainage of pseudocysts or abscesses, debridement of necrotic gland, or treatment of pseudoaneurysm may be required. Ultrasonographic localization of the main pancreatic duct (see section "Guidance techniques") should be considered during any Puestow or Frey procedure in which the pancreatic duct is not easily palpable.

Acute Pancreatitis Findings: Generally shows hypoechogenicity or a mixed echo pattern of the parenchyma due to edema or associated necrotic and hemorrhagic tissue. CEUS may be utilized to delineate non-enhancing areas of necrosis for debridement [16].

Chronic Pancreatitis Findings: Non-autoimmune etiologies are characterized by heterogeneous hyperechogenicity of a hard and atrophic parenchyma, frequently associated with calcifications and acoustic shadowing. The pancreatic duct appears hypoechoic, is often dilated (can appear as a series of dilations and strictures, the so-called chain of lakes),

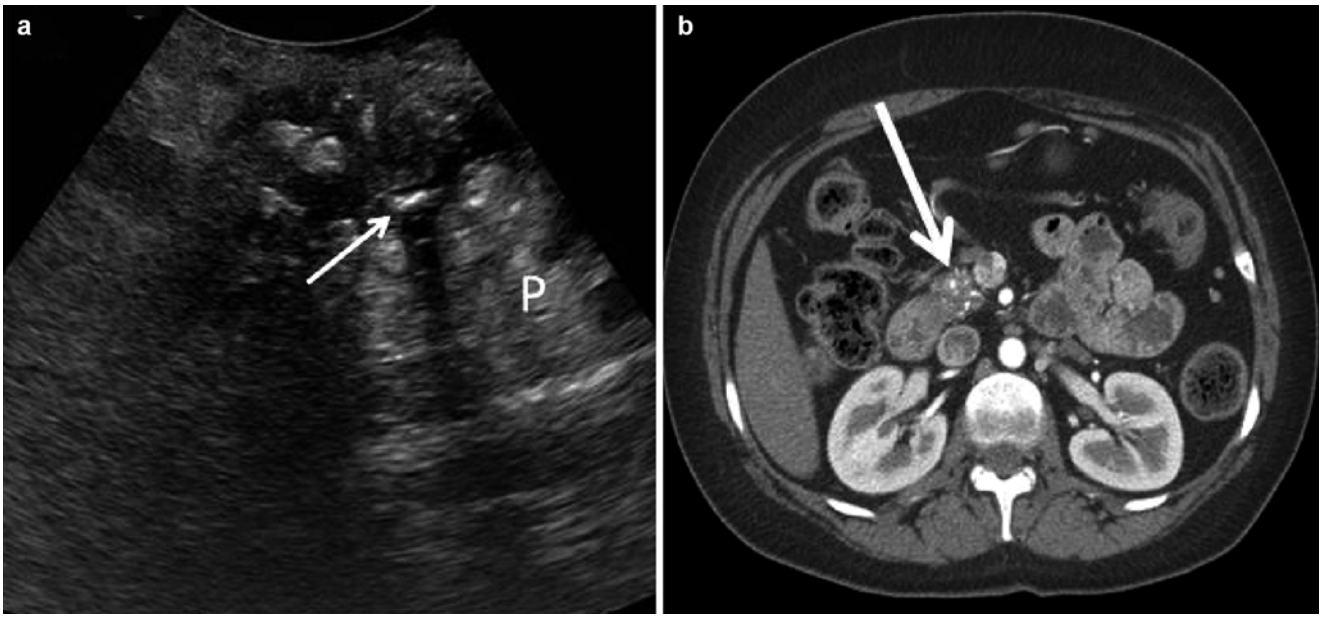

Fig. 12.13 *Chronic pancreatitis* – A transverse view (**a**) shows a hyperechoic parenchyma with calcifications (*P*) and a narrow pancreatic duct stone with acoustic shadowing (*thin white arrow*). A corresponding CT scan (**b**) shows an atrophic head with multiple calcifications (*thick white arrow*)

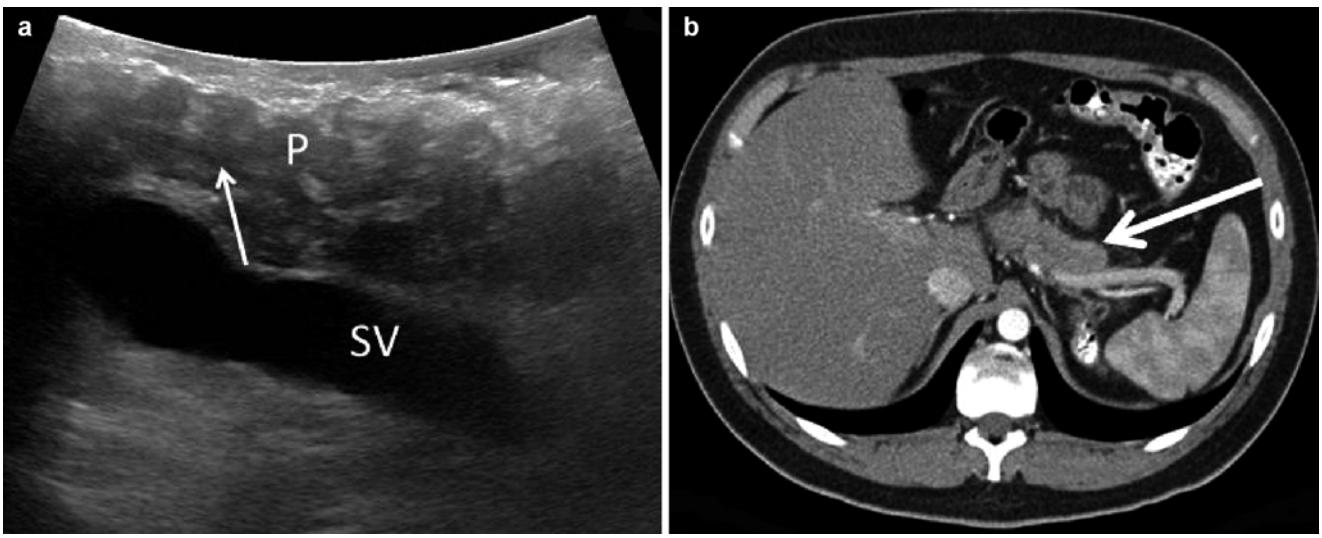

Fig. 12.14 *Autoimmune pancreatitis* – A longitudinal view (**a**) shows a hypoechoic parenchyma (*P*) and a narrow pancreatic duct (*thin white arrow*). The splenic (*SV*) vein is also noted. A corresponding CT scan (**b**) shows a thickened gland with a smooth surface (*thick white arrow*), often described as "sausage-like"

and may contain intraductal calcifications with associated acoustic shadowing (Fig. 12.13). This is in stark contrast to autoimmune pancreatitis which is characterized by heterogenic hypoechogenicity of an enlarged gland, often with a strictured duct, and rare calcifications (Fig. 12.14).

Pseudocyst Findings: Pseudocysts as small as 2–3 mm can be accurately detected by IOUS. They appear as well-defined hypoechoic masses with associated posterior enhancement and can contain debris of mixed echogenicity (Fig. 12.15). Ultrasonography can help to differentiate pseudocysts from abscesses (less well-defined cystic masses with mixed echogenicity and/or presence of luminal gas), hematomas (mixed echogenicity, fluid-fluid levels suggesting clot), or malignancy (intraluminal nodules and/or irregular pseudocyst wall) [17]. CEUS has a 100 % sensitivity and specificity for characterizing pseudocysts, which appear as a non-enhancing lesion in all phases with a nonvascular core. However, traversing vessels may be found in the early stages [18, 19].

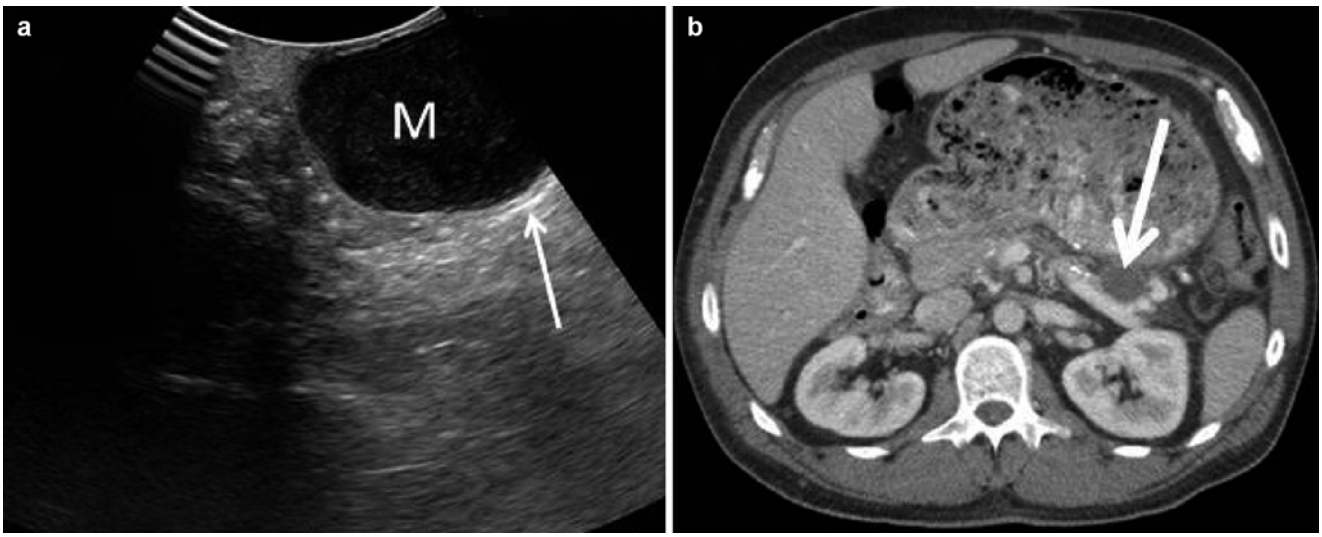

Fig. 12.15 *Pseudocyst* – (**a**) The typical pseudocyst (*M*) will appear well circumscribed and uniformly hypoechoic with posterior enhancement (*thin white arrow*). The corresponding CT scan (**b**) shows the pseudocyst (*thick white arrow*)

Pseudoaneurysm Findings: The development of a pseudoaneurysm involving a peripancreatic vessel is a known complication of pancreatitis and can be fatal if it ruptures. IOUS with color Doppler can assist localization of the lesion, identify the extent of the vessel involvement, and help gain proximal and distal control prior to exposure.

Pancreatic Cysts

Indications: Intraoperative ultrasound plays an integral part in the management of cystic lesions of the pancreas, particularly the characterization of suspected intraductal mucinous neoplasms (IPMNs). The malignant potential of IPMNs is directly related to its relationship with the main pancreatic duct. Main branch or mixed subtypes have a mean invasive malignancy rate of 43 % and should be resected. The side-branch subtype has a lower associated mean invasive malignancy rate of 17 % and is recommended for selective resection or enucleation based on the "Sendai criteria." Included in these criteria are lesions greater than 3 cm and those that are clinically symptomatic or have high-risk features (main duct involvement, thickened cyst wall, mural nodules, positive cytology, main duct size 5–9 mm, or abrupt change in caliber of pancreatic duct with distal pancreatic atrophy) [20]. Each of these features is identifiable by ultrasound. IOUS has been shown to be more sensitive than, and equally specific as EUS or CT for the diagnosis of IPMN, with improved ability to assess the extent of ductal involvement [21]. If there is no suggestion of main duct involvement, IOUS may be utilized to determine the extent of the resection required. Recent studies have shown that enucleation for solitary cystic lesions not involving the main duct may be a viable option for resection [22, 23]. IOUS is an important tool for safely performing localized resection of small lesions, as it can delineate surrounding vessels and ducts. Anatomic proximity of a cyst to the main pancreatic duct may influence the decision to enucleate versus resect because of the risk for pancreatic fistula. Cysts that are less than 2 mm from the main pancreatic duct have a risk of pancreatic fistula development nearing 60 %, whereas those more than 2 mm from the main pancreatic duct are associated with a 19 % incidence of fistulization [24]. Intraoperative ultrasound may also be useful to characterize non-IPMN cyst anatomy or assist in obtaining aspirates for diagnosis [25, 26]. However, as most of this can now be done via EUS preoperatively, the role of IOUS is to delineate anatomy for resection.

Intraductal Pancreatic Mucinous Neoplasm (IPMN) Findings: IPMNs appear as a heterogeneous hypoechoic dilated duct with possible echogenic intramural nodules. IOUS should be utilized to evaluate the relationship of the lesion with the main duct and any major vessels. Side-branch IPMNs can often be seen communicating with the main pancreatic duct (Fig. 12.16). The use of CEUS in IPMN evaluation is limited but can help to differentiate non-perfused intramural clot from perfused intramural nodules [27].

Serous Cyst Findings: Serous cystadenomas typically are characterized by a solitary hypoechoic microcystic (cysts <2 cm in diameter) mass with a thin wall and a lobulated margin. Infrequently they may contain a central scar, possibly calcified. Occasionally the septation of the cyst will be so dense that the lesion appears echogenic (Fig. 12.17). These cysts are hyperenhancing on CEUS with vascularized septa [28, 29].

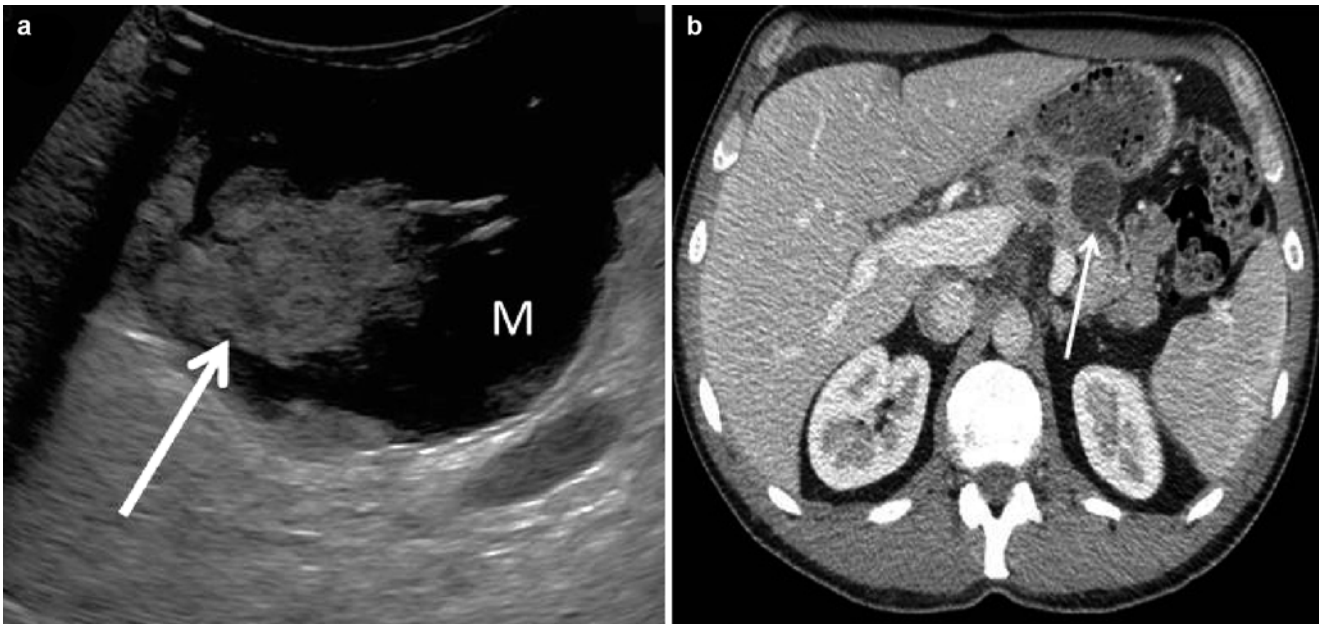

Fig. 12.16 *Intraductal papillary mucinous neoplasm* – This transverse view of the pancreas (**a**) shows a heterogeneous cystic mass (*M*) containing a large mural nodule (*thick white arrows*). The corresponding CT scan (**b**) shows a cystic mass in continuity with a dilated main duct (*thin white arrow*), consistent with a side-branch IPMN

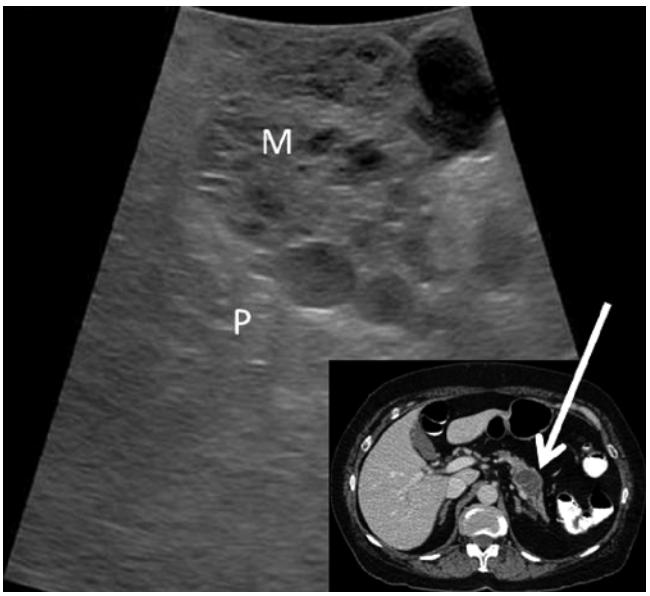

Fig. 12.17 *Microcystic lesion* – A complex multiloculated cystic mass (*M*) with a lobular border contains many subcentimeter hypoechoic cysts. The surrounding parenchyma (*P*) appears normal. The *inset* shows the relative location by CT scan

Mucinous Cyst Findings: Mucinous cystadenomas and cystadenocarcinomas are generally characterized by a hypoechoic macrocystic (cysts >2 cm in diameter) mass with irregular thick walls and internal complexity (mural irregularity and/or septations) (Fig. 12.18). The differentiation between micro- and macrocystic is not directly correlated with a malignant diagnosis [30, 31]. CEUS frequently shows hyperenhancement of the cyst wall, internal inclusions, and septa [18, 19, 28].

Ductal Adenocarcinoma

Indications: Advancements in multi-detector computerized tomography (MDCT) have supplanted the routine use of laparoscopic ultrasound in pancreatic adenocarcinoma staging, as MDCT has been shown to be more specific and has a higher negative predictive value for determining resectability [3]. However, intraoperative ultrasound still has selected utility in pancreatic cancer treatment with a 93 % sensitivity for determining resectability [3, 32]. MDCTs lack the sensitivity, the positive predictive value, and the ability to accurately determine vessel patency or guide treatment in real time [33–38]. The use of laparoscopic ultrasound for staging has been shown to change management in 7–17 % of cases in which it is performed [39, 40]. Intraoperative ultrasonography for pancreatic adenocarcinoma should still be considered for the following: confirmation of anatomy for operative planning, staging of disease when CT scan is equivocal, evaluation of vessel patency/involvement in real time, or guiding the of biopsy of potential metastatic lesions or suspicious lymph nodes.

Findings: Pancreatic adenocarcinoma appears as a homogeneous hypoechoic mass with ill-defined margins. Large

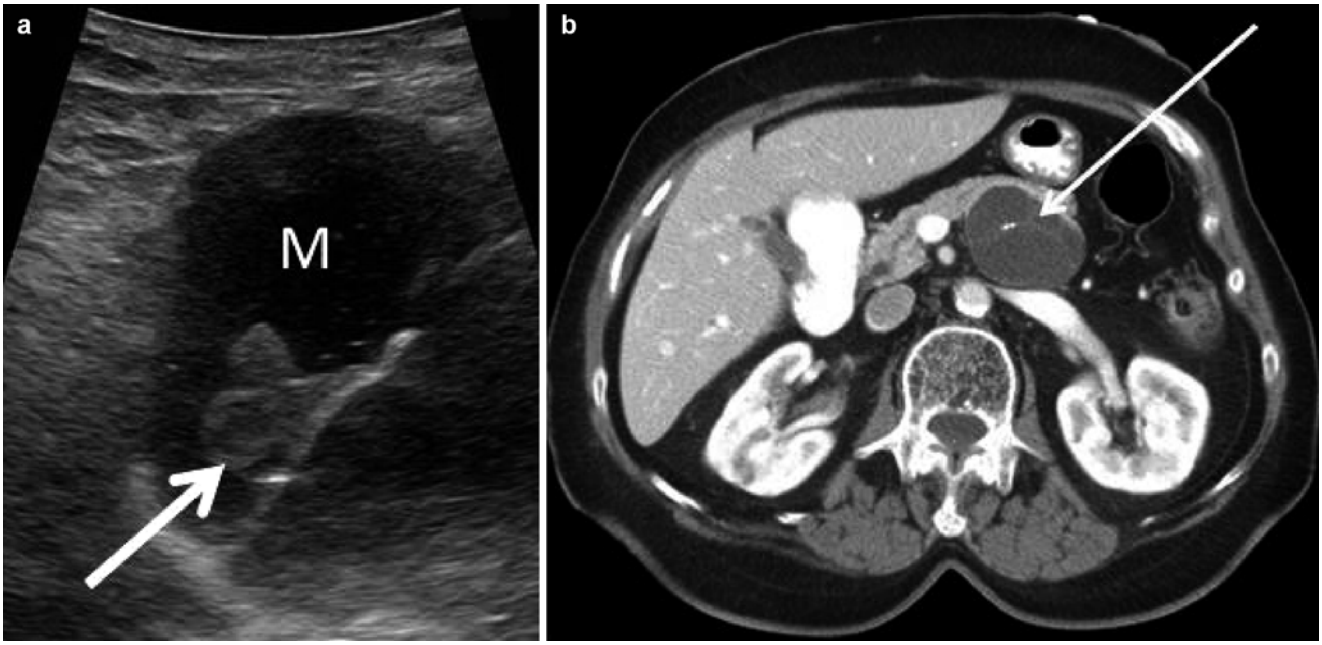

Fig. 12.18 *Macrocystic lesion* – The single hypoechoic mass (*M*) with a thick well-circumscribed border is typical of macrocystic lesions. These mass may have internal septations or mural irregularity (*thick white arrow*). The corresponding CT scan shows internal septations (*thin white arrow*)

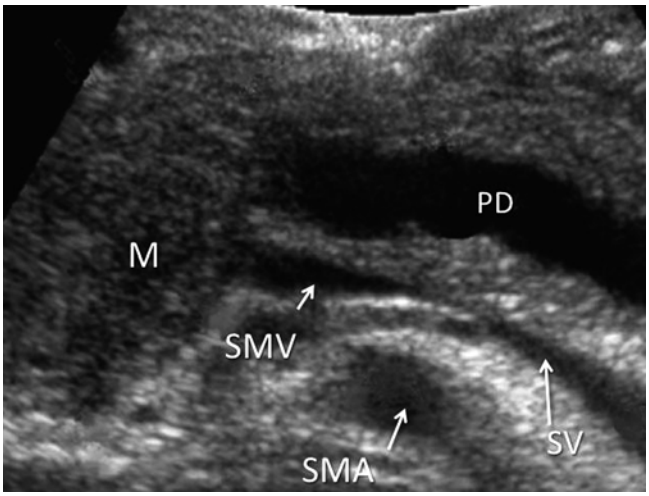

Fig. 12.19 *Adenocarcinoma* – The homogeneous hypoechoic mass (*M*) with ill-defined borders is classic for adenocarcinoma. This tumor in the head has caused pancreatic duct (*PD*) dilatation secondary to compression. In this plane, the SMA, SMV, and splenic vein (*SV*) appear to be uninvolved

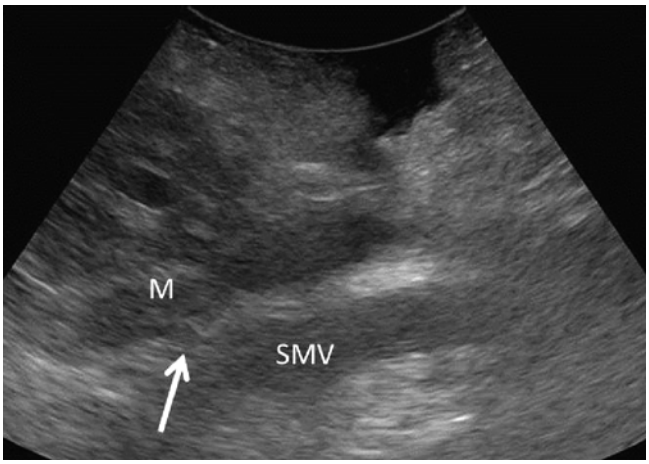

Fig. 12.20 *Vessel invasion* – The ill-defined border of the homogeneous mass (*M*) is invading into the superior mesenteric vein (*SMV*), as evidenced by a loss of the vessel margin (*white arrow*)

tumors can display a mixed echogenicity. A concomitant pancreatitis secondary to ductal obstruction can increase the echogenicity of tissue surrounding a suspected lesion, thereby creating a perceived decrease in echogenicity of the mass. This can increase the sensitivity of detecting smaller lesions, with IOUS normally having a detection threshold of 1 cm in diameter (Fig. 12.19). CEUS will show hypoenhancement of all vascular phases in 90 % of cases [1, 18, 41–44]. Margins and vessel involvement are typically better visualized with CEUS as well [45, 46].

Resectability of ductal adenocarcinoma is generally determined according to one of various consensus criteria [47, 48]. Although there are slight differences within these criteria, they all limit resectability based on presence of metastasis and some degree of major local vessel involvement. Invasion of the portal or mesenteric vessels is evidenced on IOUS by encasement of the vessel wall, stricturing of lumen, presence of thrombus, or intraluminal tumor mass (Fig. 12.20).

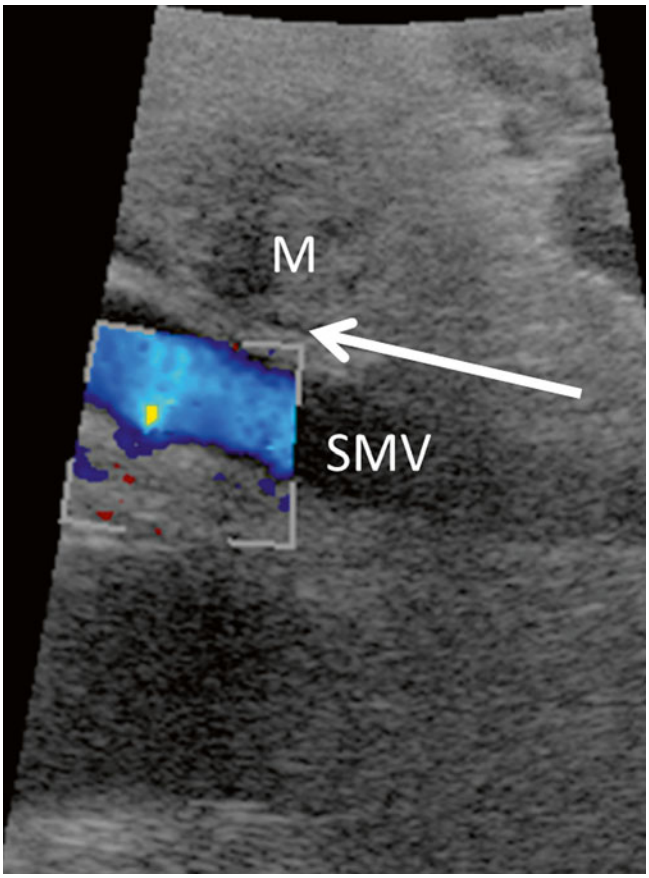

Fig. 12.21 *Vessel abutment* – The ill-defined homogeneous hypoechoic mass (*M*) is abutting the SMV but not invading it. Note that there is a loss of the plane between the parenchyma and the vessel wall (*white arrow*), but there is no distortion of the vein. Doppler may be used to confirm patency

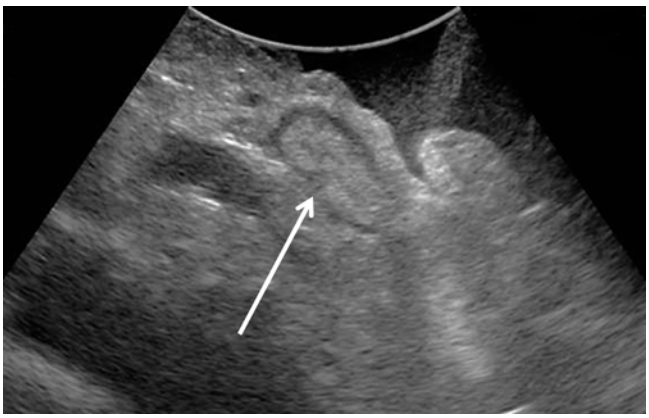

Fig. 12.22 *Suspicious lymph node* – An abnormal appearing lymph node (*white arrow*) will typically be heterogeneous, larger than a centimeter, and rounder than a normal lymph node and may have an irregular border

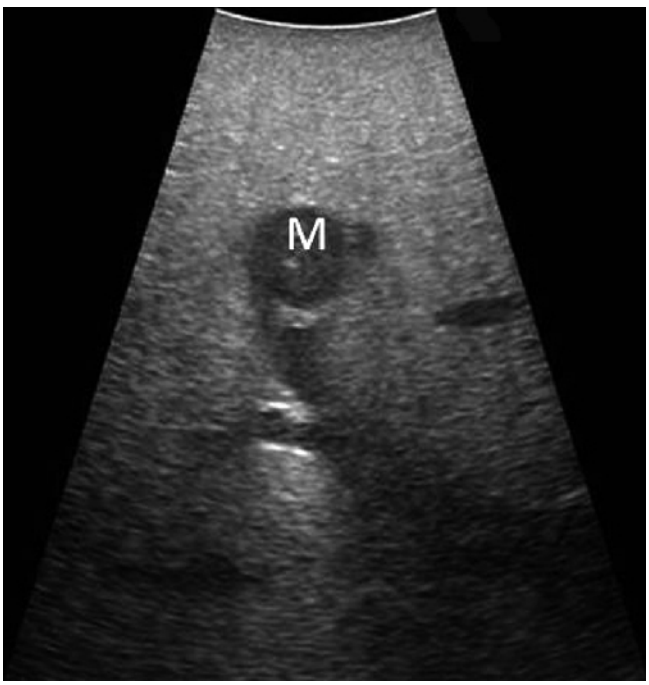

Fig. 12.23 *Liver metastases* – The liver may be easily scanned if there is concern for metastases. The mass (*M*) depicted here is of a mixed echogenicity, but pancreatic metastases may appear as hyper- or hypoechoic as well

Involvement should be highly suspected if the mass abuts the vessel and causes the normally echogenic vessel wall to become distorted and lose some degree of echogenicity (Fig. 12.21).

Sonographic evaluation and/or biopsy of suspicious lymph nodes or metastatic lesions should be considered anytime involvement would preclude resection or provide information that might change therapy. Lymph nodes highly suspicious for malignancy will typically appear diffusely hypoechoic or of mixed echogenicity, be larger (10–15 mm), and be rounder (long/short axis >0.5) than their benign counterparts (Fig. 12.22). Metastatic liver lesions generally have a hypoechoic or mixed pattern but can occasionally be hyperechoic (Fig. 12.23).

Neuroendocrine Tumors

Indications: In contrast to its variable utility in adenocarcinoma, IOUS in pancreatic neuroendocrine tumors (NETs) is quite useful for diagnosis and treatment [49, 50]. NETs derive from the islet of Langerhans and are generally classified based on their functional status and which hormone is produced. Functional NETs may often require resection secondary to symptomatology when they are too small to be detected by other modalities. IOUS allows surgeons to locate insulinomas as small as 2–3 mm with 95–100 % sensitivity and can assist in planning parenchyma-sparing enucleations [4, 22, 49–57]. The detection rate for extrahepatic gastrinomas is much less at 58 % [58]. Nonfunctional NETs do not often require IOUS for

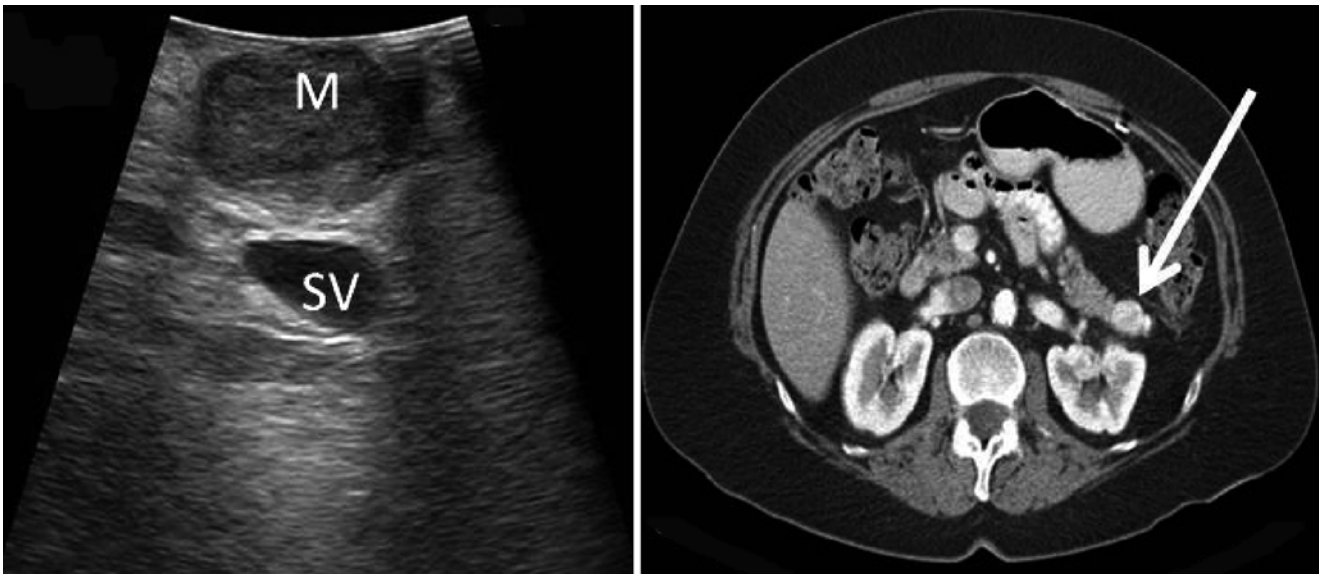

Fig. 12.24 *Neuroendocrine tumor* – This surface lesion is best viewed utilizing the "standoff" technique. The mass (*M*) appears as a well-defined, homogeneous, hypoechoic mass. There is an associated mild compression of the splenic vein (*SV*). The corresponding CT scan shows an enhancing lesion in the tail (*white arrow*)

precise localization as they are generally larger on first presentation, likely due to lack of symptoms leading to discovery [59]. Eighty-five percent of NETs are functional, 60 % are insulinomas, and 16 % are gastrinomas [60]. NETs may be associated with the hereditary multiple endocrine neoplasia type 1 (MEN1) syndrome, and IOUS should be utilized to assess for multiple lesions anytime a NET is suspected. This is especially important for gastrinomas, of which a third may be associated with MEN1 [60]. Ninety percent of insulinomas are benign, solitary, and located within the pancreas [61, 62]. While most insulinomas are benign, the peripancreatic and liver regions should still be scanned for metastasis [51]. The presence of multiple lesions with suspected insulinomas is suggestive of malignancy and/or MEN1. Gastrinomas tend to be far more ominous. They are frequently multiple small lesions, with 30 % occurring outside the pancreas and a 60–90 % incidence of malignancy [61, 63]. The most common site of metastasis is within the "gastrinoma triangle" (bounded by the cystic/common bile duct junction, third part of the duodenum, and the pancreatic neck). This zone and the liver should always be evaluated in suspected cases of gastrinomas. Saline infusion of duodenum via a nasogastric tube may help evaluate the lumen for occult nodules [1].

Findings: Neuroendocrine tumors typically appear as well-defined, homogeneous, hypoechoic masses (Fig. 12.24). However, up to 10 % of insulinomas may appear as iso- or hyperechoic with or without internal cystic change [51, 59, 61, 64, 65]. NETs are generally hyperenhancing in the arterial phase, but larger NETs may have avascular segments secondary to necrosis resulting in a variable enhancement pattern [29, 64, 66].

Emerging Uses

Since the final chapter of this book is dedicated to the future use of IOUS, we will discuss briefly those applications pertaining to pancreatic surgery. As mentioned previously, High-Intensity Focused Ultrasound (HIFU) is currently being developed as a transcutaneous treatment for pancreatic cancer. It has mainly been used outside of the United States, and no large trials have been conducted of its efficacy, but early data is promising for reducing pain and improving survival in nonoperative adenocarcinoma [67–70].

Contrast-enhanced ultrasound utilizes microbubbles (MBs) to better delineate vascular characteristics for diagnosis; however, these same MBs may have therapeutic uses. The application of high-frequency ultrasound to tissues will result in thermal injury and cavitation (the release of gas bubbles from tissue/fluid secondary to vibration). The energy required to initiate cavitation is less in the presence of MBs, leading to decreased thermal injury to surrounding tissue. Cavitation itself can lead to transient (sonoporation) or permanent increased permeability of cell membranes, thereby improving drug uptake. Additionally, the MBs can be covered or filled with chemotherapeutic agents and delivered systemically. When directed IOUS is applied to the target tissue, the drug will be released and tumor uptake will be enhanced via the cavitation effect [71].

The use of IOUS to guide placement of fiducial markers for stereotactic body radiotherapy has had some investigation for adjuvant and neoadjuvant treatment of pancreatic cancer [72–74]. The hope is that larger radiation doses may be given in a focused manner with reduced regional effects. Early data

is promising, but currently there is insufficient evidence that this is superior to other available therapies [75].

Another potential use would be providing retrograde access to an anastomotic stricture of the pancreatic duct following resection. Often when stricturing of the neo-ampulla occurs postoperatively, the os is extremely difficult to locate endoscopically. We anticipate being able to use IOUS to introduce a wire via needle localization into the dilated duct, through the strictured os, and rendezvous with an endoscopist for advancement of a stent in patients where revision of the anastomosis is too dangerous.

Conclusion

Operative ultrasound has proven to be an invaluable resource to pancreatic surgeons. The benefits of real-time imaging, high sensitivity, and minimal invasiveness can assist surgeons in the diagnosis of disease, operative planning, and guiding intervention. While its use in staging pancreatic adenocarcinoma has largely been supplanted by modern CT scanning, the expansion of its use to other pancreatic pathologies has been instrumental in advancement of surgical treatment of these conditions. With the combination of ultrasonography and endoscopic management, rarely do the sequelae of pancreatitis require major operative intervention. IOUS has allowed surgeons to precisely delineate anatomy and reduce the area of resection for cystic and neuroendocrine tumors. Contrast enhancement is proving to be useful in differentiating between cystic lesions and further aiding in delineating anatomy. As High-Intensity Focused Ultrasound becomes more widely available, we anticipate the next logical step being miniaturization of the equipment thereby allowing for focused laparoscopic treatment.

References

1. Sun MRM, Brennan DD, Kruskal JB, Kane RA. Intraoperative ultrasonography of the pancreas. Radiographics. 2010;30(7):1935–53.
2. Shin LK, Brant-Zawadzki G, Kamaya A, Jeffrey RB. Intraoperative ultrasound of the pancreas. Ultrasound Q. 2009;25(1):39–48; quiz 48.
3. Long EE, Van Dam J, Weinstein S, Jeffrey B, Desser T, Norton JA. Computed tomography, endoscopic, laparoscopic, and intraoperative sonography for assessing resectability of pancreatic cancer. Surg Oncol. 2005;14(2):105–13.
4. Jakimowicz JJ. Intraoperative ultrasonography in open and laparoscopic abdominal surgery: an overview. Surg Endosc. 2006;20 Suppl 2:S425–35.
5. Lane RJ, Glazer G. Intra-operative B-mode ultrasound scanning of the extra-hepatic biliary system and pancreas. Lancet. 1980;2(8190):334–7.
6. Sigel B, Machi J, Ramos JR, Duarte B, Donahue PE. The role of imaging ultrasound during pancreatic surgery. Ann Surg. 1984;200(4):486–93.
7. Khokhlova TD, Hwang JH. HIFU for palliative treatment of pancreatic cancer. J Gastrointest Oncol. 2011;2(3):175–84.
8. Jacobs JE, Coleman BG, Arger PH, Langer JE. Pancreatic sparing of focal fatty infiltration. Radiology. 1994;190(2):437–9.
9. Bertolotto M, Dalla Palma L, Quaia E, Locatelli M. Characterization of unifocal liver lesions with pulse inversion harmonic imaging after Levovist injection: preliminary results. Eur Radiol. 2000;10(9):1369–76.
10. Xu H-X. Contrast-enhanced ultrasound: the evolving applications. World J Radiol. 2009;1(1):15–24.
11. Piscaglia F, Nolsøe C, Dietrich CF, Cosgrove DO, Gilja OH, Bachmann Nielsen M, et al. The EFSUMB guidelines and recommendations on the clinical practice of Contrast Enhanced Ultrasound (CEUS): update 2011 on non-hepatic applications. Ultraschall Med. 2012;33(1):33–59.
12. Claudon M, Cosgrove D, Albrecht T, Bolondi L, Bosio M, Calliada F, et al. Guidelines and good clinical practice recommendations for contrast enhanced ultrasound (CEUS) – update 2008. Ultraschall Med. 2008;29(1):28–44.
13. D'Onofrio M, Martone E, Malagò R. Contrast-enhanced ultrasonography of the pancreas. JOP. 2007;9(5):560–6.
14. Gluck M, Ross A, Irani S, Lin O, Gan SI, Fotoohi M, et al. Dual modality drainage for symptomatic walled-off pancreatic necrosis reduces length of hospitalization, radiological procedures, and number of endoscopies compared to standard percutaneous drainage. J Gastrointest Surg. 2012;16(2):248–56; discussion 256–7.
15. Irani S, Gluck M, Ross A, Gan SI, Crane R, Brandabur JJ, et al. Resolving external pancreatic fistulas in patients with disconnected pancreatic duct syndrome: using rendezvous techniques to avoid surgery (with video). Gastrointest Endosc. 2012;76(3):586–93.e3.
16. Ripollés T, Martínez MJ, López E, Castelló I, Delgado F. Contrast-enhanced ultrasound in the staging of acute pancreatitis. Eur Radiol. 2010;20(10):2518–23.
17. Ros PR, Hamrick-Turner JE, Chiechi MV, Ros LH, Gallego P, Burton SS. Cystic masses of the pancreas. Radiographics. 1992;12(4):673–86.
18. D'Onofrio M, Barbi E, Dietrich CF, Kitano M, Numata K, Sofuni A, et al. Pancreatic multicenter ultrasound study (PAMUS). Eur J Radiol. 2012;81(4):630–8.
19. Rickes S, Wermke W. Differentiation of cystic pancreatic neoplasms and pseudocysts by conventional and echo-enhanced ultrasound. J Gastroenterol Hepatol. 2004;19(7):761–6.
20. Tanaka M, Fernández-del Castillo C, Adsay V, Chari S, Falconi M, Jang J-Y, et al. International consensus guidelines 2012 for the management of IPMN and MCN of the pancreas. Pancreatology. 2012;12(3):183–97.
21. Kaneko T, Nakao A, Inoue S, Sugimoto H, Hatsuno T, Ito A, et al. Intraoperative ultrasonography by high-resolution annular array transducer for intraductal papillary mucinous tumors of the pancreas. Surgery. 2001;129(1):55–65.
22. Cauley CE, Pitt HA, Ziegler KM, Nakeeb A, Schmidt CM, Zyromski NJ, et al. Pancreatic enucleation: improved outcomes compared to resection. J Gastrointest Surg. 2012;16(7):1347–53.
23. Turrini O, Schmidt CM, Pitt HA, Guiramand J, Aguilar-Saavedra JR, Aboudi S, et al. Side-branch intraductal papillary mucinous neoplasms of the pancreatic head/uncinate: resection or enucleation? HPB (Oxford). 2011;13(2):126–31.
24. Brient C, Regenet N, Sulpice L, Brunaud L, Mucci-Hennekine S, Carrère N, et al. Risk factors for postoperative pancreatic fistulization subsequent to enucleation. J Gastrointest Surg. 2012;16(10):1883–7.
25. Machi J, Sigel B, Kurohiji T, Zaren HA, Sariego J. Operative ultrasound guidance for various surgical procedures. Ultrasound Med Biol. 1990;16(1):37–42.
26. Johnson CD, Stephens DH, Charboneau JW, Carpenter HA, Welch TJ. Cystic pancreatic tumors: CT and sonographic assessment. AJR Am J Roentgenol. 1988;151(6):1133–8.

27. Itoh T, Hirooka Y, Itoh A, Hashimoto S, Kawashima H, Hara K, et al. Usefulness of contrast-enhanced transabdominal ultrasonography in the diagnosis of intraductal papillary mucinous tumors of the pancreas. Am J Gastroenterol. 2005;100(1):144–52.
28. D'Onofrio M, Megibow AJ, Faccioli N, Malagò R, Capelli P, Falconi M, et al. Comparison of contrast-enhanced sonography and MRI in displaying anatomic features of cystic pancreatic masses. AJR Am J Roentgenol. 2007;189(6):1435–42.
29. D'Onofrio M, Gallotti A, Pozzi Mucelli R. Imaging techniques in pancreatic tumors. Expert Rev Med Devices. 2010;7(2):257–73.
30. Khurana B, Mortelé KJ, Glickman J, Silverman SG, Ros PR. Macrocystic serous adenoma of the pancreas: radiologic-pathologic correlation. AJR Am J Roentgenol. 2003;181(1):119–23.
31. Yeh HC, Stancato-Pasik A, Shapiro RS. Microcystic features at US: a nonspecific sign for microcystic adenomas of the pancreas. Radiographics. 2001;21(6):1455–61.
32. Barabino M, Santambrogio R, Pisani Ceretti A, Scalzone R, Montorsi M, Opocher E. Is there still a role for laparoscopy combined with laparoscopic ultrasonography in the staging of pancreatic cancer? Surg Endosc. 2011;25(1):160–5.
33. Vargas R, Nino-Murcia M, Trueblood W, Jeffrey RB. MDCT in pancreatic adenocarcinoma: prediction of vascular invasion and resectability using a multiphasic technique with curved planar reformations. AJR Am J Roentgenol. 2004;182(2):419–25.
34. Prokesch RW, Chow LC, Beaulieu CF, Nino-Murcia M, Mindelzun RE, Bammer R, et al. Local staging of pancreatic carcinoma with multi-detector row CT: use of curved planar reformations initial experience. Radiology. 2002;225(3):759–65.
35. Conlon KC, Dougherty E, Klimstra DS, Coit DG, Turnbull AD, Brennan MF. The value of minimal access surgery in the staging of patients with potentially resectable peripancreatic malignancy. Ann Surg. 1996;223(2):134–40.
36. Callery MP, Strasberg SM, Doherty GM, Soper NJ, Norton JA. Staging laparoscopy with laparoscopic ultrasonography: optimizing resectability in hepatobiliary and pancreatic malignancy. J Am Coll Surg. 1997;185(1):33–9.
37. Machi J, Sigel B, Zaren HA, Kurohiji T, Yamashita Y. Operative ultrasonography during hepatobiliary and pancreatic surgery. World J Surg. 1993;17(5):640–5; discussion 645–6.
38. Sugiyama M, Hagi H, Atomi Y. Reappraisal of intraoperative ultrasonography for pancreatobiliary carcinomas: assessment of malignant portal venous invasion. Surgery. 1999;125(2):160–5.
39. Rumstadt B, Schwab M, Schuster K, Hagmüller E, Trede M. The role of laparoscopy in the preoperative staging of pancreatic carcinoma. J Gastrointest Surg. 1997;1(3):245–50.
40. Hann LE, Conlon KC, Dougherty EC, Hilton S, Bach AM, Brennan MF. Laparoscopic sonography of peripancreatic tumors: preliminary experience. AJR Am J Roentgenol. 1997;169:1257–62.
41. Kitano M, Kudo M, Maekawa K, Suetomi Y, Sakamoto H, Fukuta N, et al. Dynamic imaging of pancreatic diseases by contrast enhanced coded phase inversion harmonic ultrasonography. Gut. 2004;53(6):854–9.
42. D'Onofrio M, Zamboni G, Tognolini A, Malago R, Faccioli N, Frulloni L, et al. Mass-forming pancreatitis: value of contrast-enhanced ultrasonography. World J Gastroenterol. 2006;12(26):4181–4.
43. Kersting S, Konopke R, Kersting F, Volk A, Distler M, Bergert H, et al. Quantitative perfusion analysis of transabdominal contrast-enhanced ultrasonography of pancreatic masses and carcinomas. Gastroenterology. 2009;137(6):1903–11.
44. Numata K, Ozawa Y, Kobayashi N, Kubota T, Shimada H, Nozawa A, et al. Contrast-enhanced sonography of pancreatic carcinoma: correlations with pathological findings. J Gastroenterol. 2005;40(6):631–40.
45. Faccioli N, D'Onofrio M, Malagò R, Zamboni G, Falconi M, Capelli P, et al. Resectable pancreatic adenocarcinoma: depiction of tumoral margins at contrast-enhanced ultrasonography. Pancreas. 2008;37(3):265–8.
46. Grossjohann HS, Rappeport ED, Jensen C, Svendsen LB, Hillingsø JG, Hansen CP, et al. Usefulness of contrast-enhanced transabdominal ultrasound for tumor classification and tumor staging in the pancreatic head. Scand J Gastroenterol. 2010;45(7–8):917–24.
47. Vauthey J-N, Dixon E. AHPBA/SSO/SSAT Consensus conference on resectable and borderline resectable pancreatic cancer: rationale and overview of the conference. Ann Surg Oncol. 2009;16(7):1725–6.
48. Margaret T. NCCN guidelines: pancreatic adenocarcinoma. http://www.nccn.org/professionals/physician_gls/pdf/pancreatic.pdf. Accessed Mar 4 2014.
49. Fendrich V, Bartsch DK, Langer P, Zielke A, Rothmund M. Diagnosis and surgical treatment of insulinoma – experiences in 40 cases. Dtsch Med Wochenschr. 2004;129(17):941–6.
50. Norton JA, Cromack DT, Shawker TH, Doppman JL, Comi R, Gorden P, et al. Intraoperative ultrasonographic localization of islet cell tumors. A prospective comparison to palpation. Ann Surg. 1988;207(2):160–8.
51. Gorman B, Charboneau JW, James EM, Reading CC, Galiber AK, Grant CS, et al. Benign pancreatic insulinoma: preoperative and intraoperative sonographic localization. AJR Am J Roentgenol. 1986;147(5):929–34.
52. Grover AC, Skarulis M, Alexander HR, Pingpank JF, Javor ED, Chang R, et al. A prospective evaluation of laparoscopic exploration with intraoperative ultrasound as a technique for localizing sporadic insulinomas. Surgery. 2005;138(6):1003–8; discussion 1008.
53. Isla A, Arbuckle JD, Kekis PB, Lim A, Jackson JE, Todd JF, et al. Laparoscopic management of insulinomas. Br J Surg. 2009;96(2):185–90.
54. Huai JC, Zhang W, Niu HO, Su ZX, McNamara JJ, Machi J. Localization and surgical treatment of pancreatic insulinomas guided by intraoperative ultrasound. Am J Surg. 1998;175(1):18–21.
55. Grant CS, Van Heerden J, Charboneau JW, James EM, Reading CC. Insulinoma. The value of intraoperative ultrasonography. Arch Surg. 1988;123(7):843–8.
56. Hiramoto JS, Feldstein VA, LaBerge JM, Norton JA. Intraoperative ultrasound and preoperative localization detects all occult insulinomas. Arch Surg. 2001;136(9):1020–5; discussion 1025–6.
57. Akerström G, Hellman P. Surgery on neuroendocrine tumours. Best practice & research. Clin Endocrinol Metab. 2007;21(1):87–109.
58. Machi J, Oishi AJ, Furumoto NL, Oishi RH. Intraoperative ultrasound. Surg Clin North Am. 2004;84(4):1085–111, vi–i.
59. Buetow PC, Parrino TV, Buck JL, Pantongrag-Brown L, Ros PR, Dachman AH, et al. Islet cell tumors of the pancreas: pathologic-imaging correlation among size, necrosis and cysts, calcification, malignant behavior, and functional status. AJR Am J Roentgenol. 1995;165(5):1175–9.
60. King CM, Reznek RH, Dacie JE, Wass JA. Imaging islet cell tumours. Clin Radiol. 1994;49(5):295–303.
61. Buetow PC, Miller DL, Parrino TV, Buck JL. Islet cell tumors of the pancreas: clinical, radiologic, and pathologic correlation in diagnosis and localization. Radiographics. 1997;17(2):453–72; quiz 472A–B.
62. Service FJ, McMahon MM, O'Brien PC, Ballard DJ. Functioning insulinoma–incidence, recurrence, and long-term survival of patients: a 60-year study. Mayo Clinic Proc. 1991;66(7):711–9.
63. McLean AM, Fairclough PD. Endoscopic ultrasound in the localisation of pancreatic islet cell tumours. Best practice & research. Clin Endocrinol Metablism. 2005;19(2):177–93.
64. Malagò R, D'Onofrio M, Zamboni GA, Faccioli N, Falconi M, Boninsegna L, et al. Contrast-enhanced sonography of nonfunctioning pancreatic neuroendocrine tumors. AJR Am J Roentgenol. 2009;192(2):424–30.
65. D'Onofrio M, Vecchiato F, Faccioli N, Falconi M, Pozzi Mucelli R. Ultrasonography of the pancreas. 7. Intraoperative imaging. Abdom Imaging. 2007;32(2):200–6.

66. Dietrich CF, Braden B, Hocke M, Ott M, Ignee A. Improved characterisation of solitary solid pancreatic tumours using contrast enhanced transabdominal ultrasound. J Cancer Res Clin Oncol. 2008;134(6):635–43.
67. Sofuni A, Moriyasu F, Sano T, Yamada K, Itokawa F, Tsuchiya T, et al. The current potential of high-intensity focused ultrasound for pancreatic carcinoma. J Hepatobiliary Pancreat Sci. 2011;18(3):295–303.
68. Wu F, Wang Z-B, Zhu H, Chen W-Z, Zou J-Z, Bai J, et al. Feasibility of US-guided high-intensity focused ultrasound treatment in patients with advanced pancreatic cancer: initial experience. Radiology. 2005;236(3):1034–40.
69. Xiong LL, Hwang JH, Huang XB, Yao SS, He CJ, Ge XH, et al. Early clinical experience using high intensity focused ultrasound for palliation of inoperable pancreatic cancer. JOP. 2009;10(2):123–9.
70. Zhao H, Yang G, Wang D, Yu X, Zhang Y, Zhu J, et al. Concurrent gemcitabine and high-intensity focused ultrasound therapy in patients with locally advanced pancreatic cancer. Anticancer Drugs. 2010;21(4):447–52.
71. Alzaraa A, Gravante G, Chung WY, Al-Leswas D, Bruno M, Dennison AR, et al. Targeted microbubbles in the experimental and clinical setting. Am J Surg. 2012;204(3):355–66.
72. Goyal K, Einstein D, Ibarra RA, Yao M, Kunos C, Ellis R, et al. Stereotactic body radiation therapy for nonresectable tumors of the pancreas. J Surg Res. 2012;174(2):319–25.
73. Kim JH, Hong SS, Kim JH, Park HJ, Chang Y-W, Chang AR, et al. Safety and efficacy of ultrasound-guided fiducial marker implantation for CyberKnife radiation therapy. Korean J Radiol. 2012;13(3):307–13.
74. Rwigema J-CM, Heron DE, Parikh SD, Zeh HJ, Moser JA, Bahary N, et al. Adjuvant stereotactic body radiotherapy for resected pancreatic adenocarcinoma with close or positive margins. J Gastrointest Cancer. 2012;43(1):70–6.
75. Herman JM, Chang DT, Goodman KA, Wild AT, Laheru D, Zheng L, et al. A phase II multi-institutional study to evaluate gemcitabine and fractionated stereotactic body radiotherapy for unresectable, locally advanced pancreatic adenocarcinoma. ASCO Meeting Abstr. 2012;30(15_suppl):4045.
76. Lichtenstein DA. Whole body ultrasonography in the critically ill. Heidelberg: Springer; 2010.

Intraoperative Ultrasound During Laparoscopic Cholecystectomy

13

Ezra N. Teitelbaum and Nathaniel J. Soper

Abbreviations

CBD	Common bile duct
ERCP	Endoscopic retrograde cholangiopancreatography
IOC	Intraoperative cholangiography
LUS	Laparoscopic ultrasound

Introduction

Ultrasound has long been used as an anatomic and diagnostic guide during surgery of the liver and biliary tree. The introduction of B-mode ultrasound technology in the 1970s allowed for real-time viewing of two-dimensional sonographic images, which facilitated its use in a variety of contexts including open cholecystectomy to evaluate the common bile duct (CBD) for stones and define ductal and vascular anatomy [1–3]. However, due to the relative ease of access to tactile manipulation and exploration of the CBD, neither ultrasound nor intraoperative cholangiography (IOC) was routinely employed during cholecystectomy in the open surgical era. The rapid adoption of laparoscopic cholecystectomy in the early 1990s was initially associated with a sharp increase in the rate of CBD injury [4]. A call to remedy this increase in severe complications, in addition to the need for a reliable method for assessing for choledocholithiasis laparoscopically, brought about a renewed interest in both intraoperative laparoscopic ultrasound (LUS) and IOC. While debate still exists regarding the utility of these modalities in decreasing rates of CBD injury, there is no doubt that they are valuable tools that have advanced surgeons' understanding and appreciation of the anatomic relationships of the biliary tree when viewed and approached laparoscopically.

Currently, LUS and IOC each exist as excellent options for both detecting CBD stones and delineating anatomy during laparoscopic cholecystectomy. LUS offers several distinct advantages including a lack of radiation and contrast dye, the ability to perform repeat examinations without the need to cannulate the cystic duct, and comparatively superior time and cost-effectiveness. Additionally, because laparoscopy is a surface imaging modality, LUS allows an assessment of structures beyond the visible surface. This chapter describes the techniques for performing LUS during laparoscopic cholecystectomy and interpreting the resulting sonographic images and additionally provides a review of the available clinical data regarding its effectiveness in comparison with IOC.

Indications

The use of ultrasound during laparoscopic cholecystectomy serves two main functions: the identification of CBD stones and the examination and confirmation of biliary and vascular anatomy. LUS can be used selectively or in a routine fashion in regard to both functions. When applied in a selective manner (similar to selective IOC), LUS is employed when there is a preoperative or intraoperative suspicion of choledocholithiasis. This evaluation can be based on a number of preoperative factors, including jaundice, elevated bilirubin or transaminase levels, a dilated CBD or common duct stones seen on transabdominal ultrasound, or an elevated lipase level or history of gallstone pancreatitis. Intraoperatively, observation of a dilated CBD or cystic duct, and/or the presence of stones within the cystic duct, can also alert to the presence of choledocholithiasis. When applied selectively for anatomic identification, LUS is used when a question exists regarding the anatomic orientation of the hepatocystic triangle, to confirm the location of the CBD and common hepatic duct in relation to the plane of dissection, or to

E.N. Teitelbaum, MD (✉) • N.J. Soper, MD (✉)
Department of Surgery,
Northwestern University Feinberg School of Medicine,
251 E. Huron St., Galter 3-150,
Chicago, IL 60611, USA
e-mail: e-teitelbaum@northwestern.edu, nsoper@nmh.org

E.J. Hagopian, J. Machi (eds.), *Abdominal Ultrasound for Surgeons*,
DOI 10.1007/978-1-4614-9599-4_13,

confirm an aberrant ductal or vascular configuration that is identified during initial dissection.

We advocate a routine approach to the use of LUS during laparoscopic cholecystectomy, in which a LUS examination is performed during every case regardless of preoperative suspicion of choledocholithiasis or the ease of intraoperative anatomic identification. There are several advantages to a routine usage approach. It allows the surgeon to more quickly amass an extensive LUS experience and gain familiarity with the sonographic appearance of normal ductal anatomy. This allows for greater confidence in interpreting LUS images during difficult and potentially stressful cases, such as those with inflammatory conditions or aberrant anatomy. If surgical residents are assisting in the cases, routine use gives them increased exposure to the techniques of LUS and allows for enhanced cognitive correlation of the anatomy seen laparoscopically with a second visualization modality. Additionally, a protocol of routine LUS use allows the other operating room staff to become familiar with the procedure and guarantees that the necessary equipment will be available for every case.

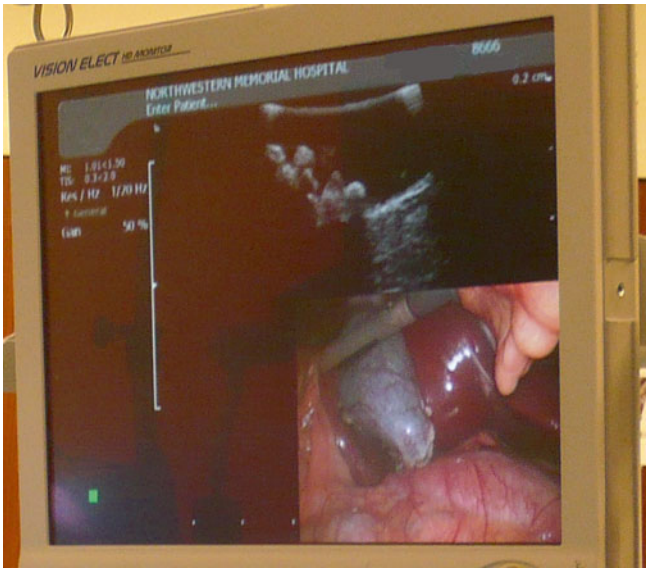

Fig. 13.1 The operating room monitor is configured to show the sonographic and laparoscopic images simultaneously in a "picture-in-picture" view

Equipment

Modern laparoscopic ultrasound probes are designed to enable efficient and reliable intraoperative use. Several probes with a 10 mm diameter that can be inserted through standard 10 or 11 mm laparoscopic trocars are commercially available [5]. These probes use primarily B-mode (i.e., two-dimensional) ultrasound with frequencies between 5 and 10 MHz [6]. Seven and 7.5 MHz are the most commonly used frequencies during laparoscopic evaluation of the biliary system. A linear or curvilinear ultrasound array between 3 and 7 cm in length is optimal.

Probes with both vertically and horizontally deflectable tips are helpful in obtaining variable viewing angles and most incorporate Doppler sonography to simultaneously overlay flow measurements onto the primary sonographic image. This feature is useful in differentiating between bile ducts and adjacent vasculature, especially when imaging the biliary tree proximal to the bifurcation of the common hepatic duct and proper hepatic artery. Modern probes can be sterilized after each usage, obviating the need for sterile probe covers, which can tear causing contamination of the operative field and are often difficult to introduce through laparoscopic trocars.

Essential to efficient use of LUS is an endoscopic operating suite equipped to transmit two images to the viewing monitors simultaneously, in a "picture-in-picture" display (Fig. 13.1). This allows the surgeon to correlate the ultrasound images with their anatomic position laparoscopically, as well as efficiently maneuver the LUS probe in the operative field. Additionally, the ability to record both the laparoscopic and sonographic images is helpful for medical documentation and retrospective teaching purposes.

LUS Technique

Initial Dissection

Although some authors have described the use of LUS during laparoscopic cholecystectomy immediately upon establishment of pneumoperitoneum, during routine cases we prefer to perform an initial dissection of the hepatocystic triangle prior to sonographic examination. Using a standard four-port technique, a combination of blunt and electrocautery dissection is used to remove all of the fibrous and fatty tissue from the hepatocystic triangle in order to establish a "critical view of safety" [7]. Reserving use of LUS until after this dissection has been performed offers several advantages. The most important is that a meticulous and thorough dissection is the most essential means to preventing CBD injury [4]. By completing this dissection prior to the LUS examination, the surgeon does not run the risk of being misled by a seemingly normal anatomic configuration on ultrasound. Additionally, opening the hepatocystic triangle via dissection allows for an easier and more complete LUS examination. The gallbladder is freed from the inferior aspects of its peritoneal attachments to the liver bed, enabling retraction of the infundibulum further laterally from the cystic duct-CBD junction. This allows for easier LUS identification and delineation of the ductal structures and enables the surgeon to manipulate the

infundibulum with more mobility during LUS to create a variety of viewing angles.

If there is uncertainty regarding the anatomy during the course of the dissection to create a "critical view," LUS can be employed earlier to examine the ducts in relation to the area in question. In the case of a difficult or confusing dissection, LUS and IOC can be employed conjointly to establish a more robust anatomic examination. However, LUS and IOC should be only considered tools that provide additional information, rather than definitive evaluations. If any uncertainty exists regarding the anatomic relationships of the critical ductal and/or vascular structures after the use of these modalities, the surgeon should not hesitate to convert to an open procedure in order to ensure optimal safety.

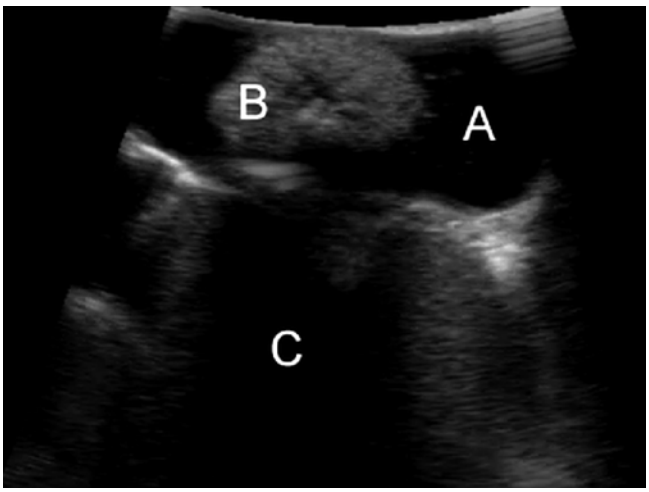

Fig. 13.2 The gallbladder is imaged, showing anechoic gallbladder fluid (*A*), a large hyperechoic stone (*B*), and sonographic shadowing (*C*) created by the stone

Intraoperative Scanning

Once a dissection to a "critical view" has been completed, the ultrasound probe is connected to the scanner and the monitors are switched to a "picture-in-picture" view. Using the standard "American" four-port configuration, the ultrasound probe can be introduced through either the epigastric or umbilical trocar. While we prefer the epigastric technique, each method has its own advantages and disadvantages. Often when a certain structure or segment of the CBD cannot be visualized via one trocar, the probe position must be switched, and some authors have advocated routine imaging from both orientations in every case. While we have found this to be infrequently necessary, surgeons must have a good familiarity with both techniques.

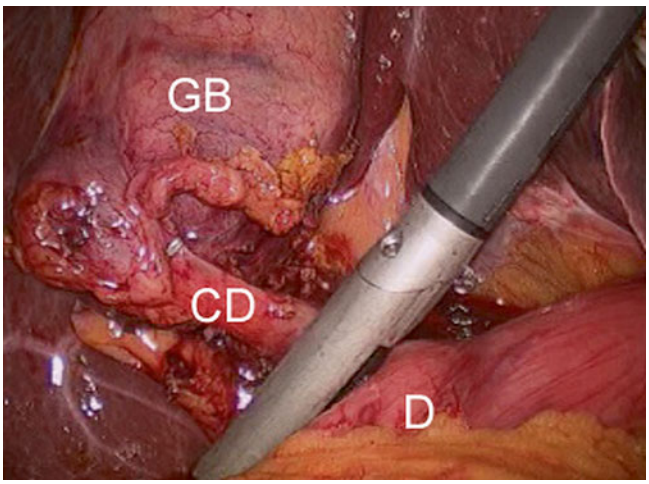

Fig. 13.3 The starting position for imaging the biliary tree when scanning through the epigastric trocar. The probe is placed over the midportion of hepatoduodenal ligament, superior to the duodenum (*D*) and inferior to the cystic duct (*CD*) and gallbladder (*GB*)

Epigastric Scanning Technique

When scanning through the epigastric trocar, the surgeon stands on the patient's left side and manipulates the probe with his or her right hand while the left hand retracts the gallbladder infundibulum using a grasper placed through the more medial of the two right-subcostal trocars. The assistant retracts the gallbladder fundus superiorly over the liver through the lateral subcostal trocar and operates the camera. The probe is inserted in the direction of the gallbladder, with the scanning array facing posteriorly. It is helpful to hold the probe with your index finger positioned on the side opposite to the scanning array in order to maintain spatial orientation during subsequent probe maneuvering.

The probe is first positioned directly over the gallbladder wall. The sonographic depth of field and gain can then be adjusted to optimize the image. Fluid inside the gallbladder should appear anechoic (i.e., black), and any stones should be hyperechoic (i.e., white) and create "shadowing" in the sonographic field beyond their location (Fig. 13.2). When scanning through the gallbladder, other pathology such as polyps can be identified. In contrast to stones, polyps will appear less hyperechoic, will not create shadowing, and will not fall to a dependent location within the gallbladder. (Refer to Chap. 5 for more detail.)

Once the sonographic view has been fine-tuned and the gallbladder inspected, the probe is placed over the midportion of the hepatoduodenal ligament with the scanning array facing posteriorly (Fig. 13.3). The probe is then manipulated in order to visualize the portal triad structures: the CBD, proper hepatic artery, and portal vein. The probe is positioned perpendicular to the hepatoduodenal ligament, and as a result, all three structures are seen in a transverse orientation and appear as circles on the sonographic image. The CBD and

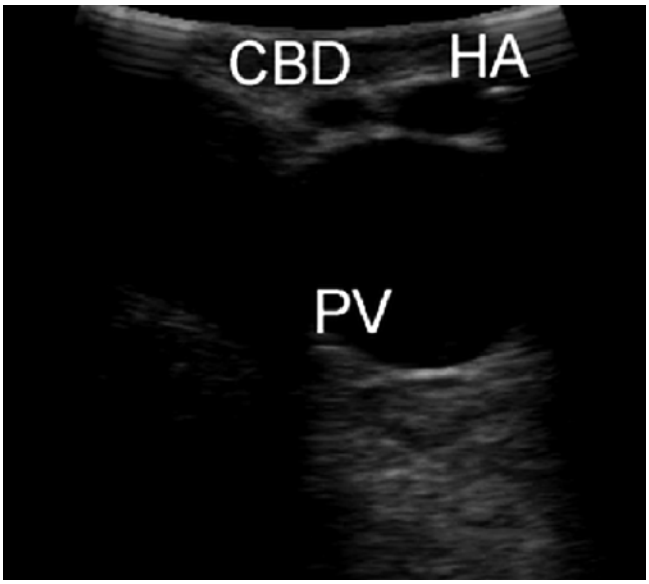

Fig. 13.4 The portal triad is visualized, creating a "Mickey Mouse head" appearance of the common bile duct (*CBD*) and proper hepatic artery (*HA*) anteriorly and portal vein (*PV*) posteriorly, all seen in transverse section

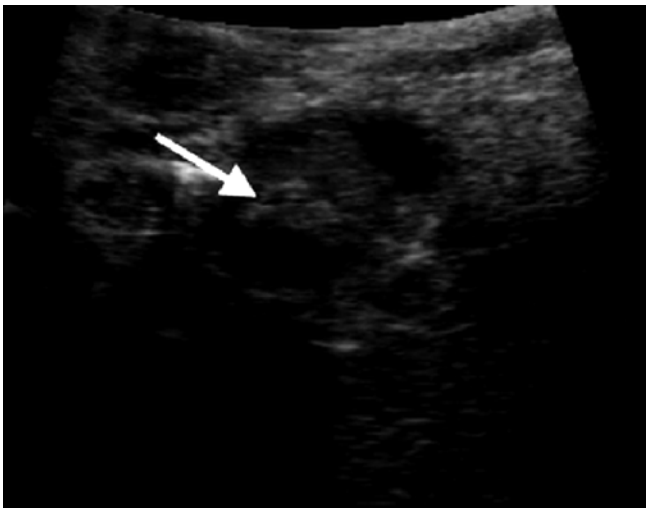

Fig. 13.5 A hyperechoic stone (*arrow*) visualized within the common bile duct

hepatic artery are usually smaller in diameter and aligned in the same anterior-posterior plane, ventral to the larger portal vein. This normal configuration creates a so-called Mickey Mouse head sonographic appearance (Fig. 13.4).

The probe is then moved caudad down the hepatoduodenal ligament and toward the duodenum in order to scan the length of the CBD. During this step the surgeon should manipulate the probe slowly, while only moving in a single plane without rotation. This will allow for visualization of the entire length of the suprapancreatic CBD and minimize the risk of skipping over a segment of duct that contains a stone. The probe should rest gently on the hepatoduodenal ligament during this step. If too much pressure is applied, the CBD will be compressed and obscured from view. Conversely, if the probe is lifted off the surface of the ligament, the acoustic window and sonographic image will be lost. This can be an issue in very thin patients in whom the hepatoduodenal ligament is devoid of fat. To remedy this problem, saline can be infused to flood the right upper quadrant and act as an acoustic coupler in order to create a better acoustic window [8]. However, in actual practice we have found this to be rarely necessary, as well as additionally time consuming.

As the CBD is sequentially imaged, the surgeon should be primarily looking for intraductal stones and sludge. Stones appear intensely hyperechoic and create acoustic shadowing on the side opposite to the scanning array (i.e., toward the bottom side of the sonographic image) (Fig. 13.5). Once detected, the diameter of a stone can be measured using the sonographic calipers function. This can be helpful in determining the most effective means of stone removal via laparoscopic or open CBD exploration or endoscopic retrograde cholangiopancreatography (ERCP). Sludge is defined as echogenic intraductal debris consisting of particles less than 1 mm in diameter and does not usually result in shadowing [9]. During our initial experience with LUS, we would attempt to treat all findings of CBD sludge with flushing via a catheter introduced into the cystic duct [10]. However, we have found this sludge to most often be of no clinical consequence and now reserve intervention for cases in which it is causing biliary obstruction or pancreatitis [11].

After imaging of its suprapancreatic portion, the CBD is followed distally as it enters the pancreatic parenchyma. As the CBD enters the pancreas, its path deviates to the patient's right side, toward the ampulla of Vater. In order to follow the duct along this course, the LUS probe is held in a stationary position abutting the superior edge of the duodenum and slowly rotated in a clockwise direction. With this motion, the CBD should be kept in a transverse orientation on the sonographic image (Fig. 13.6). The duct should be followed until its entrance into the duodenum. The muscular sphincter of the ampulla can be seen as a hypoechoic ring surrounding the distal most segment of the duct (Fig. 13.7). Additionally, the pancreatic duct can often be seen traversing the pancreas inferior to the CBD. In certain patients a long common segment of CBD-pancreatic duct exists and can be documented sonographically, which may predispose to the development of gallstone pancreatitis.

Pancreatic tissue is relatively hyperechoic compared with the fatty tissue of the hepatoduodenal ligament. This can make detection of CBD stones more difficult in the ductal segment within the pancreas. In many series, rates of complete visualization and stone detection in the intrapancreatic (distal) CBD are lower than the suprapancreatic portion, and

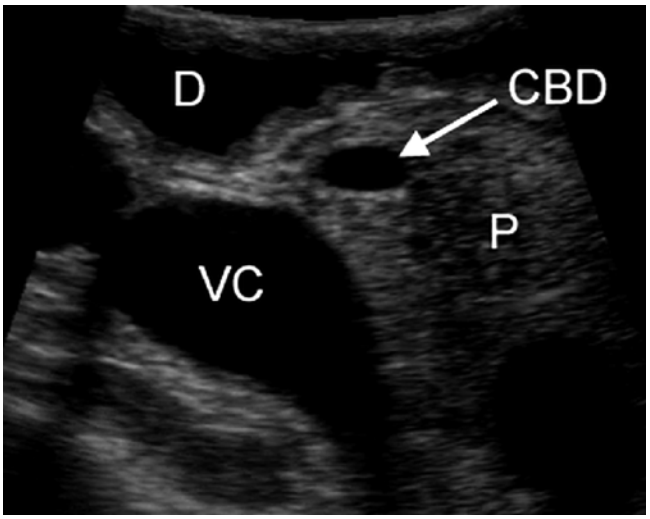

Fig. 13.6 The common bile duct (*CBD*) is seen transversing the relatively hyperechoic pancreatic parenchyma (*P*). The duodenum (*D*) anteriorly and inferior vena cava (*VC*) posteriorly are also visualized

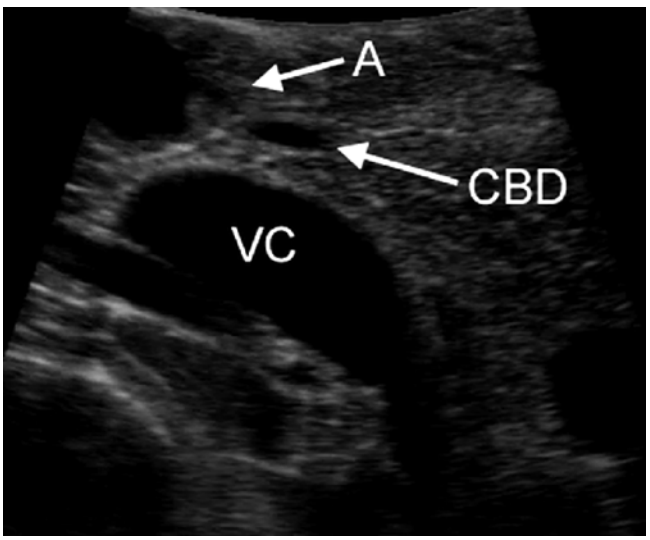

Fig. 13.7 The distal common bile duct (*CBD*) is seen just as it enters the duodenum through the ampulla of Vater (*A*). The inferior vena cava (*VC*) is seen posterior to the pancreas

some authors have described imaging of the distal CBD as the "Achilles heel" of LUS during laparoscopic cholecystectomy [12–14]. If visualization of the distal CBD is inadequate, several maneuvers can be performed to improve the image quality. Usually, simply placing the LUS probe directly on the duodenum with the transducer directed posteriorly and scanning while exerting gentle downward pressure (to displace air) will result in excellent imaging of the intrapancreatic CBD. If this maneuver does not provide adequate visualization, saline can be instilled into the stomach and duodenum via a nasogastric tube, creating a better acoustic window. The probe can also be repositioned through the

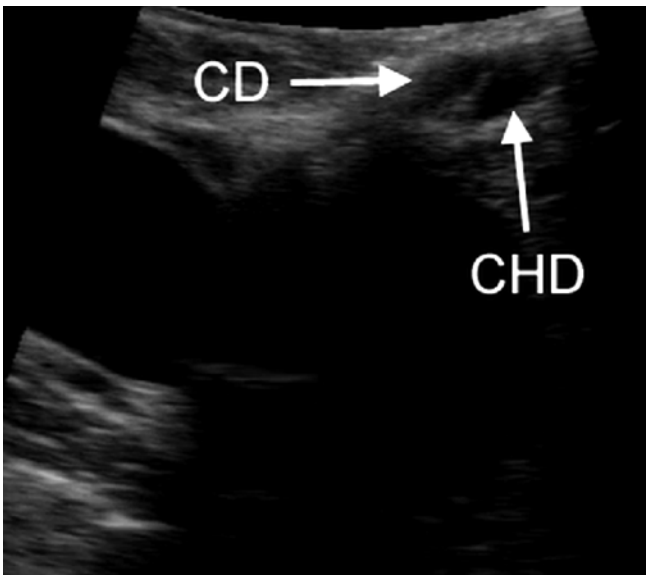

Fig. 13.8 The cystic duct (*CD*) and common hepatic duct (*CHD*) are imaged just as they join to form the common bile duct

umbilical trocar if epigastric visualization is insufficient. In patients with a narrow CBD, saline can be injected into the duct via a catheter introduced through a cystic ductotomy. This acts to dilate the CBD and may enable better visualization of distal CBD stones but requires the same ductotomy and cannulation as an IOC.

After the entire length of the CBD has been satisfactorily evaluated for the presence of stones, attention is turned to examining the anatomy of the hepatocystic triangle. The probe is returned to its original position above the hepatoduodenal ligament and then moved cephalad until the junction between the CBD and cystic duct is visualized (Fig. 13.8). The location of this junction is noted on the laparoscopic image to ensure that the anatomic assumptions made after the initial dissection to a "critical view of safety" were in fact correct. LUS can also be used to measure the length of the cystic duct, to ensure adequate space for clip application. To do this, the gallbladder infundibulum is retracted laterally, to orient the cystic duct perpendicular to the CBD. A longitudinal image of the cystic duct can occasionally be obtained and its length measured directly using the sonographic caliper function. If the anatomy does not allow for a longitudinal view, the cystic duct length can be estimated by flooding the right upper quadrant with saline and scanning down the gallbladder in transverse section until the transition from infundibulum to narrow cystic duct is observed. The distance from this point (i.e., the origin of the cystic duct) to the transverse image of the CBD to the right of the sonographic image is then measured. Using this technique, a study determined the measured cystic duct length to be within 5 mm of the length determined by either IOC or complete dissection of the cystic duct to the CBD junction in 87 % of cases [15].

After examining the cystic duct and cystic-CBD junction, the probe is slid further cephalad to visualize the common hepatic duct and right and left hepatic ducts. Often during this step the liver edge obstructs the probe when scanning through the epigastric trocar. If this occurs, the probe tip can be flexed to the right to create a longitudinal view of the hepatic ducts.

Umbilical Scanning Technique

In contrast to the transverse views seen when scanning through the epigastric trocar, the umbilical technique creates longitudinal images of the CBD. This allows for entire segments of the duct to be viewed simultaneously, and for this reason it is the preferred technique of many authors [12, 13]. However, scanning from an umbilical position requires removal and reinsertion of the laparoscope through the epigastric trocar. With the laparoscope viewing cephalad to caudad and the monitors positioned toward the head of the table, the movements of the probe are seen in a "mirror image" and are counterintuitive. This makes probe maneuvering awkward, especially for those new to the technique, and can therefore lengthen the time required to perform the examination. For this reason we prefer epigastric scanning, although surgeons should become proficient in both techniques as often a certain segment of the CBD cannot be viewed via the initial approach.

Umbilical scanning begins with the gallbladder released from both fundal and infundibular retraction. The probe is positioned over the liver and the gallbladder is visualized using segment V as an acoustic window. As in the epigastric technique, this view is used to adjust the sonographic image and the gallbladder is examined for stones and polyps. The probe is then moved medially over liver segment IV and the confluence of the hepatic ducts and hepatic arteries is visualized. Use of Doppler mode to identify arterial flow can be helpful in orienting the anatomy proximal to the branching of these structures.

Once the common hepatic duct has been identified, it is examined for stones and sludge. With the probe entering through the umbilical trocar, the hepatic duct and CBD will be seen in longitudinal section (Fig. 13.9). The more proximal portion of the duct will appear toward the left side of the sonographic image using typical settings. In order to examine the entire width of the ducts, the probe is slowly rotated back and forth. Once a segment of the duct has been scanned in its entirety, the probe is slid caudad in order to scan distally. As the CBD enters the pancreatic head, its sonographic image will switch from longitudinal to oblique, as the duct curves to the patient's right side and into the duodenum.

Once the CBD has been scanned completely for stones, the anatomy of the cystic duct-CBD junction is examined. To obtain this view, the gallbladder should be regrasped and the infundibulum retracted laterally. From the umbilical trocar, the cystic duct can be seen in transverse section and followed along its length. It can be more difficult to identify the cystic-CBD junction using the umbilical scanning technique because often the two structures cannot be visualized concurrently. This can be remedied by deflecting the probe tip to the left in order to obtain an image of both the cystic duct and CBD in transverse section, in a sense replicating the view obtained via epigastric scanning.

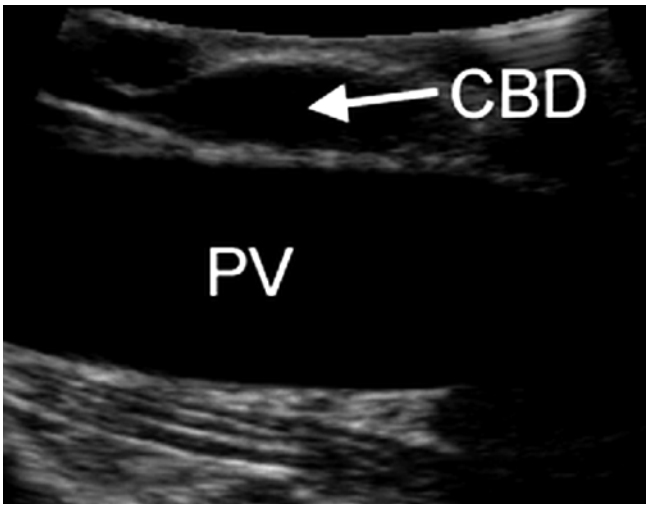

Fig. 13.9 The common bile duct (*CBD*) and portal vein (*PV*) seen in longitudinal section when scanning through the umbilical trocar

Clinical Outcomes and Comparison with IOC

As LUS and IOC are generally used for the same two purposes, detecting CBD stones and identifying biliary anatomy, it is natural that the two modalities should be compared in regard to their efficacy in these tasks. However, while it is necessary to know the relative strengths and weaknesses of each technique, surgeons should not become solely reliant on one or the other. In many instances it is necessary to use both imaging methods during a single operation in order to confirm the presence of choledocholithiasis or interpret confusing or aberrant anatomy. For this reason, routine practice with both methods is recommended, especially during a surgeon's early experience and when teaching surgical trainees.

LUS has several discrete advantages as compared with IOC. LUS does not use x-rays and thus can be performed safely during pregnancy, does not expose operating room personnel to potentially harmful radiation, and does not require assistance from a dedicated radiology technician. No contrast dye is used, which may contraindicate IOC for patients with iodine allergies. IOC also requires cannulation

Table 13.1 Success rates, LUS vs. IOC

		Success rate (%)		Time (min)	
Study	Number	LUS	IOC	LUS	IOC
Siperstein et al. [16]	300	100	94	–	–
Thompson et al. [17]	306	–	–	7	11
Machi et al. [14]	100	95	92	9	16
Birth et al. [12]	518	>99	92	7	16
Catheline et al. [18]	900	100	85	10	18
Tranter et al. [19]	135	98	90	–	–

Table 13.2 Success rates, detection of CBD stones

	Number	Sensitivity (%)		Specificity (%)	
Study		LUS	IOC	LUS	IOC
Siperstein et al. [16]	300	96	96	100	100
Thompson et al. [17]	360	90	98	100	98
Machi et al. [14]	100	89	88	100	98
Birth et al. [12]	518	83	100	100	99
Catheline et al. [18]	900	80	75	99	99
Tranter et al. [19]	135	96	86	100	99

of the cystic duct and therefore poses a risk of CBD injury if the biliary anatomy has been misinterpreted on initial dissection. LUS, on the other hand, is essentially without complication risk and unlike IOC can easily be performed multiple times during an operation to reassess the anatomy as dissection proceeds. In contrast, IOC generally affords a more comprehensive "road map" of biliary anatomy and is the first technical step in performing a laparoscopic common bile duct exploration.

In general, LUS has greater feasibility than IOC, with rates of scanning success approaching 100 % with experience (Table 13.1). Reported failures are generally due only to malfunctioning equipment, whereas IOC has a defined failure rate of approximately 10 % due to inability to cannulate small cystic ducts and obstruction of contrast passage due to cystic duct valves or tortuosity. In studies comparing the two modalities, LUS has been shown uniformly to have shorter completion times [12, 14, 17, 18].

Detection of CBD Stones

Several studies have evaluated the relative success of LUS and IOC for detecting CBD stones (Table 13.2). While both LUS and IOC were performed on each patient in these studies and the findings compared, there are still several methodological issues that must be taken into account when evaluating their results. The most important is the absence of a gold standard examination with which to compare the respective modalities and verify either the true presence or absence of stones. These authors assumed that a negative result on both LUS and IOC is indicative of a true absence of CBD stones, barring later clinical presentation of a missed stone. This assumption has the potential to underestimate the number of false-negative exams, as missed stones can pass without causing symptoms. In most studies, a positive exam (on either LUS or IOC) was investigated via either surgical CBD exploration or ERCP, in order to confirm the result and clear the duct. This methodology however has the potential to overestimate the number of false positives, as CBD stones detected intraoperatively may have passed by the time of the CBD exploration or ERCP. Additionally, in the majority of studies, the surgeon viewed both exams without blinding, thus potentially influencing the performance and interpretation of the second test (in most cases IOC) in the instance of a positive initial result. One should evaluate the following data with these limitations in mind.

Sensitivity for detecting CBD stones ranges from 80 to 96 % for LUS and 75–100 % for IOC depending on the study [12, 14, 16–19]. It is instructive to take a closer look at several of the series that found LUS to be less sensitive than IOC. Thompson and colleagues found a cumulative sensitivity of 90 % with LUS, as compared with 98 % for IOC [17]. However, when the authors subdivided their series into three time periods, they found a sensitivity of 77 % for LUS in the first cohort of 140 patients, as compared to 100 and 96 % in the latter 78 and 142 patients. This improvement was primarily due to better detection of stones in the intrapancreatic portion of the distal CBD. During the second patient cohort, the authors routinely cannulated the cystic duct and injected saline in order to dilate the CBD. In the third group of patients, the authors performed this maneuver on a selective basis, only when the distal CBD could not be adequately visualized on initial examination.

Birth and colleagues found a sensitivity of 83 % for LUS, as opposed to 100 % for IOC [12]. Similar to the previously discussed study, all of the four stones missed by LUS were in a preampullary position in the distal CBD. Three of these missed stones were visualizable by LUS after instilling 400 ml of saline into the stomach and duodenum via a nasogastric tube. However, the authors still counted these as false negatives, as they were initially missed by LUS and only discovered after performing an IOC. The results of these two studies show that both increased operator experience and adjunct maneuvers to improve distal CBD imaging can increase LUS sensitivity to a level equal or superior to IOC. However, surgeons should keep in mind that imaging the distal CBD can be a challenging aspect of LUS. If the intrapancreatic portion of the duct cannot be clearly examined, an IOC should be performed to confirm the absence of stones.

Although both modalities are highly specific in the detection of CBD stones, LUS is superior to IOC in this respect, with a nearly zero incidence of false positives. Although rare, false-positive results do occur during IOC, primarily

due to the misinterpretation of air bubbles in the CBD as stones. For this reason, some authors have proposed using LUS as a confirmatory test when a CBD stone is detected on IOC [20].

Examination of Anatomy

In general, IOC provides a better delineation of biliary anatomy than LUS. This is because IOC allows the surgeon to simultaneously visualize the entire biliary tree, so that presumed relationship of the cystic duct with the hepatic and common bile ducts can be confirmed. In contrast, LUS is only able to visualize a single cross-sectional plane at a time. A complete view of the biliary anatomy must therefore be mentally constructed by correlating these two-dimensional images with their position laparoscopically. This can be challenging, especially in cases with severe inflammation or aberrant anatomic configurations. One study found that LUS was only able to detect 82 % of the anatomic anomalies found on IOC [21]. Another showed that IOC showed variant anatomy in 14 % of cases, but LUS was unable to visualize any of these [22]. While most of these variants were in the proximal biliary tree, above the cystic duct-CBD junction, these findings caution the use of LUS for interpretation of unknown or confusing anatomy. Our preference is to use IOC during cases in which a difficult dissection or unusual anatomy makes identification of the ductal relationships uncertain.

LUS does however provide several advantages over IOC with regard to anatomic examination. The ability to overlay color Doppler signaling on the sonographic image can be extremely helpful in delineating vascular from ductal structures. This can aid in confirming variations in arterial anatomy, such as a replaced right hepatic artery, that could be potentially injured during dissection of the hepatocystic triangle. LUS also provides a more accurate measure of distance than IOC, important in reliably determining ductal diameters, stone size, and the interval between two anatomic structures. In general, IOC tends to overestimate the true diameter of the CBD due to dilation after contrast injection, blurring of duct edges, and the lack of a reliable reference length on the same plane as the duct [12]. Lastly, LUS does not require cystic duct cannulation and can be used multiple times throughout an operation. These characteristics often make its use advantageous to IOC during cases of severe cholecystitis, if the ductal structures cannot be easily identified early in the dissection [23].

Several studies have addressed the issue of whether the use of routine LUS for anatomic identification leads to a decrease in rates of CBD injury and other biliary complications. Similar to IOC, there is only circumstantial evidence regarding this assertion, and the ability of either routine imaging modality to decrease CBD injury remains controversial even after 20 years of debate and study. Biffl and colleagues compared rates of biliary complications at a single institution in which two surgeons used LUS on a routine basis while the other three surgeons used IOC selectively [24]. The routine LUS group had no biliary complications, whereas the non-LUS surgeons had a 2.5 % biliary complication rate, including a 0.8 % rate of CBD injury and 0.7 % rate of retained CBD stones. This disparity occurred despite the fact that the non-LUS surgeons performed more operations on average, with a lower percentage of patients operated on for acute cholecystitis. Another multicenter study showed that over a series of 1,381 laparoscopic cholecystectomies with routine LUS, no CBD injuries occurred [25]. In these cases, use of LUS to delineate biliary anatomy was able to prevent conversion to open surgery in 6 % of cases. Additionally, the authors found that supplementary IOC was only truly necessary in 2 % of the cases.

Cost

While patient safety and the avoidance of biliary complications should be the primary concerns when evaluating the use of LUS or IOC, the cost associated with these modalities is an important secondary consideration, especially if they are to be employed on a routine basis. Although the initial purchase cost of an ultrasound scanner is substantial, it can be used during a multitude of operations across several surgical subspecialties. Several studies have shown LUS to be less expensive than IOC on a per-case basis, primarily due to the use of disposable catheters and the cost of a radiology technician during IOC. One study found that LUS cost on average $131, as opposed to $408 for IOC [26]. The authors calculated that even if IOC was used on a selective basis, its cost would average out to $157 per cholecystectomy performed and thus still be more expensive than routine LUS. Another study found a per-case cost of $362 and $665 for LUS and IOC, respectively, and that based on this differential, the cost of the ultrasound scanner itself would be recouped after 95 uses [27]. An examination of our own data based on disposable equipment and additional operating time required showed a cost savings of $145 per case with LUS as compared with IOC [10].

Conclusion

LUS provides an excellent means of examining the biliary tree during laparoscopic cholecystectomy, with the primary goals of defining anatomic relationships and detecting choledocholithiasis. Beyond achieving these objectives, LUS allows the surgeon to look within the hepatocystic triangle and the hepatoduodenal ligament prior to and during the progression of surgical dissection. This allows for a more in depth understanding of the often

disorienting and potentially dangerous two-dimensional laparoscopic view of these complex anatomic structures. For this reason, we employ LUS in a routine fashion and make a point of incorporating its use into the curriculum for medical students and surgical residents. While LUS offers many advantages over IOC, the two modalities should be seen as complementary. Whether utilized in a routine or selective manner, it is essential for the modern laparoscopic surgeon to have a familiarity and facility with both techniques, in order to optimize patient safety and streamline the detection and treatment of CBD stones during laparoscopic cholecystectomy.

References

1. Lane RJ, Coupland GA. Ultrasonic indications to explore the common bile duct. Surgery. 1982;91(3):268–74.
2. Sigel B, Machi J, Beitler JC, Donahue PE, Bombeck CT, Baker RJ, et al. Comparative accuracy of operative ultrasonography and cholangiography in detecting common duct calculi. Surgery. 1983;94(4):715–20.
3. Jakimowicz JJ, Rutten H, Jurgens PJ, Carol EJ. Comparison of operative ultrasonography and radiography in screening of the common bile duct for calculi. World J Surg. 1987;11(5):628–34.
4. Strasberg SM, Hertl M, Soper NJ. An analysis of the problem of biliary injury during laparoscopic cholecystectomy. J Am Coll Surg. 1995;180(1):101–25.
5. Hakamada K, Narumi S, Toyoki Y, Nara M, Oohashi M, Miura T, et al. Intraoperative ultrasound as an educational guide for laparoscopic biliary surgery. World J Gastroenterol. 2008;14(15):2370–6.
6. Soper NJ. The utility of ultrasonography for screening the common bile duct during laparoscopic cholecystectomy. J Laparoendosc Adv Surg Tech A. 1997;7(5):271–6.
7. Strasberg SM, Brunt LM. Rationale and use of the critical view of safety in laparoscopic cholecystectomy. J Am Coll Surg. 2010;211(1):132–8.
8. Perry KA, Myers JA, Deziel DJ. Laparoscopic ultrasound as the primary method for bile duct imaging during cholecystectomy. Surg Endosc. 2008;22(1):208–13.
9. Santambrogio R, Bianchi P, Opocher E, Verga M, Montorsi M. Prevalence and laparoscopic ultrasound patterns of choledocholithiasis and biliary sludge during cholecystectomy. Surg Laparosc Endosc Percutan Tech. 1999;9(2):129–34.
10. Wu JS, Dunnegan DL, Soper NJ. The utility of intracorporeal ultrasonography for screening of the bile duct during laparoscopic cholecystectomy. J Gastrointest Surg. 1998;2(1):50–60.
11. Halpin VJ, Dunnegan D, Soper NJ. Laparoscopic intracorporeal ultrasound versus fluoroscopic intraoperative cholangiography: after the learning curve. Surg Endosc. 2002;16(2):336–41.
12. Birth M, Ehlers KU, Delinikolas K, Weiser HF. Prospective randomized comparison of laparoscopic ultrasonography using a flexible-tip ultrasound probe and intraoperative dynamic cholangiography during laparoscopic cholecystectomy. Surg Endosc. 1998;12(1):30–6.
13. Catheline JM, Turner R, Rizk N, Barrat C, Buenos P, Champault G. Evaluation of the biliary tree during laparoscopic cholecystectomy: laparoscopic ultrasound versus intraoperative cholangiography: a prospective study of 150 cases. Surg Laparosc Endosc. 1998;8(2):85–91.
14. Machi J, Tateishi T, Oishi AJ, Furumoto NL, Oishi RH, Uchida S, et al. Laparoscopic ultrasonography versus operative cholangiography during laparoscopic cholecystectomy: review of the literature and a comparison with open intraoperative ultrasonography. J Am Coll Surg. 1999;188(4):360–7.
15. Tomonaga T, Filipi CJ, Lowham A, Martinez T. Laparoscopic intracorporeal ultrasound cystic duct length measurement: a new technique to prevent common bile duct injuries. Surg Endosc. 1999;13(2):183–5.
16. Siperstein A, Pearl J, Macho J, Hansen P, Gitomirsky A, Rogers S. Comparison of laparoscopic ultrasonography and fluorocholangiography in 300 patients undergoing laparoscopic cholecystectomy. Surg Endosc. 1999;13(2):113–7.
17. Thompson DM, Arregui ME, Tetik C, Madden MT, Wegener M. A comparison of laparoscopic ultrasound with digital fluorocholangiography for detecting choledocholithiasis during laparoscopic cholecystectomy. Surg Endosc. 1998;12(7):929–32.
18. Catheline JM, Turner R, Paries J. Laparoscopic ultrasonography is a complement to cholangiography for the detection of choledocholithiasis at laparoscopic cholecystectomy. Br J Surg. 2002;89(10):1235–9.
19. Tranter SE, Thompson MH. A prospective single-blinded controlled study comparing laparoscopic ultrasound of the common bile duct with operative cholangiography. Surg Endosc. 2003;17(2):216–9.
20. Kimura T, Umehara Y, Yoshida M, Sakuramachi S, Kawabe A, Suzuki K. Laparoscopic ultrasonography and operative cholangiography prevent residual common bile duct stones in laparoscopic cholecystectomy. Surg Laparosc Endosc Percutan Tech. 1999;9(2):124–8.
21. Rothlin M, Largiader F. The anatomy of the hepatoduodenal ligament in laparoscopic sonography. Surg Endosc. 1994;8(3):173–80.
22. Teefey SA, Soper NJ, Middleton WD, Balfe DM, Brink JA, Strasberg SM, et al. Imaging of the common bile duct during laparoscopic cholecystectomy: sonography versus videofluoroscopic cholangiography. AJR Am J Roentgenol. 1995;165(4):847–51.
23. Pfluke JM, Bowers Jr SP. Laparoscopic intraoperative biliary ultrasonography: findings during laparoscopic cholecystectomy for acute disease. J Laparoendosc Adv Surg Tech A. 2011;21(6):505–9.
24. Biffl WL, Moore EE, Offner PJ, Franciose RJ, Burch JM. Routine intraoperative laparoscopic ultrasonography with selective cholangiography reduces bile duct complications during laparoscopic cholecystectomy. J Am Coll Surg. 2001;193(3):272–80.
25. Machi J, Johnson JO, Deziel DJ, Soper NJ, Berber E, Siperstein A, et al. The routine use of laparoscopic ultrasound decreases bile duct injury: a multicenter study. Surg Endosc. 2009;23(2):384–8.
26. Machi J, Oishi AJ, Tajiri T, Murayama KM, Furumoto NL, Oishi RH. Routine laparoscopic ultrasound can significantly reduce the need for selective intraoperative cholangiography during cholecystectomy. Surg Endosc. 2007;21(2):270–4.
27. Falcone Jr RA, Fegelman EJ, Nussbaum MS, Brown DL, Bebbe TM, Merhar GL, et al. A prospective comparison of laparoscopic ultrasound vs intraoperative cholangiogram during laparoscopic cholecystectomy. Surg Endosc. 1999;13(8):784–8.

Intraoperative Ultrasound During Biliary Tract Surgery

14

Ewen M. Harrison and O. James Garden

Introduction

The use of ultrasonography during biliary surgery was first proposed in the mid-1960s by Knight in the UK and Eiseman in the United States [1, 2]. These pioneers made use of A-mode ultrasonography which is unidirectional with the signal displayed on an oscilloscope. These were notoriously difficult to interpret with Eiseman noting:

> Small stones may be overlooked unless the surgeon is alert to rescan any suspicious "pips" and to observe the oscilloscopic deflection as the probe closes on the point under question.

Yet, many of the difficulties described are similar to those faced today, with duodenal air making it "particularly difficult to interpret signals from the ampullary region of the duct" and the need for care "in using the intraluminal probe to avoid air bubbles within the duct … [as] the sonar reflections of intraductile bubbles are similar to calculi". The development of B-mode ultrasonography in the 1980s saw a dramatic improvement in quality, with two-dimensional images conveying for the first time the structure of the underlying organs [3]. This aided interpretation and allowed the recording of findings with Polaroid images. While the main driver of these innovations was the need to identify common bile duct calculi, the low resolution of preoperative imaging left the surgeon making important intraoperative decisions regarding the nature of common bile duct lesions and the nature or degree of infiltration of pancreatic lesions. Intraoperative cholangiography was in common use, was effective and was usually straightforward to perform. It may not be surprising that intraoperative ultrasonography was not widely employed, given the relative ease with which the anatomy could be delineated with cholangiography.

In more recent years, two factors have acted to rekindle an interest in operative ultrasonography: the development of hepato-pancreaticobiliary surgery as a specialty with a widening range of operative procedures and aggressive strategies to manage cancer, and the development of laparoscopic surgery including cholecystectomy, pancreatectomy and liver resection. The requirement for the surgeon to accurately delineate the position of lesions in the biliary system has provided a stimulus for the development of this technique.

The aim of this chapter is to describe the anatomy of the normal biliary tract with specific reference to intraoperative ultrasonography. Using images and video, the assessment of the biliary tract is described and the influence of ultrasonography on the management of common pathologies is highlighted.

Anatomy of the Biliary Tree

The biliary tract is a set of anatomical structures that convey bile secreted from the liver to the duodenum. Small intrahepatic biliary radicles coalesce into larger segmental ducts, which form the left and right hepatic ducts (Fig. 14.1). The course of the left duct is extrahepatic to its confluence with the right duct, where the common hepatic duct is formed (Fig. 14.1a). This lies within the hepatoduodenal ligament and runs anterior and to the right of the portal vein. The anatomy of the portal pedicle is highly variable, hence the importance of ultrasonography in delineating it. The lower part of the common hepatic duct lies to the right of the proper hepatic artery, with the right hepatic artery branch usually running behind the common hepatic duct (Fig. 14.1a). The right hepatic artery can run over the anterior surface of the common hepatic duct, which is an important variation to identify to avoid injury to this vessel.

E.M. Harrison, MB, ChB, PhD, FRCS (✉)
O.J. Garden, CBE, FRCSEd, FRSE
Department of Clinical Surgery, The University of Edinburgh, Royal Infirmary of Edinburgh, 51 Little France Crescent, Edinburgh EH16 4SA, UK
e-mail: ewen.harrison@ed.ac.uk; o.j.garden@ed.ac.uk

Electronic supplementary material The online version of this chapter (doi:10.1007/978-1-4614-9599-4_14) contains supplementary material, which is available to authorized users. Videos can also be accessed at http://www.springerimages.com/videos/978-1-4614-9598-7

E.J. Hagopian, J. Machi (eds.), *Abdominal Ultrasound for Surgeons*,
DOI 10.1007/978-1-4614-9599-4_14, © Springer Science+Business Media New York 2014

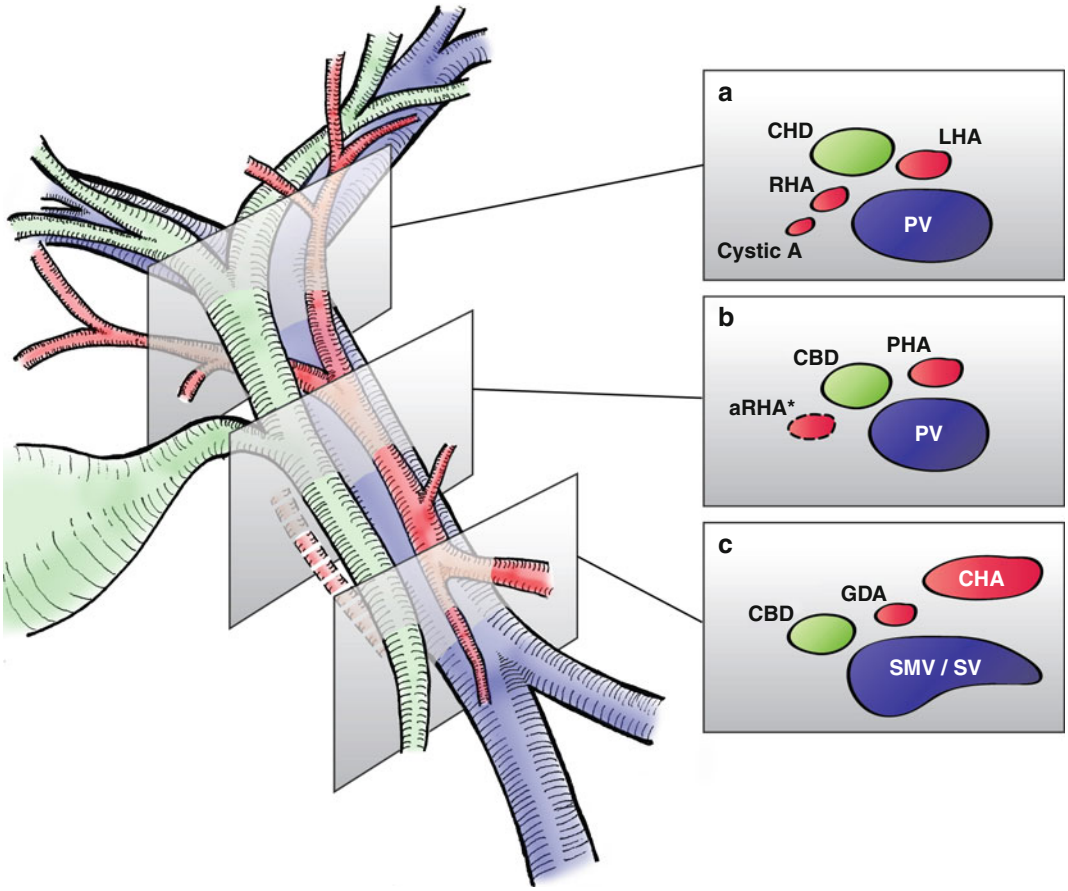

Fig. 14.1 Anatomy of the extrahepatic biliary tree with typical transverse ultrasonographic planes through the portal pedicle. The right hepatic artery (*RHA*) usually runs behind the common hepatic duct (*CHD*), with the origin of the cystic artery (*Cystic A*) being variable (**a**). An important variant is an accessory right hepatic artery (*aRHA*) arising from the superior mesenteric artery present in 15 % of patients (**b**). The superior mesenteric vein/splenic vein confluence is tear-shaped and often easy to identify (**c**). *LHA* left hepatic artery, *PHA* proper hepatic artery, *CHA* common hepatic artery, *GDA* gastroduodenal artery, *CBD* common bile duct

The cystic artery arises from a variable origin along the length of the proper and right hepatic arteries. Similarly, the insertion of the cystic duct into the common bile duct varies, either running a short course and inserting directly or, more commonly, travelling beside the common hepatic duct for a length prior to insertion. The posterior sectoral duct can also insert low into the common hepatic duct or, rarely, directly into the cystic duct. An uncommon configuration in posterior sectoral duct anatomy is sometimes implicated in the occurrence of bile duct injury at laparoscopic cholecystectomy.

An anatomical variant occurring in 15 % of patients is an accessory or replaced right hepatic artery arising from the superior mesenteric artery (Fig. 14.1b) [4]. Identifying and protecting aberrant vessels is important, particularly during resectional surgery such as extrahepatic bile duct resection and pancreaticoduodenectomy. An accessory left hepatic artery arising from the left gastric artery crosses the lesser omentum in a position out with the portal pedicle. This vessel will not usually be seen on standard sonography of the portal pedicle, unless the probe is moved left and the vessel looked for specifically.

The common hepatic artery is prominent in transverse planes low in the pedicle, appearing greater than its size given the angle of approach (Fig. 14.1c). It can be used to identify the gastroduodenal artery which usually arises at the same level and should not be confused with the right gastric artery (see Fig. 14.4b). The coeliac trunk can usually be visualised dropping behind the pancreas, with the splenic and left gastric artery origins usually visible.

The confluence of the splenic vein and superior mesenteric vein can be identified by its tear-shaped appearance in the transverse plane on ultrasound. Potentially troublesome venous tributaries can often be identified in this area, prior to dissection in pancreaticoduodenectomy. The portal vein can be followed up behind the pancreas towards the liver, a manoeuvre which can often aid the assessment of resectability of malignant disease.

Lymph nodes are present throughout the portal pedicle and may be enlarged as a consequence of disease (see discussion of section "Benign obstruction of the biliary tree"). These are easily identified and measured.

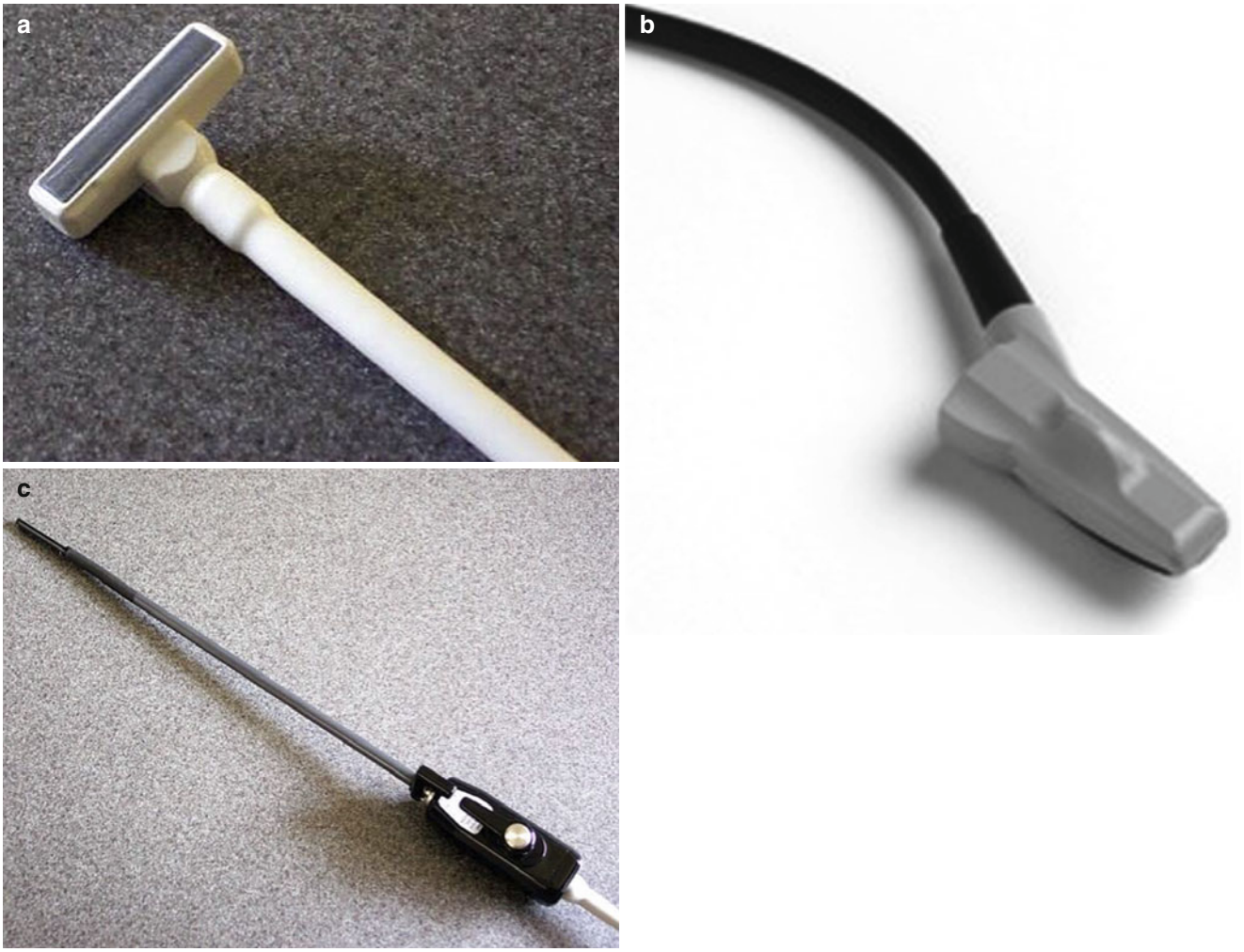

Fig. 14.2 Ultrasound transducers designed for use in surgery: (**a**) T-style linear probe, (**b**) I-style convex probe, and (**c**) laparoscopic probe

Equipment

A number of different companies now produce versatile high-resolution equipment providing excellent image quality. Real-time B-mode ultrasound images are of course essential, but the ability to add colour flow, power flow and spectral Doppler is now standard. This allows visualisation of blood flow in vessels, which at its simplest can be used in the initial orientation of structures. The technology is now such that even flow in the smallest vessels can be visualised with high sensitivity and resolution. Facilities on the most advanced systems include multi-planar image reconstruction and 3D automated volume measurement.

Various probe options are available including the authors' preferred T-transducer (Fig. 14.2a) and the I-style finger-grip transducer (Fig. 14.2b). These can be configured with linear or convex arrays, with the former providing a rectangular field of view and the best spatial resolution at the tissue depths typically encountered in hepatobiliary and pancreatic surgery. Laparoscopic probes in the past required to be placed within a sterile plastic sheath containing conductive gel which was awkward and yielded poor image quality. Probes can now be sterilised in ethylene oxide, allowing direct organ contact with improved image in quality. A 12-mm port is required for use and port placement is described below. The tip of the probe is flexible in two planes, allowing most required angles to be achieved through one port (Fig. 14.2c).

Remote control units are available for sterile use and image/video storage can be integrated with institution picture archiving and communication systems (PACS). Specialised probes have been designed that include a needle guide and come with specific software to aid accurate placement for radiofrequency/microwave ablation.

Technique in Open Surgery

The access to the organs of the abdomen afforded by open surgery provides an ideal opportunity for contact ultrasonography. The high-frequency, compact equipment now available

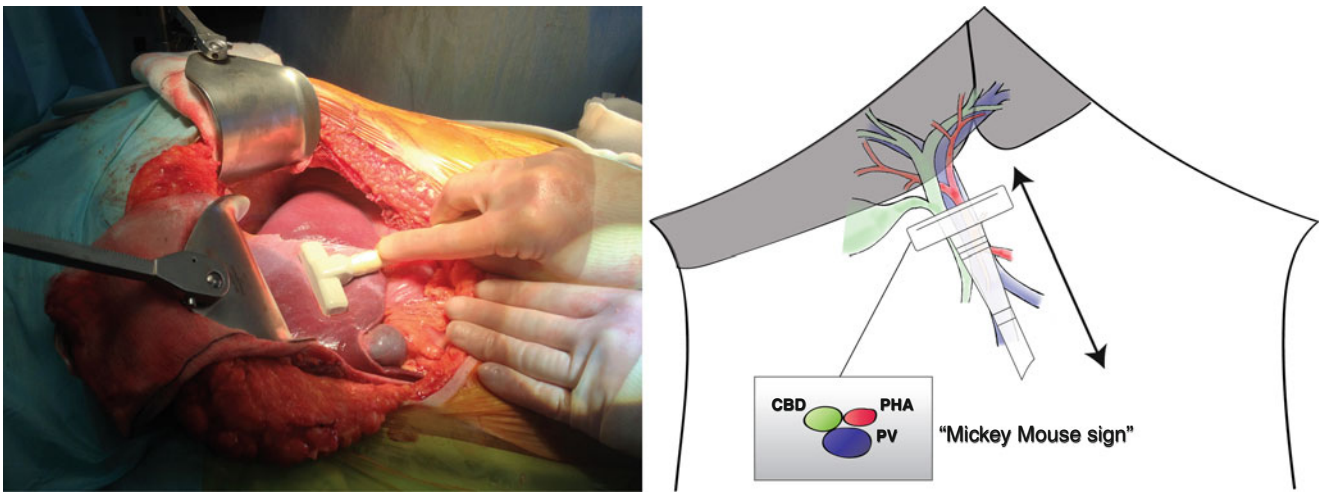

Fig. 14.3 Ultrasonography of the portal pedicle starts with identification of "Mickey Mouse", formed by the larger portal vein (*PV*) sitting posteriorly with the common bile duct (*CBD*) and proper hepatic artery (*PHA*) in front

can be fully sterilised and placed directly on abdominal viscera to obtain high-resolution real-time images of intra-abdominal structures. This gives the operating surgeon an accurate and flexible tool to assess the anatomy, the nature and the extent of disease, aiding operative decision-making.

Intraoperative ultrasound may be useful in surgery for benign or malignant disease and in both cases the approach is the same. A full visual inspection and manual examination is useful and should be performed initially at laparotomy [5]. Together with the preoperative imaging, this will provide valuable information about the nature and extent of disease. Ultrasonography starts at the hepatoduodenal ligament with examination of the structures of the portal pedicle. Placement of fixed surgical retractors including a specific liver retractor on segment IV may aid access. The use of warm saline around the ligament can help if image quality is poor, but is not always required. It often helps if the operator retracts gently on the duodenum, placing the hepatoduodenal ligament under some tension.

To aid initial orientation, the "Mickey Mouse sign" can be useful (Fig. 14.3). The larger portal vein sitting posteriorly, with the bile duct and hepatic artery in front are reminiscent of the face and ears of the famous cartoon character. "Mickey" can be followed up and down, which acts to keep the probe at right angles to the structures. Care must be taken not to compress structures with the probe. The common bile duct is normally around 8 mm in diameter and can be difficult to visualise when not dilated. It can be differentiated from other portal structures by its hyperechoic wall and absence of flow on Doppler.

Benign Obstruction of the Biliary Tree

Non-malignant obstruction of the biliary tree can result from congenital abnormalities but is more commonly associated with gallstones, benign biliary strictures or a consequence of acute or chronic pancreatitis. In 997 consecutive patients selected for laparoscopic cholecystectomy, operative cholangiography was accomplished in 962 (96 %) [6]. Forty-six patients (4.6 %) had at least one filling defect in the common bile duct, although 12 of these patients had a normal cholangiogram within 48 h (26 % possible false-positive rate) and a further 12 (26 %) had spontaneously passed a stone by 12 weeks. Twenty-two patients (2.2 % of total population) had persistent CBD stones 6 weeks after laparoscopic cholecystectomy.

Figures 14.4 and 14.5 and accompanying videos (Videos 14.1, 14.2 and 14.3, respectively) show typical images obtained with ultrasonography during open surgery. This patient presented with obstructive jaundice and cholangitis on a background of upper abdominal pain. A CT showed dilatation of the extra- and intrahepatic biliary tree with no pancreatic duct dilatation and an obstructing 1.5 cm gallstone in the distal common bile duct. Endoscopic retrograde cholangiopancreatography (ERCP) with sphincterotomy was performed and a biliary stent placed. The bilirubin remained elevated and the cholangitis persisted and a second ERCP was performed, with placement of a second biliary stent. The stone was impacted and could not be removed at ERCP. Drainage was achieved and the symptoms of sepsis settled. Given the size and position of stone, clearance by open exploration was performed.

"Mickey Mouse" is identified and the common bile duct seen to be significantly distended at 1.5 cm (Fig. 14.4a). What initially appears to be the proper hepatic artery is actually a prominent gastroduodenal artery. This is followed up and the origin of the right gastric artery is seen (Fig. 14.4b), just before a large common hepatic artery is visualised (Fig. 14.4c). The cystic duct is long and clearly inserts in a low position (Fig. 14.4b). A lymph node is seen behind the common bile duct which does not look enlarged on ultrasonography and is not suspicious on palpation. Towards the

confluence of the left and right hepatic duct, plastic stents are seen within the common hepatic duct, with associated acoustic shadowing (Fig. 14.4d). Some debris can be seen at different levels in the duct.

Longitudinal views are seen in Fig. 14.5. With the right side of the images being the anatomical superior position, the pancreas and pancreatic duct are seen anterior to the confluence of the superior mesenteric/splenic vein (Fig. 14.5a). The bile duct is abnormally thickened and a large stone is present just superior to the neck of the pancreas (Fig. 14.5b). A prominent acoustic shadow is cast behind the stone, obscuring the view of structures in this area. Moving superiorly, two plastic

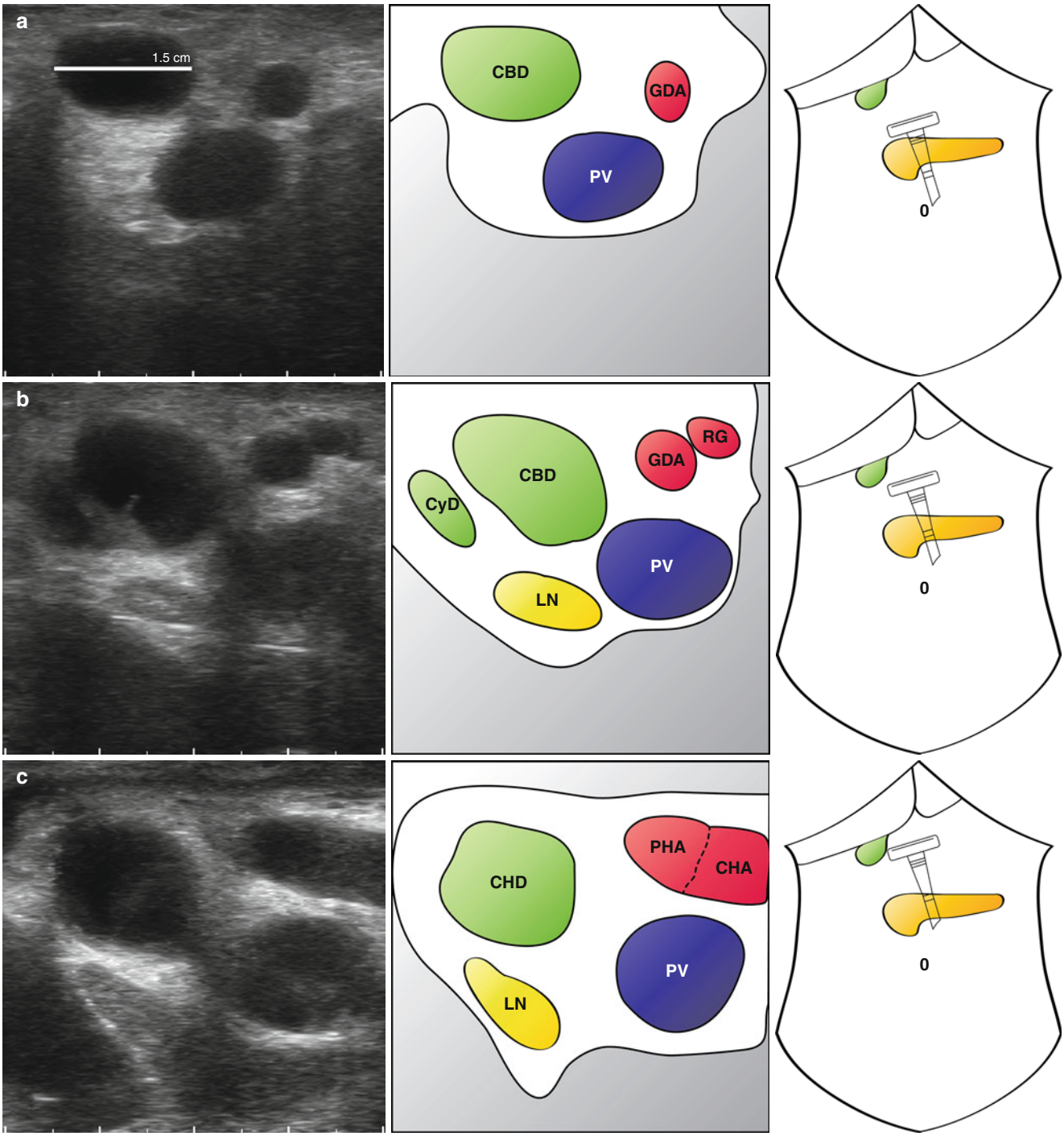

Fig. 14.4 Transverse views of portal pedicle in a patient with biliary obstruction. A full description is provided in the main text. A dilated common bile duct (*CBD*) is followed up with the portal pedicle (**a**). The arterial anatomy is clearly seen (**a**–**d**) and two plastic stents can be seen within the common hepatic duct (**d**) (Also see accompanying Video 14.1) *GDA* gastroduodenal artery, *PV* portal vein, *CHD* common hepatic duct, *RG* right gastric artery, *CyD* cystic duct, *LN* lymph node, *PHA* proper hepatic artery, *CHA* common hepatic artery

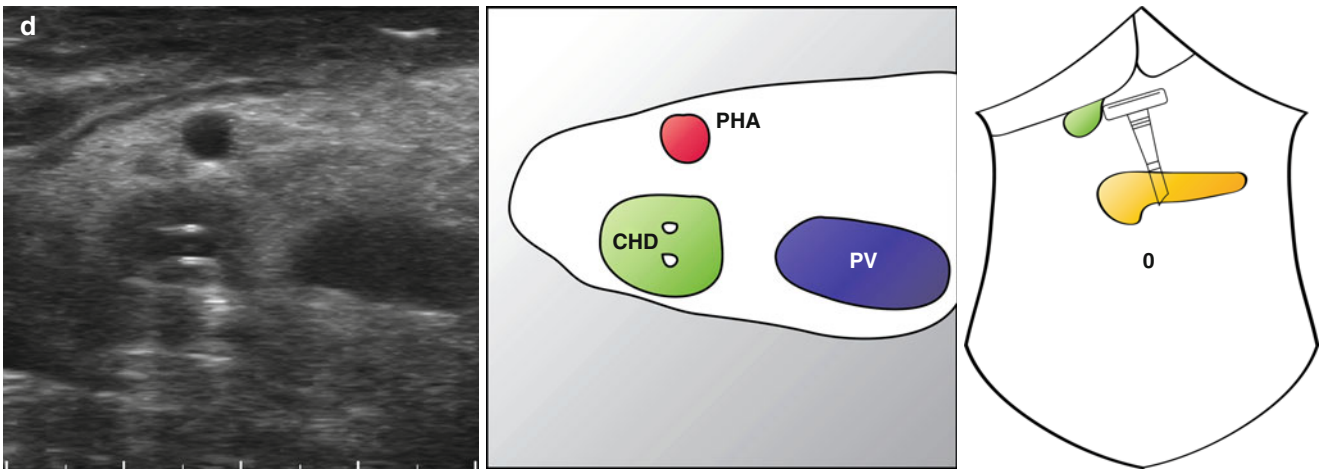

Fig. 14.4 (continued)

stents are seen in the common bile duct (Fig. 14.5c). With careful manipulation of the probe, the stents are seen to pass the stone into the distal CBD (Fig. 14.5d).

An open common bile duct exploration was performed and the stone removed in fragments. The duct was visualised with a choledochoscope, and the operating surgeon was satisfied that all stone fragments had been cleared. The duct was primarily closed without a t-tube and the patient discharged from hospital 6 days later.

Malignant Obstruction of the Distal Biliary Tree

Malignant obstruction of the distal biliary tree is most commonly caused by adenocarcinoma of the head of the pancreas. Other causes include cholangiocarcinoma arising in the distal common bile duct, duodenal or ampullary adenocarcinoma and obstruction resulting from malignant portal lymph nodes.

Figure 14.6 with the accompanying video (Videos 14.4 and 14.5) shows images obtained with ultrasonography during open exploration of a patient who presented with painless jaundice and weight loss. A CT showed dilatation of the extra- and intrahepatic biliary tree and pancreatic duct. No gallstones or large mass were seen on cross-sectional imaging and a presumed diagnosis of distal/ampullary cholangiocarcinoma was made. No evidence of locally advanced disease or distant metastases was seen on CT. Endoscopic retrograde cholangiopancreatography (ERCP) was performed and a short metal stent inserted. Brushings of the bile duct showed cellular atypia but no frankly malignant cells.

At open exploration, ultrasonography in the transverse plane showed a grossly dilated pancreatic duct (Fig. 14.6a). The metal stent was clearly visualised in the CBD and an inhomogeneous mass seen in the head of the pancreas. The dilated pancreatic duct could be followed into the tail of the pancreas (Fig. 14.6b). The confluence of the SMV/SV and SMA were well visualised and did not appear involved in the mass. In the longitudinal plane, the portal vein was followed up through the head of the pancreas and the wall appeared smooth and regular with no suggestion of malignant involvement. No large nodes were seen around the coeliac trunk or in the aortocaval window.

The patient went on to have a pancreaticoduodenectomy and was found to have a T3N1 ductal adenocarcinoma of the head of pancreas which was completely excised.

Malignant Obstruction of the Proximal Biliary Tree

Hilar and intrahepatic cholangiocarcinoma remain difficult tumours to treat with poor outcomes. A spectrum of tumours of the biliary tree exist which is summarised in Table 14.1. Risk factors for cholangiocarcinoma include age (65 % cases are greater than 65 years old), smoking, primary sclerosing cholangitis (PSC, lifetime risk 5–15 %), Caroli's disease (lifetime risk 7 %), choledochal cysts (5 % will transform) and chronic intraductal inflammation (from gallstones, liver fluke and typhoid) [7]. The origin of the tumour is most commonly the perihilar biliary tree (50–60 %) but can also arise within the liver (20–25 %) and in the distal bile duct (20–25 %) or can be multifocal (5 %).

Fewer than 20 % of patients presenting with hilar cholangiocarcinoma are suitable for a potentially curative resection. Of those that undergo surgery with curative intent, 30 % are shown to have an incomplete resection. The recently updated British Society of Gastroenterology guidelines are a useful resource for the diagnosis and treatment of cholangiocarcinoma [7]. Laparoscopic ultrasound may be considered in the staging of cholangiocarcinoma and this is discussed in Chap. 10.

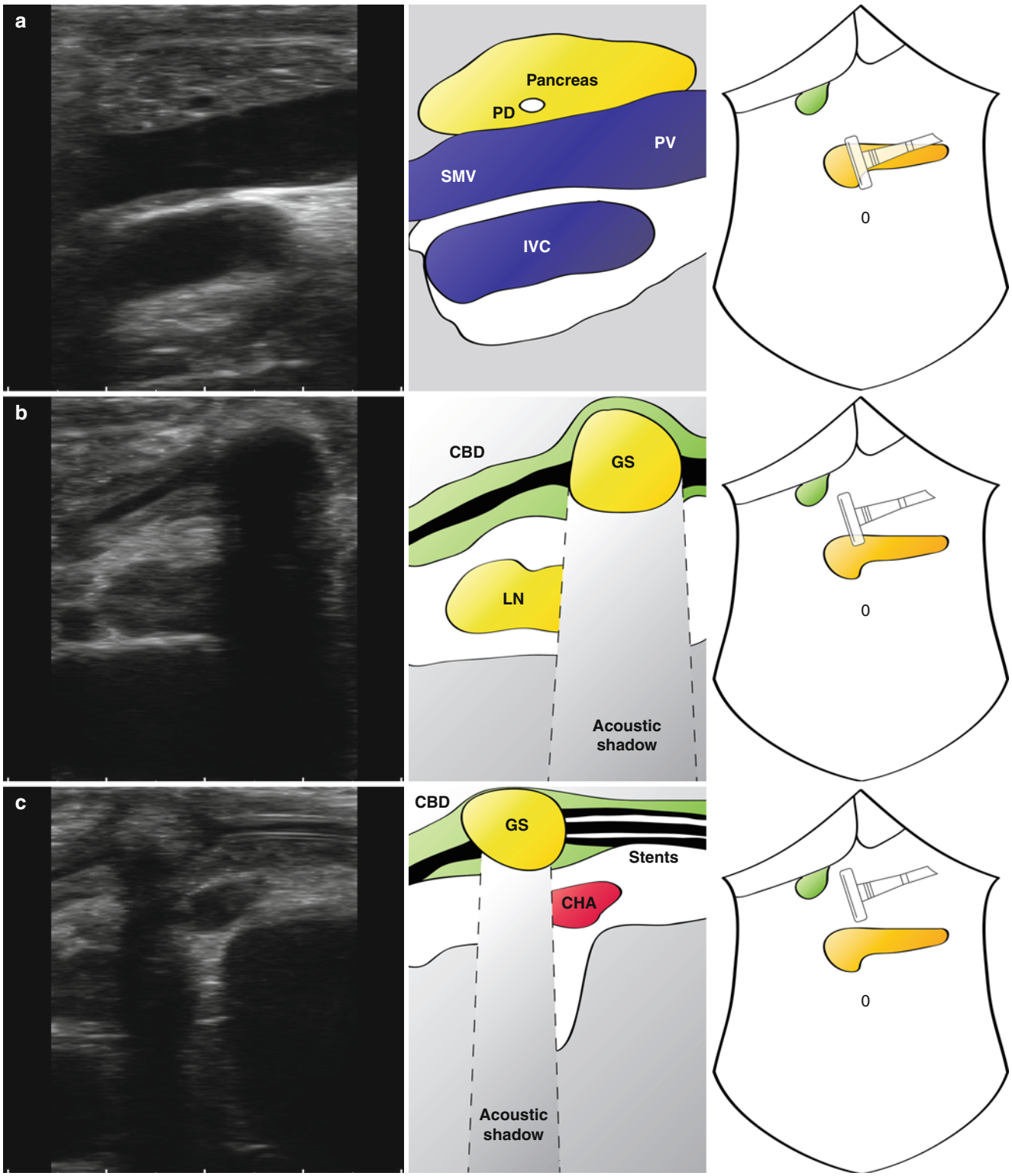

Fig. 14.5 Longitudinal views of portal pedicle in patient with biliary obstruction. The neck of the pancreas can be seen with a visible but non-dilated pancreatic duct (**a**; *PD*). A large gallstone (*GS*) is seen in a thickened common bile duct (**b**; *CBD*) (note the prominent acoustic shadow). Stents can be seen in the CBD (**c**) extending below the level of the stone (**d**) (Also see accompanying Videos 14.2 and 14.3). *SMV* superior mesenteric vein, *PV* portal vein, *LN* lymph node, *CHA* common hepatic artery

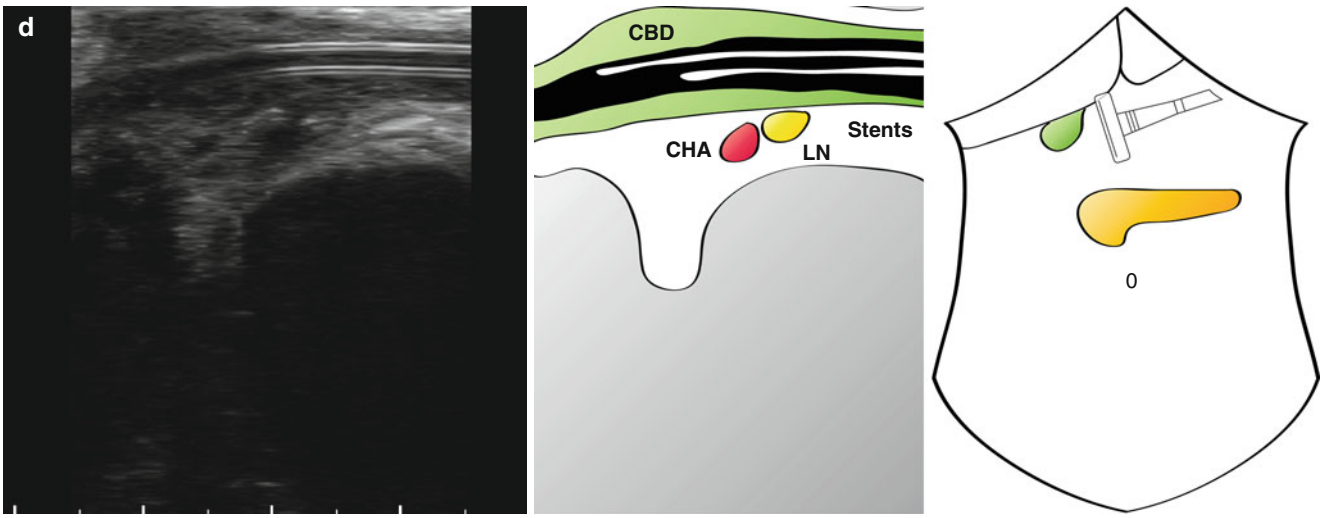

Fig. 14.5 (continued)

Accurate assessment of the extent of tumour within the biliary tree is essential prior to attempted resection. This assessment is now primarily performed using magnetic resonance cholangiopancreatography (MRCP). Triple-phase CT is also essential for assessing arterial and portal venous involvement, as well as determining the presence of distant metastases. If biliary drainage is required, then this should be performed by a percutaneous transhepatic technique to the side of the liver with least disease. The Bismuth-Corlette classification of biliary strictures provides a useful taxonomy for describing and treating hilar cholangiocarcinoma (Fig. 14.7). At laparoscopy/laparotomy, intraoperative ultrasound may be used to assess extent of disease, guiding which resection is appropriate [7]. For types I and II, en bloc resection of the extrahepatic bile ducts and gallbladder, regional lymphadenectomy and Roux-en-Y hepaticojejunostomy are appropriate. In type III disease, these approaches can be extended to include a right (IIIa) or left (IIIb) hepatectomy, which may require resection of two or three liver sections. Type IV is often not resectable, but an extended right or left hepatectomy may be possible.

Other malignant causes of high biliary obstruction include metastatic liver disease and hepatocellular carcinoma (HCC). Figure 14.8 shows images from a 52-year-old male patient presenting with segmental biliary obstruction as a result of a large HCC. The patient had no apparent background liver disease and was not jaundiced. The position of the tumour just anterior and superior to the liver hilus resulted in compression to the segment V (Fig. 14.8a) and IV (Fig. 14.8b) ducts. See also Video 14.6.

Given the position of the tumour, a portal vein embolisation was performed preoperatively with significant hypertrophy of the left lateral section. An extended right hepatectomy was able to be performed with preservation of the extrahepatic biliary tree.

Intraoperative Ultrasound in Laparoscopic Surgery

Assessment of the biliary tree by laparoscopic ultrasonography (LUS) may be required in the context of benign or malignant disease. The former is dominated by the complications of gallstones, typically when choledocholithiasis is suspected during cholecystectomy. LUS may be useful in the staging of biliary tract malignancies (see Chap. 10). The current standard of management should be to perform staging laparoscopy with LUS prior to proceeding to resection for patients with cholangiocarcinoma, as it will prevent unnecessary laparotomies in up to 30 % of patients [7]. Laparoscopic resection of bile duct cancers is still rare, although laparoscopic pancreaticoduodenectomy is now performed by enthusiastic individuals. LUS can be useful in the assessment of gallbladder wall thickening or polyps in the presence of gallstones, when malignancy has not been excluded by preoperative imaging. With confident use of LUS to exclude an infiltrating mass in the gallbladder wall, a laparoscopic cholecystectomy can be performed, avoiding an open radical cholecystectomy.

Port position is important and should be based on the most likely operative procedure to be performed. Modern laparoscopic ultrasound probes (Fig. 14.2c) have a flexible tip that can be manipulated in two planes allowing most necessary positions to be obtained from a single 12 mm port and all positions from two 12 mm ports. A common situation faced by the surgeon is using LUS to image the common bile duct during gallbladder surgery with laparoscopic bile duct

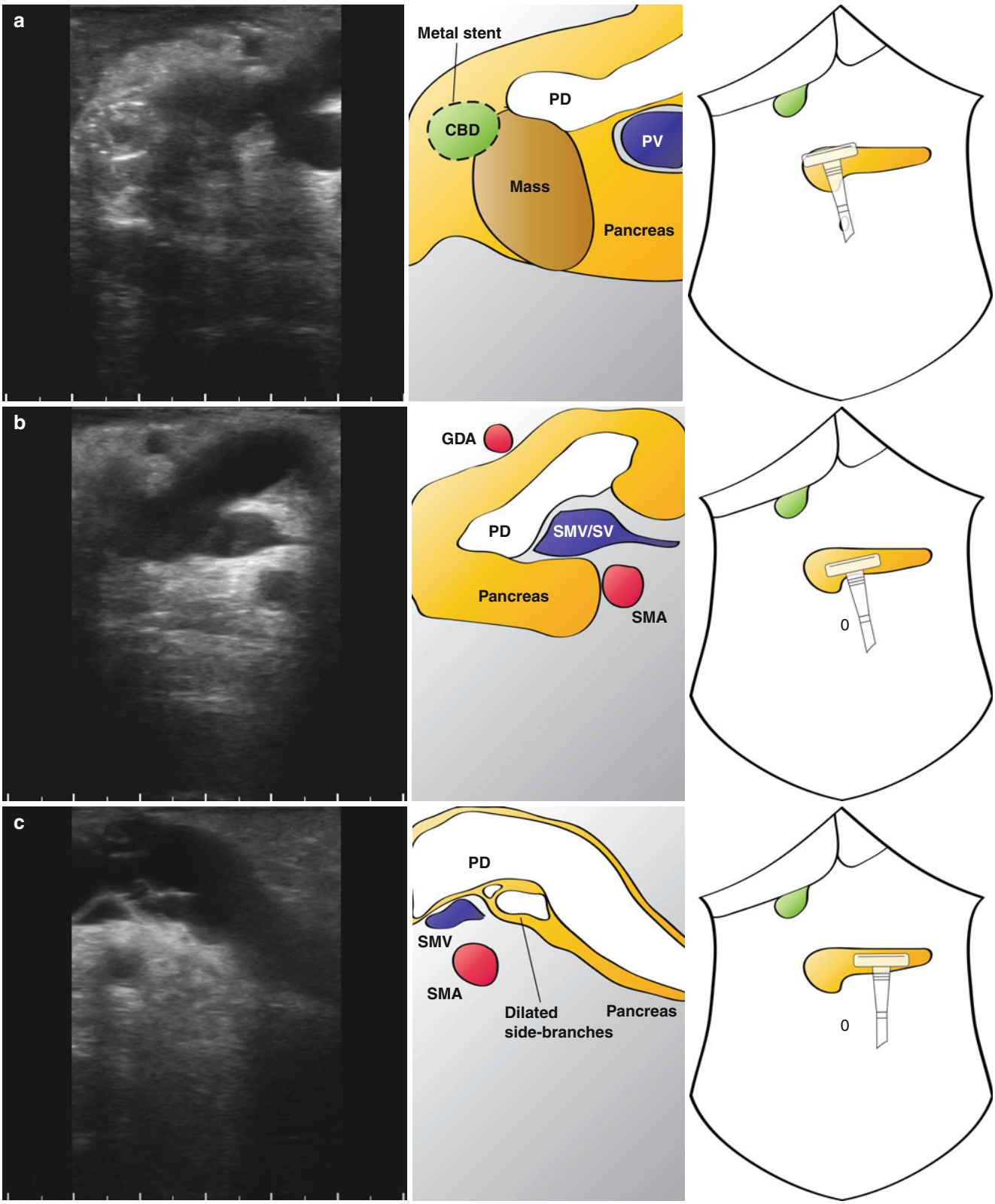

Fig. 14.6 Malignant obstruction of the biliary tree. An indistinct mass is seen in the head of the pancreas with dilatation of the pancreatic duct (*PD*) and a metal stent in the common bile duct (*CBD*; **a**). The confluence of the superior mesenteric vein (**b**; *SMV*) and splenic vein (*SV*) becomes the portal vein (**d**; *PV*) which can be followed beneath the neck of the pancreas. Both the vein and the superior mesenteric artery (**c**; *SMA*) appear free of tumour (Also see accompanying Videos 14.4 and 14.5)

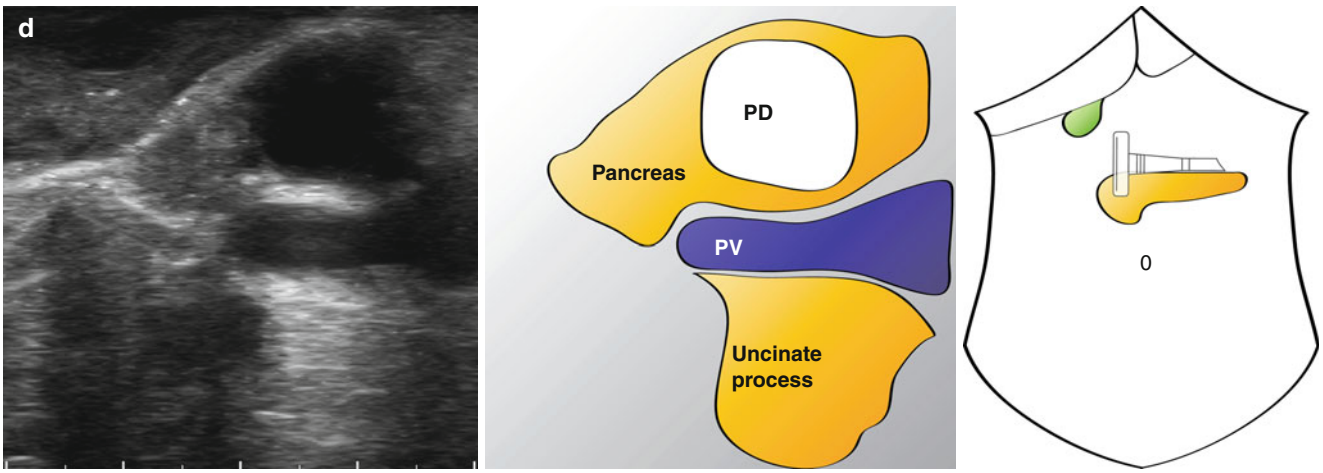

Fig. 14.6 (continued)

Table 14.1 World Health Organization (WHO) classification of biliary malignancies

	Benign	Premalignant	Malignant
Tumours of intrahepatic ducts	Bile duct adenoma	Biliary adenofibroma	Intrahepatic cholangiocarcinoma
	Microcystic adenoma	Biliary adenofibroma	Intraductal papillary neoplasm with associated invasive neoplasia
	Biliary adenofibroma	Mucinous cystic neoplasm	Mucinous cystic neoplasm with associated invasive neoplasia
Tumours of extrahepatic bile ducts		Adenoma	Adenocarcinoma
		Biliary intraepithelial neoplasia	Adenosquamous carcinoma
		Intracystic (gall bladder) or intraductal (bile duct) papillary neoplasm	Intracystic (gall bladder) or intraductal (bile duct) papillary neoplasm + associated invasive neoplasia
		Mucinous cystic neoplasm	Mucinous cystic neoplasm with associated invasive neoplasia
			Squamous cell carcinoma
			Undifferentiated carcinoma

Modified from Khan et al. [7]

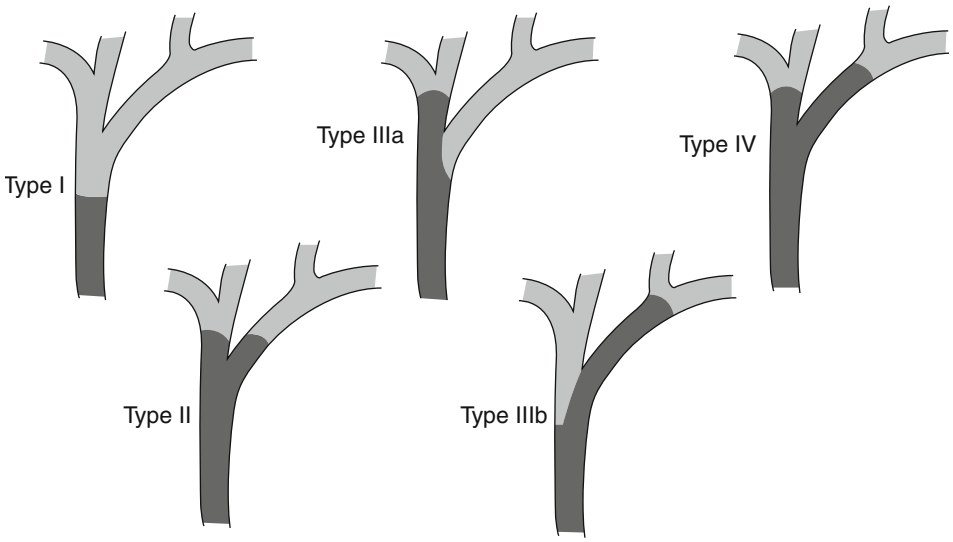

Fig. 14.7 Bismuth-Corlette classification of biliary strictures (From Khan et al. [7])

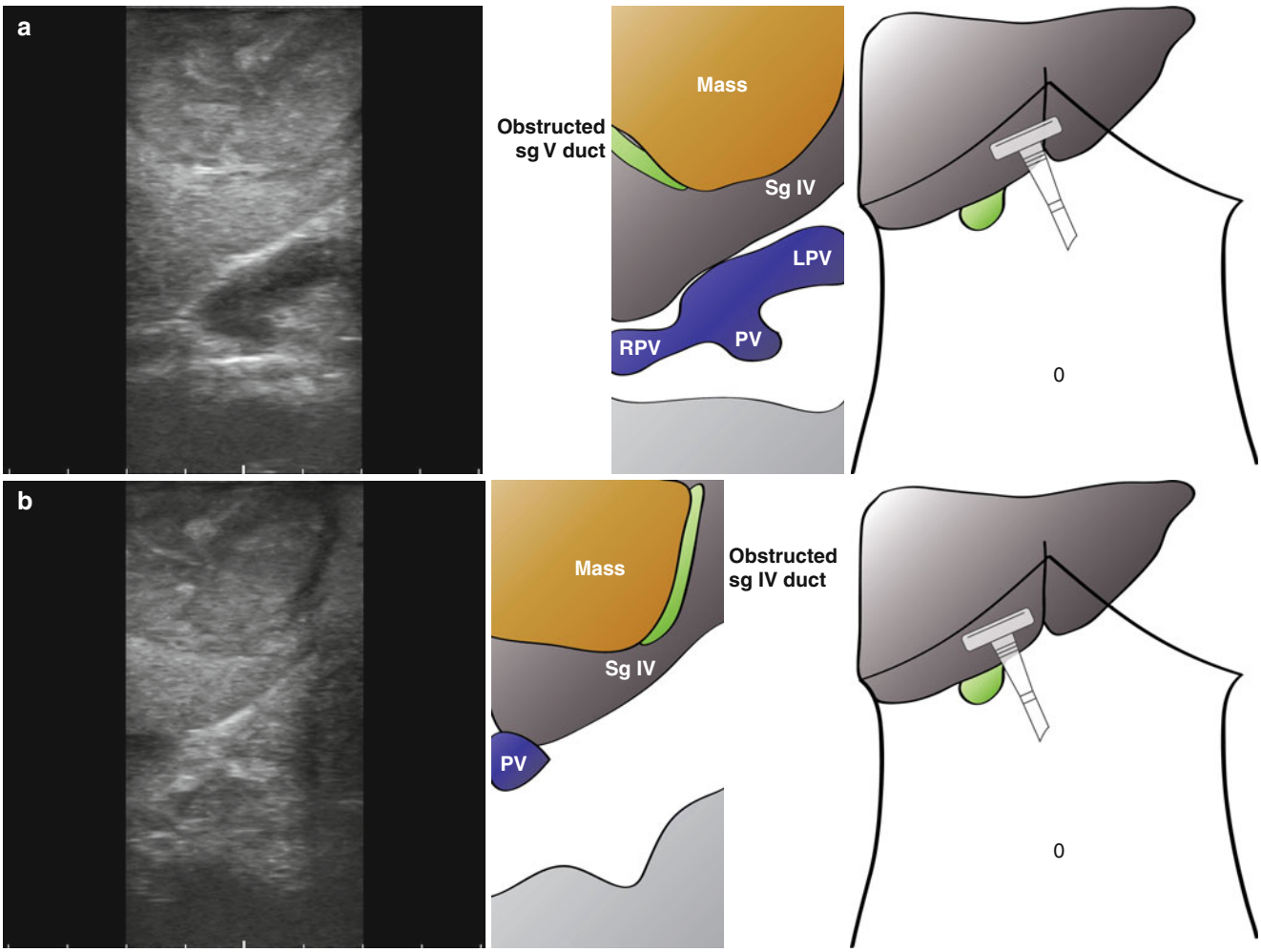

Fig. 14.8 Segmental obstruction of biliary tree by large hepatocellular carcinoma (HCC). The tumour sits anterior and superior to the liver hilus resulting in compression to the segment V (**a**) and IV (**b**) ducts. See also Video 14.6

exploration. When it is expected that a choledochotomy will be performed, the midline epigastric port site should be placed slightly lower than normal (~3 cm) to aid the laparoscopic placement of sutures to close the duct.

Figure 14.7 demonstrates a common approach to obtaining longitudinal (left panel) and transverse (right panel) views of the hepatoduodenal ligament from two 12 mm ports placed in the epigastrium and below the umbilicus. Rotation of the probe is useful and will ensure good contact with tissues. Instilling saline into the peritoneal cavity may help to improve image quality, although is usually not required. Particularly during cholecystectomy for gallstones, it is the authors' usual practice to perform ultrasonography prior to any dissection. Maintaining complete tissue planes initially ensures unimpeded views of the biliary tree. In operators with good experience of LUS, demonstrating a non-dilated biliary tree without stones usually obviates a requirement for cholangiography.

Early prospective studies showed laparoscopic ultrasound compared favourably with intraoperative cholangiography in the detection of ductal stones [8]. Contemporary series have confirmed these findings [9], suggesting that routine use of laparoscopic ultrasound can reduce the need for cholangiography [10]. It has been proposed that LUS should be considered the primary method of imaging the bile duct during laparoscopic cholecystectomy [11] and using LUS to define anatomy may reduce the incidence of bile duct injury [12]. It is accepted, however, that neither operative cholangiography nor ultrasonography obviates the need for safe dissection and neither eliminates the risk of injury to the main bile duct (Fig. 14.9).

Abnormal Gallbladder Wall Thickening with Gallstones

A 45-year-old female patient presented with longstanding right upper quadrant pain associated with eating. She had never been jaundiced and had no weight loss. A transabdominal ultrasound of the gallbladder had raised the possibility of an underlying neoplasm and revealed significant thickening of the gallbladder wall on the liver side in the absence of

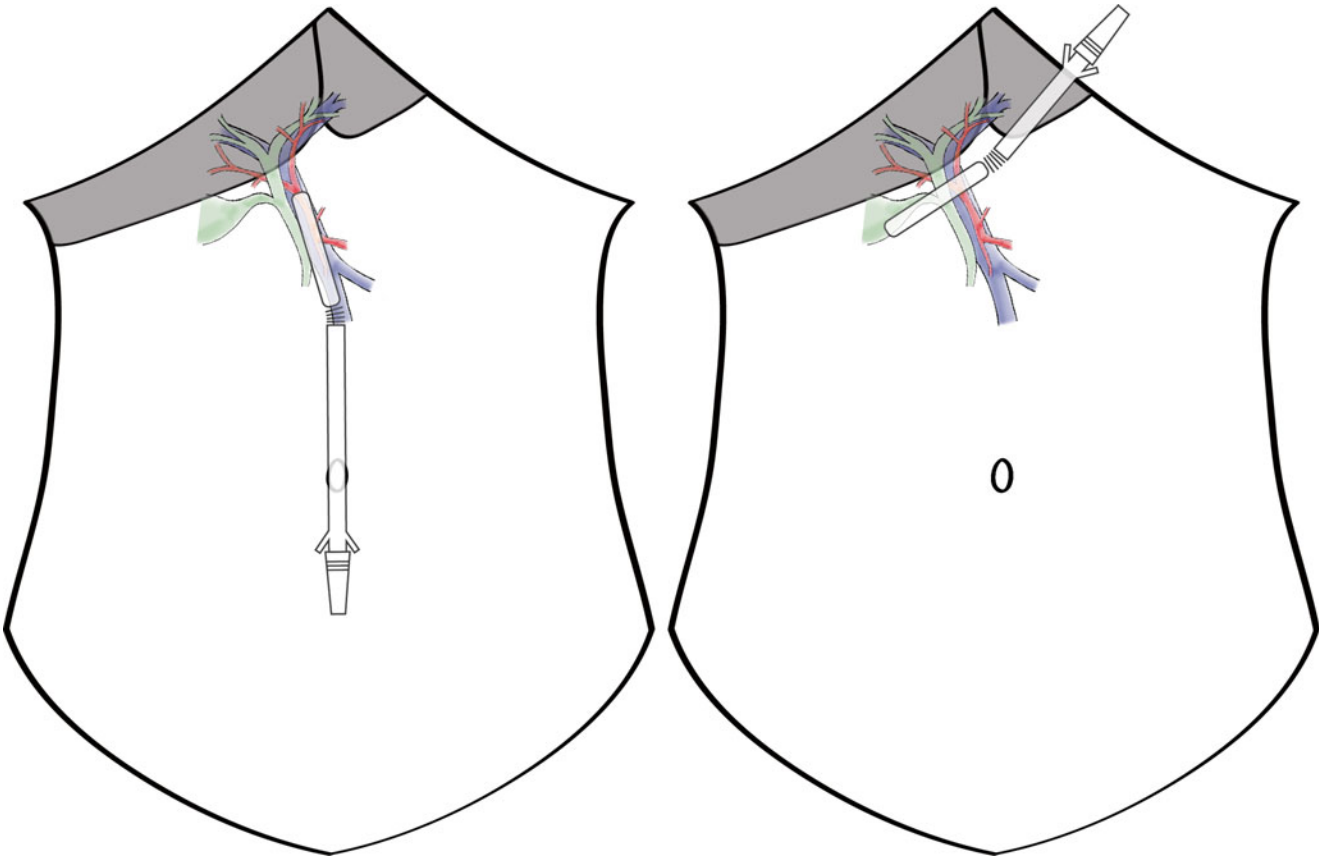

Fig. 14.9 Obtaining longitudinal (*left panel*) and transverse (*right panel*) views of the portal pedicle through a 10–12 mm umbilical and epigastric laparoscopic port

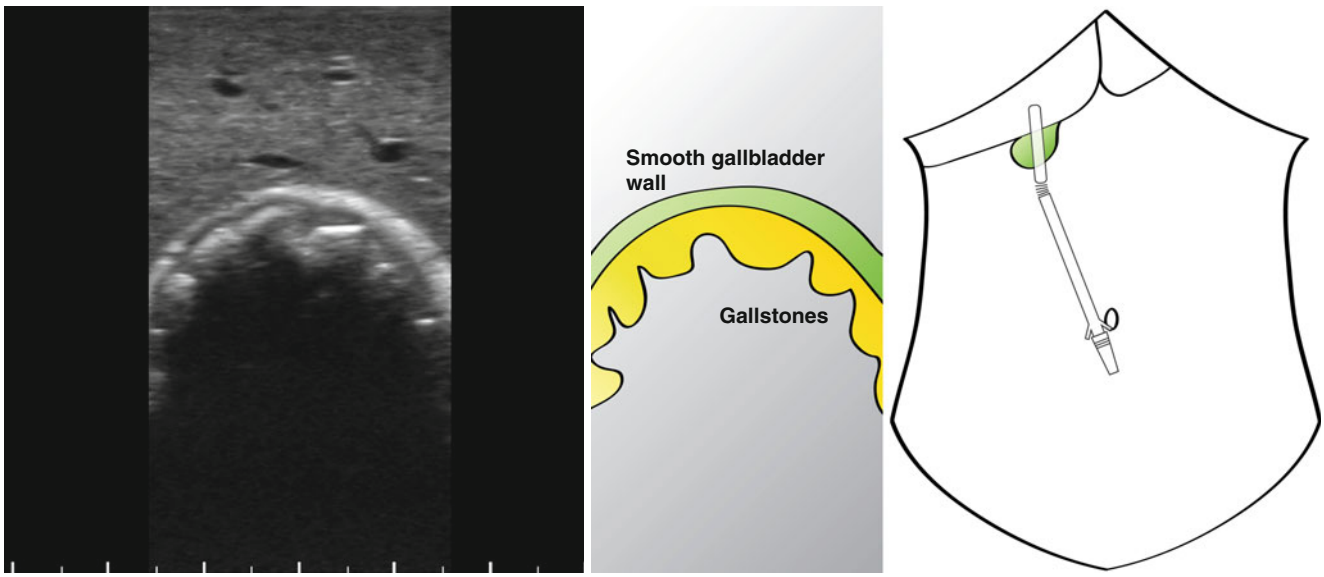

Fig. 14.10 Laparoscopic ultrasound examination of gallbladder described as suspicious on preoperative imaging. The gallbladder is seen to be smooth and relatively thin walled, with multiple gallstones present within the lumen. No infiltrating lesion was seen (Also see Video 14.7)

evidence of acute inflammation. No definite infiltrating lesion was seen and no other evidence of malignancy was present.

Laparoscopic ultrasound of the gallbladder was performed (Fig. 14.9). The gallbladder was seen to be smooth with multiple gallstones present. On careful LUS, it was clear there was no gallbladder wall lesion and a laparoscopic cholecystectomy was performed. Pathological examination confirmed no malignant lesion (Fig. 14.10; see also Video 14.7).

Conclusions

Intraoperative ultrasonography of the biliary tree remains an essential part of the armamentarium of the hepatobiliary surgeon. It allows the operating surgeon to clearly delineate anatomy (bile ducts and vessels) and make judgements on the nature and extent of disease. It is efficacious in the detection of common bile duct stones and in experienced hands obviates the need for cholangiography, avoiding exposure to ionising radiation and the potential introduction of infection to the biliary tree.

Intraoperative ultrasonography has high success rates in published studies and the advantage of the ability to repeat the examination during dissection. In general, it is quicker than alternative imaging modalities and has a lower overall cost.

There is a learning curve and the surgeon will require specific training in technique and interpretation of images. It can be technically difficult in certain patients and can be limited by the presence of air in the duodenum. In experienced hands, intraoperative laparoscopic ultrasonography can be as good as cholangiography in delineating anatomy and detecting bile duct stones. There is some evidence that it may be associated with a reduction in the risk of bile duct injury (Level II, Grade B).

References

1. Eiseman BB, Greenlaw RH. Localization of common duct stones by ultrasound. Arch Surg. 1965;91(1):195–9.
2. Knight PR, Newell JA. Operative use of ultrasonics in cholelithiasis. Lancet. 1963;1(7289):1023–5.
3. Lane RJ, Glazer G. Intra-operative B-mode ultrasound scanning of the extra-hepatic biliary system and pancreas. Lancet. 1980;316(8190):334–7.
4. Hiatt JR, Gabbay J, Busuttil RW. Surgical anatomy of the hepatic arteries in 1000 cases. Ann Surg. 1994;220(1):50–2.
5. Hata S, Imamura H, Aoki T, Hashimoto T, Akahane M, Hasegawa K, et al. Value of visual inspection, bimanual palpation, and intraoperative ultrasonography during hepatic resection for liver metastases of colorectal carcinoma. World J Surg. 2011;35(12):2779–87.
6. Collins C, Maguire D, Ireland A, Fitzgerald E, O'Sullivan GC. A prospective study of common bile duct calculi in patients undergoing laparoscopic cholecystectomy: natural history of choledocholithiasis revisited. Ann Surg. 2004;239(1):28–33.
7. Khan SA, Davidson BR, Goldin RD, Heaton N, Karani J, Pereira SP, et al. Guidelines for the diagnosis and treatment of cholangiocarcinoma: an update. Gut. 2012;61(12):1657–69.
8. Greig JD, John TG, Mahadaven M, Garden OJ. Laparoscopic ultrasonography in the evaluation of the biliary tree during laparoscopic cholecystectomy. Br J Surg. 1994;81(8):1202–6.
9. Tranter SE, Thompson MH. A prospective single-blinded controlled study comparing laparoscopic ultrasound of the common bile duct with operative cholangiography. Surg Endosc. 2003;17(2):216–9.
10. Machi J, Oishi AJ, Tajiri T, Murayama KM, Furumoto NL, Oishi RH. Routine laparoscopic ultrasound can significantly reduce the need for selective intraoperative cholangiography during cholecystectomy. Surg Endosc. 2007;21(2):270–4.
11. Perry KA, Myers JA, Deziel DJ. Laparoscopic ultrasound as the primary method for bile duct imaging during cholecystectomy. Surg Endosc. 2008;22(1):208–13.
12. Machi J, Johnson JO, Deziel DJ, Soper NJ, Berber E, Siperstein A, et al. The routine use of laparoscopic ultrasound decreases bile duct injury: a multicenter study. Surg Endosc. 2009;23(2):384–8.

Intraoperative and Laparoscopic Ultrasound During Liver Surgery

15

Gabriella Pittau, Michele Tedeschi, and Denis Castaing

Intraoperative ultrasound (IOUS) was used primarily in 1960 to localize renal calculi during surgery for nephrolithotomy [1]. The first application of IOUS in hepatobiliary surgery was described by Yamakawa in 1951 to detect cholelithiasis using A-mode ultrasound [2]. With the progress in ultrasound technology and the refinement of instruments, by the mid-1970s, real-time two-dimensional B-mode imaging systems became available. In 1977, Makuuchi was the first to use an electronic linear array (2.5- and 3.5-MHz transducers) for IOUS examination of the liver and pancreas [3]. Since then, IOUS of the liver has become an essential tool for hepatobiliary surgery and is essential in planning surgical strategies. Current applications of intraoperative ultrasound include assessment of tumor(s) and vascular involvement in addition to guidance of hepatic resection, whole or split-liver transplantation, and tumor ablation. Traditional ultrasound does not provide information about tumor vascularity and tissue microcirculation; however, contrast agents are becoming available to allow this evaluation [4, 5].

The purpose of this chapter is to explain how to perform IOUS of the liver. Normal anatomy and anatomic variations, typical features of hepatic tumors, and the different applications of IOUS will be discussed.

Technique

Equipment

Dedicated transducers should be used for IOUS of the liver. The frequency of the probe is inversely proportional to the depth of penetration, but proportional to the image definition. The ideal probe is therefore a compromise between depth and detail. The most common probes are the multifrequency (5, 7.5, 10 MHz) T-probe linear or curvilinear array, T-style finger-grip, and I-style finger-grip and should have color Doppler capability. The probe should fit comfortably in the palm of the hand and between the fingers to easily explore the upper part and the right lateral segments of the liver (Fig. 15.1). If the probe is not sterilizable, a condom sheath can be used to provide sterility of the probe. The sheath must be long at least 2 m to make sure that the entire length of the electric supply cord is covered, and it should snugly fit to the

G. Pittau, MD (✉) • M. Tedeschi, MD
HPB Surgery and Liver Transplantation,
AP-HP, Hôpital Paul Brousse, Centre Hépato-biliaire,
12-14 Avenue Paul Vaillant Couturier,
Villejuif 94800, France
e-mail: gabriella.pittau@pbr.aphp.fr; mictedeschi@yahoo.it

D. Castaing, MD
HPB Surgery and Liver Transplantation,
AP-HP, Hôpital Paul Brousse, Centre Hépato-biliaire,
12-14 Avenue Paul Vaillant Couturier,
Villejuif 94800, France

University Paris-Sud, UMR-S 785, Villejuif F-94800, France

Inserm, Unité 785, Villejuif F-94800, France
e-mail: denis.castaing@pbr.aphp.fr

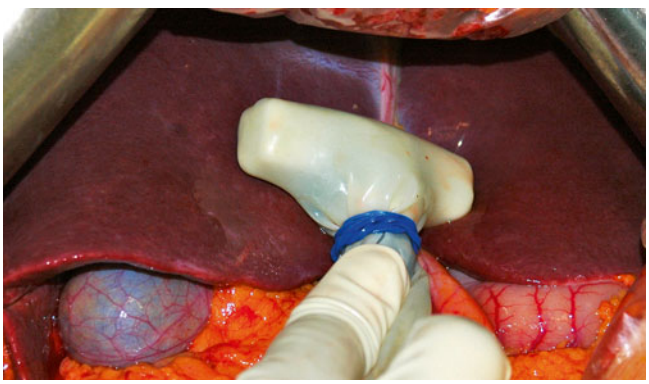

Fig. 15.1 T-style finger-grip intraoperative probe

E.J. Hagopian, J. Machi (eds.), *Abdominal Ultrasound for Surgeons*,
DOI 10.1007/978-1-4614-9599-4_15, © Springer Science+Business Media New York 2014

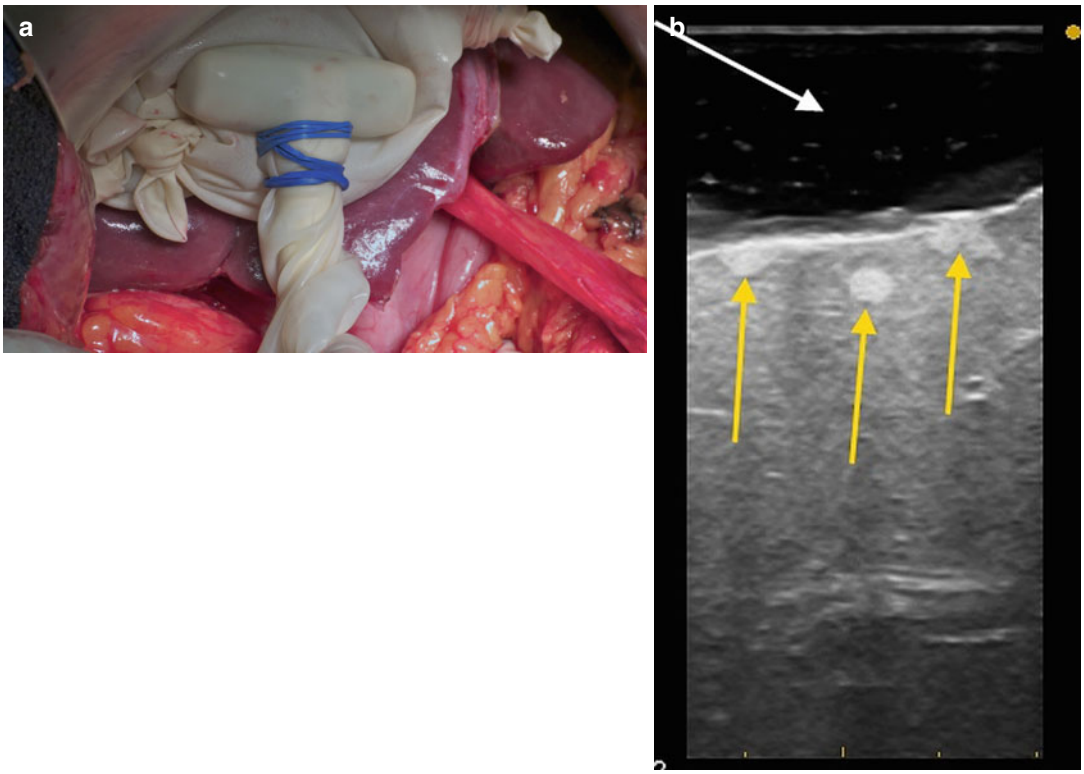

Fig. 15.2 (**a**) Probe standoff technique: a saline-filled glove is placed between the probe and the liver in order to examine the superficial aspect of the liver. (**b**) Probe standoff (*white arrow* indicates saline interface) allows better visualization of superficial lesions (*yellow arrows* indicate lesions)

transducer to avoid artifacts. The covered cord must be kept off the ground and away from all equipment.

IOUS of the Liver

Open Approach

The ultrasound scanner and monitor screen are placed to the right of the patient. The surgeon can begin with a small incision as it is easy to slide the hand between the liver and the diaphragm. If there are no contraindications to the planned operation, the incision can be extended and the liver mobilized to perform a complete IOUS.

The probe is placed directly on the surface of the liver. Typically, no gel is required, as the natural surface moisture of the liver is adequate for acoustic coupling. In some cases, however, some moisture on the liver surface is required. Only light pressure should be applied to the liver surface to avoid vascular compression. It is important to note that there is decreased resolution for about the first 5 mm between the probe and liver surface. In order to explore this area, probe standoff can be used with saline immersion (Fig. 15.2a, b) (refer to "Probe standoff scanning" for further information). The probe is moved in different directions by making small rotational movements around its axis. A standardized approach and technique is essential in order to ensure complete exploration of the organ. The liver is scanned completely from the upper to the caudal edge, moving from the left to the right through the entire organ in a systematic manner in order not to leave any area unexplored.

Aims of the liver ultrasound exploration are:

- To identify tumors
- To discover tumor thrombi and vascular invasion
- To define the relation of these lesions with respect to the vascular anatomy

The initial step of IOUS of the liver is to identify each hepatic vein as it arises from the inferior vena cava. The probe is held in a transverse midline position on the anterior surface of the liver and angled toward the beating heart (Fig. 15.3). All three hepatic veins must be followed to their peripheral tributary branches by moving the probe along the hepatic veins' axes.

The next step is to identify and follow the portal pedicles in order to define segmental anatomy of the liver. This is best achieved by placing the transducer on the surface of the liver, at the level of the segment IV, and angling the transducer toward the porta hepatis. Beginning from the left of the round ligament, the left portal branches for segments 2, 3, and 4 are identified and followed. Thereafter, moving over to the right side of the round ligament, the anterior and the posterior branches of the right portal vein and the feeding vessels for segments 5, 6, 7, and 8 are identified and followed. By using the intraoperative Doppler and color flow setting, dilated bile ducts can be discriminated from adjacent vascular structures

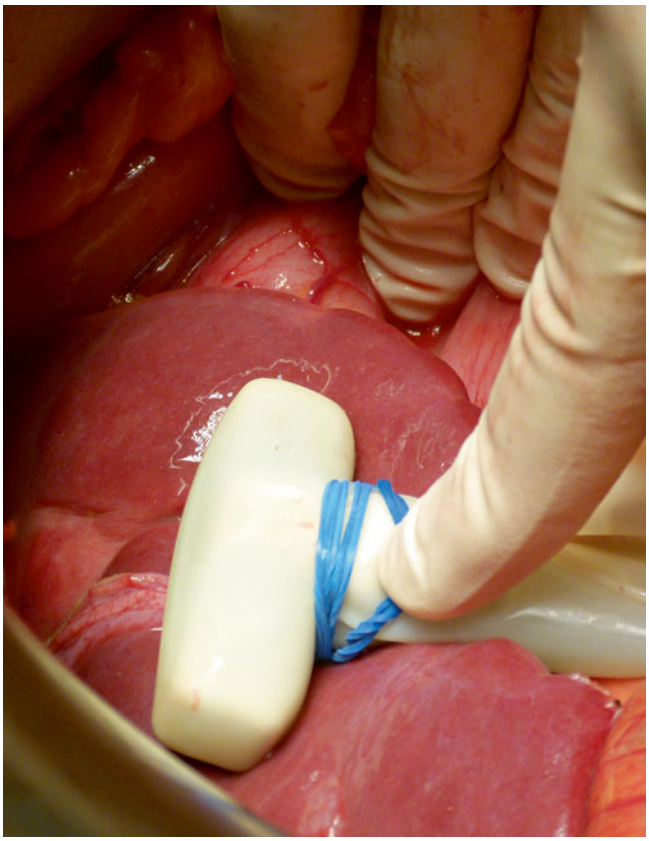

Fig. 15.3 The probe is angled toward the heart in order to identify hepatic veins

and define the flow direction. The examination is completed with ultrasound of gallbladder and the porta hepatis.

Laparoscopic Approach

As the use of laparoscopic procedures and minimally invasive surgery continues to increase, the role of IOUS during laparoscopy has become even more important. The laparoscopic approach has some limits as the surgeon is unable to palpate the liver and potential lesions. The technique of laparoscopic IOUS is similar to the open approach. The probe is introduced through a 12-mm epigastric or umbilical port for longitudinal imaging and a lateral abdominal port for transverse imaging. We use a 7.5-MHz linear-array transducer. A flexible probe is preferable as it allows better contact with the liver surface, which is limited by using a rigid probe (Fig. 15.4a, b). As in the open IOUS, the posterior segments of the liver are difficult to visualize. To explore this "blind area," it is essential to obtain maximal medial displacement of the liver by placing the patient in the semi-lateral position with the right side elevated.

Contrast-Enhanced Intraoperative Ultrasound (CE-IOUS)

There are limitations in liver ultrasound. In cirrhotic patients, IOUS is able to identify new lesions in 15–33 % of patient with hepatocellular carcinoma (HCC), which can change the surgical strategy [4, 6, 7]. On the other hand, tiny metastases from colorectal cancer may be not detected during IOUS [5].

Fig. 15.4 (**a**) The laparoscopic ultrasound probe with a flexible tip. (**b**). Angulation of the laparoscopic ultrasound probe allows for better exploration of the liver surface

Contrast-enhanced intraoperative ultrasound (CE-IOUS) has improved the ultrasound capability in detection and characterization of hepatic nodules [8]. Second-generation microbubble contrast agents have further improved the sensitivity of CE-IOUS [9, 10]. The microbubble is an ideal ultrasound contrast agent as it is extremely echogenic, as well as biocompatible, multifunctional, and inexpensive. Microbubbles are gas spheres between 0.1 and 10 μm in diameter and are much smaller than the wavelength of diagnostic ultrasound, which is typically 100–1,000 μm [11]. The gas core has a low density and is highly compressible, allowing it to shrink and expand

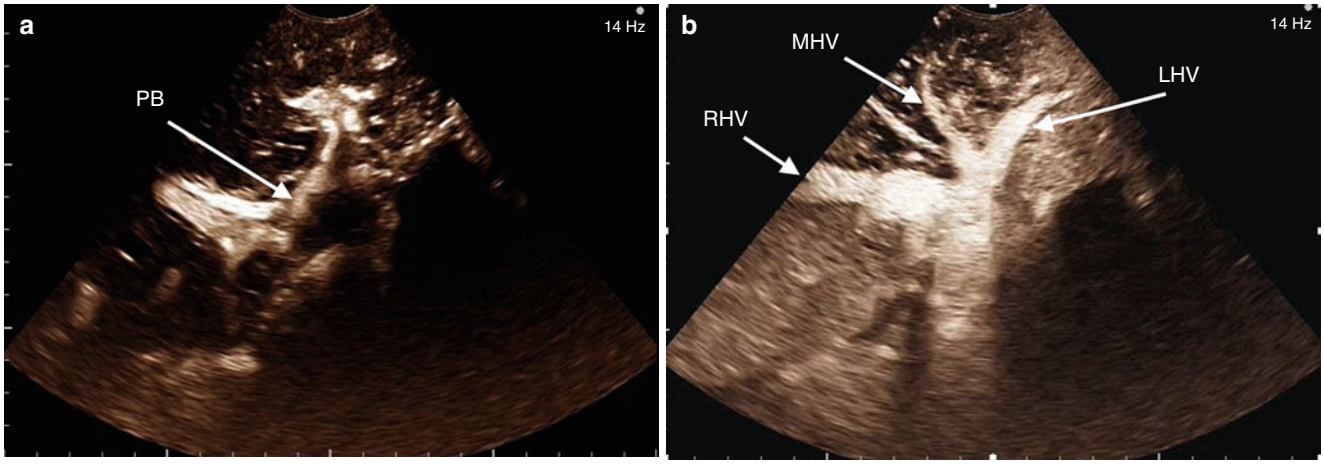

Fig. 15.5 Contrast-enhanced intraoperative ultrasound (CE-IOUS). (**a**) Arterial and portal features after injection of SonoVue. Portal bifurcation (*PB*) is showed by *white arrow*. (**b**) Hepatic veins in the late phase of CE-IOUS: right hepatic vein (*RHV*), middle hepatic vein (*MHV*), and left hepatic vein (*LHV*)

with the passage of an acoustic wave. The most widely used contrast agent is SonoVue (Bracco Imaging, Milan, Italy®) commercialized in Italy since the end of 2001. It is a pure intravascular contrast agent made of stabilized microbubbles containing sulfur hexafluoride, an echogenic and poorly soluble gas. Microbubbles have approximately the same size of red blood cells and are able to move into the vessels, but not through the vascular endothelium into the interstitial space. Recently, a new ultrasound contrast agent, Sonazoid (GE Healthcare, Oslo, Norway ®), has been developed, but it is not available in every country. It accumulates in hepatic Kupffer cells, providing a parenchyma-specific image in addition to demonstrating tumor vascularity [12, 13]. IOUS is initially performed in order to search for new nodules and to establish a surgical strategy. Following IOUS, CE-IOUS is performed in order to detect new nodules. CE-IOUS is also performed at the end of restorative face of liver transplantation (LT) in order to check the vascular anastomoses patency and the parenchyma perfusion. We use a dedicated probe for CE-IOUS and utilize SonoVue as contrast agent. The anesthesiologist injects 4.8 ml of SonoVue through a peripheral vein, which is followed by 10 ml of normal saline. The ultrasound is then performed using an US machine, which has contrast-specific software. Each phase of the ultrasound examination is recorded (arterial phase, portal phase, and late phase) (Fig. 15.5a, b). (Refer to section "Intraoperative contrast-enhanced ultrasound" in Chap. 23, for further information.)

Normal Anatomy

Knowledge of the anatomy of the liver is very important in order to understand and analyze under ultrasound the different aspects of the hepatic parenchyma, segmental anatomy, and structures, such as the vessels and biliary tract.

Ultrasound Anatomy of the Liver

The normal liver parenchyma is of a medium echogenicity and is made of many thin spots creating a homogenous appearance. In comparison to the kidney, the liver is less echogenic. However, in the case of steatosis, there is an increase in liver echogenicity as compared to the kidney. The liver surface is normally very smooth. Irregular and nodular appearance with protrusions or indentations are typical features found in liver cirrhosis.

Segmental Anatomy of the Liver

The liver is a large organ without many landmarks. Its blood vessels are not identified or defined on the surface. These difficulties in defining liver anatomy and its vasculature can be resolved by performing IOUS. The importance of the intrahepatic vasculature as a guide for the recognition of the segmental anatomy of the liver is extremely important for liver resection and, in particular, for repeat liver resection. In cases of repeat liver resection, the liver surface is different and IOUS is paramount in defining the segmental anatomy and vasculature. IOUS is also very useful for marking vessels on the liver surface to guide the resection and to perform anatomic hepatectomies. To obtain the most useful information by performing IOUS, the surgeon must be familiar with the relevant intraoperative and vascular anatomy and the spectrum of normal and abnormal findings.

Segmental anatomy of the liver is based on the hepatic veins and the intrahepatic branches of portal system. As described by Healy and Schroy, hepatic territories are defined as Glissonian segments, which are based on Glissonian pedicles with an arterial branch, portal branch,

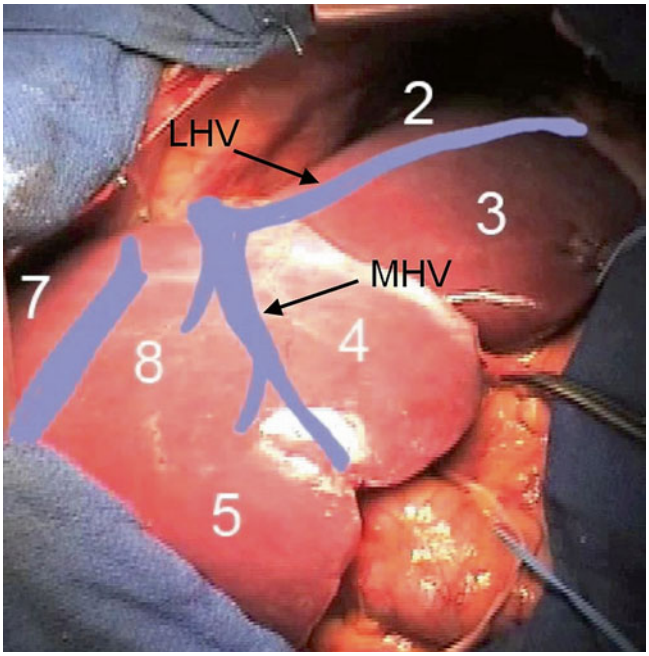

Fig. 15.6 Liver anatomy according to Couinaud segmentation. The middle hepatic vein (*MHV*) divides the right and left livers. The left hepatic vein (*LHV*) runs between segments *2* and *3*

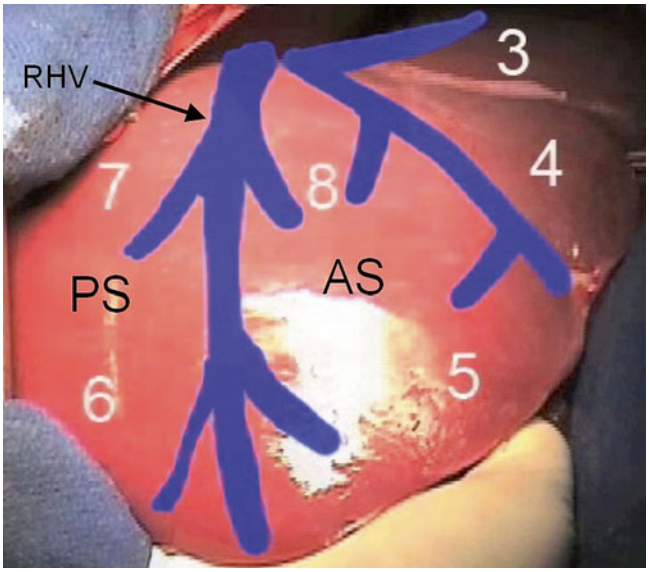

Fig. 15.7 The right liver is divided by the right hepatic vein (*RHV*): the anterior sector (*AS*) and the posterior sector (*PS*)

and intrahepatic bile duct [14]. The pedicles are surrounded by the intrahepatic extension of the Glisson's capsule that covers the liver surface. Alternatively, Couinaud described eight liver segments, whereby the left liver consists of segments 2, 3, and 4 and the right liver consists of segments 5, 6, 7, and 8 [15]. Note that in this terminology, the left lobe consists of segments 2 and 3 and the right lobe consists of the right liver (segments 5, 6, 7, and 8) and segment 4. The left hepatic vein travels between segments 2 and 3 in the left lobe. The middle hepatic vein divides the left and the right livers, whereby the right hepatic vein divides the right liver into the anterior sector (5 and 8) and the posterior sector (6 and 7) (Figs. 15.6 and 15.7).

The hepatic veins are identified beginning at their junctions with the IVC and are followed along their main axes. The hepatic veins divide the liver into different sectors. The plane between the middle hepatic vein and the IVC (inferior vena cava) divides the right (supplied by the right portal vein) and the left hepatic parenchymas (supplied by the left portal vein) (Fig. 15.6). The junction between the IVC and hepatic veins is easy to identify (Fig. 15.8). Since they are not surrounded by Glisson's capsule, the walls of the hepatic veins are recognized as a thin echogenic line. Typically, the left and the middle hepatic veins have a common trunk (Fig. 15.8). Several branches including one large posterior and some small anterior tributaries usually form the left hepatic vein. Two anterior veins from segments 4 and 5 form the middle hepatic vein. Less frequently, there are small veins draining the upper part of the segment 4 and segment 8

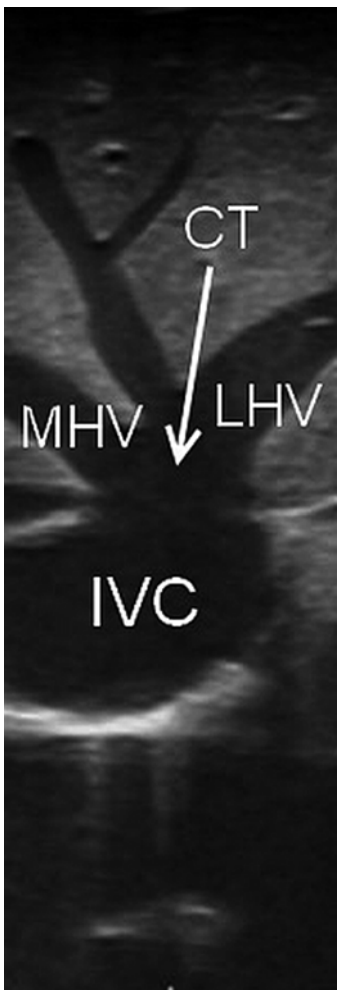

Fig. 15.8 The common trunk (*CT*) is formed by the left (*LHV*) and middle (*MHV*) hepatic veins to empty into the inferior vena cava (*IVC*)

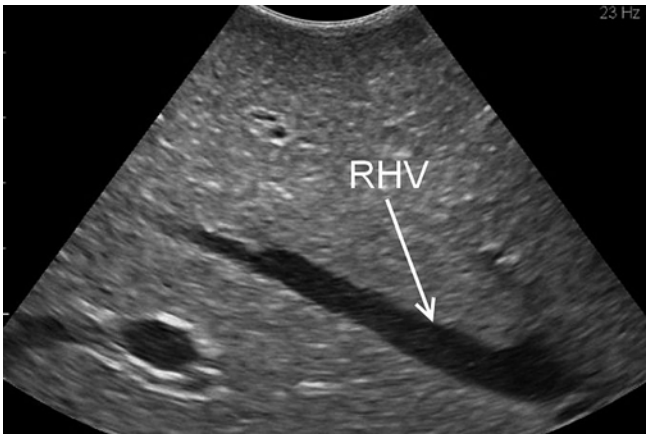

Fig. 15.9 The right hepatic vein (*RHV*) divides the right liver in the anterior and posterior sectors

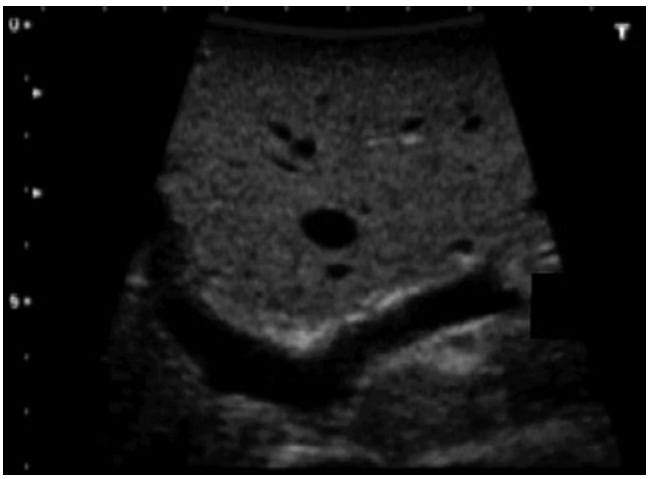

Fig. 15.11 Portal bifurcation at the hepatic hilum

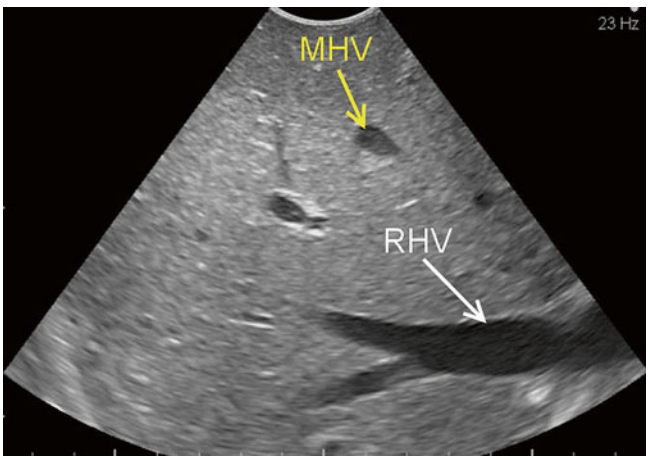

Fig. 15.10 Here, depicted are the right hepatic vein (*RHV*, *white arrow*) and the middle hepatic vein (*MHV*, *yellow arrow*)

into the middle hepatic vein. As indicated above, the plane between the IVC and the middle hepatic vein splits the liver in two different parts, each with its own portal supply. The line passing through this plane is called main portal scissure and is very useful to discriminate the limit between the right and left hepatectomies.

The junction between the IVC and the right hepatic vein is located on the right side of the IVC and typically (70 %) consists of a single large trunk (Figs. 15.9 and 15.10). There are usually three or four hepatic veins which drain segment 1 and very difficult to recognize due to their small size. The surgeon should also recognize the location of accessory hepatic veins, as this can be clinically important. For example, a right accessory hepatic vein draining the inferior right liver allows the surgeon to preserve the inferior portion of the right liver (segments 5, 6), even in case of ligature of the right hepatic vein [16, 17]. This vein is present in 13 % and joins the IVC directly at the level of the hepatic hilum.

The portal vein is the most important element of the hepatic hilum, and the intrahepatic branches are used to determine the segmental anatomy. The portal bifurcation is easily detectable under ultrasound by placing the probe transversely over the lower portion of segment 4 targeted on the hilum and through a horizontal plane. The arterial branch and the biliary system are typically anterior and superior to the portal system and can be difficult to identify (Fig. 15.11).

Keeping the probe in the same plane and moving it toward the left side, the extrahepatic portion of the left branch of the portal vein (i.e., the horizontal portion of the left portal vein) is followed. At this level, in the posterior plane, the segment 1 portal branches are identified. The left portal vein then turns anteriorly (i.e., the umbilical portion of the left portal vein) and extends to the round ligament, where the round ligament appears as a well-defined hyperechoic zone. Here, the left portal vein terminates in a cul-de-sac named the recess of Rex (Fig. 15.12a–d). At the "elbow" of the left portal vein, the branch to segment 2 arises (Fig. 15.13). At the level of the recess of Rex, the left portal vein terminates into two branches to segment 3 (to the left) and to segment 4 (to the right) (Fig. 15.14).

The right branch of the portal vein is short as it divides early into its anterior and posterior branches (Fig. 15.15). The anterior branch of the right portal vein is located between the right and middle hepatic veins and supplies the anterior sector of the right liver with separate branches to segments 5 and 8. The posterior trunk of the right portal vein supplies the posterior sector of the right liver but is more variable as it supplies multiple branches to segments 6 and 7. One of the most important anatomic variations of the portal system is the trifurcation of the portal vein, where the main portal vein divides into the left, right anterior, and right posterior branches. Also important is the "slipping" of the right anterior branch, where this branch arises from the left portal vein.

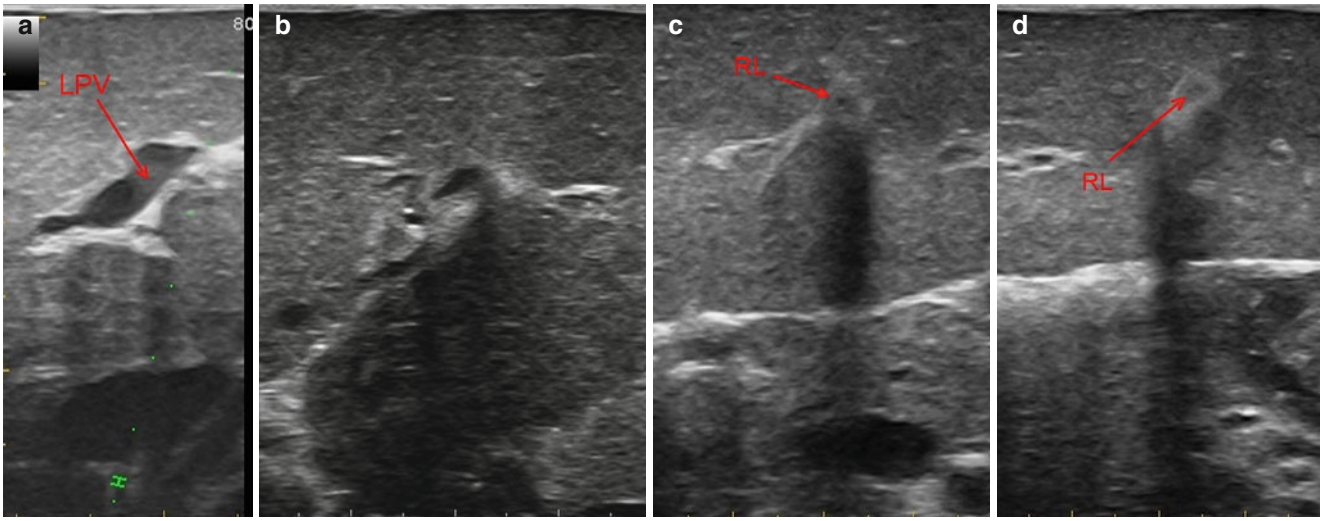

Fig. 15.12 (**a**–**d**) This series of images shows the left portal vein (*LPV*) (**a**) where it extends to the round ligament and as it terminates in the recess of Rex (**b**) at the round ligament (*RL*). The round ligament appears as a well-defined hyperechoic zone (**c**, **d**)

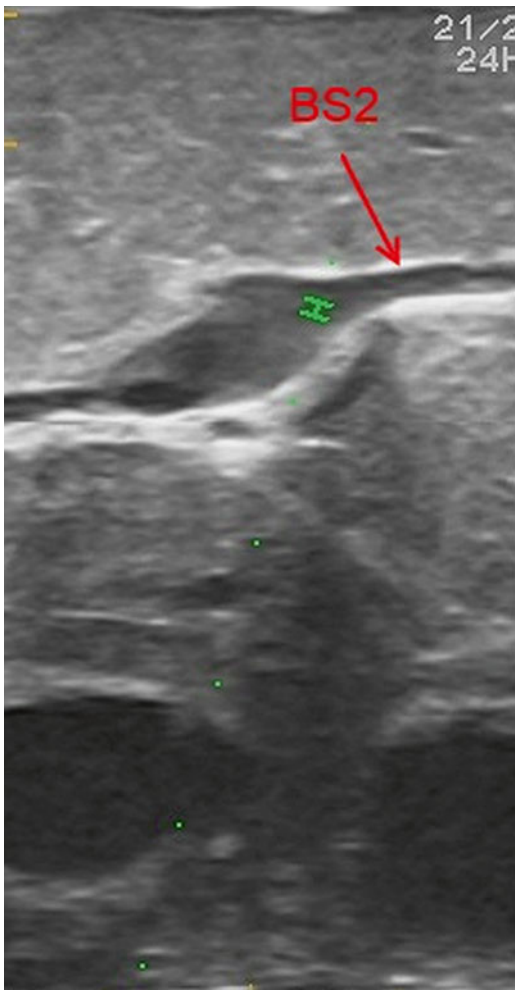

Fig. 15.13 The picture shows the origin of the portal branch to segment 2 (*BS2*)

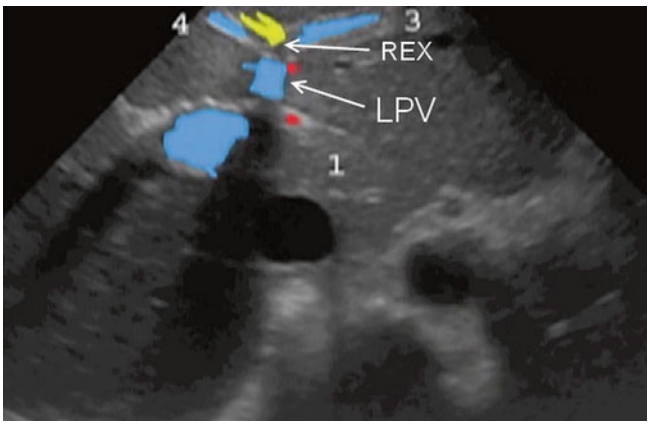

Fig. 15.14 Left portal vein (*LPV*). Portal branches to segments 3 (*3*) and 4 (*4*) can be recognized at the level of the recess of Rex (*REX*). Also seen here is the portal branch to segment 1 (*1*)

An arterial variation that is frequently relevant is a replaced right hepatic artery, which arises from the superior mesenteric artery and travels posterior to the portal vein. A replaced or accessory left hepatic artery arising from the left gastric artery and running through the ligamentum venosum may also be encountered. Intrahepatic arteries are not usually visible but may be enlarged in the case of arterialization of the liver (pathological finding) or after a major hepatectomy. The right and left bile ducts, as well as their confluence, are normally identifiable and their typical diameter is approximately 5 mm. The peripheral bile channels are not evident unless they are dilated for pathological reasons, such as in biliary obstruction.

The exploration of some areas of the liver is particularly challenging in the intraoperative setting.

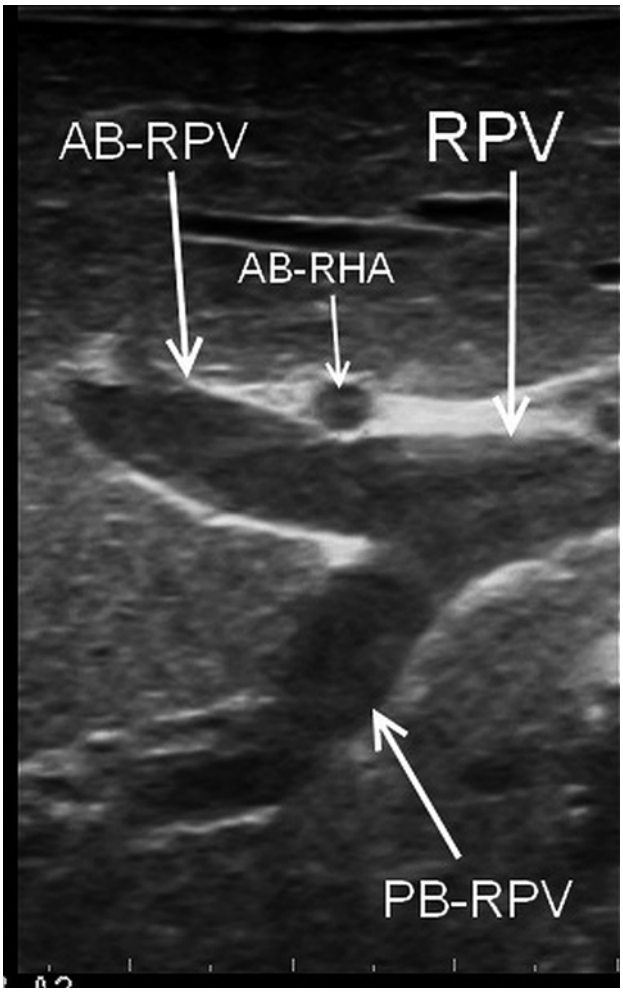

Fig. 15.15 Right portal vein (*RPV*) and its anterior (*AB-RPV*) and posterior branches (*PB-RPV*). Also seen here is the anterior branch of right hepatic artery (*AB-RHA*)

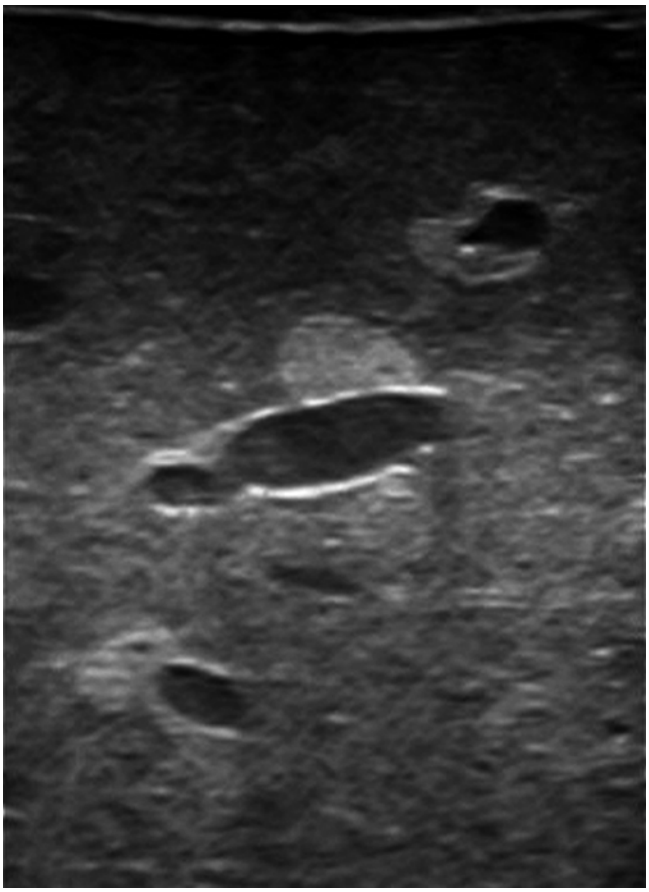

Fig. 15.16 Hepatic adenoma. It appears as a hyperechoic round lesion placed side to hepatic vein without any signs of compression

For example, upper and lateral aspects of the right liver, whose access typically requires dissection of the falciform and triangular ligaments, can be difficult to image. In that case, it might be necessary to place the probe on the inferior surface of the liver. Lesions very close to the liver surface can also be difficult to image. In this case, a probe standoff technique, as discussed earlier, can be used or placing the probe on the opposite surface of the liver can image the lesion.

Ultrasound Features of Hepatic Tumors

IOUS can identify certain hepatic tumors due to different sonographic characteristics as compared to the normal liver parenchyma. Tumors are characterized as being an-, hyper-, or hypoechoic when compared to normal hepatic parenchyma. Anechoic (appears black) lesions are typically cystic and may be, for example, biliary cysts or hydatid cysts. Hyperechoic (appears brighter than the background liver) lesions are more commonly benign tumors such as hemangiomas and adenomas (Fig. 15.16). Less frequently, malignant lesions are hyperechoic. Finally, hypoechoic (appears darker than the background liver) lesions are typically malignant tumors (Fig. 15.17a–c), such as colorectal liver metastasis (CRLM), neuroendocrine tumor, or HCC. Homogenous isoechoic tumors are the most difficult to recognize. They may be identified only by their mass effect on neighboring vascular structures or by the presence of a hypoechoic border. Tumors may be either homo- or heterogeneous (mixed), compared to normal parenchyma, and the ultrasound beam beyond the lesion may be attenuated, increased, or completely absent. The usefulness of IOUS is even more important for unknown lesions detected intraoperatively. In this section, the ultrasound features of CRLM, HCC, and benign tumors as well as the role of IOUS in the detection of the primary and metastatic tumors will be discussed.

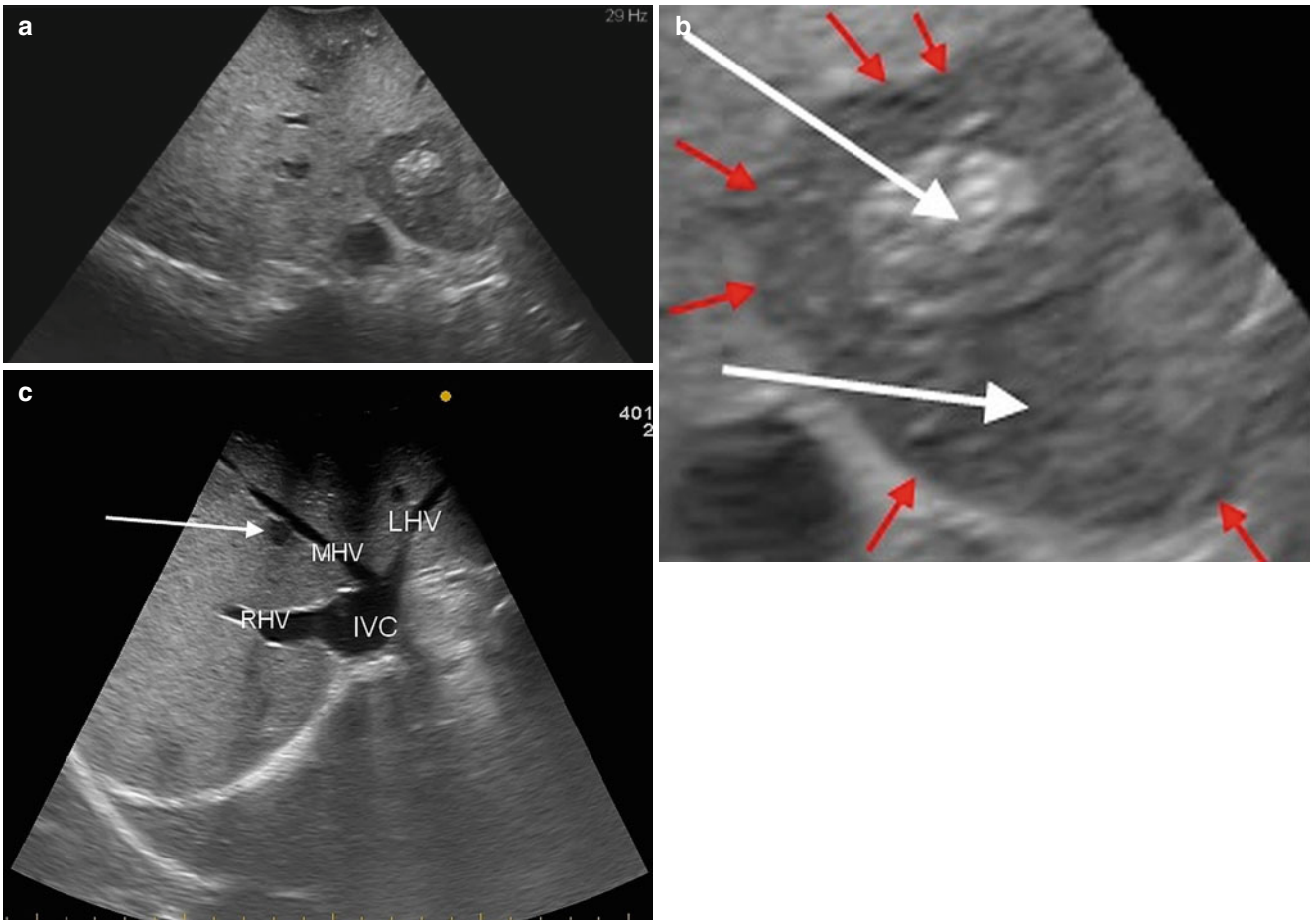

Fig. 15.17 Liver metastases. (**a**, **b**) The ultrasound characteristics of a lesion may be influenced by the degree of necrosis in response to chemotherapy. (**a**) This post-chemotherapy-treated colorectal liver metastasis is a heterogeneous lesion, which is predominantly hypoechoic with a central hyperechoic zone. The hyperechoic zone may represent calcification. (**b**) The border of the lesion is irregular as showed by *red arrows*. *White arrows* indicate the hypo- and hyperechoic characteristics of this lesion. (**c**) This hypoechoic lesion corresponds to a liver metastasis from neuroendocrine tumor. Note the proximity to the middle hepatic vein (*MHV*). *RHV* right hepatic vein, *MHV* median hepatic vein, *LHV* left hepatic vein, *IVC* inferior vena cava

Liver Metastasis

Approximately half of patients with colorectal cancer develop liver metastases [18, 19]. The only potentially curative option for these patients is surgical resection in order to reach a 5-year survival rate of 25–58 % [20, 21]. Intraoperative ultrasound has been recognized for years to be beneficial in those undergoing liver resection for colorectal liver metastases (CRLM). In particular, IOUS allows the surgeon to detect additional small CRLM not seen on preoperative cross-sectional imaging, typically those less than 2 cm and those metastases which have "disappeared" following chemotherapy (i.e., "missing" metastases). Several reports identify the additional detection rate of IOUS to be as high as 10–20 % [22, 23]. Sensitivity of more than 90 % has been reported with positive and negative predictive values of 90 and 70 %, respectively [24, 25]. Recent studies have suggested that with the improvement of preoperative imaging, there is no additional benefit of IOUS. However, Van Vledder and colleagues have demonstrated that IOUS leads to the detection of additional lesions in 10 % of patients and subsequently changes the surgical strategy in 9 % of patients [26]. Furthermore, they found that the probability of finding additional metastases varied considerably based on specific clinical and ultrasound features. Those who had more than four metastases or those who had hypoechoic lesions were found to have a higher chance of identifying additional lesions in 26 and 18 %, respectively. The detection of additional lesions may change the surgical approach and may contribute to improved outcomes. Recently, D'Hondt et al. reported that IOUS could change the operative strategy in 16.5 % of patients [27]. Furthermore, IOUS is useful to detect metastases, which have "disappeared" after chemotherapy. To improve surgical outcomes, there is an increasing trend to administer preoperative chemotherapy to patients with resectable CRLM. This leads to more patients who have a major radiological response but also leads to liver metastases which

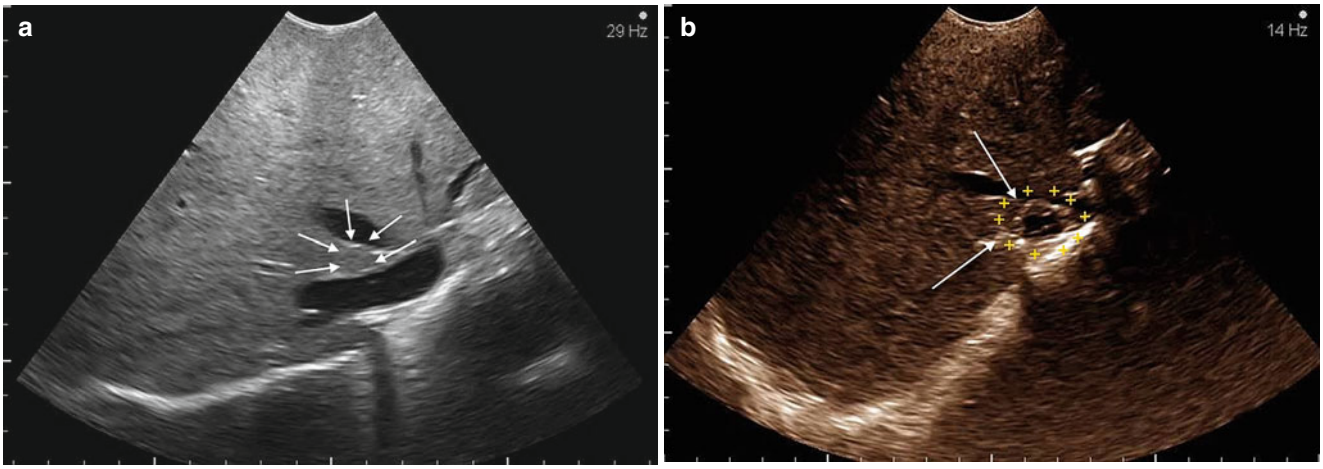

Fig. 15.18 Contrast-enhanced ultrasound. (**a**) IOUS is unable to detect this isoechoic lesion. The lesion is marked by the *white arrows*. (**b**) Following injection of contrast medium, the liver metastasis appears (*white arrows* and *yellow* +). This particular lesion had disappeared on the preoperative imaging following chemotherapy. This demonstrates the utility of CE-IOUS during standard IOUS, especially in those "missing" metastases following chemotherapy

"disappear" after chemotherapy. A recent paper reports that IOUS increases the intraoperative detection of these "disappearing" metastases in more than 50 % of cases [28]. The ability of IOUS to detect additional metastases is also improved by the use of contrast agents (Fig. 15.18a, b). CE-IOUS is more sensitive than conventional IOUS for detecting CRLM [32], with a sensitivity rate reported around of 97 % [29]. Recent papers have shown that CE-IOUS leads to a change in the surgical strategy in 14–30 % of CRLM cases [30, 31].

Hepatocellular Carcinoma

HCC is the fifth most common malignancy and represents the principal cause of death of cirrhotic patients [33–35]. Among the local treatments available, surgical resection is the most radical approach [36–39]. Intraoperative ultrasound enables identification of new occult lesions in 15–33 % of patients with HCC, and it is responsible for a change in operative strategy in more than 15 % of cases [27, 40] (Fig. 15.19).

IOUS is very important in those with cirrhosis and HCC. The hard and irregular surface of the cirrhotic liver makes detection of liver lesions by palpation very difficult, especially in the case of deep and small HCC [49]. Furthermore, atrophy or hypertrophy of the cirrhotic liver can make the localization of liver lesions and the definition of the liver vascularization more difficult. The use of IOUS allows for parenchymal-sparing resection and limits the number of patients undergoing major hepatectomy [50, 51].

However, IOUS has some limitations. In cirrhotic patients, less than half of the new lesions detected by IOUS are HCC.

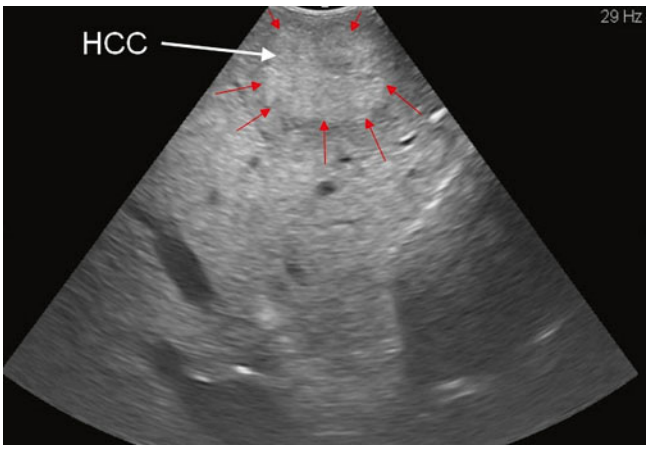

Fig. 15.19 Hepatocellular carcinoma. Note that it is isoechoic (*white arrow*) with a hypoechoic irregular rim (*red arrows*)

These lesions may be benign, which include regenerative and dysplastic nodules. The diagnosis of HCC is a critical point in cirrhotic patients to avoid resection and sacrifice of functioning parenchyma. In those with cirrhosis, the possibility to assess the vascularity of nodules detected by IOUS may improve the ability in discriminating malignant from benign lesions. In fact, except for those nodules with a mosaic ultrasound pattern, which are malignant in 80 % of cases, only 24–30 % of hypoechoic and 0–1 % of hyperechoic nodules are malignant when evaluating for HCC [4, 6]. A needle biopsy of a new lesion can be performed, but the false-negative rate is as high as 30 % [40–42]. Furthermore, a needle biopsy can lead to tumor seeding and ultimately may worsen the prognosis of a patient [43–45]. The analysis

of a nodule's vascularity may provide the crucial information for differentiation.

Recently, CE-IOUS has been reported to evaluate tumor vascularization as is done with other contrast imaging modalities [46, 47]. CE-IOUS using SonoVue has been advocated as an alternative to differentiate HCC from benign lesions found during IOUS [7]. Using CE-IOUS, a change in the surgical strategy has been reported in 35–79 % of cases [7, 48]. Even using the newer contrast agent Sonazoid, CE-IOUS is able to detect new lesions in more than 20 % of cirrhotic patients. In a prospective study, Arita and colleagues showed that the sensitivity and specificity of CE-IOUS with Sonazoid for differentiating HCC were 65 and 94 %, respectively, and with an accuracy of 87 % [40]. (Refer to section "Intraoperative contrast-enhanced ultrasound" in Chap. 23, for further information.)

Using CE-IOUS, hypoechoic or hyperechoic nodules are considered malignant if the lesion [52]:

- Becomes hyperechoic (i.e., full enhancement) in the arterial phase and becomes hypoechoic in the delayed portal and late phase
- Remains hypoechoic with thin vessels supplying the nodule in the arterial and delayed phases
- Does not show early enhancement (i.e., full enhancement on the arterial phase) but remains hypoechoic in the delayed phases without peripheral and/or intralesional neovascularization (refer to section "Intraoperative contrast-enhanced ultrasound" in Chap. 23, for further information)

IOUS allows an accurate three-dimensional reconstruction of the relationship between the tumor, the portal branches, and the hepatic veins: This is a fundamental step in the definition of the proper surgical strategy. It remains unclear whether hepatectomy for HCC should be performed as anatomic resection or nonanatomic resection. The majority of recurrences occur in the liver as a result of subclinical metastases, which originate from the primary tumor through microscopic vascular invasion and peripheral spread along the intrasegmental branches. This is the most important factor associated with a poor prognosis [53–55].

On this basis, the routine removal of the hepatic segment fed by tumor-bearing portal tributaries (i.e., the entire functional unit through an anatomic resection) has been suggested to be more effective for tumor eradication [56]. On the other hand, most surgeons prefer, in cirrhotic patients, to preserve functional liver parenchyma with a nonanatomic resection in order to reduce the risk of postoperative liver failure. Two recent meta-analyses of observational studies addressed this still debated topic. The meta-analysis of Zhou et al. [57] found that disease-free survival was better in those undergoing anatomic resection as compared to nonanatomic resection. Chen and colleagues [58] demonstrated similar results in terms of disease-free survival in their meta-analysis, however found no difference in overall survival between the two groups. Improved disease-free and overall survival in those undergoing anatomic as opposed to nonanatomic resection was also found by Cucchetti and colleagues [59]. However, in this meta-analysis, the nonanatomic resection group had a higher proportion of cirrhosis, which affected both disease-free and overall survival. These meta-analyses are limited as they include only retrospective observational studies and not randomized studies. Limited resection guided by IOUS is simpler than the routine segmentectomy as there is no need to identify and ligate the portal branch, which supplies the area of the liver to be resected. If resection is not feasible, either because of the extent of the tumor or because of a high risk of postoperative liver failure, percutaneous ultrasound-guided embolization of the portal branch supplying the tumor may be performed. Embolization can prevent a massive portal invasion that may further increase the preexistent portal hypertension and lead to a GI bleeding.

Benign Tumors

The most important role of IOUS in the benign tumors is to discriminate between them from malignant lesions. Usually, metastases that arise from the same primary malignancy have a similar size and similar ultrasound appearance. Therefore, if two or more lesions of similar size have different ultrasound appearances, it is possible that one lesion represents malignancy while the other may represent a different diagnosis, such as a benign lesion. Hemangiomas vary widely in appearance, but are typically soft. On Doppler ultrasound, hemangiomas do not have increased flow as compared to the adjacent liver parenchyma. They are solitary in 90 % of cases and are typically hyperechoic. Among the other solid tumors, such as adenoma and focal nodular hyperplasia, an ultrasound-guided biopsy is necessary if the diagnosis is in doubt.

Applications in the Hepatic Surgery

Hepatectomy

Certain steps should be followed in performing IOUS of the liver prior to liver resection. First, the tumor must be localized after performing a meticulous ultrasound. The probe should be moved slowly and gain should be modified to better characterize the tumor. The use of probe standoff with saline immersion, as described earlier, is useful to localize superficial lesions as is the placement of the probe on the opposite face of the liver. Secondly, anatomic variations

should be noted and taken into consideration prior to liver resection. The hepatic and portal venous systems must be evaluated, especially since hepatocellular carcinomas frequently invade major vessels as can colorectal cancer metastases. Once the tumor is localized and all segments of the liver have been evaluated, the relationship of the tumor and vessels in terms of vascular proximity, occlusion, and invasion is integrated by the surgeon. Color flow and Doppler US are frequently used to discriminate dilated bile ducts and blood vessels. If a vascular thrombus is identified, it may be important to distinguish between a tumor-associated thrombus, which is avascular, and a tumor thrombus, which has an arterial waveform at pulsed Doppler evaluation. It is always important to exclude the presence of a thrombus in critical areas such as the hepatic venous confluence.

Once a full evaluation of the liver anatomy and tumor features is complete, the best surgical strategy is chosen. In cases of deep lesions, the liver capsule can be marked with cautery overlying the lesion under ultrasound. Furthermore, the hepatic veins and portal branches can be marked to define the limits of resection. Ultrasound can be used during parenchymal resection to confirm the resection line and to ensure completeness of resection. During parenchymal transection, the air bubbles within the resection line are visible under ultrasound. A wet compress within the resection line also allows ultrasound visualization of the resection margin. Thus, during resection, the correct resection line can be verified using ultrasound.

Intraoperative ultrasound is imperative to evaluate the extent of the tumor in the liver. Ultrasound findings in the operating room can lead to a change in the surgical strategy or a contraindication of the planned surgery. For example, consider a CRLM case where the preoperative imaging demonstrates disease to be localized to the right liver; however, IOUS demonstrates disease to extend to the left liver and compress the left hepatic vein. Here, the planned resection is contradicted. On the other hand, consider a case where a small metastasis is found to be abutting or invading a segmental portal branch by IOUS; a parenchymal-sparing, such as segmentectomy or subsegmentectomy, may be undertaken [60]. Lastly, if multiple metastases of colorectal cancer are found to be bilateral under IOUS, consideration can be given to a two-stage hepatectomy (classic or ALPPS) [61–64].

Biopsy

Despite the improvement of preoperative imaging, the diagnosis of a lesion may be difficult to establish, such as in the case of small lesions in cirrhotic patients. If IOUS or CE-IOUS fails to discriminate between a benign and malignant diagnosis, an ultrasound-guided biopsy of the lesion is preferable (Fig. 15.20). Biopsy under ultrasound guidance can be performed and the specimen is analyzed as a fresh frozen section by pathology. We prefer to biopsy using a Menghini or Tru-Cut needle, which obtains a specimen that measures up to 2 mm of diameter.

To avoid hemorrhage, the biopsy needle is passed through normal parenchyma to reach the tumor for biopsy. If the biopsy demonstrates malignancy, resection of the liver parenchyma between the liver surface and the lesion where the needle passed during biopsy is necessary. This is to ensure completeness of resection as tumor seeding via the needle track can occur during biopsy.

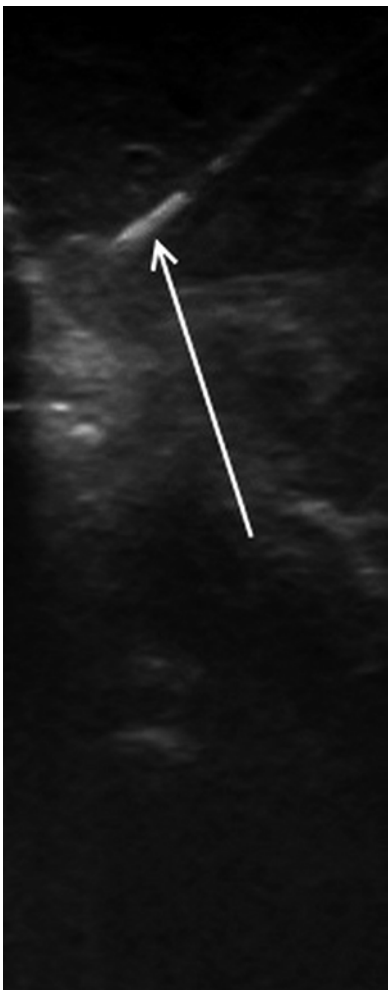

Fig. 15.20 A practical application of intraoperative ultrasound is biopsy. Depicted here is the intraoperative biopsy of a hypoechoic lesion (*white arrow*: biopsy needle)

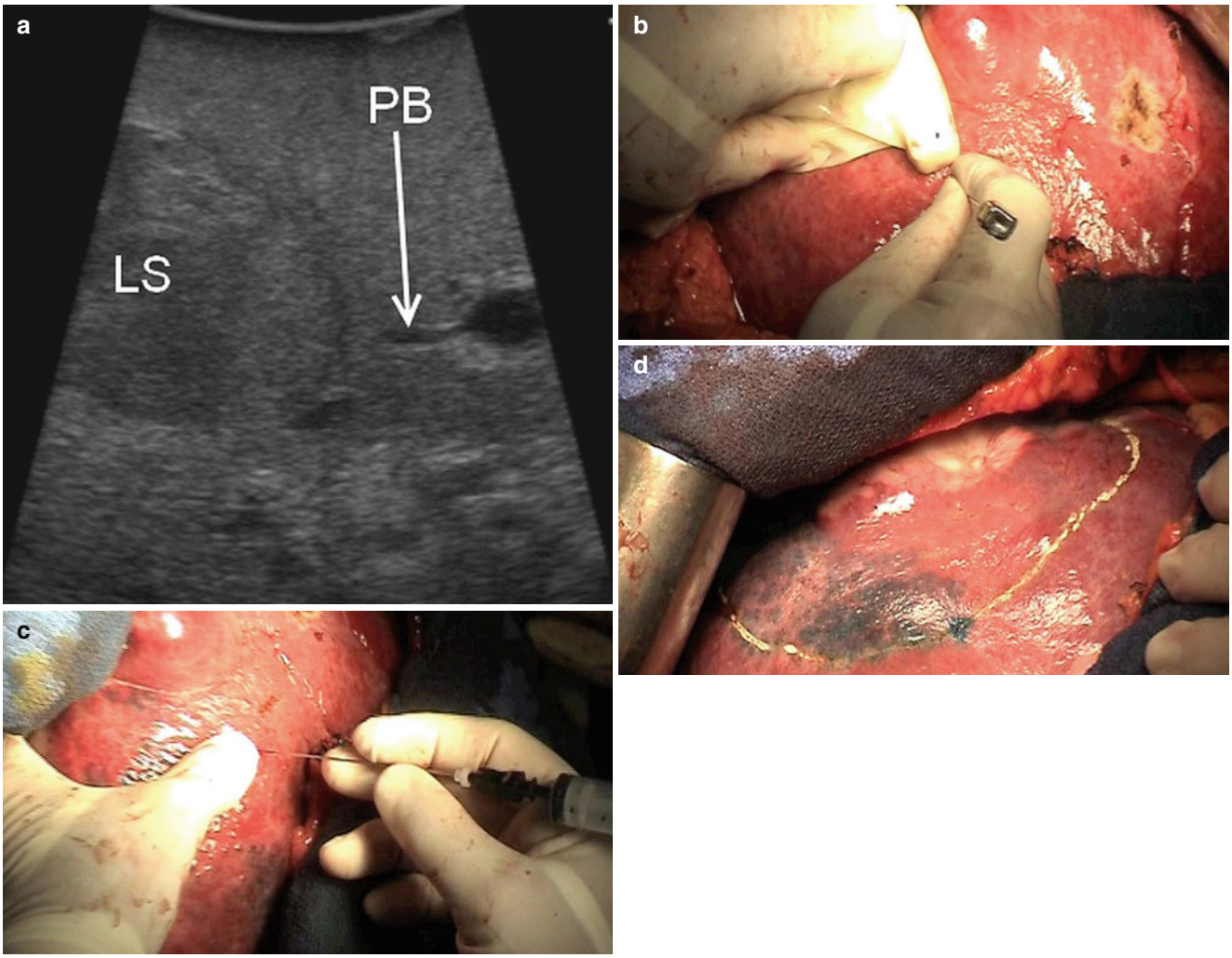

Fig. 15.21 Ultrasound-guided anatomic hepatectomy by dye injection. (**a**). Using US, the lesion (*LS*) with feeding portal branch (*PB*) is identified. (**b**) A Chiba needle is inserted under US guidance into the portal vein supplying the tumor. (**c**) Injection of methylene blue via the Chiba needle into the portal vein. (**d**) Methylene blue marks the extent of resection required by the portal supply

Ultrasound-Guided Anatomic Hepatectomy by Dye Injection

As described above, HCC can invade the portal venous branches either by direct invasion or by spread of cancer cells via the portal vein, which supplies the tumor. In patients with impaired hepatic function, a limited resection should be carried out in order to prevent postoperative hepatic failure. Therefore, in cirrhotic patients, a complete resection limited to the portal space containing the tumor is mandatory. This type of resection can be carried out by using blue dye injection guided by IOUS and is termed subsegmentectomy by a Japanese team [65]. After the tumor is identified by IOUS, the portal vein supplying the tumor is accessed under ultrasound and blue dye (methylene blue) is injected. The stained area defines the limits of the resection and is marked by electric cautery. In patients with HCC, an arterial-portal shunt is not uncommon, and, therefore, hepatic artery branch should be occluded during injection. This will ensure containment of the blue dye to the portal unit requiring resection (Fig. 15.21).

Ultrasound-Guided Vessel Compression

It is generally considered that for anatomic sectionectomy, preventive division of the sectional vascular pedicles by an extrahepatic approach is required for definition of the hepatic

area to be resected. However, many of the proposed techniques are technically demanding and time consuming and have associated drawbacks [66–71]. According to Torzilli and colleagues, IOUS-targeted bimanual liver compression can be an effective method to identify subsegmental and segmental areas of the liver and to remove them in an anatomic fashion [72, 73]. IOUS and, if needed, CE-IOUS are performed before using the US-guided vessel compression technique. Once the tumor is identified, the most peripheral portal pedicle supplying the tumor is located under IOUS. The hemiliver where the lesion is located is partially mobilized. The surgeon's left or right hand is placed below the right or the left hemiliver, respectively, while the IOUS probe, handled by the surgeon's other hand, is placed above the liver. Both hands are positioned at the level of interest under IOUS, which is at the most distal portion of the vessel, but proximal to the tumor to be removed. The surgeon uses his/her fingertips and the IOUS probe to compress bilaterally the liver at the targeted position. This results in compression of the portal pedicle supplying the tumor, as previously identified. This maneuver is constantly monitored by real-time US. The IOUS probe is maintained on the liver surface until discoloration is noted. Once the first assistant marks the discolored area with the electrocautery, the compression is released. Due to the thickness and the shape of the liver profile, bimanual compression is more difficult to apply for lesions located in segments 1, 8, or superior 4. These areas should be demarcated by compressing the segmental branches of the adjacent segment, section, or hemiliver. Once the area is demarcated, IOUS is used to guide liver resection.

The main advantage of this technique is that it is not invasive, as it does not require any additional vascular access, dissection, or clamping. The technique is always feasible and totally reversible. It does not require vascular division, injection, or ablation. Once the compression is released, there is full return of the liver to the initial condition. Mobilization of the liver to accomplish the targeted compression may be required to perform the liver dissection. Furthermore, this maneuver can minimize the area of resection by choosing, under IOUS, the most peripheral and suitable level of compression of the feeding portal and arterial branches. This has the potential added value of further sparing liver parenchyma, as compared with a complete segmentectomy. It may be potentially applied in each segment of liver as long as the thickness of the parenchyma and the anatomy of liver are suitable [60]. This technique has even been described for resection of segment 8 [74].

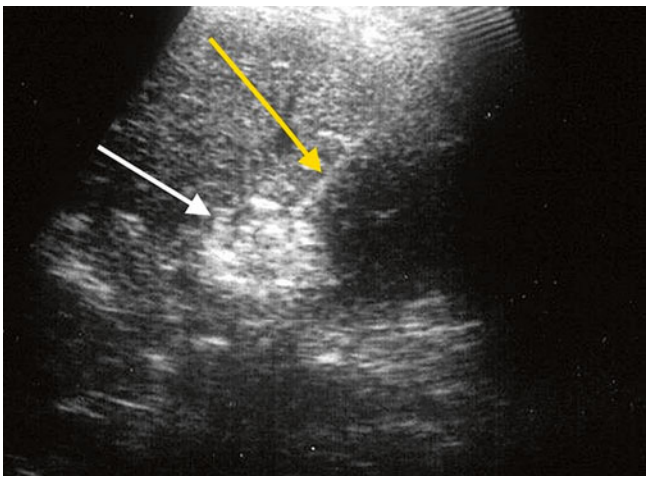

Fig. 15.22 Radiofrequency (RFA) liver tumor ablation. The radiofrequency needle (*yellow arrow*) is inserted into the lesion (*white arrow*) under US guidance. Once the radiofrequency energy is applied, the efficacity of the procedure can be monitored by the appearance of a hyperechoic rim around the lesion

Guidance of Intraoperative and Percutaneous Radiofrequency Ablation and Other Ablative Techniques

Hepatic resection is the most effective treatment for patients with primary or metastatic hepatic malignancies. Unfortunately, liver resection can be limited by a poor functional reserve of the remnant liver in cirrhosis and by the presence of multifocal bilateral lesions in metastatic disease. Nowadays, radiofrequency ablation (RFA) has been accepted as a treatment for primary and liver metastases when liver resection is contraindicated. Four prospective randomized studies showed superiority of RFA compared to ethanol injection in terms of local recurrence and overall survival in those with HCC [75–78]. Furthermore, there are now at least five reports, including one randomized trial, comparing RFA with resection for HCC. RFA has been shown to have similar local tumor control with a lower rate of complication for small HCC [79–83]. IOUS guidance during RFA is useful to identify the tumor, to guide the RFA needle into the tumor, and to check the efficacity of ablation (Fig. 15.22). (Refer to Chap. 17 for further information.)

Application in Liver Transplantation

IOUS has an important role in liver transplantation (LT). It is routinely used to assess the status of vascular anastomoses. Pulsed and color Doppler evaluation of the hepatic

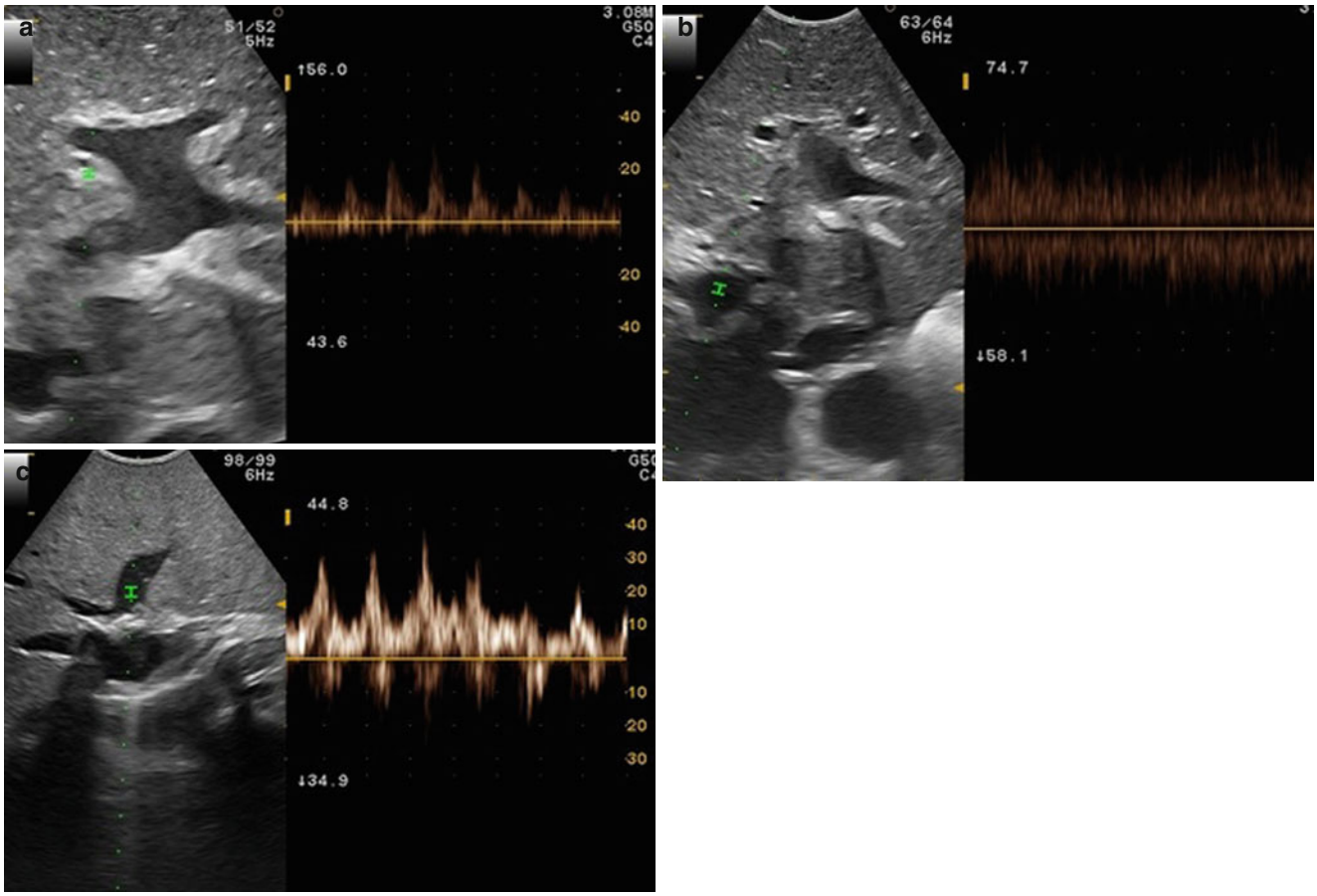

Fig. 15.23 Intraoperative ultrasound during liver transplantation. Each vessel is evaluated using Doppler in this series of figures. (**a**) The arterial flow, (**b**) portal flow, and (**c**) hepatic venous flow are verified. In each slide, the green notch indicates the vessel being assessed

artery as well as the study of the portal vein and the inferior vena cava (IVC) should be included in the ultrasound exam.

Sometimes, primary graft nonfunction is related to vascular complications, which can be addressed during the operation. Therefore, its detection during LT is extremely important.

We perform color Doppler IOUS (CE-IOUS) once the vascular anastomoses are done. A complete examination should show good flow within the main hepatic artery, proximal and distal to the anastomosis, as well as in the right and left hepatic branches (Fig. 15.23a–c). Usually, the hepatic artery has low-impedance waveform pattern with flow during the diastolic phase. The absence of flow in the hepatic artery would suggest a hepatic artery thrombosis (HAT). The normal hepatic vein waveform pattern shows cyclical variations of flow velocity during inspiration and flow reversal flow the contraction of the right heart. Nonphasic hepatic vein waveforms can be found in vena caval stenosis or thrombosis (i.e., Budd-Chiari syndrome). The typical pattern of the portal vein demonstrates almost continuous flow, with variations related to breathing movements.

CE-IOUS at the end of LT has been useful for us to better evaluate portal, arterial, and hepatic venous flow. CE-IOUS can be useful to detect arterial flow where classic IOUS has failed to demonstrate flow. On the other hand, in patients with normal flow on IOUS, altered arterial perfusion may be detected by CE-IOUS (Fig. 15.24a–c). IOUS examination is also required during the harvesting phase of living donor liver transplantation (LDLT). Ultrasound examination of the hepatic veins is essential in planning and guiding resection during LDLT.

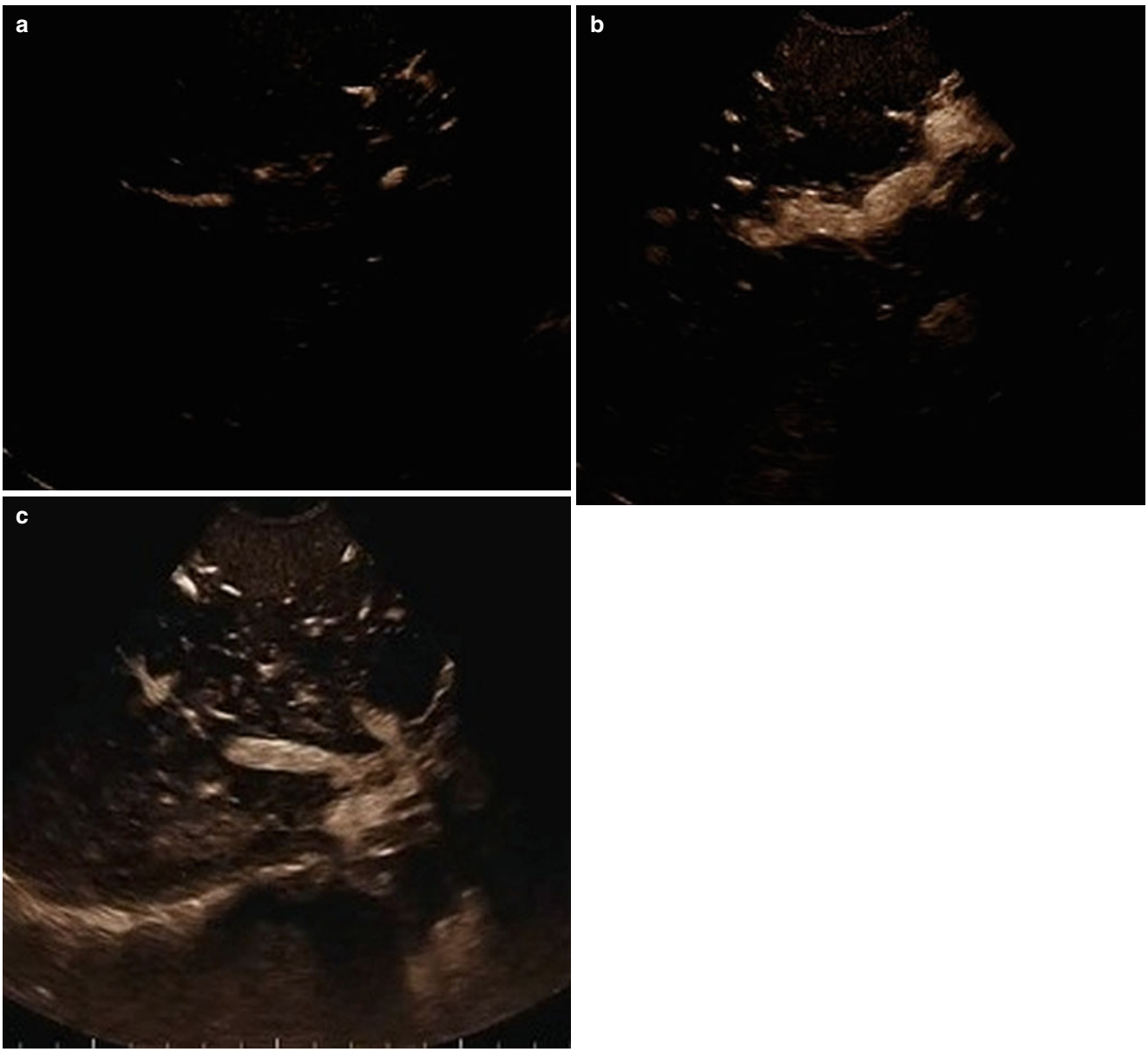

Fig. 15.24 CE-IOUS during liver transplantation. CE-IOUS is performed at the end of liver transplantation to verify patency of the (**a**) arterial, (**b**) portal, and (**c**) hepatic venous phases

Conclusion

IOUS provides crucial diagnostic and staging information to the surgeon during liver surgery.

The use of IOUS is mandatory during hepatic surgery and should be part of surgeons' professional training and experience. Despite the high quality of preoperative imaging, IOUS is still an essential tool in detecting lesions and planning and executing the surgical strategy.

References

1. Schlegel JU, Diggdon P, Cuellar J. The use of ultrasound for localizing renal calculi. J Urol. 1961;86:367–9.
2. Yamakawa K, Naito S, Azuma K, et al. Laparoscopic diagnosis of intraabdominal organs: ultrasound diagnosis through laparoscopy. Jpn J Gastroenterol. 1958;55:741.
3. Makuuchi M, Kamiya K, Sugiura M, et al. Ultrasonic examination by electronic scanning during operation. Proceedings of the 32nd meeting of the Japan Society of Ultrasonics in Medicine, Tokyo, Japan. 1977. p. 129–30.
4. Takigawa Y, Sugawara Y, Yamamoto J, et al. New lesions detected by intraoperative ultrasound during liver resection for hepatocellular carcinoma. Ultrasound Med Biol. 2001;27(2):151–6.
5. Yamada H, Kondo S, Okushiba S, et al. Analysis of predictive factors for recurrence after hepatectomy for colorectal liver metastases. World J Surg. 2001;25(9):1129–33.
6. Kokudo N, Bandai Y, Imanishi H, et al. Management of new hepatic nodules detected by intraoperative ultrasonography during hepatic resection for hepatocellular carcinoma. Surgery. 1996;119:634–40.
7. Torzilli G, Palmisano A, DelFabbro D, et al. Contrast-enhanced intraoperative ultrasonography during surgery for hepatocellular

carcinoma in liver cirrhosis: is it useful or useless? A prospective cohort study of our experience. Ann Surg Oncol. 2007;14:1347–55.
8. Solbiati L, Tonolini M, Cova L, et al. The role of contrast-enhanced ultrasound in the detection of focal liver lesions. Eur Radiol. 2001;11 Suppl 3:15–26.
9. Leen E, Ceccotti P, Moug SJ, et al. Potential value of contrast-enhanced intraoperative ultrasonography during partial hepatectomy for metastases: an essential investigation before resection? Ann Surg. 2006;243:236–40.
10. Torzilli G, Botea F, Procopio F, et al. Use of contrast-enhanced intraoperative ultrasonography during liver surgery for colorectal cancer liver metastases – its impact on operative outcome. Analysis of a prospective cohort study. Eur J Cancer Suppl. 2008;6:16–23.
11. Borden MA, Shengping Q, Ferrara KW. Ultrasound contrast agents. In: Molecular imaging: principles and practice. Shelton: PMPH-USA; 2011. p. 425–44.
12. Kindberg GM, Tolleshaug H, Roos N, et al. Hepatic clearance of Sonazoid perfluorobutane microbubbles by Kupffer cells does not reduce the ability of liver to phagocytose or degrade albumin microspheres. Cell Tissue Res. 2003;312:49–54.
13. Yanagisawa K, Moriyasu F, Miyahara T, et al. Phagocytosis of ultrasound contrast agent microbubbles by Kupffer cells. Ultrasound Med Biol. 2007;33:318–25.
14. Healy JE, Schroy PC. Anatomy of the biliary ducts within the human liver; analysis of prevailing pattern of branching and the major variations of the biliary ducts. Arch Surg. 1953;66:599–616.
15. Couinard C. Lobes et segments hepatiques. Presse Med. 1954;62:709.
16. Rashleigh-Belcher HJC, Russel RCG, Lees WR. Cutaneous seeding of pancreatic carcinoma by fine needle aspiration biopsy. Br J Rdiol. 1986;59:182–3.
17. Sakuarai M, Seki K, Okamura J, et al. Needle tract implantation of hepatocellular carcinoma after percutaneous liver biopsy. Am Surg Pathol. 1983;7:191–5.
18. Jemal A, Siegel R, Xu J, Ward E. Cancer statistics, 2010. CA Cancer J Clin. 2010;60:277–300.
19. Manfredi S, Lepage C, Hatem C, et al. Epidemiology and management of liver metastases from colorectal cancer. Ann Surg. 2006;244:254–9.
20. de Haas RJ, Wicherts DA, Salloum C, et al. Long-term outcomes after hepatic resection for colorectal metastases in young patients. Cancer. 2010;116:647–58.
21. Robertson DJ, Stukel TA, Gottlieb DJ, et al. Survival after hepatic resection of colorectal cancer metastases: a national experience. Cancer. 2009;115:752–9.
22. Rifkin MD, Rosato FE, Branch HM, et al. Intraoperative ultrasound of the liver. An important adjunctive tool for decision making in the operating room. Ann Surg. 1987;205:466–72.
23. Clarke MP, Kane RA, Steele Jr G, et al. Prospective comparison of preoperative imaging and intraoperative ultrasonography in the detection of liver tumors. Surgery. 1989;106:849–55.
24. Guimaraes CM, Correia MM, Baldisserotto M, et al. Intraoperative ultrasonography of the liver in patients with abdominal tumors: a new approach. J Ultrasound Med. 2004;23:1549–55.
25. Wagnetz U, Atri M, Massey C, et al. Intraoperative ultrasound of the liver in primary and secondary hepatic malignancies: comparison with preoperative 1.5-T MRI and 64-MDCT. AJR Am J Roentgenol. 2011;196:562–8.
26. Van Vledder MG, Pawlik TM, Munireddy S, et al. Factors determining the sensitivity of intraoperative ultrasonography in detecting colorectal liver metastases in the modern era. Ann Surg Oncol. 2010;17:2756–63.
27. D'Hondt M, Vandenbroucke-Menu F, Préville-Ratelle S, et al. Is intraoperative ultrasound still useful for the detection of a hepatic tumour in the era of modern pre-operative imaging? HPB. 2011;13:665–9.
28. Ferrero A, Langella S, Russolillo N, et al. Intraoperative detection of disappearing colorectal liver metastases as a predictor of residual disease. J Gastrointest Surg. 2012;16:806–14.
29. Ruzzenente A, Conci S, Iacono C, et al. Usefulness of contrast-enhanced intraoperative ultrasonography (CE-IOUS) in patients with colorectal liver metastases after preoperative chemotherapy. J Gastrointest Surg. 2013;17(2):281–7.
30. Takahashi M, Hasegawa K, Arita J, et al. Contrast-enhanced intraoperative ultrasonography using perfluorobutane microbubbles for the enumeration of colorectal. Br J Surg. 2012;99:1271–7.
31. Schulz A, Dormagen JB, Drolsum A, et al. Impact of contrast-enhanced intraoperative ultrasound on operation strategy in case of colorectal liver metastasis. Act Radiol. 2012;10:1081–7.
32. Shah AJ, Callaway M, Thomas MG, et al. Contrast-enhanced intraoperative ultrasound improves detection of liver metastases during surgery for primary colorectal cancer. HPB. 2010;12:181–7.
33. Parkin DM, Bray F, Ferlay J, et al. Estimating the world cancer burden. Globocan 2000. Int J Cancer. 2001;94:153–6.
34. Hashem B, El-Serag. Hepatocellular carcinoma. N Engl J Med. 2011;365:1118–27.
35. Fattovich G, Giustina G, Degos F, et al. Morbidity and mortality in compensated cirrhosis type C: a retrospective follow-up study of 384 patients. Gastroenterology. 1997;112:463–72.
36. Cha CH, Saif MW, Yamane BH, et al. Hepatocellular carcinoma: current management. Curr Probl Surg. 2010;47:10–67.
37. Arii S, Yamaoka Y, Futagawa S, et al. Results of surgical and non surgical treatment for small-sized hepatocellular carcinomas: a retrospective and nationwide survey in Japan. The Liver Cancer Study Group of Japan. Hepatology. 2000;32:1224–9.
38. Hanish SI, Knechtle SJ. Liver transplantation for the treatment of hepatocellular carcinoma. Oncology (Williston Park). 2011;25:752–7.
39. Kruskal JB, Kane RA. Intraoperative US of the liver: techniques and clinical applications. Radiographics. 2006;26:1067–84.
40. Arita J, Takahashi M, Hata S, et al. Usefulness of contrast-enhanced intraoperative ultrasound using sonazoid in patients with hepatocellular carcinoma. Ann Surg. 2011;254:992–9.
41. Bru C, Maroto A, Bruix J, et al. Diagnostic accuracy of fine-needle aspiration biopsy in patients with hepatocellular carcinoma. Dig Dis Sci. 1989;34:1765–9.
42. Forner A, Vilana R, Ayuso C, et al. Diagnosis of hepatic nodules 20 mm or smaller in cirrhosis: prospective validation of the noninvasive diagnostic criteria for hepatocellular carcinoma. Hepatology. 2008;47:97–104.
43. Shuto T, Yamamoto T, Tanaka S, et al. Resection of needle-tract implantation after percutaneous puncture for hepatocellular carcinoma. J Gastroenterol. 2004;39:907–8.
44. Silva MA, Hegab B, Hyde C, et al. Needle track seeding following biopsy of liver lesions in the diagnosis of hepatocellular cancer: a systematic review and meta-analysis. Gut. 2008;57:1592–6.
45. Young AL, Malik HZ, Abu-Hilal M, et al. Large hepatocellular carcinoma: time to stop preoperative biopsy. J Am Coll Surg. 2007;205:453–62.
46. Ogawa S, Kumada T, Toyoda H, et al. Evaluation of pathological features of hepatocellular carcinoma by contrast-enhanced ultrasonography: comparison with pathology on resected specimen. Eur J Radiol. 2006;59:74–81.
47. Sugimoto K, Moriyasu F, Kamiyama N, et al. Analysis of morphological vascular changes of hepatocellular carcinoma by microflow imaging using contrast-enhanced sonography. Hepatol Res. 2008;38:790–9.
48. Lu Q, Luo Y, Yuan CX, et al. Value of contrast-enhanced intraoperative ultrasound for cirrhotic patients with hepatocellular carcinoma: a report of 20 cases. World J Gastroenterol. 2008;14:4005–10.
49. Van Sonnenberg E, Ferrucci JT, Mueller PR, et al. Percutaneous drainage of abscesses and fluid collections: technique, results and application. Radiology. 1982;142:1–10.
50. Torzilli G, Montorsi M, Donadon M, et al. "Radical but conservative" is the main goal for ultrasonography-guided liver resection: prospective validation of this approach. J Am Coll Surg. 2005;201(4):517–28.

51. Torzilli G, Montorsi M, Del Fabbro D, et al. Ultrasonographically guided surgical approach to liver tumors involving the hepatic veins close to the caval confluence. Br J Surg. 2006;93(10):1238–46.
52. Torzilli G. Intraoperative ultrasound in surgery for hepatocellular carcinoma. Ann Ital Chir. 2008;79:99–106.
53. Cucchetti A, Zanello M, Cescon M, et al. Improved diagnostic imaging and interventional therapies prolong survival after resection for hepatocellular carcinoma in cirrhosis: the university of bologna experience over 10 years. Ann Surg Oncol. 2011;18: 1630–7.
54. Park JH, Koh KC, Choi MS, et al. Analysis of risk factors associated with early multinodular recurrences after hepatic resection for hepatocellular carcinoma. Am J Surg. 2006;192:29–33.
55. Vauthey JN, Lauwers GY, Esnaola NF, et al. Simplified staging for hepatocellular carcinoma. J Clin Oncol. 2002;20:1527–36.
56. Yuki K, Hirohashi S, Sakamoto M, et al. Growth and spread of hepatocellular carcinoma. A review of 240 consecutive autopsy cases. Cancer. 1990;66:2174–9.
57. Zhou Y, Xu D, Wu L, et al. Meta-analysis of anatomic resection versus nonanatomic resection for hepatocellular carcinoma. Langenbecks Arch Surg. 2011;396:1109–17.
58. Chen J, Huang K, Wu J, Zhu H, et al. Survival after anatomic resection versus nonanatomic resection for hepatocellular carcinoma: a meta-analysis. Dig Dis Sci. 2011;56:1626–33.
59. Cucchetti A, et al. A comprehensive meta-regression analysis on outcome of anatomic resection versus nonanatomic resection for hepatocellular carcinoma. Ann Surg Oncol. 2012;19(12):3697–705.
60. Torzilli G, et al. Systematic subsegmentectomy by ultrasound-guided finger compression for hepatocellular carcinoma in cirrhosis. Ann Surg Oncol. 2009;16:1843.
61. Adam R, Laurent A, Azoulay D, et al. Two-stage hepatectomy: a planned strategy to treat irresectable liver tumors. Ann Surg. 2000;232(6):777–85.
62. Narita M, Oussoultzoglou E, Jaeck D, et al. Two-stage hepatectomy for multiple bilobar colorectal liver metastases. Br J Surg. 2011; 98(10):1463–75.
63. Schnitzbauer AA, Lang SA, Goessmann H, et al. Right portal vein ligation combined with in situ splitting induces rapid left lateral liver lobe hypertrophy enabling 2-staged extended right hepatic resection in small-for-size settings. Ann Surg. 2012;255(3):405–14.
64. de Santibañes E, Clavien PA. Playing Play-Doh to prevent postoperative liver failure: the "ALPPS" approach. Ann Surg. 2012;255(3): 415–7.
65. Makuuchi M, Hasegawa H, Yamazaki S, et al. The use of operative ultrasound as an Aid to liver resection in patients with hepatocellular carcinoma. World J Surg. 1987;11:615–21.
66. Makuuchi M, Hashikura Y, Kawasaki S, et al. Personal experience of right anterior segmentectomy (segments V and VIII) for hepatic malignancies. Surgery. 1993;114:52–8.
67. Takasaki K, Kobayashi S, Tanaka S, et al. Highly anatomically systematized hepatic resection with Glissonean sheath code transection at the hepatic hilus. Int Surg. 1990;75:73–7.
68. Launois B, Jamieson GG. The posterior intrahepatic approach for hepatectomy or removal of segments of the liver. Surg Gynecol Obstet. 1992;174:155–8.
69. Launois B, Jamieson GG. The importance of Glisson's capsule and its sheaths in the intrahepatic approach to resection of the liver. Surg Gynecol Obstet. 1992;174:7–10.
70. Batignani G. Hilar plate detachment and extraglissonian extrahepatic anterior approach to the right portal pedicle for right liver resections. J Am Coll Surg. 2000;190:631–4.
71. Strasberg S, Linehan DC, Hawkins WG. Isolation of right main and right sectional portal pedicles for liver resection without hepatotomy or inflow occlusion. J Am Coll Surg. 2008;206:390–6.
72. Torzilli G, Makuuchi M. Ultrasound-guided finger compression in liver subsegmentectomy for hepatocellular carcinoma. Surg Endosc. 2004;18:136–9.
73. Torzilli G, Procopio F, Cimino M. Anatomical segmental and subsegmental resection of the liver for hepatocellular carcinoma: a new approach by means of ultrasound-guided vessel compression. Ann Surg. 2010;251:229–35.
74. Torzilli G, Procopio F, Palmisano A. Total or partial anatomical resection of segment 8 using the ultrasound-guided finger compression technique. HPB. 2011;13:586–91.
75. Shiina S, Teratani T, Obi S, et al. A randomized controlled trial of radiofrequency ablation with ethanol injection for small hepatocellular carcinoma. Gastroenterology. 2005;129:122–30.
76. Lin SM, Lin CJ, Lin CC, et al. Randomised controlled trial comparing percutaneous radiofrequency thermal ablation, percutaneous ethanol injection, and percutaneous acetic acid injection to treat hepatocellular carcinoma of 3 cm or less. Gut. 2005;54:1151–6.
77. Lencioni RA, Allgaier HP, Cioni D, et al. Small hepatocellular carcinoma in cirrhosis: randomized comparison of radio-frequency thermal ablation versus percutaneous ethanol injection. Radiology. 2003;228:235–40.
78. Brunello F, Veltri A, Carucci P, et al. Radiofrequency ablation versus ethanol injection for early hepatocellular carcinoma: a randomized controlled trial. Scand J Gastroenterol. 2008;43:727–35.
79. Chen MS, Li JQ, Zheng Y, et al. A prospective randomized trial comparing percutaneous local ablative therapy and partial hepatectomy for small hepatocellular carcinoma. Ann Surg. 2006;243:321–8.
80. Montorsi M, Santambrogio R, Bianchi P, et al. Survival and recurrences after hepatic resection or radiofrequency for hepatocellular carcinoma in cirrhotic patients: a multivariate analysis. J Gastrointest Surg. 2005;9:62–7.
81. Abu-Hilal M, Primrose JN, Casaril A, et al. Surgical resection versus radiofrequency ablation in the treatment of small unifocal hepatocellular carcinoma. J Gastrointest Surg. 2008;12:1521–6.
82. Liang HH, Chen MS, Peng ZW, et al. Percutaneous radiofrequency ablation versus repeat hepatectomy for recurrent hepatocellular carcinoma: a retrospective study. Ann Surg Oncol. 2008;15:3484–93.
83. Peng ZW, Zhang YJ, Chen MS, et al. Radiofrequency ablation as first-line treatment for small solitary hepatocellular carcinoma: long-term results. Eur J Surg Oncol. 2010;36:1054–60.

Techniques in Laparoscopic and Intraoperative Ultrasound Guidance

16

David J. Niemeyer, Kerri A. Simo, and David A. Iannitti

Introduction

The use of intraoperative ultrasound is beneficial for many abdominal surgical procedures. While used for other purposes, intraoperative ultrasound is an essential tool for the hepatobiliary surgeon to localize tumors and define vascular anatomy in the liver and pancreas. It is useful during resection and is essential for all but the most superficial liver tumor ablations [1–4]. Ablation and biopsy of tumors requires facile use of intraoperative ultrasound guidance techniques to achieve reproducible and effective ablations with minimal chance of incomplete ablation and local tumor recurrence. Ultrasound can be utilized in both open and laparoscopic surgery with the use of a variety of transducers.

A disciplined and comprehensive ultrasound of the organ of interest is paramount to a successful operation. Primarily, intraoperative ultrasound localizes lesions found on preoperative imaging. It can also find previously undetected lesions [3, 5]. It is therefore essential that the chosen ultrasound scanning technique provide a thorough examination of all parenchyma.

Identified lesions can be targeted for needle biopsy/ablation or avoided during resection in order to achieve negative margins. Ultrasound guidance of biopsy needles, ablation electrodes, or antennae require the operator to perform a maneuver in three dimensions while referencing a two-dimensional ultrasound image. This can be technically challenging, even when the lesion is well visualized by the ultrasound transducer. Multiple errant attempts may result in unnecessary trauma so correct technique is helpful in reducing these errant attempts [6, 7]. This chapter discusses techniques in ultrasound surveillance as well as advanced techniques of biopsy and ablation device guidance for both laparoscopic and open surgery.

Transducer Selection/Positioning

Transducer Selection

The image produced by an ultrasound transducer is affected by the configuration of the piezoelectric crystals that make up the transducer surface as well as the frequency they transmit. Higher-frequency ultrasound waves create sharper, higher-resolution images at the expense of penetration depth. High-frequency ultrasound waves attenuate very quickly in the tissue, and imaging of deep tissues with high-frequency transducers is poor. One of the benefits of operative ultrasound is that high-frequency probes that do not give good transabdominal images can be used directly on the organ of interest. This results in much more detailed images than would be available outside the operating room. In our practice we use frequencies of 5–10 MHz when imaging the liver to a depth up to 9 cm. For the pancreas we use 10 MHz and a depth up to 4 cm. For high-resolution vascular imaging, we use 15 MHz with a depth of 3 cm.

The shape of the transducer also affects the shape of the plane of tissue imaged. Curvilinear probes create a fan-shaped image with a larger amount of deep tissue visualized, whereas linear probes produce rectangular images of tissue directly beneath the transducer. We use both linear and curved arrays in open surgery, and the laparoscopic ultrasound probes are curved arrays in line with the shaft of the instrument (Fig. 16.1).

Transducer Orientation

The ultrasound transducer produces an image of the narrow plane of tissue beneath it. The transducer of most open ultrasound probes is perpendicular to the cord and handle and is

D.J. Niemeyer, MD • K.A. Simo, MD • D.A. Iannitti, MD (✉)
Hepatobiliary and Pancreas Surgery,
Department of General Surgery, Carolinas Medical Center,
1025 Morehead Medical Drive, Suite 300, Charlotte, NC 28203, USA
e-mail: david.niemeyer@carolinashealthcare.org;
kerri.simo@carolinashealthcare.org; david.iannitti@carolinas.org

E.J. Hagopian, J. Machi (eds.), *Abdominal Ultrasound for Surgeons*,
DOI 10.1007/978-1-4614-9599-4_16,

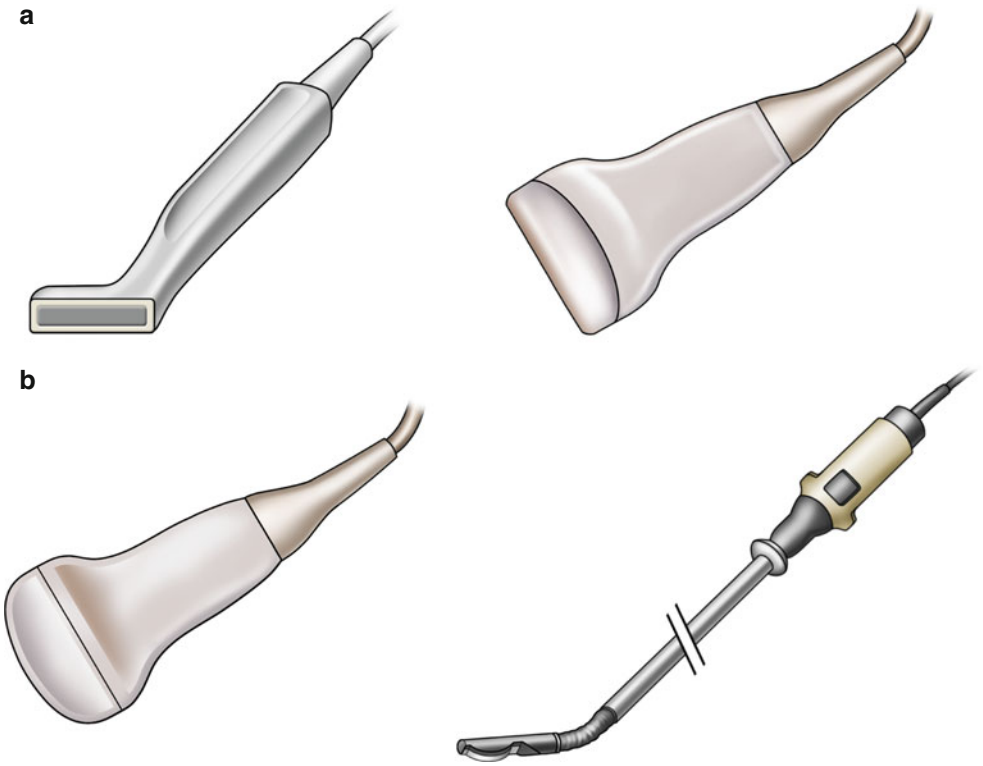

Fig. 16.1 Ultrasound probes are designed with both ergonomics and imaging characteristics in mind. Handpieces can be shaped for a particular use, and straight and curved arrays provide different imaging qualities. (**a**) Linear transducers in two ergonomic configurations. (**b**) Curved array transducers in both open and laparoscopic varieties

therefore described as having a "left" and "right" side (Fig. 16.2). The laparoscopic probe is oriented such that the transducer is in line with the shaft. The distal tip of the device is termed the "toe" and the proximal end of the transducer the "heel" (Fig. 16.3). The image on the ultrasound screen can be manipulated in regard to the "left-right" orientation viewed on the screen. Thus, the toe portion of the image can be on the right-hand side of the screen or on the left. This applies in a similar manner to an open probe. It is at the operator's discretion as to which orientation to choose, and the preferred view will depend on how each individual visually processes the spatial relationship seen on the screen [8]. Either orientation is acceptable, but it is critically important to know the orientation prior to beginning a scan for accurate planning and execution of biopsy or ablation. The recommended technique for determining orientation of the probe is to place only the tip of the laparoscopic probe, or one side of the open probe, in contact with the tissue and then look at the screen to determine which side of the tissue is being projected (Fig. 16.4a, b). The orientation is now known and the image can then be reversed as needed.

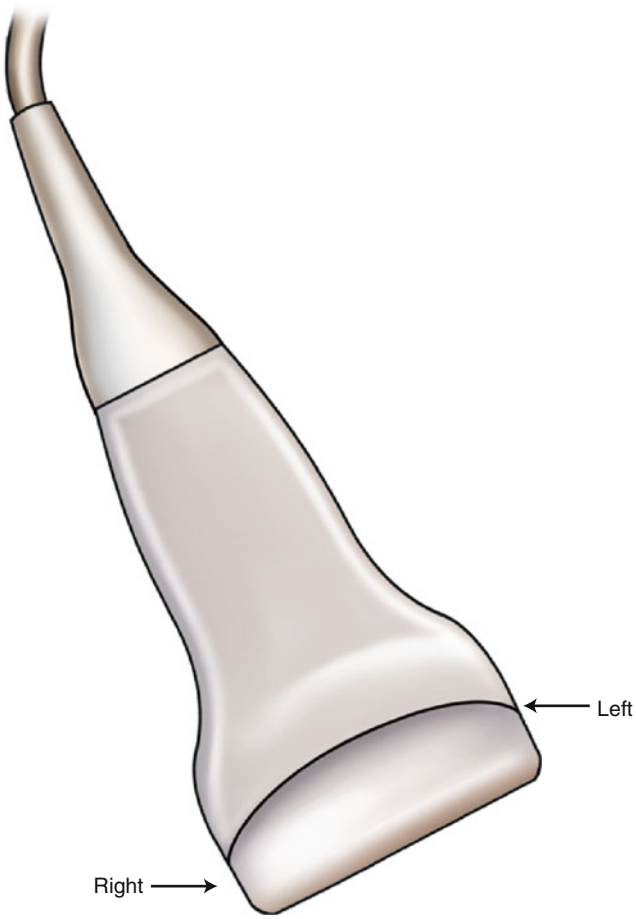

Fig. 16.2 Handheld ultrasound transducer marked left and right. The image on-screen can be flipped so that the right edge of the transducer corresponds to either the right or left edge of the screen to fit the user's spatial orientation preference

Transducer Head Position

The laparoscopic transducer can be flexed up and down as well as left to right. This allows for great flexibility in scanning an organ's contour. Rigid laparoscopic ultrasound devices are available, but the limitations of movement make them inadequate for full hepatic ultrasound. A common pitfall is to place the transducer in contact with the tissue and then rotate the transducer head while stationary in order to scan the tissue. This results in large amounts of deep tissue scanned, but very little tissue scanned on the surface. Figure 16.5 shows the result of rotating the transducer head without moving across the tissue (Fig. 16.5). When this maneuver is performed sequentially at different positions along a path, it is very easy to think that all tissue along the path has been scanned. However, in reality this is not the case. Figure 16.6 illustrates how a superficial lesion can be missed entirely by placing the transducer in two positions and rotating while remaining in place (Fig. 16.6). Therefore, the recommended technique for scanning is to move the transducer over the tissue while keeping it parallel to the tissue. In this way, an equal amount of deep and superficial tissue will be visualized, reducing the chance of missed lesions at any depth (Fig. 16.7). With an open ultrasound probe, this error is easier to avoid by keeping the ultrasound probe flat on the tissue of interest.

There are circumstances when moving an ultrasound probe smoothly over the surface of an organ is not possible. For example, a cirrhotic liver is very challenging to transduce accurately because it is difficult to get all points of the transducer touching the surface at one time. This can be overcome with a "standoff" technique where saline solution is used to submerge the liver (Figs. 16.8 and 16.9). The ultrasound transducer can then be positioned above the surface without the loss of image quality that would result from transmission through air. This can also be very useful for superficial lesions located around corners. Figure 16.10 demonstrates the standoff technique allowing visualization of a lesion that would be difficult to access with a flexed ultrasound transducer (Fig. 16.10)

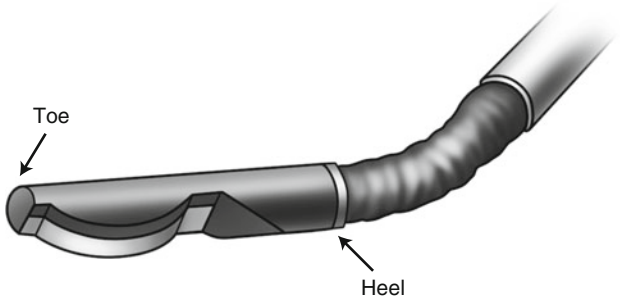

Fig. 16.3 Laparoscopic transducer head shown in flexed position marked with heel and toe. The image on-screen can be flipped to fit the user's preference

Scanning Techniques

Regardless of the tissue scanning method employed, it is important that it be methodical and complete. With any organ, a scanning technique can follow anatomic landmarks within the tissue, such as vasculature, or can be performed in a standardized fashion along the surface of the organ. For liver ultrasound, two different approaches are recommended. The portal vasculature can be followed in a "pedicle" technique, or the surface of the liver can be followed in a "lawnmower" fashion. These techniques will be described for the liver in this section, but other organs in the abdomen can be scanned with similar techniques requiring only small modifications for anatomy.

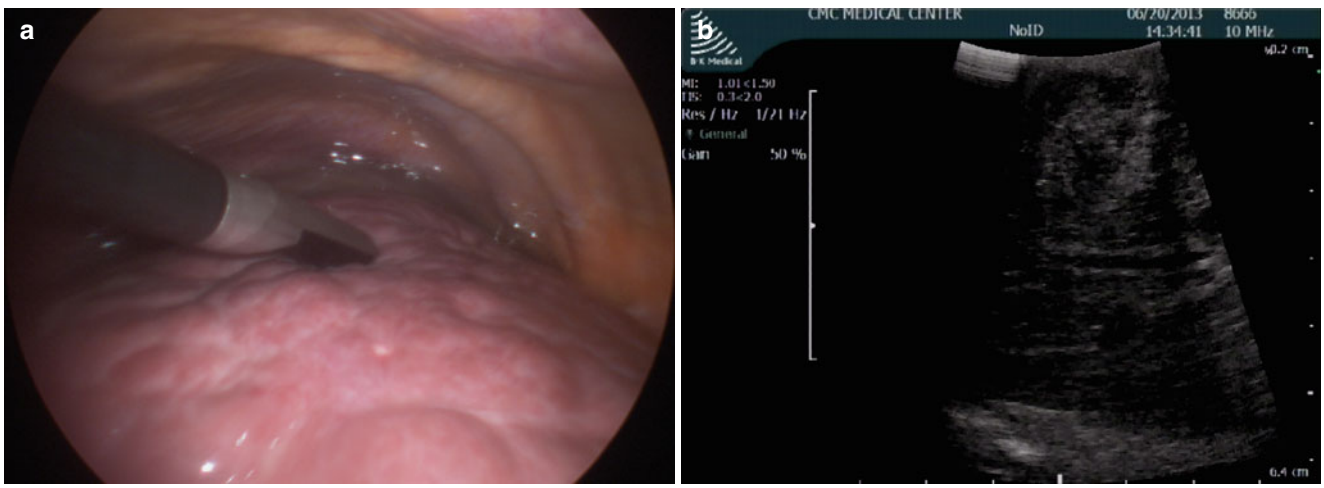

Fig. 16.4 (**a**) Intraoperative image of ultrasound toe touching the tissue. (**b**) A corresponding ultrasound image showing half of field with visible tissue, orienting the toe of the probe to the right of the screen

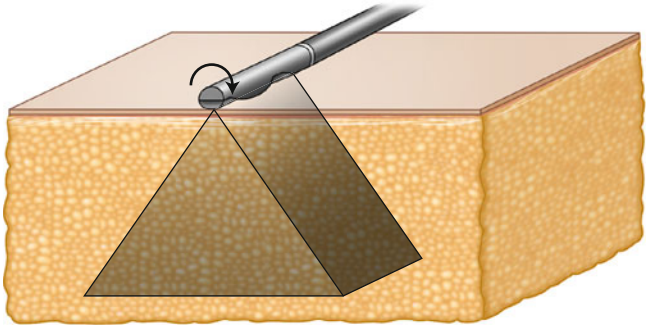

Fig. 16.5 The tissue is visualized perpendicular to the transducer. Rotation of the laparoscopic transducer without linear movement along the tissue visualizes a large amount of deep tissue with relatively little superficial tissue visualized

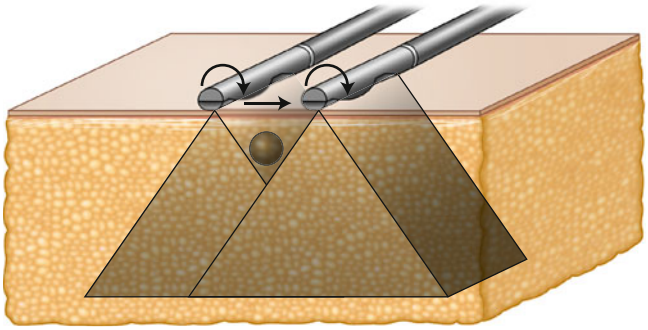

Fig. 16.6 When two sequential positions are used for transducer rotation, superficial lesions can be missed even though complete visualization is assumed. In this figure the laparoscopic transducer is rolled on the surface, moved laterally, and rolled in position again. A superficial mass is not imaged by either rolling motion, and if not picked up during the lateral movement of the probe, it will be missed entirely

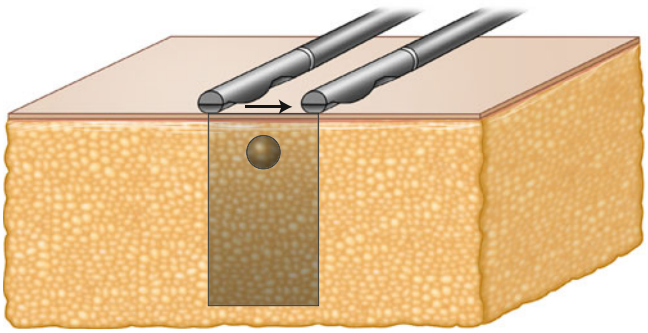

Fig. 16.7 By moving the transducer linearly along the tissue while maintaining perpendicular position relative to the tissue surface, an equal amount of superficial and deep tissue is visualized, and a superficial lesion is located

Lawnmower Technique

The "lawnmower" technique is used to scan the liver irrespective of intrahepatic anatomical landmarks. The entire surface is scanned by moving the transducer back and forth

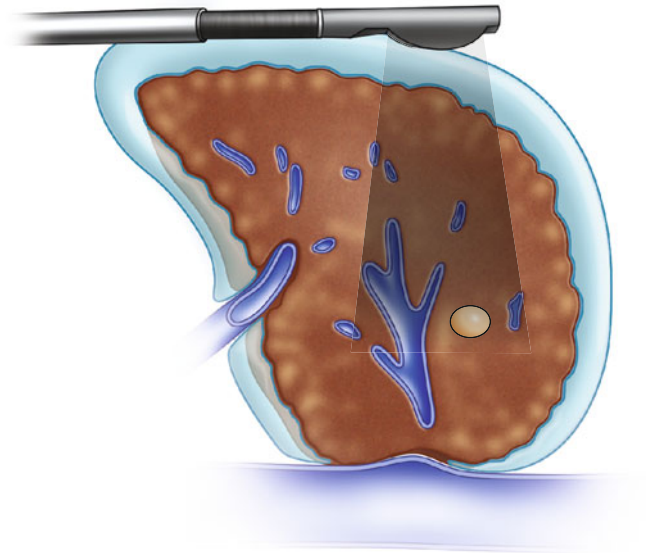

Fig. 16.8 The standoff technique used for a nodular cirrhotic liver using saline as an acoustic window. Ultrasound waves pass through the water layer and into the tissue seamlessly, providing a superior image

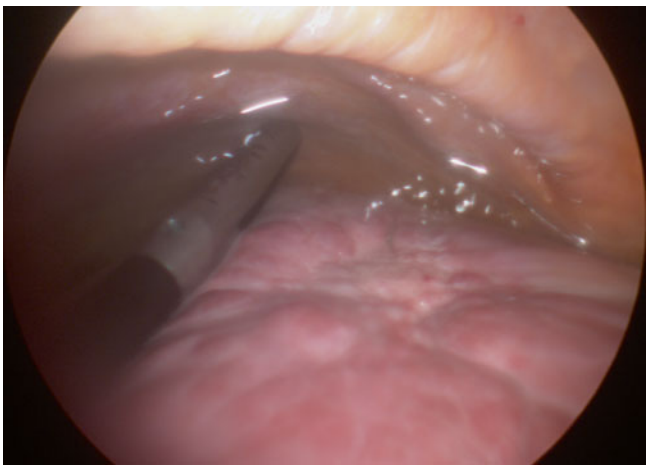

Fig. 16.9 A laparoscopic view of the standoff technique in use. Note the nodular appearance of the liver and the saline surrounding it. The transducer is submerged in saline in order to visualize pathology close to the surface of the liver

in narrow stripes beginning away from and moving toward the operator. Figure 16.11 shows the pattern used for this technique (Fig. 16.11). We perform this technique beginning in the right lobe and use the following pattern every time for consistency: segments VII–VI, VIII–V, IVa–IVb, II–III, and lastly I. Stripes should overlap so that no tissue is missed. The transducer should be moved slowly over the liver while the operator maintains constant attention to the ultrasound image. Recall that the laparoscopic transducer can be flexed to facilitate imaging over the dome of the liver. In an open approach the transducer motion can be modified to overlap stripes formed in a forward-and-back motion without

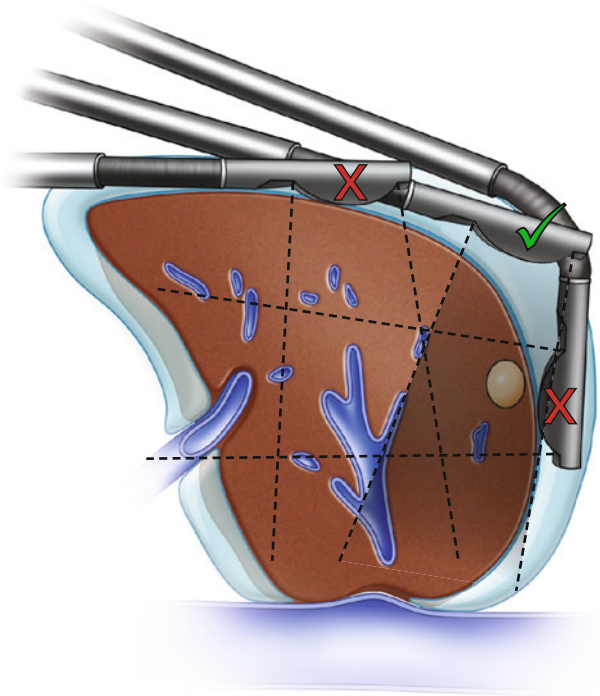

Fig. 16.10 The standoff technique used to visualize a superficial lesion high on the dome of the liver, which would be difficult to access directly with the ultrasound probe. This allows the lesion to be visualized through both the liver tissue and water layer with a clear image on-screen. The inferior (*red X*, *top*) probe position is the farthest a straight probe can achieve while maintaining contact directly with the liver tissue. The lesion is missed. The superior (*red X*, *right*) probe position requires the probe to be flexed around the edge of the liver to visualize the tumor, making targeting extremely difficult. The middle (*green check mark*) probe position allows the surgeon to visualize the tumor with a straight probe, making targeting for ablation most straightforward

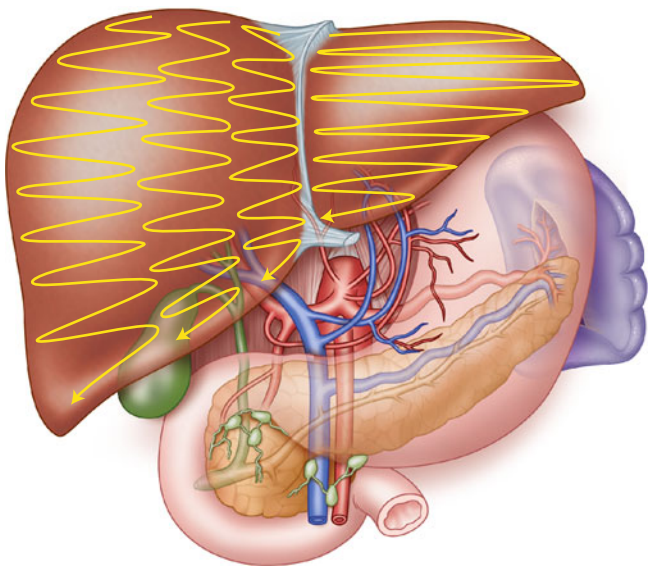

Fig. 16.11 The lawnmower technique. The probe is moved side to side in small stripes beginning away and moving toward the surgeon. The entire liver is visualized without regard to intrahepatic anatomy

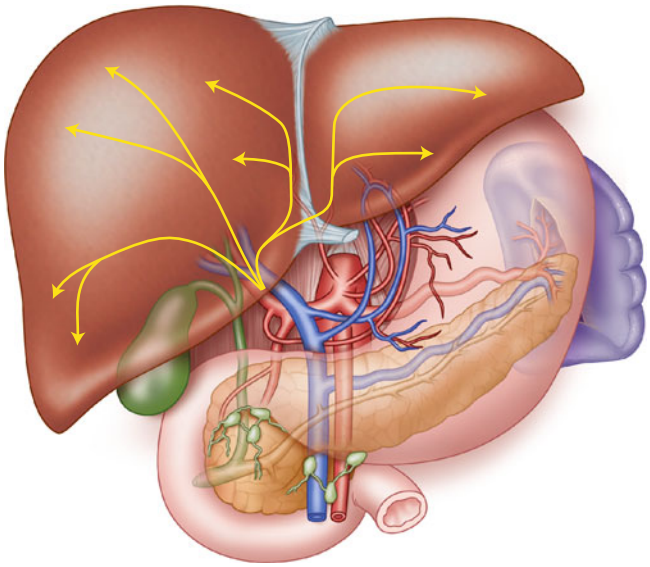

Fig. 16.12 The pedicle technique. Beginning at the porta hepatis, the portal pedicles are traced systematically. We begin with the right portal vein and move along the anterior, posterior, and segmental branches to the periphery of each segment. The left portal vein is traced in similar fashion, followed by the caudate lobe. This technique is especially useful to help identify lesions known to be in proximity to specific pedicles seen on preoperative imaging

side-to-side motions within stripes. This technique is especially useful when the surgeon is not looking for specific lesions based on preoperative imaging, but rather scanning for potential lesions.

Pedicle Technique

The basis of the "pedicle" technique is to use the liver anatomy as a guide. The surface of the liver is scanned in the direction of the portal pedicles (Fig. 16.12). Beginning with the portal vein, the right portal vein is followed along its anterior, followed by posterior segmental branches to the periphery of each segment. The left portal vein is scanned along the branches of IVa and IVb followed by the branches of II/III. Segment I is scanned last. During this technique we find it more natural to flip the left-right orientation of the screen when moving from the right to the left portal pedicles. When all pedicles are traced to their periphery, the liver is considered to be effectively visualized in its entirety. When preoperative cross-sectional imaging demonstrates lesions with nearby vasculature, the pedicle technique allows the surgeon to follow vessels to or near the lesion. This technique can be performed by itself or as a localizing technique for specific lesions followed by a lawnmower scan to evaluate the entire liver for additional lesions.

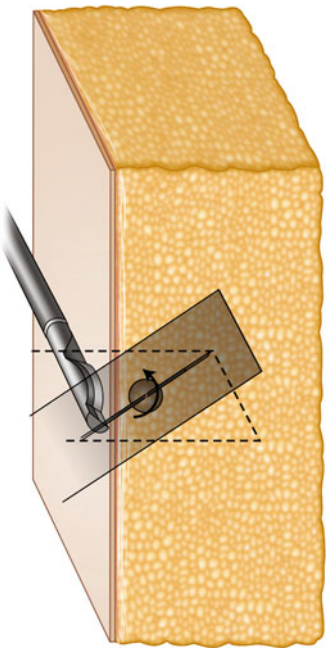

Fig. 16.13 If the transducer head is rotated without being recognized, an identified lesion will be mistakenly thought to be beneath the probe, when in fact it is perpendicular to the probe off to one side. This leads to errant passes and unneeded tissue trauma

Guidance Techniques

After lesion identification with ultrasound, targeting for biopsy or ablation can be performed under ultrasound guidance. Needle guidance can be performed either "in plane" with the transducer or "out of plane." Prior to any attempt at needle insertion, it is essential to have the transducer correctly positioned. Again, the ultrasound image presented on-screen is a thin plane of the tissue directly beneath, and in line with, the transducer head. Therefore, only objects passed directly underneath the transducer head will be imaged, including the needle and the lesion itself. It is important that the laparoscopic or open transducer head be flat against the tissue to provide a clear image along the entire length of the probe. It is also imperative to avoid rotating the transducer head as previously discussed. When a lesion has been identified with a rotated transducer head, the temptation is to assume the lesion is perpendicular to the tissue surface under the transducer. However, the image is actually of the tissue perpendicular to the transducer head. So if the transducer is rotated, the lesion will not be directly beneath the transducer, but rather off to the side. Figure 16.13 demonstrates the position of a lesion relative to the ultrasound probe when rotated

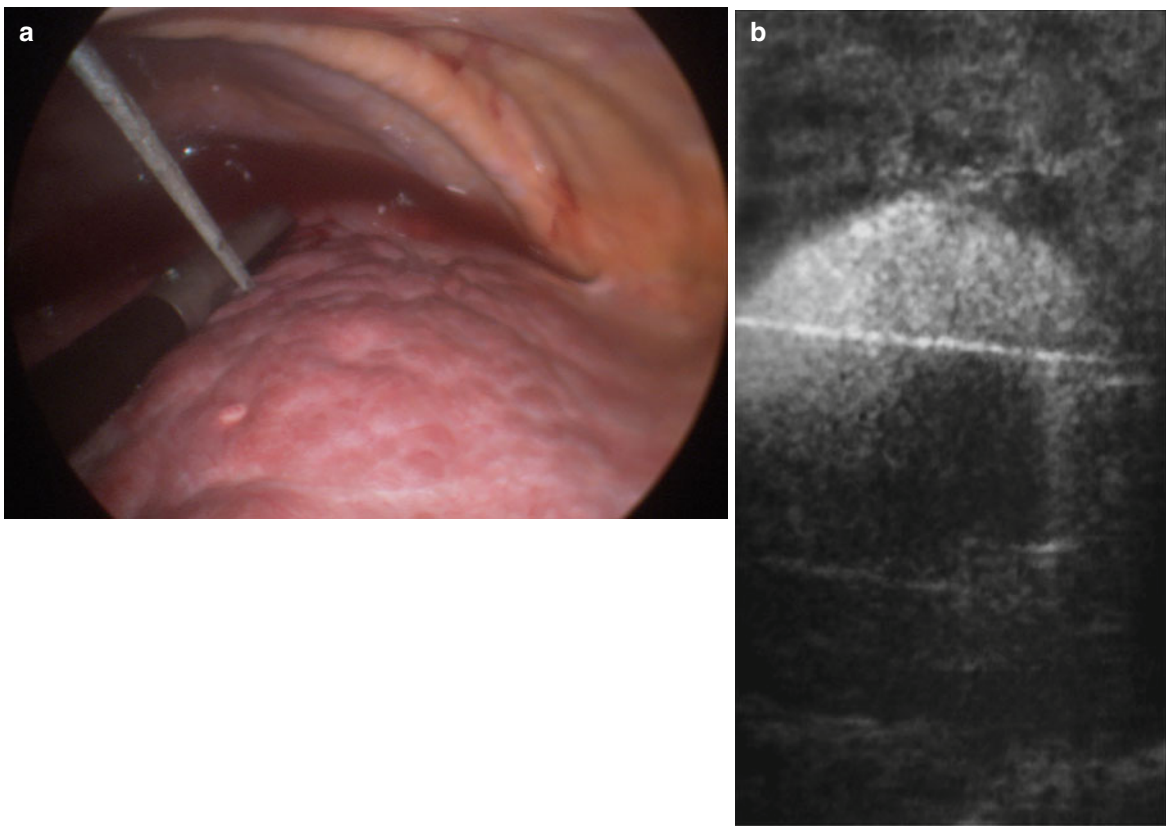

Fig. 16.14 (**a**) A microwave antenna is advanced in plane with the lesion. The antenna is visualized throughout its course, with the lesion still in view on-screen (**b**). Adjustments can be made quickly to minimize unnecessary errant attempts

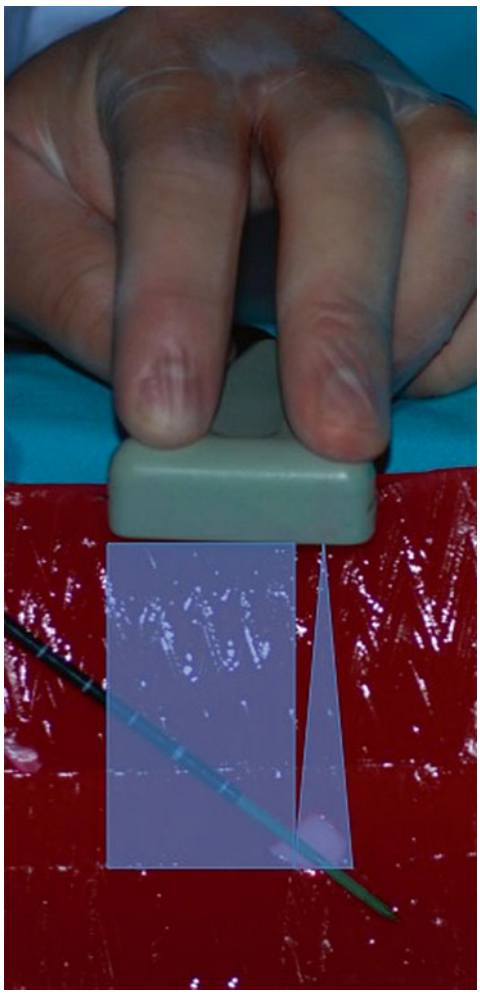

Fig. 16.15 Placing the lesion of interest at the far edge of the probe allows an "in-plane" antenna to be visualized traversing the entire screen. Adjustments are easier, and no screen space is wasted on the tissue not to be traversed

(Fig. 16.13). This makes targeting much more difficult and should be avoided.

In-Plane Targeting

In-plane targeting refers to passing the biopsy/ablation needle through the tissue parallel to and directly beneath the ultrasound transducer. This allows the surgeon to monitor the track of the needle throughout insertion. Figure 16.14a, b shows an image of an in-plane technique with a representative ultrasound image (Fig. 16.14a, b). When possible, placement of the lesion at the ultrasound probe toe laparoscopically, or at the edge opposite from needle entry of an open probe, as seen in Fig. 16.15 is recommended (Fig. 16.15). This allows for the greatest amount of needle track to be visualized and affords the opportunity to make angle adjustments early in the course of the maneuver. This must be done with care and attention to the tip of the needle, however, as it will travel the most during an angle adjustment and structures near the tip can be lacerated.

Open surgery affords great flexibility of motion in the absence of abdominal wall interference, making an in-plane approach feasible most of the time. In-plane targeting laparoscopically is more challenging not only because of the additional abdominal layer but also because all maneuvers are performed referencing the two-dimensional image produced by the laparoscope. Laparoscopic ultrasound probe shafts are in line with the transducer. It is ideal if the needle can be advanced from the heel of the probe directly beneath the transducer head. This should be kept in mind when determining where and at what angle to insert the needle through the skin.

Some laparoscopic ultrasound devices have built-in biopsy channels or attachment needle guides that can be placed on the tip of the transducer. Tracking guides can then be displayed on the screen in the path of a needle passed through the guide. This allows the surgeon to visualize the path of the needle before insertion and can reduce the number of errant passes. It is not always possible to orient the ultrasound device and needle to use the channel guide, and some large diameter devices do not fit through the channels. However, it is a useful adjunct when available. It is often necessary, as well as advantageous, to flex the ultrasound probe left or right in order to bring the heel into better position for needle insertion. When it is not feasible to use a needle guide or to pass under the probe from directly behind the heel, it is recommended to insert the needle alongside the transducer head at no greater than a 30° angle. This will bring the majority of the needle's path within the ultrasound image.

Once the transducer has been positioned appropriately for an in-plane technique, the surgeon must assess the lesion's depth by ultrasound and mentally determine the entry point and angle of approach to intersect with the lesion at the correct depth. During laparoscopy, this determines the entry and passage through both the abdominal wall as well as liver tissue. This determination is more difficult for deep lesions. However, when using the in-plane technique, error in angle of insertion can be ascertained quickly and adjustments made without making multiple full-depth passes through the tissue.

There are many benefits to utilizing the in-plane technique. The ability to rapidly assess needle angle helps avoid additional unnecessary tissue trauma. Adjustments in needle position are more difficult once the abdominal wall has been traversed. It may be necessary to entirely withdraw and replace the needle. The preferred approach is set up so that the needle passes through the abdominal wall at the same angle as through the intra-abdominal tissue. In thin patients adjustments can more easily be made without requiring great effort or strain on the needle. Obese patients will often

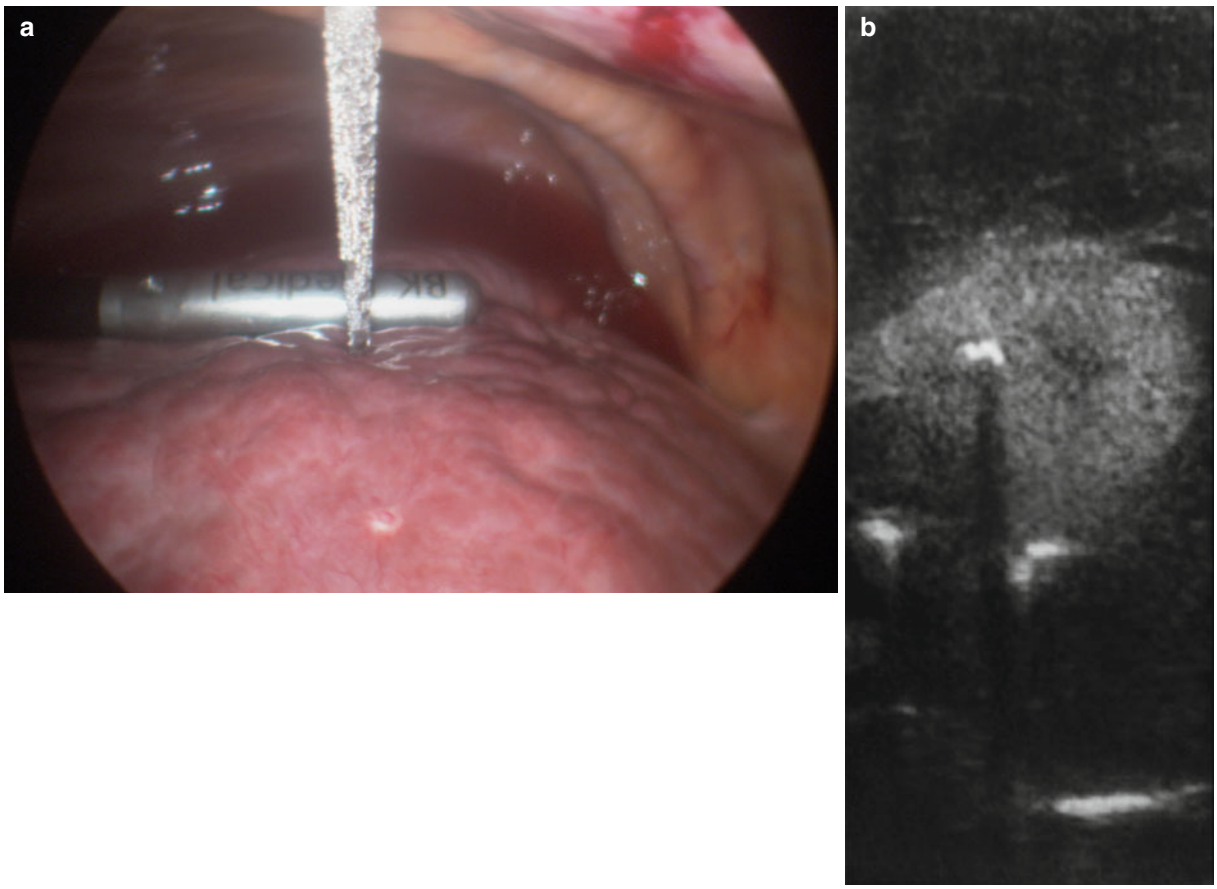

Fig. 16.16 (**a**) A microwave antenna is advanced out of plane with the lesion. The lesion and antenna are visualized on-screen together only in the single instance of the antenna crossing the plane of the ultrasound image (**b**). Adjustments are more difficult to make from an out-of-plane approach

require replacement of the needle if more than minor adjustments are required in the angle of the approach. An additional benefit to the in-plane technique is the ability to visualize in real time the needle traverse parenchyma prior to reaching the target. This allows the surgeon an approach that avoids large vessels during entry.

Out-of-Plane Targeting

It is common that an in-plane approach is not feasible for biopsy/ablation. This can occur when the approach through the abdominal wall is limited by port placement or when a lesion can only be viewed with the ultrasound probe in one position. When this occurs, an out-of-plane needle insertion is required. Figure 16.16a, b illustrates this technique with a corresponding ultrasound image (Fig. 16.16a, b). When a needle is inserted out of plane and the ultrasound transducer is held in a single position, the needle is only visible briefly as it breaks the plane of the visualized tissue. This can make it very technically difficult to assess needle trajectory and often results in full-depth passes being performed before the error in trajectory is recognized. The surgeon can move the ultrasound probe during the insertion to follow the needle, and it is important to do so to avoid injury to vessels, but this removes the lesion from the ultrasound image and the lesion must be reacquired during insertion. The combination of needle and lesion is only seen together on the ultrasound image when a correct placement results in the needle being within the lesion. A recent study looking at a novel 3D guidance system tested operators of varying experience in standard 2D targeting. The out-of-plane success rate in the hands of experts was 60 % [6]. When misses occur it is often difficult to correctly assess the cause of the miss in order to make adjustments for additional attempts. When a miss occurs it is recommended to leave the needle in position and pass the ultrasound between lesion and needle to assess the cause of the miss. In this situation, the probe can be rotated while in a single position, which will give the surgeon the ability to assess more of the needle track and extent of the lesion without needing to navigate around the needle. This will also lessen the chance of making a similar mistake on a second attempt. Patience is emphasized to avoid making similar errant passes repeatedly.

Future Directions

Innovations in ultrasound imaging and targeting are currently at various stages of development. Devices that provide a three-dimensional solution to lesion targeting are currently being developed and actively used, some within the confines of a prospective trial [6, 7, 9]. One of the most difficult and often frustrating parts of ultrasound guidance is performing a three-dimensional procedure using a two-dimensional image. The surgeon must simultaneously process the ultrasound image, the angle and flex of the ultrasound probe, and the position of the needle in three dimensions relative to the lesion and must mentally project the trajectory of the needle to intersect with the lesion. Newer technologies perform many of these tasks automatically by providing a three-dimensional view of the spatial relationships of instruments and the virtual path of the needle. Chapter 18 will discuss these evolving technologies in greater detail. These new devices will result in fewer errant attempts, more precise targeting, and ultimately more consistently complete tumor ablations.

Conclusions

Intraoperative ultrasound can be an incredibly useful tool for guidance of biopsy/ablation when used correctly. Consistent methods of surveillance will increase the ability to detect both known and unknown lesions. When possible, in-plane needle insertion is recommended. However, even out-of-plane targeting can be very successful when patience and proper technique are employed. Emerging technologies will further enhance the surgeon's ability to target lesions for biopsy and ablation with greater precision.

References

1. Belli G, D'Agostino A, Fantini C, et al. Laparoscopic hand-assisted right hemihepatectomy by ultrasound-directed intrahepatic approach. J Hepatobiliary Pancreat Surg. 2009;16:781–5.
2. Navarra G, Bartolotta M, Scisca C, et al. Ultrasound-guided radiofrequency-assisted segmental arterioportal vascular occlusion in laparoscopic segmental liver resection. Surg Endosc. 2008;22:1724–8.
3. Santambrogio R, Opocher E, Ceretti AP, et al. Impact of intraoperative ultrasonography in laparoscopic liver surgery. Surg Endosc. 2007;21:181–8.
4. Torzilli G, Makuuchi M. Intraoperative ultrasonography in liver cancer. Surg Oncol Clin N Am. 2003;12:91–103.
5. Lo CM, Lai EC, Liu CL, et al. Laparoscopy and laparoscopic ultrasonography avoid exploratory laparotomy in patients with hepatocellular carcinoma. Ann Surg. 1998;227:527–32.
6. Sindram D, McKillop IH, Martinie JB, Iannitti DA. Novel 3-D laparoscopic magnetic ultrasound image guidance for lesion targeting. HPB (Oxford). 2010;12:709–16.
7. Sindram D, Swan RZ, Lau KN, et al. Real-time three-dimensional guided ultrasound targeting system for microwave ablation of liver tumours: a human pilot study. HPB (Oxford). 2011;13:185–91.
8. Franconeri SL, Scimeca JM, Roth JC, et al. Flexible visual processing of spatial relationships. Cognition. 2012;122:210–27.
9. Kingham TP, Scherer MA, Neese BW, et al. Image-guided liver surgery: intraoperative projection of computed tomography images utilizing tracked ultrasound. HPB (Oxford). 2012;14:594–603.

Ultrasound Techniques for Liver Tumor Ablation

17

Paul D. Hansen, W. Cory Johnston, and Chet Hammill

Introduction

Chemical and thermal ablations have been used for centuries to treat surface tumors. With the development of modern imaging technologies and surgical techniques, it became possible to visualize and treat tumors, not only inside the body, but inside the parenchymal confines of visceral organs. The introduction of B-mode ultrasound, for example, allows modern-era hepatobiliary surgeons to accurately map the internal architecture of the liver in real time and to identify and precisely target lesions deep within the liver using high-quality two-dimensional and three-dimensional imaging with Doppler capabilities.

Livraghi et al. first reported the use of percutaneous, ultrasound-guided intratumoral alcohol injection in 1986 [1]. They described injections of 95 % alcohol into nine patients with hepatocellular cancer and four patients with liver metastases from other primary cancers. The success of these early attempts engendered an interest in further development of ablative techniques. Progress in ultrasound technology allowed for better imaging resolution, improving our ability to accurately target smaller and deeper tumors. Improved perioperative care and the development of laparoscopy enabled surgeons to offer safe, minimally invasive, effective therapies to high-risk patients with limited hepatic function.

Numerous ablative methods have been developed over the years. They typically fall into two categories: chemical ablation and thermal ablation. Chemical ablations have most commonly used ethyl alcohol or acetic acid, both of which can be applied using direct intratumoral injection. Cell death is rendered via microvascular thrombosis, protein denaturation, and cellular dehydration, resulting in tumor necrosis. Experience has shown that this works best in encapsulated and relatively soft tumors such as hepatocellular cancer and neuroendocrine tumors [2–4]. The ablative chemical infiltrates the tumor parenchyma, remaining largely within the capsule. Intratumoral injections do not work well in dense tumors such as metastatic adenocarcinomas because they do not allow even infiltration and distribution of the ablative chemical. Rather, the ablative chemicals tend to fracture out of the tumor or leak back along the injection tract.

A better technology for these dense tumors is thermal ablation, which uses either intense cold or intense heat to destroy the tumor. Cryotherapy, freezing of tumors, has largely fallen out of favor for liver tumor ablation due to high rates of periprocedural complication and treatment failure [5]. When tumors are rapidly frozen and thawed, tissue destruction occurs via microvascular thrombosis and ice crystal formation, resulting in cellular disruption. While not all cells are killed in each freeze-thaw cycle, repeating the cycle more than once generates cell kill rates of over 99.9 % [6]. Periprocedural complications include probe tract bleeding, freeze fractures, and thrombocytopenia or renal failure. Cryotherapy is most commonly performed using liquid nitrogen or liquid argon which requires a probe with a 3–5 mm diameter. These probes can cause significant bleeding along the insertion tract. Freeze fractures occur during the freeze-thaw cycle, much like dropping an ice cube in warm water, and can result in vascular injuries and subsequent hemorrhage. Finally, platelet-antibody complex formation resulting from antigen release when hepatocytes are injured can cause severe thrombocytopenia or renal failure in some patients.

Thermal ablation using heating relies on the fact that human tissue raised above 60 °C will die instantly due to protein denaturation, cell wall degradation, and microvascular thrombosis [7]. Therefore, focal application of energy to

P.D. Hansen, MD (✉) • C. Hammill, MD
Department of Surgical Oncology, Gastrointestinal and Minimally Invasive Surgery, The Oregon Clinic, Portland, OR, USA

Providence Cancer Center, 4805 NE Glisan Street, Suite 6N60, Portland, OR 97213, USA
e-mail: phansen@orclinic.com; chammill@orclinic.com

W.C. Johnston, MD
Department of Surgical Oncology, Providence Cancer Center, 4805 NE Glisan Street, Suite 6N60, Portland, OR 97213, USA
e-mail: coryjohnston@gmail.com

E.J. Hagopian, J. Machi (eds.), *Abdominal Ultrasound for Surgeons*,
DOI 10.1007/978-1-4614-9599-4_17,

induce tissue heating can be an effective method of tumor ablation. Several types of energy have been studied and can produce enough heat to create effective areas of tissue ablation. The limiting factor in effectiveness is not the source of energy (e.g., radiofrequency, microwave, laser, etc.), but rather the failure to apply the energy accurately and thoroughly enough to generate a 100 % target tumor kill while sparing surrounding vital tissue.

The most commonly utilized modalities today are radiofrequency ablation (RFA) and microwave ablation (MWA). Radiofrequency ablation uses a rapidly alternating electrical current, ~450,000 Hz, which causes the ions within the effected tissue field to realign with the current flow 450,000 times per second. This realignment motion causes frictional heating, resulting in tissue temperatures well over 100 °C. The power of an electrical field falls off at $1/r^4$ (r = radius). This rapid falloff in power requires careful probe design to prevent overheating of tissues immediately adjacent to the source of the energy while generating adequate heat to thoroughly ablate tumors and a margin of normal tissue up to 6 cm in diameter. Combinations of power algorithms and liquid coolants have been used to overcome these problems. Treatment failures adjacent to vascular pedicles is another potential problem, as vessels larger than 3 mm are generally not thrombosed and persistent blood flow can act as a heat sink, cooling surrounding tissues. Ensuring adequate heating requires aggressive ablations, often on both sides of large vessels.

Microwave ablation also uses electromagnetic waves but typically at 915 MHz or 2.14 GHz [8]. These high-energy waves penetrate biologic tissues effectively, are not hindered by tissue charring or desiccation, and can create thorough areas of tissue necrosis quickly. Drawbacks of microwave technologies have included less precision in tissue heating, overheating of cables attached to the probe, and limitations in ablation diameter and shape. These drawbacks will likely be overcome with further refinements in probe design.

The common goal for a successful tumor ablation includes the complete destruction of the tumor and 1 cm margin of surrounding tissue while protecting the surrounding normal liver and its architecture. Limiting factors for thermal tumor ablation include (1) the size of the target tumor and (2) the risk of thermal injury to the central bile ducts.

Using current technologies, ablation of tumors greater than 3 cm in diameter is associated with a higher rate of failure and subsequent local tumor recurrence. In addition, bile ducts are susceptible to thermal destruction. Thermal ablations should generally not be performed within 1 cm of the primary branches of the central biliary structures and ablations within 2 cm should be less aggressive. While this reduces the risk of biliary injury, it increases the risk of local treatment failure, and, therefore, patients undergoing ablation of tumors in this region must be selected carefully. Given these restrictions, aggressive ablations with meticulous ultrasound-guided placement of the ablation probes performed on tumors 3 cm in diameter or smaller, and more than 2 cm from central biliary structures, can be expected to generate local tumor failure rates of less than 2 % [9].

This chapter will describe the technical factors utilized to obtain a high success rate while minimizing periprocedural complications. We will discuss preoperative planning, operating room setup, staging procedures, and tumor-targeting strategies focusing on the ultrasound-related aspects of the procedure. We will also review tips for overcoming some of the more common technical difficulties encountered during surgical ablative procedures.

Note should be made of the fact that liver resection is still widely considered the treatment of choice for resectable liver tumors [10–12]. There are two important factors that have led surgeons to look for safe and effective alternatives to surgical resection in the treatment of liver tumors. The first is that, historically, liver resection was associated with high perioperative morbidity and mortality. While the safety of liver resection has improved over the last two decades, it is still considered a major surgical intervention and complication rates are not trivial. The second factor is that following resections, patients must be left with adequate functional liver reserve. This is especially problematic in cirrhotic patients. More than 85 % of primary liver tumors develop in the setting of cirrhosis. These patients typically have minimal functional liver reserve and are not candidates for major hepatic resections. Parenchymal sparing techniques improve the ability of these patients to tolerate potentially curative therapies. We view liver resection and liver tumor ablation as complementary treatments. There are advantages and disadvantages to each. They are simply tools, which should be used wisely and selectively by well-trained surgeons experienced in both technologies.

Overview of Surgical Approach

Preoperative Planning

The most important step in performing successful liver tumor ablation is appropriate patient selection. It is vital to understand fundamental oncologic principles, and to know whether destruction of a tumor or tumors is likely to have a meaningful impact on the patient's overall outcome. If so, it is important to understand whether the particular tumor(s) is amenable to an ablative approach, and whether the risk/benefit ratio is in the patient's favor. Finally, it is vital to select an ablative technology and approach that offers the highest chance of success while minimizing risk.

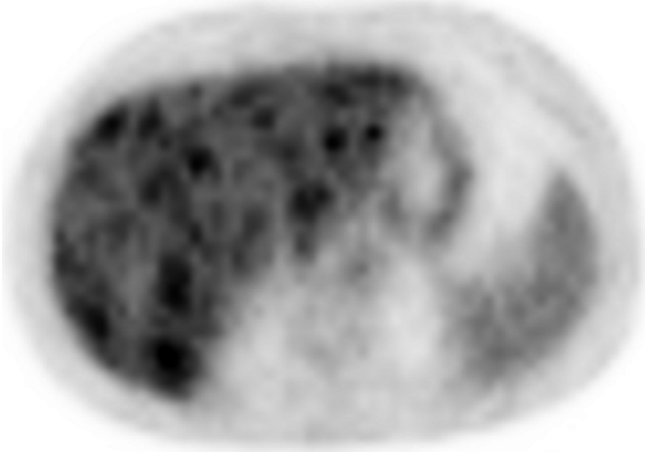

Fig. 17.1 PET scan demonstrating too many lesions to be able to safely and effectively perform ablation with curative intent

After an appropriate presurgical evaluation, imaging plays the primary role in preoperative planning. Key factors to determine include the number and size of lesions; the location of target lesions relative to portal structures, hepatic veins, and other viscera; and the volume of liver destruction required to affect a durable response. There is no established absolute cutoff in the number or size of lesions that may be ablated. The number of lesions, whether primary or metastatic, effects prognosis. From a technical perspective, ablation of more than 5 or 6 lesions during a single operative event is challenging. This is due to both the volume of liver ablated and the difficulties in accurately mapping and targeting this number of tumors (Fig. 17.1).

Tumors which are 3 cm in size require the creation of a 5 cm ablation zone. While RFA and MWA ablation technologies can create reliable ablation zones up to this size, larger zones become progressively more unreliable and dangerous to central portal structures. Local treatment failure rates for tumors less than 3 cm in size are typically well below 10 % but increase sharply above this size [9]. Similarly, tumors of any size can be ablated using chemical infiltration, but the larger the lesion, the less likely the cell kill will be 100 %. This problem can be overcome, to some degree, by using multiple ablation sessions. However, recurrence rates following ethanol injection for tumors larger than 3 cm are often reported to be above 20 % [13].

Operating Room Setup

Whether using open or laparoscopic techniques, the optimal setup for surgical ultrasound-guided tumor ablation is to have the surgeon and the ultrasound image on opposite sides of the target tumor. For liver tumor ablations, this typically involves the surgeon standing on the patient's left side, about hip level. The ultrasound monitor (and laparoscopic monitor) is on the patient's right side, usually about shoulder level. This allows the surgeon to comfortably look directly across the table, with the surgeon's line of sight in alignment with the target tumor and imaging displays. This will facilitate the surgeon's ability to create a three-dimensional mental image of the target and optimize the approach with an ablative probe (Fig. 17.2a).

Laparoscopic Staging

Laparoscopic staging includes a thorough peritoneoscopy. Specifics of the case will determine the degree to which visceral manipulation will be required to assess the possibility of extrahepatic disease. For patients with colorectal liver metastases who have a high-quality CT scan and are otherwise at low risk for intra-abdominal recurrence, we use a two-port technique (Fig. 17.2b). We start by viewing the easily visible, non-hepatic surfaces of the peritoneal cavity with little visceral manipulation. If there are specific concerns for extrahepatic recurrence, we will add additional ports to mobilize the abdominal viscera sufficiently to explore the entire abdominal and pelvic cavities.

The liver surface is scanned visually. Adhesiolysis is performed as necessary to visualize the anterior surface and dome of the liver. Visualization of the under surface of the liver is facilitated using an instrument through the second port. The falciform, triangular, and coronary ligaments are divided selectively, as it is usually possible to perform through ultrasound examination of the liver without doing so. The porta hepatis may be visualized with ultrasound through segment 4 of the liver (Fig. 17.3a) or by direct contact through the hepatoduodenal ligament (Fig. 17.3b). Identification of portal, peripancreatic, or para-celiac lymphadenopathy may alter the intended treatment strategy, particularly in cases when extrahepatic pathology is a contraindication to liver-directed therapies (Fig. 17.4).

Biopsies are obtained at the discretion of the surgeon. Unexpected findings in the liver, such as fibrosis or cirrhosis, may be of importance in planning the ablation or in the planning of future medical management. Wedge or core needle biopsies of non-tumoral liver tissue may be obtained for pathologic analysis. Unexpected lesions within the liver are biopsied if there is a question regarding their etiology. Wedge biopsies of surface lesions and core needle biopsies penetrating directly into surface lesions are discouraged as they may result in tumor seeding of the peritoneal cavity. Core biopsies are best obtained by transiting a minimum of 1 cm of normal liver parenchyma prior to entering the target tumor. This will reduce the risks associated with tumor spillage (Fig. 17.5).

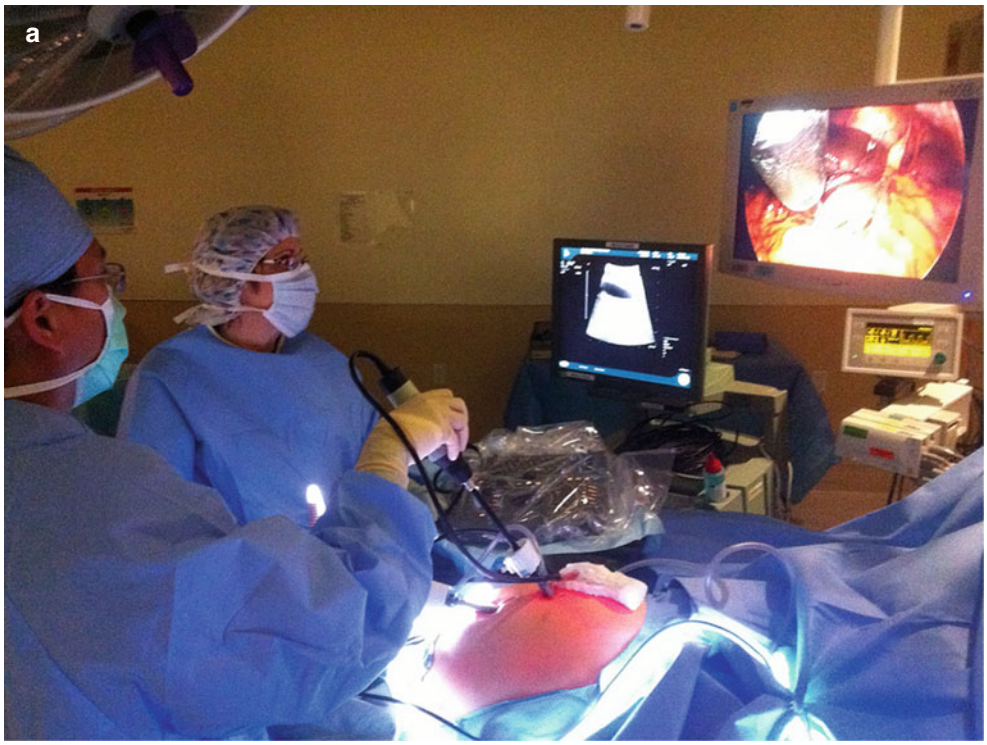

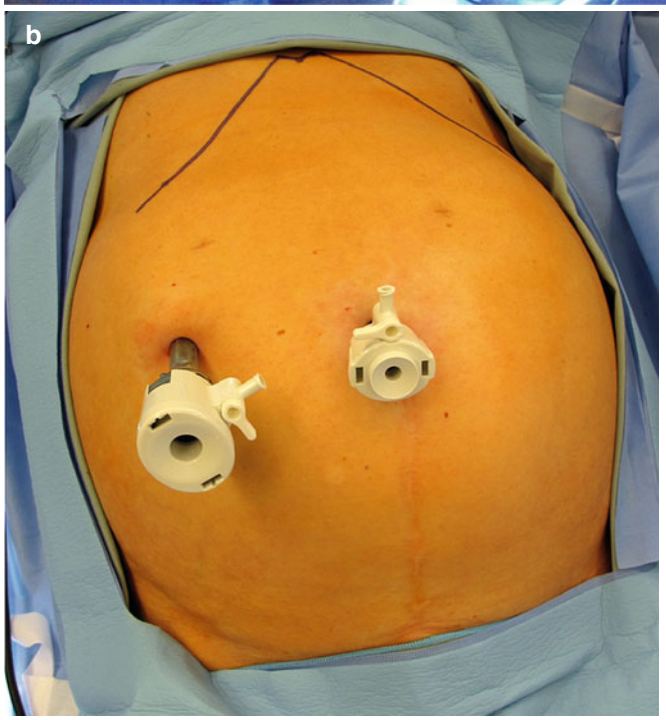

Fig. 17.2 (**a**) Operating room with the surgeon standing on the patient's left and the US and laparoscopy monitors diametrically opposite the liver. (**b**) Inset demonstrates typical port positions for a staging laparoscopy, intraoperative US, and tumor ablation

Surgical Approach

Like the difference between tumor ablation and liver resection, a laparoscopic or open approach should not be considered universally applicable. Each of these approaches is a tool to be used as needed by knowledgeable and skillful surgeons. A laparoscopic approach has the advantages of being less invasive. This has been clearly demonstrated to yield lower perioperative morbidity and mortality rates and allow faster recovery. Faster recovery is especially important considering that many patients have a poor prognosis and a short anticipated time of survival. One practical limitation of the laparoscopic approach is that many surgeons have not had adequate training to feel fully competent in the technique of

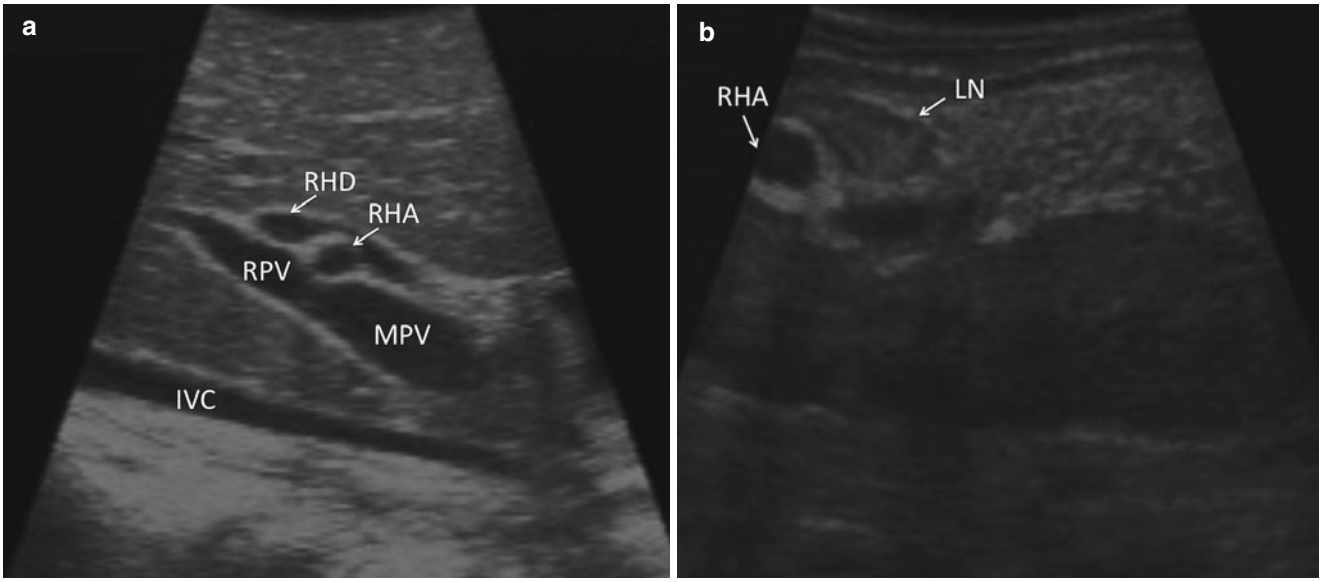

Fig. 17.3 (**a**) US demonstrates an image of the porta hepatis as seen when scanned through segment 4b of the liver (*IVC* inferior vena cava, *MPV* main portal vein, *RPV* right portal vein, *RHA* right hepatic artery, *RHD* right hepatic duct). (**b**) US demonstrates an image of the porta as seen with direct application of the US probe to the porta hepatis (*RHA* right hepatic artery, *LN* lymph node)

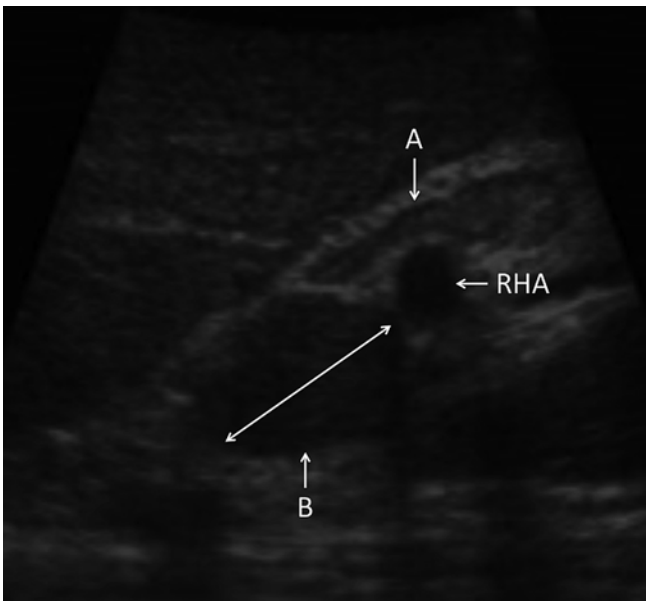

Fig. 17.4 US image demonstrating portal lymph nodes. Node A is normal. Node B is infiltrated with tumor (*RHA* right hepatic artery)

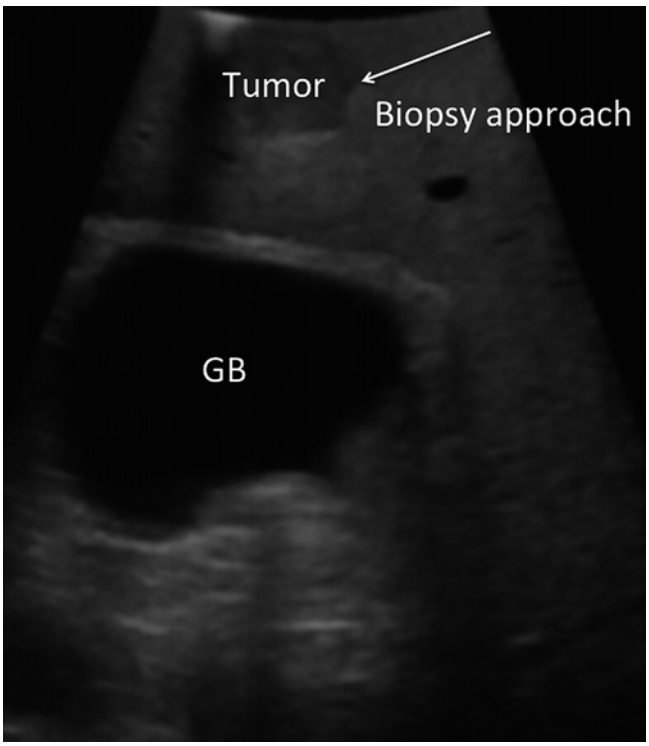

Fig. 17.5 US image demonstrates a tumor near the surface of the liver. Biopsy of surface lesions should be performed via an angle that allows transit of at least 1 cm of normal tissue prior to penetrating tumor. This approach will reduce the risk of peritoneal seeding of the tumor (*GB* gallbladder)

laparoscopic ultrasound or the application of laparoscopic ablation. While there are no areas of the liver that cannot be accessed using laparoscopic techniques, addressing lesions in segments 4a, 7, and 8 can be challenging. These may require advanced laparoscopic techniques not currently universally available.

The advantages of an open approach include the ability to add a manual component to the staging procedure. There is no surgical instrument as refined or sensitive as the human hand at identifying subtle changes in texture or firmness, which may be indications of additional pathology. The other primary utilization of an open ablative approach is in

combination with open surgical resection. Some tumor burdens, for example, may require a combination of a formal left or right hepatectomy and ablation of one or more lesions in the contralateral, remnant liver.

Liver Mapping

Prior to initiation of liver mapping, it is important to make sure that the ultrasound is optimized for the conditions at hand. Optimizing ultrasound settings and technique for the liver are covered in Chaps. 4 and 15. In general, it is best to use the highest frequency that penetrates to adequate depths within the liver. For most livers, 10 MHz is appropriate. For fatty or cirrhotic livers, 5–7.5 MHz may allow better imaging of deeper structures. Familiarity with Doppler features is occasionally helpful in differentiating between vascular and biliary structures or determining whether there is flow in a vessel.

It is important to perform a thorough screening of the liver at the time of ablation. This is done by locating key structures within the liver, dividing the liver into known anatomic sections/sectors and segments, and screening each in a standardized fashion. Using this regimented approach, additional lesions not seen on preoperative imaging may be found in 10–25 % of cases [14–16]. Intraoperative ultrasound may identify lesions as small as 3 mm. Although it may be difficult to accurately biopsy such lesions, knowledge of their presence may significantly alter the course of the operation.

Using the Brisbane terminology [17], the liver is divided into sections (or sectors) using the hepatic veins. We start by advancing the ultrasound probe to the diaphragm on the patient's right side of the falciform ligament, where the vena cava and the orifices of the left, middle, and right hepatic veins are identified (Fig. 17.6a, b). The middle hepatic vein divides the liver into left and right livers. The right hepatic vein divides the right liver into the right anterior section/sector and the right posterior section/sector. The left hepatic vein is used to divide the left liver into medial (segments 3 and 4) and lateral (segment 2) sections. For clarification, it should be noted that many surgeons divide the left liver into a left medial sector (segment 4) and a left lateral sector (segments 2 and 3) [18].

With the sections/sectors demarcated, the ultrasound probe is drawn back until the portal bifurcation is identified (Fig. 17.7). Sweeping left and right, the branches of the left and right portal veins can be followed to locate the individual segments of the liver. Each segment can then be screened individually for lesions. Thorough screening of the liver requires a combination of two different types of motion with the ultrasound probe. A sweeping motion is used to move across the surface of the liver (Fig. 17.8a). This motion is used to move from segment to segment and to scan immediately under the surface of the liver. A side-to-side rolling

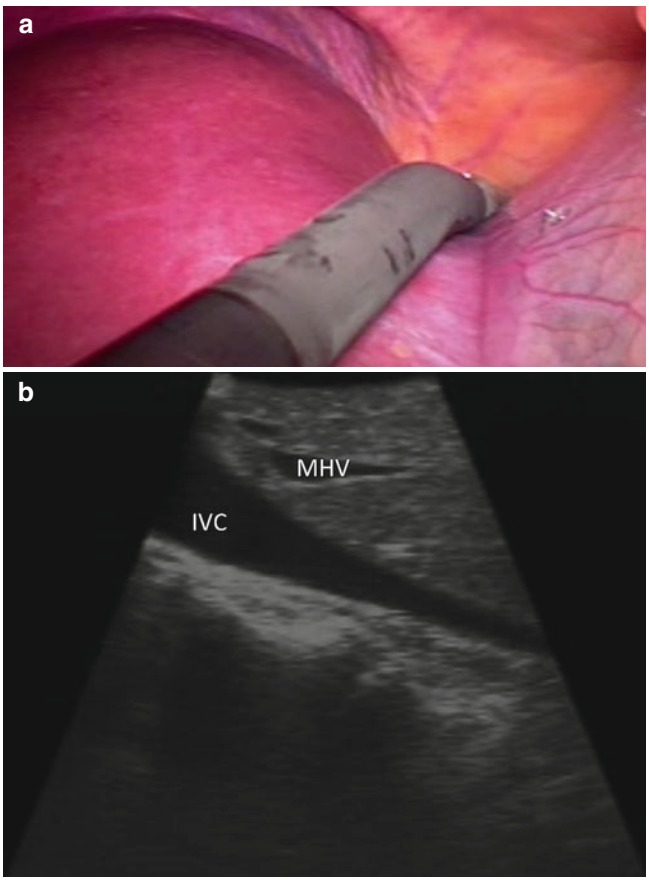

Fig. 17.6 (**a**) Laparoscopic view demonstrates the tip of the US probe over segment 4a, from which the inferior vena cava and the base of the hepatic veins can be identified. (**b**) US image demonstrates the inferior vena cava (*IVC*) and middle hepatic vein (*MHV*). The MHV can be identified as it empties into the IVC near the toe of the US probe and runs toward the heel of the US probe. The left and right hepatic veins can be viewed by rolling the probe to the patient's left and right, respectively

motion is used to scan within the parenchyma of each segment (Fig. 17.8b). This allows a more careful examination of deeper tissues. It is important to keep the shaft of the ultrasound straight during the rolling motion. The combination of these two probe maneuvers is required to assure a complete evaluation of all hepatic tissue (Fig. 17.8c, d). (Refer to Chap. 4 for further information.)

If a targeted lesion is identified early in the screening process, it is helpful to note its ultrasound characteristics. Some tumors demonstrate characteristic morphologic features. For example, metastatic adenocarcinomas tend to have a hypoechoic halo surrounding a heterogeneous, hyperechoic center (Fig. 17.9) [19]. In practice, however, there is a great deal of variability in how lesions appear on ultrasound. Once a known lesion's ultrasound characteristics are evaluated, it is easier to know what to look for during the remainder of the staging process. Metastatic lesions within an individual patient tend to have a similar appearance.

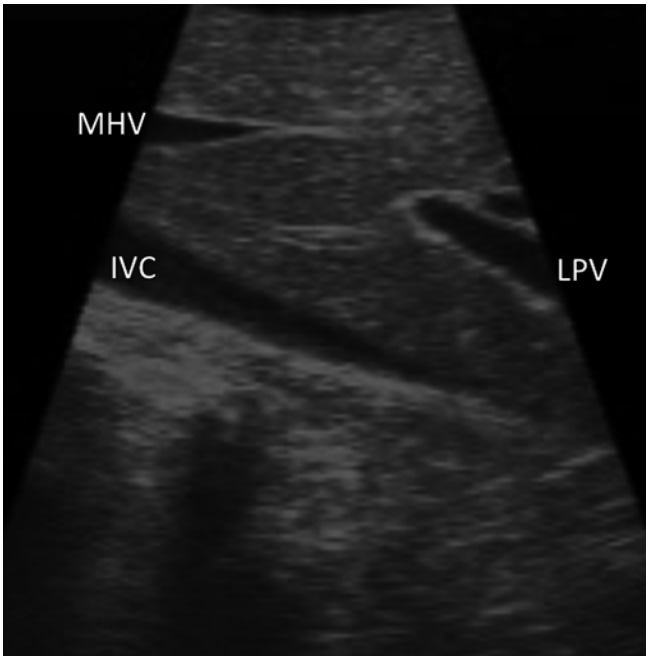

Fig. 17.7 US image demonstrating that the LPV (*LPV*, portal vein) is seen when the US probe is drawn straight back from segment 4a (*MHV* middle hepatic vein, *IVC* inferior vena cava)

Targeting Tumors

During staging, the precise locations of target lesions are noted. As the liver is surveyed, the surgeon develops a three-dimensional mental map of the liver, its key structures, and the tumors. This allows the surgeon to then develop a strategy for ablation.

The easiest method for targeting a tumor with either a biopsy needle or an ablation probe is to approach the tumor in a parallel plane to the ultrasound image. The tumor is positioned beneath the tip of the ultrasound probe, and the ablation probe is advanced under direct vision toward the target from the heel of the ultrasound probe (Fig. 17.10). This allows the operator to use the entire imaging field while targeting tumors and enhances the accuracy of the approach. The ultrasound probe can be gently swept from side to side or advanced and retracted as needed to guide the probe toward the target. (Refer also to Chap. 16 for further information.) Advancement of the probe into the tumor should be performed only after the surgeon is certain of the optimal position for ablation. This will prevent repeated punctures of the target tumor, potentially spilling cancer cells into the surrounding tissue, needle tract, or into the peritoneum.

Monitoring the Ablation

Once thermal heating begins, ultrasound imaging becomes progressively difficult. There is a combination of nitrogen outgassing and steam formation within the tissues. These gaseous changes prevent ultrasound wave transmission, which obscures the target image. Thus, exact placement of the probe is required prior to the beginning of ablation. This is part of the reason that multiple overlapping ablations are prone to failure. After completion of the ablation, imaging characteristics will improve as the tumor cools. Thus, secondary placements of the ablation probe, when required, are best performed after the tissue has been allowed to cool sufficiently.

For chemical injections of liver tumors, monitoring under ultrasound guidance is also helpful. Once the tumor has been penetrated by the injection needle, infiltration of the chemical agent is seen due to gas microbubbles in the injectate. As the needle is passed forward and backward during injection within the tumor, all aspects of the tumors should be seen to "gas out."

Maximizing the Chance of a Successful Ablation

Beyond appropriate patient selection and thorough mapping of the liver, the two most critical components of a high success rate for liver tumor ablation are accuracy of probe placement and aggressiveness of ablation. As stated, successful ablations require not only destruction of 100 % of all tumor cells but also a 1 cm margin of normal surrounding tissue [20]. Thus, successful ablation of a 1 cm tumor requires an accurate 3 cm ablation. When targeting a 1 cm tumor, the probe may be off-center by several mm, and the 3 cm ablation is still likely to destroy the whole tumor (Fig. 17.11a, b). When targeting a 3 cm tumor, however, if the probe is not well centered, it is easy for some portion of the tumor to lie near the edge of the ablation margin. This is especially true if the tumor is not perfectly round, as many larger lesions are not. If some portion of the tumor is not ablated, a treatment failure will result. It is thus imperative that probe placement be highly accurate, centered from all three-dimensional perspectives. This degree of accuracy requires significant skill with the ultrasound, a thoughtful triangulated approach to the tumor, and patience with precisely placing the probe tip in line with the center of the target.

Further patience is required during the actual heating portion of the ablation process. The surgeon must take the time to allow the tumor and margin to be brought to the temperature required to achieve a complete kill. When using RFA devices, such as the AngioDynamics XLie, we recommend and routinely practice a double ablation technique. The empirically derived temperature algorithms provided by AngioDynamics are utilized. After completion of the initial ablation, however, we retract the tines, turn the probe 30°, and then redeploy the tines and repeat one more ablation (Fig. 17.12). This assures that the area at highest likelihood for treatment failure, the area midway between the tines on

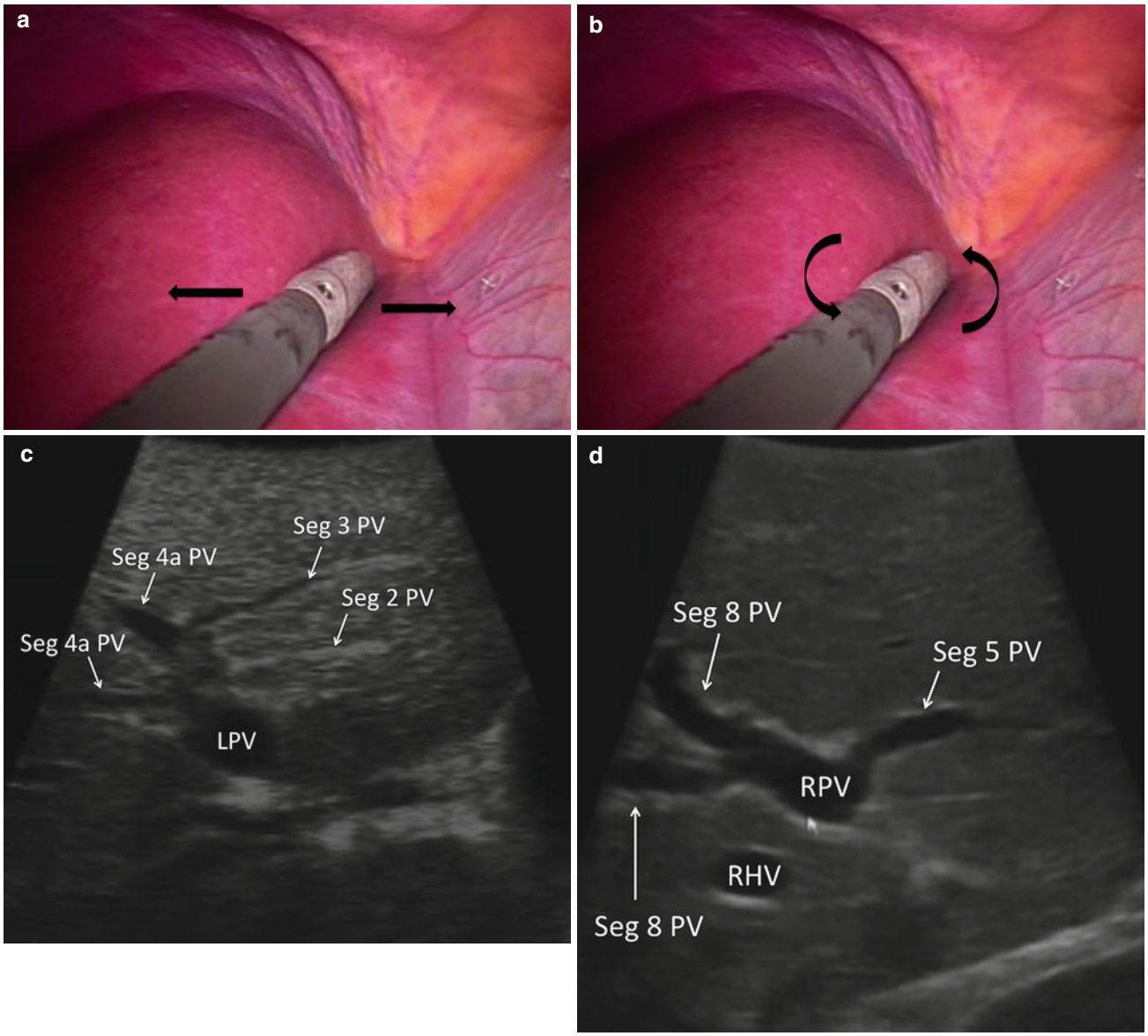

Fig. 17.8 (**a**) Laparoscopic image showing the US probe sweeping left to right. (**b**) Laparoscopic image showing the US probe rolling. Note the shaft of the US probe is straight. (**c**) US image demonstrating the segmental anatomy of the left liver (*LPV* left portal vein, *Seg* segment, *PV* portal vein). (**d**) US image demonstrating the segmental anatomy of the right liver anterior section (*RPV* right portal vein, *Seg* segment, *PV* portal vein, *RHV* Right Hepatic Vein)

initial deployment, is now adjacent to the tines. Utilizing meticulous probe placement and aggressive ablation techniques, the chance of local treatment failure can be minimized.

Technical Tips for Challenging Tumors

Deep-Seated Lesions

While lesions lying deeper in the liver can be more challenging to identify and target, there are no segments in the liver that cannot be approached either laparoscopically or with open surgery. Segment 7 and deep segment 8 lesions can be accessed by entering the liver anteriorly and traversing the full thickness of the liver. For superficial posterior lesions, this may risk thermal injury to the diaphragm. Small areas of thermal injury to the diaphragm are typically well tolerated. If curative ablation will require a larger area of diaphragmatic injury, it is recommended that the patient be placed in the left lateral decubitus position and the liver mobilized anteriorly by division of the right triangular and coronary ligaments. This will allow direct access to the target lesion while protecting the diaphragm.

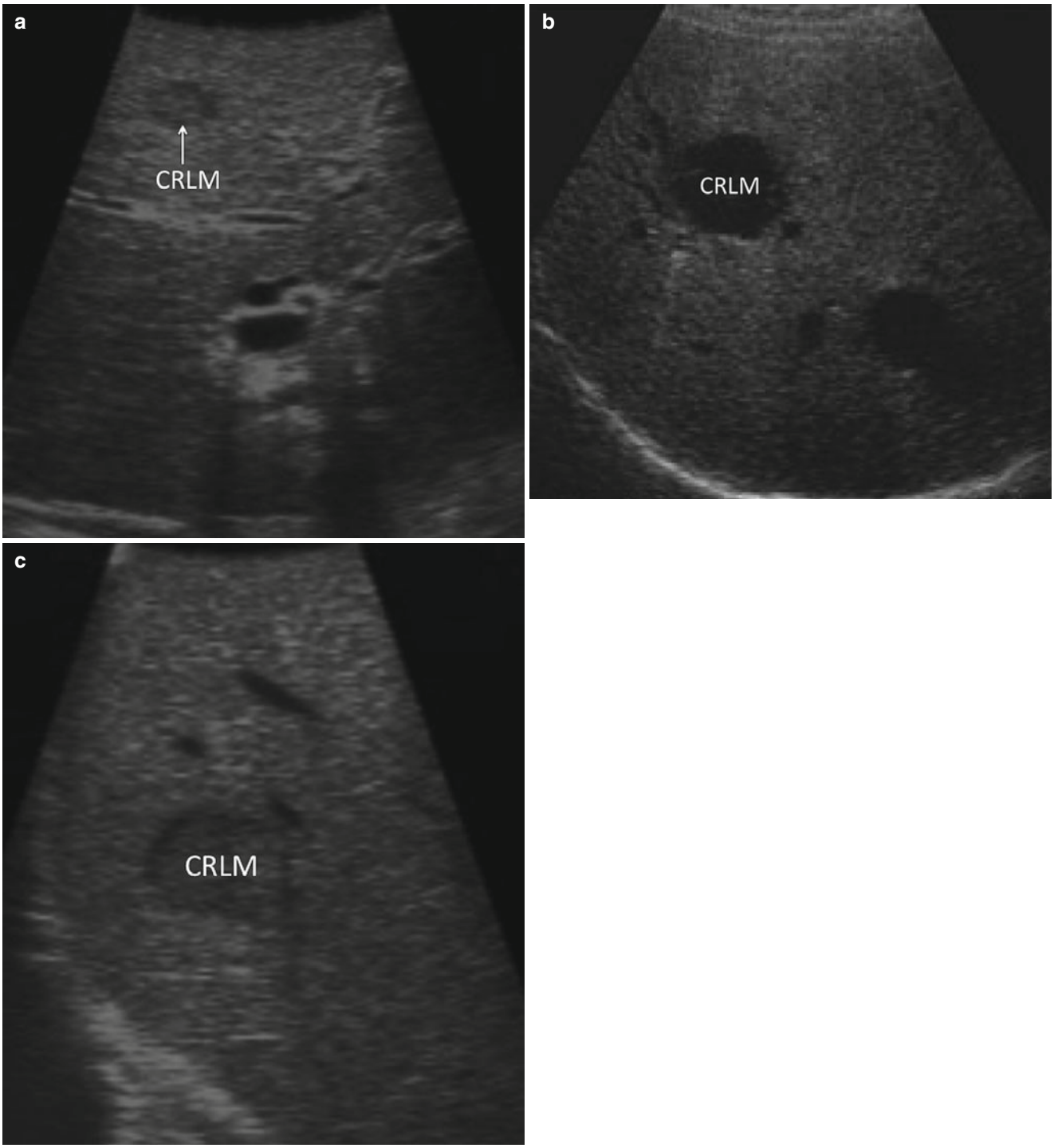

Fig. 17.9 US images demonstrating different US imaging characteristics of colorectal liver metastases (*CRLM*). (**a**) Demonstrates a mixed iso- and hypoechoic lesion; (**b**) is a hypoechoic lesion; and (**c**) shows an iso-/hypoechoic lesion with a hypoechoic rim

Retro-portal

Lesions lying at a safe distance, but directly behind the hilum of the liver, can be difficult to target safely. We recommend avoiding direct transgression of primary portal venous or biliary structures by selecting a path that bypasses the hilum (Fig. 17.13). This can be done by using a probe access point on the abdominal wall that is far to the patient's right or left. Occasionally, this requires deforming the liver with compression or mobilization of the ligaments. Alternatively, this can be achieved with a more advanced technique, requiring the arcing of the ablation probe, curving the approach to the tumor.

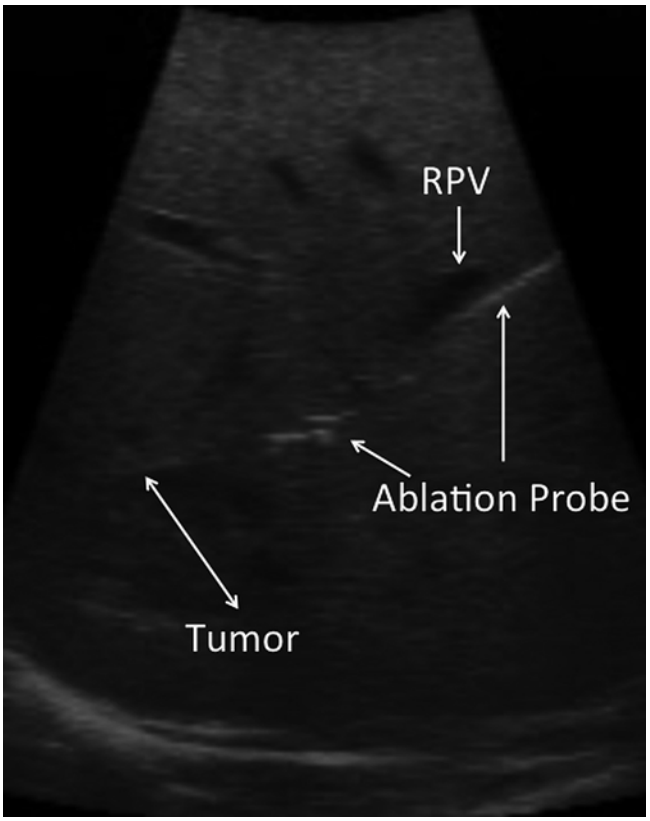

Fig. 17.10 US image demonstrating the approach of the ablation probe "in plane" with the US probe. The "in-plane" approach allows the surgeon to visualize the direction and angulation of the probe over a distance as it nears the tumor. This will optimize the surgeon's ability to target the center of the tumor (*RPV* right portal vein)

Caudate Lesions

Caudate lesions need to be selected for ablation with great care. It is uncommon for a caudate lobe lesion to be more than 2 cm from the central hilar structures. If the lesion is a hepatocellular cancer or a neuroendocrine tumor, a chemical ablation can be performed. If the lesion is an adenocarcinoma, thermal ablation must be performed with great care, acknowledging a higher likelihood of biliary injury or local recurrence. It is possible to dissect the portal structures up and away from the caudate to some degree, but the left hepatic duct remains at risk.

Nearby Viscera

The gallbladder will tolerate small areas of partial ablation on its hepatic surface. If the ablation requires larger areas of gallbladder injury or peritoneal surface injury to the gallbladder, cholecystectomy is recommended (Fig. 17.14). Care should be taken to mobilize the hepatic flexure of the colon or duodenum away from the liver if these structures lie close to the ablation zone.

Hostile Abdomen

For patients who have had multiple prior surgeries, intra-abdominal sepsis, or prior hepatectomies making a transabdominal approach to the liver unfeasible, we recommend a transthoracic approach. With a 3-port technique, the right

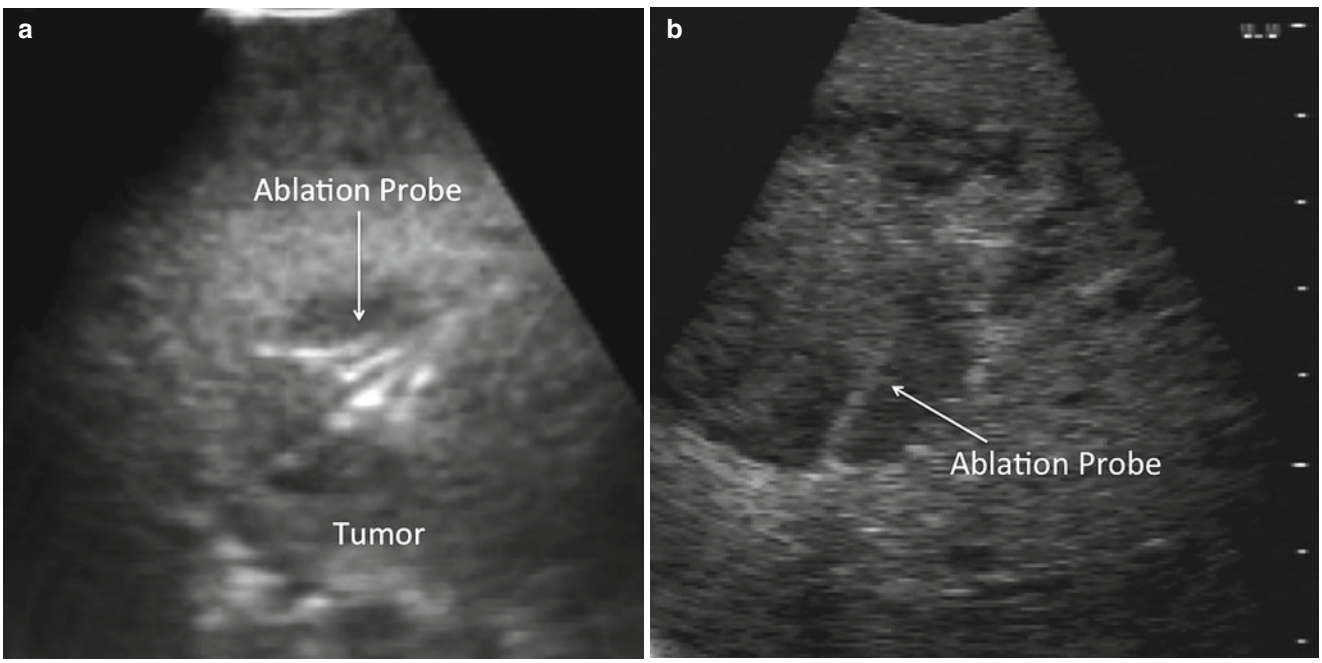

Fig. 17.11 (**a**) US image demonstrates the ablation of a tumor deep in the liver, segment 7 near the diaphragm. The ablation probe tines are well centered in the tumor. (**b**) US image demonstrates an off-center ablation probe

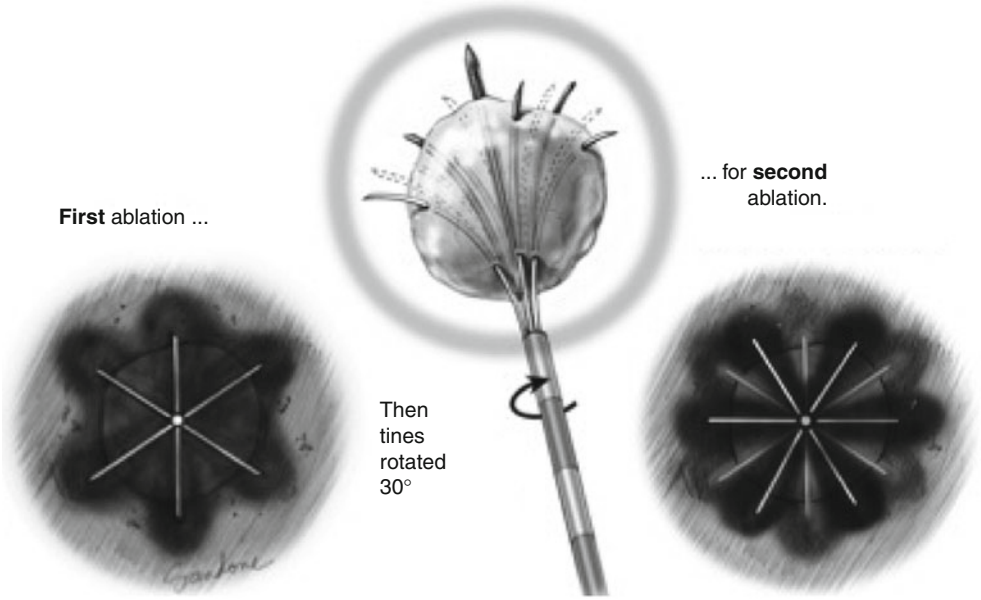

Fig. 17.12 Image demonstrates the double overlapping ablation using an AngioDynamics XLie-type radiofrequency ablation device (Used with permission from Hammill et al. [21])

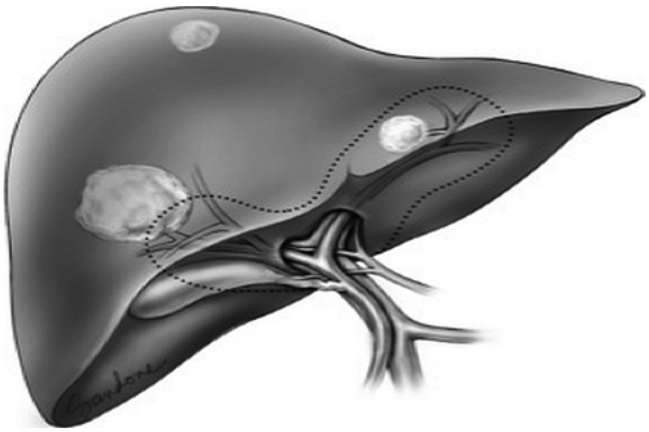

Fig. 17.13 Image demonstrates the zone within the liver where injury to the central biliary structures is high risk (Used with permission from Hammill et al. [21])

thorax can be accessed, the lung swept to the side, and the ultrasound evaluation of the liver performed transdiaphragmatically. The ablation probe may be passed through the chest wall and thorax with thoracoscopic visualization and then transdiaphragmatically under ultrasound guidance. The same principles used for a transabdominal approach will generally apply. Anatomic orientation is obviously more challenging, and the hepatic hilum and adjacent viscera are still at risk for injury.

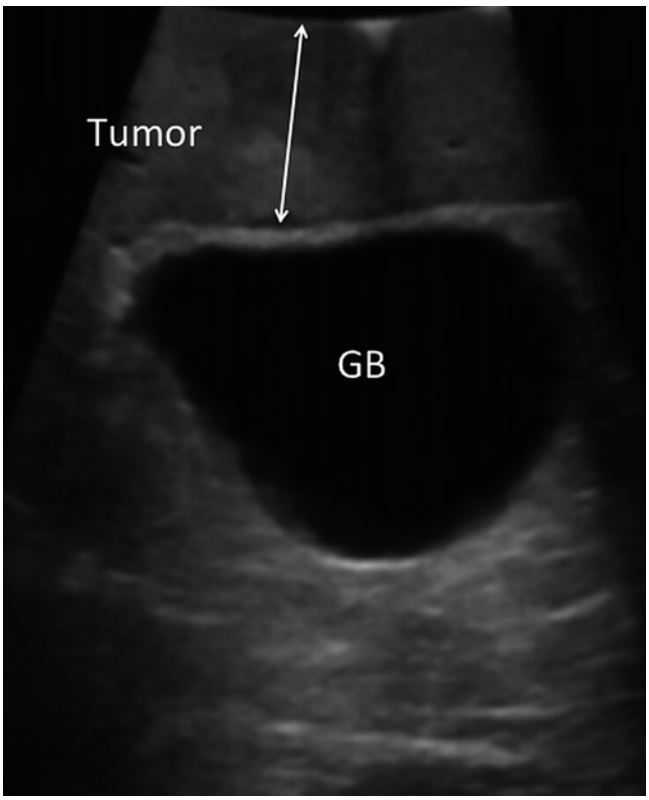

Fig. 17.14 US image demonstrates a tumor adjacent to the gallbladder (*GB*). Ablation of this tumor will injure the gallbladder wall and may be an indication for a cholecystectomy

Stacked Lesions

When lesions are aligned within the liver such that one lesion is deep to another, it is always recommended to ablate the deeper lesion first (Fig. 17.15). As noted above, the thermal ablation process obscures the ability to target lesions with ultrasound. If it is necessary to target a nearby lesion in an obscured ablation zone, simply waiting until the tissue cools will often improve visualization.

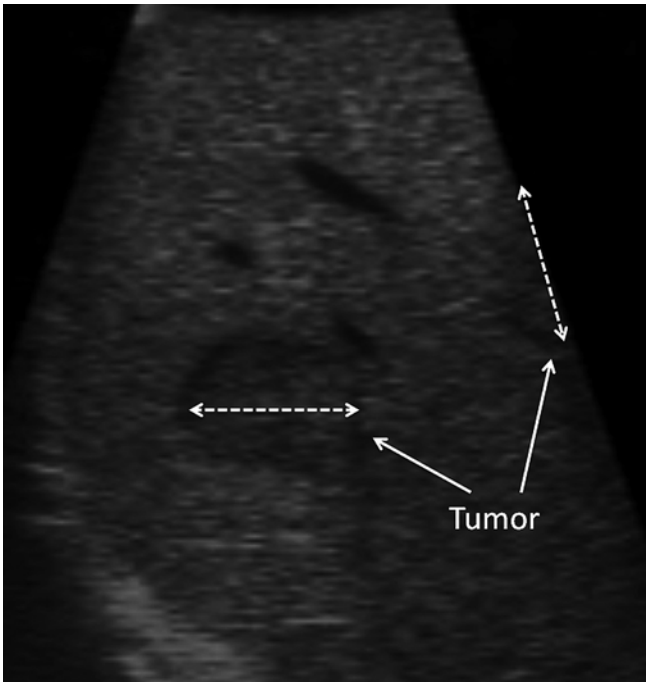

Fig. 17.15 US image demonstrates stacked tumors within the liver. Ablation of the deeper lesion first will produce less obscuration when targeting the more anterior tumor

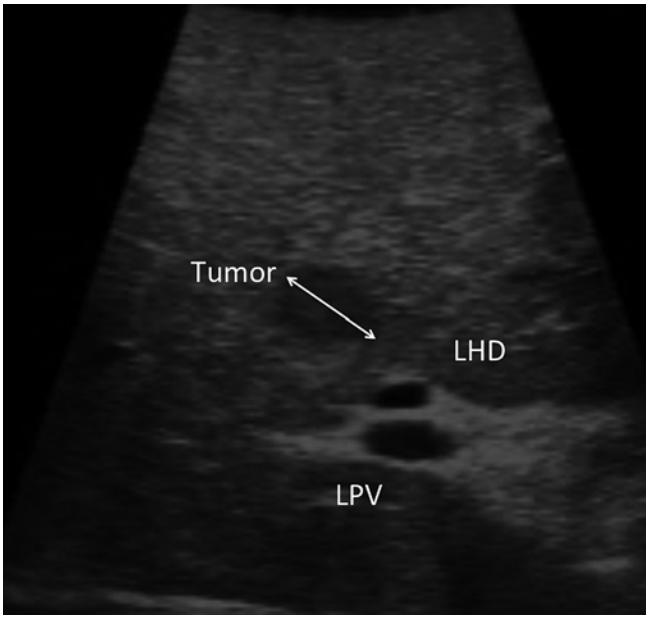

Fig. 17.16 US image demonstrates tumors lying adjacent to the central biliary structures. Attempted curative ablation of this lesion will likely result in destruction of the biliary structures. Attempts to cool the biliary tree during thermal ablation yield unpredictable levels of protection of the ducts and may increase the likelihood of local treatment failure

Lesions Near Hilar Structures

For curative ablations, we recommend a margin of at least 1 cm of normal liver tissue be ablated beyond the edge of the tumor. To achieve a low local recurrence rate, we believe in aggressive local ablation. Therefore, ablations within 2 cm of the central hilar structures risk injury to the common hepatic duct or its primary branches (Fig. 17.16). Injury to the duct in this area can result in severe complications, such as bilomas, strictures, portal vein thrombosis, etc. We recommend avoiding thermal ablation for any tumor within 1 cm of the common hepatic duct, right or left hepatic ducts, or the right anterior and posterior sectoral ducts. Small lesions between 1 and 2 cm from these structures may be thermally ablated, but care must be taken to ablate less aggressively than normal and the higher risk of significant injury or local recurrence must be acknowledged. For hepatocellular cancer and neuroendocrine tumors in this area, we use chemical ablations.

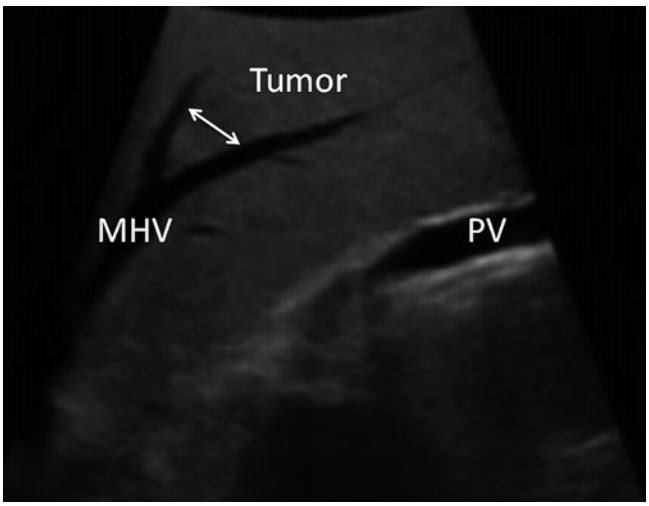

Fig. 17.17 US image demonstrating a tumor immediately adjacent to the middle hepatic vein. Such lesions are at higher risk for recurrence and need to be ablated more aggressively (*MHV* middle hepatic vein, *PV* portal vein)

Lesions Adjacent to the Vena Cava or Hepatic Veins

Ablations of lesions immediately adjacent to hepatic veins require careful consideration. The larger veins will act as a heat sink, cooling the adjacent tissue (Fig. 17.17). Thus, a well-placed and somewhat more aggressive ablation may be required to guarantee success. For tumors that have significant components of their mass on either side of a large vein, multiple ablations from different angles may be required to achieve complete tumor destruction.

There are similar concerns when ablating tumors adjacent to the vena cava. In addition, following an ablation immediately adjacent to the vena cava, the liver and vena cava will become fused. This precludes any future surgical resection of the adjacent liver tissue without a caval resection. As staged surgical procedures are more commonly performed in

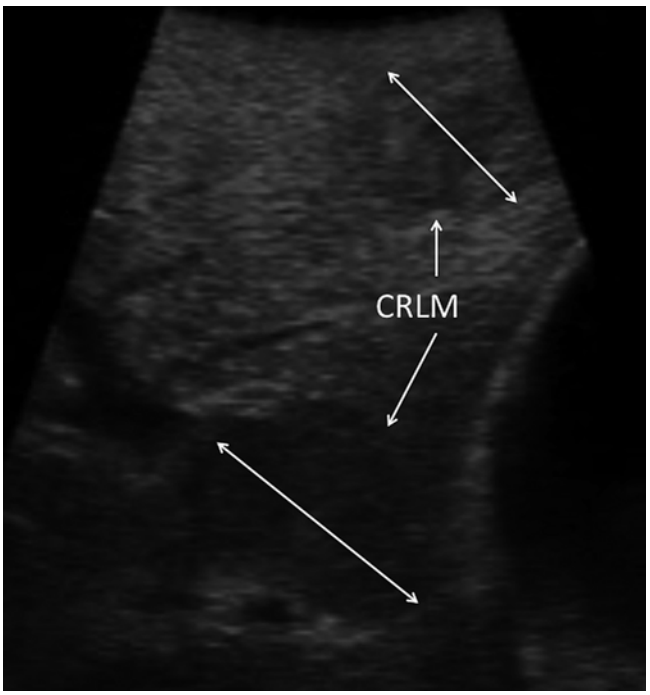

Fig. 17.18 US image demonstrates a colorectal liver metastasis (*CRLM*) after neoadjuvant chemotherapy. Partial tumor response results in regression of the tumor and loss of definitive imaging characteristics making targeting more difficult. Tumors are indicated by *arrows*

the management of colorectal liver metastases, this potential difficulty must be considered.

Disappearance of Pretreated Lesions

Modern chemotherapeutic regimens are associated with tumor regression rates of nearly 70 %. With the increasing utilization of neoadjuvant chemotherapy in the treatment of patients with colorectal liver metastases, targeting pretreated lesions can be challenging. Tumor regression of larger lesions may lead to central necrosis and rounding of the tumor. Smaller lesions tend to regress by losing their characteristic appearance on ultrasound, becoming more amorphous and less discreet, rendering them difficult or impossible to identify (Fig. 17.18).

We do not recommend the blind ablation of an approximated tumor position. If a tumor is not clearly visible, we recommend a blind resection of the involved region of the liver or aborting the ablative procedure with close follow-up of the patient.

Summary

There have been substantial improvements in technology (ultrasound and minimally invasive instrumentation), which now afford us the opportunity to perform highly successful, low risk ablations of liver lesions. Successful treatment strategies require thoughtful patient selection, careful planning, and strict adherence to the basic principles of accurate probe placement and thorough destruction of the target lesion and a surrounding margin of normal tissue.

Surgeon familiarity with ultrasound theory, equipment, and application is critical to the practice of hepatobiliary surgery today. Ultrasound skills are obtained through careful study but, more importantly, hands-on experience. Tumor ablation is an advanced skill and should only be attempted by experienced surgeons. That said, it is imperative that we teach the next generation of hepatobiliary surgeons to be facile enough with surgical ultrasound and ablation technologies, so that these techniques become an integral part of their practice.

References

1. Livraghi T, Festi D, Monti F, Salmi A, Vettori C. US-guided percutaneous alcohol injection of small hepatic and abdominal tumors. Radiology. 1986;161(2):309–12.
2. Shiina S, Tateishi R, Imamura M, Teratani T, Koike Y, Sato S, Obi S, Kanai F, Kato N, Yoshida H, Omata M, Koike K. Percutaneous ethanol injection for hepatocellular carcinoma: 20-year outcome and prognostic factors. Liver Int. 2012;32(9):1434–42.
3. Siperstein AE, Berber E. Cryoablation, percutaneous alcohol injection, and radiofrequency ablation for treatment of neuroendocrine liver metastases. World J Surg. 2001;25(6):693–6.
4. Ansari D, Andersson R. Radiofrequency ablation or percutaneous ethanol injection for the treatment of liver tumors. World J Gastroenterol. 2012;18(10):1003–8.
5. Bala MM, Riemsma RP, Wolff R, Kleijnen J. Cryotherapy for liver metastases. Cochrane Database Syst Rev. 2013;(6):CD009058.
6. Mu F, Niu L, Li H, Liao M, Li L, Liu C, Chen J, Li J, Zuo J, Xu K. Percutaneous comprehensive cryoablation for metastatic hepatocellular cancer. Cryobiology. 2013;66(1):76–80.
7. Hong K, Georgiades C. Radiofrequency ablation: mechanism of action and devices. J Vasc Interv Radiol. 2010;21(8 Suppl):S179–86.
8. Brace CL. Microwave tissue ablation: biophysics, technology, and applications. Crit Rev Biomed Eng. 2010;38(1):65–78.
9. Veltri A, Guarnieri T, Gazzera C, Busso M, Solitro F, Fora G, Racca P. Long-term outcome of radiofrequency thermal ablation (RFA) of liver metastases from colorectal cancer (CRC): size as the leading prognostic factor for survival. Radiol Med. 2012;117(7):1139–51.
10. Huang J, Hernandez-Alejandro R, Croome KP, Yan L, Wu H, Chen Z, Prasoon P, Zeng Y. Radiofrequency ablation versus surgical resection for hepatocellular carcinoma in Childs A cirrhotics-a retrospective study of 1,061 cases. J Gastrointest Surg. 2011;15(2):311–20.
11. Feng K, Yan J, Li X, Xia F, Ma K, Wang S, Bie P, Dong J. A randomized controlled trial of radiofrequency ablation and surgical resection in the treatment of small hepatocellular carcinoma. J Hepatol. 2012;57(4):794–802.
12. Berber E, Tsinberg M, Tellioglu GJ, Simpfendorfer CH, Siperstein AE. Resection versus laparoscopic radiofrequency thermal ablation of solitary colorectal liver metastasis. Gastrointest Surg. 2008;12(11):1967–72.
13. Khan KN, Yatsuhashi H, Yamasaki K, Yamasaki M, Inoue O, Koga M, Yano M. Prospective analysis of risk factors for early intrahepatic recurrence of hepatocellular carcinoma following ethanol injection. J Hepatol. 2000;32(2):269–78.
14. van Vledder MG, Pawlik TM, Munireddy S, Hamper U, de Jong MC, Choti MA. Factors determining the sensitivity of intraoperative

ultrasonography in detecting colorectal liver metastases in the modern era. Ann Surg Oncol. 2010;17(10):2756–63.
15. Elias D, Sideris L, Pocard M, de Baere T, Dromain C, Lassau N, Lasser P. Incidence of unsuspected and treatable metastatic disease associated with operable colorectal liver metastases discovered only at laparotomy (and not treated when performing percutaneous radiofrequency ablation). Ann Surg Oncol. 2005;12(4):298–302.
16. Thaler K, Kanneganti S, Khajanchee Y, Wilson C, Swanstrom L, Hansen PD. The evolving role of staging laparoscopy in the treatment of colorectal hepatic metastasis. Arch Surg. 2005;140(8):727–34.
17. Belgihiti J, Clavien PA, Gadzijev E, et al. The Brisbane 2000 terminology of liver anatomy and resections. HPB. 2000;2:333–9.
18. Bismuth H. Surgical anatomy and anatomical surgery of the liver. World J Surg. 1982;6(1):3–9.
19. Xu LH, Cai SJ, Cai GX, Peng WJ. Imaging diagnosis of colorectal liver metastases. World J Gastroenterol. 2011;17(42):4654–9.
20. Park MJ, Kim TH, Lee KM, Cheong JY, Kim JK. Radiofrequency ablation of metastatic liver masses: recurrence patterns and prognostic factors based on radiologic features. Hepatogastroenterology. 2012;60(123):563–7.
21. Hammill CW, Billingsley KG, Cassera MA, Wolf RF, Ujiki MB, Hansen PD. Ann Surg Oncol. 2011;18(7):1947–54. doi:10.1245/s10434-010-1535-9. Epub 2011 Mar 12.

Computer-Assisted Navigation for Ultrasound "3-D Ultrasound"

18

John B. Martinie and Sharif Razzaque

This comprehensive textbook is uniquely designed with surgeons in mind, with the understanding that ultrasound can be a somewhat difficult imaging tool to master. Simply visualizing ultrasound images for the first several times, which often appear as black and white abstract portraits without well-defined borders or distinct anatomic landmarks, can be challenging. Recall, if you will, the first time you, as a fresh out of the classroom medical student, gazed upon an ultrasound image and thought, "I have no idea what I am looking at." And although most experienced general surgeons can easily identify a gallbladder filled with stones on an abdominal ultrasound, interpreting less common or more complex images is often difficult. Even more so is the art of using ultrasound as a tool for guidance of a diagnostic or therapeutic endeavor, such as a core-needle biopsy, central line placement, or tumor ablation. It would be a *tremendous understatement* to say that mastering ultrasound takes significant dedication, practice, and perseverance. Despite being mentioned as a curriculum requirement by the American Board of Surgery, formal training in ultrasound for surgical residents in the majority of programs in the United States has not yet become standard. Furthermore, many surgeons who completed surgical training prior to the development of more user-friendly ultrasound machines and widespread use of these machines during residency find it difficult to adopt the new skills required for ultrasound. It is not uncommon, even today in 2013, to hear that even accomplished surgeons call a radiologist to the operating room to interpret ultrasound images. This textbook aims to eliminate the need for this practice and to help enable practicing general surgeons with the skills necessary to perform ultrasound with confidence and proficiency.

It is hard for most of us to imagine a world without computers, which have become fixtures in our daily lives. Some of these computers are more subtle than others and embedded in standard household refrigerators or microwave ovens, items that we often overlook. A growing percentage of automobiles on the roads today have GPS (Global Positioning System) navigation built in or have add-on aftermarket devices to help us get around without getting lost. Cell phones are no longer just a means of communication; they have become powerful computers that allow us to search the Internet, find the nearest coffee shop, or direct us with infinitely detailed maps and "GPS" directions. Almost all air traffic in the United States, commercial or private, utilize computerized navigation devices that have become so accurate as to virtually eliminate older means of manual navigation (using compasses and maps). Computers have also become standard in fields such as automobile and aircraft construction as well as parts manufacturing, where they enable precision and efficiency that exceeds human capacity. In some cases these computers allow humans to perform tasks quicker and safer, while in other cases the computers can take over and perform the task completely without human intervention. Surgical robots and unmanned military combat aircraft (drones) are becoming household vocabulary. Such is the world we are entering.

Computer-assisted navigation systems are not new to medicine; there has been research in this field for over 50 years [1]. As they apply to ultrasound in particular, there are a number of systems coming on the market which will be discussed which incorporate elements of computerized positional tracking into standard ultrasound platforms. This chapter will focus on these different systems, how they work, and how they incorporate ultrasound, specifically, into their navigation system. The preceding chapters have extensively discussed the theory and means by which to perform ultrasound examination of the liver, pancreas, and biliary tree. Transabdominal, open surgical, and laparoscopic ultrasound techniques all

J.B. Martinie, MD (✉)
Department of Surgery, Carolinas Medical Center,
1025 Morehead Medical Drive, Suite 300, Charlotte, NC 28204, USA
e-mail: john.martinie@carolinashealthcare.org

S. Razzaque, PhD
InnerOptic Technology, Inc.,
106A Churton St., Hillsborough, NC 27278, USA
e-mail: sharif@inneroptic.com

E.J. Hagopian, J. Machi (eds.), *Abdominal Ultrasound for Surgeons*,
DOI 10.1007/978-1-4614-9599-4_18, © Springer Science+Business Media New York 2014

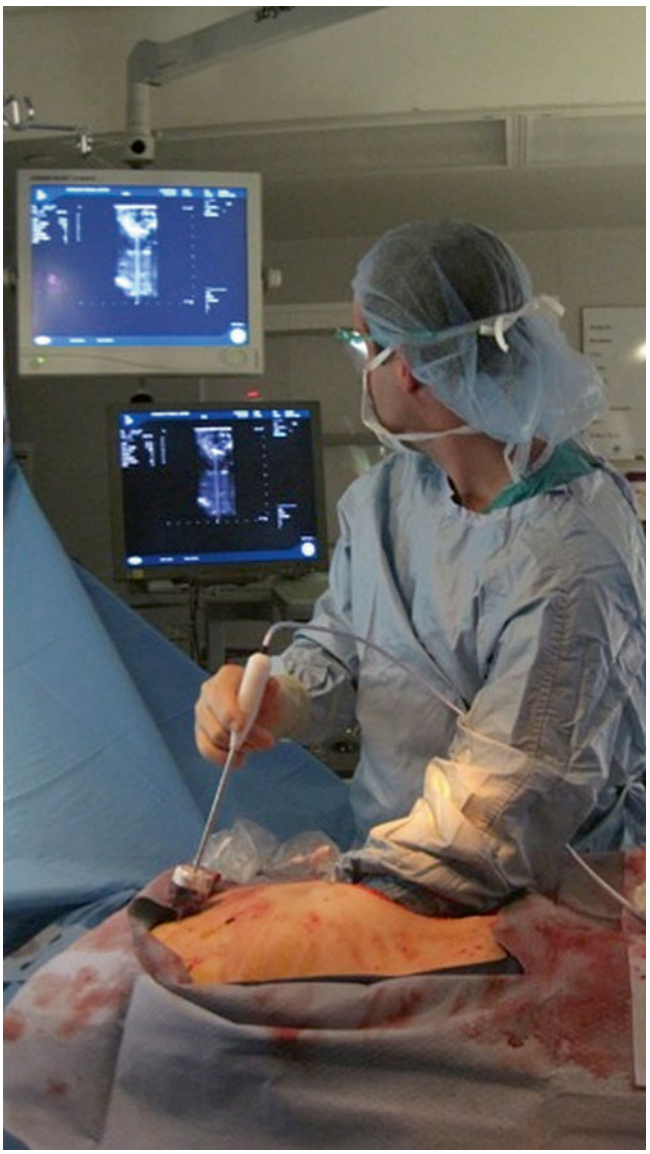

Fig. 18.1 Laparoscopic, hand-assisted, ultrasound-guided ablation of a hepatic malignancy. The patient had undergone a sigmoid resection and already had a lower abdominal hand port in place. Notice the surgeon is performing the procedure by looking back over his shoulder in the opposite direction

require skills and practice in order to consistently identify target anatomy with precision and efficiency. Simply identifying a small neuroendocrine tumor of the pancreas or a small hepatoma in a cirrhotic liver can be difficult. Doing this with a flexible-tip laparoscopic ultrasound probe is doubly so. Placing a biopsy needle or ablation antennae into a small tumor such as the ones mentioned above and using a laparoscopic approach represents the ultimate achievement and requires multiple skills which, quite simply, are not easily taught or attained. The surgeon must mentally fuse information from the laparoscopic camera, commonly displayed on one flat-panel monitor, with information from the ultrasound probe, which is often displayed on a second monitor or on the ultrasound machine itself. Then, in what is commonly referred to as "biaxial" image interpretation, the surgeon must move their instrument in the direction desired [1]. What "biaxial" means, in plain English, is that the operator is looking at a television monitor, not down at their hands. This is a skill that many older surgeons, brought up before the age of video games or laparoscopic surgery, have never fully mastered. It is probably safe to say that this is a skill required from all graduating surgical residents. Add to this the ultrasound image, which often is not oriented in the same position as the laparoscopic image or the patient's body. Finally, the ultrasound image itself is a thin, two-dimensional data set and will not identify a biopsy needle or ablation antennae until they actually cross the ultrasound "plane." It is this complex amalgam of data – laparoscopic and ultrasound image, target organ location, and surgeon's hand and instrument positioning – that must be processed by the surgeon's brain in this procedure (see Fig. 18.1). It is this process or skill that computers, can play a significant role in making it easier for the surgeon to first locate a tumor and then successfully target the lesion [1].

"Computerized Proprioception"

There are several commercially available computer-assisted navigational systems currently available, or under development, which have been developed specifically with liver and pancreas surgeons in mind. These systems include those produced by InnerOptic Technology (Hillsborough, NC), Pathfinder Technology (Nashville, TN), and CAScination AG (Bern, Switzerland). They all share some technical design characteristics, and even have some identical third-party components in common, but perhaps nothing more important than the similar concept *behind* the hardware. Essentially, these systems allow the computer to "know" where certain things are in space, such as a biopsy needle, an ablation antenna, or an ultrasound handpiece transducer. For lack of a better term, we might call this *computerized proprioception.* We begin by creating a three-dimensional "space" in the computer construct and allow the computer to place certain items in correct position *and orientation*, in this case an ultrasound probe and its corresponding ultrasound 2-D image. The computer then can add additional objects into that space in a location and orientation determined by the *tracking system* (also called *the localization system*) that it employs [1]. These objects, ranging from biopsy needles to microwave ablation antennae to surgical instruments, are computer-generated models (or avatars) of the actual instruments (see Fig. 18.2). This allows the surgeon to visualize the particular instrument relation to the ultrasound image and target lesion long before intersecting the plane of the

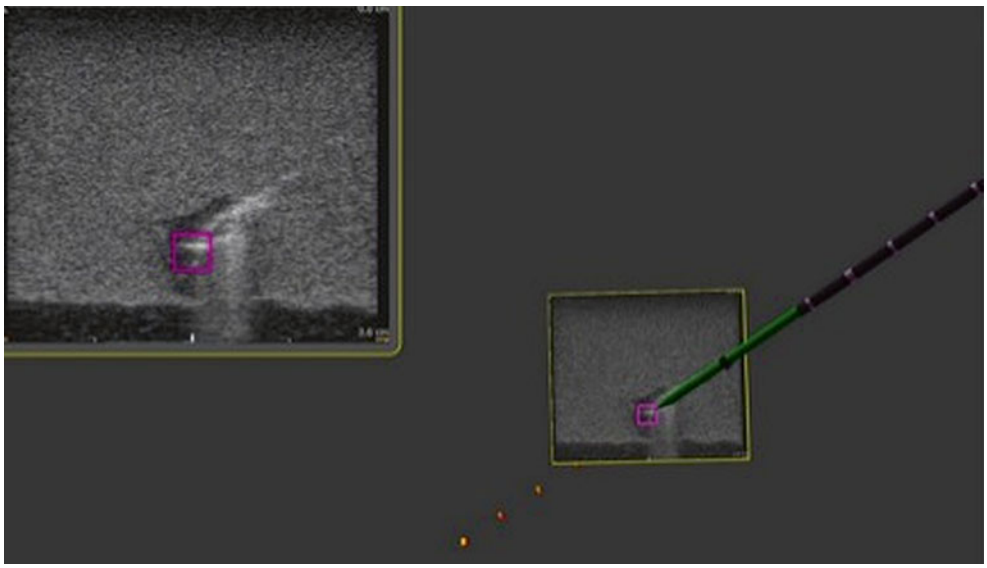

Fig. 18.2 Ultrasound guidance system image including 2-D ultrasound image in the left upper corner and stereoscopic 3-D image with microwave antenna avatar in the center. Notice the *purple square* target on the ultrasound image

ultrasound. (Remember that the surgeon does not normally see the antenna once it disappears into the target organ, until it crosses the ultrasound plane. Even then, it is often difficult to actually "see" the instrument.) Early systems utilized actual mechanical arms or calipers, which relayed information about instrument position to the computer to determine the location and orientation of certain items held in those arms. These systems utilized what is referred to as "mechanical digitizers" in order to relay positional information about the end instrument's location and position to the computer [1] (see Figs. 18.3 and 18.4). One of these systems, which was developed at the University of North Carolina, Chapel Hill, Department of Computer Science, even added stereoscopic three-dimensional goggles (or head-mounted displays) to allow the surgeon to "look" directly at the target organ, rather than at a television monitor [2, 3].

Although functional and certainly revolutionary, these systems had the drawback of being somewhat bulky and impractical for certain OR environments. With the advancement of technology, infrared cameras and optical sensors became the systems of choice for several of the image guidance systems and made the mechanical arms somewhat obsolete. These systems, collectively termed optical tracking systems (OTSs), have been used by the above-mentioned companies, yet the actual hardware (infrared camera and optical reflectors) was developed by a third-party company

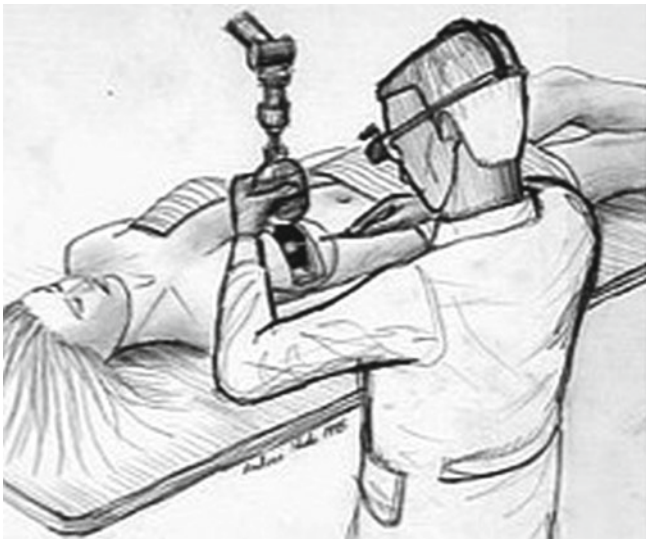

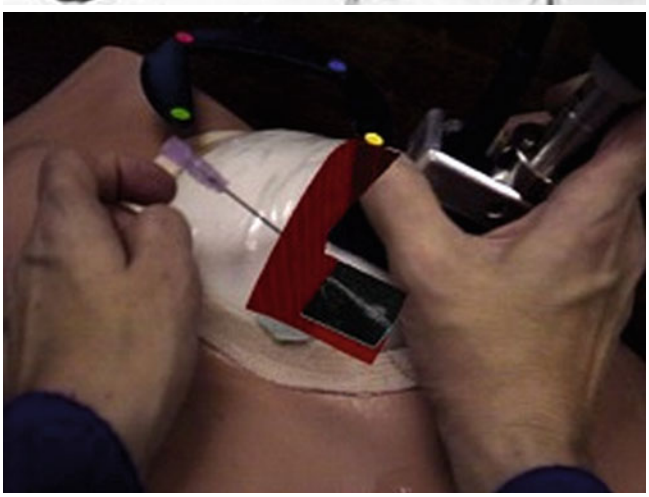

Figs. 18.3 and 18.4 Breast biopsy system (ca 1996). A mechanical arm is used to track the position and orientation of the ultrasound probe, and the live U/S scan appears inside the breast, via an augmented-reality head-worn display. *Left*: conceptual sketch (Courtesy of Andrei State). *Right*: view from the head-mounted display, showing the U/S scan on a breast phantom, with an aspiration needle (Courtesy of Andrei State)

(Northern Digital Inc., Ontario, Canada). Several OTSs for orthopedic and neurosurgical procedures, as well as for general surgery, are currently available and all share certain similar tracking components, *although not all systems utilize ultrasound.* The Brainlab® system (Feldkirchen, Germany), for example, uses CT and MR imaging of the patient's skull and brain along with an optical tracking system to help perform complex and precise neurosurgical procedures.

At least two companies have used similar strategies specifically for computer-navigated liver surgery, namely, Pathfinder® (Nashville, TN, USA) and CASination® (Bern, Switzerland). Both of these companies utilized sophisticated computer software to first construct complex 3-D models of each patient's liver, including vascular anatomy and tumor characteristics. Both systems incorporate an OTS described above to *co-register* the patients' actual liver and surgical instruments to the CT-based, computer-generated, 3-D model of the patient's liver on a video monitor. In this way, the surgeon is able to "see" how close a particular instrument is to certain vital structures such as a major portal vein branch or hepatic vein. Both of these systems have been employed in actual human clinical surgeries for open hepatic resections and/or ablations with remarkable efficacy. These systems depend on static, preoperative CT- or MR-generated models rather than real-time intraoperative ultrasound (IOUS). With the mobilization and manipulation of the liver during open surgery, there often is *distortion* of the actual organ and the relationship of, say, a tumor to internal hepatic structures. Furthermore, there is continual movement of the patient's liver during surgery from mechanical ventilation and diaphragmatic motion. As such, it was critical for these navigation systems to integrate live ultrasound.

The first system to successfully integrate real-time intraoperative ultrasound and an OTS for the purpose of liver surgery was produced by InnerOptic (Hillsborough, NC). This system grew out of the earlier research in the Department of Computer Science at the University of North Carolina, Chapel Hill, and has undergone multiple improvements and modifications since the first prototype was developed, some out of trial and error and some out of continuous improvements in hardware technology [2, 3]. The initial systems utilized rather large infrared cameras and optical LEDs mounted on clip-on adaptors for the ultrasound handpiece and the microwave ablation antennae (see Fig. 18.5). Yet this system proved functional enough to produce significant targeting improvements both in the laboratory setting and, after multiple generations of refinements and modifications, in the operating room. This data was presented at the American Hepato-Pancreato-Biliary Association annual meeting in 2008 and subsequently published, demonstrating an improvement in targeting of small phantom tumors in gelatin models by both experience and novice operators [4] (see Fig. 18.6). Furthermore, this system was shown to be both accurate and safe in an actual OR environment consisting of open hepatic ablation procedures [5]. Once again, lessons learned in both the laboratory and in the OR led to design modifications and improvements. Some of the other systems, previously described, which initially relied solely on preoperative CT or MR eventually modified their systems to include ultrasound. These systems now allow the surgeon to visualize both the preop CT mapping of the liver with real-time intraoperative ultrasound, all on a single flat-panel monitor (see Fig. 18.7).

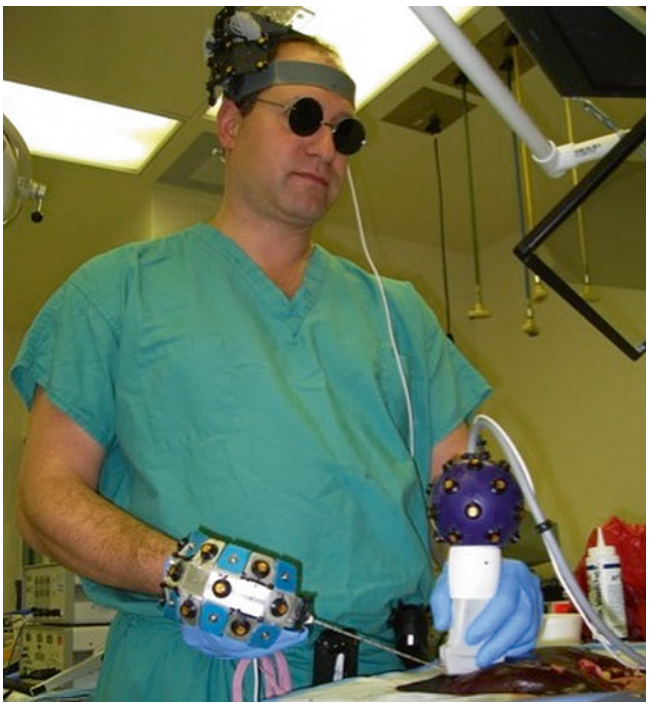

Fig. 18.5 Early guidance system prototype (ca. 2007) utilizing "active" optical sensors attached to ultrasound probes and microwave antennae and including a "head positional mount." This system was modified and refined over time

"What Do You Mean by 3-D?"

A bit of clarification is in order regarding what is meant by "3-D," in ultrasound navigation systems. To begin with, most ultrasound transducers in use today by surgeons (to include BK Medical, Aloka®, and SonoSite®) all utilize a single linear array of crystals and therefore produce a single-plane, two-dimensional ultrasound image. Much more sophisticated ultrasound systems utilize a grid of crystal transducers, or have a linear array, and a motor to quickly sweep it back and forth inside the ultrasound probe housing and can produce true multi-planar, three-dimensional ultrasound images. These machines are commonly used in obstetrics, where eager parents-to-be can see hauntingly detailed, 3-D images of their developing baby. However, when we speak of 3-D

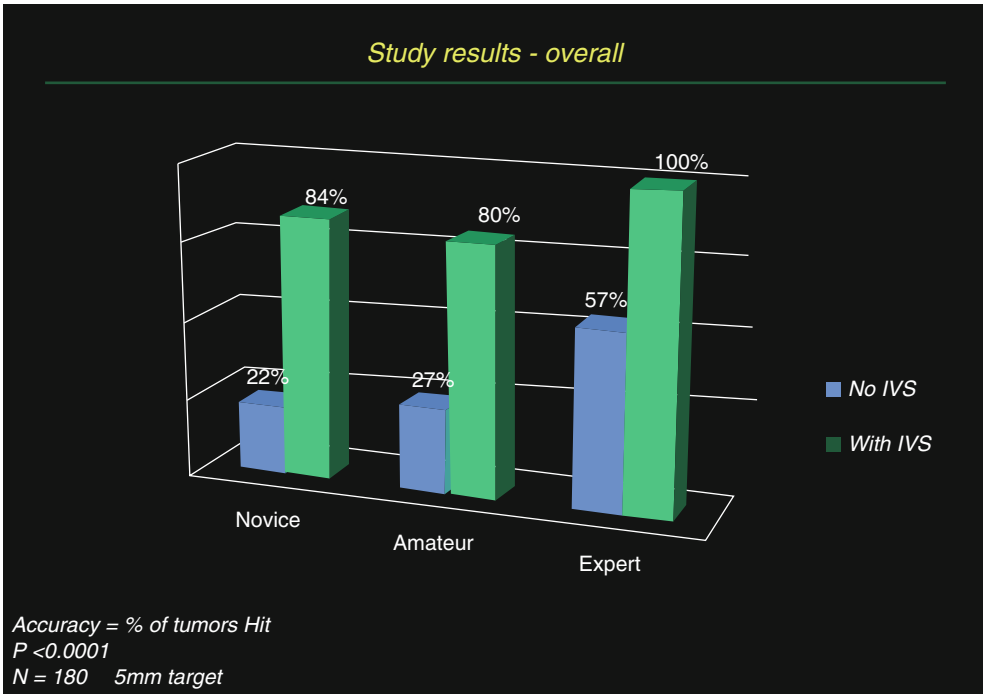

Fig. 18.6 Results from targeting studies utilizing a 3-D guidance system for ultrasound, with optical tracking, in gelatin agar targets

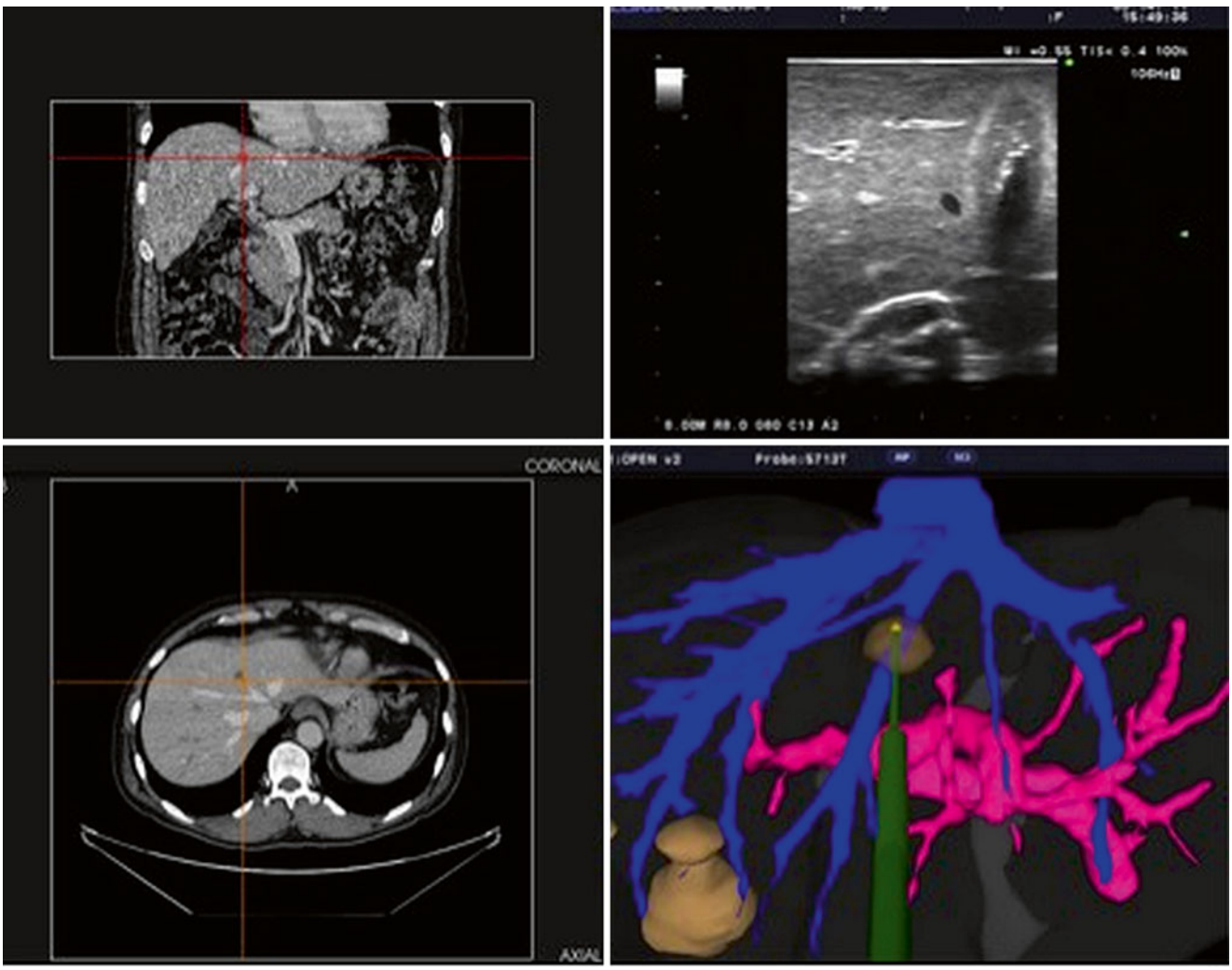

Fig. 18.7 Screenshot of a guidance system incorporating coronal and axial CT images, an ultrasound image, and a computer model of the hepatic vascular anatomy and phantom ablation antenna (Image courtesy of Pathfinder Technologies)

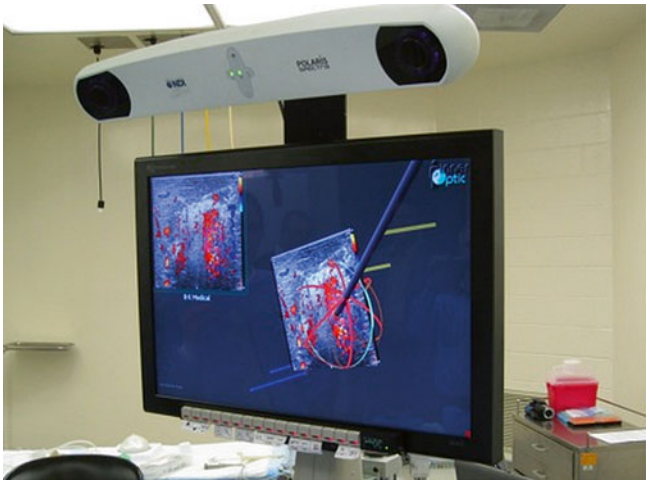

Fig. 18.8 3-D optical tracking system incorporating a high-resolution 3-D monitor and overhead infrared camera (Polaris, NDI, Waterloo, Ontario, Canada)

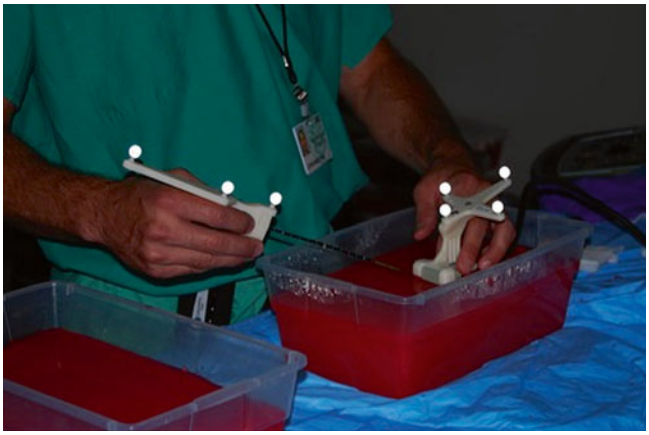

Fig. 18.9 Optical reflectors attached on plastic mounts to an ultrasound handpiece and ablation antenna. This system demonstrated superior accuracy when targeting small tumor targets in gelatin models (see Fig. 18.6)

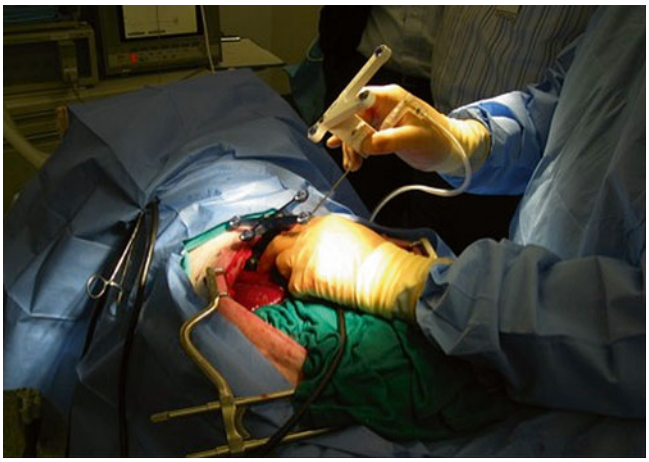

Fig. 18.10 Optical tracking system used during open liver ablation trials in porcine models

ultrasound guidance systems, we do not mean to imply a true 3-D ultrasound image; rather, some aspect of the navigation system is in 3-D. When we see a typical ultrasound image on a typical ultrasound monitor, we are seeing a 2-D image on a 2-D screen. And when we see a typical laparoscopic image, say during a laparoscopic cholecystectomy, we are seeing a 2-D image on a 2-D monitor. The InnerOptic system utilizes a high-resolution stereoscopic 3-D monitor that affords the surgeon depth perception not possible on even a high-definition 2-D television monitor. In these systems, the ultrasound image itself remains a 2-D image within a larger 3-D monitor "window." Imagine, if you will, the ultrasound image is a sheet of paper floating in a virtual "box" in the 3-D monitor. That ultrasound image, as a sheet of paper, can be rotated and adjusted by the surgeon to the optimal position for the procedure. The computer then can a 3-D computer-generated model of the particular device in the precise position and orientation determined by the systems tracking components. Essentially, there are both 2-D and 3-D components within a 3-D space. The combination of these elements gives the surgeon the information needed to target a tumor with greater ease and precision (see Fig. 18.8). (*Keep in mind that images depicted in this chapter are, in fact, 2-D representations of actual stereoscopic 3-D computer images*).

Open Optical Tracking Systems (OTS)

As described above, there are several systems available which incorporate optical tracking systems (OTS) including optical reflectors and infrared (IR) cameras for navigation in hepatic surgery. And although each system has unique features, all systems share the same basic concepts. These cameras emit infrared light which bounces off of the small, round, optical reflectors and back to the camera. Each camera system actually utilizes multiple infrared emitters and multiple receivers, which are needed to "triangulate" the position of the reflectors and their spatial orientation. These optical "reflectors" are a type of a "passive system" of targeting that eliminated the need for wires to the surgical instruments. Older systems utilized "active" reflectors, which actually consisted of LEDs, which were connected by wire to the OTS computer (Fig. 18.5). Additionally, there are multiple reflectors clustered in unique geometric patterns on specially designed clip-on mounts. These mounts, in turn, are attached to the surgical instruments, biopsy needles, or ultrasound handpieces (see Figs. 18.9 and 18.10). When the camera receives the infrared light from the reflectors, it then transmits this information to the systems computer, usually a laptop computer. The computer then processes this data and is able to determine the precise location and spatial

orientation of each reflector, and in turn, each instrument. These OTSs function similar to the way sailors of old were able to determine their location in the middle of oceans by the position of the stars in the sky. The real advantage of these systems is their ability to incorporate a computer-generated three-dimensional model of an ablation antenna (or other device) and place that image into the 3-D television monitor for the surgeon to see. Some systems have even added trajectory tools to their systems, which allow the surgeon to simply aim the ablation device or biopsy needle at the target and advance straight in.

Yet as good as some of these systems were for aiding surgeons in performing ultrasound-guided tasks, there were limitations to each. One common difficulty was "line of sight" limitations. What this means, simply, is that when a surgeon performs an ultrasound as part of an open liver operation, their hand is often obscured from view by the right costal margin or by the surgical retractors or drapes. This is particularly true when the surgeon's hand and ultrasound transducer are placed over the dome of the liver. These factors limited the ability of the infrared camera to "see" the optical reflectors, which prompted many successive tweaks and modifications to the shape of the reflectors (e.g., making the handles much longer, wider, etc.). Yet, despite continual changes to the designs, ergonomic and logistical limitations persisted and to a certain degree hampered the surgeons' ability to perform ultrasound-guided procedures.

From Open to Laparoscopic

Technology marches on and waits for no one. Even as many of these systems were developed, put through preclinical and clinical trains, and passed FDA approval, many have become obsolete. This happened, in part, because technology improved but, equally so, because surgical practice has evolved. Over the past several years, there has been a significant trend toward performing liver tumor ablations in a minimally invasive fashion, to the point that, at many high-volume hepatobiliary centers, the vast majority of ablations are now performed laparoscopically [6, 7]. At Carolinas Medical Center, a 900-bed tertiary referral center for liver surgery, we perform approximately 100 liver tumor ablations per year. The vast majority of these procedures are now performed laparoscopically [8]. And because many surgeons who perform laparoscopic liver tumor ablations utilize an *articulating* or *flexible* laparoscopic ultrasound probe, the position of the transducer head cannot be determined using externally applied optical tracking reflectors. (Although it should be said that utilizing a rigid ultrasound probe, it is possible to use the OTSs described above, using IR cameras and optical reflectors. This system was actually tested in 2008, but its benefits were limited, because of the lack of articulation of the ultrasound probe, and

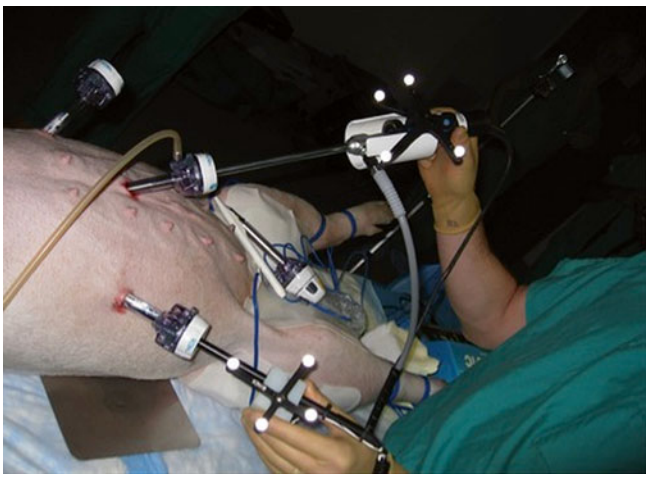

Fig. 18.11 Prototype of laparoscopic version of optical tracking system in porcine model, utilizing a rigid ultrasound probe (*left hand*)

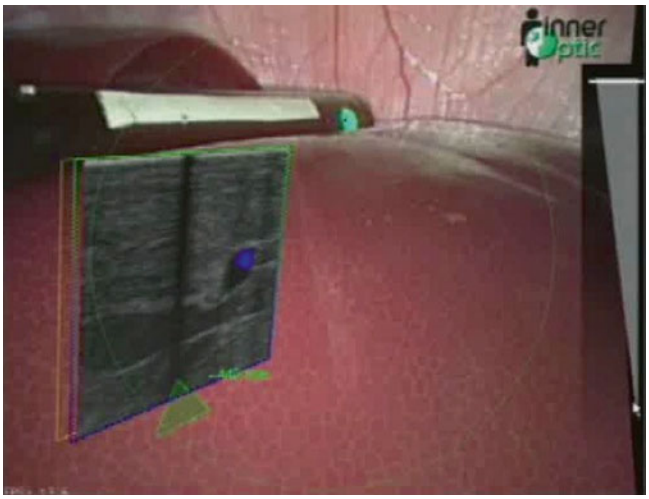

Fig. 18.12 Video monitor view of laparoscopic image and superimposed ultrasound image (from Fig. 18.11)

because surgeons sometimes had to hold the instruments at awkward angles to keep line of sight between the reflectors on the handles and the IR tracking cameras [unpublished researched]) (see Figs. 18.11 and 18.12).

Another problem with using the optical reflectors attached to the handle of ablation antennae is that these devices have a fair amount of flexibility. If these antennae or needles are not placed extremely carefully, there can be a "deflection" of the tip by up to roughly a centimeter. The computer will not be able to account for this deflection, and thus accuracy will suffer. As a result in this rather significant change in surgical practice, and in addition to the limitations discussed above, systems employing infrared cameras and optical reflectors have, according to some opinions, become obsolete. Systems had to be totally rethought and redesigned to accommodate the evolution to minimally invasive approaches.

Electromagnetic Tracking Systems (EMTSs)

As opposed to optical tracking, electromagnetic tracking systems do not require line of sight between the surgical instruments and cameras. Instead, these systems consist of a magnetic field generator, either mounted to a cart or the operating table, and tiny sensor coils, inside the surgical instruments. These systems utilize the principle of electromagnetic induction – which underlies almost all modern electrical technology: transformers, motors, radio, etc. Imagine a source coil, inside the field generator on a cart. If we run an alternating electrical current through the source coil, the coil generates a varying magnetic field, which passes through the patient (see Fig. 18.13). Imagine a second, much smaller, receiver/sensor coil, inside the surgical instrument, nearby the source coil. The magnetic field induces a small electrical current signal in the sensor coil. The strength of this signal depends approximately on the sensor's distance from the source coil and on sensor's orientation to the magnetic field. Modern electromagnetic tracking systems have several source coils inside the field generator, at different positions and or orientations relative to the operating table. A computer drives each of these source coils with (possibly) different frequencies and strengths of currents and measures the resulting current signal in the sensor coil, to estimate the position and orientation of the sensor coil. Some systems incorporate feedback – based on where they last found the sensor coil, the computer might alter the signals that drive the source coils, to more accurately home in on subsequent small movements of the sensor coil [9].

These electromagnetic systems were first developed in the 1970s by Polhemus Navigation Systems as a way to track a pilot's helmet in an aircraft cockpit, so that the pilot could aim weapons or steer radar with his head motion. In the 1980s the applications were expanded to include capturing the motion of actors for movies and capturing a person's head and limb positions for virtual reality [10]. In the 1990s, the first systems for medical procedures appeared. Today, there are several companies making medical electromagnetic tracking systems, particularly for interventional radiology and cardiac catheterization procedures. These include Ascension (Milton, Vermont), Northern Digital Inc. (Ontario, Canada), superDimension (Minneapolis, MN), and Biosense Webster (Diamond Bar, CA).

Metal objects (such as in the operating table and in the surgical instruments) can be a problem for electromagnetic tracking systems, because the varying magnetic field, produced by the source coil, can cause eddy currents inside the metal objects near the patient. These unintended eddy currents produce their own magnetic fields that can distort the primary field detected by the sensor coils, which in turn can lead to inaccurate position readings or tracking system failures. Various manufacturers have developed different proprietary and confidential techniques for handling metal materials in the area of the procedure. Regarding the patient table, some tracking systems require keeping the field generator and sensor coils close to each other and far from the metal in the patient table. Other systems have a large field generator that is magnetically shielded from the table and must be positioned underneath the patient. Regarding metals in the surgical instruments, most modern tracking systems tolerate stainless steel and titanium, but not ferrous metals or aluminum. The EMTS-based guidance system developed by InnerOptic Technology Inc. (Hillsboro NC) was first tested

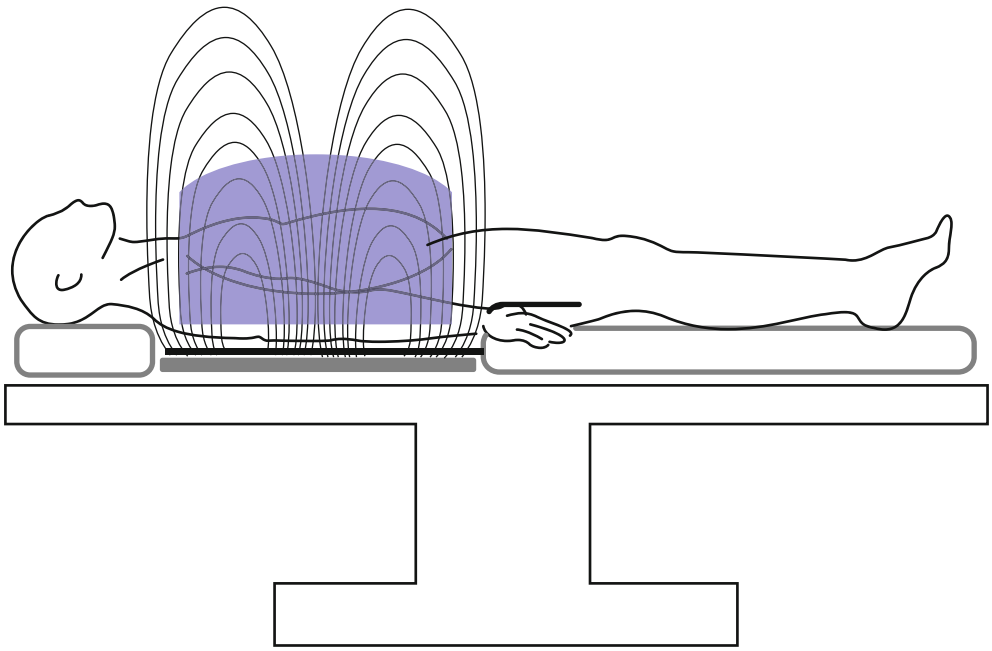

Fig. 18.13 Schematic representation of the authors' estimate of the electromagnetic field produced by tabletop field generator which envelopes the patient's body

Fig. 18.14 Essential components of an electromagnetic tracking system (EMTS). A large, flat field generator, an articulating ultrasound probe, and a microwave ablation antenna

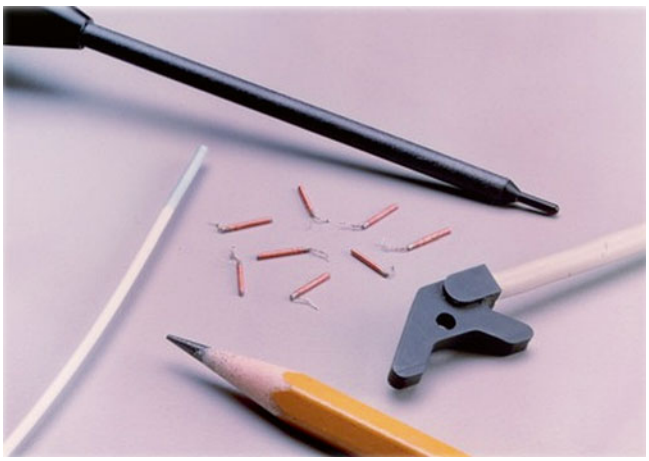

Fig. 18.16 Sensor coils which can be incorporated into ultrasound probes or surgical instruments. These probes function similarly to the optical reflectors in OTSs (Image courtesy of Northern Digital Inc.)

Fig. 18.15 Tabletop, flat EM field generator in position on the OR table, underneath the foam padding and patient. The device itself measures only a few cm in thickness and produces a relatively large, homogenous EM field

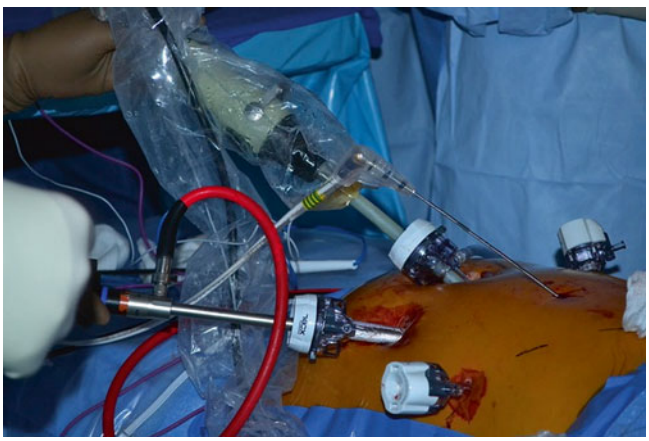

Fig. 18.17 Laparoscopic liver ablation performed using an EMTS during human clinical trials

at Carolinas Medical Center in 2010 and performed well in preclinical testing and subsequent IRB-approved human clinical trials [4, 5, 11]. The system incorporated a thin, flat magnetic field generator (NDI, Ontario, Canada) with source coils that was designed to be placed under the patient (see Figs. 18.14 and 18.15). Tiny sensor coils were placed into the tip of an articulating ultrasound probe (BK Medical, Denmark) as well as microwave ablation antennae (Microsulis, England) (see Fig. 18.16). The large, overhead OTS cameras were thus eliminated, as were the clumsy, clip-on optical reflectors on the surgical instruments. Furthermore, since the miniature sensor coils are placed in the actual tip of the instruments, the bending or deflecting of the antennae virtually becomes less of a potential for error (see Figs. 18.17, 18.18, and 18.19). As of the time of writing of this chapter, several companies are developing EMTSs to be placed into their clinical inventory, and these will likely replace the older OTSs as the modality of choice for image guidance for ultrasound.

Future Directions

Despite many years of research and development and incorporation into functioning, clinically available products, ultrasound guidance systems remain a relative rarity in the operating rooms of the overwhelming majority of surgeons throughout the world. Part of this is due to the relative lack of widespread availability of these products, and part of this is due to the actual cost of the systems. Some of the systems discussed in this chapter reportedly have sticker prices of almost 500 thousand US dollars, several times the cost of many modern surgical ultrasound machines. It is not

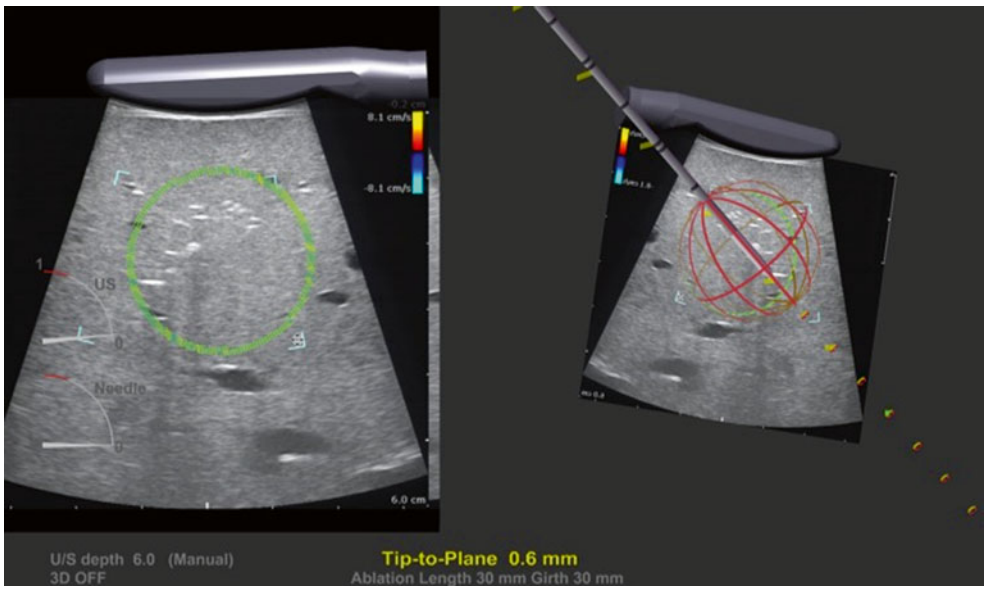

Fig. 18.18 Video monitor image of a 3-D EMTS showing a standard 2-D ultrasound image on the *left* and stereoscopic 3-D image with computer model (avatar) of motion-tracked microwave antenna on the *right*

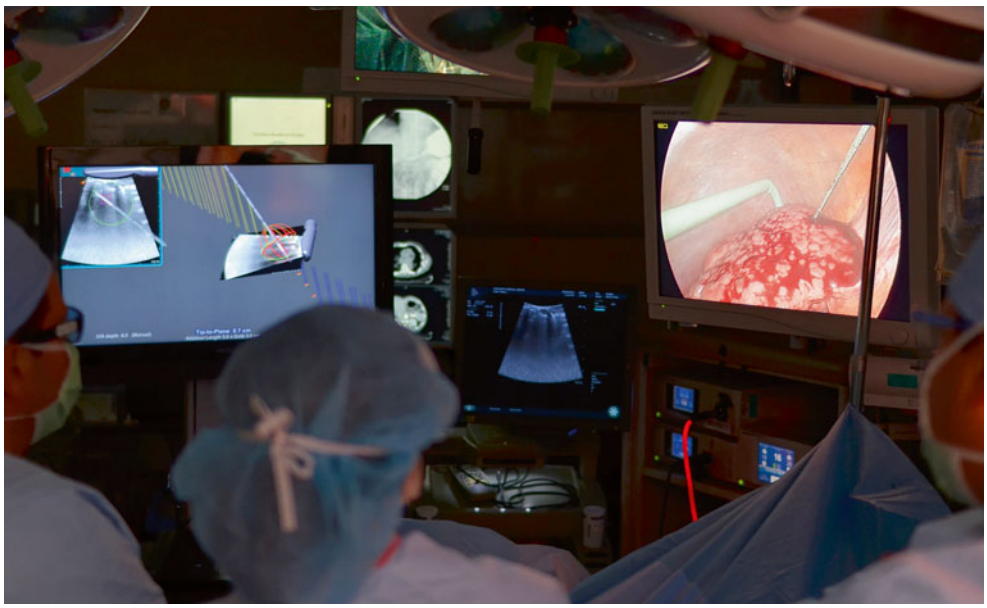

Fig. 18.19 Intraoperative photo of a laparoscopic liver tumor ablation using the EMTS. Note side-by-side monitors with stereoscopic 3-D ultrasound navigation image and laparoscopic image. Some of the surgeons are wearing lightweight passive 3-D stereo glasses

hard to understand that in this current economic healthcare climate, adoption of these types of systems will be extremely difficult. Perhaps the optimal solution would be the incorporation of ultrasound imaging, a 3-D image guidance EMTS, and an ablation device, into a single, affordable unit. But that would take cooperation from multiple medical products companies, not always an easy task. It is clear, however, that these guidance systems will continue to play an ever-growing role in the future of medicine (see Fig. 18.20).

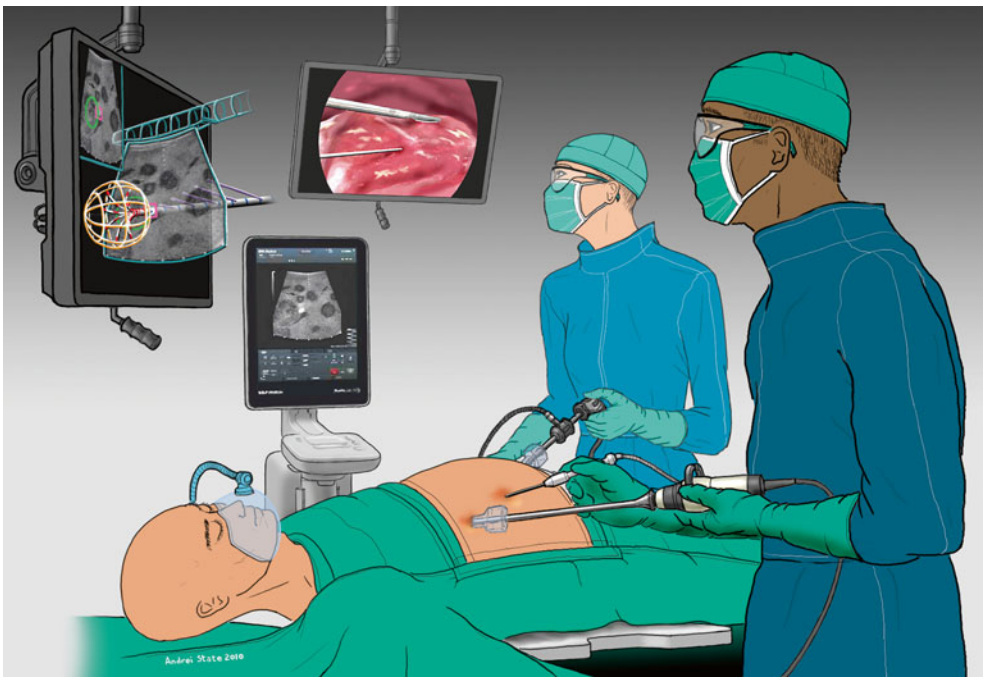

Fig. 18.20 Illustration of the EMTS developed for minimally invasive hepatic tumor ablations (Courtesy of Andrei State and InnerOptic)

References

1. Birkfellner WHJ, Wilson E, Cleary K. Tracking devices. In: Peters T, Cleary K, editors. Image-guided interventions. 1st ed. New York: Springer; 2008. p. 23–36.
2. Bajura MFH, Ohbuchi R. Merging virtual objects with the real world: seeing ultrasound imagery within the patient. In: 19th annual conference on Computer Graphics and Interactive Techniques; Chicago; 1992. p. 203–10.
3. State A, Livingston M, Garrett WF, Hirota G, Whitton MC, Pisano ED. Technologies for augmented-reality systems: realizing ultrasound-guided needle biopsies. In: 23rd annual conference on Computer Graphics and Interactive Techniques; New Orleans; 1996. p. 439–46.
4. Sindram D, McKillop IH, Martinie JB, Iannitti DA. Novel 3-D laparoscopic magnetic ultrasound image guidance for lesion targeting. HPB (Oxford). 2010;12:709–16.
5. Sindram D, Swan RZ, Lau KN, McKillop IH, Iannitti DA, Martinie JB. Real-time three-dimensional guided ultrasound targeting system for microwave ablation of liver tumours: a human pilot study. HPB (Oxford). 2011;13:185–91.
6. Hammill CW, Billingsley KG, Cassera MA, Wolf RF, Ujiki MB, Hansen PD. Outcome after laparoscopic radiofrequency ablation of technically resectable colorectal liver metastases. Ann Surg Oncol. 2011;18:1947–54.
7. Kennedy TJ, Cassera MA, Khajanchee YS, Diwan TS, Hammill CW, Hansen PD. Laparoscopic radiofrequency ablation for the management of colorectal liver metastases: 10-year experience. J Surg Oncol. 2013;107:324–8.
8. Swan RZ, Sindram D, Martinie JB, Iannitti DA. Operative microwave ablation for hepatocellular carcinoma: complications, recurrence, and long-term outcomes. J Gastrointest Surg. 2013;17:719–29.
9. Raab FH, Blood EB, Striner TO, Jones HR. Magnetic position and orientation tracking system. IEEE Trans Aerosp Electron Syst. 1979;15:709–18.
10. Ellis SR. Virtual environments and environmental instruments. In: Carr K, England R, editors. Simulated and virtual realities: elements of perception. 1st ed. Boca Raton: CRC Press; 1995. p. 28.
11. Sindram D, Simo K, Swan RZ, Niemeyer DJ, Lee SB, McKillop IH, Iannitti DA, Martinie JB. Laparoscopic microwave ablation of liver tumors using 3D guidance system in humans. HPB (Oxford). 2013;15:71.

Endoluminal Ultrasound: Anatomy, Technique, and Intervention of the Anorectum

19

Joseph L. Frenkel and John H. Marks

Introduction

Surgeons currently have the ability to use endoscopic ultrasound for diagnostic purposes in the anus and rectum. The most common uses for this technology include rectal cancer staging and fecal incontinence. As treatment options have evolved in the management of rectal cancer, especially after the introduction of neoadjuvant therapy, this data has become even more important. In addition to these two indications, it is less frequently used for identification of occult perianal and perirectal abscesses and fistula tracts. This chapter will discuss the indications for the study, review the anatomy of the rectum and anus, and discuss the technique of endoscopic ultrasound of the anus and rectum and the interpretation of the images acquired.

Endorectal ultrasound (ERUS) is a fairly unique imaging modality in that the study is performed directly by the surgeon. The surgeon, endoscopist, or radiologist has the ability to see the anatomic layers of the rectal wall as well as the layers of the sphincter muscle in the anal canal. This technology was developed in the mid-1980s as a way of advancing both the accuracy and reproducibility of tumor staging as well as giving the ability to stage tumors beyond the reach of the examining finger [1, 2]. Because we can see the various layers of the anatomy with such detail, we are able to use ultrasound data to stage rectal cancer and to describe with very specific detail the presence of sphincter defects in the anal canal. More importantly, as surgeons we are also able to correlate these finding with the still-essential clinical exam and other clinically important data to arrive at the most accurate staging possible. This information is critical in deciding on treatment options for these diseases and is central to the TNM staging system which is currently universally applied for the description and management of rectal cancer [3] (Table 19.1).

Table 19.1 AJCC colon and rectum cancer staging

Stage	Definition
Tis	Carcinoma in situ
T1	Tumor invades submucosa
T2	Tumor invades muscularis propria
T3	Tumor invades through muscularis propria into pericolorectal tissues
T4a	Tumor penetrates to surface of visceral peritoneum
T4b	Tumor directly invades or is adherent to other organs/structures
N0	No regional lymph node metastasis
N1	Metastasis in 1–3
N1a	Metastasis in 1 regional lymph node
N1b	Metastasis in 2–3
N1c	Tumor deposit(s) in subserosa, mesentery, or non-peritonealized pericolorectal tissues without regional nodal metastasis
N2	Metastasis in 4+ regional lymph nodes
N2a	Metastasis in 4–6
N2b	Metastasis in 7+
M0	No distant metastasis
M1	Distant metastasis
M1a	Metastasis confined to one organ/site
M1b	Metastases in more than one organ/site

J.L. Frenkel, MD (✉)
Division of Colorectal Surgery, Lankenau Medical Center and Lankenau Institute for Medical Research, Mainline Health Systems, 100 East Lancaster Avenue, Medical Office Building West, Suite 330, Wynnewood, PA 19096, USA
e-mail: frenkelj@mlhs.org

J.H. Marks, MD, FACS, FASCRS (✉)
Division of Colorectal Surgery, Lankenau Medical Center and Lankenau Institute for Medical Research, Mainline Health Systems, 100 East Lancaster Avenue, Medical Office Building West, Suite 330, Wynnewood, PA 19096, USA

Department of General Surgery and Digestive Oncology, University Nice Sophia-Antipolis, Centre Hospitalier University, Nice, France
e-mail: marksj@mlhs.org

E.J. Hagopian, J. Machi (eds.), *Abdominal Ultrasound for Surgeons*,
DOI 10.1007/978-1-4614-9599-4_19,

Indications

Rectal Cancer

For decades the mainstay of rectal cancer management has been an abdominal perineal resection (APR). With this as the treatment strategy, nuances of the cancer stage are not as important. However, with the increased focus on sphincter preservation and local excision treatment options with transanal endoscopic microsurgery (TEM) or other endoluminal approaches, rectal cancer staging has come to the forefront. Two issues are of central importance in this regard. First, how far does the lesion penetrate the rectal wall? Second, is there lymph node involvement? While hope exists in the future for a better predictor of nodal disease, at present, the best predictor of the N stage for rectal cancer is the T stage [4–7] (Table 19.2). The depth of invasion therefore is the most important predictor of lymph node metastasis and local recurrence in rectal cancer and is essential knowledge in its management.

Endorectal ultrasound is used in the initial evaluation of both rectal polyps as well as invasive rectal cancer. If a lesion is not invasive, management consists of local excision. For invasive lesions, ERUS is performed shortly after initial diagnosis of a tumor prior to initiation of neoadjuvant therapy. It is far less accurate to stage a tumor after the start of neoadjuvant therapy, as ultrasound cannot differentiate between tumor and postradiation fibrosis [8]. Additionally, the exam may be prohibitively uncomfortable as the patient's radiation therapy progresses. For smaller, polypoid tumors, it is fairly common to be asked to evaluate a patient after an attempt at polypectomy by another physician, and this situation is frequently hard to avoid. However, the accuracy of ERUS in this situation may suffer. Following electrothermal injury from snare cautery or biopsy, the accuracy of the study decreases as the resulting inflammation and scar can cause significant artifact and lead to over-staging of the lesion.

ERUS is the best available means to delineate the depth of invasion of a tumor, and this will assist in decisions regarding the use of neoadjuvant chemoradiation prior to any surgical intervention. Although numbers vary from study to study, the overall accuracy of T stage interpretation in experienced hands is approximately 70 %, and this does vary depending on the skill level of the examiner and the T stage [9, 10]. uT3 lesions are the most accurately diagnosed, whereas uT1 lesions are the least accurate. In addition to the depth of penetration of a lesion, ERUS has the ability to visualize lymph nodes in the perirectal fat. Lymph node accuracy is slightly lower at approximately 65 %. Although the accuracy of this information is slightly poorer compared to tumor depth, it does add significant information to the staging process. Unfortunately, the specifics of decision making based on these results are beyond the scope of this chapter. If the tumor is obstructing in nature, it cannot be examined in a transanal fashion and a high-quality MRI is the preferred option.

Table 19.2 Relationship between T stage and node positivity in rectal cancer

T stage	Node positivity (%)
T0	0
T1	6–12
T2	17–22
T3	>60

Incontinence

Endoanal ultrasound (EAUS) is used to evaluate the sphincter mechanism in patients suffering from fecal incontinence. The most common cause of anal sphincter complex injury is obstetrical trauma, in particular third- and fourth-degree perineal injuries. Risk factors for these injuries include forceps deliveries, nulliparity, increasing fetal birth weight, labor length, and performance of a midline episiotomy [11]. Other causes of sphincter injury include iatrogenic injury from previous anorectal surgery (hemorrhoidectomy, fistulotomy, sphincterotomy) and other trauma to the perineum.

Sphincter injuries are very common after vaginal delivery and are frequently occult even in the setting of a perineal tear. EAUS can be used to evaluate for these sphincter defects and is used as a main determinant as to whether someone is a surgical candidate for sphincteroplasty in the treatment of fecal incontinence. EAUS can be used to identify and evaluate both the internal and external anal sphincter. In addition, the puborectalis muscle at the top of the anal canal is seen, as is the superficial external sphincter at the bottom of the anal canal. Pudendal nerve terminal motor latency testing is an adjunct test in addition to ultrasound to evaluate the effectiveness of nerve conduction, as prolonged nerve conduction times can indicate nerve damage as a contributor to fecal incontinence. If the conduction study is abnormal, this may predict poorer outcomes after sphincter reconstructive surgery [12].

Perianal Abscess and Fistula

On occasion, EAUS and ERUS have been used in the diagnosis of perianal abscesses and fistulas. It is generally employed when diagnostic difficulty during an exam under anesthesia is encountered. One can use the technology to identify a fistula tract or internal opening in the anal canal for a presumed perianal fistula, and EAUS can increase the rate of both fistula tract identification and internal opening identification when compared with physical exam alone [13].

The injection of hydrogen peroxide into the fistula tract will cause it to become hyperechoic and has been shown to improve the rate of fistula identification. In the settings of anorectal Crohn's disease, it can be particularly helpful, as the tracts and abscesses can be quite complex. In addition, it is useful in evaluating rectovaginal and anovaginal fistulas. In this instance, visualized sphincter defects may cause one to consider sphincteroplasty along with an advancement flap procedure as opposed to a simple advancement flap in order to heal an anterior fistula in women.

Anatomy of the Rectum and Anus

The rectum is approximately 12–15 cm in length and descends through the pelvis from the sigmoid colon. There are three semilunar mucosal valves (Houston's valves) that are viewed endoscopically and must be avoided when entering any instrument. More importantly, the direction of the rectum follows the morphology of the sacrum. After a slight anterior direction in entering the anus, the rectum ascends posteriorly first and then anteriorly to the sacral promontory. When first inserting the rigid sigmoidoscope, the tip is pointed anteriorly at the umbilicus. After inserting it a couple of centimeters to traverse the anal canal, the scope is pointed posteriorly along the sacral hollow and then anteriorly once again. This is essential to understand when entering the rigid sigmoidoscope or ultrasound probe.

The histologic layers of the rectal wall must be understood in order to perform and interpret ERUS. The layers include the mucosa, submucosa, muscularis propria, and perirectal fat. The depth of invasion of a tumor through these layers indicates the T stage of a tumor (Table 19.1).

The anal canal begins at the level of the puborectalis muscle. There are two muscular layers in the canal. The outer muscle begins as the puborectalis, which is really a medial continuation of the levator ani muscles at the pelvic floor. This muscle acts as a sling to control bowel function by creating an angle between the rectum and anal canal. With the relaxation of this muscle, there is posterior straightening of the anorectal junction to allow for defecation. Distal to this is the external sphincter muscle, which is separated into deep, superficial, and subcutaneous layers. This muscle is under voluntary control to aid with continence. Traumatic defects in this muscle can lead to incontinence.

The inner muscular layer of the anal canal is the internal sphincter, which is a continuation of the circular muscle layer of the muscularis propria of the rectum. This is an involuntary muscle that creates a baseline tone in the anal canal for continence of liquid stool and gas. Relaxation of this muscle allows for defecation. Reduced tone in this muscle may lead to fecal soiling or leakage. Lateral to all the muscular layers of the rectum is the ischiorectal fat.

Superficial to the muscle layers of the anal canal is the mucosa and submucosa which contain the hemorrhoidal plexuses. The dentate line is grossly visible and separates two distinct histologic areas of the anus. Above it is the anal transition zone which is a purplish epithelial layer of cuboidal cells which lead to the true columnar epithelium of the rectum. Beneath it is a modified squamous epithelium leading to the true squamous epithelium of the perianal skin. Although histologically and embryologically one may view the dentate line as the end of the rectum, from the surgeon's perspective, the beginning of the anal canal should be viewed as the anorectal ring. This ring is the most proximal part of the muscular anus at the puborectalis. The importance of this lies in the ability of the surgeon to measure on digital exam the level of a palpable lesion above or below this point so he can both describe the location of a lesion without ambiguity as well as make surgical decisions regarding sphincter preservation surgery. Conversely, some may use the anal verge in describing the location of anorectal lesions. This is a poor substitute, as the length of the anal canal varies significantly, and this value will not be able to guide further management.

Technique

Instrument Setup

The BK Medical ultrasound probe (BK Medical, Herlev, Denmark) is the most widely utilized, and although there are other systems, this section will describe the assembly and use of this instrument (Fig. 19.1a, b). The ultrasound probe rotates a transducer continually to provide a 360° cross-sectional image of the rectum and anus. The setup for ERUS and EAUS is similar; however, a different probe tip is utilized. The probe contains a wire at its base which is attached to the computer and monitor console. A metal shaft is placed over the inner ultrasound shaft and secured at its base. An ultrasound crystal is then inserted at the top of the probe.

The two most common crystals are the 7 and 10 MHz frequency crystals. Newer instruments have a crystal contained within the shaft of the probe that is able to transmit differing frequencies using the console to select them. In general the higher the frequency of the probe, the higher the resolution of the image, but the lower the depth of tissue penetration and what ultimately can be seen. Typically the 7 MHz crystal is used for imaging of the rectum and the 10 MHz crystal is used for imaging of the anus. The reasoning behind this relates to the focal length. Because the focal length of the 7 MHz crystal is between 2 and 5 cm versus only 1 and 4 cm with the 10 MHz crystal, there is a better opportunity to evaluate the perirectal fat for pathologic lymphadenopathy. This being said, one can use increasing frequencies to enhance clarity of the image at the expense of focal distance. It is

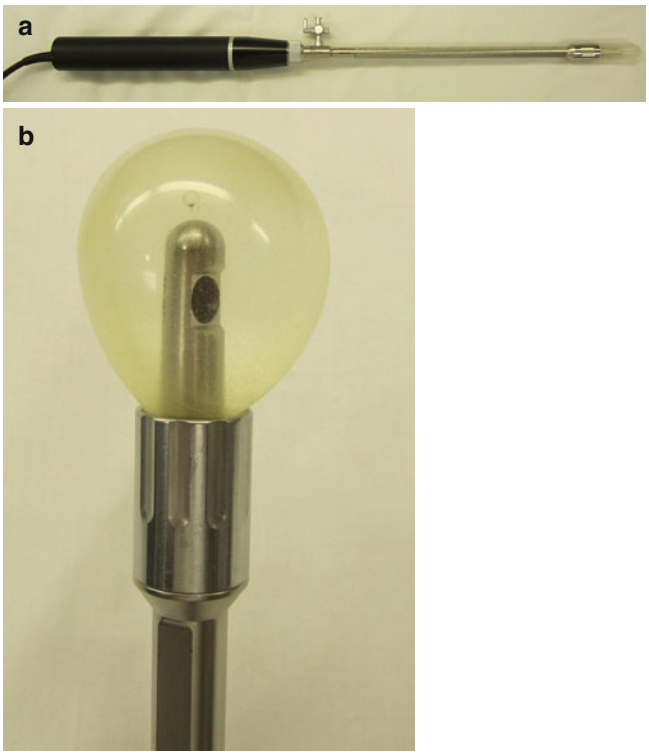

Fig. 19.1 (**a**) Depicts the standard ultrasound probe with the clear plastic cap used for endoanal ultrasound. (**b**) Shows a balloon tip inflated with water. The crystal is in the *center* of the balloon. This tip is used for endorectal ultrasound

particularly easy to change between frequencies as desired with newer machine models, which is done by selecting frequencies via the console as opposed to replacing the crystal at the tip of the instrument in older models.

Endorectal Ultrasound

For ERUS, a balloon is placed over the 7 MHz crystal and secured with a rubber ring to the probe. This is further secured with a metal ring. Insufflation of the balloon is necessary to gain contact with the rectal wall, and this is accomplished with sterile water or saline solution. The water is injected through the probe at its side port. Initially, it is necessary to inject water, rotate the probe vertically downward, and withdraw air from the balloon. Water is used as an acoustic window, similar to the "standoff" technique used in abdominal ultrasound (see Chap. 4). Air or bubbles in the fluid of the balloon cause significant artifact and must be removed as fully as possible. This process may need to be repeated several times to ensure no artifacts in the image.

After enema preparation, the patient is placed in a left lateral decubitus position. Digital rectal exam is performed and is ideally followed by rigid sigmoidoscopy to identify the location of the lesion. If the lesion being evaluated is in the very lower rectum (e.g., beneath the first rectal value), rigid sigmoidoscopy can be omitted at the operator's discretion. Although some may not employ rigid sigmoidoscopy and use a blind insertion technique, sigmoidoscopy is extremely useful as it allows one to accurately and safely place the probe proximal to the lesion. This gives one assurance that the entirety of the lesion has been evaluated. In addition, visible lymph nodes are often found just proximal to the lesion as opposed to at the level of the lesion, so one should begin the evaluation proximal to the lesion if possible.

After advancing the sigmoidoscope proximal to the lesion, the lens of the scope is removed and the ultrasound probe lubricated and gently placed through the sigmoidoscope until resistance is met. The sigmoidoscope is then withdrawn over the probe to its base as low as possible and the light source of the sigmoidoscope turned off. The balloon is insufflated with between 30 and 60 ml of water. The total amount relates to the diameter of the rectum and can be adjusted during the procedure. The goal is clear visualization of the layers of the rectum. Underdistention may create an artifact if there is no contact between the balloon and the mucosa, whereas overdistention may not allow one to see the delineation between layers.

The button on the probe is pressed to begin rotating the crystal, and the syringe on the side port is oriented toward the patient's right shoulder. This positioning will result in proper orientation of the lesions on the monitor, with anterior lesions at 12 o'clock, posterior lesions at 6 o'clock, left-sided lesions at 3 o'clock, and right-sided lesions at 9 o'clock. Orientation can be confirmed with visualization of the prostate in men and vagina in women. The prostate and seminal vesicles are very straightforward to identify, whereas the vagina can be identified both visually as well as with concurrent digital exam.

The probe is then slowly withdrawn through the tumor. One attempts to visualize any lymph nodes in the perirectal fat as well as the tumor itself. Lymph nodes can be distinguished from vessels as they disappear over a distance whereas vessels are continuous. After the tumor is fully passed, the process can be repeated. Typically we repeat this process three times to be confident in our reading. This often necessitates the removal of the probe and reinsertion of the rigid sigmoidoscope to be sure one is once again above the lesion prior to reinsertion of the probe. Prior to removal of the probe, the balloon is always fully desufflated.

With regard to fine tuning of the imaging, some adjustments should be mentioned. One can increase and decrease the size of the image on the monitor, and this can be helpful. Additionally, the gain knob can be adjusted as necessary for clarity of image. As mentioned previously, the balloon itself can be insufflated or desufflated further if one cannot see all layers of the rectum on the ultrasound image. Lastly, the

angle at which the probe is held will influence the quality of the image. Ideally, it is held perpendicular to the rectum at all levels. One must strive to have the probe centered in the ultrasound image by moving the probe handle in different directions to accomplish this.

Endoanal Ultrasound

Endoanal ultrasound is less technically challenging to perform than ERUS. The initial setup is similar; however, a 10 MHz frequency is used instead of the 7 MHz frequency. Instead of placing a balloon over the crystal, a solid plastic cap is placed over the crystal and attached to the probe (Fig. 19.1). The cap is then filled with sterile water through the same stopcock used for ERUS. Care must once again be taken to avoid air bubbling in the cap, although the cap has a pinhole in the tip so once the cap is filled, air usually has been displaced by the water.

The patient is placed in the same left lateral decubitus position and digital exam is performed. There is no need for sigmoidoscopy in EAUS. The probe is lubricated and placed in the distal rectum with the syringe in line with the right shoulder and the button on the probe pressed to begin rotating the crystal. Several passes are taken to evaluate the internal and external sphincter. There will be artifact if the tip of the probe is either in the rectum or out of the canal, as either situation results in loss of contact of the probe with a surface. In women it can be particularly helpful to place a finger in the vagina. This will confirm orientation as well as give the ability to measure the perineal body on the monitor if desired. Pressing down on the posterior wall of the vagina with a gloved finger will be seen by morphologic change in the image as well as a curvilinear hyperechoic line.

Gain and image size can be adjusted similarly to TRUS. If evaluating a fistula, peroxide can be injected into the fistula tract to identify it and highlight its course. During either EAUS or ERUS, images can be captured and printed utilizing controls on the probe.

Image Interpretation

Endorectal Ultrasound

In evaluating the rectum, there are a series of circular hyperechoic bright lines and surrounding circular hypoechoic dark areas with a most peripherally outer bright area (Fig. 19.2a, b). These will be described from the center outward. The probe is a small bright circular lucency visualized in the center of the image. This is surrounded by a circular dark area which represents the water-filled balloon. The inner bright line surrounding this dark area depicts the interface between the balloon and the rectal mucosa. The inner dark area beyond this represents the mucosa and muscularis mucosa. The middle bright line represents the submucosa. The outer dark area beyond this represents the muscularis propria. The outer bright area beyond this last dark layer represents the perirectal fat.

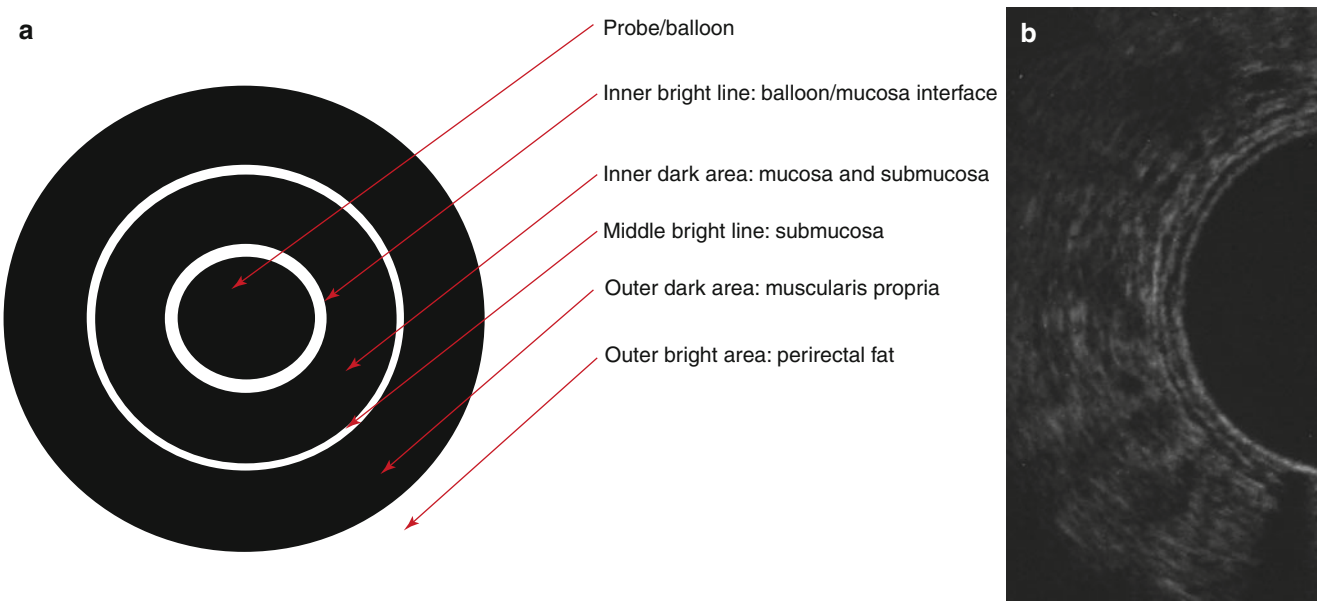

Fig. 19.2 (**a**) Diagram of the visualized layers of the rectal wall. The *dark center* represents the ultrasound balloon. The *inner bright line* is interface between balloon and mucosa. The *inner dark area* is mucosa and submucosa. The *middle bright line* is submucosa. The *outer dark area* is muscularis propria. The *outer bright area* is perirectal fat. (**b**) Portion of a normal ultrasound of the rectal wall. If you look from the center outward to the left, you can see a similar progression of bright lines and dark areas

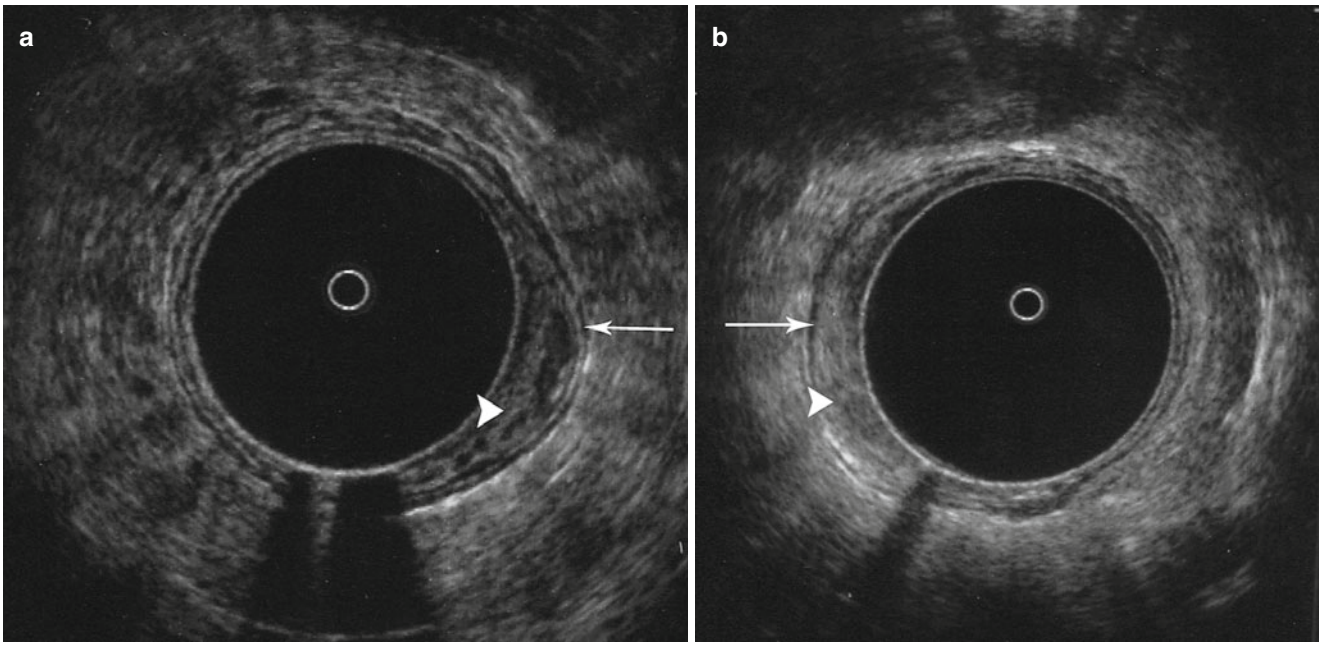

Fig. 19.3 uT0 lesions are noninvasive polyps. In both (**a**) and (**b**), *arrowheads* show a tumor in the mucosa and *arrows* point to *middle bright line* (submucosa) which remains uniform and intact. Notice some outward bowing of this line in both examples which is frequently seen

A rectal mass is typically hypoechoic in nature. When evaluating the depth of a rectal mass, one attempts to visualize which layer this hypoechoic structure reaches in the above pattern. Beyond focusing on the mass itself, one uses the uniform, irregular, or broken nature of the middle bright line and outer bright area to determine if their boundaries have been broken. For uT0 lesions (e.g., polyps), the mass can be seen within the inner dark area (Fig. 19.3a, b). For uT1 lesions (submucosal invasion), the mass is seen in the inner dark area extending to the middle bright line causing irregular stippling of the line but with no clear break (Fig. 19.4). This is perhaps the most subtle diagnosis to make. For uT2 lesions (muscularis propria invasion), the mass is seen extending to the outer dark area with a clear break in the middle bright line (Fig. 19.5a, b). The border between the outer dark area and outer bright area is still uniform in appearance. For uT3 lesions (perirectal fat invasion), one can see an extension of the mass into the outer bright area or significant scalloping of the border between the outer dark area and outer bright area (Fig. 19.6a, b). In the case of uT4 lesions, there is invasion into surrounding structures such as the prostate, vagina, cervix, uterus, bladder, or bony structure. In these instances, the hypoechoic mass is seen extending to the outer bright area and the hyperechoic signals of the outer bright area are lost between the mass and the structure.

As stated previously, the evaluation of lymph nodes can be inaccurate. To begin with, evidence that one is visualizing a node must be proven by moving the probe above and below it. Vasculature and lymphatic channels will be continuous, whereas lymph nodes will appear and disappear with movement of the probe. Also as stated previously, lymphadenopathy often occurs above a lesion so one should be sure to begin the study above it. The typical appearance of a malignant lymph node is a hypoechoic structure with regular borders (Fig. 19.7). Hyperechoic structures or those with irregular borders are more often inflammatory

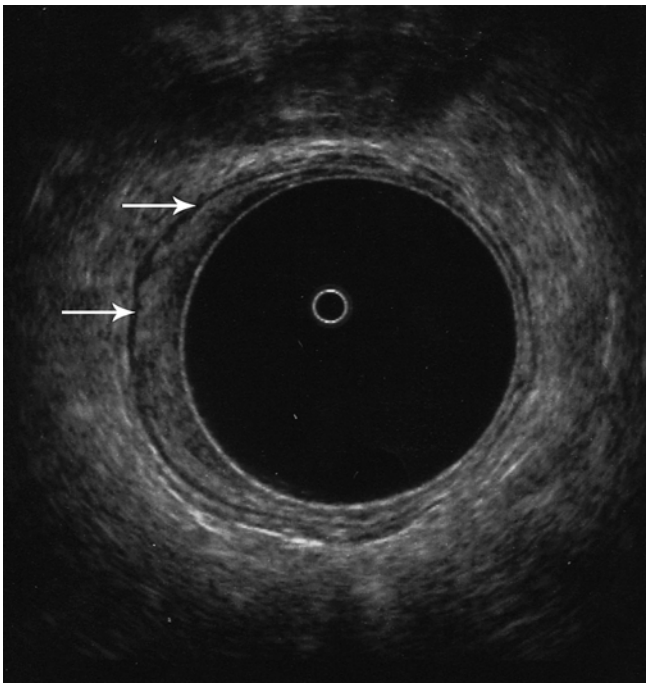

Fig. 19.4 uT1 lesions invade the submucosa. Notice the lack of uniformity or stippling of the *middle white line* (submucosa), demonstrated with *arrows*

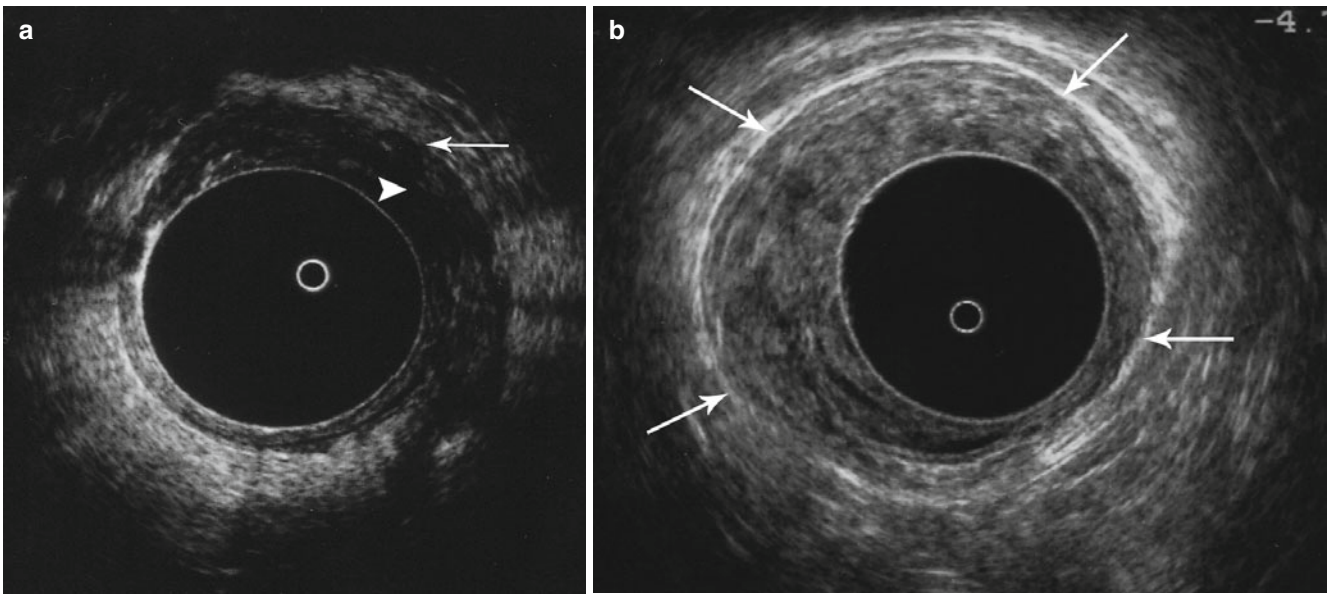

Fig. 19.5 uT2 lesions invade the muscularis propria. In (**a**) the *arrowhead* shows the tumor extending to the *outer dark area* (muscularis propria), and the *arrow* shows the interface between the *outer dark area* and *outer bright area* to be uniform without penetration or stippling by the tumor. In (**b**) the *arrows* depict the interface between the tumor and the *outer bright area* to be uniform. In this example, we see a circumferential tumor in the muscularis propria, and all hypoechoic areas beyond the interface of the balloon and mucosa (*the inner bright line*) represent a tumor

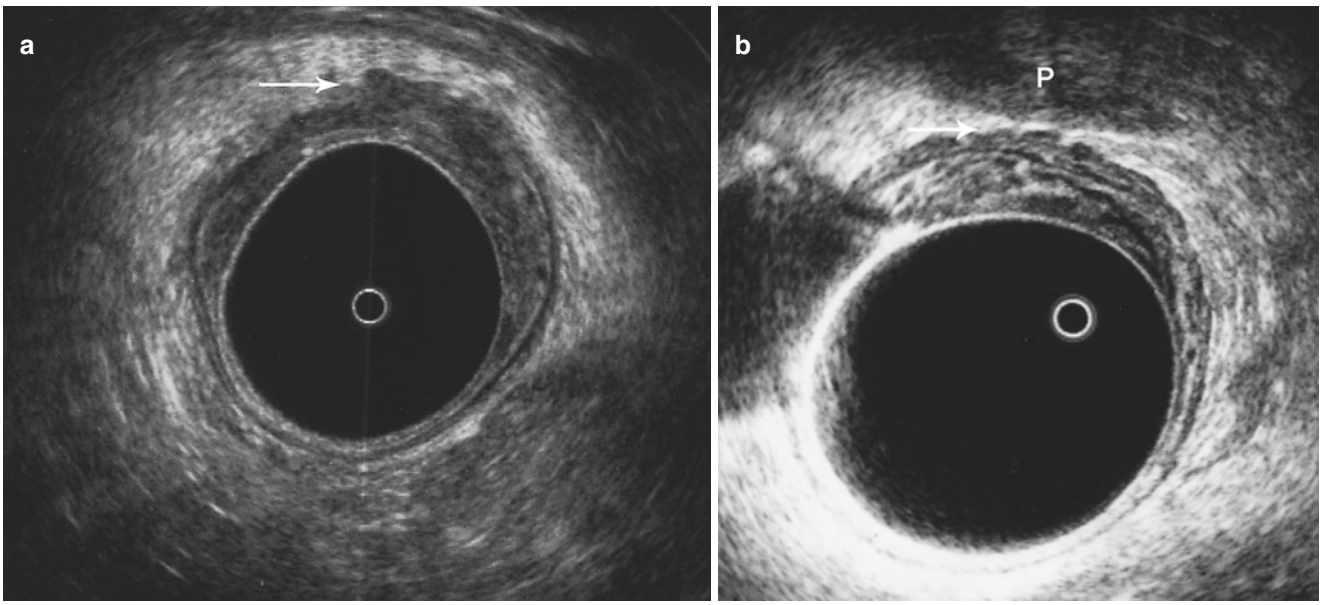

Fig. 19.6 uT3 lesions invade into the perirectal fat. In (**a**) the *arrow* shows the edge of the tumor extending into the *outer bright area* (perirectal fat). Compare the irregularity of this interface between the *outer dark area* and *outer bright area* to elsewhere in the image where it is uniform and normal. In (**b**), the *arrow* shows scalloping of the outer dark area and outer bright area interface, also indicative of a uT3 tumor with invasion into the perirectal fat. The prostate is visualized anteriorly as a dark structure (labeled *P*). In this instance one can still see a thin bright plane between the tumor and prostate. If there is no visualized bright plane between these two hypoechoic structures, it would be consistent with a uT4 lesion

in nature. Many feel that the presence of a lymph node on ultrasound imaging denotes some form of pathology, and it has been shown that the larger the size of the node (e.g., greater than 5 mm), the more often the node contains metastatic disease [14].

Endoanal Ultrasound

The appearance of the anal canal on ultrasound is very straightforward. They will be described from the center outward as was done in the ERUS section (Fig. 19.8).

The probe is at the center and appears the same in both ERUS and EAUS image types as a small bright circle. After a large dark area which depicts the water-filled probe tip used in EAUS, there is an inner bright line which represents the interface between the probe tip and the anal mucosa. Beneath this is an inner bright area which represents the mucosal, hemorrhoidal plexuses and submucosal tissues. The internal sphincter is seen as a middle dark area and the external sphincter is seen as an outer bright area surrounding it. On a normal study, the internal sphincter appears uniform throughout the anal canal. The external sphincter begins most proximally at the puborectalis as a u-shaped structure (Fig. 19.9a, b). As one moves distally, this outer bright area becomes circular in the mid-anal canal (Fig. 19.10). Distally as one moves beyond the internal sphincter in the anal canal, the middle dark area is lost and the remaining bright area beyond the inner bright line represents the superficial external sphincter (Fig. 19.11).

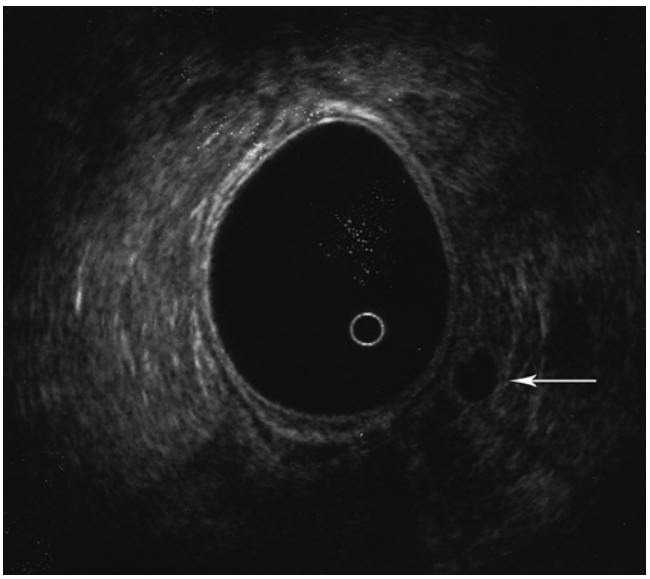

Fig. 19.7 uN1 with visualized lymph node in the perirectal fat (*arrow*). The node is visualized above the main tumor (not seen in this image), a common finding. This emphasizes the need to start imaging above the tumor, for both complete analysis of the tumor as well as lymph node evaluation

Using the above as the normal, one can evaluate for defects in the musculature from prior trauma. This is normally seen as hypoechoic defects in the outer bright area of the external sphincter and loss of uniformity with thinning or destruction of the middle dark area which represents the internal sphincter (Fig. 19.12a, b). These defects are often seen anteriorly in women as a result of obstetrical trauma. They can also be seen from iatrogenic injury due to surgical management of hemorrhoids, fistulas, and fissures anywhere in the anal canal.

Hypoechoic defects can be seen in the case of fistulas (Fig. 19.13). With the addition of hydrogen peroxide, fistula tracts can be elucidated and made hyperechoic for ease of identification. Hydrogen peroxide is commonly used as an adjunct technique in the identification of an internal opening of a perianal fistula that is difficult to find with easy passage of a fistula probe. Injection of hydrogen peroxide using an angiocath through the external opening in the perianal skin can result in bubbles at the internal opening along the mucosa of the anal canal (often at the level of the dentate line). A similar injection technique, when used in combination with EAUS, can elucidate the fistula tract for identification and ultimately safe passage of a fistula probe or draining seton.

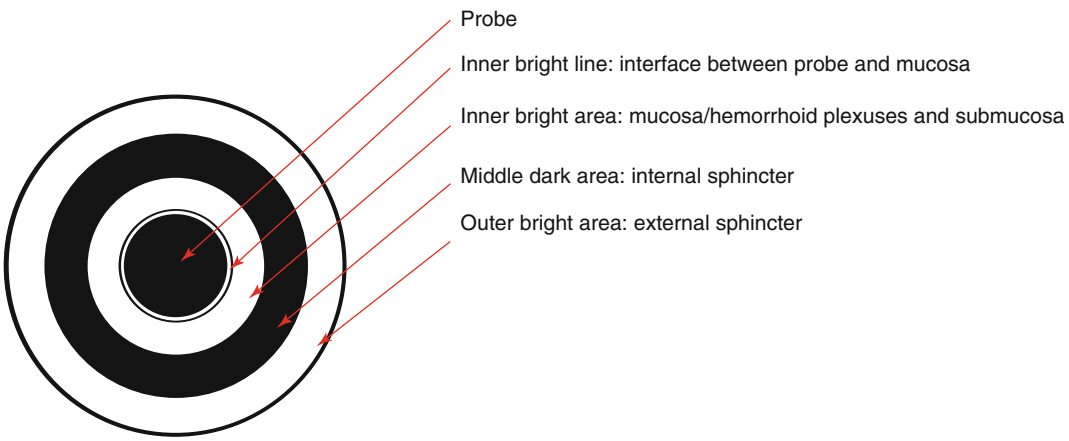

Fig. 19.8 Diagram of the normal anatomy of the middle anal canal. After the *inner dark area* which represents the water-filled cap is an *inner bright line*. This represents the interface between the probe and anal mucosa. This is followed by an *inner bright area* which depicts the mucosa, hemorrhoidal plexuses and submucosa of the anal canal. The *middle dark area* represents the internal sphincter muscle, and the *outer bright area* represents the external sphincter muscle. Compare this with Fig. 19.10 as an example

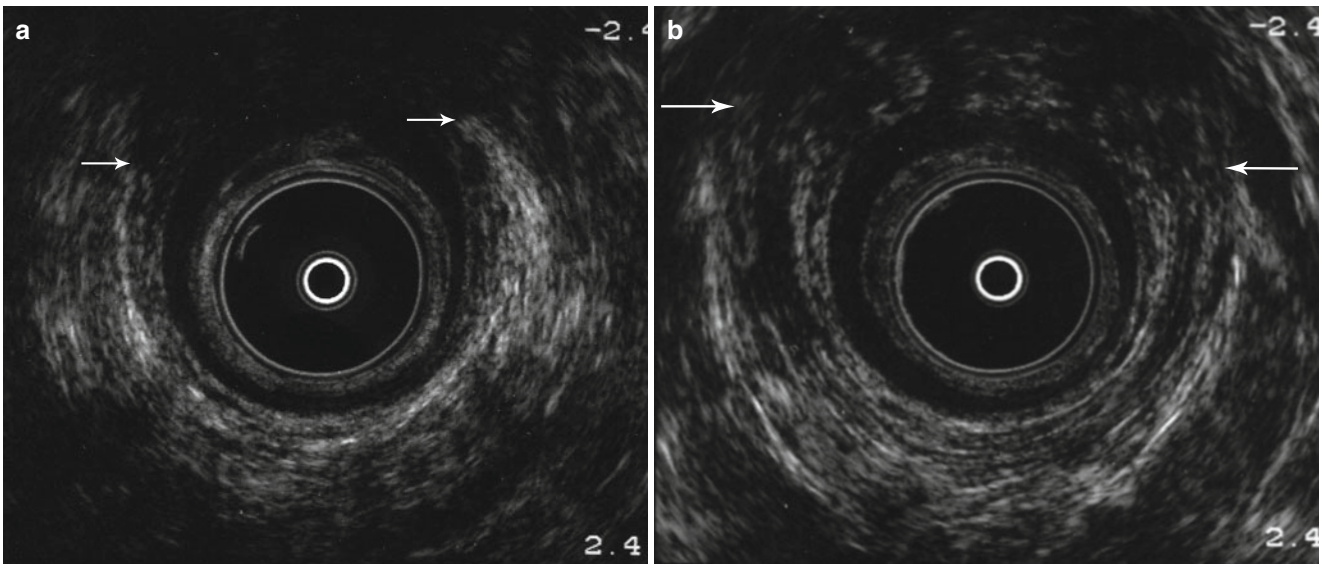

Fig. 19.9 Normal anatomy of the proximal anal canal. In (**a**) and (**b**), the *outer bright structure* depicts puborectalis. This is a U-shaped structure at this level, with *arrows* at the ends of the structure. Incorrectly interpreted, one might see this as a sphincter defect, but this is a normal anatomic finding at this most proximal level of the canal

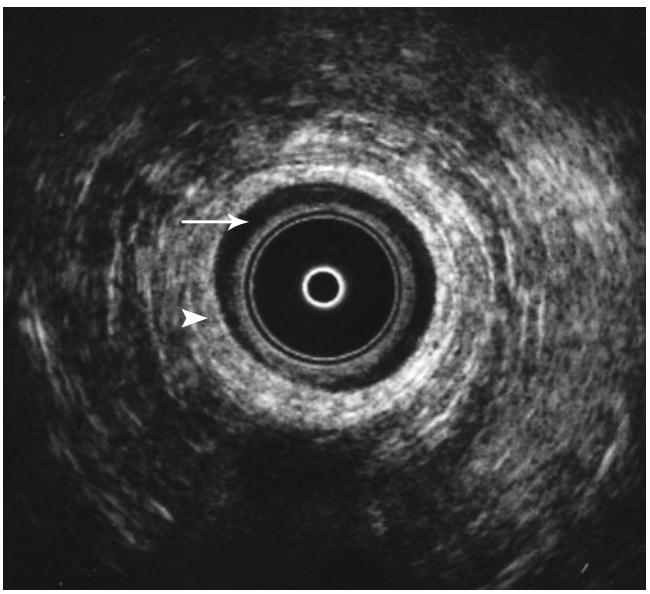

Fig. 19.10 Normal anatomy of the middle anal canal. The *middle dark area* represents internal sphincter (*arrow*) and *outer bright area* depicts external sphincter (*arrowhead*). Note the relative uniformity of both structures

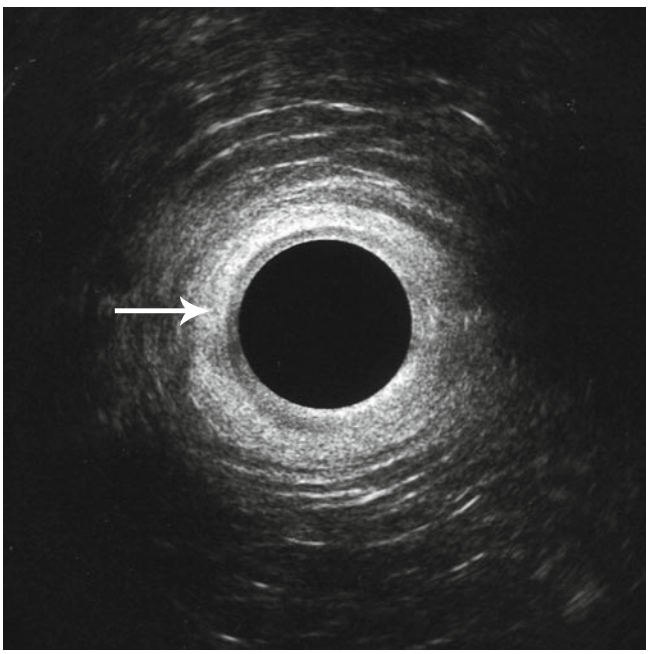

Fig. 19.11 Normal distal anal canal. The *bright uniform area* shows the superficial external sphincter only (*arrow*). The probe has passed the most superficial portion of the internal sphincter, and this *middle dark area* is no longer visualized

Three-Dimensional Endorectal Ultrasound

Three-dimensional endorectal ultrasound is based on the same principles as two-dimensional ultrasound and newer ultrasound machines carry the capability to produce these images. In addition to cross-sectional images, coronal and sagittal reconstructions can also be produced and may help in image interpretation. In these machines the ultrasound crystal is contained within the probe itself, and this allows for movement of the crystal back and forth by depressing buttons on the probe handle. This allows for easier image acquisition and is a more comfortable exam for the patient, as the probe usually only needs to be inserted once. As stated above, the frequency can be adjusted on the console depending on the circumstances in these newer models which can be

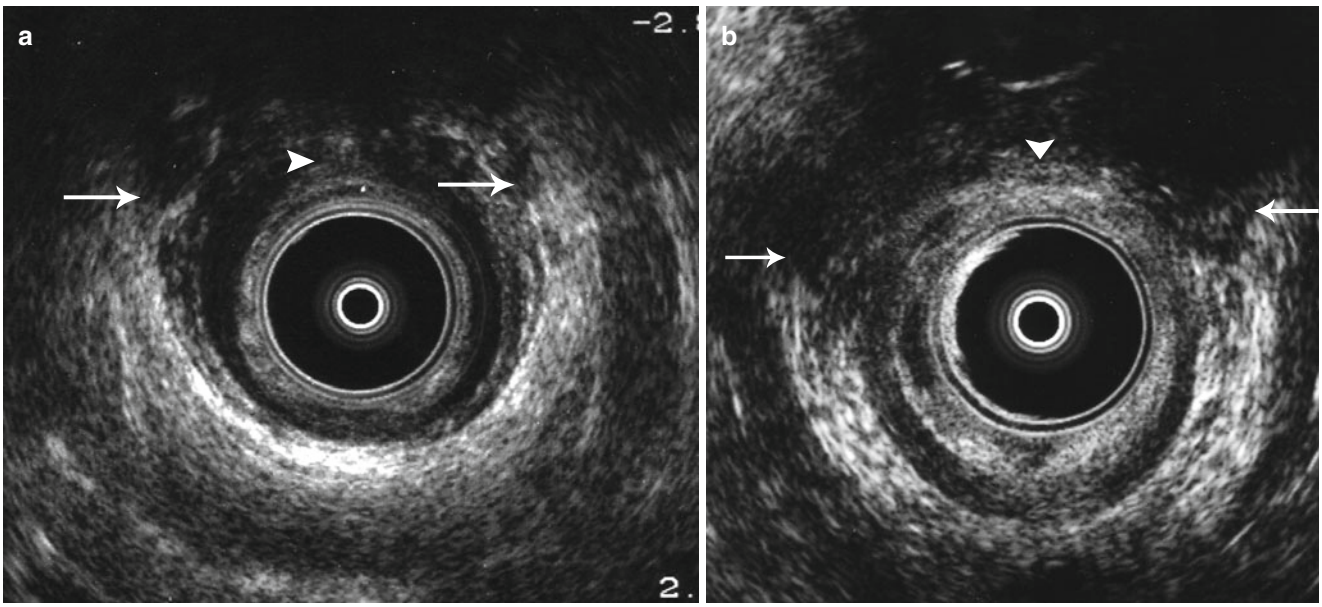

Fig. 19.12 Anterior sphincter disruption. In both (**a**) and (**b**), we see loss of the outer bright area anteriorly (*arrows* point to the edges of normal *outer bright areas*) and loss of the internal sphincter (*middle dark area*) as well (*arrowhead*). In (**a**) in particular, note the mixed echogenicity of the area between the *two arrows* at the *top* of the image. This depicts external sphincter scar from prior trauma

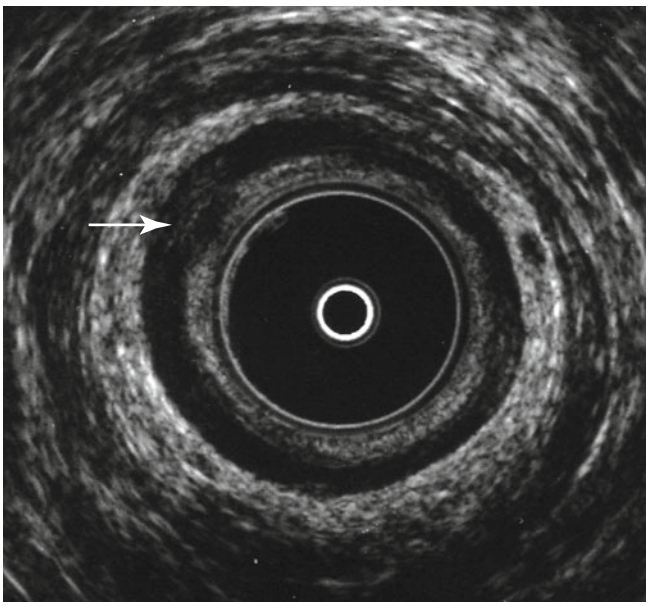

Fig. 19.13 Perianal fistula shown with *arrow*. Notice the subtle heteroechoic area surrounded by normal hypoechoic internal sphincter

helpful in certain circumstances. Although the three-dimensional images acquired are visually appealing, studies attempting to show increased accuracy in rectal cancer staging have been equivocal [15, 16].

Conclusion

Endorectal and endoanal ultrasound are useful diagnostic studies in the evaluation of rectal cancer, fistulas, and incontinence. One can visualize the anatomic layers of the rectal wall and anal canal in great detail. This is essential in the initial staging of rectal cancer and guides subsequent management, whether it is neoadjuvant chemoradiation or surgery. Endoanal ultrasound accurately identifies and delineates anal sphincter defects. This information is essential in the planning of the surgical management of fecal incontinence. ERUS can also be helpful in the identification of perianal abscesses and fistulas that are difficult to diagnose clinically. By placing the ultrasound in the hands of the surgeon, critical imaging for the optimal surgical management of the patient can be obtained.

References

1. Hildebrandt U, Feifel G. Preoperative staging of rectal cancer by intrarectal ultrasound. Dis Colon Rectum. 1985;28(1):42–6.
2. Benyon J, Roe AM, Foy DMA, Channer JL, Virjee J, Mortensen NJ. Preoperative staging of local invasion in rectal cancer using endoluminal ultrasound. J R Soc Med. 1987;80:23–4.
3. Edge SB, Byrd DR, Compton CC, Fritz AG, Greene FL, Trotti A. Colon and rectum. In: Edge SB, Byrd DR, Compton CC, Fritz AG, Greene FL, Trotti A, editors. AJCC cancer staging manual. 7th ed. New York: Springer; 2010. p. 143–64.
4. Brodsky JT, Richard GK, Cohen AM, Minsky BD. Variables correlated with the risk of lymph node metastasis in early rectal cancer. Cancer. 1992;69(2):322–6.
5. Killingback M. Local excision of carcinoma of the rectum: indications. World J Surg. 1992;16(3):437–46.
6. Blumberg D, Paty PB, Guillem JG, Picon AI, Minsky BD, Wong WD, et al. All patients with small intramural rectal cancers are at risk for lymph node metastasis. Dis Colon Rectum. 1999;42(7):881–5.

7. Sitzler PJ, Seow-Choen F, Ho YH, Leong APK. Lymph node involvement and tumor depth in rectal cancers: an analysis of 805 patients. Dis Colon Rectum. 1997;40(12):1472–6.
8. Gavioli M, Bagni A, Piccagli I, Fundaro S, Natalini G. Usefulness of endorectal ultrasound after preoperative radiotherapy in rectal cancer: comparison between sonographic and histopathologic changes. Dis Colon Rectum. 2000;43(8):1075–83.
9. Garcia-Aguilar J, Pollack J, Lee S, Hernandez de Anda E, Mellgren A, Wong WD, et al. Accuracy of endorectal ultrasonography in preoperative staging of rectal tumors. Dis Colon Rectum. 2002;45(1):10–5.
10. Kauer WKH, Prantl L, Dittler HJ, Siewert JR. The value of endosonographic rectal carcinoma staging in routine diagnostics: a 10-year analysis. Surg Endosc. 2004;18:1075–8.
11. Christianson LM, Bovbjerg VE, McDavitt EC, Hullfish KL. Risk factors for perineal injury during delivery. Am J Obstet Gynecol. 2003;189(1):255–60.
12. Pla-Martí V, Moro-Valdezate D, Alos-Company R, Solana-Bueno A, Roig-Vila JV. The effect of surgery on quality of life in patients with faecal incontinence of obstetric origin. Colorectal Dis. 2007;9:90–5.
13. Toyonaga T, Tanaka Y, Song JF, Katori R, Sogawa N, Kanayama H, et al. Comparison of accuracy of physical examination and endoanal ultrasonography for preoperative assessment in patients with acute and chronic anal fistula. Tech Coloproctol. 2008;12:217–23.
14. Katsura Y, Yamada K, Ishizawa T, Yoshinaka H, Shimazu H. Endorectal ultrasonography for the assessment of wall invasion and lymph node metastasis in rectal cancer. Dis Colon Rectum. 1992;35(4):362–8.
15. Kim JC, Kim HC, Yu CS, Han KR, Kim JR, Lee KH, et al. Efficacy of 3-dimentional endorectal ultrasonography compared with conventional ultrasonography and computed tomography in preoperative rectal cancer staging. Am J Surg. 2006;192:89–97.
16. Kim JC, Cho YK, Kim SY, Park SK, Lee MG. Comparative study of three-dimensional and conventional endorectal ultrasonography used in rectal cancer staging. Surg Endosc. 2001;16:1280–5.

Part III

Ultrasound in Surgical Practice

Getting Started

20

Christopher J. Kim and Junji Machi

Introduction

Realizing the value of surgical ultrasound is fundamental to getting started, and motivating the practitioner to persevere as a beginner toward proficiency is paramount. Commitment of time, resources, and realistic expectations are important. A consistent effort to gain ultrasound experience is essential. For physicians in training, ultrasound is commonly integrated within surgical residency and fellowship programs. Ultrasound is used for examinations in the clinics and hospitals, including emergency rooms and intensive care units, and for procedures at the bedside and during open and minimally invasive operations. For practicing physicians, incorporating ultrasound in patient care activities will be within their own scope of practice. Additional matters include access to equipment, acquisition costs, mentoring, sufficient opportunity to perform and interpret ultrasound scans, and meeting institution-dependent requirements on credentialing and privileges.

Scope of Surgical Ultrasound

Technology advances resulting in improved transducers, contrast-enhanced imaging, high-intensity focused ultrasound, three-dimensional imaging, equipment usability, portability, and minimally invasive applications all have expanded the applications of ultrasound to every surgical specialty. Simultaneous diagnostic and therapeutic ability, real-time information, noninvasiveness, and safety profile make ultrasound widely suitable. As described in detail in other chapters, for the general surgeon, ultrasound is most often used for abdominal diseases and endocrine diseases. Focused assessment with sonography for trauma (FAST) is an adjunct to the Advanced Trauma Life Support (ATLS) primary survey. The use of ultrasound in the emergency and critical care settings extends the physical examination and facilitates bedside procedures. Liver ultrasound is commonly used for surveillance of hepatocellular carcinoma and for screening and evaluation of liver metastases. Intraoperative ultrasound (IOUS) during oncologic procedures accurately assesses the extent of malignancy. IOUS is an essential component in the armamentarium for hepatopancreatobiliary surgery. Esophageal, gastric, and rectal cancer staging and endoluminal treatments utilizing ultrasound are becoming standard. Endobronchial ultrasound (EBUS) is becoming a minimally invasive diagnostic tool for evaluation of the mediastinum. Duplex ultrasound in diagnosing vascular disease and intravascular ultrasound (IVUS) use in procedures continues to expand.

Surgeon Challenges

Competence in surgical ultrasound depends on proper experience and regular performance. Further, ultrasound examinations differ significantly in required technique and interpretation. Competence in one area does not assure crossover competence to other areas. The requisite skills to perform and interpret a FAST exam are markedly different than those required for laparoscopic IOUS during hepatectomy. Proper acquisition, interpretation, limitations, and pitfalls in imaging can confound even the most experienced surgeon but who is a novice at surgical ultrasound. While the scope of surgical ultrasound is wide, so can requirements upon the surgeon. Previous training, overall experience, and

C.J. Kim, MD
Department of Surgery,
Regional Medical Center of San Jose,
200 Jose Figueres Avenue, Suite 225, San Jose, CA 95128, USA
e-mail: kimjinyong@gmail.com

J. Machi, MD, PhD, FACS (✉)
Department of Surgery, John A. Burns School of Medicine,
University of Hawaii and Kuakini Medical Center, Honolulu, HI, USA

Noguchi Medical Research Institute, JADECOM-NKP GME Center Tokyo Bay, Urayasu-Ichikawa Medical Center, (Noguchi Hideyo Memorial International Hospital), Urayasu, Chiba, Japan
e-mail: junji@hawaii.edu

E.J. Hagopian, J. Machi (eds.), *Abdominal Ultrasound for Surgeons*,
DOI 10.1007/978-1-4614-9599-4_20, © Springer Science+Business Media New York 2014

areas of clinical application should guide the practitioner in focusing his efforts. "Hands-on" or even observational experience is most important to gaining ultrasound proficiency. However, text and online resources, ultrasound courses, ultrasonography technicians, radiologists, and fellow colleagues are invaluable as well and should supplement proper ultrasound training.

Ultrasound Education

In the United States, exposure to ultrasound often begins in medical school. Ultrasound is included in the basic curriculum to complement student understanding of anatomy and physiology. Clerkship rotations expose students to ultrasound as a point-of-care or bedside clinical tool. The availability of handheld ultrasound devices increases its use and application as an extension of the physical examination and is now provided to medical students in many programs. Emphasis on the clinical applications of ultrasound in both diagnostic and therapeutic roles increases during the postgraduate educational years. The majority of surgical residency and fellowship programs incorporate formal ultrasound training. Areas of ultrasound application may vary between universities versus community-based training programs. However, recent graduates of surgical training programs are expected to be facile in surgical ultrasound fundamentals.

Surgical fellows in breast, trauma/surgical critical care, oncology, hepatopancreatobiliary, transplant, cardio thoracic, and minimally invasive surgery are expected to demonstrate experience and proficiency in ultrasound techniques. This is a considerable change from the 1990s, when programs incorporating formal ultrasound training were in the minority and expectations for ultrasound competence were low.

American College of Surgeons Role in Ultrasound Education

In 1995, the American College of Surgeons (ACS) Committee on Emerging Surgical Technology and Education (CESTE) established the ACS National Ultrasound Faculty (NUF), developing a structured ultrasound educational program for surgeons and residents [1–3]. The basic ultrasound course emphasizes ultrasound physics, instrumentation, scanning technique, and pitfalls. Successful completion of the basic module is required before taking advanced modules. In coordination with surgical specialty societies, the NUF has developed advanced modules addressing specific ultrasound applications. After completion of advanced training modules, the surgeon becomes "proctor ready." An ultrasound instructor course and instructor candidate monitoring is part of a faculty development program.

Advanced ultrasound modules/courses which the ACS has previously provided and is currently providing include:

- Breast Ultrasound
- Abdominal Ultrasound (including Intraoperative, Laparoscopic, and Endoscopic Ultrasound)
- Vascular Ultrasound
- Thyroid and Parathyroid Ultrasound (Head and Neck Ultrasound)
- Advanced Hepatopancreatobiliary (HPB) Ultrasound
- Ultrasound for Instructors
- Ultrasound for Residents
- FAST Ultrasound
- Ultrasound in the ICU: ECHO and Thoracic

To promote surgical ultrasound education and encourage standardization among course offerings, the ACS developed a process for exporting courses offered at the Annual ACS Clinical Congress. By exporting ultrasound courses, residents and practicing surgeons can learn new skills at their location appropriate to their practice. Several surgical specialty societies conduct ACS ultrasound courses.

Exporting an ultrasound course entails the following steps:

1. Identify a course chair (NUF faculty member).
2. Identify faculty and activity planners (ACS member).
3. Application approval by NUF and the ACS Division of Education.
4. Maintain a faculty/student ratio of 1:6 or less.
5. Complete post-course report.

The ACS currently offers four ultrasound courses for export:

- Ultrasound for Residents
- FAST Ultrasound
- Thyroid and Parathyroid Ultrasound
- Ultrasound in the ICU: ECHO and Thoracic

At the recent ACS Annual Clinical Congress in 2012, the College's first offering of *Advanced Hepatopancreatobiliary Ultrasound* course was well received. Similarly, the *HPB Ultrasound and Advanced Technology course* was offered at the Americas Hepato-Pancreato-Biliary Association (AHPBA) Annual Meetings in 2012, 2013, and 2014 and is planned to continue.

Each ultrasound skill course has as a prerequisite, successful completion of *The Ultrasound for Surgeons: A Basic Course, 2nd Edition CD*, or an equivalent basic ultrasound course.

Verification and Documentation for Surgeons Using Ultrasound

The ACS does not verify experience or competence in surgeon-performed ultrasound. The ACS verification model addresses ultrasound education, not expertise. Essential to the model is documentation of ultrasound activities.

The ACS has approved a five-level model for verification and documentation of knowledge and skills, following participation in the educational programs of the ACS:

- Level I: Verification of attendance
- Level II: Verification of satisfactory completion of course objectives
- Level III: Verification of knowledge and skills
- Level IV: Verification of preceptor experience
- Level V: Verification of satisfactory patient outcomes

The Postgraduate Didactic and Skill-Oriented courses offered at the Clinical Congress of the ACS have been assigned verification levels I–III based on the requirements of each level.

The importance of ultrasound documentation is pertinent for local credentialing, maintaining continuing medical education (CME), continuing quality improvement (CQI), and meeting specialty society guidelines.

To ensure practitioners are qualified and the facilities and equipment used are appropriate and meet and maintain quality standards, a voluntary verification process is made available to ACS fellows. The ACS verification program entails four components:

1. The surgeon must meet the requirements for education and/or experience.
2. The facilities and equipment should meet recommended standards.
3. The surgeon should maintain qualifications through continued experience and formal continuing medical education in the technique and its applications.
4. Surgeons' outcomes using ultrasound should be assessed through a program of continuous quality improvement.

Example of Specialty Society Certification Guidelines

Recognizing the effectiveness of ultrasound in multiple clinical aspects relating to management of breast diseases and the need for surgeons trained in ultrasound, the American Society of Breast Surgeons (ASBS) offers certification in breast ultrasound and stereotactic procedures.

The ASBS requirements for ultrasound certification include meeting criteria in areas of clinical experience, training, and quality assurance. The framework of the program is based on principles for the proper performance and interpretation of diagnostic and interventional breast ultrasound, appropriate clinical application, and use of interventions to guide further management.

There are two components to the breast ultrasound certification process: clinical and written examinations.

Eligibility criteria for surgeons seeking breast ultrasound certification include:

- Board certification by the American Board of Surgery (ABS) or American Osteopathic Board of Surgery (AOBS) or evidence of international equivalent
- Documented appropriate level of training and a minimum of 1-year experience in the performance and interpretation of breast ultrasound
- Documented performance of no fewer than 100 breast ultrasound exams per year with review of a minimum of 100 mammography exams annually that include authenticated reports
- Documented completion of 15 AMA Category 1 CME credits in breast ultrasound toward the AMA Physician's Recognition Award

While membership in the ASBS is not required for certification, the candidate must agree to comply with ASBS standards, policies, and procedures. Breast ultrasound certification is valid for 3 years.

A major goal of the ASBS breast ultrasound certification program is to improve the quality of care for patients with breast disease by encouraging education and training to advance expertise and clinical competency for surgeons who use ultrasound and ultrasound-guided procedures in their practice.

Other surgical specialty societies have similar certification guidelines reflecting the importance of meeting quality standards for ultrasound training and performance.

Steps to Getting Started

- Find an ultrasound machine.
- Familiarize yourself with the equipment.
- Gain experience by scanning and focus on proper technique: *scan, scan, and scan*!!!
- Start with simple and focused scanning and then add complex scanning gradually.
- Identify a mentor.
- Document everything.
- Plan credentialing strategies based on your ultrasound application.
- Learn coding and billing last.

Ultrasound machines are readily accessible. Various types of machines with different functions at different prices are available. Just for focused ultrasound of the thyroid or breast, mainly for needle guidance for aspiration or biopsy, no sophisticated machines are necessary; a simple grayscale B-mode ultrasound (without color Doppler function) with high-frequency transducers suffices. In the typical community hospital, each department may have several machines. Accessing an ultrasound machine for the operating room (OR) may not be as easy. In this scenario, burden sharing is a cost-effective strategy for ultrasound equipment purchasing. Multiple services can share through "team buying" to distribute equipment cost and improve utilization efficiency. Discuss with the chief of staff and OR purchasing manager what is most feasible.

Gain experience by scanning. Like any technical activity, practice is required for skill. Experiences matter. Scan whatever is available – yourself, friends, phantoms, and

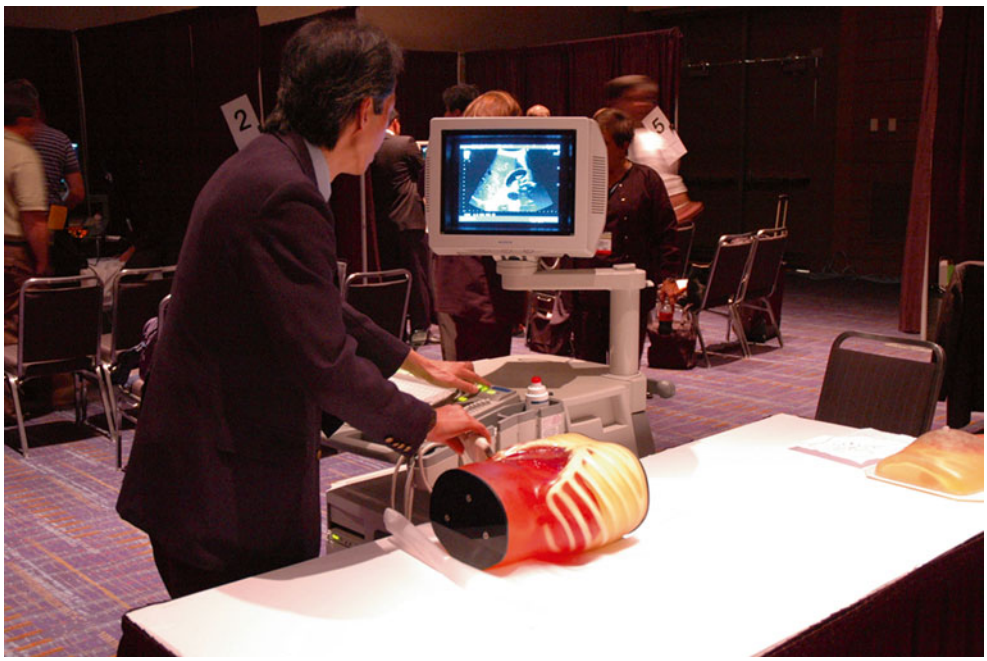

Fig. 20.1 Scanning of a transabdominal ultrasound phantom (Courtesy of Kyoto Kagaku Co., Ltd., Kyoko Japan)

patients. Focus on proper ultrasound practice. Performing an ultrasound examination and interpreting images are not always intuitive. Further, establishing bad habits from the beginning is hard to break. Scan with proper technique and optimal patient positioning, use appropriate equipment calibrated to the right settings, and become familiar with imaging interpretation and pitfalls. There are excellent ultrasound phantoms commercially available (Figs. 20.1, 20.2, 20.3, 20.4, 20.5, 20.6, 20.7, 20.8, 20.9, and 20.10).

SCAN, SCAN, SCAN!!! Ultrasound – guide, guide, guide!!! Experiences matter. How many experiences does a surgeon need for gaining ultrasound proficiency and expertise? There is no simple answer to this question. The required numbers of ultrasound scanning and interpretation experiences vary depending on the complexity of the task in each ultrasound application. Requisite experience for learning FAST is different from the learning curve for IOUS or laparoscopic ultrasound. In general, roughly 30–50 cases in which someone performs ultrasound by himself/herself may be needed to obtain confidence and competence in a specific examination. These cases should include sufficient numbers of abnormal findings. In addition to diagnostic ultrasound, ultrasound-guided procedures such as needle biopsy require probably about 15–30 cases of independent performance. Because ultrasound guidance is for invasive procedures, it is encouraged to practice such ultrasound procedures using ultrasound phantoms including target lesions before performing on patients.

Seek out opportunities to perform ultrasound. For example, if seeing a consult in the ER for possible cholecystitis, perform your own right upper quadrant ultrasound. This experience will require finding appropriate acoustic windows, identifying surrounding organs aside from the gallbladder, including the liver, kidney, and pancreas. Proper interpretation of the scans will require distinguishing between a normal and an inflamed gallbladder and gallstones versus artifact or appreciating findings suggesting alternative diagnoses. "Close the loop" by comparing your own ultrasound scans and interpretation to the formal radiology examination. If a radiologist or an expert surgeon-sonographer is available and amenable, ask for feedback.

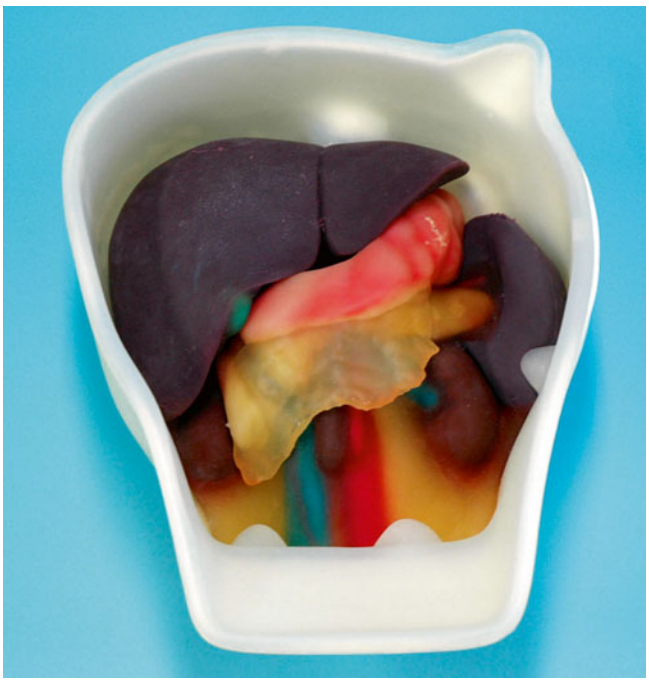

Fig. 20.2 Intraoperative/laparoscopic ultrasound phantom (Courtesy of Kyoto Kagaku Co., Ltd., Kyoko Japan)

Learn in a graduated approach – start first with simple ultrasound tasks. Mastery of basic skills is required before complex tasks can be accomplished. Learning ultrasound

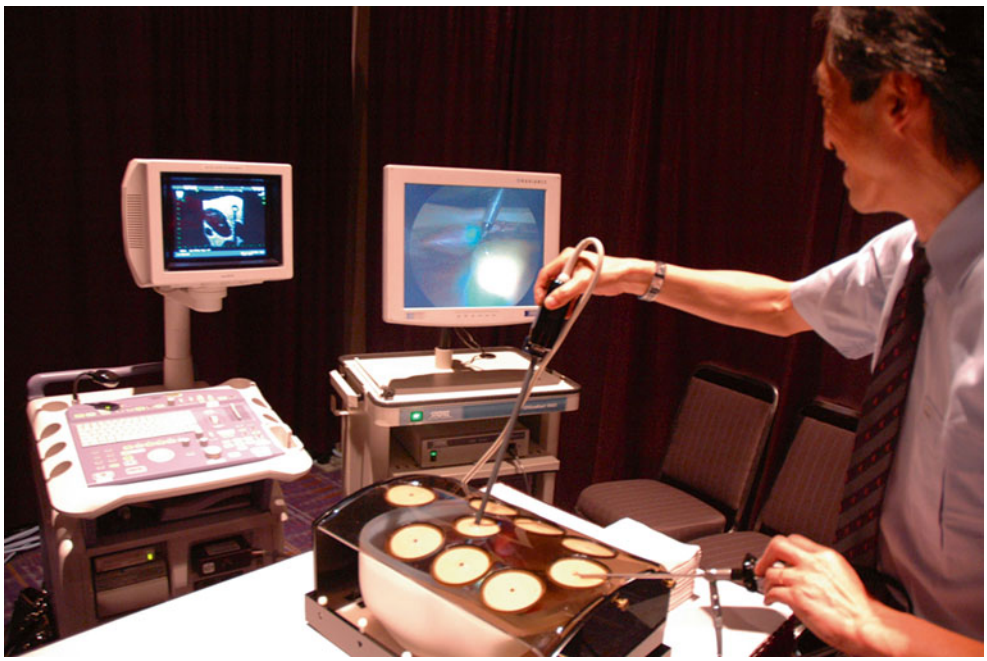

Fig. 20.3 Laparoscopic ultrasound training using intraoperative/laparoscopic ultrasound phantom, which is placed in a laparoscopic trainer box (Courtesy of Kyoto Kagaku Co., Ltd., Kyoko Japan)

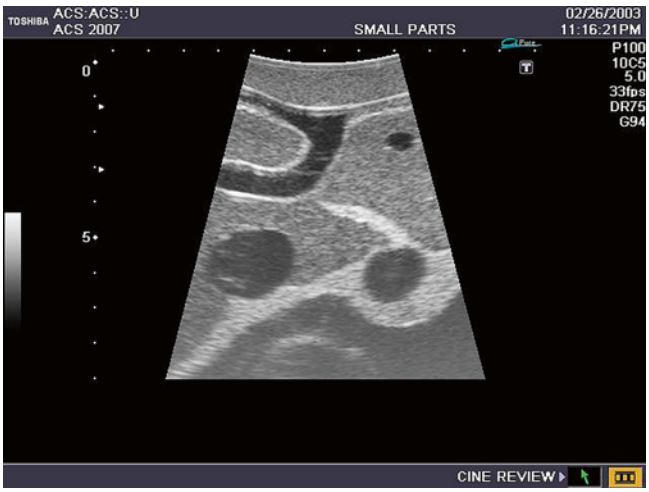

Fig. 20.4 Intraoperative ultrasound phantom scanning image: liver (Courtesy of Kyoto Kagaku Co., Ltd., Kyoko Japan)

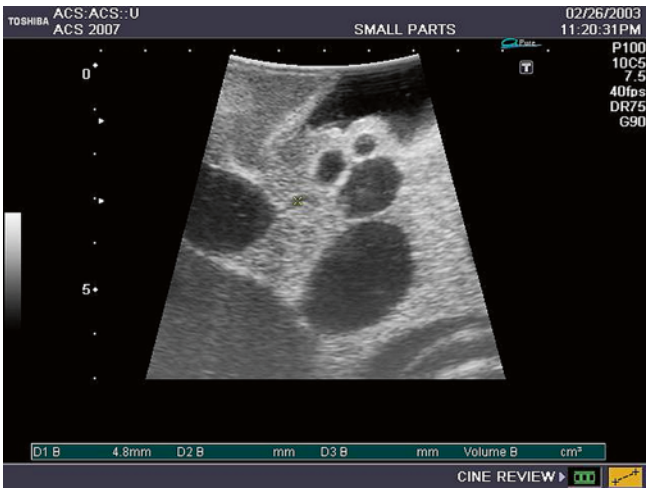

Fig. 20.5 Intraoperative ultrasound phantom scanning image: biliary system and associated surrounding structures. A cursor indicates the cystic duct (Courtesy of Kyoto Kagaku Co., Ltd., Kyoko Japan)

can be divided into five phases, paralleling the ACS Ultrasound Education Program:

1. Learning basic ultrasound concepts (cognitive)
   - Basic ultrasound physics (pulse-echo principle, propagation speeds, impedance, attenuation, reflection, resolution, etc.)
   - Basic ultrasound instrumentation (machine components)
   - Basic ultrasound scanning techniques (probe orientation, probe handling [rocking, rotating, sliding], ultrasound planes)
   - Basic ultrasound interpretation principles (machine assumptions, hypoechoic, hyperechoic, isoechoic, artifacts [shadowing, enhancement, reverberation, mirror image, etc.])
2. Learning advanced ultrasound applications (cognitive)
   - Advanced concepts for specific ultrasound applications
3. Learning real-time ultrasound scanning (practical, hands-on experience)
   - Supervised experience to guide learning of specific scanning techniques, interpretive skills, and interventions
4. Mentored/monitored practice of specific ultrasound applications
5. Independent, credentialed practice of specific ultrasound applications

The concepts and applications characterizing the first three phases are commonly covered during residency or fellowship training. Alternatively, this can also be achieved through

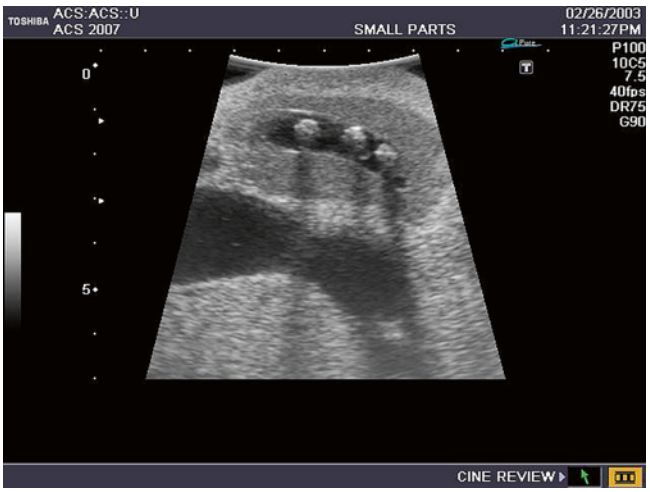

Fig. 20.6 Intraoperative ultrasound phantom scanning image: bile duct stones with shadowing (Courtesy of Kyoto Kagaku Co., Ltd., Kyoko Japan)

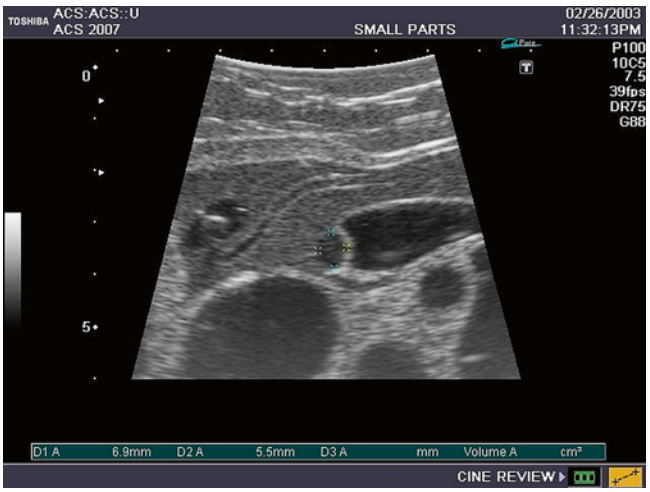

Fig. 20.7 Intraoperative ultrasound phantom scanning image: pancreas and pancreatic head tumor (cursors) (Courtesy of Kyoto Kagaku Co., Ltd., Kyoko Japan)

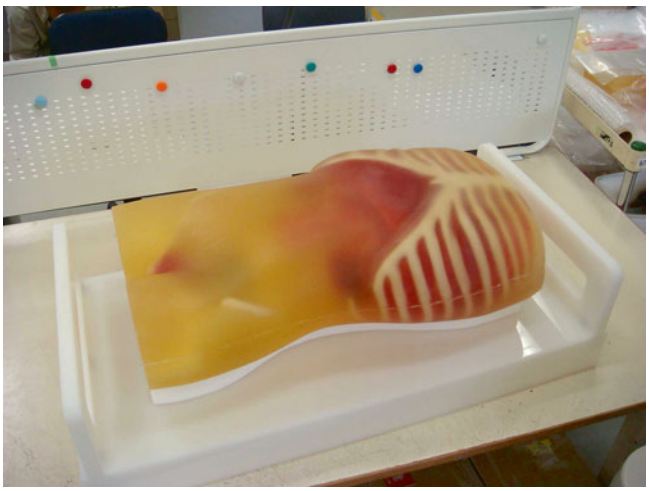

Fig. 20.8 FAST/ER phantom: abdominal/thoracic ultrasound phantom including abdominal pathology such as intra-abdominal bleeding, acute cholecystitis, and others (Courtesy of Kyoto Kagaku Co., Ltd., Kyoko Japan)

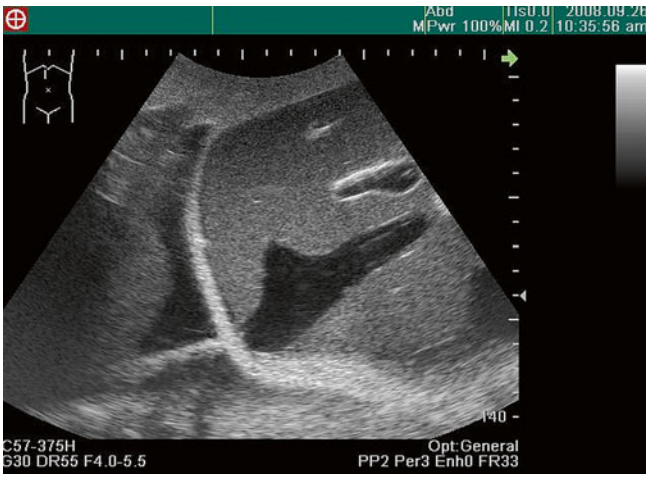

Fig. 20.9 FAST/ER phantom scanning image: cardiac tamponade (Courtesy of Kyoto Kagaku Co., Ltd., Kyoko Japan)

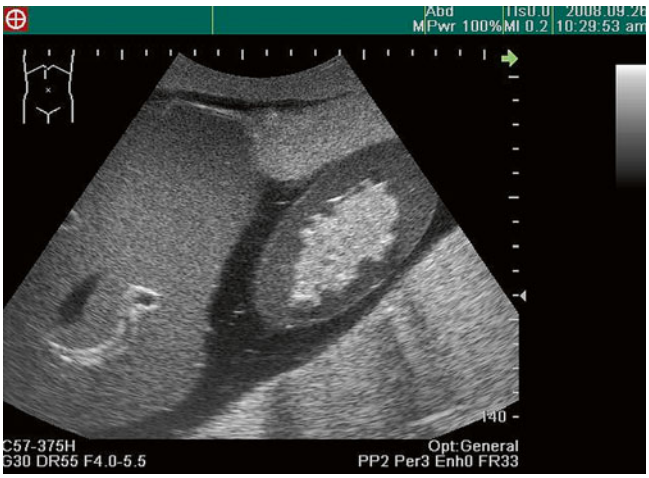

Fig. 20.10 FAST/ER phantom scanning image: intra-abdominal bleeding (Courtesy of Kyoto Kagaku Co., Ltd., Kyoko Japan)

successful completion of ultrasound courses. The ACS Ultrasound Education Program verifies completion of the first three phases. For a surgeon to become "proctor ready" for the fourth phase, a mentor or local proctor is required. Finally, independent ultrasound practice represents the last phase.

Having a mentor is invaluable to gain valuable insight beyond your own education and experience. A beneficial mentorship will facilitate progressing effectively and efficiently toward reaching ultrasound competence. Residents, colleagues, sonographers, and radiologists can all serve as mentors. Some residents and sonography technicians are very capable in performing ultrasound examinations. Radiologists may be expected to be highly proficient at image interpretation and/or ultrasound-guided procedures. Colleagues and senior surgeons may provide all of the aforementioned guidance, in

DOCUMENTATION OF ULTRASOUND EXPERIENCE DURING RESIDENCY

Name: _____ Date of Completion of Residency: _____

Ultrasound Courses Attended:
Date: _____ Location: _____

Type of Course: _____ Sponsoring Organization: _____

Ultrasound Rotation at Kuakini Medical Center (one month) Date: _____

Ultrasound Didactic Lectures Attended:
- Dr. Machi's lectures on ultrasound principles _____Hours
- Instrumentation / Scanning Techniques _____Hours
- Clinical Applications _____Hours
- Other Lectures _____Hours
- Subjects _____

Ultrasound Hands-On Training Attended:
- Dr. Machi's Skills Training _____Hours
- Other Training _____Hours

Tests Answered and Returned:
- Ultrasound Basics Yes _____ No_____
- Abdominal Ultrasound Yes_____ No _____

Practical Ultrasound experience during residency:

	# Examinations Observed	#Examinations Performed
Diagnostic Ultrasound		
Head & Neck	_____	_____
Breat	_____	_____
Trauma/Acute Setting	_____	_____
Abdominal	_____	_____
Intraoperative/Laparoscopic	_____	_____
Vascular	_____	_____
Endorectal/Endoscopic	_____	_____
Ultrasound-Guided Procedures		
Thyroid Interventional	_____	_____
Breast Interventional	_____	_____
Abdominal Interventional	_____	_____

Reviewed by and discussed with Dr. Junji Machi Date: _____

Fig. 20.11 Sample of ultrasound documentation form for surgical residents at the University of Hawaii, Department of Surgery

addition to strategies to implement ultrasound successfully in the context of career and practice.

Documentation

Documentation of ultrasound experience is important at all levels of training. The medical student may be expected to document ultrasound examinations and imaging interpretations to fulfill academic course requirements. Surgical residents and fellows need appropriate ultrasound documentation to fulfill rotation and program requirements. Additionally, proper documentation during training may fulfill future prerequisites and/or requirements for verification, certification, advanced course enrollment, and surgical specialty society credentialing. Furthermore, providing proper ultrasound documentation is mandatory in many processes for gaining privileges, appropriate medical communication, assessing outcomes, as well as seeking reimbursements (Fig. 20.11).

Credentialing

There is no standard credentialing process for surgical ultrasound. Credentialing implies adequate judgment and training to perform ultrasonography safely and accurately interpret the findings. However, the requirements in skill and interpretation for performing ultrasound can differ

significantly based on the application. Again, adequate experience and training in one area of ultrasound does not necessarily confer adequate experience and training in another. Then it is not surprising, but rather appropriate, that there are no general standards for ultrasound credentialing. Reflecting the importance of specificity in ultrasound credentialing, the majority of surgical specialty societies now provide either guidelines, specific requirements, or their own ultrasound certification program. Contacting the relevant surgical specialty society may be the first step in ascertaining preferred or existing credentialing requirements.

Privileges

After obtaining credentials in ultrasound, privileging qualified surgeons is typically determined by the surgeon's individual hospital, chief of surgery, appropriate institutional committee, board, or governing body, in conjunction with the Joint Commission on Accreditation of Healthcare Organizations (JCAHO or JC) guidelines for granting hospital privileges.

The processes of granting, maintaining, and renewing privileges should not differ significantly from processes applying to other surgical procedures. A period of provisional privileges may be given, during which time the number of cases, patient selection, indications for ultrasound application, quality, and outcomes will be reviewed. Monitoring ultrasound performance may be done through quality assurance mechanisms or the relevant institutional committee. Renewal of privileges should entail continuing clinical activity, satisfactory performance, and continuing medical education (CME).

Conclusions

Ultrasonography is a potentially powerful and versatile tool for the surgeon. In the past, ultrasound was utilized mostly within a diagnostic capacity. Enabling the clinician to "see" in a new dimension and extending the physical examination, ultrasound was referred to as "the modern equivalent of the stethoscope." As equipment and imaging improved, bulky ultrasound machines confined to examination rooms and radiology suites have now moved toward handheld devices, which can facilitate ultrasound use almost anywhere. Increasing use of ultrasound by surgeons has progressively expanded its utilization to therapeutic applications in a multitude of procedures and specialties. The limitations on surgical ultrasound no longer appears to be technology or local practice patterns, but previous reluctance of the surgical community as a whole to realize its value. A large part of this phenomenon is most likely related to obstacles in gaining the required experience to make ultrasound a tool which feels easy to use. Early exposure and formal ultrasound experience during medical school, residency and fellowship training, educational leadership and course offerings by the ACS and NUF, utilization of local resources to gain ultrasound experience, and coordination with surgical specialty societies to export ultrasound courses and set quality standards for ultrasound training and performance will be instrumental to widespread adoption of this valuable tool. Finally, the most important is surgeons' recognition and commitment in the use of ultrasound for improvement of patient outcome.

Resources

Accreditation Council for Continuing Medical Education
515 North State Street
Suite 7340
Chicago, IL 60610
Phone: (312) 464–2500
Website: www.accme.org

American College of Radiology
1891 Preston White Drive
Reston, VA 22091
Phone: (703) 648–8900
Website: www.acr.org
Email: info@acr.org

American College of Surgeons
National Ultrasound Faculty
633 North Saint Clair Street
Chicago, IL 60611–3211
Phone: (312) 202–5000
Website: www.facs.org/education/ultrasound/index.html

American Institute of Ultrasound in Medicine
14750 Sweitzer Lane
Suite 100
Laurel, MD 20707–5907
Phone: (301) 498–4100 or (800) 638–5352
Website: www.aium.org

American Registry for Diagnostic Medical Sonography
51 Monroe Street
Plaza East 1
Rockville, MD 20850–2400
Phone: (301) 738–8401 or (800) 541–9754
Website: www.ardms.org

The American Society of Breast Surgeons
5950 Symphony Woods Road
Suite 212
Columbia, MD 21044
Phone: (410) 992–5470 or (877) 992–5470
Website: www.breastsurgeons.org

Radiological Society of North America
820 Jorie Boulevard
Oak Brook, IL 60523
Phone: (630) 571–2670
Website: www.rsna.org

Society of American Gastrointestinal and Endoscopic Surgeons
11300 West Olympic Boulevard
Suite 600
Los Angeles, CA 90064
Phone: (310) 437–0544
Website: www.sages.org

Society of Ultrasound in Medical Education
Website: www.susme.org
Email: info@susme.org

Society of Radiologists in Ultrasound
44211 Slatestone Court
Leesburg, VA 20176–5109
Phone: (703) 858–9210 or (800) 438–2777
Website: www.sru.org

Society for Vascular Ultrasound
4601 Presidents Drive
Suite 260
Lanham, MD 20706
Phone: (301) 459–7550
Website: www.svunet.org

References

1. Staren ED, Knudson MM, Rozycki GS, et al. An evaluation of the American College of Surgeons ultrasound education program. Am J Surg. 2006;191(4):489–96.
2. Freitas ML, Frangos SG, Frankel HL. The status of ultrasonography training and use in general surgery residency programs. J Am Coll Surg. 2006;202(3):453–8.
3. Statement on Ultrasound Examinations by Surgeons. Committee on Emerging Surgical Technology and Education, American College of Surgeons. Bull Am Coll Surg 1998;83:47–40.

Abdominal Ultrasound: Credentialing and Certification

21

R. Stephen Smith, William R. Fry, and Richard A. Hoppman

Introduction

The use of clinical ultrasound as a diagnostic tool by surgeons has rapidly increased over the past two decades. The use of ultrasound has found its way into essentially all of the surgical subspecialties. Ultrasound provides a real-time diagnostic modality that enhances the surgeon's ability to make therapeutic decisions. Utilization of ultrasound during operative procedures is an extension and expansion of other diagnostic modalities, such as computed tomography. A number of studies have documented that surgeons can perform ultrasound with a high degree of sensitivity, specificity, and accuracy. Other papers have documented that the interpretation of specific ultrasound images by surgeons is equivalent to the high-quality interpretation provided by radiologists and other imaging specialists.

The Credentialing Process

A basic principal of the privileging and credentialing process is that a surgeon must have adequate judgment and excellent training to perform ultrasound with safety and accuracy. However, guidelines for credentialing must be flexible and reasonable. While general guidelines may be applicable to all surgeons, subspecialty differences in practice, ultrasound utilization, and clinical applications must be considered. All surgical ultrasound examinations are not the same in scope, complexity, or difficulty.

R.S. Smith, MD, RDMS, FACS (✉)
W.R. Fry, MD, RVT, RDMS, FACS
Department of Surgery, University of South Carolina School of Medicine, 2 Medical Park Rd. #306, Columbia, SC 29203, USA
e-mail: flysurg@yahoo.com; chaoticdoc@aol.com

R.A. Hoppman, MD
Department of Internal Medicine,
University of South Carolina School of Medicine,
6311 Garners Ferry Road, 29209 Columbia, SC, USA
e-mail: richard.hoppmann@uscmed.sc.edu

Criteria for establishing the standards required for a surgeon to be granted ultrasound privileges should take into account the surgeon's overall experience and extensive skills obtained through residency and fellowship training and the application of these skills during ongoing patient care activities. Standards should be uniform when considering a surgeon's application for privileges in ultrasound. Privileges should be considered and granted for each category of ultrasound after a careful process of consideration and a thorough review of the surgeon's training and experience. While ultrasound principles and instrumentation are similar regardless of the clinical activity, the ability of a surgeon to perform one ultrasound examination in an acceptable fashion does not automatically guarantee competency to perform another type of ultrasound study. For example, skill and certification in performance of the focused assessment with sonography for trauma (FAST) examination do not imply that a surgeon possesses adequate skills in laparoscopic, intraoperative, vascular, or breast ultrasound. Each area of surgical ultrasound has different requirements for training and mandates different skill sets. One size does not fit all.

The process for credentialing a surgeon to perform ultrasound examinations is the responsibility of each individual hospital. It is the responsibility of the Department of Surgery, as directed by the chair, to recommend an individual surgeon for privileges in ultrasound. This process should not be substantively different from the process leading to a recommendation for privileges for other surgical procedures. Credentialing decisions must be based on the objective assessment of the individual's capabilities and not due to the specialty of the applicant. Equal skills mandate equal privileges.

Requirements for Training

The field of surgical ultrasound has undergone dramatic changes over the past two decades. Twenty years ago, most surgeons were not formally trained in ultrasound

E.J. Hagopian, J. Machi (eds.), *Abdominal Ultrasound for Surgeons*,
DOI 10.1007/978-1-4614-9599-4_21,

applications. Since that time, however, formal ultrasound training has been incorporated into many general surgery residency and subspecialty fellowship training programs. The contemporary graduate of a surgical training program has, in all likelihood, received a structured experience in surgical ultrasound. Most residency and fellowship directors can now provide documentation of the resident's training and expertise in multiple areas of surgical ultrasound. The residency program director should be prepared to verify the graduate's skill in surgical ultrasound to any credentialing body. The surgical resident should include in his or her case logs, the number and types of ultrasound examinations performed during training. The ability to provide this information to the credentials committee of an institution will streamline the surgeon's ability to gain privileges in surgical ultrasound at individual hospital. To ensure the availability of a structured program in ultrasound education for general surgery residencies, the American College of Surgeons National Ultrasound Faculty offers an introductory course in surgical ultrasound specifically tailored for residents. This Resident Course is very similar in design and content to the Basic Ultrasound Module offered by the American College of Surgeons to practicing surgeons. Successful completion of the resident ultrasound course allows residents to enter into a number of advanced training modules offered by the American College of Surgeons and other surgical specialty organizations. Through participation in these advanced training programs, the surgeon can gain new skills and become "proctor ready" in advanced ultrasound examinations.

For practicing surgeons without formal residency or fellowship training in ultrasound, there must be documentation of adequate prior experience in surgical ultrasound or evidence of participation in a structured training program that is accepted by the hospital's credentialing process. The requirements for this training curriculum, as well as a defined level of experience (number of ultrasound examinations), should be clearly delineated by the institution. Such a training curriculum should include a formal course of instruction, as outlined by the American College of Surgeons or other bona fide specialty societies, as well as opportunities for the practicing surgeon to observe, assist, and serve as the primary surgical sonographer in the specific area of surgical ultrasound in which privileges are requested. An acceptable ultrasound course should include didactic sessions and a hands-on experience with models or stimulators. The surgeon must demonstrate an acceptable fund of knowledge as well as technical and procedural expertise.

Practical Experience

The applicant for credentials in surgical ultrasound should be able to document an appropriate volume of ultrasound studies during which the surgeon obtained the images and provided an initial interpretation. The minimum number of procedures required for the granting of privileges is determined by the complexity of the examination. For example, several series have shown that considerable expertise with the FAST examination can be gained after 15–25 studies. For more complex clinical situations such as hepatobiliary or intraoperative ultrasound studies, the volume of examinations to reach an acceptable level of skill may be greater. The chief of surgery at the specific hospital should set the volume standard for each individual surgical ultrasound examination. Additionally, requirements for proctoring must be standardized and established in advance.

The criteria to determine competency in each surgical ultrasound examination should be fair, uniform, and straightforward. Areas of assessment should include familiarity with ultrasound physics, ultrasound instrumentation and equipment, appropriate patient selection, efficient performance of the ultrasound examination, and of course, accurate interpretation of the images obtained. The acceptable standards for each examination should be set by the chair of surgery with input from the appropriate division or section chief. The assessment of the applicant's skills and qualifications must be unbiased, objective, and transparent in all cases. The credentialing process should never be viewed as a mechanism to protect "turf" for other practitioners or other departments. This practice is morally, ethically, and legally indefensible and can interfere with optimal patient care. Institutions that deny, withdraw, or restrict a surgeon's privileges in surgical sonography must have an appropriate appeal mechanism in place. This process must be in accordance with medical staff bylaws and follow the guidelines of the Joint Commission.

Maintenance and Renewal of Privileges

Once a surgeon has been credentialed in ultrasound, the chair of the Department of Surgery or the hospital's credentialing body should assure that competency is maintained. There should be a mechanism in place to monitor and record the number of ultrasound procedures performed and the accuracy of these diagnostic images. This process should be incorporated into the hospital's performance improvement program. Areas of monitoring could include the frequency of the utilization of ultrasound, image quality and standard

orientation, and appropriate patient selection. Participation in continuing medical education programs and surgical ultrasound should be expected and required.

Further Reading

Granting of Endoscopic Ultrasonography Privileges for Surgeons. Society of American Gastrointestinal Endoscopic Surgeons (SAGES). Surg Endosc. 2000;14:691–2.

Society of American Gastrointestinal Endoscopic Surgeons (SAGES). Guidelines for Granting of Ultrasound Privileges for Surgeons. 2014. http://www.sagescms.org.

Shepherd AE, Gogalniceanu P, Kashef E, et al. Surgeon-performed ultrasound: a call for consensus and standardization. J Surg Educ. 2012;69:132–3.

Staren ED, Knudson MM, Rozycki GS, et al. An evaluation of the American College of Surgeons ultrasound education program. Am J Surg. 2006;191:489–96.

Statement on Ultrasound Examinations by Surgeons. Committee on Emerging Surgical Technology and Education, American College of Surgeon. Bull Am Coll Surg. 1998;83:37–40.

Coding and Billing for Ultrasound Examinations

22

Junji Machi

Introduction

Surgical procedures should be appropriately performed for appropriate indications and documented and then coded/billed. Surgeon-performed ultrasound examinations are the same. Once the surgeon becomes proficient in performing independent ultrasound examinations and the credentialing for performing ultrasound is achieved locally, he or she can consider billing for ultrasound examinations. Table 22.1 is the summary of important points for coding and billing for ultrasound examinations.

Documentation of Ultrasound Findings

Adequate documentation is an essential component to patient care, but it is also required for billing. There should be a permanent record of the ultrasound examination and its interpretation. Comparison with previous relevant imaging studies is helpful and always performed when available. Images of all appropriate areas, both normal and abnormal, should be recorded in appropriate storage format. Variations from normal size or dimension should be accompanied by measurements. Images should be labeled with the examination date, patient identification, and image orientation. A report of the ultrasound findings should be included in the patient's medical record, regardless of where and when the study is performed.

Coding and Billing

For coding, first of all, documentation is essential. In addition to ultrasound findings, appropriate indications for examinations should be documented. For the process of billing, the correct coding with appropriate modifiers must be used. The coding may change, and, therefore, the surgeon should update the coding using the current "CPT" and "ICD." Like all procedures in today's environment, surgeons or their billers must follow up on reimbursement for ultrasound. If appropriate reimbursement is not received, the surgeon should discuss the issue with the insurer and, when necessary, with local or national professional societies.

For all ultrasound examinations, there are professional and technical components. Surgeons performing office ultrasound (e.g., transabdominal ultrasound) by themselves using their own equipment can code for both the professional and the technical components. In such a case, no modifier is required. For surgeons performing ultrasound in a facility or hospital (e.g., ultrasound in the emergency room, intensive care unit, or operating room), the situation is more complex. If a surgeon performs ultrasound examinations (with or without a technician) using the hospital's machine, he or she should use modifier -26 to charge only for the professional component. In a facility or hospital, a surgeon performing ultrasound by himself or herself (without the help of a hospital technician) using his or her own machine can charge only for the professional component for Medicare patients. In this

Table 22.1 Coding and billing for ultrasound examinations

1. Proficiency and credentialing
2. Adequate ultrasound examination for appropriate indications
3. Adequate documentation; indications and ultrasound findings with record of images
4. Use of correct coding and modifier: understanding of professional and technical components
5. Updating of coding using current "CPT" and "ICD"
6. Follow-up of reimbursement

J. Machi MD, PhD, FACS
Department of Surgery, John A. Burns School of Medicine, University of Hawaii and Kuakini Medical Center, Honolulu, HI, USA

Noguchi Medical Research Institute, JADECOM-NKP GME Center Tokyo Bay, Urayasu-Ichikawa Medical Center, (Noguchi Hideyo Memorial International Hospital), Urayasu, Chiba, Japan
e-mail: junji@hawaii.edu

E.J. Hagopian, J. Machi (eds.), *Abdominal Ultrasound for Surgeons*,
DOI 10.1007/978-1-4614-9599-4_22,

Table 22.2 Coding for ultrasound examinations frequently performed by surgeons and Medicare reimbursement[a]

		Medicare reimbursement of 2013[b] (average of all states)	
Code	Procedure (ultrasound examination)	Total service	Professional component
76700	US of the abdomen, including the liver, biliary, pancreas, and spleen, *complete*[c]	$235.60	
76705	US of the abdomen, *limited* (e.g., *single organ, quadrant, follow-up)*[c]	$172.77	
76770	US of the retroperitoneum (e.g., renal, aorta, nodes) *complete*[d]	$214.66	
76775	US of the retroperitoneum, *limited*[d]	$162.30	
76856	US of the pelvis (nonobstetric)[e]	$172.77	
76942	US guidance for needle placement (biopsy, aspiration, injection, localization device, etc.)[f]	$235.60	
76970	US study follow-up (for repeat US for follow-up of specific organs)	$125.65	
76975	Gastrointestinal endoscopic US (modifier -26)		$188.48 (modifier -26)
76998	US guidance, intraoperative[g]	$324.61	
76700/76705	Intraoperative abdominal US and laparoscopic US[h]	$235.60	
76940	US guidance for tissue ablation (modifier -26)[i]		$198.95 (modifier -26)

Notes
US ultrasound, *FAST* focused abdominal sonography for trauma
[a]As of March 2014, some procedures listed here have become bundled. Surgeons and billers need to update bundle information
[b]Coding and reimbursement shown here are based on information (Medicare Reimbursement of 2013) as of May 2013
[c]76700 and 76705 are frequently used by surgeons performing abdominal US, including FAST. Use 76705 for US of the abdominal wall (e.g., hernia evaluation)
[d]76770 and 76775 are not commonly used by surgeons. Instead, 76700 and 76705 are used, because the retroperitoneum US is usually performed as part of abdominal US
[e]76856 is not frequently used. A possible utility for surgeons is the pelvic US during evaluation of appendicitis or lower abdominal pain. In such circumstances, 76700 or 76705 may be a better code
[f]US guidance (76942) is just for the US portion of the procedure and is added to the procedure itself
Examples: 49082 and 76942: US-guided paracentesis
47000 and 76942: US-guided percutaneous liver biopsy
47001 and 76942: US-guided open liver biopsy
[g]Intraoperative US guidance (76998) is used when US is performed to guide procedures (e.g., hepatic resection) during surgery. However, for open liver biopsy, it is better to use 76942
[h]Currently, there is no code specific for "intraoperative abdominal US" and "laparoscopic US." For this reason, 76700 or 76705 is used for intraoperative abdominal US and laparoscopic US, as well as transabdominal US. This code is for diagnostic US, and you can add these codes. Example: Laparoscopic US during laparoscopic cholecystectomy is coded as 47562 and 76700 or 76705
[i]When US is used for guidance of tissue ablation, such as radiofrequency thermal ablation and cryoablation, 76940 is used. Do not report 76998 in addition to 76940. For liver ablation procedures (radiofrequency and cryotherapy) themselves, see codes 47370–47382

case, the surgeon must add modifier -26 (they must include this; otherwise, the claim will be rejected) because Medicare pays only for the professional component on the HCFA 1500. For other insurers (such as Blue Cross/Blue Shield), both components may be paid; however, the surgeon should first discuss this issue with a medical director of the insurance company. Otherwise, the modifier -26 should be used for the professional charge only.

Table 22.2 is a list of coding for ultrasound examinations commonly performed in a surgical practice of the abdomen, including office-based ultrasound and hospital-based ultrasound.

Surgeons who evaluate a patient, determine that an ultrasound examination is indicated, and perform the ultrasound by themselves can charge for both the evaluation and management (E/M) service and the ultrasound examination. E/M services are separately payable if the documentation indicates that the visit led to the decision to perform a procedure (the ultrasound examination). Generally, when a procedure is performed (e.g., incision and drainage) after an E/M service, it is reported by adding the modifier -25 to the appropriate level of E/M service. However, it is not necessary to add -25 for an ultrasound examination. For example, if the surgeon is asked (consulted) to evaluate a patient with right upper quadrant abdominal pain and performs ultrasound after E/M service, the codes are as follows:

992XX	Office consultation
76700	Ultrasound of the abdomen

The surgeon should make sure that the information in the documentation is substantive enough to demonstrate medical necessity for the ultrasound examination.

For multiple surgical procedures, generally, the modifier -51 is added. For distinct procedural service, the modifier -59 is added. However, it is not necessary to add -51 or -59 for additional ultrasound coding. For example, when billing for the professional component of intraoperative ultrasound (guidance for hepatic lobectomy), ultrasound guidance for liver biopsy, followed by right hepatic lobectomy, the codes are:

47130	Hepatic lobectomy
47001-51	Open liver biopsy
76700-26	Intraoperative ultrasound or
76998-26	Intraoperative ultrasound guidance
76942-26	Ultrasound guidance for biopsy

Note that newer coding/billing, many procedures have become "bundled", and insurers may not pay for multiple procedures. Surgeons and their billers, therefore, need to update this "bundle" information.

Medicare has been paying physicians for diagnostic and therapeutic ultrasound services regardless of specialty. To receive reimbursement for ultrasound services, it may be necessary to submit documentation of credentialing for performing ultrasound in accordance with the local insurer's policies.

The above guideline regarding coding and billing is applicable to Medicare. Other insurers may use a slightly different coding system, and, therefore, one may have to confirm each insurer's policy regarding ultrasound practice.

Conclusion

Surgeons first need to learn and master ultrasound examinations and then perform ultrasound appropriately with sufficient technical competency for appropriate indications. Once examinations are done in such way, surgeons do not need to hesitate to do billing for reasonable payment. However, precise documentation and accurate coding are critical. For coding and billing of all ultrasound examinations, there are professional and technical components. The coding changes periodically, and, therefore, the surgeon should update the coding with modifiers using the current "CPT" and "ICD." It is imperative for surgeons and their billers to understand and use appropriate and timely coding and billing to obtain suitable payment.

Useful References

Coders' Desk Reference for Procedures 2013, Optum (Ingenix). www.optumcoding.com

Future Perspective in Abdominal Ultrasound

23

Junji Machi, Fuminori Moriyasu, Shigeki Arii, Masahiko Yano, and Emi Saegusa-Beecroft

History of the Use of Ultrasound by Surgeons

The history of surgeon-performed ultrasound went back to a half century ago; surgeons in the United States were behind in the use of ultrasound. In European and Asian countries, surgeons started ultrasound examination by themselves as preoperative and intraoperative tools in the 1970s. One of the examples is an ultrasound probe specifically for intraoperative use which was created by Dr. Masatoshi Makuuchi to evaluate and localize nonpalpable liver tumors in the operative field in the mid-1970s.

In the United States, one of the earliest surgeon-performed ultrasound examinations was in the operating room. Dr. Bernard Sigel, a general surgeon and a pioneer of intraoperative ultrasound (IOUS), introduced this modality during surgery in 1979 for intraoperative diagnosis of biliary calculi. In the early 1980s, IOUS was employed during neurosurgery, endocrine surgery, and cardiovascular surgery. Since 1980, the Sigel's group (which Junji Machi joined) expanded the application of IOUS to various fields including hepatobiliary, pancreatic, and other abdominal surgery. Although benefits of IOUS were clearly reported, gaining acceptance of IOUS among surgeons was slow in the 1980s, particularly in the United States.

However, in the mid-1990s, many surgeons recognized the value of IOUS during surgical procedures, and with the availability of various types of IOUS and laparoscopic ultrasound (LUS) probes, the use of ultrasound has become more widespread during a variety of operations, especially for abdominal surgery. In certain operations such as hepatectomy, IOUS is presently considered as an essential modality, making liver surgery without IOUS suboptimal.

In addition, in the 1990s, surgeons started ultrasound examinations in the emergency room for patients with trauma and in the office for breast and thyroid evaluation with ultrasound-guided needle biopsy or aspiration and for abdominal examination pre- and postoperatively. Vascular surgeons were at that time already using ultrasound in their noninvasive vascular laboratory.

Because of expansion and future expectation of increased use of ultrasound by surgical practices, the American Board of Surgery made an announcement in the mid-1990s that during surgical training, residents should learn ultrasound examination. Soon after that, the American College of Surgeons set up a team of surgeon-sonographers as National Ultrasound Faculty and provided postgraduate skill courses in various fields such as trauma, breast, vascular, thyroid/parathyroid, and ICU cardiothoracic in addition to abdominal

J. Machi, MD, PhD, FACS (✉)
Department of Surgery, John A. Burns School of Medicine, University of Hawaii and Kuakini Medical Center, Honolulu, HI, USA

Noguchi Medical Research Institute, JADECOM-NKP GME Center Tokyo Bay, Urayasu-Ichikawa Medical Center, (Noguchi Hideyo Memorial International Hospital), Urayasu, Chiba, Japan
e-mail: junji@hawaii.edu

F. Moriyasu, MD, PhD
Department of Gastroenterology and Hepatology, Tokyo Medical University, 6-7-1 Nishishinjuku, Shinjuku-ku, Tokyo, 160-0023, Japan
e-mail: moriyasu@rb4.so-net.ne.jp

S. Arii, MD, PhD
Department of Hepato-Biliary-Pancreatic Surgery, Tokyo Medical and Dental University, 1-5-45, Yushima, Bunkyo-ku, Tokyo, 113-8510, Japan
e-mail: sh-arii@hamamatsuh.rofuku.go.jp

M. Yano
Ultrasound Systems Division, Ultrasound Systems Development Department, Tokyo Medical Systems Corporation, 1385 Shimoishigami, Otawara-Shi, Tochigi, 324-8550, Japan
e-mail: masahiko.yano@toshiba.co.jp

E. Saegusa-Beecroft, MD, PhD
Department of Surgery, JABSOM, University of Hawaii and Kuakini Medical Center, 405 N. Kuakini Street, Suite 601, Honolulu, HI 96817, USA
e-mail: esaegusa@hawaii.edu

Electronic supplementary material The online version of this chapter (doi:10.1007/978-1-4614-9599-4_23) contains supplementary material, which is available to authorized users. Videos can also be accessed at http://www.springerimages.com/videos/978-1-4614-9598-7

E.J. Hagopian, J. Machi (eds.), *Abdominal Ultrasound for Surgeons*,
DOI 10.1007/978-1-4614-9599-4_23, © Springer Science+Business Media New York 2014

ultrasound including IOUS, LUS, and transabdominal ultrasound (TAUS). Currently, there are ultrasound courses for residents and instructors as well. Other societies in the United States including Society of American Gastrointestinal and Endoscopic Surgeons and Americas Hepato-Pancreato-Biliary Association are holding abdominal ultrasound courses with hands-on sessions. Taking such courses is helpful for surgeons, especially for the ultrasound neophyte, who are interested in getting started in surgical ultrasound.

Perspective of Surgeon-Performed Ultrasound

Surgeons are currently using ultrasound in a variety of surgical settings such as the office, the ward bedside, the emergency room, the intensive care unit (by means of TAUS), and the endoscopic suite (by means of endoscopic or endorectal ultrasound (EUS)) as well as in the operating room (by means of IOUS and LUS). The state of the art of surgeon-performed abdominal ultrasound is described in this book. How about the future of abdominal ultrasound?

In the 1980s, the standard ultrasound was performed by 2-dimensional (2D) real-time B-mode ultrasound. One renovation of ultrasound occurred in the early 1990s, when color Doppler and then power Doppler imaging was introduced. Color/power Doppler imaging displays blood flow in real-time color on B-mode gray-scale images and has been used during operation as well as in the radiology department. By offering blood flow information in addition to anatomical information, this modality enhances the efficacy of IOUS and LUS during general and cardiovascular surgery. Intraoperative color/power Doppler imaging can detect and localize smaller vessels, can promptly distinguish them from ductal structures and tissue spaces, and can confirm blood flow to organs after surgical operations such as transplantation or major organ resection. These capabilities improve reading of images of surgeon-performed ultrasound.

More uses of ultrasound in future during various procedures (intra-procedural ultrasound including IOUS and LUS) will be brought about by a combination of ultrasound and other technological advances and surgeons' interest and experience. Some predictable occurrences include expansion of ultrasound applications, improvement in instrumentation, and incorporation of new ultrasound technologies.

IOUS/LUS will be used by surgeons steadily and increasingly, along with more formal training in ultrasound for residents and surgeons. Having IOUS/LUS instruments always available in the operating room and having competent surgeons available performing IOUS/LUS will permit IOUS/LUS to become not just an occasional but an everyday tool for acquiring intraoperative information; it will allow surgeons to "see" organs and lesions in a new dimension. This is particularly true in the use of LUS because of ongoing broader applications of laparoscopic or minimally invasive operations.

New innovative ultrasound technologies will lead to further improvement in image resolution and deeper sound penetration of IOUS/LUS. More user-friendly probes and scanners for surgeons are being developed. New ultrasound technological developments, such as harmonic imaging with contrast agents (intravenous ultrasound contrast is not available yet for abdominal organs in the United States as of November 2013), will improve the diagnostic accuracy of IOUS/LUS. The refinement of 3-dimensional (3D) images will simplify IOUS and LUS for planning and guiding tumor ablation or organ resections, such as hepatectomy. Anatomical and pathological information provided by 3D IOUS/LUS will enable quicker and more assured IOUS/LUS-guided surgical procedures. Thereby, 3D images may increase the diagnostic confidence of the surgeons, which is often an obstacle for the broader usage of ultrasound.

Introduction and advances of various other medical or nonmedical technologies will continuously influence or alter imaging methods and surgical procedures. In addition, less and less invasive surgery with smaller access sites will keep surgeons' hands further away from organs, thus requiring more image guidance as seen in minimally invasive and percutaneous image-guided procedure. Therefore, there will be a less distinctive border between open and percutaneous interventional ultrasound; these ultrasound techniques can eventually be categorized as "intra-procedural ultrasound." Natural orifice transluminal endoscopic surgery (NOTES) is another newer surgical-endoscopic field, in which EUS will play a role. EUS-guided radiofrequency ablation of abdominal tumors is one example of NOTES. Eventually, many of the surgical procedures that have been done with open, laparoscopic, or percutaneous approaches may be performed by endoscopic approaches, which in many cases may be guided by EUS. As technology evolves, new advances in imaging methods and image-guided procedures including IOUS, LUS, and EUS should be carefully assessed to define its practical role and cost-effectiveness in future.

Learning of Abdominal Ultrasound in Future

Performance of 2-dimensional real-time ultrasound images requires familiarity with how the position of the probe (transducer) relates to the image on the monitor screen. This probe-image orientation requires hand-eye coordination by the operator in order to understand where a particular anatomical region is shown on the screen. To acquire this type of orientation, the surgeon who is not familiar with the ultrasound probe and scan display on the monitor is well advised to practice ultrasound examination on a daily basis;

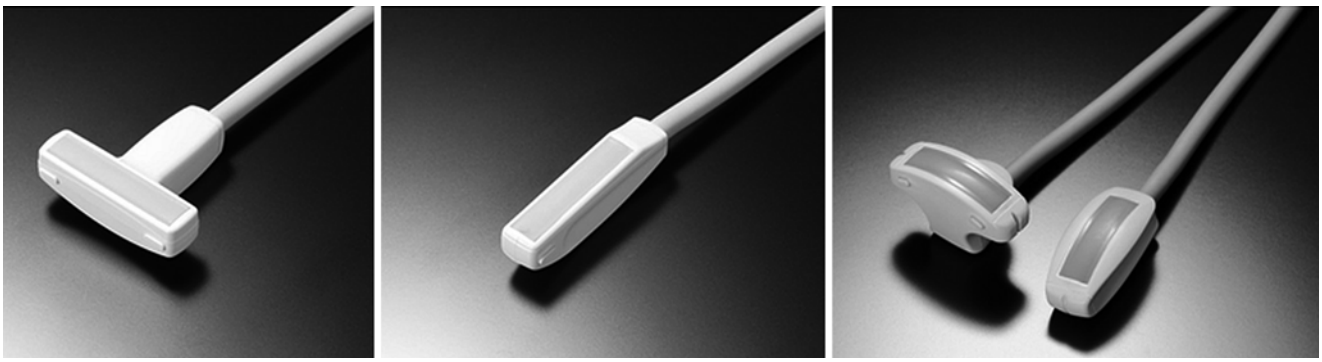

Fig. 23.1 Various types of intraoperative ultrasound (IOUS) probes

"Scan, Scan, Scan" is probably the best way to learn ultrasound. Eventually, a surgeon becomes capable of creating 3-dimensional images in his or her brain from 2-dimensional images in real time.

Before or while clinically scanning patients (human being), "Scan" can be practiced using new tools such as phantoms and stimulators. Ultrasound phantoms are available for practicing TAUS, IOUS, and LUS scanning techniques. Ultrasound simulation systems can be used to learn EUS as well as IOUS. Virtual reality technology will continually advance so that more realistic simulation of TAUS/IOUS/LUS examinations as well as surgical procedures will become available. Computer-based ultrasound simulators will greatly help future education and training in abdominal ultrasound. For general surgeons, particularly hepatobiliary, pancreatic, and endocrine surgeons, surgical oncologists, and laparoscopic surgeons, it will become critically important to master abdominal ultrasound, particularly IOUS and LUS. Collaboration with radiologists may be important initially; however, I believe it is imperative that surgeons themselves eventually should perform surgical ultrasound such as IOUS and LUS.

New and Promising Technology in Abdominal Ultrasound (Including Video Clips)

Intraoperative Contrast-Enhanced Ultrasound

Applications

In 2007, Sonazoid® (microbubbles contained in the agent which remain stable when subject to ultrasonic sound waves, enabling continuous vascular and Kupffer imaging) was approved as an ultrasound contrast for clinical use in Japan. Since that time, the use of Sonazoid in surgical procedures has been attracting a great deal of attention.

In particular, imaging in the delayed phase approximately 10 min after the intravenous injection of Sonazoid is becoming a focus of interest. This imaging technique exploits the fact that Sonazoid is phagocytized by Kupffer cells. Since Kupffer cells are not present in malignant tumors such as HCCs and metastases, echoes from contrast medium are not observed in such lesions, which therefore appear black (anechoic-hypoechoic) in ultrasound images. Such images are referred to as Kupffer images. Kupffer images make it possible to assess a tumor and its degree of invasion before surgery and are also sometimes used to select the most appropriate surgical procedure. In addition, the use of high-frequency probes in Kupffer imaging enables the detection of hepatic metastases measuring 5 mm or less, which can contribute to more accurately determine prognosis and treatment options.

Setup and Imaging Conditions

High-frequency intraoperative probes such as those shown in Fig. 23.1 and an ultrasound system that supports contrast-enhanced imaging are required for examinations using Sonazoid. The MI (mechanical index) should be in the range from 0.1 to 0.15, and the frame rate should be approximately 15 fps to ensure real-time display and avoid the collapse of bubbles. Lower frequencies are generally the most suitable for the stable detection of bubble signals. However, when determining the optimal frequency, it should be kept in mind that there is a tradeoff between resolution and tissue signal detection. The focal point should be set at the inferior border of the region of interest or the inferior border of the field of view.

Clinical Usefulness

Kupffer imaging makes it possible to visualize the location, size, and shape of tumors that are difficult to visualize in B-mode images and at the same time allows the courses of vessels near tumors to be confirmed before resection. This is a great advantage for surgical application. As shown in Fig. 23.2, the difference between conventional B-mode and Kupffer images are obvious. The exact shape of the tumor, which cannot be determined accurately in the B-mode image, is clearly depicted in the Kupffer image.

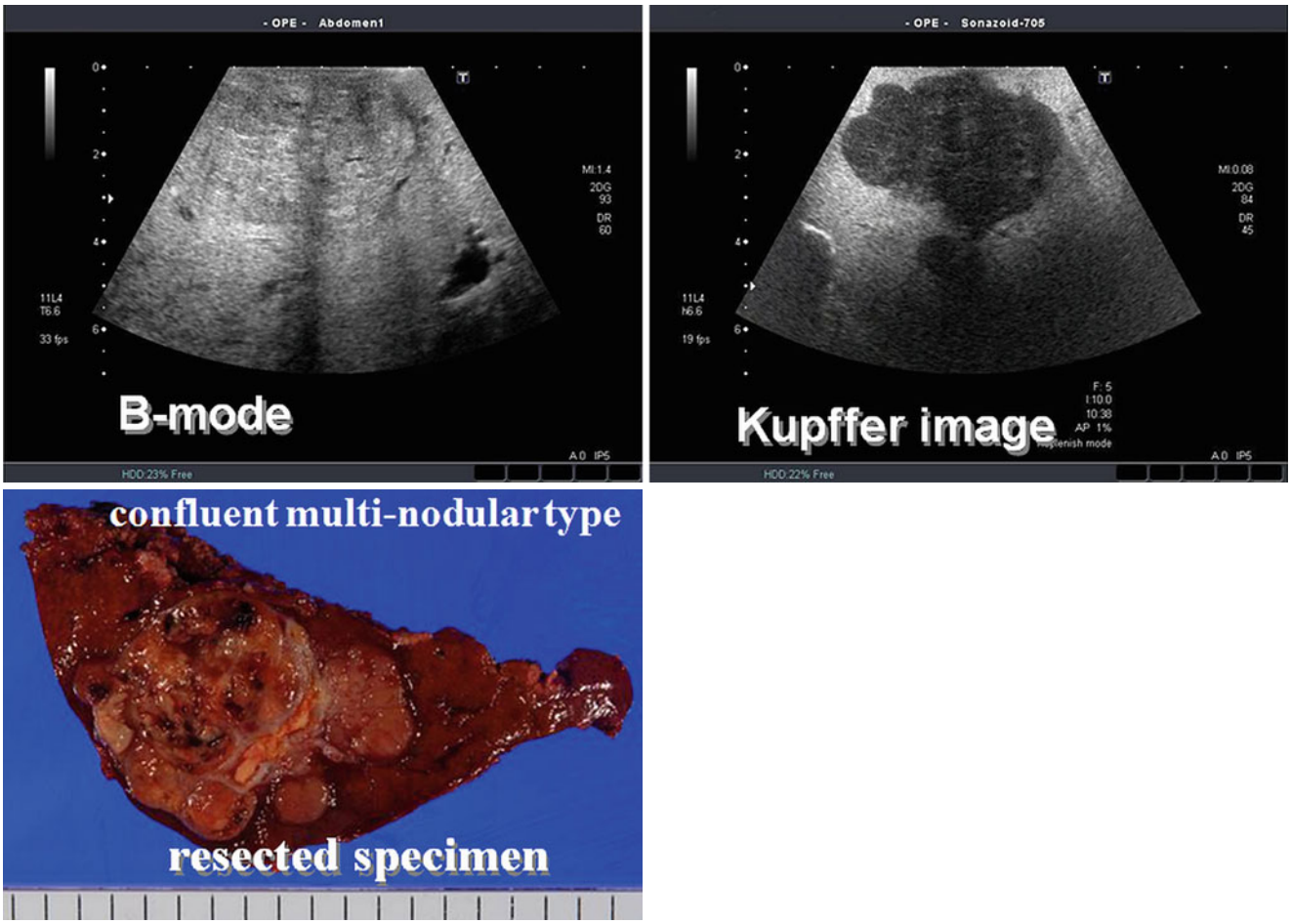

Fig. 23.2 IOUS B-mode and Kupffer images of a malignant liver tumor with a resected specimen

Kupffer imaging is also useful for detecting small malignant lesions. Metastases measuring less than 5 mm cannot be often visualized by B-mode. Kupffer imaging, on the other hand, is able to detect smaller intrahepatic metastases, as shown in Fig. 23.3.

Attempts have also been made to assess the degree of tissue differentiation by observing the courses of vessels within the tumor in the vascular phase. When micro-flow imaging (MFI), which displays bubble motion as a summed residual image, is used, fine blood vessels exhibiting various degrees of differentiation can be observed within an HCC, as shown in Fig. 23.4 (see also Video 23.1). It has been found that well-differentiated carcinomas exhibit the so-called "cotton pattern" and moderately differentiated carcinomas exhibit the "vascular pattern."

Portal Invasion by Tumors

The degree of portal invasion must be carefully assessed before surgery. Using MFI, it is possible to observe portal invasion in the early stages, as shown in Fig. 23.5 (see also Video 23.2). This image shows the leakage of portal vein blood in a pattern known as the "thread and streak sign," in which small straight lines are seen in areas of portal invasion.

Conclusion

Contrast-enhanced ultrasound (CEUS) is useful for navigation in surgery of the liver. In addition, liver metastases can be more accurately diagnosed before surgery. The clear depiction of such tumors including primary and metastatic tumors provides extremely valuable information before liver surgery. (As of 2013, in the United States, Sonazoid® is not approved by FDA).

Intraoperative Ultrasound 3D Display Techniques and Cavity and FlyThru Methods

Introduction

Various 3D display techniques have recently been introduced in the field of ultrasound diagnosis. Such 3D techniques, which provide images that depict structures more accurately

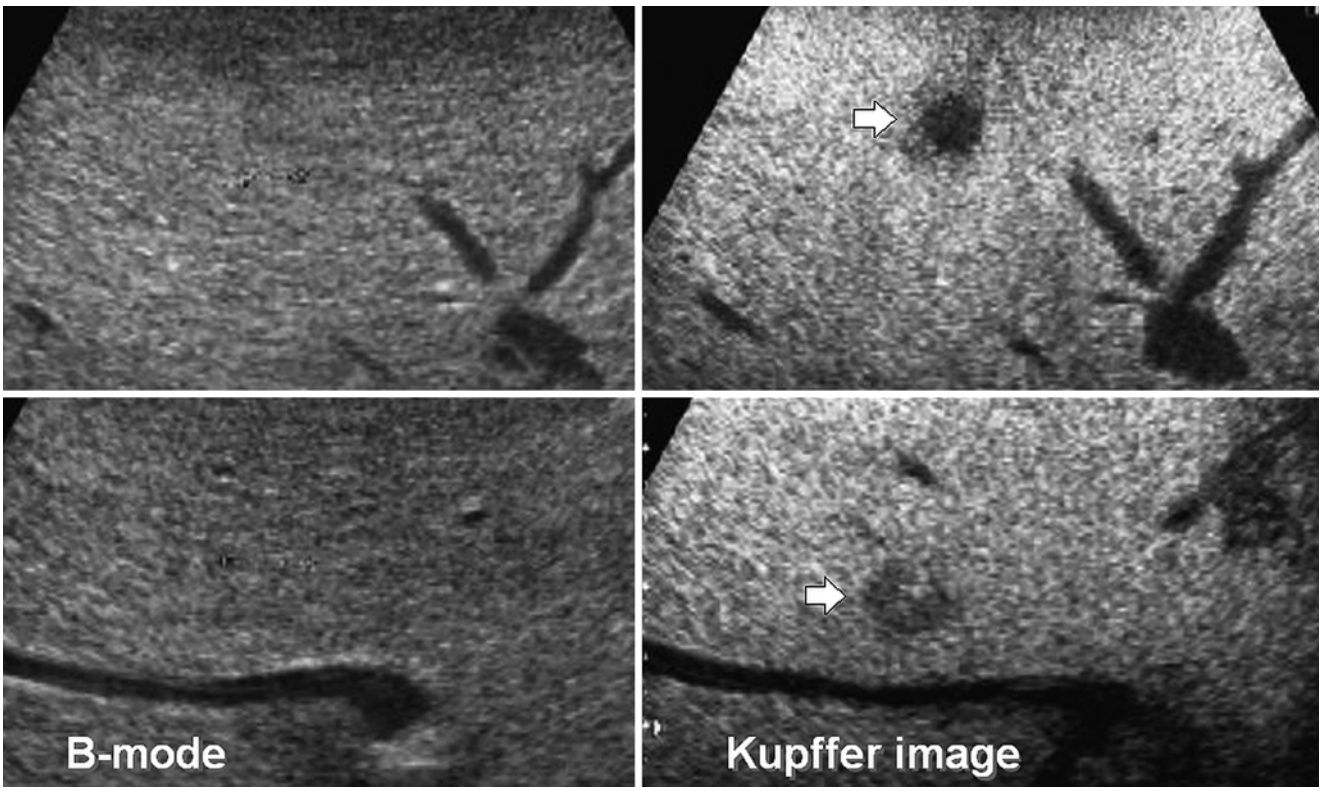

Fig. 23.3 IOUS B-mode and Kupffer images showing liver metastases (*arrows*) from a pancreatic cancer. While these tumors are difficult to recognize by B-mode, these are readily detected by Kupffer images

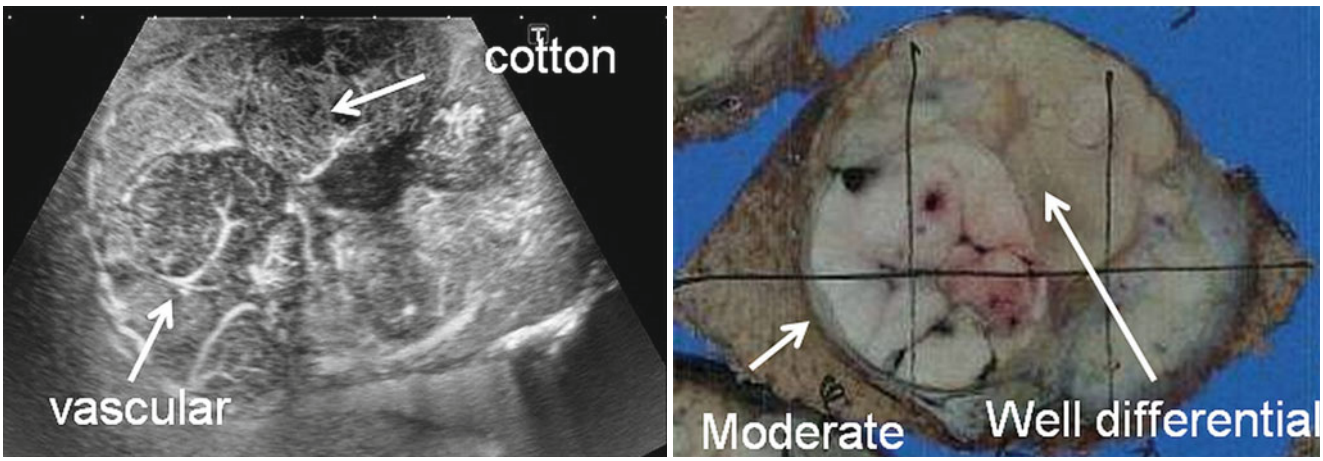

Fig. 23.4 IOUS image of multinodular HCC (hepatoma) (*left*) and a section of corresponding area of a resected specimen (*right*). See also Video 23.1

than 2D images, have been clinically employed for the examination of the fetus, luminal structures in the abdomen, and the internal structure of the heart as well as for the evaluation of the cardiac valves and myocardium. In particular, recent advances in graphics workstations and computer graphics have led to the development of 3D display techniques for CT and MRI images, and 3D display is now employed proactively in clinical practice. Here, intraoperative ultrasound 3D display techniques and the cavity and FlyThru methods, which are based on virtual reality technology, are briefly discussed.

How Are 3D Images Obtained?

Precisely determining the positions of the imaging planes is essential for accurately depicting 3D structures. Two techniques are available (Fig. 23.6): the matrix array (2D array)

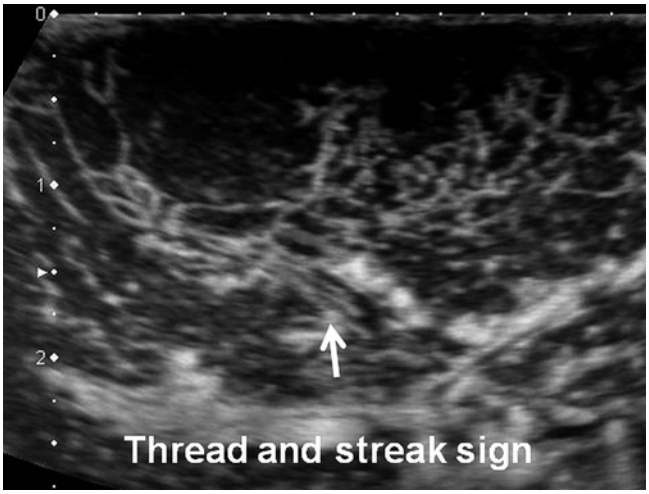

Fig. 23.5 IOUS image showing thread and streak sign in vascular MFI (micro-flow imaging). See also Video 23.2

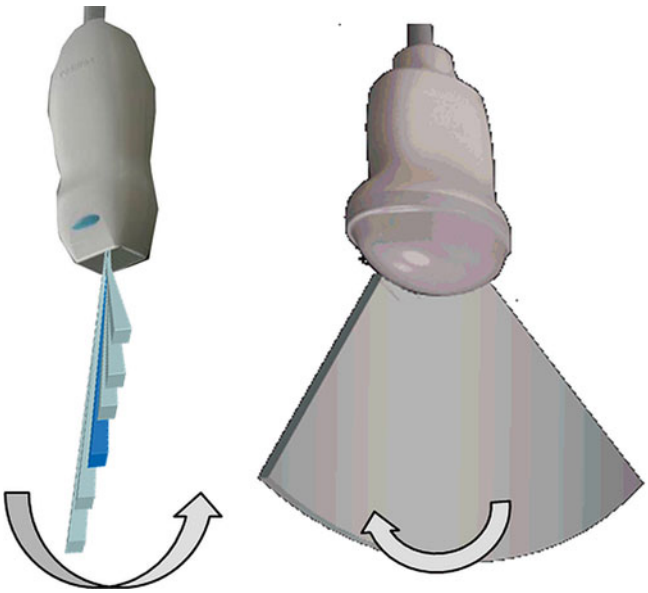

Fig. 23.6 Acquisition method for 3D data. *Left*: 2D array method. *Right*: mechanical method

technique, which electronically aims the ultrasound beam in the desired direction, and the mechanical scanning technique, which swings the transducer elements of the 2D probe back and forth. The former technique requires advanced micromachining technology, complex electronic processing, and large-scale integrated circuits but controls beam acquisition electronically and provides a high degree of flexibility during scanning (Fig. 23.6, left). A major disadvantage of this technique is that the number of transducer elements and amount of circuitry required increases as the square of that for conventional systems, and systems employing this technique are therefore expensive. The latter technique can be implemented by combining existing technology and mechatronics, and the required circuitry can be incorporated by simply adding a mechanical control section to the standard 2D imaging circuits. This helps to control (save) the cost (Fig. 23.6, right). In both techniques, 3D information is obtained based on the ultrasound beams in the scanning field as shown in Fig. 23.6, and 3D images are reconstructed from this three-dimensionally extended fan-shaped ultrasound echo information.

How Is 3D Information Displayed?

Details of the 3D information display (3D rendering) technique have been discussed elsewhere [1, 2], and therefore a brief summary of 3D rendering is provided here.

Multiplanar reconstruction (MPR) is the standard technique for displaying a 3D volume as slice images. In MPR, the three orthogonal planes in a 3D volume are displayed simultaneously as shown in Fig. 23.7 (see also Video 23.3). Normally, the plane of ultrasound scanning is defined as the A-plane; the scanning plane perpendicular to the A-plane is defined as the B-plane (i.e., the plane in which the transducer elements swing in the mechanical technique); and the plane perpendicular to both the A-plane and the B-plane is defined as the C-plane. Such images are intuitive and easy to interpret, but the simultaneously displayed area is limited, and it is therefore necessary to align the planes with the region of interest.

In the multiview method, many slice images at different slice positions in one of the MPR planes are displayed (Fig. 23.8) (see also Videos 23.4, 23.5, and 23.6). This is the basic 3D display method and is suitable for observing the 3D information in its entirety by selecting the desired display plane from among A, B, and C.

What Is the Cavity Method?

In the cavity method, which is also referred to as the inversion method, the brightness of the image is inverted and the image is then displayed three-dimensionally so that areas of low brightness, such as the lumens of hollow structures, can be clearly visualized. This is useful for observing the overall luminal morphology and vascular structures (Fig. 23.9) (see also Video 23.7). When this method is employed for Kupffer imaging in contrast-enhanced ultrasound examinations, the positional relationships between a tumor and nearby vessels can be clearly observed in real time. This technique is expected to be useful for real-time navigation during surgical procedures.

What Is the FlyThru Method?

The terms "fly-through" and "virtual endoscopy" have been used in 3D diagnostic imaging modalities such as CT and MRI. "Fly-through" refers to "flying through the human body," and virtual endoscopic 3D display in which the observer appears to be flying through luminal

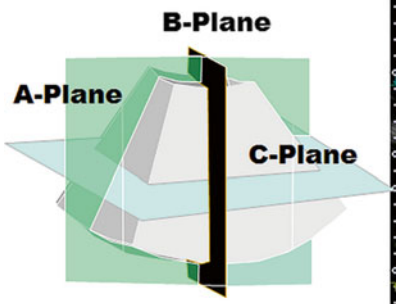

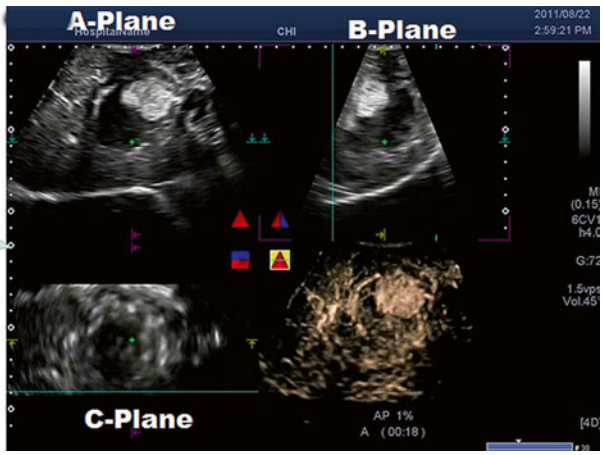

Fig. 23.7 Three planes of 3D (*left*) and MPR (multi-planar reconstruction) display method in CEUS (*right*). See also Video 23.3

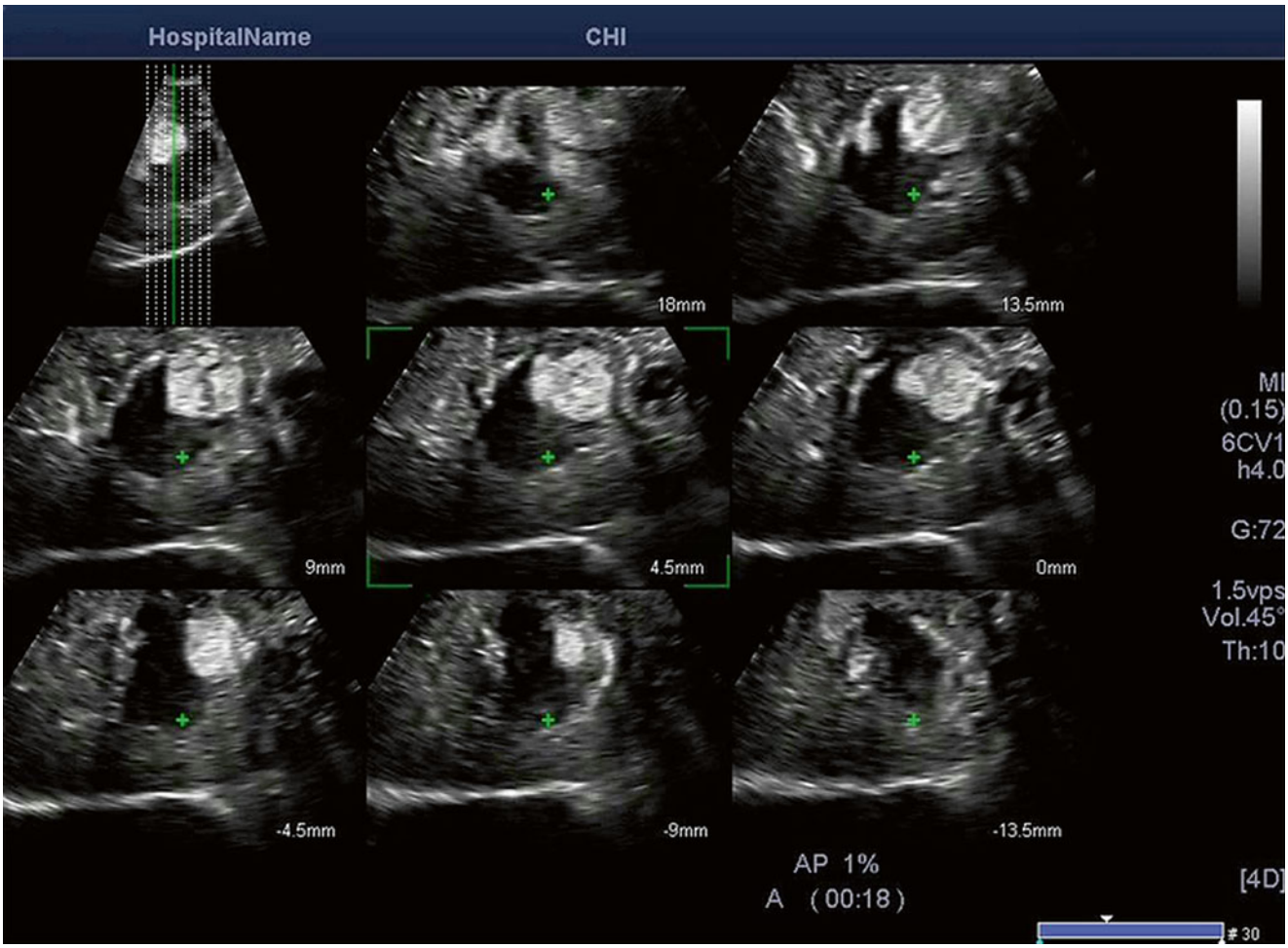

Fig. 23.8 Multiview method (example of A-plane display): many slice images. See also Videos 23.4, 23.5, and 23.6 showing A-plane, B-plane, and C-plane

structures such as the trachea or blood vessels is known as FlyThru. This method makes it possible to observe the courses of luminal structures and blood vessels and also to detect the presence of plaque, protrusions (e.g., tumor invasion), or external compression from any desired viewpoint within the lumen. Examples of typical clinical applications are shown in Fig. 23.10 (see also Video 23.8 and 23.9).

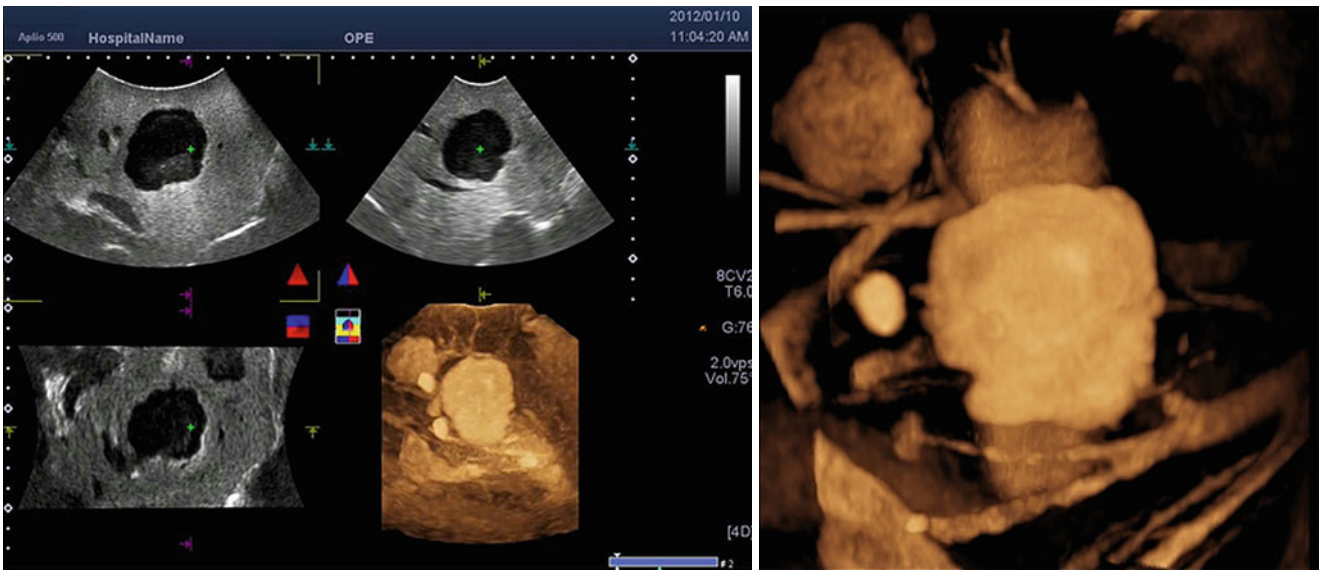

Fig. 23.9 Cavity display in IOUS Kupffer imaging of metastases. See also Video 23.7. *Left*: multiview three planes and cavity display. *Right*: cavity display

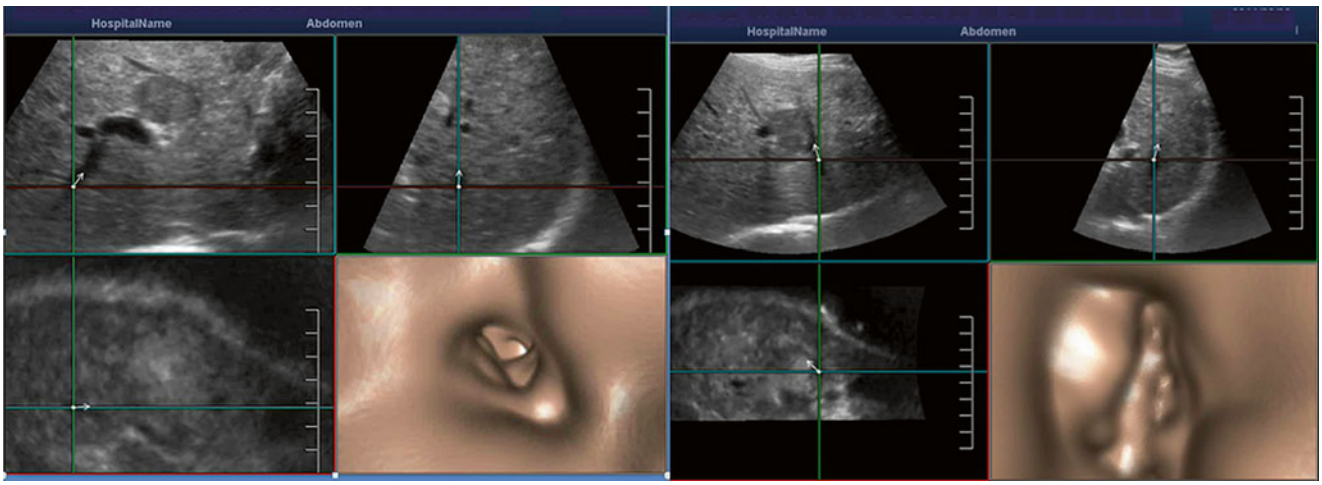

Fig. 23.10 FlyThru display of HCC and portal and hepatic veins. See also Videos 23.8 and 23.9. *Left*: multiview three planes and FlyThru (right lower) of PV (portal vein). *Right*: multiview three planes and FlyThru (right lower) of HV (hepatic vein)

Conclusion

The usefulness of 3D display in ultrasound has been discussed for many years. Cardiovascular examinations have led the way in the clinical application of 3D display, and the value of 3D display has been confirmed, particularly for the detailed evaluation of the cardiac valves. The value of 3D has also been confirmed in its application to obstetric examinations. Recently, with the development of 2D array technology, new 3D display techniques with improved real-time performance characteristics are being explored.

Fusion Technique for Combining Ultrasound with CT and MR

Introduction

The fusion technique allows the volume-to-volume fusion of images acquired by two different modalities. Real-time ultrasound images can be viewed in the same cross-sectional planes as in previously acquired CT or MR volume data. This makes it possible to observe structures from the same locations and to navigate in the region of interest. The fusion

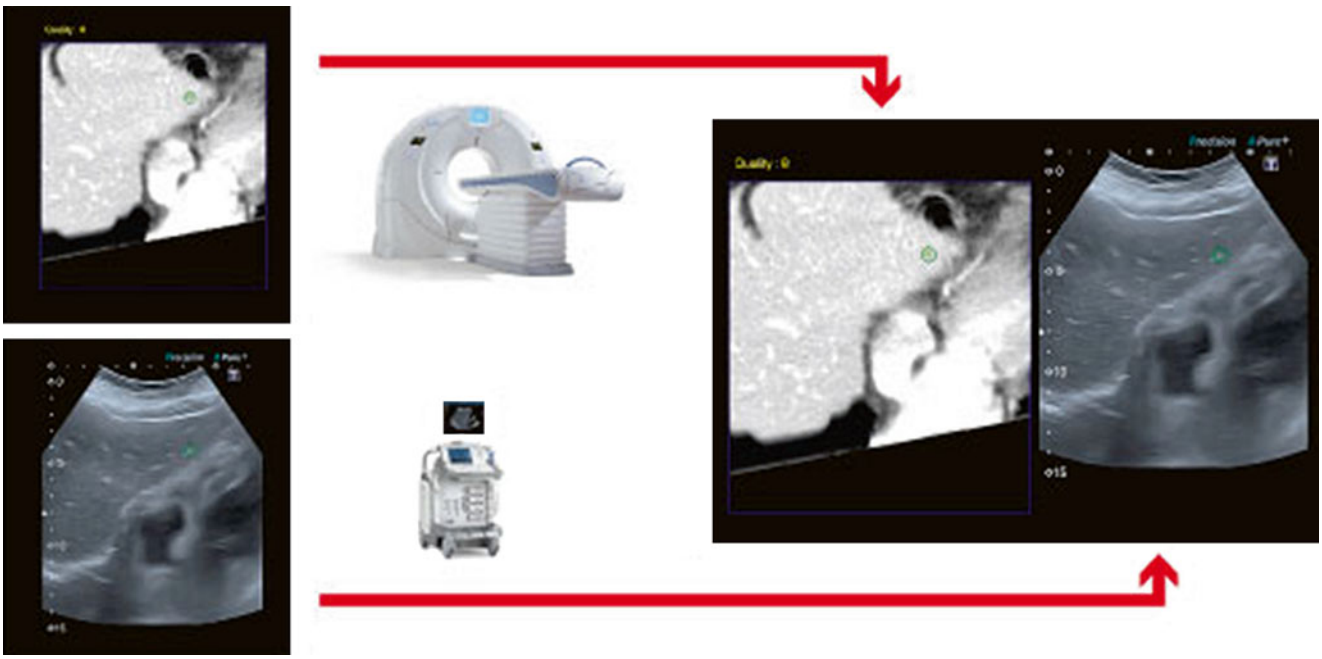

Fig. 23.11 Fusion technology. The fusion technique displays both a CT image and an ultrasound image simultaneously

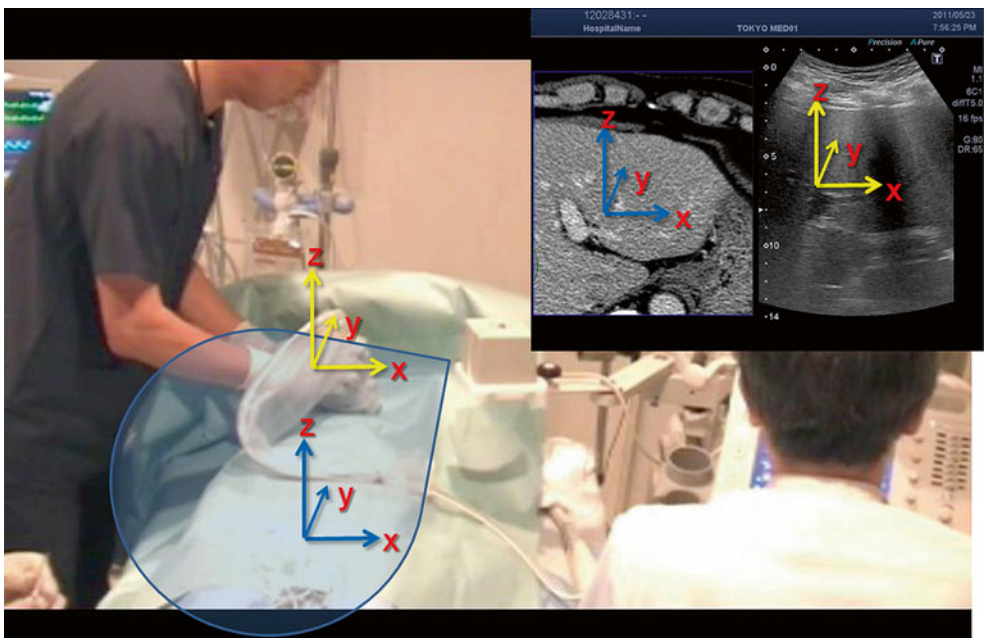

Fig. 23.12 Setting up the directions in both images (axes lock)

technique reads 3D DICOM datasets from all major imaging modalities and displays the corresponding images in real time next to the live ultrasound display, as shown in Fig. 23.11. To permit comprehensive pre- and post-intervention evaluation, Smart Fusion is available in all ultrasound imaging modes, including color Doppler and contrast-enhanced ultrasound.

Easy Setup

Image alignment is required in order to synchronize the ultrasound images and CT/MR volumes. Figure 23.12 shows how the image directions are set using an ultrasound probe. A position sensor attached to the ultrasound probe receives position information from a magnetic field generator. After

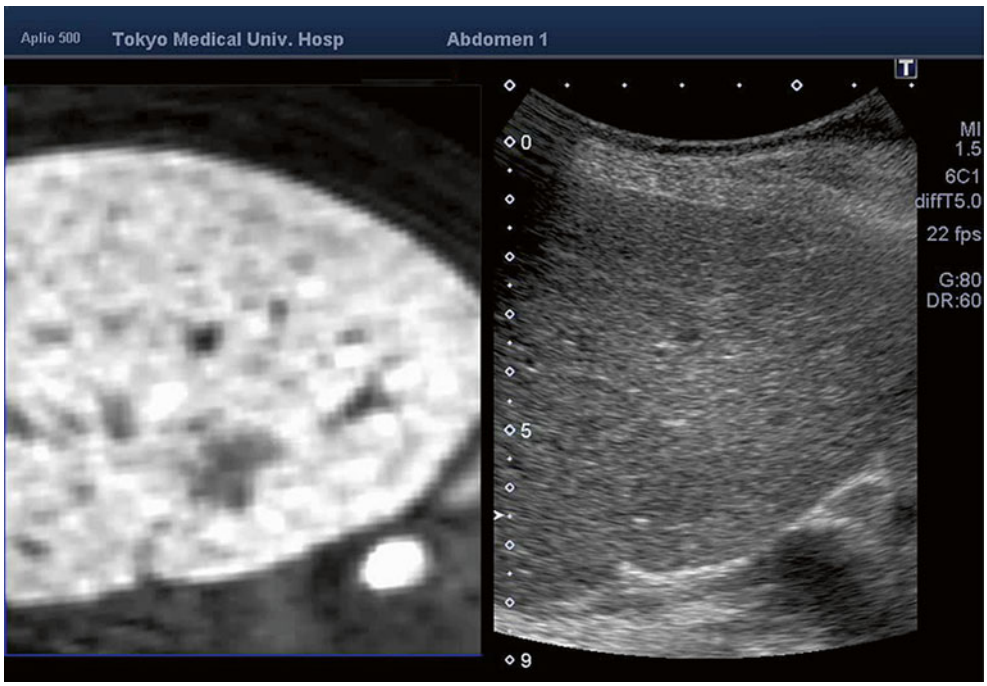

Fig. 23.13 Smart fusion. EOB MRI (*left*) vs. B-mode US (*right*)

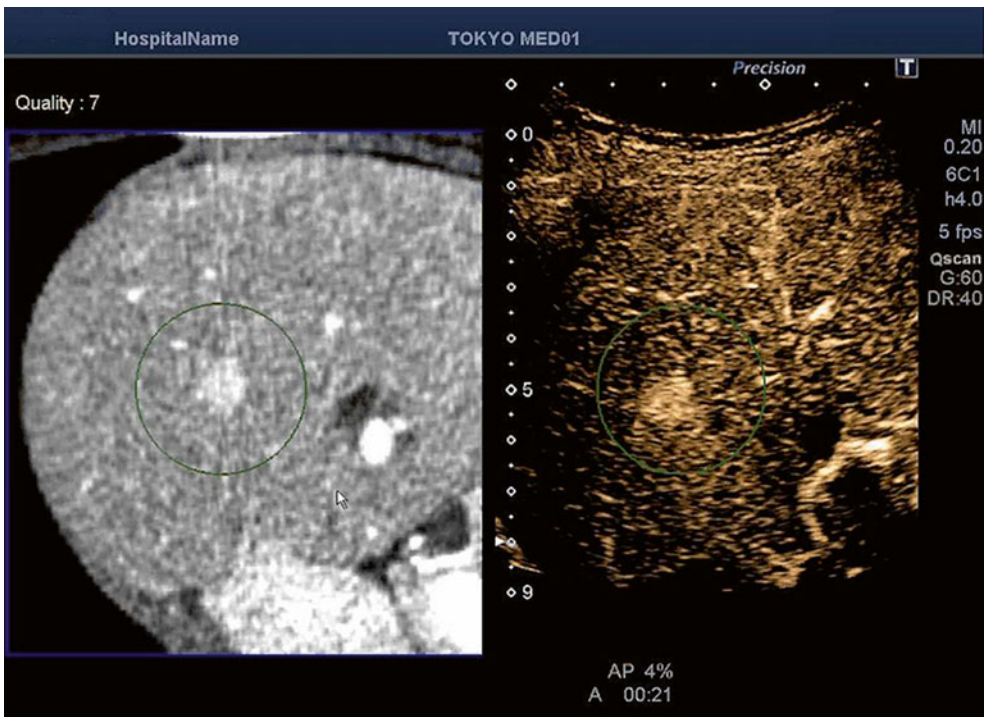

Fig. 23.14 Fusion. CTA vs. CEUS (Sonazoid®). See also Video 23.10. CTA (*left*) and CEUS (*right*) showing enhancement of a tumor (*circle area*) by CEUS

setup, the ultrasound image and the CT or MR image are precisely synchronized, and after synchronization, the positions of the images are adjusted automatically.

Diagnostic Applications

Ultrasound is useful for characterizing focal lesions, but it suffers from a number of limitations such as artifacts, acoustic shadowing, and attenuation. CT and MRI are the standard modalities for evaluating patients in clinical practice, particularly in the preoperative settings. Ultrasound has the advantages of lower cost and no radiation exposure, but the disadvantage of operator dependency. The fusion technique can be used to observe multiple lesions within a solid organ. Figure 23.13 shows an example of synchronization. Contrast-enhanced MR imaging with EOB (Gd-EOB-DTPA) clearly shows the location of the tumor, but on the other hand, the tumor is difficult to observe in the ultrasound image. This technique is helpful for the localization in addition to the diagnosis and characterization of tumors. Figure 23.14 (see also Video 23.10) shows an example of

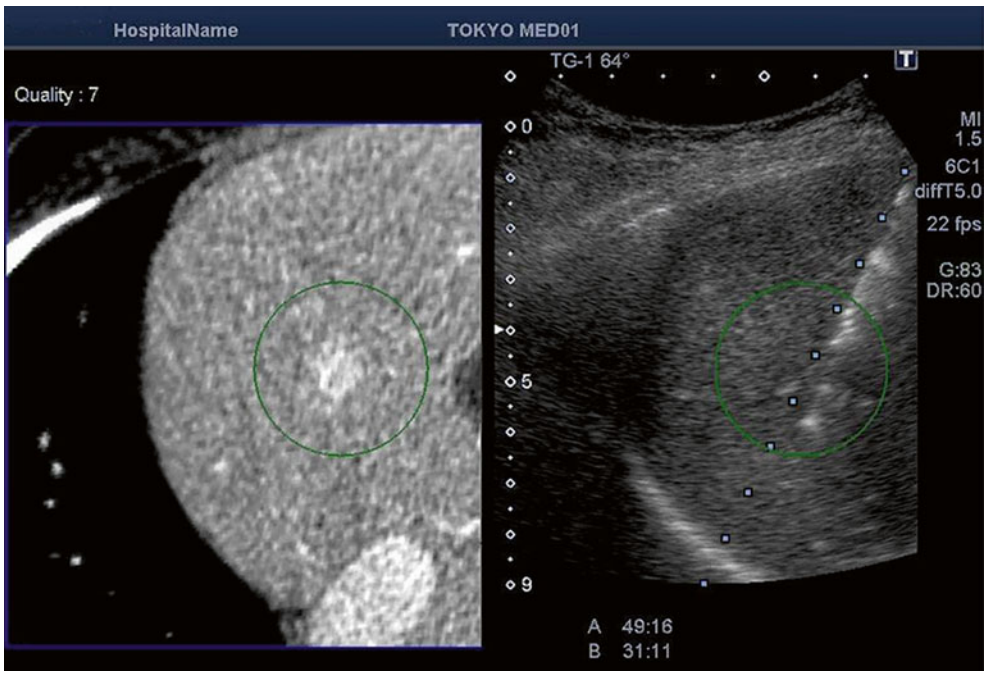

Fig. 23.15 Fusion. CTA vs. RFA (RITATM) puncture. See also Video 23.11. CTA (*left*) and CEUS (*right*). CTA shows an enhanced (hyperdense) tumor (*circle*), while CEUS shows a puncture of an RFA needle into a hypoechoic tumor (*circle*)

synchronization between CTA and CEUS in the arterial phase. This is useful for estimating the margins of the area to be ablated.

Interventional Applications

The fusion technique is useful in interventional applications because it reduces procedure times and provides a more accurate treatment. From a technical point of view, the fusion technique allows different access points and orientations to be used, which is not possible with CT or MR. Figure 23.15 (see also Video 23.11) shows real-time puncture of an RFA (radiofrequency ablation) needle using the fusion technique.

Conclusion

Matching the transducer position with previously acquired 3D datasets is a simple and quick two-step process. By moving the transducer over the region of interest, it is possible to browse through the region in both real-time ultrasound images and previously acquired volume data simultaneously. In addition, intelligent target and marker points can be set to facilitate navigation in the region of interest during surgical or interventional treatment.

Elastic Imaging: Elastography

Introduction

Physicians commonly employ palpation as an important diagnostic technique in the examination of various organs such as the breast, thyroid gland, liver, and digestive tract. When an organ is palpated, malignant tumors feel more rigid (firmer, harder) than benign lesions. This physical characteristic is related to their elastic properties. Important causes of an increase in tissue stiffness are tissue transformation, fibrosis, and steatosis. Ultrasound elastography is expected to be a useful adjunct technology for the detection of tumors, for the precise determination of the extent of cancer such as breast cancer, for the differential diagnosis and confirmation of benign and malignant lesions, and for guidance during biopsy procedures. More accurate targeting of biopsies helps to increase specificity. With regard to the prostate gland, this significantly reduces the number of biopsies required in an individual patient.

Basic Theory of Ultrasound Elastography

There are two methods for measuring the stiffness of a tumor: the strain method and the shear wave method [3].

Strain Method

There is a relationship between the amount of applied force and the degree of deformation. Two quantitative values are related to each other: pressure and strain. When force is applied to a tumor, it will deform. The relative amount of tissue distortion is called strain. The strain rate is defined as shown in Fig. 23.16.

Figure 23.16 shows the relative stiffness of the hard and soft components at the same pressure. Compression (stress) is manually applied to the tissues, and the values with and without compression are compared. In real-time ultrasound elastography, mild pressure is applied. The lesion is positioned at the center of the region of interest (ROI), and the transducer is pressed and released 3–5 times using mild pressure. It is important to ensure that pressure is applied vertically and that the target is centered and does not shift out of the scan plane.

A strain (elasticity) image is obtained by comparing the tissue data acquired in a selected ROI with and without compression. The degree of tissue distortion (strain) is measured by real-time imaging and displayed as a color-coded image. Figure 23.17 shows a typical screen display in strain elastography.

Shear Wave Method

Shear wave elastography is another method for obtaining elasticity images. It is based on the combination of the radiation force induced in the tissues by the ultrasound beam and a fast imaging sequence that displays the propagation of the resulting shear waves in real time.

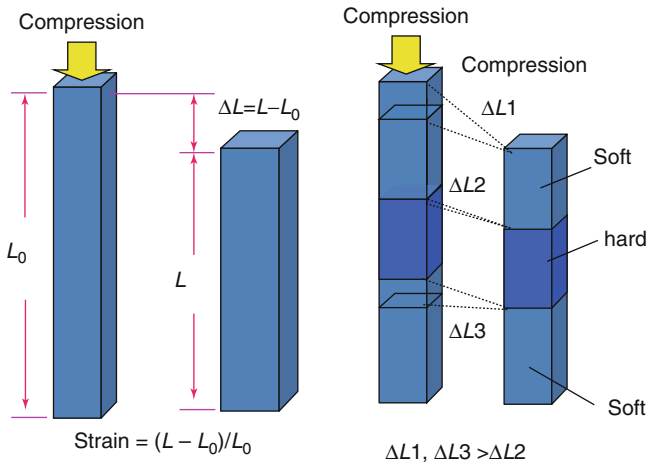

Fig. 23.16 Relationship between compression value and strain

This radiation force or "push pulse" consists of focused beams of acoustic energy (ultrasound) and is generated by the probe, unlike the manual compression technique. The shear waves, or transverse waves, move in a perpendicular manner (i.e., motion is perpendicular to the direction of wave propagation). Figure 23.18 shows the relationship between the push pulse and the shear waves.

Clinical Applications

Elastography is used to evaluate the malignancy of tumors [4–6]. There are two methods for evaluating tumors. The first method is to determine the strain ratio between the tumor and tissues around the tumor, and the other method is to categorize the strain pattern of the tumor as an elasticity score (Tsukuba score).

Figure 23.19 shows a residual fibroadenoma of the breast examined using compressed strain imaging. It shows a typical benign appearance.

In shear wave elastography, the distribution of shear wave velocities can be observed in real time. The average velocity in the ROI can also be calculated.

Figure 23.20 shows an image of a hepatocellular carcinoma (HCC) obtained by intraoperative ultrasound (IOUS). It shows a typical color pattern and Young's modulus in the small ROI based on $E = 3\sigma Vs^2$.

The color scale indicates the value of Young's modulus (kPa). Red corresponds to hard tissues and blue corresponds to soft tissues, which is the opposite of the color scale in strain elastography.

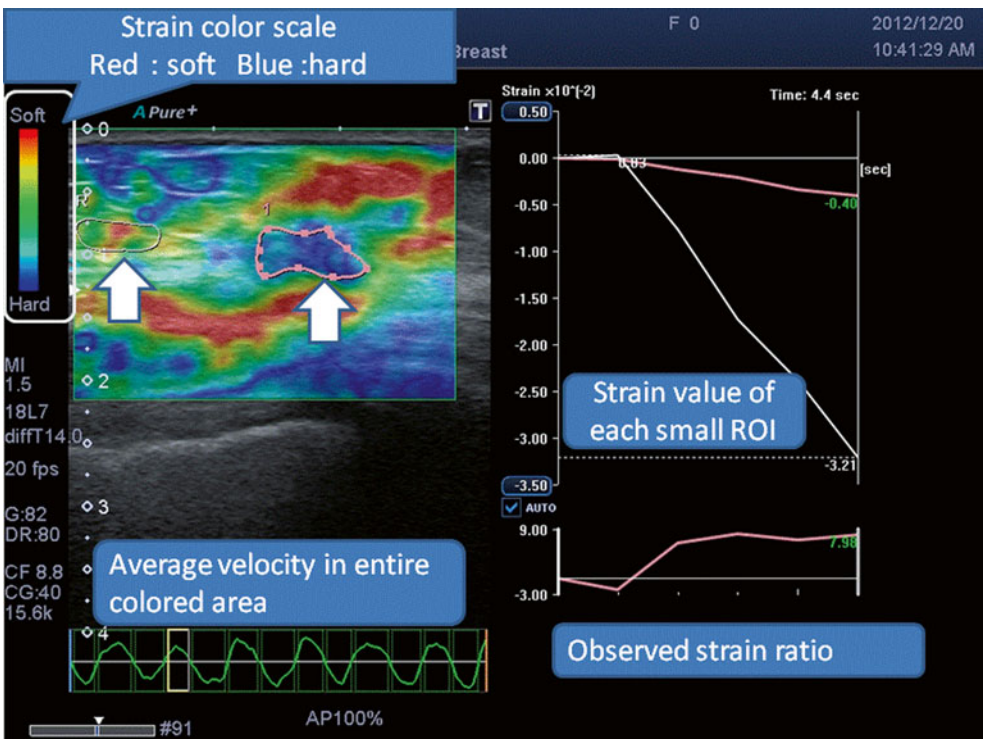

Fig. 23.17 Typical screen display in strain elastography. Strain ratio of two ROIs (tumor and fat area) shows the location of malignant tumor. *Red* shows a soft area (fat), while *blue* shows a hard area (tumor)

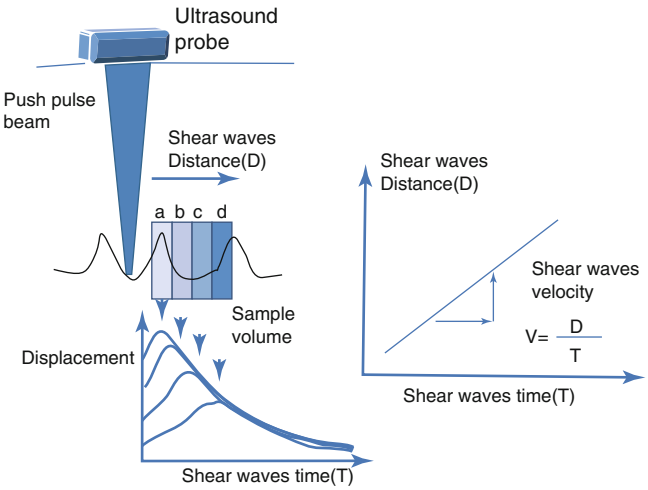

Fig. 23.18 Push pulse and shear wave velocity of shear wave elastography

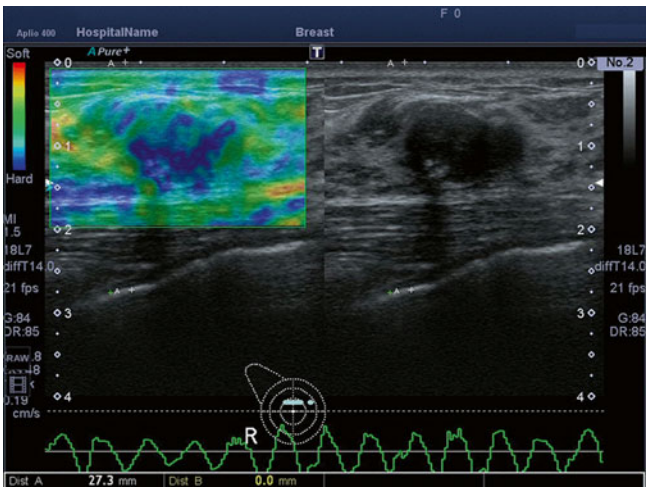

Fig. 23.19 Clinical example of strain elastography (breast). Areas inside the tumor are seen to be hard (seen in *blue color*), which is the typical pattern for a benign breast tumor, fibroadenoma. Courtesy of Dr. Tokiko Endo (Nagoya Medical Center)

Quantitative Ultrasound

Introduction

Quantitative ultrasound (QUS) has been investigated for a long time, but its clinical use is very limited. Making tissue diagnosis by ultrasound, the so-called ultrasonic tissue characterization, cannot be achieved by B-mode imaging ultrasound alone. New ultrasound technology is required; in this chapter, potential QUS is briefly described based on our recent clinical investigation on the diagnosis of cancer in the lymph nodes.

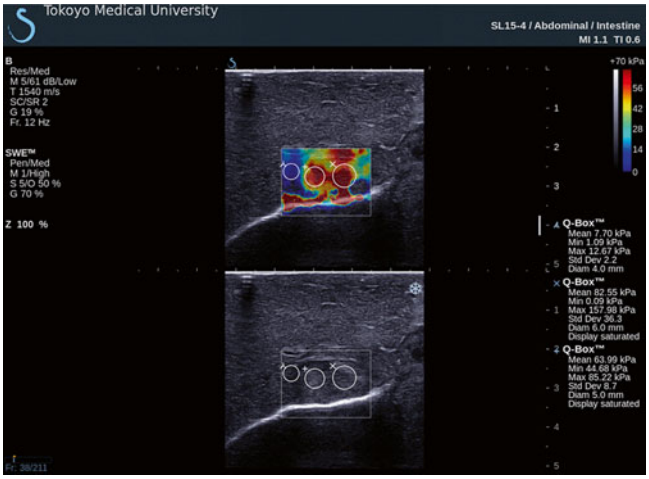

Fig. 23.20 Clinical example of shear wave elastography (IOUS of HCC). *Red* shows large value of Young's modulus (hard) and *blue* shows small value. The center of tumor is observed as hard areas

QUS for Lymph Node Metastases: Investigational Study

Detection of metastases in the lymph nodes (LN) is critical for cancer management. Conventional histopathological methods may overlook small metastatic foci because typically only one histological section is evaluated per LN. There are no current, practical means to evaluate LNs in their entire volume. As a result, clinically significant metastases may be missed.

A prospective study, funded in part by the National Institutes of Health and conducted at the University of Hawaii and Kuakini Medical Center in Hawaii and Riverside Research in New York, aims to create an operator-independent, fast, reliable system to scan and evaluate LNs in their entire volume utilizing high-frequency (HF) quantitative ultrasound (QUS). Over the past three decades, clinical applications of QUS have been investigated [7]. Unlike B-mode ultrasound images used clinically, HF QUS methods provide a quantitative means of estimating microscopic-scale tissue properties and are operator independent. Studies have further shown that HF QUS can effectively distinguish between metastatic and benign LNs [8, 9].

In this blinded study, freshly excised LNs were scanned at 26 MHz and echo-signal data were digitally acquired over the entire three-dimensional (3D) volume using a custom scanning system. LNs were step-sectioned at 50-μm intervals and stained with H&E and then later compared to 13 QUS parameters associated with tissue microstructures.

QUS parameters based on spectrum analysis and envelope statistics were estimated from the acquired RF echo-signal data [8, 9]. Linear-discriminant analysis classified LNs as metastatic or non-metastatic, and areas under receiver-operator

characteristic curves (Az) were computed to assess classification performance. QUS-estimates and cancer-probability values derived from discriminant analysis were depicted in 3D images for comparison with 3D histology [10].

An interactive graphical user interface (GUI) was developed to permit virtual 3D dissection and exploration of freshly dissected LNs; the GUI displays linked, orthogonal, cross-sectional views of the node with a histology plane that matches the XY ultrasound plane. The interactive display consisted of a gray-scale B-mode plane of the 3D volume with overlaid color-encoded QUS-estimate or cancer-probability values. Cancer probabilities were estimated and color-coded for display using a Bayesian approach based on the discriminant score [10].

Clinical Examples of QUS to Detect Lymph Node Metastases

Typical examples of clinical cases demonstrating the value of QUS in detecting macro- and micrometastases in lymph nodes are shown in Figs. 23.21 and 23.22 [10]: see legends of figures in details.

Future Potential of QUS

Future in situ applications of these QUS methods will enable surgeons to identify suspicious axillary sentinel LNs of breast cancer patients in the operating room, in addition to non-sentinel axillary LNs. Additionally, intraoperative identification of suspicious LNs in situ by surgeons during colorectal and gastric cancer surgery may be possible. These QUS applications may contribute to more accurate staging, improving surgical treatment and management of breast, colorectal, and gastric cancer patients.

Future ex vivo applications will enable pathologists to identify suspicious LNs of breast, colorectal, and gastric cancer patients in the pathology lab. The number of regional LN metastases changes the node status of the tumor-node-metastases staging and therefore affects the cancer staging and prognosis in all three cancer types. This may contribute to more-sensitive detection of metastases and therefore more-accurate tumor-node-metastases staging by targeting the permanent histology section to the suspicious region.

These techniques and promising future devices may enable detection of the clinically relevant fraction of micrometastases that are missed by conventional single-section histology. The high probability of missed clinically significant metastases is of great concern because detection of all micrometastases is essential for accurate staging and effective treatment.

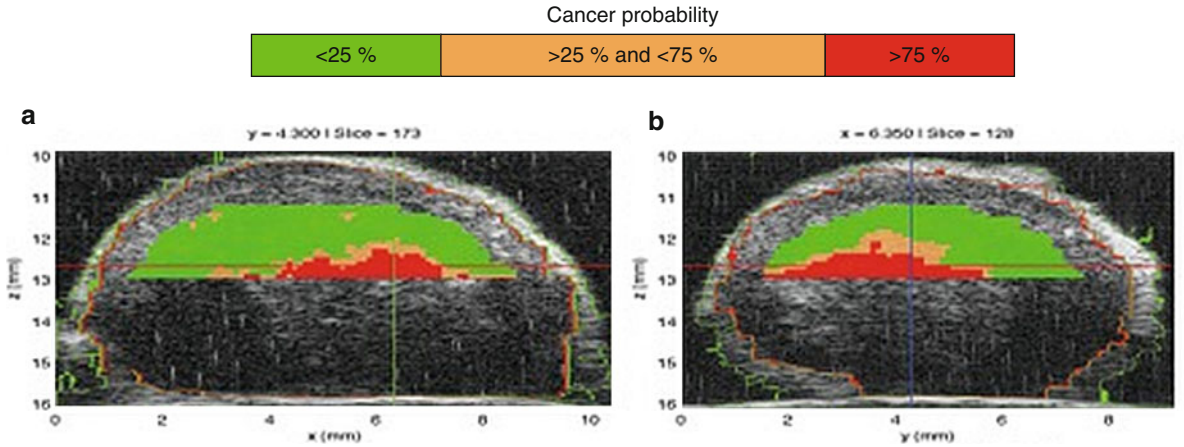

Fig. 23.21 *Top* (**a**–**d**): 3D interactive GUI with cancer-probability images of a locoregional lymph node (LN) with partially metastatic adenocarcinoma from a patient with colorectal cancer. The LN is 9.54 mm in its largest dimension, and the metastasis is 5.09 mm in its largest dimension. The graphical user interface (GUI) displays three orthogonal gray-scale B-mode cross sections from a three-dimensional (3D) rendering in (**a**–**c**). The cross sections depict color-encoded cancer-probability values using *red* to indicate a probability greater than 75 %, *orange* to indicate a probability between 25 and 75 %, and *green* to indicate a probability less than 25 %. Figure (**d**) shows a co-registered hematoxylin and eosin (H&E)-stained histology photomicrograph that corresponds to the same section as in (**c**). These images show that excellent concurrence is achieved between the *red* cancer-probability region and the definitive histology result shown in (**d**) showing the demarcated metastatic tumor. *Bottom* (**e**–**h**): 3D interactive GUI with cancer-probability images of a benign locoregional lymph node (LN) from a patient with colorectal cancer. The LN is 4.41 mm in its largest dimension. The graphical user interface (GUI) displays three orthogonal gray-scale B-mode cross sections from a three-dimensional (3D) rendering in (**e**–**g**). (**h**) shows a co-registered hematoxylin and eosin (H&E)-stained histology photomicrograph that corresponds to the same section shown in (**g**). The cross sections depict color-encoded cancer-probability values using *red* to indicate a probability greater than 75 %, *orange* to indicate a probability between 25 and 75 %, and *green* to indicate a probability less than 25 %. These images show that excellent concurrence is achieved between the *green* (probably cancer-free) cancer-probability region and the definitive histology result of the benign LN shown in (**h**)

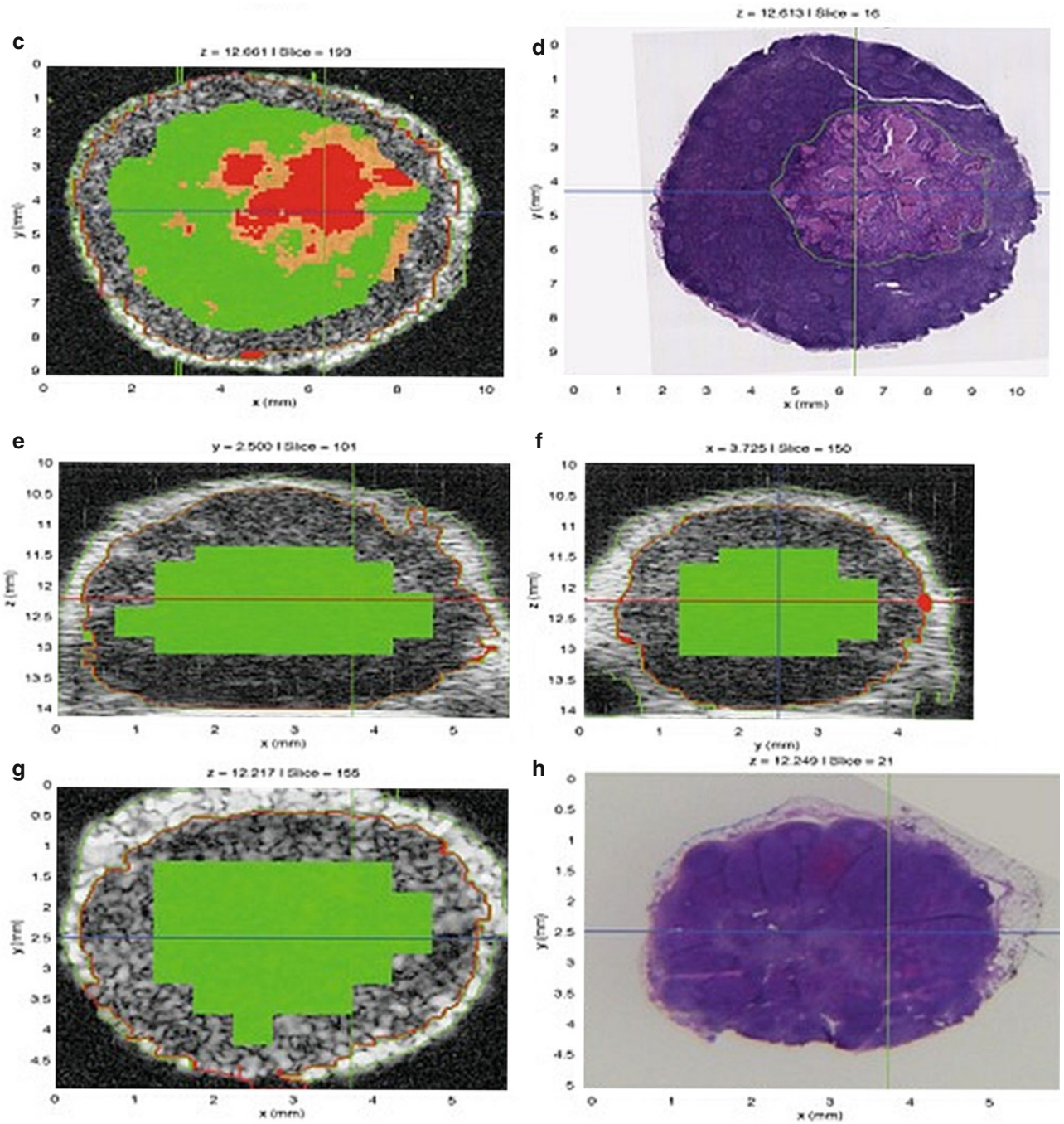

Fig. 23.21 (continued)

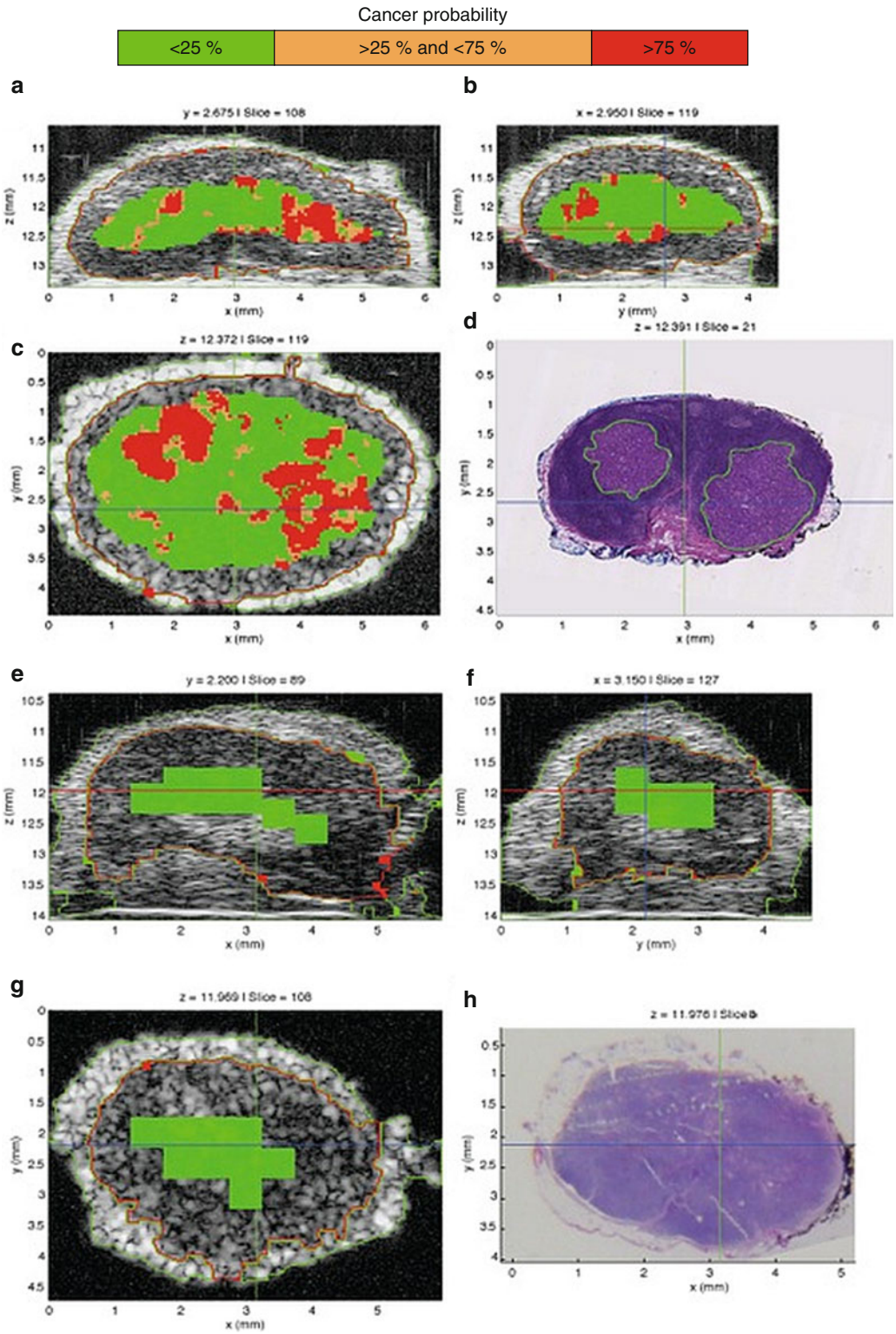

Fig. 23.22 *Top* (**a**–**d**): Cancer-probability images of an axillary sentinel lymph node (LN) of an invasive ductal breast cancer patient. The LN is 5.86 mm in its largest dimension, and it contains two micrometastatic foci. The bigger focus is 1.82 mm in its largest dimension. The graphical user interface (GUI) displays three orthogonal gray-scale B-mode cross sections from a three-dimensional (3D) rendering in (**a**–**c**). The cross sections depict color-encoded cancer-probability values using *red* to indicate a probability greater than 75 %, *orange* to indicate a probability between 25 and 75 %, and *green* to indicate a probability less than 25 %. (**d**) shows a co-registered hematoxylin and eosin (H&E)-stained histology photomicrograph that corresponds to the same section shown in (**c**). Like Fig. 23.21, this figure shows excellent concurrence between the *red* high-probability region and the corresponding metastatic region in the histology result. *Bottom* (**e**–**h**): Cancer-probability images of a benign axillary sentinel lymph node (LN) of an invasive ductal breast cancer patient. The LN is 5.51 mm in its largest dimension. The cross sections depict color-encoded cancer-probability values using *red* to indicate a probability greater than 75 %, *orange* to indicate a probability between 25 and 75 %, and *green* to indicate a probability less than 25 %. Like Fig. 23.21, this figure (**e**–**g**) shows that excellent concurrence is achieved between the *green* cancer-probability region and the definitive histology result of the benign (cancer-free) LN shown in (**h**)

Conclusions

Abdominal ultrasound including TAUS, IOUS, LUS, and EUS can provide various types of diagnostic information which are otherwise not easily or practically available. In addition, ultrasound can guide or assist various surgical procedures in real time much easier than other imaging methods. Advantages of TAUS/IOUS/LUS, including high accuracy, safety, and speed, with comprehensive anatomical information, dynamic blood flow information, and real-time guidance capability, outweigh its disadvantages such as specific instrumentation requirement and slow learning curve. The use of abdominal ultrasound by surgeons is expected to increase along with more formal training in ultrasound for surgeons. New ultrasound technologies such as ultrasound contrast enhancement, 3/4-dimensional ultrasound, and others which are described in this chapter will be employed more during future abdominal ultrasound and will facilitate interventional procedures. Being like the surgeon's stethoscope and versatile transabdominally and intraoperatively, ultrasound is a valuable technique which is recommended to master for surgeons in various fields to improve surgical decision-making and surgical outcomes.

References

1. Mitsunori Y, Tanaka S, Nakamura N, Ban D, et al. Contrast-enhanced intraoperative ultrasound for hepatocellular carcinoma: high sensitivity of diagnosis and therapeutic impact. J Hepatobiliary Pancreat Sci. 2013;20:234–42. Published online: 08 March 2012.
2. Arita J, Takahashi M, Hata S, Shindoh J, Beck Y, Sugawara Y, et al. Usefulness of contrast-enhanced intraoperative ultrasound using Sonazoid in patients with hepatocellular carcinoma. Ann Surg. 2011;254:992–9.
3. Ophir J, Céspedes I, Ponnekanti H, et al. Elastography: a quantitative method for imaging the elasticity of biological tissues. Ultrason Imaging. 1991;13:111–34.
4. Itoh A, Ueno E, Tohno E, et al. Breast disease: clinical application of US elastography for diagnosis. Radiology. 2006;239(2):341–50.
5. Fischer T, Peisker U, Fiedor S, et al. Significant differentiation of focal breast lesions: raw data-based calculation of strain ratio. Ultraschall in der Medizin. 2012;33(4):372–9.
6. Tanter M, Bercoff J, Athanasiou A, et al. Quantitative assessment of breast lesion viscoelasticity: initial clinical results using supersonic shear wave imaging. Ultrasound Med Biol. 2008;34:1373–86.
7. Lizzi FL, Greenebaum M, Feleppa EJ, Elbaum M, Coleman DJ. Theoretical framework for spectrum analysis in ultrasonic tissue characterization. J Acoust Soc Am. 1983;73:1366–73.
8. Mamou J, Coron A, Hata M, Machi J, Yanagihara E, Laugier P, Feleppa EJ. Three-dimensional high-frequency characterization of cancerous lymph nodes. Ultrasound Med Biol. 2010;36:361–75.
9. Mamou J, Coron A, Oelze M, Saegusa-Beecroft E, Hata M, Lee P, Machi J, Yanagihara E, Laugier P, Feleppa EJ. Three-dimensional high-frequency backscatter and envelope quantification of cancerous human lymph nodes. Ultrasound Med Biol. 2011;37:345–57.
10. Saegusa-Beecroft E, Machi J, Mamou J, Hata M, Coron A, Yanagihara E, Yamaguchi T, Oelze M, Laugier P, Feleppa E. 3D quantitative ultrasound for detecting lymph-node metastases. J Surg Res. 2013;183:258–69.

Index

A
Abdominal aortic aneurysms (AAA)
  acute diagnosis, 124, 125
  B-mode ultrasound, 124
  chronic diagnosis and follow-up, 124–126
Abdominal/retroperitoneal vascular structures
  abdominal aorta, 123
  aneurysmal disease, 124–126
  deep venous thrombosis, 126
  intervention, 127
  obesity, 123
  portal venous blood flow, 126, 127
  vascular stenoses and occlusions, 126
  vena cava, 123–124
  visceral/renal arteries, 123, 124
Abdominal ultrasound
  cavity method, 292, 294
  CEUS
    clinical use, 289–291
    portal invasion by tumors, 290
    Sonazoid, 289
    types of, 289
  3D display techniques
    acquisition method, 291, 292
    depict structures, 290
    disadvantage, 292
    fan-shaped ultrasound echo information, 292, 293
    multiplanar reconstruction, 292, 293
    multiview method, 292, 293
  elastography
    clinical applications, 298, 299
    physical characteristic, 297
    shear wave method, 298, 299
    strain method, 297–298
  FlyThru method, 292–294
  fusion technique, CT and MR
    3D DICOM datasets, 295
    diagnostic applications, 296–297
    image directions, 295–296
    interventional applications, 297
    Smart Fusion, 295
    volume-to-volume fusion, 294
  maintenance and renewal, privileges, 280–281
  phantoms and stimulators, 289
  privileging and credentialing process, 279
  probe-image orientation, 288
  quantitative ultrasound (QUS)
    future potential of, 300
    lymph node metastases, 299–302
    ultrasonic tissue characterization, 299
  training requirements
    documentation, 280
    formal ultrasound training, 280
    practical experience, 280
Abdominal wall
  anatomy
    anterior abdominal wall musculature and fascia, 72
    lateral abdominal wall, 72, 73
    linea alba, 72
    linea semilunaris, 72, 73
    medial abdominal wall, 72, 73
    preperitoneal space and peritoneum, 73
    ultrasonographic appearance of, 72
    vascular supply, 73, 75
  inguinal region
    femoral canal anatomy, 82
    femoral hernias, 85–86
    groin masses, 83–84
    inguinal hernia, 84–85
    normal anatomy, 82
  interventional ultrasound
    mapping of, 86
    perioperative nerve block, 86–87
    techniques, 71–72
  pathology and intervention
    abdominal wall fluid collections, 76–77
    benign tumors, 77–78
    desmoid tumor, 78
    hernias, 80–81
    neoplasms, 77, 78
    rectus diastasis, 74
    rectus sheath hematomas, 74–76
    sarcoma, 78–79
    scar-related masses, 79–80
    urachal cyst, 79
    vascular anomalies, 79
Abulfaraj, M., 151–159
Acute pancreatitis, 167
Adams, R.B., 31–60
Advanced trauma life support (ATLS), 109, 269
Ahmed, S.I., 145
Andrén-Sandberg, A., 145
Aneurysmal disease, 124–126
Arii, S., 287–303
Arregui, M.E., 151–159

B
Bahlmann, J., 90
Bang, J., 90
Bartels, E.D., 90

E.J. Hagopian, J. Machi (eds.), *Abdominal Ultrasound for Surgeons*,
DOI 10.1007/978-1-4614-9599-4, © Springer Science+Business Media New York 2014

Bedside echocardiographic assessment for trauma/critical care (BEAT) examination, 117
Bemelman, W.A., 145
Berber, E., 17–30
Berlyne, G.M., 89
Biffl, W.L., 184
Biliary tract surgery
  abnormal gallbladder wall thickening, gallstones, 197–199
  biliary obstruction
    Bismuth-Corlette classification of, 193, 196
    ERCP, 190
    hepatocellular carcinoma (HCC), 193, 197
    pancreas dilatation, 192, 195
    portal pedicle, longitudinal views, 190, 193–194
    portal pedicle, transverse views, 190–192
    World Health Organization (WHO) classification of, 192, 196
  biliary tree anatomy
    cystic artery, 188
    hepatic artery, 188
    left and right hepatic ducts, 187
    lymph nodes, 188
    splenic vein and superior mesenteric vein, 188
  equipment
    B-mode ultrasound, 189
    PACS, 189
    T-transducer, 189
  laparoscopic ultrasonography (LUS)
    vs. intraoperative cholangiography, 197
    port position, 194, 197
  mickey mouse sign, 190
  retractors placement, 190
Biondi, A., 137
Birth, M., 183
Blot, W.J., 141
Bodtger, U., 158
Brooks, A., 117

C
Calderon, D.R., 121–127
Castaing, D., 201–216
Catheline, J.M., 183
Chemical ablations, 229
Chen, J., 211
Cholangiocarcinoma
  laparoscopic ultrasound (LUS)
    hilar, 139, 141–142
    intrahepatic, 142, 143
  risk factor, 192
Chronic pancreatitis, 167–168
Colorectal liver metastases (CRLM)
  clinical risk score (CRS), 137
  Dutch guidelines for, 136
  hepatic outflow, 138, 139
  indication for, 137
  liver resection, 136
  meta-analysis, 136, 137
  vascular structures, 139, 140
Computer-assisted navigation systems
  breast biopsy system, 245
  3-D optical tracking system, 246, 248
  2-D ultrasound image, 244, 245
  electromagnetic tracking systems (EMTSs)
    components of, 250, 251
    guidance systems, 252, 253
    intraoperative photo of, liver tumor, 251, 252
    laparoscopic liver ablation, 251
    schematic representation of, 250
    sensor coils, 251
    tabletop, 251
    video monitor image, 251, 252
  global positioning system, 243
  guidance system prototype, 246, 247
  hand and instrument positioning, 244
  laparoscopic ultrasound
    prototype of, 249
    video monitor, 249
  open optical tracking systems (OTS)
    IR camera, 248
    limitations of, 249
    during open liver ablation, 248
    optical reflectors, 248
Conlon, K.C., 145
Connor, S., 142
Contrast-enhanced ultrasound (CEUS)
  abdominal ultrasound
    clinical use, 289–291
    portal invasion by tumors, 290
    Sonazoid, 289
    types of, 289
  pancreatic surgery, 166–167
Cook, J.H., 3
CRLM. *See* Colorectal liver metastases (CRLM)
Cucchetti, A., 211

D
De Castro, S.M., 137
Dempah, D., 151–159
Desmoid tumor, 77, 78
Dewitt, J., 158
D'Hondt, M., 209
Doran, H.E., 145
Doucas, H., 145
Ductal adenocarcinoma
  concomitant pancreatitis, 171
  homogeneous hypoechoic mass, 171
  indications, 170
  liver metastases, 172
  resectability, 171
  suspicious lymph nodes, 172
  vessel abutment, 172
  vessel invasion, 171
Dulchavsky, S.A., 117
Duplex ultrasound (DUS)
  physics
    aliasing, 122
    B-mode image, 121, 122
    pencil Doppler, 121
    rarefaction, 121
    spectral broadening, 121–122
  vascular structures (*see* Abdominal/retroperitoneal vascular structures)
Durup Scheel-Hincke, J., 145

E
EFAST. *See* Extended focused assessment with sonography for trauma (EFAST)
Electromagnetic tracking systems (EMTSs)
  components of, 250, 251
  guidance systems, 252, 253
  intraoperative photo of, liver tumor, 251, 252

laparoscopic liver ablation, 251
schematic representation of, 250
sensor coils, 251
tabletop, 251
video monitor image, 251, 252
Ellis, E.B., 99
Endoanal ultrasound (EAUS)
anterior sphincter disruption, 262, 264
external sphincter, 261–263
10 MHz frequency, 259
perianal fistula, 262, 264
puborectalis, 262, 263
Endoluminal ultrasound
AJCC colon and rectum cancer staging, 255
BK medical ultrasound probe, 257
endoanal ultrasound
anterior sphincter disruption, 262, 264
external sphincter, 261–263
10 MHz frequency, 259
perianal fistula, 262, 264
puborectalis, 262, 263
endorectal ultrasound
circular hypoechoic dark areas, 259
lymph nodes visualization, 258
orientation of lesion, 258
patient positioning, 258
rigid sigmoidoscopy, 258
three-dimensional, 263–264
uN1, lymph node, 260, 262
uT0 lesions, 260
uT1 lesions, 260
uT2 lesions, 260, 261
uT3 lesions, 260, 261
indications
incontinence, 256
perianal abscess and fistula, 256–257
rectal cancer, 256
7 MHz crystal, 257
rectum and anus anatomy, 257
Endorectal ultrasound (ERUS)
circular hypoechoic dark areas, 259
lymph nodes visualization, 258
orientation of lesion, 258
patient positioning, 258
rigid sigmoidoscopy, 258
three-dimensional, 263–264
uN1, lymph node, 260, 262
uT0 lesions, 260
uT1 lesions, 260
uT2 lesions, 260, 261
uT3 lesions, 260, 261
Endoscopic retrograde cholangiopancreatography (ERCP), 152, 153, 155, 190, 192
Endoscopic ultrasound (EUS)
celiac artery, 154
clinical uses
biliary disease, 155–156
esophageal disease, 154–155
gastric disease, 155
pancreatic disease, 156–158
upper abdominal masses diagnosis, 158
console function, 153
development of, 151
echoendoscopes
duodenoscope, 153
forward-viewing echoendoscopes, 152
linear tip echoendoscope, 151, 152
radial tip echoendoscope, 151–152
transpapillary IDUS catheters, 153
forceful intubation, 153
pharyngeal intubation, 153
upper abdomen, 158–159
Zenker's diverticulum, 153
Endo, T., 299
Enestvedt, C.K., 145
Epigastric hernias, 80, 81
ERUS. *See* Endorectal ultrasound (ERUS)
EUS. *See* Endoscopic ultrasound (EUS)
Extended focused assessment with sonography for trauma (EFAST)
barcode sign, 116, 117
clinical data, 116–117
comet-tail sign, 113, 116
high-frequency transducer, 113
ICU Setting, 117–118
low-frequency transducer, 113, 115
lung sliding, 113
pneumothorax/hemothorax, 113, 116
seashore sign, 116

F
Femoral hernias, 85–86
Ferrada, P., 118
FlyThru method, 292–294
Focused assessment with sonography for trauma (FAST)
abdominal examination
free fluid, 110
hepatorenal recess, 110–112
pubic symphysis, 111, 114, 115
splenorenal recess, 110, 112, 113
ATLS algorithm, 109
clinical data
blunt torso injury, 111–112
penetrating torso injury, 112–113
pericardial examination, 110, 111
Frankel, H.L., 109–119
Freehand technique, 95, 96
Frenkel, J.L., 255–264
Friese, R.S., 111
Fry, W.R., 279–281

G
Gallbladder carcinoma, 146–147
Gammelgaard, P.A., 90
Garden, O.J., 129–148, 187–199
Gastric cancer, 133, 136
Gastric disease, 155
Gecelter, G., 61–68
Gholghesaei, M., 137
Giovannini, M., 155
Giuffrida, M.J., 61–68
Goel, N., 7–15
Goere, D., 142
Goldberg, B.B., 90, 100, 109
Grobmyer, S.R., 137
Groin masses, 83–84
Guidance procedures
electromagnetic tracking systems, 252, 253
surgical ultrasound, 5
ultrasound guidance (*see* Ultrasound guidance)
Gunst, M., 117

H
Hagopian, E.J., 3–5
Hammill, C., 229–241
Han, D.C., 121–127
Handheld ultrasound transducer, 220
Hansen, P.D., 229–241
Hariharan, D., 137, 142, 145
Harrison, E.M., 129–148, 187–199
Hayashi, S., 3
Healy, J.E., 204
Helton, W.S., 161–174
Hepatic tumors
  benign tumors, 211
  hepatocellular carcinoma, 210–211
  liver metastasis, 209–210
Hepatocellular carcinoma (HCC), 139, 210–211
Hernias, 80–81
  epigastric, 80, 81
  femoral, 85–86
  inguinal, 84–85
  spigelian, 80, 81
  umbilical, 80
  ventral, 80–81
Hilar cholangiocarcinoma, 139, 141–142
Holm, H.H., 90, 100
Hood, K., 89–106
Hoppman, R.A., 279–281
Hyacinthe, A.C., 117

I
Iannitti, D.A., 219–227
Inguinal hernia, 84–85
Instrumentation
  backing (damping) material, 18
  control panel
    depth setting, 24, 26
    focus control, 24, 27
    new patient control, 22
    power control, 22–23
    time gain compensation, 23, 25
    ultrasound machine presets, 22
  curvilinear (convex) array, 21
  image display
    beam former, 25, 26
    display unit, 28
    dynamic ultrasound image, 25, 30
    image processor, 27–28
    signal processor, 26–27
  linear array, 21
  matching layer, 19
  phased array, 21–22
  piezoelectric materials, 17–18
  transducer housing, 18
  transducer (probe) types
    attenuation, 19–20
    endocavitary probes, 20
    intraoperative and laparoscopic probes, 21
    mechanical sector probes, 20
Intraductal Pancreatic Mucinous Neoplasm (IPMN), 169, 170
Intrahepatic cholangiocarcinoma, 142, 143
Intraoperative ultrasound (IOUS)
  equipment setup, 32
  guidance techniques, 223–224
  handheld ultrasound transducer, 220
  in-plane targeting, 225–226
  laparoscopic transducer, 220, 221
  Lawnmower technique, 222, 223
  liver
    biopsy, 212
    contrast-enhanced intraoperative ultrasound, 203–204
    hepatectomy, 211–212
    hepatic tumors (*see* Hepatic tumors)
    laparoscopic approach, 203
    open approach, 202–203
    percutaneous radiofrequency ablation, 214
    segmental anatomy, 204–208
    transplantation, 214–216
    ultrasound-guided anatomic hepatectomy, dye injection, 213
    ultrasound-guided vessel compression, 213–214
  liver scanning technique
    contact scanning, 40
    interventions, 40
    liver mobilization, 43
    pancreas scanning technique, 47–49
    probe placement, 40, 41
    probe standoff scanning, 40
    rocking probe movement, 45–47
    rocking/tilting transducer movement., 42–43
    systematic scanning approach, 40
    transverse and longitudinal plane, 43–44
  out-of-plane targeting, 226
  pedicle technique, 223
  toe orientation, 220, 221
  transducer head position
    standoff technique, 221–223
    superficial lesion, 221, 222
    tissue visualization, 221, 222
  transducer selection, 219, 220
  T-style finger-grip intraoperative probe, 201
Intravascular ultrasound (IVUS), 127, 269

J
Jimenez, R.E., 145
Johnston, W.C., 229–241
John, T.G., 145
Jorgensen, H.E., 90
Joyner, C.R. Jr., 89

K
Karachristos, A., 145
Khan, A.Z., 137
Khan, S.A., 196
Kim, C.J., 269–277
Kirkpatrick, A.W., 117
Knight, P.R., 3
Knudtson, J.L., 117
Koea, J., 137
Kratochwil, 90
Kriplani, A.K., 142
Kristensen, J.K., 90
Kwon, A.H., 145

L
Laparoscopic transducer, 220, 221
Laparoscopic ultrasound (LUS)
  biliary scanning technique
    gallbladder, 53, 55
    retroduodenal bile duct, 56, 57

umbilical trocar, 52
upper abdominal organs., 52
biliary tract surgery, port position, 194, 197
clinical outcomes
anatomy examination, 184
CBD stones, success rates, 183
cost, 184
LUS *vs.* IOC, 182, 183
success rates, 182, 183
epigastric scanning technique
Achilles heel, 181
anechoic gallbladder fluid, 179
cystic duct (CD) and common hepatic duct (CHD), 181
epigastric trocar, 179
hyperechoic pancreatic parenchyma, 180, 181
hyperechoic stone, 180
mickey mouse head, 180
Mickey Mouse Head Sonographic Appearance, 180
muscular sphincter, ampulla, 180, 181
probe positioning, 179
equipment, 178
indications, 177–178
initial dissection, 178–179
intraoperative scanning, 179
liver scanning technique, 51–52
pancreas scanning technique, 56, 57, 59–60
probe orientation, 49
sliding probe movement, 49, 52
staging, gastrointestinal malignancy
biopsy, 133, 134
cholangiocarcinoma (*see* Cholangiocarcinoma)
colorectal liver metastases, 136–139
complications, 147
epigastric port, 130
gallbladder carcinoma, 146–147
gastric cancer, 133, 136
hepatocellular carcinoma, 139
intra-abdominal organs, 130, 131
lymph nodes, 132, 133
oesophagogastric junctional cancer, 133, 135–136
pancreatic/peri-pancreatic carcinoma (*see* Pancreatic/peri-pancreatic carcinoma)
peritoneal disease, 129
peritoneum performed, 130, 131
portal triad, 130, 132
port placement, 130
principles of, 129
tilting probe movement, 49, 52
umbilical scanning technique, 182
Laparoscopy, 129–130
Lawnmower technique, 222, 223
Liang, P., 106
Lichtenstein, D.A., 117
Liver mapping, 234, 236, 237
Liver surgery
biopsy, 212
contrast-enhanced intraoperative ultrasound, 203–204
hepatectomy, 211–212
hepatic tumors (*see* Hepatic tumors)
laparoscopic approach, 203
open approach, 202–203
percutaneous radiofrequency ablation, 214
segmental anatomy, 204–208
transplantation, 214–216
ultrasound-guided anatomic hepatectomy, dye injection, 213
ultrasound-guided vessel compression, 213–214
Liver tumor ablation
chemical ablations, 229
goal for, 230
microwave ablation (MWA), 230
preoperative planning
deep tumor ablation, 235, 238
double overlapping ablation, 235, 239
laparoscopic staging, 231, 233
lesions size and number, 231
liver mapping, 234, 236, 237
operating room setup, 231, 232
patient selection, 230
PET scan, 231
surgical approach, 232–234
target lesions, 235
radiofrequency ablation (RFA), 230
technical tips for
caudate lesions, 238
deep-seated lesions, 236
hostile abdomen, 238–239
nearby viscera, 238
near hilar structures, 240
pretreated lesions, 241
retro-portal, 237, 239
stacked lesions, 239, 240
vena cava/ hepatic veins, 240–241
thermal ablation, 229–230
ultrasound-guided intratumoral alcohol injection, 229
Livraghi, T., 103, 229
Lytton, B., 3

M
Machi, J., 3, 4, 183, 269–277, 283–285, 287–303
Makuuchi, M., 3, 101, 201, 287
Mann, C.D., 137
Ma, O.J., 116
Marks, J.H., 255–264
Martin, H.E., 99
Martinie, J.B., 243–253
Matsushima, K., 109–119
McGahan, J.P., 104
Menack, M., 145
Metcalfe, M.S., 137
Microwave ablation (MWA), 105, 106, 230
Moriyasu, F., 287–303
Mortensen, F.V., 137
Mucinous cyst, 170
Muntean, V., 137

N
Natarajan, B., 111
Neuroendocrine tumors (NETs), 172–173
Newell, J.A., 3
Niemeyer, D.J., 219–227
Nieveen van Dijkum, E.J.M., 145
Northeved, A., 90

O
Open optical tracking systems (OTS), 245–246
Otto, P., 90

P
Pancreatic cysts
indications, 169
IPMN, 169, 170
mucinous cyst, 170
serous cystadenomas, 169, 170
Pancreatic/peri-pancreatic carcinoma
ampullary carcinoma, 145
cancer-related deaths, 142
CT/MRI, 146
distal cholangiocarcinoma, 142, 145
endoscopic ultrasound, 144–145
irresectable disease, 144
meta-analysis, 144
nonoperative palliation, 143
study analysis, 144, 145
Pancreatic surgery
contrast-enhanced ultrasound (CEUS), 166–167
intraoperative ultrasound (IOUS)
direct scanning, 163, 164
ductal adenocarcinoma (*see* Ductal adenocarcinoma)
emerging uses, 173–174
imaging guidance, 164–166
indirect scanning, 163, 164
neuroendocrine tumors, 172–173
pancreatic cysts, 169–170
pancreatitis, 167–169
probe orientation, 164, 165
scanning techniques, 163–164
Standoff technique, 164, 165
systematic scanning, 164, 166
transduodenal view, 164, 165
laparoscopic ultrasound
handheld transducers, 161
pencil-like end-fire transducer, 161
preoperative setup, 162–163
side-fire transducer, 161
normal pancreatic anatomy, 164, 166
Pancreatitis
acute pancreatitis, 167
chronic, 167–168
indications, 167
pseudoaneurysm, 169
pseudocyst, 168, 169
Parks, K.R., 3–5
Pedicle technique, 221, 223
Picture archiving and communication systems (PACS), 189
Pietrabissa, A., 145
Pilkington, S.A., 137
Pittau, G., 201–216
Pollack, H.M., 90, 100
Pseudoaneurysm, 169
Pseudocysts, 156, 168
Puli, S.R., 154
Pulse repetition frequency (PRF), 122

R
Radiofrequency ablation (RFA), 104, 105, 230
Rahusen, F.D., 137
Rantanen, N.W., 117
Rarefaction, 121
Rasmussen, S.N., 90
Razzaque, S., 243–253
Rectus diastasis, 74
Rectus sheath hematomas, 74–76
Reddy, K.R., 145
Rose, J.B., 161–174
Rossi, S., 104
Röthlin, M.A., 116
Rozycki, G.S., 109

S
Saegusa-Beecroft, E., 287–303
Saitoh, M., 94
Schachter, P.P., 145
Schlegel, J.U., 3
Schrope, B.A., 7–15
Schroy, P.C., 204
Sigel, B., 3, 4, 86, 287
Simo, K.A., 219–227
Siperstein, A., 183
Sisley, A.C., 116
Smart Fusion, 295
Smith, R.S., 279–281
Soffer, D., 113
Soper, N.J., 177–185
Spectral broadening, 121–122
Spigelian hernias, 80, 81
Stewart, F.E.W., 99
Surgical ultrasound
ACS ultrasound education program, 273–274
American College of Surgeons (ACS) Committee, 270
breast ultrasound certification process, 271
clinical evaluation, 4
credentialing, 275–276
documentation, 275
FAST/ER phantom
abdominal/thoracic, 272, 274
cardiac tamponade, 272, 274
intra-abdominal bleeding, 272, 274
history, 3–4
intraoperative evaluation
guidance procedures, 5
hepatic resection, 4
malignancy, staging of, 5
intraoperative/laparoscopic ultrasound phantom, 272
intraoperative ultrasound phantom scanning image, 272, 273
bile duct stones, 272, 274
biliary system, 272, 273
liver, 272, 273
pancreas and pancreatic head tumor, 272, 274
laparoscopic ultrasound training, 272, 273
privileging qualified surgeons, 276
professional development, 5
scope of, 269
surgical residency and fellowship programs, 270
training, 4, 269–270
transabdominal ultrasound phantom, 272
universities *versus* community-based training programs, 270
verification and documentation for, 270–271

T
Taskin, H.E., 17–30
Taylor, A.M., 145
Tedeschi, M., 201–216
Teitelbaum, E.N., 177–185
Thermal ablation, 229–230, 240
Thompson, B.N.J., 145
Thompson, D.M., 183

Tilleman, E.H.B.M., 142
Tissue harmonic imaging (THI), 11–12
Torzilli, G., 213
Transabdominal ultrasound (TAUS), 288, 289
  biliary scanning technique, 36–38
  equipment setup, 31
  liver scanning technique, 36–38
  pancreas scanning techniques, 37–40
  standard scanning planes, 32–34
  transducer manipulation, 34–36
  transducer placement, 32, 34
Tranter, S.E., 183
Trauma ultrasound
  extended FAST (*see* Extended focused assessment with sonography for trauma (EFAST))
  FAST techniques (*see* Focused assessment with sonography for trauma (FAST))
  history, 109
  indications of, 118–119

U
Ultrasound (US)
  abdominal (*see* Abdominal ultrasound)
  abdominal organs and lesion characteristics
    anechoic regions, 61, 62
    brightness mode, 61
    hypoechoic tissues, 61, 62
    isoechoic regions, 62, 63
    mixed echogenicity, 61, 62
    ultrasound signals, 61
  abdominal ultrasound (*see* Abdominal ultrasound)
  abdominal wall (*see* Abdominal wall)
  artifacts (*see* Ultrasound artifacts)
  CEUS (*see* Contrast-enhanced ultrasound (CEUS))
  coding and billing
    E/M services, 284
    guideline for, 285
    Medicare reimbursement, 284
    modifier, 285
    professional and technical components of, 283–284
  documentation, 283
  DUS (*see* Duplex ultrasound (DUS))
  EAUS (*see* Endoanal ultrasound (EAUS))
  EUS (*see* Endoscopic ultrasound (EUS))
  guidance (*see* Ultrasound guidance)
  instrumentation (*See* Instrumentation)
  IOUS (*see* Intraoperative ultrasound (IOUS))
  LUS (*see* Laparoscopic ultrasound (LUS))
  physical principles
    acoustic streaming, 14
    acoustic waves, 7–8
    attenuation, 8–9
    Doppler effect, 9–10
    imaging modes, 10–11
    mechanical effects, 13–14
    newer technologies, 11–12, 15
    resolution, 9
    thermal effects, 12–13
    thermal index, 14
  surgeon-performed ultrasound, 287–288
  surgical (*see* Surgical ultrasound)
  surgical ultrasound (*see* Surgical ultrasound)
  TAUS (*see* Transabdominal ultrasound (TAUS))
  trauma ultrasound (*see* Trauma ultrasound)
Ultrasound artifacts
  absorption, 64
  attenuation, 64
  clinical classification of, 65
  correctable technical errors
    classic acoustic shadow, 66
    edge shadowing, 66, 67
    mirror imaging, 66, 67
    radiofrequency ablation, 66
    reverberation (contact) artifact, 66
    ring-down artifacts, 67
  enhancement, 64
  reflection and scatter, 64
  refraction, 65
  velocity displacement, 64–65
Ultrasound guidance
  advantages and disadvantages, 92–93
  biopsy/aspiration, 99–100
  drainage techniques
    acute cholecystitis, 103
    catheter placement, 102–103
    cholecystostomy catheter, 102, 104
    gallbladder, freehand technique, 102–104
    guidewire exchange technique, 101
    intra-abdominal abscess, 100
    intra-abdominal collections, 101–102
    postoperative biloma, 101
    trocar technique, 101
  equipment
    core-needle biopsy, 98–99
    needle visualization, 97–98
    spring-loaded automated biopsy needles, 99
  ethanol tumor ablation, 104, 105
  history, 89–90
  interventional ultrasonography, 90–92
  microwave ablation, 105, 106
  procedure preparation, 93
  radiofrequency ablation, 104, 105
  and visualization, 94–96
Umbilical hernias, 80
Urachal cyst, 79

V
Vaince, F., 71–87
Van Vledder, M.G., 209
Varadarajulu, S., 156
Vascular anomalies, 79
Velasco, J.M., 71–87, 89–106
Ventral hernias, 80–81
Vollmer, C.M., 142, 145

W
Weber, S.M., 142
White, R., 145

Y
Yamakawa, K., 201
Yano, M., 287–303
You, J.S., 119

Z
Zhao, Z.-W., 145
Zhou, Y., 211